

S-Substituted Dibenzothiophenium Triflates: Synthesis, Structure and Reactivity



Dissertation

zur Erlangung des mathematisch-naturwissenschaftlichen Doktorgrades

“Doctor rerum naturalium“

der Georg-August Universität Göttingen

im Promotionsprogramm

der Georg-August University School of Science (GAUSS)

vorgelegt von

Kevin Kafuta

aus Bad Kreuznach

Göttingen, 2021

Betreuungsausschuss:

- Prof. Dr. Manuel Alcarazo (Institut für Organische und Biomolekulare Chemie, Tammannstr. 2, 37077 Göttingen)
- Prof. Dr. Dietmar Stalke (Institut für Anorganische Chemie, Tammannstr. 4, 37077 Göttingen)

Mitglieder der Prüfungskommission:

- Referent: Prof. Dr. Manuel Alcarazo (Institut für Organische und Biomolekulare Chemie, Tammannstr. 2, 37077 Göttingen)
- Korreferent: Prof. Dr. Dietmar Stalke (Institut für Anorganische Chemie, Tammannstr. 4, 37077 Göttingen)

Weitere Mitglieder der Prüfungskommission:

- Jun.-Prof. Dr. Johannes C. L. Walker (Institut für Organische und Biomolekulare Chemie, Tammannstr. 2, 37077 Göttingen)
- Prof. Dr. Ulf Diederichsen (Institut für Organische und Biomolekulare Chemie, Tammannstr. 2, 37077 Göttingen)
- Dr. Christian Sindlinger (Institut für Anorganische Chemie, Tammannstr. 4, 37077 Göttingen)
- Dr. Matthias Otte (Institut für Anorganische Chemie, Tammannstr. 4, 37077 Göttingen)

Tag der mündlichen Prüfung: 08.04.2021

I hereby confirm that I have written the attached thesis on my own and that I did not use any other resources than those specified. This work has not been previously submitted, either in the same or in a similar form to any other examination committee and has not yet been published.

Troisdorf, 17.02.2021

Place and date

Signature

Acknowledgements

In the first place, I would like to thank Prof. Alcarazo for giving me the opportunity to supervise me as a PhD and providing laboratories in order to fulfill my work. My thanks go also to Prof. Stalke for assessing my written thesis as my second supervisor.

Many thanks also go to Jun.-Prof. Johannes Walker, Prof. Diederichsen, Dr. Sindlinger and Dr. Otte for being part of my committee.

In particular I wanted to thank Dr. Kozhushkov, Dr. Golz and Marvin Böhm for the thorough correction of my thesis.

Furthermore, I would like to thank my colleagues Adam Zielinski, Alejandro García-Barrado, Kai Aversch, Marvin Böhm, Bernd Waldecker, Martí Recort Fornals, Vijaykumar Gonela, Zhen Li and Samuel Pantiga not only for a warm and great atmosphere in the laboratory but also for sharing your knowledge and experience to me. You supported me very much in troubling times and I had a great time sharing a laboratory with you.

Great thanks go also to Christopher Golz for investigating X-ray structures for me. In addition, my special appreciation goes to Martin Simon and Martina Pretor who were always willing to help me. My thanks also go to my students André Korzun and Tianshu Liu. Moreover, my thanks go to the whole research group of Prof. Alcarazo for the great time I have had. It is an honor for me that I could be a part of this research group. Besides, I thank the NMR and Mass department for the measurements of my compounds.

I would like to thank Tiam, Ezra and Amelie. Something in my life would be missing without you. I enjoy seeing you growing up and learning things so fast. Stay the same as you are, and you will find your way through life.

Additionally, I would like to thank Lena. We have had a great time together so far and I am very happy to share a future with you.

My thanks go to my Mom & Erik and my Dad & Wiebke. I would not be where I am in my life without your support. Lastly, I would like to thank Sven, Laura, my friends, and my family who are always there whenever I need them.

“Phantasie ist wichtiger als Wissen, denn Wissen ist begrenzt.”

- Albert Einstein -

Content

Abbreviations	13
1. Introduction	16
1.1. General Properties of Sulfonium Salts	16
1.1.1. Sulfonium Salts in Nature	18
1.2. C(sp)-Substituted Sulfonium Salts	19
1.2.1. Synthesis of S-(Alkynyl) Sulfonium Salts.....	20
1.2.2. Structure of S-(Alkynyl) Sulfonium Salts.....	22
1.2.3. Reactivity of S-(Alkynyl) Sulfonium Salts	23
1.2.4. Alternative Alkynylation Reagents	26
1.2.5. Synthesis & Reactivity of S-(Cyano) Sulfonium Salts	32
1.3. C(sp ²)-Substituted Sulfonium Salts: Alkenyl substituents.....	37
1.3.1. Synthesis of S-(Alkenyl) Sulfonium Salts	38
1.3.2. Structure of S-(Alkenyl) Sulfonium Salts	41
1.3.3. Reactivity of S-(Alkenyl) Sulfonium Salts.....	43
1.3.4. Alternative Alkenylation Reagents	51
1.4. C(sp ²)-Substituted Sulfonium Salts: Aryl substituents	58
1.4.1. Synthesis of S-(Aryl) Sulfonium Salts.....	59
1.4.2. Structure of S-(Aryl) Sulfonium Salts.....	64
1.4.3. Reactivity of S-(Aryl) Sulfonium Salts	65
1.5. C(sp ³)-Substituted Sulfonium Salts.....	81
1.5.1. Synthesis of S-(Alkyl) Sulfonium Salts	81
1.5.2. Reactivity of S-(Alkyl) Sulfonium Salts.....	83
2. Project Aim.....	84
3. Results and Discussion	87
3.1. Synthesis & Applications of (Z)-Vinyl-Dibenzothio-phenium Triflates.....	87
3.1.1. Alternative Approach towards S-(Alkynyl)dibenzothiophenium Triflates	87

3.1.2.	Addition Reactions of <i>S</i> -(Alkynyl)dibenzothiophenium Triflates.....	90
3.1.3.	Michael-Type Reaction of Vinylsulfonium Salt 142b.....	94
3.1.4.	Phenanthrene Synthesis <i>via</i> Photochemical Cyclization of Vinylsulfonium Salts	103
3.1.4.1.	Synthesis of <i>S</i> -(Alkynyl)sulfonium Salt 5j	104
3.2.	Alkynylsulfone Synthesis	110
3.3.	Diyne Synthesis.....	113
3.4.	Synthesis & Reactivity of <i>S</i> -(Aryl)dibenzothiophenium Triflates	118
3.4.1.	Synthesis of <i>S</i> -(Aryl)dibenzothiophenium Triflates	118
3.4.2.	Structure of <i>S</i> -(Aryl)dibenzothiophenium Triflates 93o & 93m.....	123
3.4.3.	Nucleophilic Aromatic Substitution of <i>S</i> -(Aryl)sulfonium Triflates.....	126
3.4.4.	Palladium Catalysis with <i>S</i> -(Aryl)sulfonium Triflates	132
3.4.5.	Mechanistic investigation: Preparation of <i>S</i> -(Aryl)dibenzothiophenium Triflates	137
4.	Summary	143
5.	Experimental Part	146
	5-([1,1'-Biphenyl]-2-ylethynyl)-5 <i>H</i> -dibenzo[<i>b,d</i>]thiophen-5-ium Trifluoromethanesulfonate (5j):	147
	General Procedure for the Synthesis of Compounds 33a-33m.....	147
	Triisopropyl(phenylbuta-1,3-diyn-1-yl)silane (33a):	148
	1,4-Diphenylbuta-1,3-diyne (33a'):.....	148
	Triisopropyl[[4-(trifluoromethyl)phenyl]buta-1,3-diyn-1-yl]silane (33b):.....	148
	1,4-Bis[4-(trifluoromethyl)phenyl]buta-1,3-diyne (33b'):.....	148
	Triisopropyl[(4-methoxyphenyl)buta-1,3-diyn-1-yl]silane (33c):.....	149
	1,4-Bis(4-methoxyphenyl)buta-1,3-diyne (33c'):.....	149
	{[4-Bromo-[1,1'-biphenyl]-3-yl]buta-1,3-diyn-1-yl}triisopropylsilane (33d):.....	149
	[[4-Iodophenyl]buta-1,3-diyn-1-yl]triisopropylsilane (33e):.....	150
	Triisopropyl(thiophen-3-ylbuta-1,3-diyn-1-yl)silane (33f):	150
	3-[(Triisopropylsilyl)buta-1,3-diyn-1-yl]pyridine (33g):.....	150
	(Ferrocenylbuta-1,3-diyn-1-yl)triisopropylsilane (33h):.....	150

1,4-Diferrocenylbuta-1,3-diyne (33h'):	151
Triisopropyl[(7-methyl-1,8-diphenylnaphthalen-2-yl)buta-1,3-diyne-1-yl]silane (33i):	151
1,4-Bis(7-methyl-1,8-diphenylnaphthalen-2-yl)buta-1,3-diyne (33i'):	151
Methyl 3,4,5-Trimethoxy-2'-[(triisopropylsilyl)buta-1,3-diyne-1-yl]-[1,1'-biphenyl]-2-carboxylate (33j):	152
1-Methoxy-4-(phenylbuta-1,3-diyne-1-yl)benzene (33l):	152
General Procedure for the synthesis of Compounds 37a-37h	152
Triisopropyl[(phenylsulfonyl)ethynyl]silane (37a):	152
Triisopropyl(tosylethynyl)silane (37b):	153
{[(4-Fluorophenyl)sulfonyl]ethynyl}triisopropylsilane (37c):	153
{[(4-Bromophenyl)sulfonyl]ethynyl}triisopropylsilane (37d):	153
{[(4-Chlorophenyl)sulfonyl]ethynyl}triisopropylsilane (37e):	153
Triisopropyl{[(2-nitrophenyl)sulfonyl]ethynyl}silane (37f):	154
Triisopropyl[(thiophen-2-ylsulfonyl)ethynyl]silane (37g):	154
Diphenyl[(triisopropylsilyl)ethynyl]phosphine Oxide (37h):	154
(<i>E/Z</i>)-(4-Methoxybenzyl)[2-phenyl-2-(phenylsulfonyl)vinyl]sulfane (70c):	155
(<i>E/Z</i>)-2-[(2-Methoxy-1-phenylvinyl)sulfonyl]thiophene (70d):	155
(<i>Z</i>)-Triphenyl[2-phenyl-2-(phenylsulfonyl)vinyl]phosphonium Trifluoromethanesulfonate (70e)	156
(<i>Z</i>)- <i>N</i> ,4-dimethyl- <i>N</i> -[2-phenyl-2-(phenylsulfonyl)vinyl]benzene-sulfonamide (70f):	156
(<i>E/Z</i>)-(2-Bromophenyl)[2-phenyl-2-(phenylsulfonyl)vinyl]sulfane (70g):	157
(<i>Z</i>)-2-Phenyl-2-[2-phenyl-2-(phenylsulfonyl)vinyl]-1 <i>H</i> -indene-1,3(2 <i>H</i>)-dione (70h):	157
(<i>Z</i>)-1-Methyl-4-[[2-phenyl-2-(phenylsulfonyl)vinyl]sulfonyl]benzene (70i):	158
(<i>Z</i>)-[2-Bromo-1-(phenylsulfonyl)vinyl]benzene (70j)	158
(<i>Z</i>)-1-Methyl-4-[[2-phenyl-2-(phenylsulfonyl)vinyl]oxy]benzene (70k):	159
(<i>Z</i>)-[2-Fluoro-1-(phenylsulfonyl)vinyl]benzene (70l):	159
(<i>Z/E</i>)-1-Fluoro-4-[4-phenyl-4-(phenylsulfonyl)but-3-en-1-yn-1-yl]benzene (70m and 70m'):	160
(<i>E</i>)-1-Fluoro-4-[4-phenyl-4-(phenylsulfonyl)but-3-en-1-yn-1-yl]benzene (70m'):	160

(Z)-[(1-Phenyl-2-thiocyanatovinyl)sulfonyl]benzene (70n):	161
General Procedure for the Synthesis of Compounds 93a-93t.....	161
5-Phenyl-5 <i>H</i> -dibenzo[<i>b,d</i>]thiophen-5-ium Trifluoromethanesulfonate (93a):	161
5-(4-Ethylphenyl)-5 <i>H</i> -dibenzo[<i>b,d</i>]thiophen-5-ium Trifluoromethane-sulfonate (93b):	162
5-(4-Cyclopropylphenyl)-5 <i>H</i> -dibenzo[<i>b,d</i>]thiophen-5-ium Trifluoromethanesulfonate (93c): ..	162
5-(4-Methoxyphenyl)-5 <i>H</i> -dibenzo[<i>b,d</i>]thiophen-5-ium Trifluoromethanesulfonate (93e):	163
5-(4-Phenoxyphenyl)-5 <i>H</i> -dibenzo[<i>b,d</i>]thiophen-5-ium Trifluoromethanesulfonate (93f):	163
5-(3,4-Dichlorophenyl)-5 <i>H</i> -dibenzo[<i>b,d</i>]thiophen-5-ium Trifluoromethanesulfonate (93g):	164
5-(4-Fluorophenyl)-5 <i>H</i> -dibenzo[<i>b,d</i>]thiophen-5-ium Trifluoromethanesulfonate (93h):	164
5-(4-Chlorophenyl)-5 <i>H</i> -dibenzo[<i>b,d</i>]thiophen-5-ium Trifluoromethanesulfonate (93i):	164
5-(4-Bromophenyl)-5 <i>H</i> -dibenzo[<i>b,d</i>]thiophen-5-ium Trifluoromethanesulfonate (93j):	165
5-(4'-Iodo-[1,1'-biphenyl]-4-yl)-5 <i>H</i> -dibenzo[<i>b,d</i>]thiophen-5-ium Trifluoromethanesulfonate (93k):	165
5-(4'-{[(Trifluoromethyl)sulfonyl]oxy}-[1,1'-biphenyl]-4-yl)-5 <i>H</i> -dibenzo[<i>b,d</i>]thiophen-5-ium Trifluoromethanesulfonate (93l):	166
5-(3,4-Dibromothiophen-2-yl)-5 <i>H</i> -dibenzo[<i>b,d</i>]thiophen-5-ium Trifluoromethanesulfonate (93m):	166
[2,5'-Bidibenzo[<i>b,d</i>]thiophen]-5'-ium Trifluoromethanesulfonate (93n):	166
5-[3-(Ethoxycarbonyl)-4-methoxyphenyl]-5 <i>H</i> -dibenzo[<i>b,d</i>]thiophen-5-ium Trifluoromethanesulfonate (93o):	167
5-(Benzofuran-2-yl)-5 <i>H</i> -dibenzo[<i>b,d</i>]thiophen-5-ium Trifluoromethanesulfonate (93p):	167
5-(4-Methoxy-2,6-dimethylphenyl)-5 <i>H</i> -dibenzo[<i>b,d</i>]thiophen-5-ium Trifluoromethanesulfonate (93q):	168
5-[(8 <i>R</i> ,9 <i>S</i> ,13 <i>S</i> ,14 <i>S</i>)-3-Methoxy-13-methyl-17-oxo-7,8,9,11,12,13,14, 15,16,17-decahydro-6 <i>H</i> -cyclopenta[<i>a</i>]phenanthren-2-yl]-5 <i>H</i> -dibenzo[<i>b,d</i>]thiophen-5-ium Trifluoromethanesulfonate (93r):	168
5-(4-Oxo-2-phenyl-4 <i>H</i> -chromen-3-yl)-5 <i>H</i> -dibenzo[<i>b,d</i>]thiophen-5-ium Trifluoromethanesulfonate (93s)	168
5-(2,6-di- <i>tert</i> -Butylpyridin-3-yl)-5 <i>H</i> -dibenzo[<i>b,d</i>]thiophen-5-ium Trifluoromethanesulfonate (93t):	169

5-[(8 <i>R</i> ,9 <i>S</i> ,13 <i>S</i> ,14 <i>S</i>)-3-Methoxy-13-methyl-17-[[trifluoromethyl]-sulfonyl]oxy]- 7,8,9,11,12,13,14,15-octahydro-6 <i>H</i> -cyclopenta[<i>a</i>]phen-anthren-2-yl]-5 <i>H</i> -dibenzo[<i>b,d</i>]thiophen- 5-ium Trifluoromethanesulfo-nate (93u):	169
(3,5'-Bidibenzo[<i>b,d</i>]thiophen)-5'-ium 5,5-Dioxide Trifluoromethanesul-fonate (93y):	170
(5,2':8',5''-Terdibenzo[<i>b,d</i>]thiophenes)-5,5''-dium Trifluoromethanesul-fonate (93n'):	170
(<i>E/Z</i>)-5-[2-(4-Fluorophenyl)-2-[[trifluoromethyl]sulfonyl]oxy]vinyl]-5 <i>H</i> -dibenzo[<i>b,d</i>]thiophen-5- ium Trifluoromethanesulfonate (142a):	171
(<i>Z</i>)-5-[2-Phenyl-2-(phenylsulfonyl)vinyl]-5 <i>H</i> -dibenzo[<i>b,d</i>]thiophen-5-ium Trifluoromethanesulfonate (142b):	172
(<i>Z</i>)-5-(2-Chloro-2-phenylvinyl)-5 <i>H</i> -dibenzo[<i>b,d</i>]thiophen-5-ium Trifluoromethanesulfonate (142c):	172
(<i>E</i>)-5-(2-Chloro-1-iodo-2-phenylvinyl)-5 <i>H</i> -dibenzo[<i>b,d</i>]thiophen-5-ium Trifluoromethanesulfonate (142d):	173
(<i>E</i>)-5-(1,2-Dibromo-2-phenylvinyl)-5 <i>H</i> -dibenzo[<i>b,d</i>]thiophen-5-ium Trifluoromethanesulfonate (142e):	173
(<i>E</i>)-5-{2-Chloro-1-iodo-2-[4-(trifluoromethyl)phenyl]vinyl}-5 <i>H</i> -dibenzo[<i>b,d</i>]thiophen-5-ium Trifluoromethanesulfonate (142f):	174
5-{3-[4-(Trifluoromethyl)phenyl]bicyclo[2.2.1]hepta-2,5-dien-2-yl}-5 <i>H</i> -dibenzo[<i>b,d</i>]thiophen-5- ium Trifluoromethanesulfonate (142g):	174
(<i>E</i>)-5-{1,2-Dibromo-2-[4-(trifluoromethyl)phenyl]vinyl}-5 <i>H</i> -diben-zo[<i>b,d</i>]thiophen-5-ium Trifluoromethanesulfonate (142h):	175
(<i>Z</i>)-5-{2-([1,1'-Biphenyl]-2-yl)-2-(phenylsulfonyl)vinyl}-5 <i>H</i> -dibenzo-[<i>b,d</i>]thiophen-5-ium Trifluoromethanesulfonate (142i):	176
5-{3-([1,1'-Biphenyl]-2-yl)bicyclo[2.2.1]hepta-2,5-dien-2-yl}-5 <i>H</i> -dibenzo[<i>b,d</i>]thiophen-5-ium Trifluoromethanesulfonate (142j):	176
(<i>Z</i>)-1-Phenyl-2-[2-phenyl-2-(phenylsulfonyl)vinyl]-1 <i>H</i> -pyrrole (149)	177
[2-Phenyl-2-(phenylsulfonyl)ethene-1,1-diyl]bis(phenylsulfane) (151a):	177
2-[Phenyl(phenylsulfonyl)methylene]naphtho[1,8- <i>de</i>][1,3]dithiine (151b):	178
2,4-Diphenylfuran-3-carbonitrile (153):	178
9-(Phenylsulfonyl)phenanthrene (159):	179

1,4-Dihydro-1,4-methanotriphenylene (160):	179
1,4-Bis[(3-methoxyphenyl)thio]benzene (162a):	180
1-(4-Chlorophenoxy)-3-methoxybenzene (165b):	180
General Procedure for the Synthesis of Compounds 169a-169e	181
5-[4-(Piperidin-1-yl)phenyl]-5H-dibenzo[<i>b,d</i>]thiophen-5-ium Trifluoromethanesulfonate (169a):	181
5-[4-(Pyrrolidin-1-yl)phenyl]-5H-dibenzo[<i>b,d</i>]thiophen-5-ium Trifluoro-methanesulfonate (169b):	181
5-[4-(4-Phenylpiperidin-1-yl)phenyl]-5H-dibenzo[<i>b,d</i>]thiophen-5-ium Trifluoromethanesulfonate (169c):	182
5-(4-Morpholinophenyl)-5H-dibenzo[<i>b,d</i>]thiophen-5-ium Trifluoro-methanesulfonate (169d):	182
5-[4-{[3-(10,11-Dihydro-5H-dibenzo[<i>b,f</i>]azepin-5-yl)propyl](methyl)-amino}phenyl]-5H- dibenzo[<i>b,d</i>]thiophen-5-ium Trifluoromethanesulfo-nate (169e):	183
General Procedure for the synthesis of Compounds 175, 176a & 176b	183
Methyl 4'-Ethyl-[1,1'-biphenyl]-4-carboxylate (175):	183
(8 <i>R</i> ,9 <i>S</i> ,13 <i>S</i> ,14 <i>S</i>)-3-Methoxy-13-methyl-2-(thiophen-2-yl)-6,7,8,9,11, 12,13,14,15,16-decahydro- 17 <i>H</i> -cyclopenta[<i>a</i>]phenanthren-17-one (176a):	184
(8 <i>R</i> ,9 <i>S</i> ,13 <i>S</i> ,14 <i>S</i>)-2-(Furan-2-yl)-3-methoxy-13-methyl-6,7,8,9,11,12,13, 14,15,16-decahydro-17 <i>H</i> - cyclopenta[<i>a</i>]phenanthren-17-one (176b):	184
4-Chloro-4'-(trifluoromethyl)-1,1'-biphenyl (177a):	185
(4-Chlorophenyl){4''-(trifluoromethyl)-[1,1':2',1''-terphenyl]-2-yl}sulfane (177d):	185
4-Bromo-4'-(trifluoromethyl)-1,1'-biphenyl (178a):	186
General Procedure for the Synthesis of Compounds 179a, 180a, 181a, 182a & 182b	186
4-Iodo-4''-(trifluoromethyl)-1,1':4',1''-terphenyl (179a):	187
4''-(Trifluoromethyl)-[1,1':4',1''-terphenyl]-4-yl Trifluoromethanesulfo-nate (180a):	187
4-Iodo-1,1':4',1''-terphenyl (181a):	187
4''-Iodo-4-methoxy-3,5-dimethyl-1,1':4',1''-terphenyl (182a):	188
4,4'''-Dimethoxy-3,3''',5,5''''-tetramethyl-1,1':4',1'':4'',1'''-quaterphenyl (182b):	188

NMR Spectra.....	189
X-Ray Structures.....	295
References.....	330

Abbreviations

°	Degree	cal	Calories
°C	Degree celsius	cald.	Calculated
Å	Ångstrom (10 ⁻¹⁰ m)	cat.	Catalytic
α	Alpha	cm	Centimeter
β	Beta	COD	Cyclooctadiene
σ	Sigma	COX	Cyclooxygenase
σ*	Antibonding sigma	Cy	Cyclohexyl
δ	Chemical shift	d	Dublett
π	Pi	DABCO	1,4-Diazabicyclo[2.2. 2]octane
π*	Antibonding pi	DABSO	1,4-Diazabicyclo[2.2. 2]octane-bis(sulfur oxide)
ΔT	heat	dba	Dibenzylidenacetone
ΔG	Gibbs energy	DBT	Dibenzothiophene
Δν _{1/2}	Average line broadening	DBT ⁺	Dibenzothiophenium triflate
[2.2.2]K	2.2.2-Cryptand	DBU	Diazabicycloundecene
λ̄	Wavelength	DCM	Dichloromethane
¹ H	Hydrogen-1	ddpf	1,1'-Ferrocenediyl-bis(diphenylphosphine)
¹³ C	Carbon-13	de	Diastereomeric excess
¹⁸ F	Fluorine-18	DFT	Density-functional theory
¹⁹ F	Fluorine-19	DIPEA	<i>N,N</i> -Diisopropylethylamine
³¹ P	Phosphorus-31	DMF	<i>N,N</i> -Dimethylformamide
15-C-5	15-crown-5 ether	DMSO	Dimethylsulfoxide
Ac	Acetyl	DSC	Differential scanning calorimetry
Alk	Alkyl	<i>E</i>	Entgegen
Alphos	Di-1-adamantyl(4''-butyl-2'',3'',5'',6''-tetrafluoro-2',4',6'-triisopropyl-2-methoxy-meta-terphenyl)phosphine	E ⁺	Generic electrophile
Ar	Generic arene	e ⁻	Electron
aq	Aqueous	EBX	Ethynylbenziodoxolon
ATR	Attenuated total reflection	EI	Electron Ionisation
Boc	<i>tert</i> -Butyloxycarbonyl	equiv.	Equivalents
Bpin	Pinacolato boryl	ESI-MS	Electrospray ionisation mass spectrometry
bpy	2,2'-Bipyridine	Et	Ethyl
Bu	Butyl	<i>et al.</i>	et alia

EDG	Electron donating group	min	Minutes
EPR	Electron paramagnetic resonance	MSA	Methanesulfonic acid
eV	Electron volt	n-Bu	<i>n</i> -Butyl
EWG	Electron withdrawing group	n-BuLi	<i>n</i> -Butyllithium
FBW	Fritsch-Buttenberg Wiechell		
FG	Functional group	n-Oct	<i>n</i> -Octyl
g	Gram	nm	Nanometer
GC-MS	Gas chromatography mass spectrometry	NMR	Nuclear magnetic resonance
h	Hours	Npht	Naphthyl
HMDS	Hexamethyldisilazane	Nu⁻	Generic nucleophile
HPLC	High performance liquid chromatography	o	<i>ortho</i>
HRMS	High resolution mass spectrometry	OA	Oxidative addition
hν	Light irradiation	p	<i>para</i>
Hz	Hertz	p.	Page
<i>i</i>-Pr	<i>iso</i> -Propyl	Ph	Phenyl
IR	Infrared spectroscopy	Pr	Propyl
<i>J</i>	Coupling constant	ppm	Parts per million
J	Joule	PTH	10-Phenylphenothiazine
k	Kilo	q	Quartett
<i>k</i>	Rate constant	R	Universal gas constant
LED	Light-emitting diode	RCY	Decay-corrected radio chemical yield
M	Molar	rt	Room temperature
[M]	Generic metal	s	Singulett
<i>m</i>	<i>meta</i>	SAM	S-Adenosyl methionine
m	Multiplett	SES	2-(Trimethylsilyl)ethanesulfonyl
<i>m/z</i>	Mass-to-charge ratio	SET	Single electron transfer
<i>m</i>CPBA	<i>meta</i> -Chloroperoxybenzoic acid	SMM	S-Methylmethionine
Me	Methyl	SMC	Suzuki-Miyaura Coupling
MHz	Megahertz	S_N	Nucleophilic substitution
mg	Milligram	SPhos	2-Dicyclohexylphosphino-2',6'-dimethoxybiphenyl
mL	Milliliter	t	Triplett
μL	Mikroliter	t	Time
mmol	Millimol	T	Temperature
μmol	Mikromol	TA-Au	1,2,3-Triazole-Gold ^I
MW	Microwave	TBAF	Tetrabutylammonium fluoride

TBAX	Tetrabutylammonium halide	TPP	<i>meso</i> -Tetraphenylporphine
TBDMS	<i>tert</i> -Butyldimethylsilyl	TIPS	Triisopropylsilyl
TBDPS	<i>tert</i> -Butyldiphenylsilyl	TS	Transition state
<i>t</i>-Bu	<i>tert</i> -Butyl	Ts	Tosyl
TEBA	Tetraethylbenzylammonium chloride	vdW	Van der Waals
Tf	Trifluoromethylsulfonyl	VSEPR	Valence shell electron pair repulsion theory
TFAA	Trifluoroacetic acid	W	Watt
TFT	2,3,7,8-Tetrafluorothianthrene	Z	Zusammen
THF	Tetrahydrofuran	X⁻	Generic anion
TMS	Trimethylsilyl	Xphos	2-Dicyclohexylphosphino-2',4',6'-triisopropylbiphenyl

1. Introduction

1.1. General Properties of Sulfonium Salts

A sulfonium salt $R_3S^+X^-$ can be defined as a positively charged cationic sulfur moiety, bearing three either alkyl, alkenyl or aryl substituents as well as a lone electron pair and a counteranion. The lone pair forces the sulfonium salts to adopt a pyramidal geometry according to the VSEPR theory and is in the origin of their stereochemical properties.^{1,2} The typical C–S bond length in sulfonium salts is 1.806 Å, and the C–S–C bond angles have an average value of 102.5° in the solid state.¹ These salts are isoelectronic and isostructural to tertiary phosphines (Figure 1).²

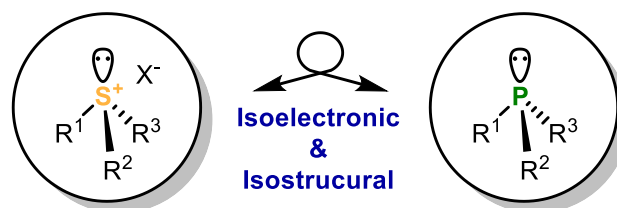


Figure 1: Isoelectronic and isostructural comparison of sulfonium salts with tertiary phosphines.

The inversion of the pyramidal structure of sulfonium salts is identical to those of tertiary phosphines.^{3,4} This process is thermodynamically hindered, which allows the isolation of both possible enantiomers. The typical energy value of the inversion barrier for triarylsulfonium salts was determined with $\Delta G^\ddagger = 25.4 \text{ kcal} \cdot \text{mol}^{-1}$ (value range 23.8–31.0 kcal · mol⁻¹) while coalescence occurred at approximately 200 °C.³ For the comparison, the isostructural oxonium salts are much less stable than their higher sulfonium analogs.⁵ In fact, many sulfonium salts turned out to be easy to handle under ambient condition; furthermore, isolation by column chromatography is not uncommon.

The chemical application of sulfonium salts is mainly divided into four categories (Figure 2). Utilizing a base converts them into sulfur ylides, which can be used to form cyclopropanes, oxiranes or aziridines.^{6–8} At least one of the substituents should be an alkyl chain to allow abstraction of the α -proton. It has been shown that sulfonium ylides can be transformed into thioethers *via* intramolecular sigmatropic shifts.^{9,10}

The formal positive charge on the sulfur atom renders the sulfonium moiety more electro-withdrawing. Thus, this leads to an inversion of the carbon neighbor's polarity, the so called "Umpolung". This property allows nucleophiles to attack the relatively low energetic $\sigma^*(S-R)$

orbital which results in a successive ligand coupling of the nucleophile and the carbon substituent. Alternatively the nucleophile attacks the α -carbon center directly and forms a bond with the sp^{-11} , sp^{2-12} or sp^3 -hybridized carbon¹³ (see Chapter 1.3.3 and 1.3.4 for detailed explanation of the mechanistic pathways). Such a reactivity is not the prerogative of sulfonium salts; thus, hypervalent iodine^{III}-based reagents show similarities in this respect (see Chapter 1.2.1).¹⁴

The delivery of an electron to a sulfonium salt, either through radical chemistry or by redox process, results in a homolytic cleavage of C–S bond with the release of an alkyl¹² or aryl radical¹⁵.

At last, transition metals like palladium can oxidatively insert into the C–S bond allowing to perform successive cross-coupling reactions.¹⁶

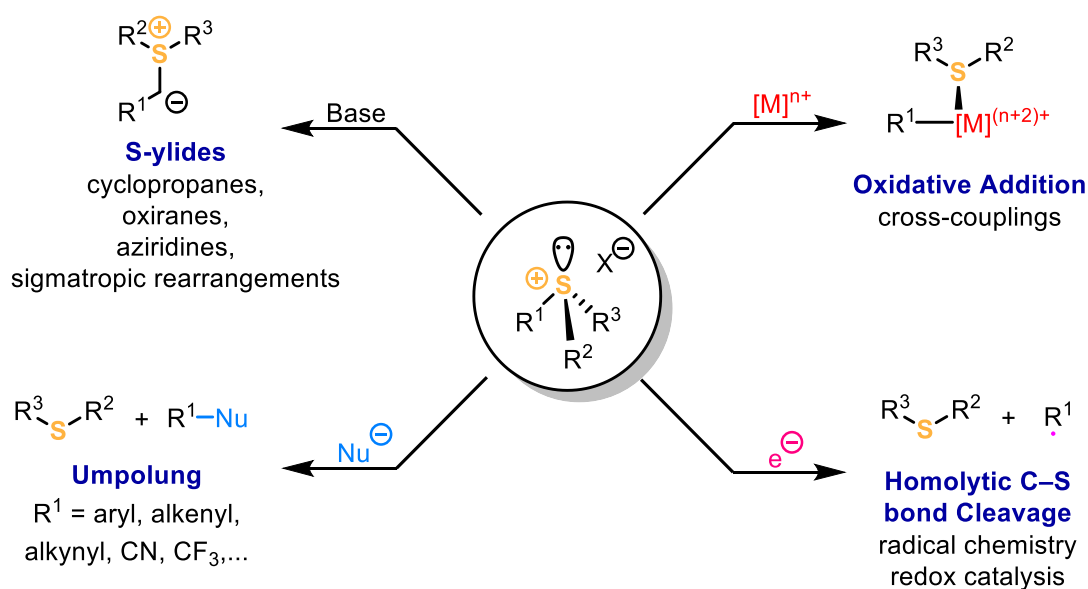
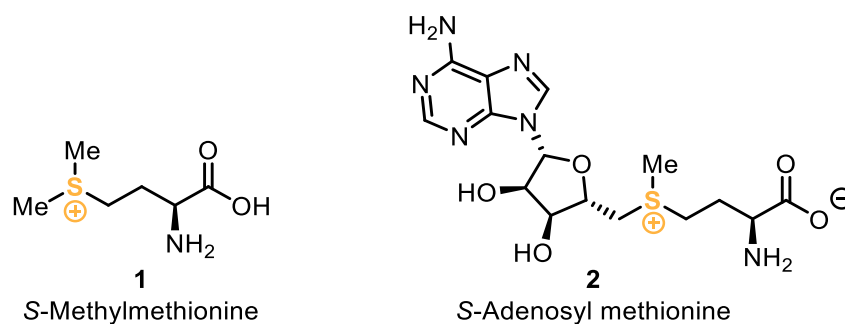


Figure 2: Four different transformation types of sulfonium salts.

Although sulfonium salts are well known and their reactivity has been widely explored since the middle of the last century, their chemistry still attracts the attention of a number of scientists nowadays. These salts appear to have great potential for expanding the known methodologies of inorganic and organic chemistry.

1.1.1. Sulfonium Salts in Nature

In nature, sulfonium salts play a key role in biosynthetic pathways. The natural abundance of *S*-methylmethionine **1** (Scheme 1), sometimes called vitamin U, is most noticeable in vegetables such as cabbage, kohlrabi, turnip, tomatoes, celery, leek, garlic leaves, beet root, raspberries and strawberries.¹⁷ This natural compound has not only a therapeutic effect in preventing gastrointestinal ulceration but moreover enhances skin regeneration and offers photoprotective properties to the skin.¹⁸



Scheme 1: *S*-Methylmethionine (**1**, SMM; left) & *S*-adenosyl methionine (**2**, SAM; right).

S-Adenosyl methionine **2** (Scheme 1) is a natural alkylating reagent, which is produced and consumed mostly in the liver. Biosynthetically this compound is used for methylation of nucleic acids, proteins, lipids and secondary metabolites. Over 40 different methylation reactions of **1** and **2** are known up to now.¹⁹

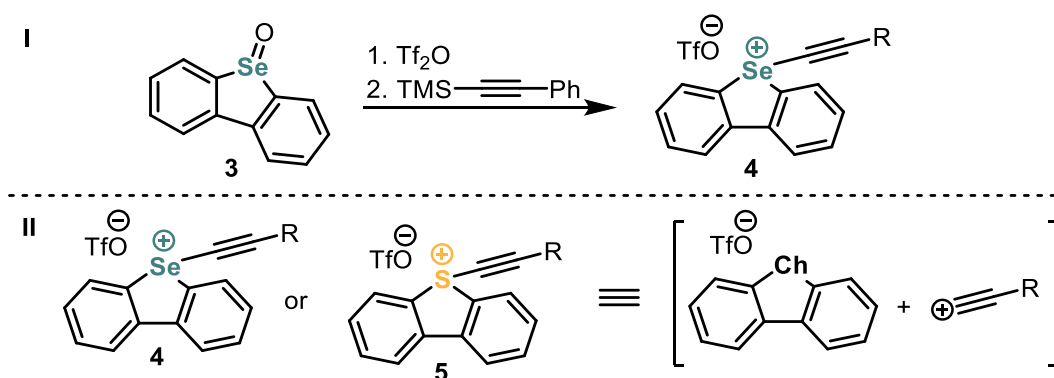
As a proof of concept, **2** is an example from nature that shows how a chiral transfer reagent should look like. This molecule could be the basis for many types of asymmetric transfer reactions.

1.2. C(sp)-Substituted Sulfonium Salts

Until very recently, the knowledge on the synthetic utility of *S*-alkynylated sulfonium salts was very limited. The main issue was the deficient accessibility towards these compounds since the main synthetic protocols either included Iodine^{III}-reagents²⁰ or sulfur-centered radicals²¹ (see Chapter 1.2.1). In 2009 another approach was considered by Liska *et al.* utilizing TMS-protected alkynes and activated sulfoxides (see Chapter 1.2.1).²² With this sophisticated procedure the chemistry of *S*-(alkynyl)sulfonium salts flourished and enabled not only the synthesis of (alkynyl)dibenzothiophenium salts but also their *S*-cyanated analogues (see Chapter 1.2.5).^{11,23,24}

It has to be noted that this synthetic approach was introduced by Nara *et al.* in 1998 to synthesize the analogous 5-(alkynyl)dibenzoselenophenium triflate **4** (Scheme 2, I).²⁵ However, the potential of this structural motif as [RC≡C]⁺-synthon has not been pointed out and therefore not explored by the authors (Scheme 2, II).

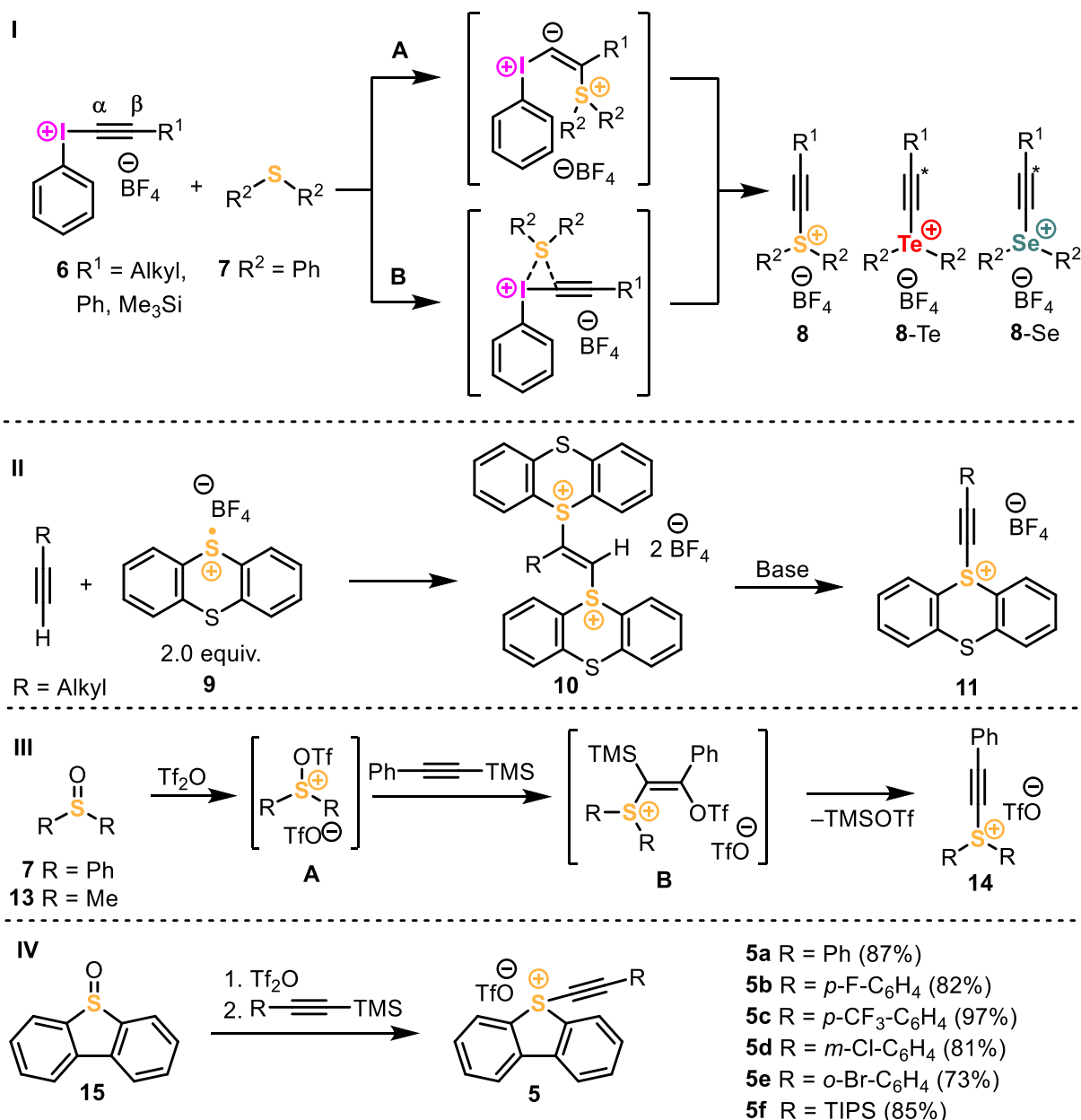
These sulfonium salts were only used as cationic polymerization photoinitiators²² but recently they were established as versatile alkylation reagents and, moreover, used in natural product synthesis (see Chapter 1.2.3).²⁶



Scheme 2: I) Synthetic method by Nara towards selenophenium salt **4**. II) Compounds **4** and **5** as ethynyl-synthons.

1.2.1. Synthesis of *S*-(Alkynyl) Sulfonium Salts

The early synthetic approaches to these compounds consisted either in treatment of diphenyl sulfide **7** with iodonium salts **6**²⁰ (Scheme 3, I) or of terminal alkyne with two equivalents of thiantrenium radical **9**²¹ (Scheme 3, II) to gain access to the corresponding sulfonium salts **8** and **11**, respectively.



Scheme 3: Three pathways to obtain *S*-alkynyl sulfonium salts I) *via* iodine^{III} salts;²⁰ II) *via* thiantrenium radical;²¹ III) *via* sulfoxides²² and IV) synthesis of *S*-(alkynyl)dibenzothiophenium triflates **5**.^{11,23}

The formation of **8** can follow two different pathways (Scheme 3, I). Pathway **A** starts with an attack by the sulfur to the β -carbon and generates intermediate **A**. After migration of the residue from β -C to α -C, the final product **8** is formed. The alternative pathway **B** starts with

the attack of the sulfur to the α -carbon. Intermediate **B** then releases iodobenzene and affords the sulfonium salt **8**. In the control ethynylation of diphenyl telluride and diphenyl selenide with β - ^{13}C -enriched **6-Ph** (99%), no randomization of the label was detected, as ^{13}C atom remained in β -position in both **8-Te** (98%) and **8-Se** (95%). However, these results did not exclude either one of the suggested mechanisms, and both pathways **A** and **B** could indeed take place.²⁰

Addition of two equivalents of thianthrene radical **9** to the terminal alkyne results in the formation of compound **10** (Scheme 3, **II**). Upon treatment of the latter with a base, a simple elimination reaction of one thianthrene occurs, and S-(alkynyl)thianthrenium tetrafluoroborate **11** is formed.

The method described in Scheme 3, **III** became the most prominent one and is used exclusively throughout the entire thesis. Treatment of a sulfoxide with an activator like triflic anhydride will generate intermediate **A**. This intermediate can react with a TMS-protected alkyne *via* an addition reaction forming **B**, which rapidly releases TMSOTf furnishing the corresponding sulfonium salt **14**.

In 2018 Alcarazo and coworkers demonstrated a convenient protocol based on the work of Liska *et al.*²² for the preparation of a series of S-(alkynyl)dibenzothiophenium triflates **5a-5f**.^{11,23}

1.2.2. Structure of S-(Alkynyl) Sulfonium Salts

The crystal structures of **5a** and **5f** in solid state are displayed in Figure 3.¹¹ Both compounds adopt distorted bipyramidal geometries around the cationic sulfur in the solid state and, as depicted in Figure 3, form dimeric structures by two bridging triflate anions, usually with a pair of shorter and longer S–O chalcogenic interactions.

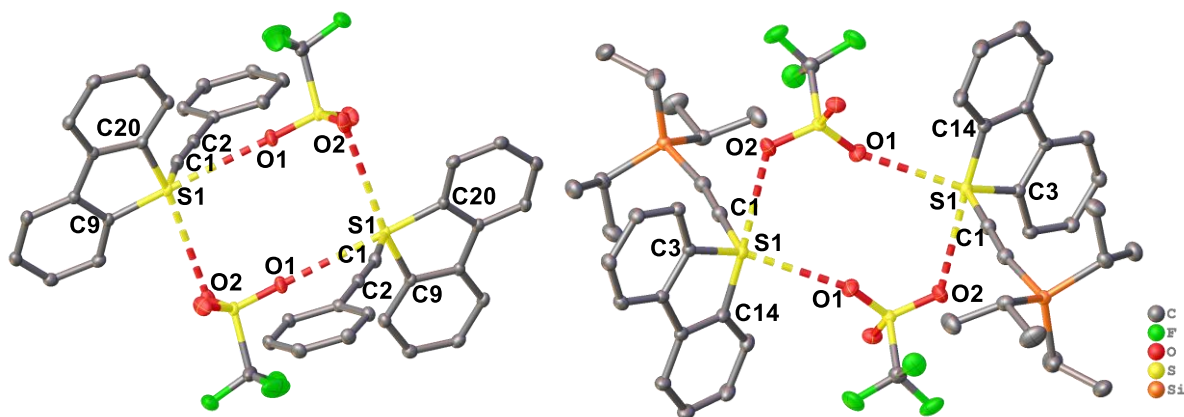


Figure 3: X-ray structures of the salts **5a** (left) and **5f** (right) in solid state. Anisotropic displacement shown at 50% probability level. Hydrogen atoms & solvent molecules were omitted for clarity. Selected bond lengths [Å] and angles [°]: **5a** (left) S1–C1 1.6871(12), S1–C20 1.7878(11), S1–C9 1.7897(11), S1–O1 3.157(1), S1–O2 3.413, O1–C1 3.179(2), C9–S1–O1 179.0(1);¹¹ **5f** (right) S1–C1 1.6980(9), S1–C3 1.7933(8), S1–C14 1.7935(8), S1–O1 3.038(1), S1–O2 2.971(9), O1–C1 3.101(1), C14–S1–O2 177.3(1).¹¹

While **5a** adopts an almost colinear angle C9–S1–O1 of 179.0(1)°, the tendency to a slightly more distorted pyramidal geometry is observed in **5f** with the angle C14–S1–O2 = 177.3(1)°. The sum of angles around S1 in **5a** is 302.3° and compared to that 294.6° in **5f**, showing somewhat stronger pyramidalization for the latter.

Additionally, consideration of the bond distances S1–O1 and S1–O2 indicates a short and a long chalcogen bond in each dimeric structure. Compound **5a** shows a short S1–O1 contact of 3.157 Å which reveals a strong interaction between the triflate anion and the sulfur center. On the other hand, the bond distance between S1 and O2 with 3.413 Å represents a rather weak interaction.

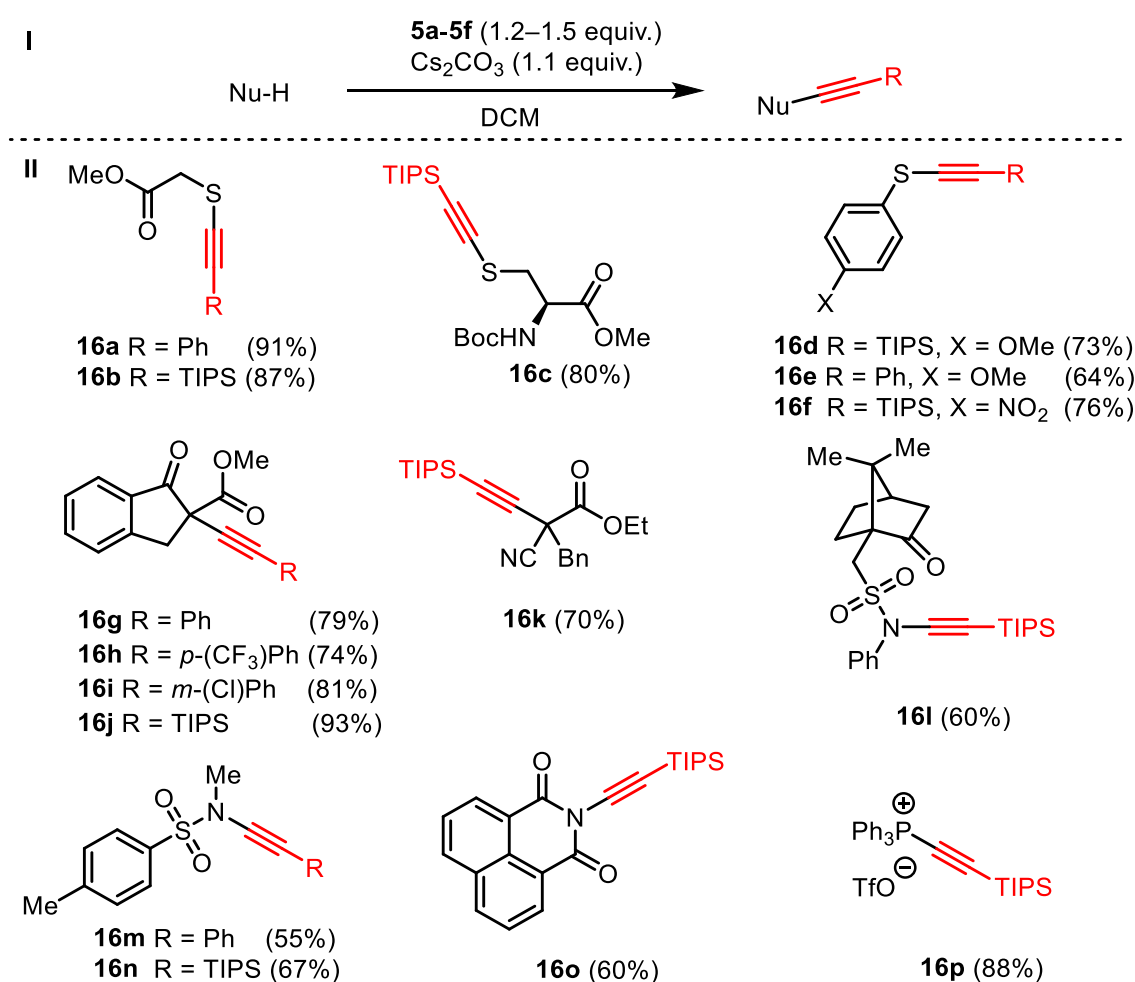
In **5f** both S–O distances are significantly shorter (3.038 Å for S1–O1 and 2.972 Å for S1–O2), even shorter than the sum of the van der Waals radii of the corresponding elements (3.32 Å). This fact hints towards an electron deficient chalcogen center in **5f** or in other words a more Lewis acidic sulfur center compared to **5a**.^[24]

This observation is in accordance with the reactivity of both reagents, since alkynylation of the nucleophiles tend to proceed via a participation of the sulfurane intermediate. The low

electron density on C1 in **5f** leads to the direct ligand coupling between C1 and nucleophile, whereas in **5a** the tendency to undergo a nucleophilic C2-attack predominates (see Chapter 1.2.3).^{2,11,27}

1.2.3. Reactivity of *S*-(Alkynyl) Sulfonium Salts

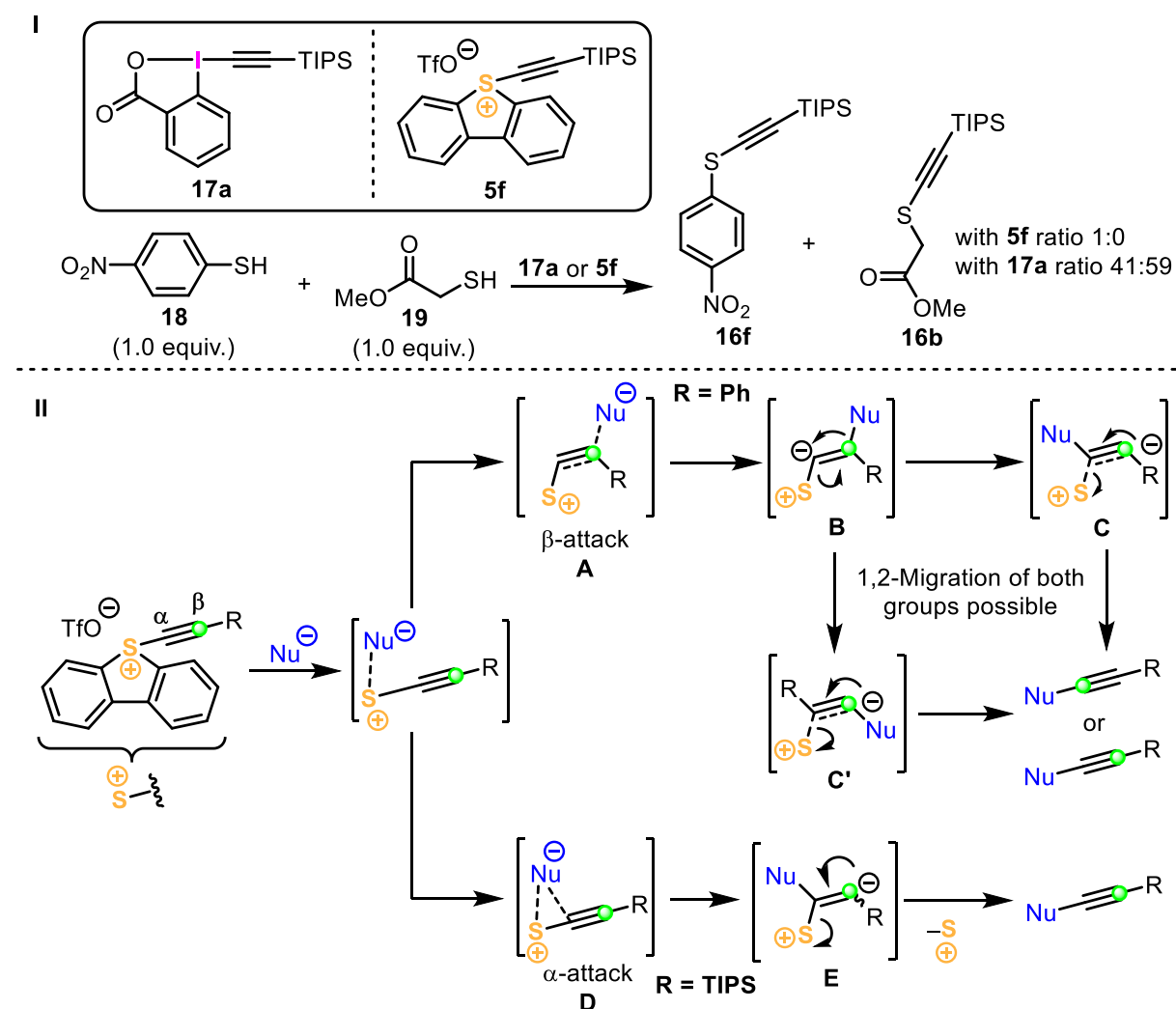
With the set of 5-(alkynyl)dibenzothiophenium triflates in hand, Alcarazo presented a variety of nucleophiles suitable for electrophilic alkylation.¹¹ In Scheme 4 a few selected examples of *S*-, C-, N- or P-centered nucleophiles are shown. To each C–H acidic nucleophile a slight excess of cesium carbonate as a base was added.



Scheme 4: Selected examples of the substrate scope for the electrophilic alkylation.¹¹

Alkyl thiols and thiophenols were easily alkylation in excellent yields, as represented by examples **16a** to **16f**. Compounds with activated C–H bonds also proved to be suitable nucleophiles, as depicted in examples **16g** to **16j**, although the reaction required 60 °C to proceed. Overall, nitrogen-based nucleophiles delivered slightly lower yields (**16l** to **16o**, 55–67%). Lastly triphenylphosphine was also utilized and gave **16p** in excellent yield.

A competition experiment of **5f** versus the EBX-TIPS analog **17a** revealed a higher selectivity for the sulfur-based transfer reagent. Hypervalent iodine^{III}-based **17a** reacts much faster but is more likely to deliver mixtures when exposed to more than one nucleophilic reaction partner (Scheme 5, I).



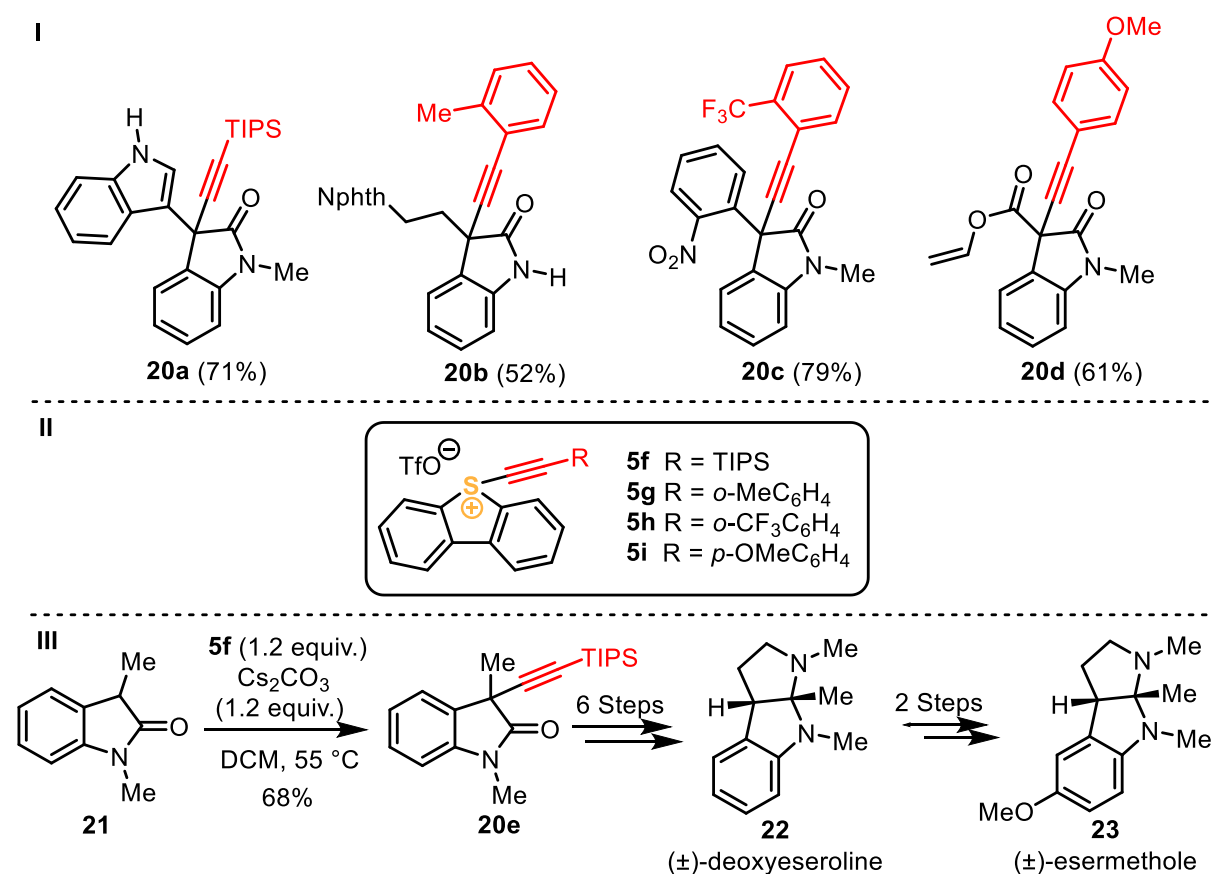
Scheme 5: I) Competition reaction between **17a** and **5f**; II) Reaction pathways for the nucleophilic attack on a generic electrophilic alkylation reagent (green dot: ^{13}C -labeled carbon atom).

Additionally, the same reactions were repeated with the specially synthesized β - ^{13}C -labeled transfer reagents **5a** and **5f** identifying the positions of the ^{13}C label in the final products. These studies revealed following mechanistic insights (Scheme 5, II): It is assumed that the nucleophile approaches the cationic sulfur center and coordinates it to form a sulfurane. This results in two potential pathways which depend on the substitution of the alkyne. If the terminal residue of the alkyne is of aromatic nature, the nucleophile preferentially attacks the β -carbon affording the coordinative intermediate **A**. Formation of the σ -bond $\text{C}_\beta\text{-Nu}$ furnished vinyl anion **B**, both substituents of which, either the nucleophile or R, are able to undergo a

1,2-shift giving **C** and **C'**, respectively. Subsequent elimination of dibenzothiophene led to the formation of the final product. Depending on which group finally migrated, the ^{13}C will be in the α - or β -position of the product.

In cases of a TIPS group as the terminal residues, coordination of the nucleophile to the α -carbon is preferred. After connection of the σ -bond $\text{C}_\alpha\text{-Nu}$ in **D**, the vinyl anionic intermediate **E** is formed, which also released dibenzothiophene *via* an elimination process and generated the Nu-C-sp^3 bond.

Just recently Bisai and coworkers demonstrated extended reactivity of *S*-(alkynyl) dibenzothiophenium triflates (Scheme 6).²⁶

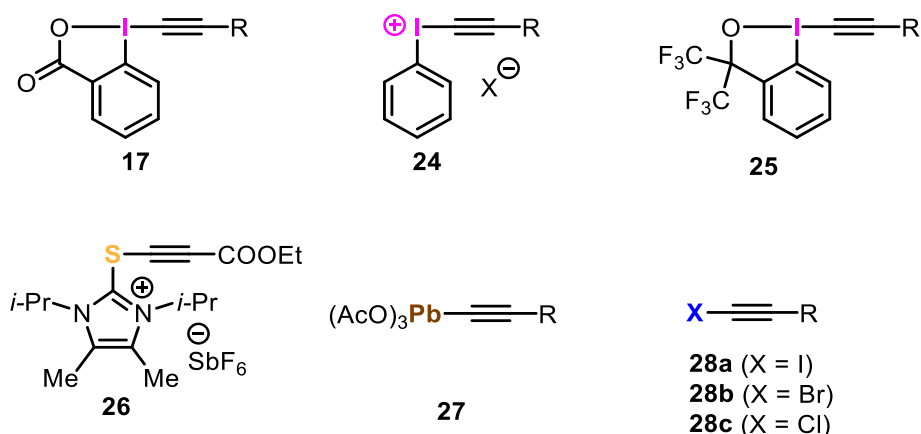


Scheme 6: I) Four selected examples of the scope for electrophilic alkylation of 2-oxindole derivatives. II) Transfer reagents used. III) Total synthetic sequence towards (\pm)-deoxyeseroline (**22**) & (\pm)-esermethole (**23**) using **5f**.²⁶

In this paper, not only a wide variety of 2-oxindoles was alkynylated – 4 selected examples **20a** to **20d** are displayed in Scheme 6, I – but also additional transfer reagents **5g-5i** were synthesized (Scheme 6, II). This methodology was used to first alkynylate **21** to **20e** in 68% yield and convert this molecule into (\pm)-deoxyeseroline **22** within six steps. Two additional steps were undertaken to synthesize (\pm)-esermethole **23** (Scheme 6, III).

1.2.4. Alternative Alkynylation Reagents

Besides *S*-(alkynyl)sulfonium salts **5** and **14**, a variety of alkynylation reagents based on various elements have been reported (Scheme 7).



Scheme 7: Alternative alkynylation reagents based on iodine (**17**, **24**, **25**), sulfur (**26**), lead (**27**) or halides (**28a–c**).

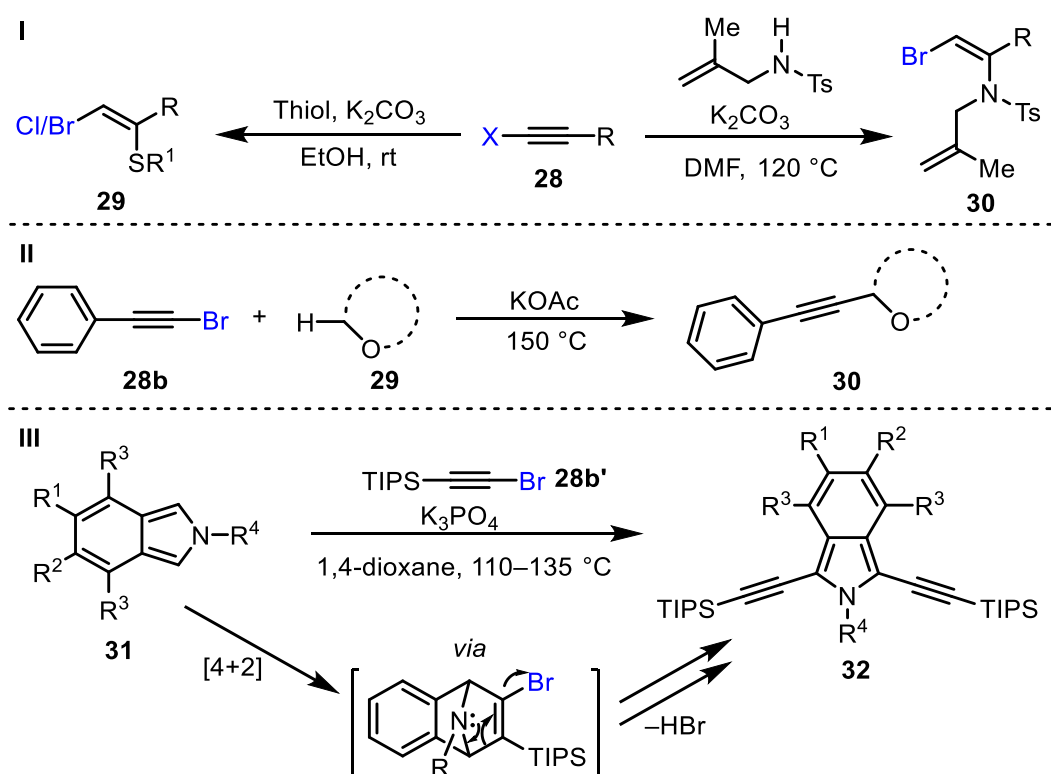
Hypervalent iodine-based alkynyl reagents **24** were first synthesized by Galton et al. in 1965.²⁸ The acyclic version **24** (with R = Ph) inspired many chemists to explore their reactivity. While Galton focused on the addition reactions onto a triple bond, they also hypothesized that **24** would act as an $[RC\equiv C]^+$ synthon. The authors could show that 2-phenylindandione could be ethynylated in 73% yield. In 1990 Nagao extended the substrate scope to terminal alkynylation with **24** (R = TMS, H) of β -dicarbonyl compounds with C–H acidic functionalities.²⁹ One year later this chemistry was further driven by Stang,³⁰ whereas Shiro published a follow up protocol on benziodoxoles **17** where additional residues (R = Cy, *n*-Oct, *t*-Bu) were introduced and analyzed by X-ray analysis.³¹ During the 90's Simonsen³² and others developed the nowadays widely used EBX analogs of **17** and **25**, finally reviewed by Waser in 2010.³³ Waser examined the alkynylation of not only thiols³⁴, but also of phosphor-centered nucleophiles³⁵. However, one drawback makes hypervalent iodine^{III}-based transfer reagents inconvenient in usage. Differential scanning calorimetry (DSC) measurements revealed spontaneous decomposition upon exposure to elevated temperatures of benziodoxoles and therefore these compounds may exhibit dangerous properties while using, especially on larger scales.³⁶

In 2015 Alcarazo developed sulfurane acetylene **26** which proved to be an alternative for electrophilic alkynylation reactions.³⁷ DSC measurements did not show any sharp exothermic combustion signals up to a temperature of 200 °C, which bypasses the unsafety aspects of **17**,

24 and **25**. Compound **26** showed comparable to the iodine-based alkylation reagents reactivity; however, the reactivity is exclusive for **26** since the ester group is needed for the alkylation of nucleophiles. Therefore, a small substrate scope of nucleophiles was demonstrated.

Additional to the popular reagents **17**, **24** and **25**, Roche and Pinhey introduced alkylation-lead triacetates **27** as reagents for the same purpose.^{38,39} However, the need to use toxic acetylene stannanes^{40,41} to synthesize these compounds makes this synthetic approach less attractive. It is noteworthy, that organolead compounds like **27** are not harmless themselves.⁴²

The structurally simplest electrophilic alkylation agents are haloalkynes **28**, at least theoretically.



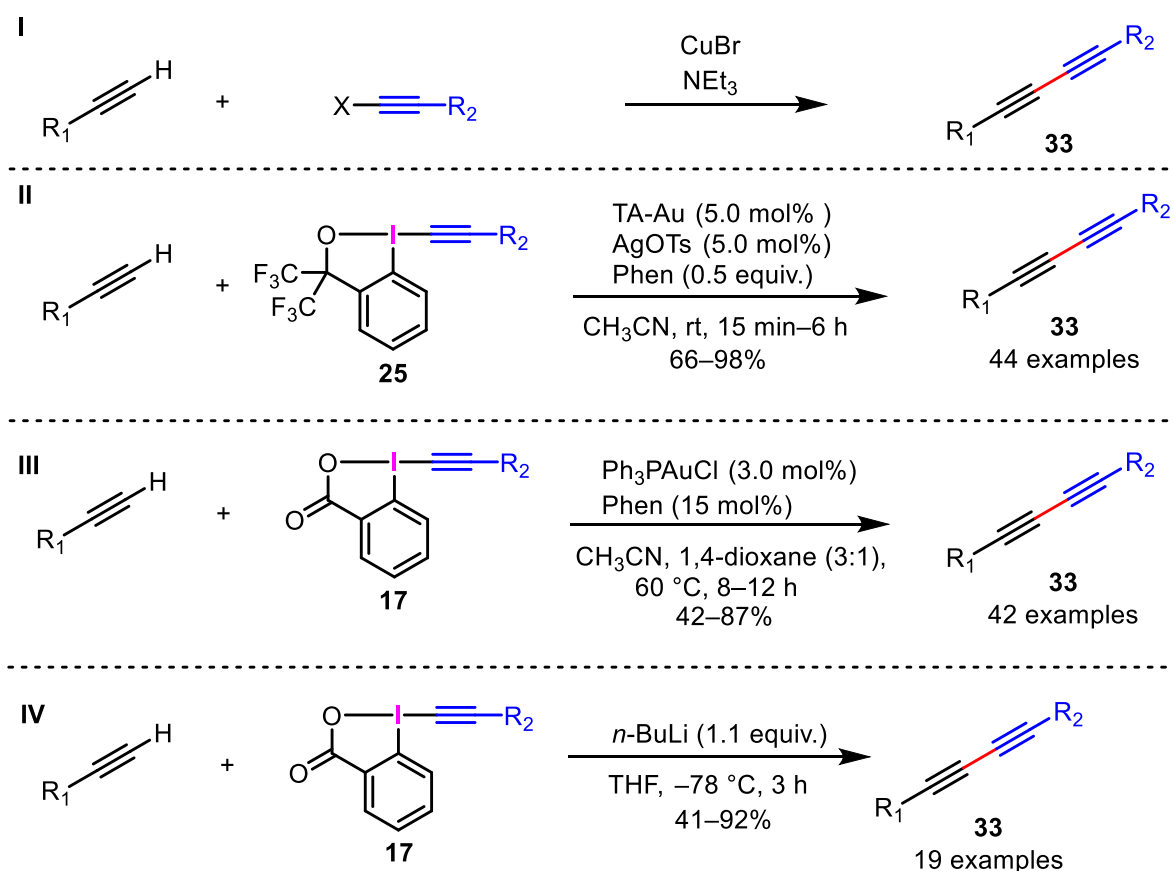
Scheme 8: I) Addition reactions to haloalkynes **28**. II) Alkylation of ethers **29**. III) C–H alkylation of isoindoles **31**.

In the presence of a nucleophile the haloalkynes **28** rather tend to undergo addition reactions than alkylation (Scheme 8, I).^{43,44} Yet there are a few examples of alkylation *with* haloacetylides. The work of Wang consisted in KOAc-promoted alkylation of α -C–H-bonds of ethers, although *via* a radical and not an electrophilic mechanism (Scheme 8, II).⁴⁵ Sugimoto showed that alkylation of isoindoles is possible with bromoacetylides, but again not *via* a classical electrophilic approach.⁴⁶ Initially a [4+2] cycloaddition under basic conditions took

place upon elevated temperatures, and then HBr was eliminated alongside with a ring opening (Scheme 8, III).

1.2.4.1. Alkynylation Reagents in Diyne Synthesis (Cadiot-Chodkiewicz Coupling)

The classical Cadiot-Chodkiewicz coupling, published in 1957, became a common method for the synthesis of unsymmetrical diynes (Scheme 9, I).⁴⁷ Catalytic amounts of copper¹ enable the generation of the carbon-carbon bond starting from a terminal alkyne and a haloalkyne. Since the past decades a number of protocols for the same purpose had been developed using either palladium⁴⁸, copper⁴⁹ or gold⁵⁰ as catalyst. Even if only substoichiometric amounts of transition metals are used in most methodologies, the development of transition metal-free protocols is of high priority because of the toxicity and pricing related with the use of transition metals.



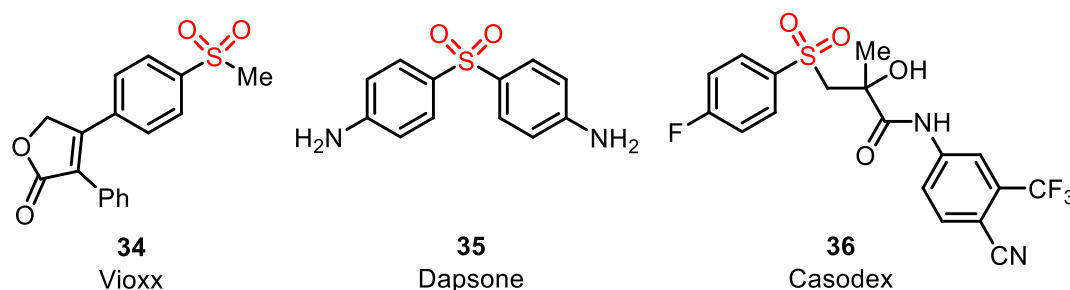
Scheme 9: I) Classical Cadiot-Chodkiewicz coupling. II) Modified Cadiot-Chodkiewicz-type coupling introduced by Liu⁵¹; III) Modified Cadiot-Chodkiewicz-type coupling introduced by Patil⁵²; IV) Modified Cadiot-Chodkiewicz-type coupling introduced by Waser⁵³.

Recently a few protocols employing the increasingly popular benzodioxoles-based reagents **17** and **25** have been published. Liu *et al.* used these alongside with catalytic amounts of

triazole-Au (TA-Au) and silver tosylate to couple them with a terminal alkyne (Scheme 9, II).⁵¹ The generality of this transformation could be represented in a large substrate scope. Homocoupling products formation which is a common problem for this reaction could also be suppressed. Patil established a similar synthesis which includes **17** and only triphenylphosphine gold^I chloride as catalyst (Scheme 9, III).⁵² In view of this thesis, however, the work of Waser is of most importance, since only a strong base is used to deprotonate the terminal alkyne and directly coupled with the acetylide unit of **17** (Scheme 9, IV).⁵³ In a part of this thesis we follow a similar approach by using deprotonated alkyne, which is then coupled with sulfur based alkynylating reagent **5f**.

1.2.4.2. Alkynylation Reagents in Alkynyl Sulfone Synthesis

Sulfone-containing compounds are widely used for pharmaceutical purposes because of their various biological activities. Three selected examples are displayed in Scheme 10.⁵⁴



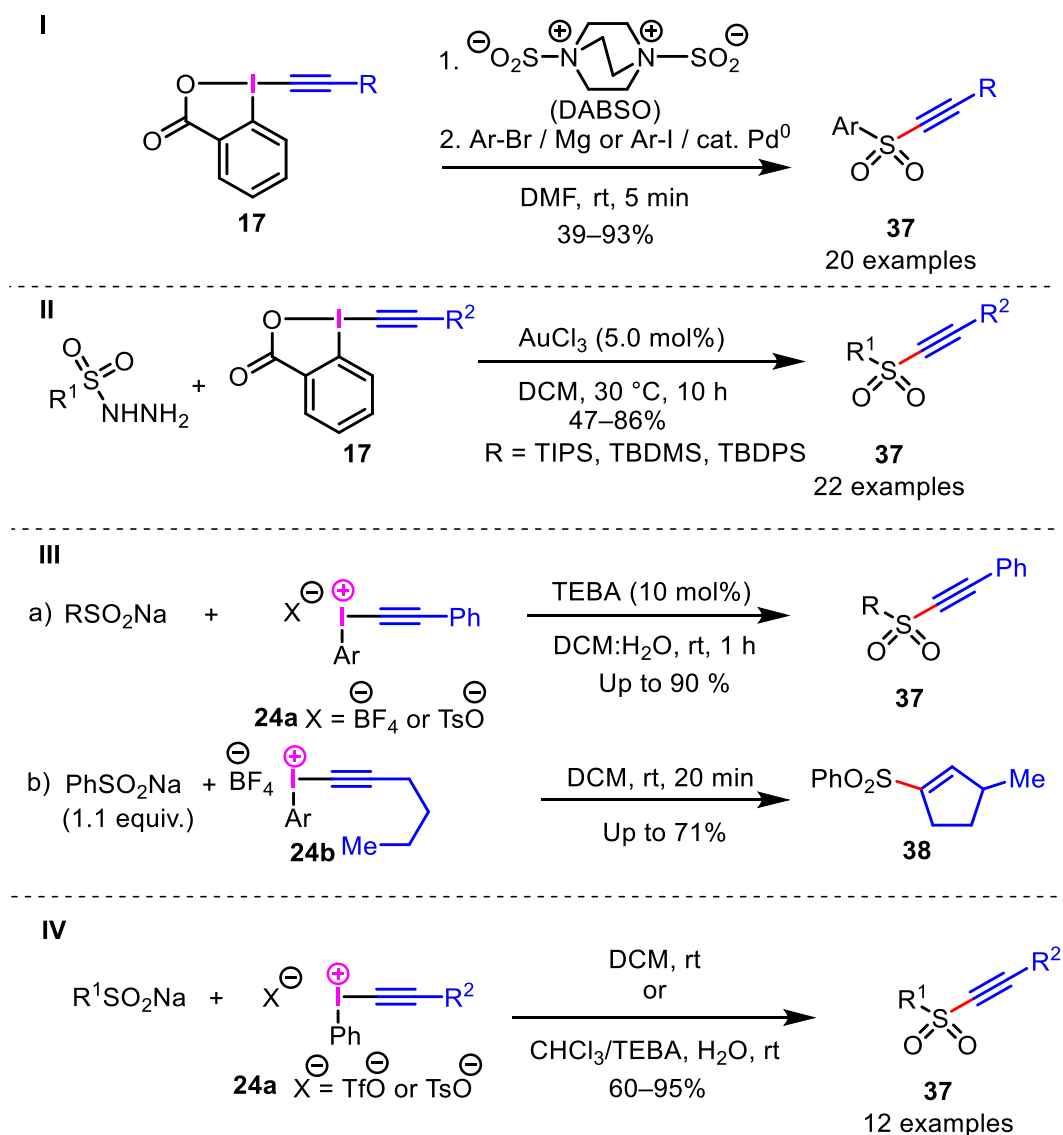
Scheme 10: Pharmaceutical compounds containing a sulfone moiety: COX-2 inhibitor Vioxx (**34**, left), antibacterial drug Dapsone (**35**, middle) & anti-androgen agent Casodex (**36**, right).

The commercial drug Vioxx **34** is a cyclooxygenase-2 inhibitor and has an anti-inflammatory effect. Dapsone **35** and Casodex **36** are also used for the treatment of human diseases and are commercialized as antibacterial and anti-androgen drugs.⁵⁴

Alongside with their pharmaceutical significance, from a synthetic point of view sulfones are important building blocks due to their versatile reactivity. A sulfone has a strong electron-withdrawing effect and therefore activates the neighboring triple bond of a sulfone-attached alkyne moiety towards electron-rich reaction partners. This property allows chemists to use these compounds in cycloadditions and conjugate addition reactions.⁵⁵

Most synthetic approaches to alkynylsulfones rely on the oxidation of the corresponding sulfides.^{56,57} Another strategy is the reaction of the corresponding sulfinate salt with an electrophile, which proved to be a convenient alternative.

In this thesis the reactions of sulfonium salts **5a** and **5f** with sulfinate salts towards alkynyl sulfones were explored. Various methods for the synthesis of alkynyl sulfones are shown in Scheme 11.



Scheme 11: Four different methods to obtain alkynylsulfones as elaborated: **I**) by Waser⁵⁴; **II**) by Patil⁵⁸; **III**) by Moran⁵⁹; **IV**) by Chen and Stang⁶⁰. TEBA = tetraethylbenzylammonium chloride.

Thus, in 2015 Waser reported a one-pot synthetic approach to sulfone alkynes using DABSO, iodine^{III}-compound **17** and either an aryl-Grignard reagent or an aryl iodide with catalytic amounts of palladium (Scheme 11, **I**).⁵⁴ This method excels in the rapid formation of sulfone alkynes in moderate to good yields. Additionally, the reaction is not restricted to formation of aryl-alkynyl substituted sulfones. The *sp*-hybridized reaction center substituent can be replaced with a one possessing *sp*² or *sp*³ carbon atom, although only a few examples were presented in this report. Patil demonstrated a dehydrazinative sulfone-alkyne coupling

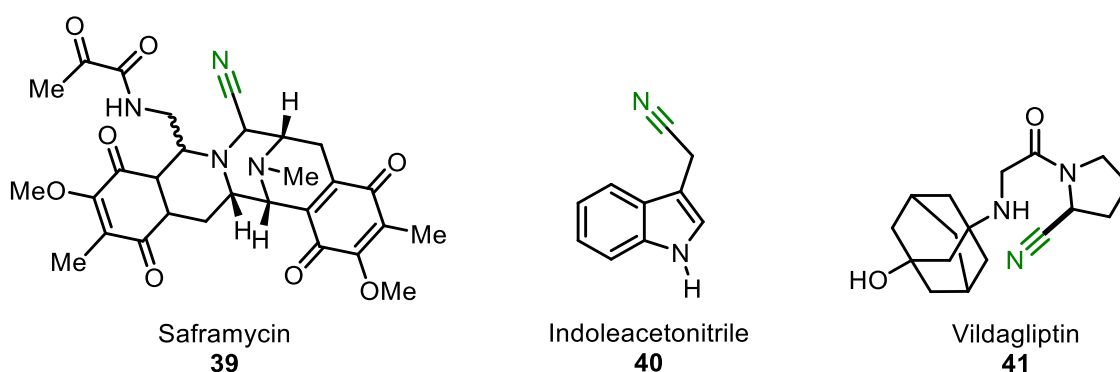
catalyzed by gold chloride (Scheme 11, II).⁵⁸ This method is not exclusive for arylsubstituted sulfone moieties: the alkyl- and alkenyl-substituted products were synthesized as a proof of concept. On the other hand, the reaction did not proceed if the terminal residue of benziodoxole **17** was a phenyl-group.

The Moran's work was focused upon the influence of the counteranion and the aryl backbone of **24a** on the reactivity (Scheme 11, III, a).⁵⁹ As concluded, the combination of tetrafluoroborate as a counteranion and *ortho*-methoxyphenyl as an aryl scaffold appeared to be the most efficient reagent. With these insights, a cyclization reaction with **24b** was undertaken and yielded 71% of sulfone **38** (Scheme 11, III, b). The authors propose that the reaction occurs *via* an intramolecular insertion of a vinyl carbene intermediate into C–H bond. The early works of Chen and Stang consist in the very minimalistic but effective reaction of a sulfinate salt and **24a** (Scheme 11, IV).⁶⁰ The triflates^[60a] or tosylates^[60b] of **24a** yielded alkynylsulfones **37** in acceptable to excellent yields under phase transfer catalytic conditions in either dichloromethane/- or chloroform/water with triethylbenzylammonium chloride as a catalyst (12 examples). Since the reaction conditions for the formation of alkynylsulfones with sulfonium salts **5a** and **5f** are comparable, the latter works are mostly related to this thesis.

1.2.5. Synthesis & Reactivity of S-(Cyano) Sulfonium Salts

Cyano groups are a prevalent structural motif in natural compounds. Saframycin (**39**) (Scheme 12), one from several α -aminonitriles found in *Streptomyces* cultures, shows high antibiotic and antitumor activities. Although being one of the first examples of such α -aminonitrile isolated from *Streptomyces (lavendulae)*, its absolute stereochemistry still remains undefined.⁶¹

Indoleacetonitrile (**40**) (Scheme 12) can be isolated from several *Cruciferae* plants. This compound is found in lightgrown cabbage (*Brassica oleracea*) and is the main factor for seedling-growth inhibition.⁶¹ The molecule participates in the mechanism of plant growth, i. e. its presence retards the growth on the light exposed side of the plant stem. This causes bending of the seedling towards the source of light. Additionally, it is proposed that the enzymatic biosynthesis is induced by exposure on light and originates from its corresponding glucosinolate.⁶¹

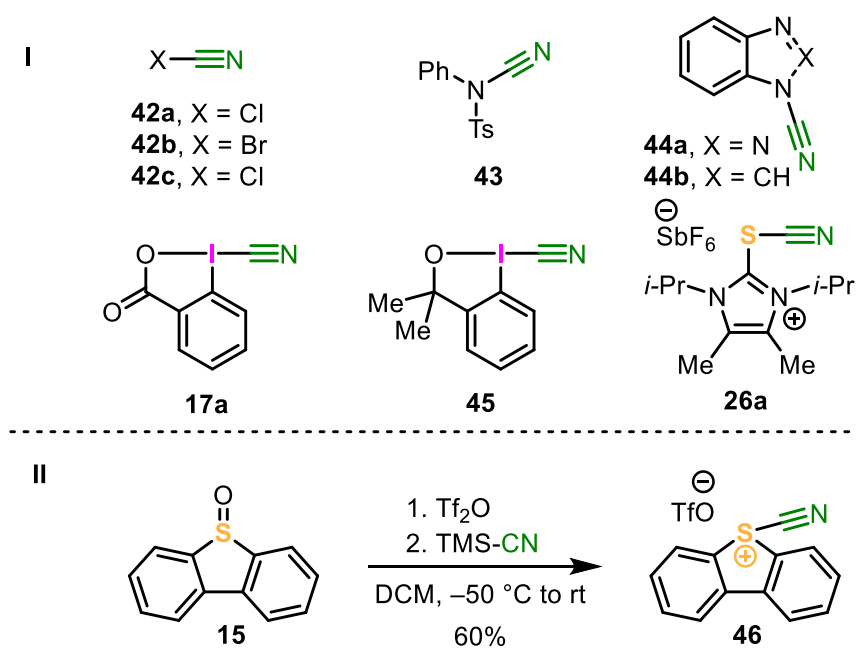


Scheme 12: Two selected examples of nitrile-containing natural compounds: Saframycin (**39**, left) and Indoleacetonitrile (**40**, middle) as well as an example of nitrile-containing pharmaceutical drugs Vildagliptin (**41**, right).

Moreover, nitrile-containing compounds are also used for pharmaceutical purposes. One selected example is a recently introduced drug named Vildagliptin (**41**) (Scheme 12), which exerts an antidiabetic effect. The metabolism of this compound has been extensively studied. The main concern using this drug was the release of cyanide caused by hydrolysis in the human body. However, this hypothesis could be revised since this metabolic pathway plays only a minor role.⁶²

It is also worth mentioning that nitriles have a wide application as agrochemicals⁶³, organic dyes⁶⁴ and in polymer chemistry⁶⁵. Additionally, nitriles are key precursors for the transformation to amines, amidines, tetrazoles, aldehydes, amides and carboxylic acids.^{66,67}

The importance of nitriles in these disciplines drove chemists to explore economic and trouble-free protocols for cyano group introduction into molecules. However, most approaches depend on the natural nucleophilicity of the cyanide anion. The 'Umpolung' of cyanide to a $[N\equiv C]^+$ -synthon is known, although not many compounds exist which provide the inverted electronic property to cyanide (Scheme 13, I).⁶⁸ Therefore, their chemistry is not extensively studied, and their limited application can also be ascribed to disadvantages of accessible electrophilic cyanation reagents.

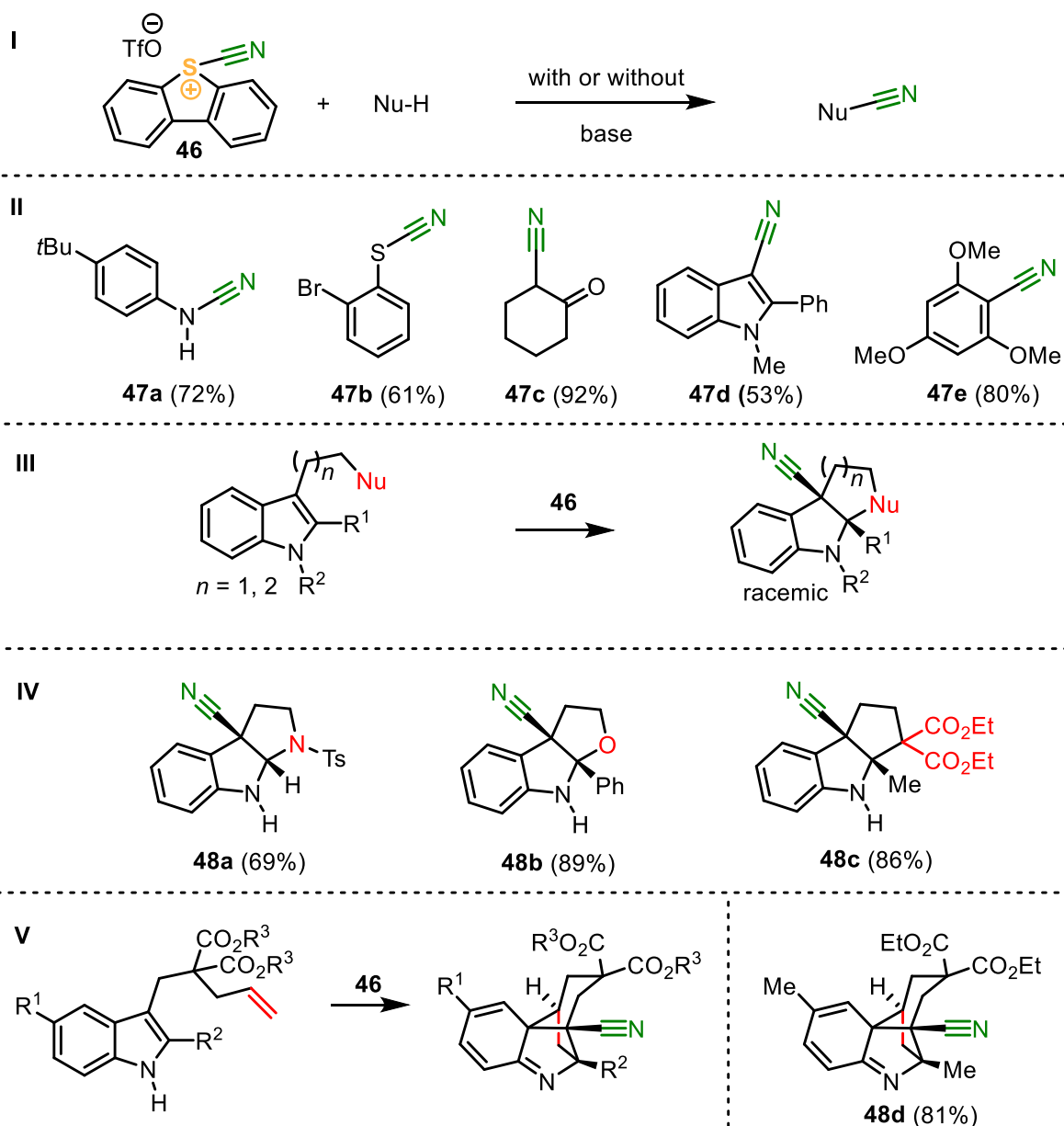


Scheme 13: I) 'Umpoled' cyanating reagents based on sulfurane (**26a**), hypervalent iodine (**17a** & **45**), halonitriles **42a-42c**, sulfonamides **43**, benzotriazole **44a** and benzimidazole **44b**.⁶⁸ II) Synthetic approach towards **46**.

The low boiling points and high toxicity of cyano halides make them very inconvenient and are therefore rather unpopular reagents (b.p. of cyanogen chloride (**42a**) and cyanogen bromide (**42b**) are 13 and 61.5 °C, respectively, whereas cyanogen iodide (**42c**) sublimes under atmospheric pressure).⁶⁹ Alternatively *N*-cyanoimidazole (**44b**),^{70,71} *N*-cyanobenzotriazole (**44a**)⁷¹ and *N*-cyanotosylamide (**43**)⁷² can be used as cyanating reagents. Their utility is restricted to either transition metal catalysis,^{68c,72} enolate chemistry⁷³ and cyanation of hard carbon nucleophiles like Grignard compounds^{74,75}.

Simonsen *et al.* introduced cyanoiodinanes **17a** and **45** in 1995 and demonstrated their ability to form C–Cyano bonds in an electrophilic fashion.⁷⁶ The reactivity was further studied by Waser and coworkers. The authors extended the range to *S*-nucleophiles⁷⁷, performed a decarboxylative light-induced cyanation of carboxylic acids⁷⁸ and used the reaction in enantiopure synthesis of 1,5-substituted hydantoin derivatives⁷⁹. Studer achieved the metal-free cyanation of alkenes.⁸⁰ Recently, Alcarazo and coworkers introduced the sulfurane-based cyanating reagent **26a**, which showed comparable reactivity to those of **17a** and **45**.³⁷ With this reagent in hand, regio- and stereoselective chloro-cyanation of triple bonds⁸¹ and, as further development of this chemistry, a cyano-cyclization towards phenanthrenes and similar compounds⁸² was elaborated. In 2019, the same group reported on the synthesis of *S*-(cyano)dibenzothiophenium triflate **46** in 60% isolated yield (Scheme 13, II).²⁴ The reaction conditions were very similar to those previously used in the preparation of *S*-(alkynyl)dibenzothiophenium triflates.^{11,23}

This reagent successfully cyanates nucleophiles, either in the presence or absence of a base (Scheme 14, I). Five selected examples representing a scope of nucleophiles ranging from amines **47a** over thiols **47b**, enolates **47c**, indoles **47d** to electron-rich arenes **47e** are shown in Scheme 14, II.

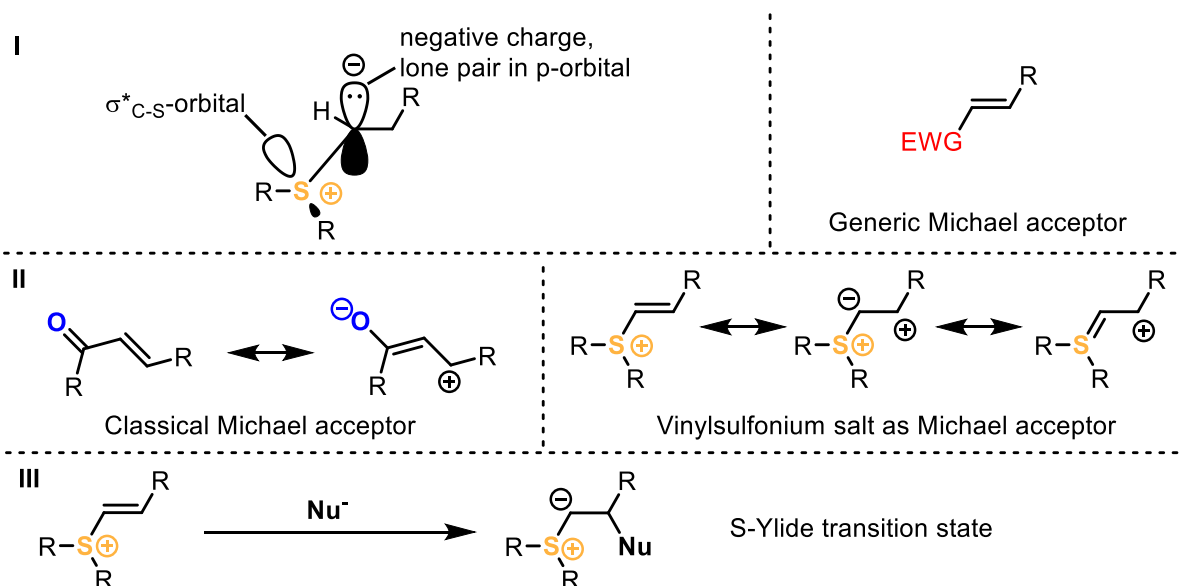


Scheme 14: I) General method of electrophilic cyanation. II) Selected examples demonstrating the substrate scope. III) General approach to the intramolecular cyclization induced with **46**. IV) Selected examples of the intramolecular cyanocyclization. V) Cyclization towards indole scaffold **48d**.²⁴

The authors took a closer look to indole derivatives and predicted the **46**-promoted intramolecular cyanocyclization with a nucleophile attached to an aliphatic chain in 3-position of the indole (Scheme 14, III). They demonstrated that intramolecular cyclization with either nitrogen-, oxygen- or enolate-based nucleophiles indeed occur in moderate to excellent yields (Scheme 14, IV). Lastly, Alcarazo and coworkers were able to transform indole derivatives bearing an olefin substituent into complex indole scaffolds like **48d** (Scheme 14, V). This approach has never been shown before and is even unknown in transition metal catalysis so far.

1.3. C(sp²)-Substituted Sulfonium Salts: Alkenyl substituents

Over the past few decades organosulfur ylide chemistry established itself as a versatile academic and industrial chemical field.^{7b} Key contributors to this topic Johnson⁸³, Corey and Chaykovsky⁸⁴ independently developed methods in the 1960's to synthesize sulfur ylides, and these zwitterionic compounds showed application in highly diastereoselective and enantioselective ways. The formation of epoxides, cyclopropanes and aziridines *via* sulfur ylides later led to the establishment of the well-known Johnson-Corey-Chaykovsky reaction.⁸⁵ An ylide consists from a positively charged sulfur atom with an adjacent carbon bearing a negative charge (Scheme 15, I). It is known that the sulfur in an ylide stabilizes the negative charge very efficiently, and this property was intensively used in synthesis^{86,87} and studied in theoretical field^{88,89}. It was long believed that the energetically low d-orbitals of the sulfur contribute to the delocalization of the electron density from the occupied p-orbital of the carbanion.⁹⁰ Nowadays the community has revised this statement, and generally accepted that the stabilization can merely be tracked back to the negative hyperconjugative interaction between the lone pair orbital of the carbanion with the σ^* -orbital of the sulfur-carbon bond.⁹¹⁻⁹⁴



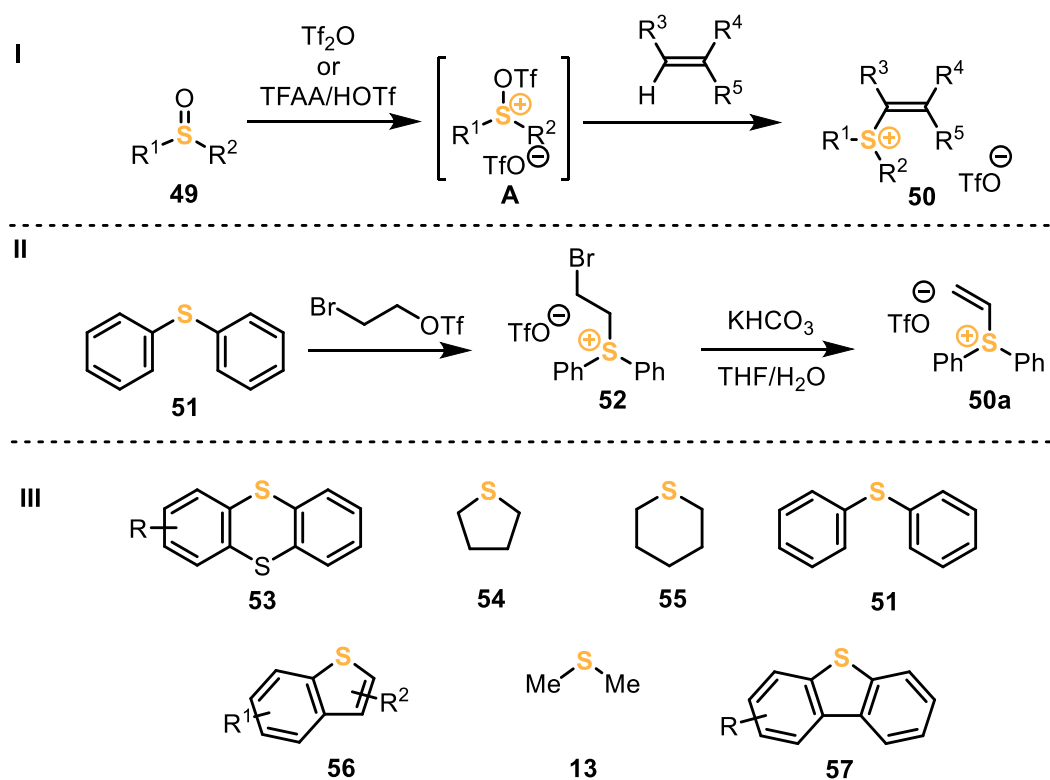
Scheme 15: I) Left: Orbital interactions in a sulfur ylide; right: generic Michael acceptor⁹⁵; II) Left: mesomeric structures of a classical Michael acceptor;⁹⁶ right: mesomeric structures between a vinylsulfonium salt, S-ylides & S-yliden (analog of phosphor ylides, see p. 465 in⁹⁷); III) Nucleophilic attack in a Michael-type reaction with a generic vinylsulfonium salt.⁹⁸

The electron deficiency at the α -carbon makes vinylsulfonium salts potent Michael acceptors, since the sulfur stabilizes the occurring ylide intermediates or transition states (Scheme 15, II

& III). Therefore, the synthetic utility of *S*-alkenyl sulfonium salts as ethylene transfer reagents was recognized and has been explored since decades.⁸⁵ With the increased knowledge about transition metal catalysis in recent time the versatility of the possible reactions of vinylsulfonium salts rose dramatically (see Chapter 1.3.3 for examples of reactivity).^{99,100}

1.3.1. Synthesis of *S*-(Alkenyl) Sulfonium Salts

The two most commonly used methods to prepare vinylsulfonium salts are shown in Scheme 16 I & II.



Scheme 16: I) Method to prepare vinylsulfonium salts **50** *via* activation of the corresponding sulfoxide followed by alkenylation. II) Alternative synthesis *via* a $\text{S}_{\text{N}}2$ -substitutive alkylation and successive dehydrobromination. III) Most common sulfonium backbones.

The activation of sulfoxides can either be achieved *via* utilization of Tf_2O , TFAA (trifluoroacetic anhydride) or triflic acid and leads to the formation of bis-triflate **A** (Scheme 16, I). Treatment of **A** with an alkene bearing at least one hydrogen substituent results in the formation of the corresponding vinylsulfonium salt **50**.

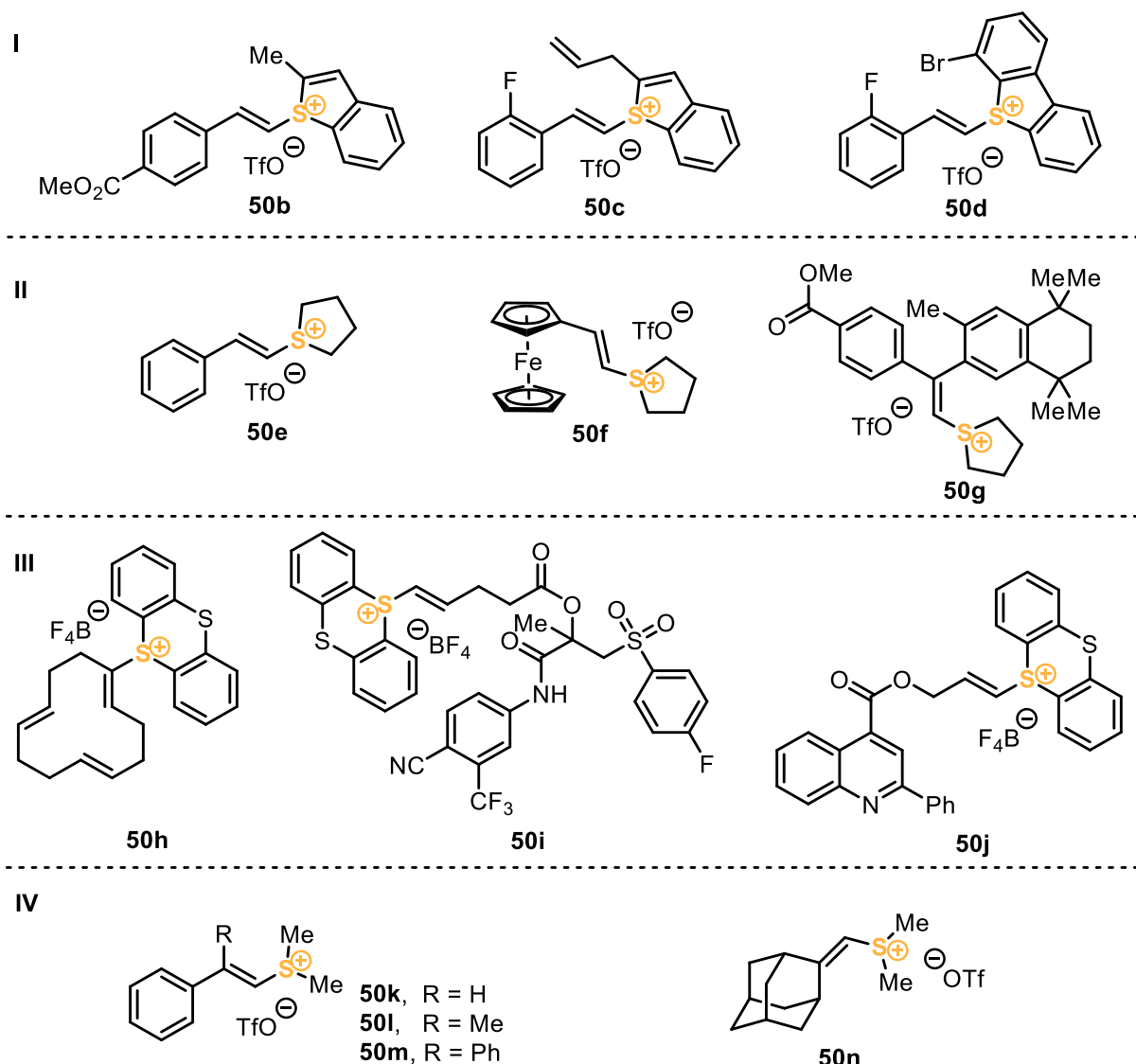
Two decades ago Mukaiyama *et al.*¹⁰¹ and Balenkova *et al.*¹⁰² demonstrated the synthetic approach to vinylsulfonium salts *via* Tf_2O activation. Recently the research group of Procter continued this chemistry and broadened the spectrum of existing vinylsulfonium salts^{100,103}, whereas Ritter and coworkers relied on the activation of TFAA with triflic acid.⁹⁹ Aggarwal

followed a different method to the target molecule **50a** (Scheme 16, II).¹⁰⁴ First the corresponding sulfide **51** reacts with 2-bromoethyl triflate affording the *S*-alkyl sulfonium salt **52**. Treatment of **52** with a potassium bicarbonate formally eliminates hydrogen bromide and the desired compound **50a** is obtained.

Scheme 16, III shows the different sulfonium backbones which were used for the formation of vinylsulfonium salts. Thianthrene **43**, diphenylsulfide **51**, benzothiophene **56**, and dibenzothiophene **57** either bear two aryl substituents or are completely aromatic themselves, whereas dimethylsulfide **13**, tetrahydrothiophene **54** and tetrahydrothiopyran **55** have simple alkyl substituents.

The reaction described in Scheme 16, I is most commonly used to obtain vinylsulfonium salts **50** and tolerant to functional groups like halogens, ethers, amides, nitriles and sulfonamides. However, this method possesses some drawbacks. Unprotected alcohols and amines could undergo undesired ester or amide formation by the direct reaction with the activator Tf₂O or TFAA, and hydrolysis of these needs to be done with care, so that the sulfonium moiety remains intact. Vinylsulfonium salts could potentially react as a Michael acceptor in the presence of an appropriate nucleophile which results in the decomposition of the sulfonium moiety. Additionally, it should be taken into account that either primary or secondary alcohols could undergo a Swern-type oxidation in the presence of activated sulfoxides like **A** (Scheme 16, I). Lastly, the substrate must not have aromatic substituents with high electron density besides the vinylic group. Otherwise both moieties would react competitive towards the activated sulfoxide **A**, and a mixture of *S*-arylated and *S*-vinylated sulfonium salts would be obtained.²

Selected examples of known vinylsulfonium salts are shown in Scheme 17.



Scheme 17: Selected examples of vinylsulfonium salts reported by: **I)** Procter¹⁰³; **II)** Procter¹⁰⁰; **III)** Ritter⁹⁹; **IV)** Nenajdenko and Balenkova¹⁰².

Procter demonstrated the *in situ* generation of vinylsulfonium salts based on benzothiopyran (**50b** & **50c**) and on dibenzothiopyran (**50d**) scaffold (Scheme 17, **I**).¹⁰³ The formation of similar salts with a tetrahydrothiopyran moiety **50e–g** was reported by Procter and coworkers as well (Scheme 17, **II**).¹⁰⁰ Only a few examples were isolated, crystallized and completely characterized; the majority was *in situ* generated and directly used for successive transformations. Ritter showed a substrate scope containing many complex structures like **50h**, **50i** or **50j** which were obtained by sulfenylation of vinylic compounds with thianthrene (Scheme 17, **III**).⁹⁹ Additionally, structures **50k–50m** and **50n** were synthesized by Balenkova in 1997.¹⁰² Therefore, the latter paper represents the pioneer work of modern vinylsulfonium chemistry.

1.3.2. Structure of *S*-(Alkenyl) Sulfonium Salts

Procter and coworkers published the crystal structures of the salts **50o**¹⁰³, **50p**¹⁰⁰ and **50q**¹⁰⁰ in the solid state which are depicted in Figure 4. In contrast to *S*-(alkynyl)dibenzothiophenium triflates (see above), these compounds do not form well defined dimeric structures. In addition to the chalcogen interactions, hydrogen bonding between the triflate anion and the vinylic protons is present.

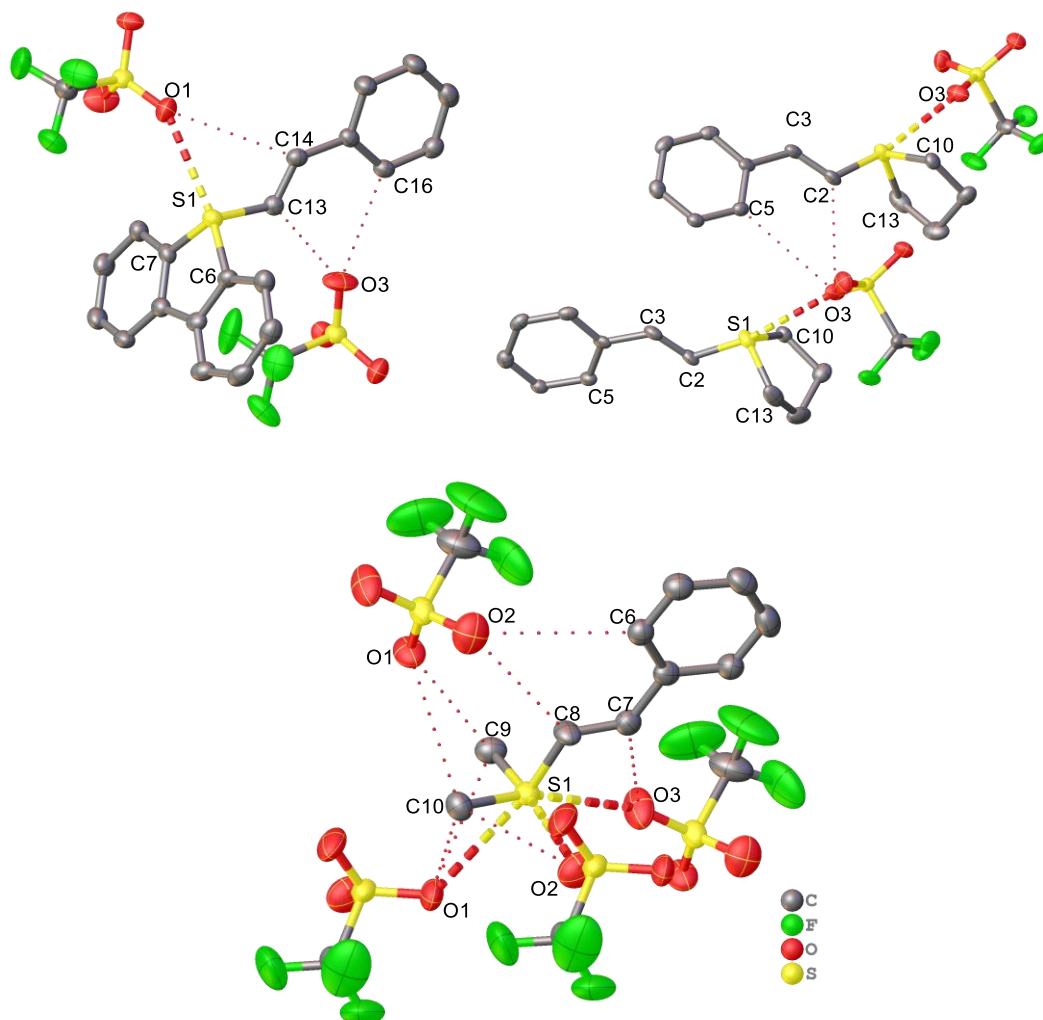


Figure 4: X-ray structure of the salts **50o** (top left; displayed with two triflate anions to show all significant interactions), **50p** (top right) & **50q** (bottom, displayed with four triflate anions to show all significant interactions) in the solid state. Anisotropic displacement shown at 50% probability level. Hydrogen atoms were omitted for clarity. Selected bond lengths [Å] and angles [°]: **50o**: S1–C6 1.782(3), S1–C7 1.784(3), S1–C13 1.761(3), S1–O1 3.038(2), O1–C14 3.388(3), O3–C13 3.462(3), O3–C16 3.256(3), C6–S1–O1 163.3; **50p**: S1–C2 1.761(4), S1–C10 1.835(4), S1–C13 1.821(5), C5–O3 3.519(5), C2–O3 3.458(5), S1–O3 3.004(3), C2–S1–O3 169.5. **50q**: S1–C8 1.771(6), S1–C9 1.802(6), S1–C10 1.794(6), C9A–O1 3.319(8), C9B–O1 3.341(8), C10A–O1 3.496(9), C10B–O1 3.347(9), C10C–O2 3.201(9), C7–O3 3.256(8), C8–O2 3.390(8), C6–O2 3.579(9), S1–O1 3.372(5), S1–O2 3.207(6), S1–O3 3.115(6), C10–S1–O3 164.8, C9–S1–O2 174.3, C8–S1–O1 171.7.

In structure **50o** the sulfur S1 expectedly adopts a distorted pyramidal geometry with the sum of angles around S1 being 297.8°. Differing from *S*-(alkynyl)dibenzothiophenium triflates, the triflate anion of **50o** rather interacts with the hydrogen atoms of the vinyl moiety *via* hydrogen bonding (O3–C13 3.462(3) Å; for others see legend to Figure 4). This hydrogen bond distance is considered to be a weak interaction between the H-donor and acceptor (2.2–2.5 Å strong, mostly covalent; 2.5–3.2 Å moderate, mostly electrostatic, 3.2–4.0 Å weak, electrostatic).¹⁰⁵ An interaction between O1–S1 could be observed additionally, whereas the triflate anion and the vinyl moiety lie in an apical array. However, the hydrogen bond interactions lead to distortion of the trigonal bipyramidal structure, which can be seen in the bond angle of C6–S1–O1 163.3°.

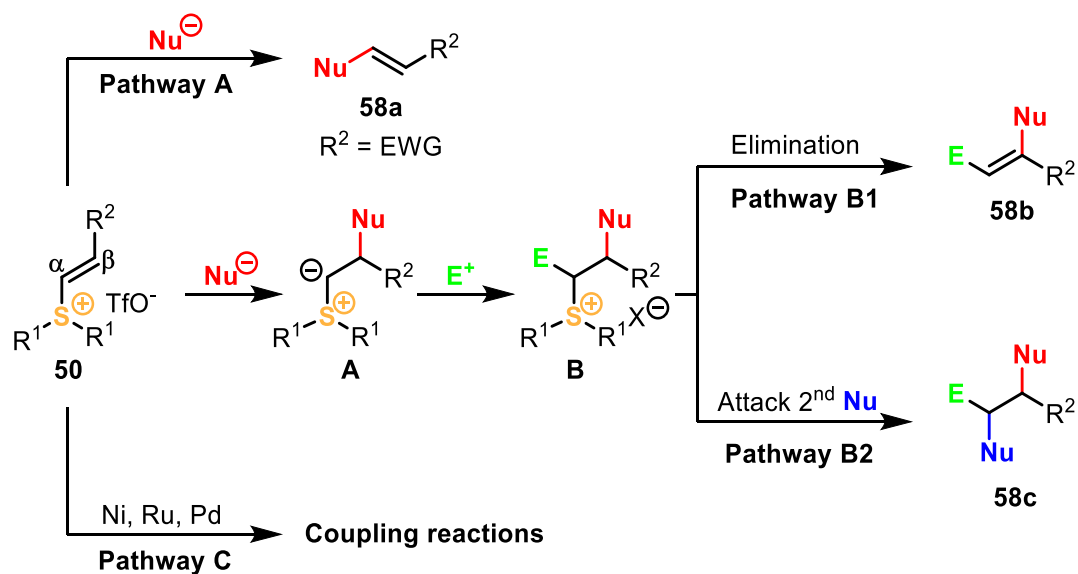
In **50p** the contact of O3–S1 is even shorter with a bond length of 3.004(3) Å. additionally to that the interaction of O3 to C2 was measured with a distance of 3.458(5) Å. The sum of angles around S1 is larger with 301.7° compared to **50o**. The triflate anion even interacts with the aromatic *ortho*-proton.

Structure **50q** shows similar hydrogen bonding interactions, which again indicates strong Brønsted acidity of the hydrogen atoms of all C–H neighboring bonds of S1. Three O–S1 contacts can be observed in this particular case, whereby the distortion of the 180° angle (O–S1–C) has a range between 164.8° to 174.3°. This structure has a sum of angles around S1 of 303.4° and tends to less pyramidalization than its cyclic analogs.

Overall, the observations in these solid-state structures reveal C–H acidic bonds besides the sulfonium moiety, which is in accordance with the reactivity of vinylsulfonium salts. The deprotonation of the vinylic proton results in well stabilized *S*-ylides which is explained in detail in chapter 1.3. Therefore, it is no surprise that the triflate anion readily forms hydrogen bonds with the corresponding sulfonium cations hydrogens.

1.3.3. Reactivity of S-(Alkenyl) Sulfonium Salts

S-Alkenyl sulfonium salts are known to possess Michael acceptor properties and therefore these salts can be used in Michael reaction-related chemistry.



Scheme 18: Reactivity modes of S-alkenyl sulfonium salts. Pathway **A**: nucleophilic α -attack; Pathway **B1**: nucleophilic β -attack followed by elimination; Pathway **B2**: nucleophilic β -attack followed by 2nd nucleophilic attack on α -carbon; Pathway **C**: coupling reactions.

The reactivity modes are divided into three main pathways (Scheme 18). Pathway **A** consists in a straight nucleophilic attack at the α -carbon of the vinylsulfonium salt **50**. This occurs when the residue on the other terminus is of electron-withdrawing nature, results in the inversion of the polarity of the vinyl-moiety and makes the α -carbon more Lewis acidic than the β -carbon. Therefore, pathway **A** is a classical Michael addition-elimination sequence, in which the sulfide moiety is substituted by the nucleophile and the product **58a** is formed.

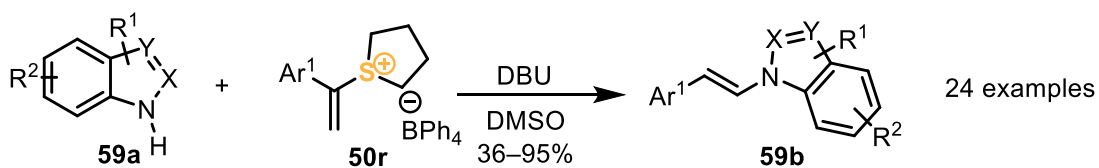
If the residue R^2 is sufficiently electron-rich, the nucleophilic attack preferentially occurs on the β -carbon. The generated sulfur ylide **A** can be quenched by an electrophile, which results in the formation of S-(alkyl)sulfonium salt **B**.

For **B**, two possible types of behavior can be predicted. Pathway **B1** results in the elimination of the sulfide alongside with the proton on the other terminus. A double bond is formed, and product **58b** is obtained. Another possibility is the attack with a second nucleophile on the α -carbon of the S-(alkyl)sulfonium salt *via* nucleophilic substitution and successive substitution of the sulfide (Pathway **B2**). In this case product **58c** will be produced.

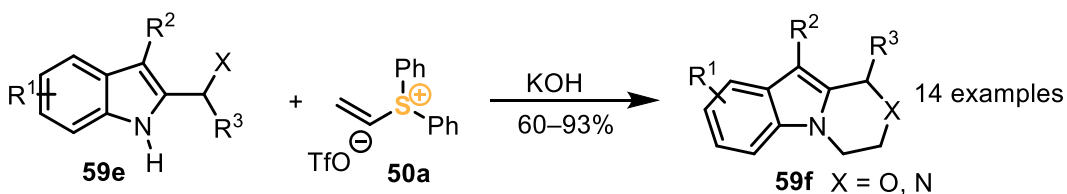
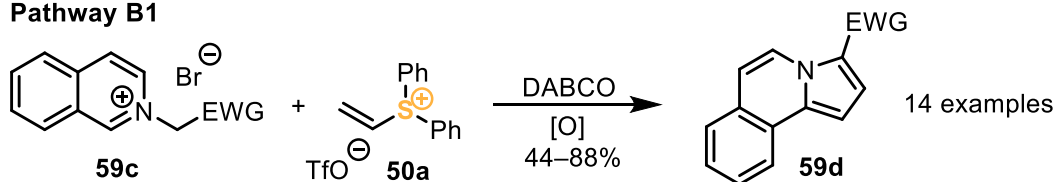
Lastly, **50** can be used in transition metal-catalyzed coupling reaction where the sulfonium moiety acts as a leaving group in analogy to halide or pseudohalide surrogates.²

Selected examples of the generic reactivity modes depicted above in Scheme 18 are shown in Scheme 19.

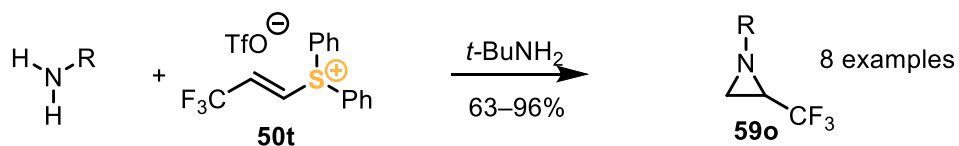
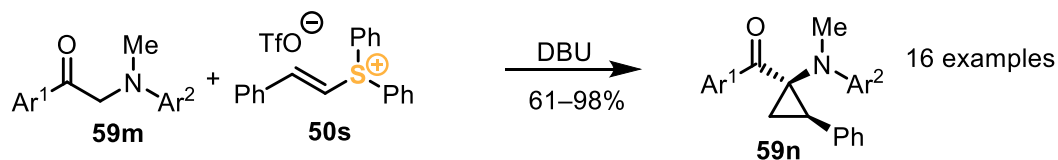
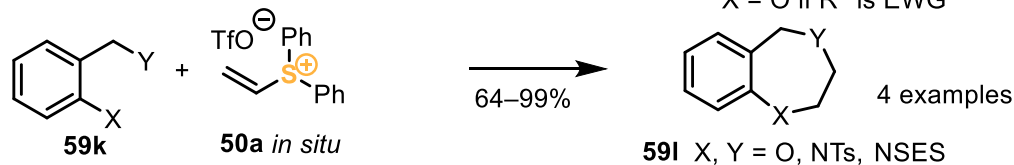
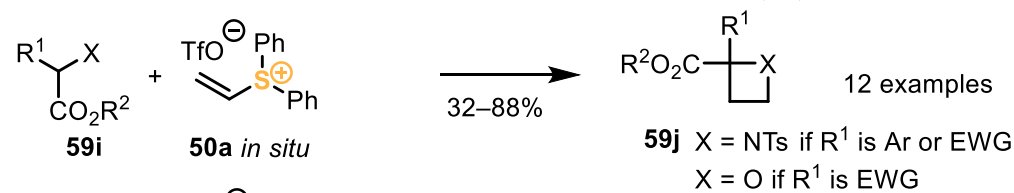
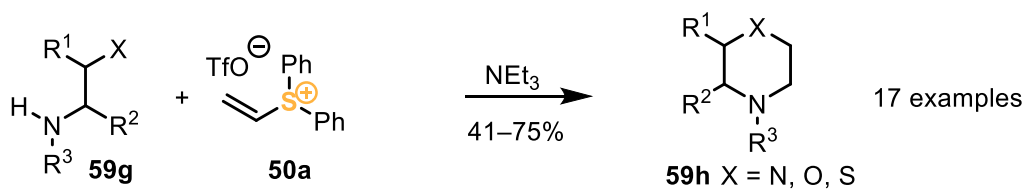
I Pathway A



II Pathway B1



III Pathway B2



Scheme 19: Representative examples for the reactivities following I) Pathway A; II) Pathway B1; III) Pathway B2.

Qian *et al.* demonstrated a chemo- and regioselective vinylation of *N*-heterocyclic compounds such as indole with the help of vinylsulfonium salts **50r** (Scheme 19, I).¹⁰⁶ Noteworthy, the counteranion in this particular transformation is tetraphenylborate which generally is used less frequently. The counteranion is incorporated during the three-step synthesis of **50r** which consists of bromination of the vinylic compound and nucleophilic substitution of the primary bromide with tetrahydrothiophene. Then the bromide counteranion is replaced with a tetraphenylborate one followed by successive dehydrobromination with K₂CO₃ in aqueous solution.

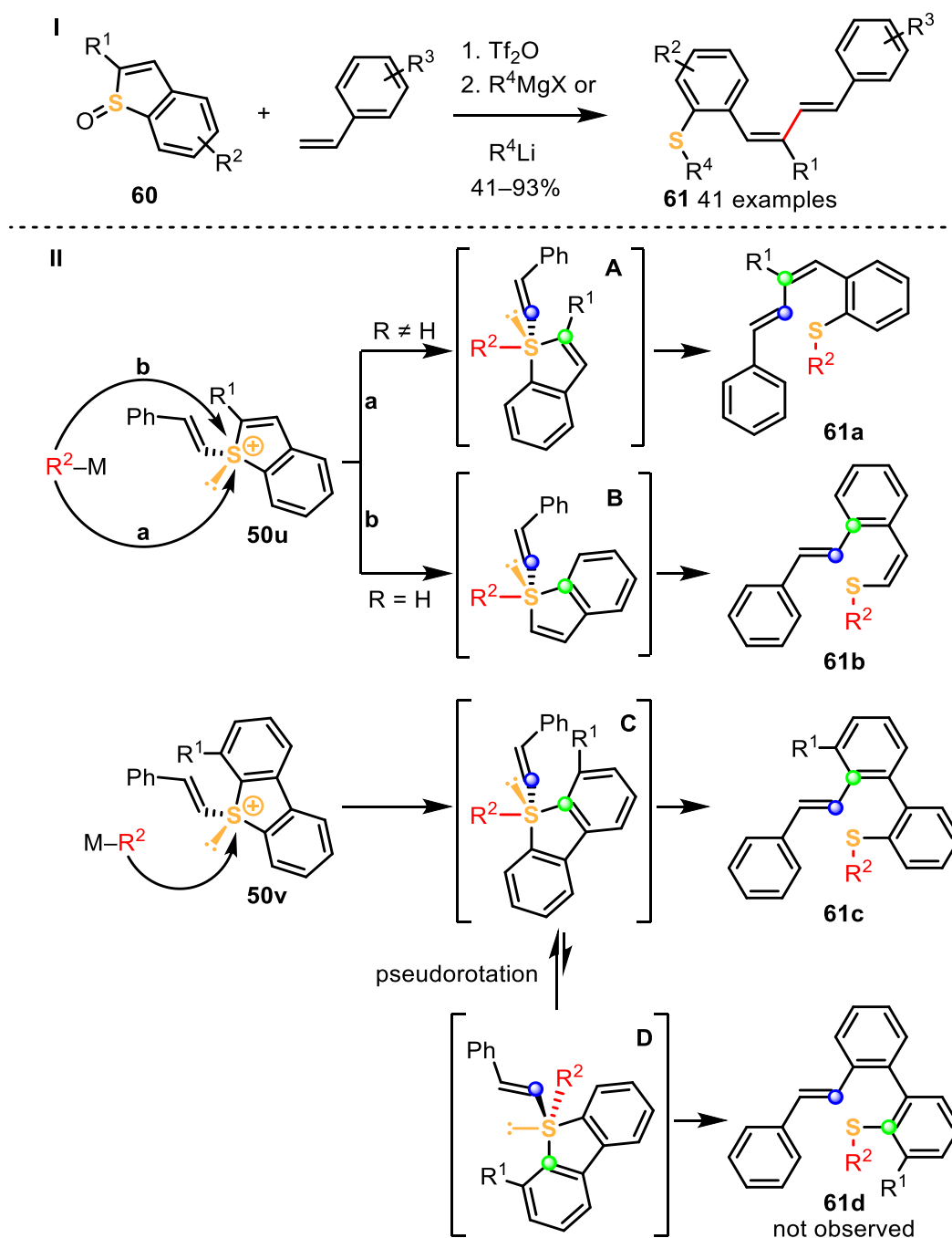
Xiao and coworkers demonstrated the synthetic utility of **50a** as an efficient ethylene transfer reagent (Scheme 19, II, first line). Starting from isoquinolinium bromides **59c**, the authors performed a mild transformation to pyrrolo[2,1-*a*]isoquinoline derivatives **59d** *via* 1,3-dipolar cycloaddition of the vinyl moiety.¹⁰⁷ DABCO was used as a base, and the terminal step was a simple oxidation to **59d** by air. Moreover, the same research group performed a similar reaction by using indole derivatives **59e** and **50a** as a Michael-acceptor with KOH as a base. The resulting *N*-fused indoles are formed *via* an intramolecular nucleophilic cyclization step (Scheme 19, II, second line).¹⁰⁸

Aggarwal and McGarrigle intensively worked in the field of vinylsulfonium salts and established protocols following reaction pathway **B2** (Scheme 19, III). In 2008 Aggarwal published a method for an annulation reactions for the synthesis of morpholines, thiomorpholines and piperazines **59h**. β -Heteroatom-substituted amines **59g** were used as starting material were treated with **50a** as ethylene transfer reagent.¹⁰⁹ However, this transformation appeared to be neither regio- nor diastereoselective. This issue has been tackled in another report of Aggarwal where it was stated that the choice of base and solvent influenced both diastereoselectivity and regioselectivity.¹¹⁰ The authors also extended the same methodology towards the synthesis of four-membered heteroatom-containing rings **59j**.¹¹¹ Azetidines and oxetanes were successfully synthesized in moderate to good yield. Additionally, Aggarwal and coworkers reported on the synthesis of seven-membered 1,4-heterocyclic systems **59i**.¹¹²

Lin *et al.* used **50s** for the formation of cyclopropanes **59n**. Remarkably, only the *Z*-diastereomers were formed upon cyclopropanation with the phenyl-substituted vinylsulfonium salt **50s**.¹¹³ Additionally, the products were later transformed into 2-benzoylquinolines by utilizing DEAD (diethyl diazenedicarboxylate) at elevated temperatures.

Aziridines **59o** were synthesized by Hanamoto *et al.* using primary amines as nitrogen source and the salt **50t**.¹¹⁴

Procter and coworkers developed a transition metal-free approach to synthesize (*E,Z*)-1,3-dienes **61**. Their strategy involved an interrupted Pummerer reaction followed by a ligand coupling (Scheme 20).¹⁰³



Scheme 20: I) One-pot transformation of styrene derivatives into (*E,Z*)-1,3-dienes **61**, as reported by Procter *et al.* II) Mechanistic proposal towards the formation of **61a**, **61b** and **61c**.¹⁰³

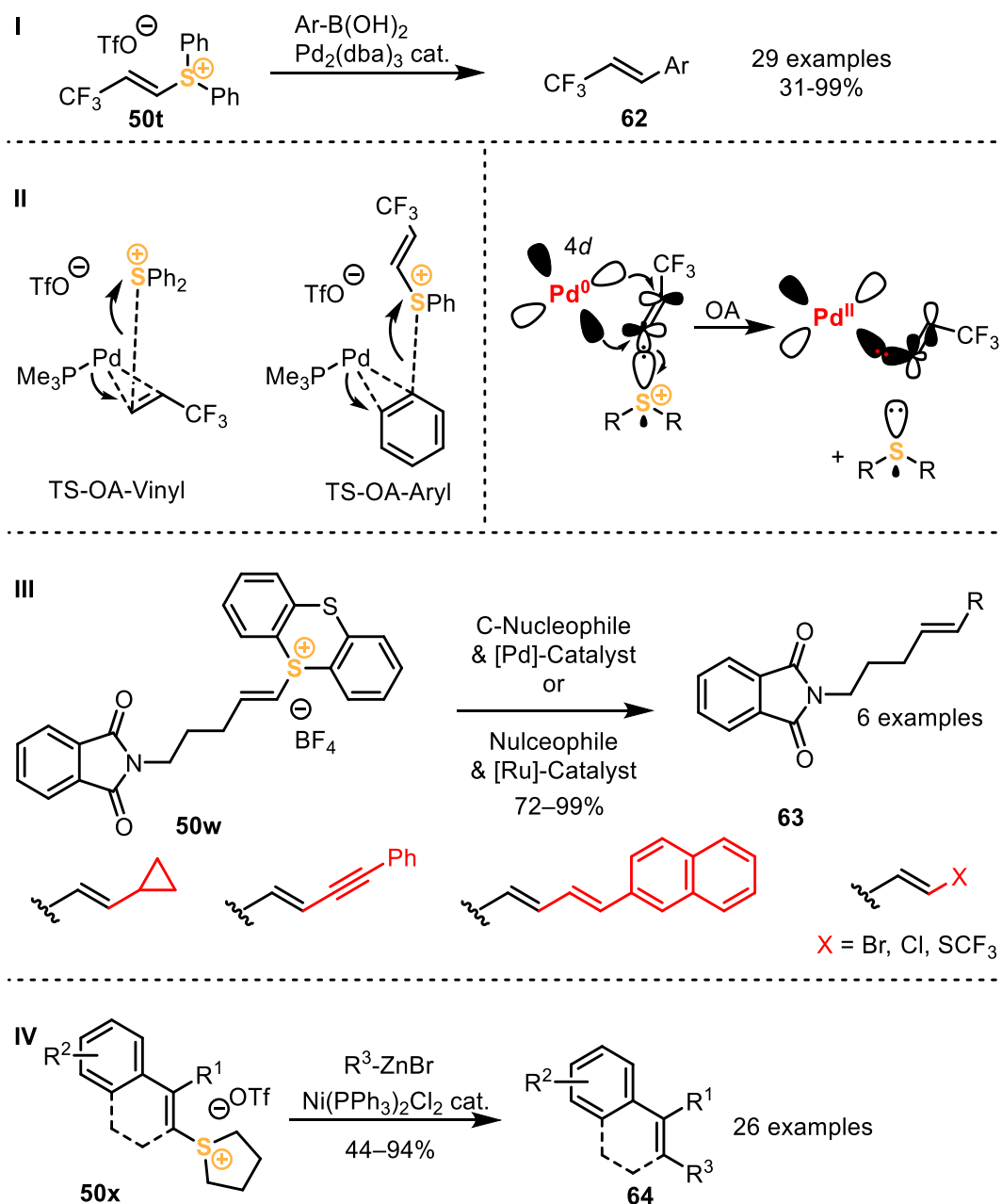
This one-pot synthesis started from readily available benzothiophene S-oxides **60** which can be easily accessed by oxidation of their parent benzothiophenes. After activation of the S-

oxide with triflic anhydride, the intermediate easily reacts with styrene derivatives affording the vinylic sulfonium salts **50u** or **50v**. Treatment of the latter with organolithium or Grignard reagents results in the formation of hypervalent sulfurane intermediates **A** or **B**. A succeeding reductive elimination step is accompanied by the degradation of the benzothiophene scaffold to form decorated derivatives of (*E,Z*)-1,3-dienes **61**. The protocol is modular in terms of the variety of *S*-oxides **60**, styrenes and the employed organometallic reagent; therefore, a large substrate scope was demonstrated by the authors.

Moreover, mechanistic proposals explaining the origin of the high selectivity of this reaction were highlighted, (Scheme 20, II). After generation of the vinylsulfonium salt **50u**, the organometallic reagent attacks the sulfur center in pathway **a** or **b**, and hypervalent (10-*S*-4) sulfuranes **A** or **B** are formed, depending on the substituent in 2-position of the benzothiophene. The nucleophile attacks the opposite to an already existing substituent side and therefore will end up in an axial position. In addition, the nucleophile will preferentially attack *via* the most accessible pathways in the coordination sphere around the sulfur center, which are opposite to the C–S bonds of the heterocycle.

If the substituent R¹ is a carbon substituent, sulfurane **A** will be formed since nucleophilic attack *via* pathway **a** is favored due to less sterical hindrance. The orbital overlap of the sp²-hybridized axial and equatorial ligands (marked as blue and green dot in Scheme 20, II) is favorable, and the product **61a** is liberated *via* ligand coupling. The 2-position of benzothiophene can also be hydrogen whereas formation of sulfurane **B** is favored (nucleophile attacks *via* pathway **b**). In this case the ligand coupling leads to formation of **61b**. The sterical effect is also important if an unsymmetrical 4-substituted dibenzothiophenium salt **50v** is used. In this case the nucleophile will attack opposite to the C–S bond nearby the steric providing substituent and sulfurane **C** is formed. The ligand coupling from this intermediate will deliver **61c**. Pseudorotation from **C** towards **D** is possible, but **D** is high in energy since the lone pair will occupy a less favorable axial position.

In 1997 Liebeskind reported the electrophilic role of *S*-(alkenyl) and *S*-(aryl) sulfonium salts in transition metal-catalyzed reactions.¹¹⁵ The authors prepared a set of tetrahydrothiophenium salts and proved their synthetic utility as coupling partners in palladium-catalyzed cross-couplings with boronic acids and organotin reagents as well as nickel-catalyzed reactions with organozinc reagents.



Scheme 21: Selected examples of transition metal-catalyzed coupling reactions with vinylsulfonium salts, as reported by **I**) Lu¹¹⁶, **III**) Ritter⁹⁹, **IV**) Procter¹⁰⁰. **II**) Optimized transition states for the oxidative addition of palladium⁰ into a vinyl C–S bond (TS-OA-Vinyl) and aryl C–S bond (TS-OA-Aryl) (left). Proposed mechanism and orbital interactions during the OA (right).¹¹⁶

Lu *et al.* examined the higher selectivity of the activation of alkenyl C–S bonds over aryl C–S bonds and reported on the selective Suzuki coupling of the (*E*)-trifluorovinyl moiety with boronic acids (Scheme 21, I).¹¹⁶ Moreover, DFT calculations have been performed and gave insight into the favorable interaction of palladium⁰ with a vinyl C–S bond comparably to an aryl C–S bond (Scheme 21, II).

The first step of the oxidative addition is the approach of the palladium⁰ center to the sulfonium salt. Then a π -complex between the 4*d*-orbital of the palladium and the π^* -orbital of the double bond is formed. During this process the electrons of the C–S⁺ bond migrate towards the sulfur center and cause the release of the corresponding sulfide as a leaving group. DFT-calculations revealed that this process is more favored with a vinyl C–S bond in comparison with an aryl C–S bond (relative free energy in solution: $\Delta G_{\text{sol}} = 11.7 \text{ kcal} \cdot \text{mol}^{-1}$). Additionally, the authors found an energetically low lying LUMO of the (trifluoromethyl)vinyl moiety through NBO (natural bond orbital) analysis. The energetic difference of the π^* -orbitals of the vinyl and both individual phenyl rings is 0.27 eV which is in accordance with the observed reactivity. The electron-withdrawing nature of the trifluoromethyl group lowers the energy of the π^* -orbital of the adjacent vinyl group significantly and therefore makes this group more prone towards oxidative additions.

The research groups of Ritter and Procter recognized the potential of the pioneer work on vinylsulfonium salts in transition metal catalysis and expanded the arsenal during the past few years.

A regio- and stereoselective thianthrenation of unactivated double bonds followed by palladium- and ruthenium-catalyzed cross-coupling reactions have been performed by Ritter.⁹⁹ The reactions were conducted for one particular substrate shown in Scheme 21, III. The authors reported not only on the palladium-catalyzed coupling of a sp^3 -, sp^2 - and sp -carbon to olefins but also found the direct replacement of the sulfonium moiety with (pseudo)halides with the help of ruthenium as a catalyst.

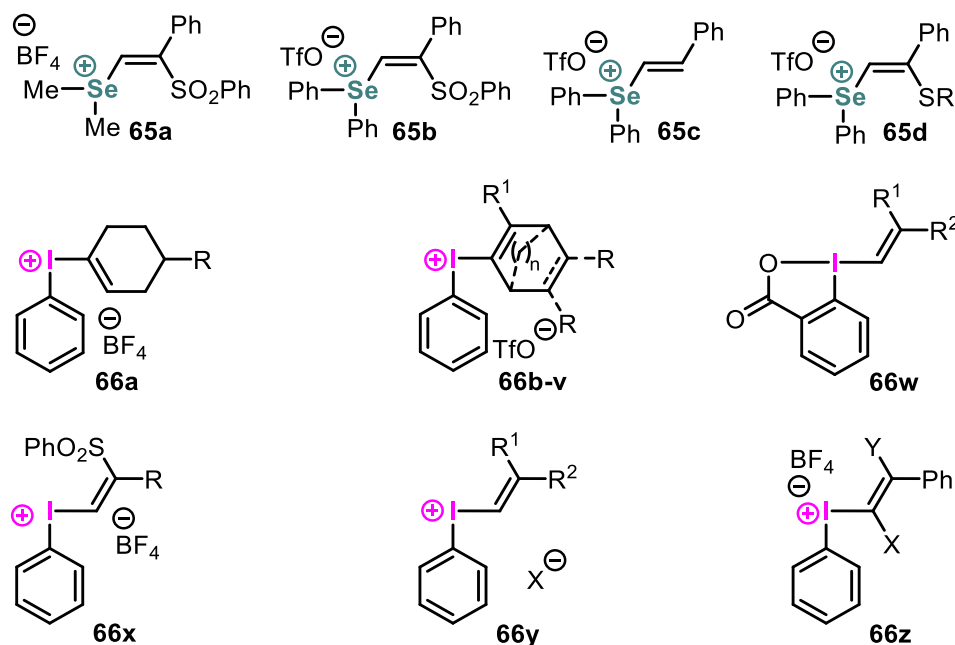
Procter and coworkers demonstrated a one-pot Pummerer reaction followed by a nickel-catalyzed cross-coupling sequence (Scheme 21, IV).¹⁰⁰ The transformation proved to be versatile in choice of both reaction participants, i. e. the vinylsulfonium salts **50x** and organozinc reagents as coupling partners. In addition to broadly used arylzinc reagents, Procter showed that sp^3 - and sp -hybridized zincates can be employed for these couplings as well. On the other hand, the sulfenylation reaction could be applied to arenes and alkynes.

Both types of substrates could be successfully coupled with an organozincate, showing not only applicability in Heck-type but also Sonogashira- and Negishi-type reactions.

It is worth noting that both reactions of Ritter and Procter used either cyclic or aliphatic sulfonium backbones to tackle the possibility of the undesired oxidative addition other than the target coupling partner.

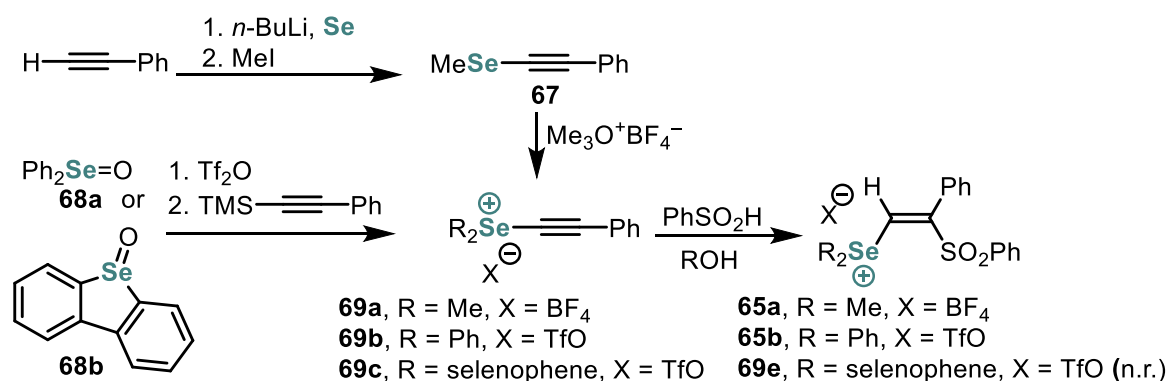
1.3.4. Alternative Alkenylation Reagents

Besides the well-established vinylsulfonium salts, structurally related iodine- and selenium-based Csp^2 -substituted salts of the types **65** and **66** play a significant role in similar chemistry as shown for sulfur-based ones. A brief overview on the structural diversity of these reagents is shown in Scheme 22.



Scheme 22: Selenium- (**65a–d**) and iodine-based (**66a–f**) alkenylating reagents.

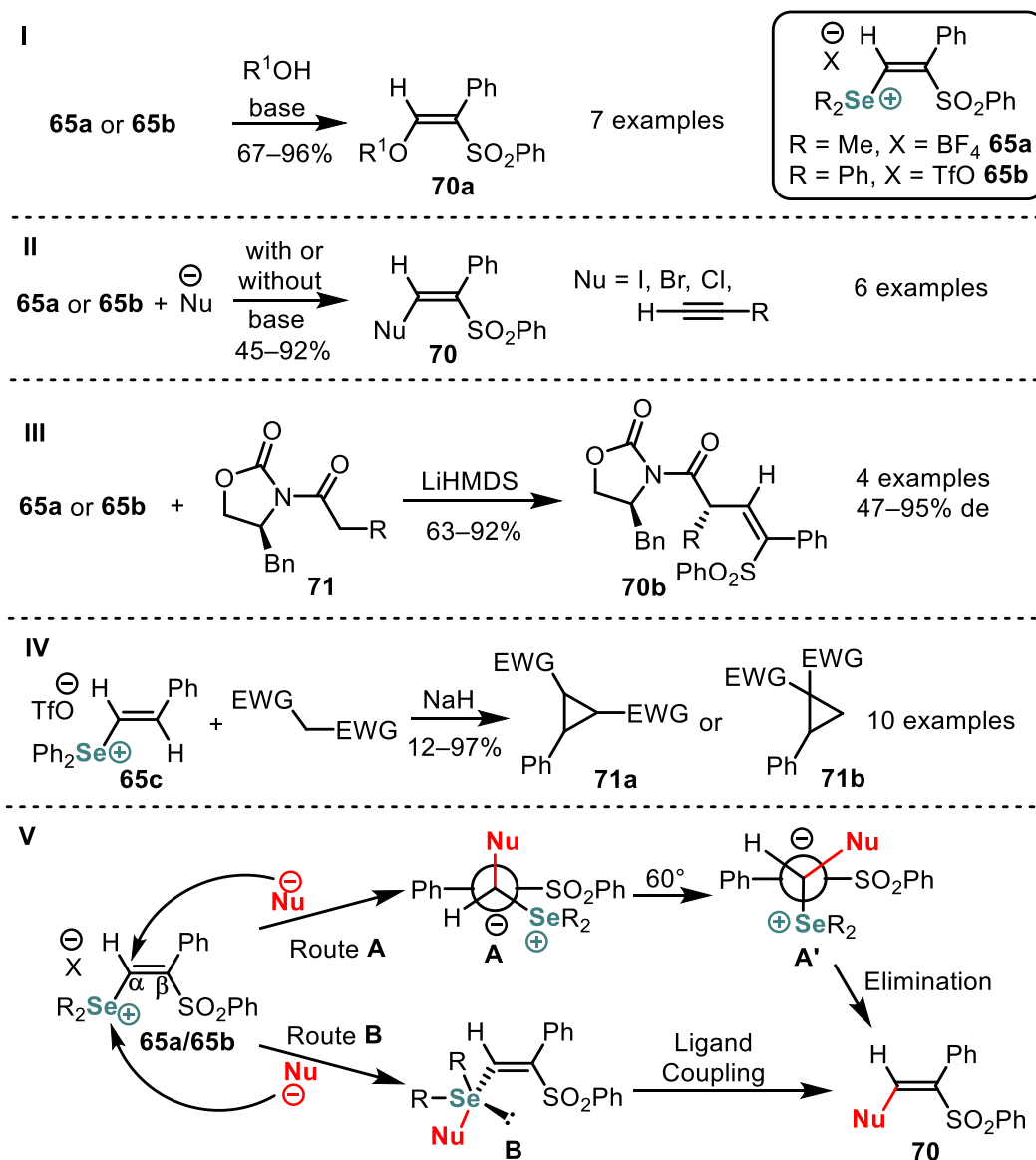
More than two decades ago Nara and Shimizu developed a synthetic strategy towards (*Z*)-(β -phenylsulfonyl)vinylselenonium salts **65a** and **65b** (Scheme 23).^{25,117} Starting from readily available phenylacetylene, compound **67** can be obtained by deprotonation with *n*-butyllithium and treatment with elemental selenium. Successive quenching with methyl iodide affords **67**. After treatment of **67** with Meerwein salt [Me₃O]⁺BF₄⁻, **69a** is obtained. The latter can add PhSO₂H furnishing **65a**.



Scheme 23: Synthetic strategies towards alkenylselenonium salts **65a** and **65b**.

A well-known method starting from selenoxides **68a** and **68b** consists in their activation with triflic anhydride followed by reaction with TMS-capped phenylacetylene to afford **69b** and **69c**. Addition of PhSO₂H in a protic solvent gives **65b**, although the reaction towards **65e** does not proceed under the same conditions.

With reagents **65a** and **65b** in hand, their properties as Michael acceptor have been tested by Kataoka and Muraoka with a variety of nucleophiles, as shown in Scheme 24.



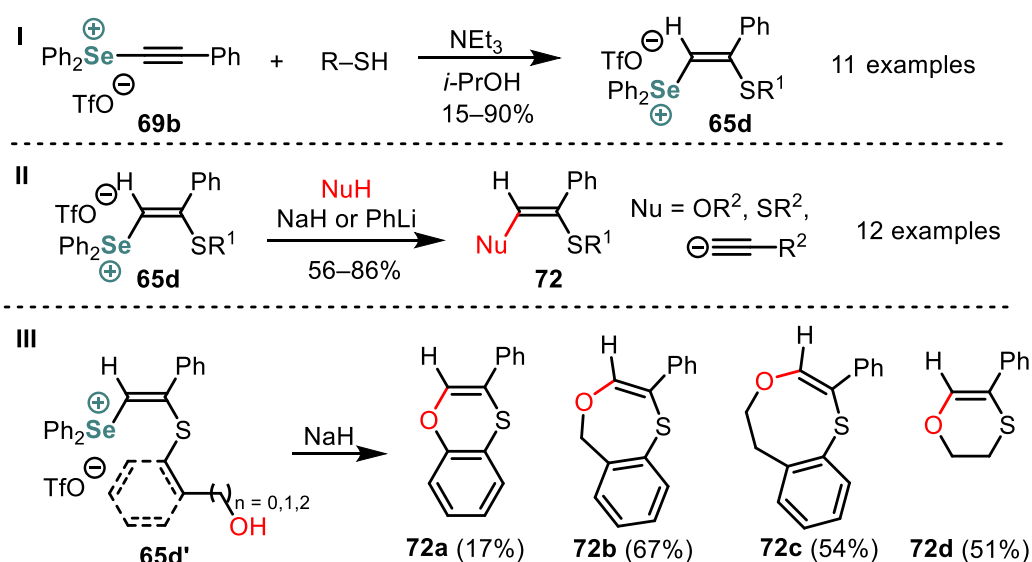
Scheme 24: Synthetic applications of vinylselenonium salts **65** as reported I) & IV) by Kataoka and II) & III) by Muraoka. V) Mechanistic proposal of the nucleophilic attack towards **70**.^{118–121}

Kataoka successfully used a variety of complex alcohols as nucleophiles to obtain **70a** in acceptable to good yields (Scheme 24, I).¹²¹ Either sodium hydride or phenyl lithium was utilized as a base. Moreover, Kataoka found out that halogenides and acetylides¹²⁰ underwent the same transformations as well as chiral oxazolidinone **71**. Alkenylation of the latter resulted

in the formation of enantiomerically enriched **70b**¹¹⁸ (Scheme 24, II & III). Lastly, under basic conditions the salt **65c** underwent cyclopropanation by the reaction with compounds possessing an activated methylene groups affording products **71a** or **71b** (Scheme 24, IV).¹¹⁹ However, this transformation appeared to be strongly dependent on the fine structure of a substrate.

In each publication discussed in Scheme 24 the same mechanistic rationalizations were proposed (Scheme 24, V). Two possible routes of the nucleophilic attack were considered. First, the nucleophile potentially can attack the α -carbon, and a stabilized negative charge remains on the β -carbon by formation of intermediate **A**. Rotation around the σ -C $_{\alpha}$ -C $_{\beta}$ -bond by 60° leads to an *anti*-periplanar conformation of the selenonium moiety and the negative charge in the conformer **A'**. The elimination of the selenide occurs and delivers **70** via a simple addition-elimination sequence. Route **B** involves the nucleophilic attack on the selenonium center forming selenurane **B**. Product **70** is subsequently formed by ligand coupling of the nucleophile and the α -carbon.¹²¹

Kataoka published a closely related work on selenonium salts with a sulfide as a β -substituent.¹²² Treatment of the triflate **69b** with a thiol in the presence of triethylamine gave a series of selenonium salts **65d** (Scheme 25, I).

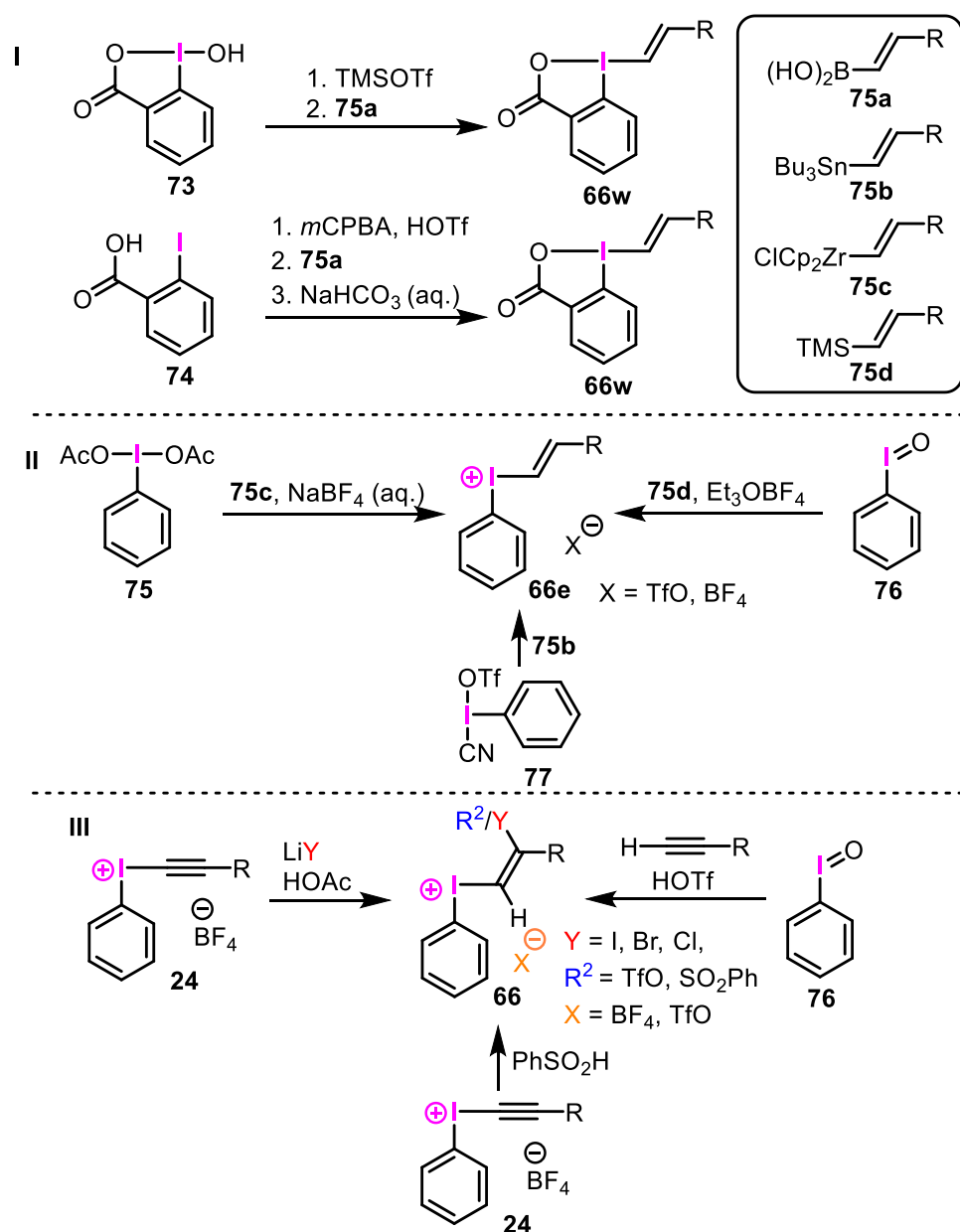


Scheme 25: I) Addition reaction onto **69b** affording **65d**. II) Nucleophilic attacks towards products **72**. III) Intramolecular nucleophilic cyclization reactions of selenonium salts **65d'**.¹²²

These salts showed the same behavior in the presence of nucleophiles as their sulfone-derived analogs. *O*- and *S*-nucleophiles as well as the generated from alkynes ones are suitable, and the corresponding products were obtained in moderate to good yields (Scheme 25, II).

Moreover, Kataoka synthesized a selenonium salts **65d'** with an alcohol group attached on aliphatic chains of different lengths (Scheme 25, III). The authors successfully performed their intramolecular cyclization by deprotonation of the alcohol function which then undergoes a nucleophilic attack *via* the mechanism described in Scheme 24, V. The ring sizes of the resultant 5,6-dihydro-4,1-benzoxathiocine skeleton extends from six-membered over eight membered ones (**72a–72d**), although **72d** in particular was obtained only in 17% yield.

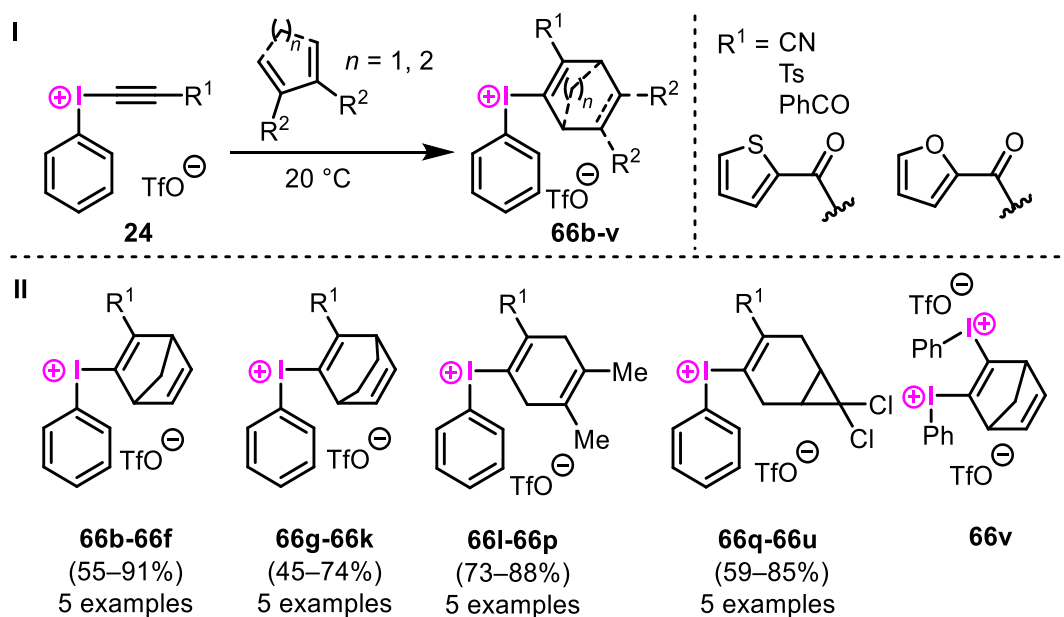
Besides the versatile applicability of vinylsulfonium salts, the chemistry of alkenyl-containing iodine^{III} reagents has been extensively explored. A general overview of the synthetic strategy towards vinyliodine reagents **66** is given in Scheme 26.



Scheme 26: I-III) General strategies for the synthesis of alkenyliodine reagents **66**.

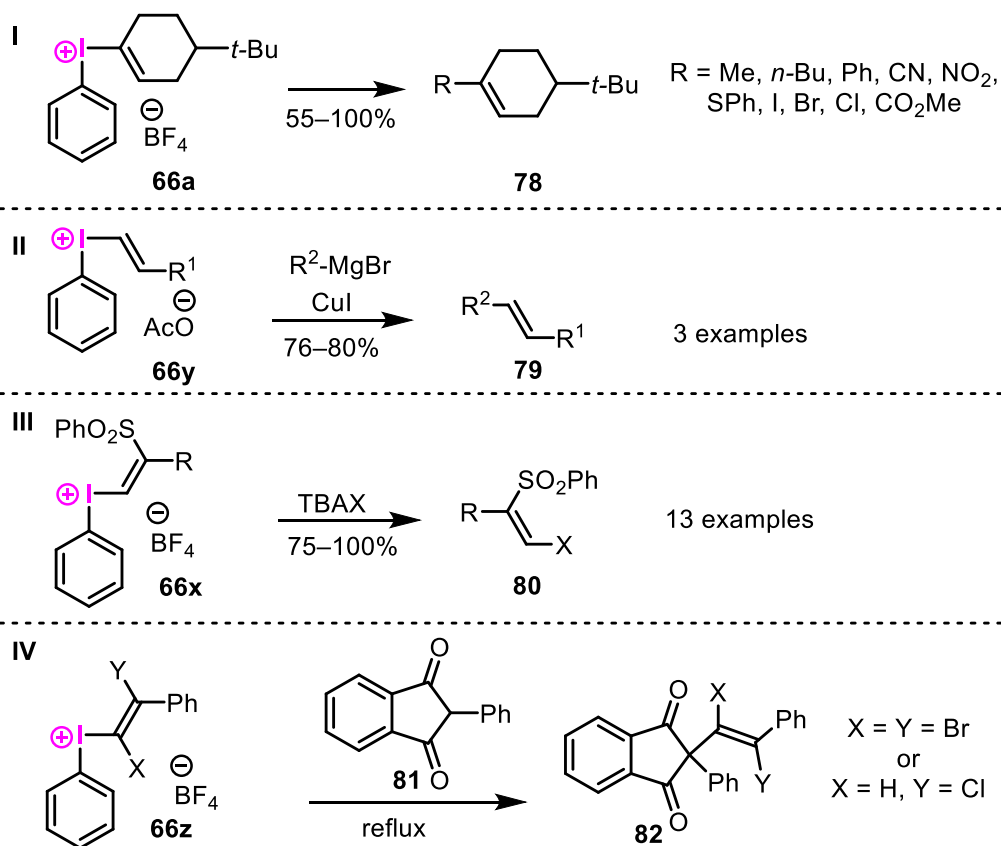
Compound **66w** was obtained upon treatment of 2-iodosylbenzoic acid (**73**) with TMSOTf¹²³ or oxidation of 2-iodobenzoic acid (**74**) with *m*CPBA followed by reaction with vinyl boronic acid **75a**¹²⁴ (Scheme 26, I). Alternatively, (*E*)-styryl(phenyl)iodonium salts **66y** were synthesized by treatment of (diacetoxy)iodobenzene (**75**), aryl(cyano)iodonium triflate (**77**) and iodosobenzene (**76**) with alkenylzirconium- (**75c**),¹²⁵ alkenyltrimethylsilane- (**75d**)¹²³ or alkenylstannane compound **75b**,¹²⁶ respectively (Scheme 26, II). The formation of vinyliodonium salt **66** was also carried out by hydrohalogenation of the corresponding alkynyl iodonium salt **24** under acidic conditions (Scheme 26, III).¹²⁷ Stang and coworkers reported on the direct synthesis of (*E*)-(β -trifluoromethylsulfonyloxyvinyl) iodonium triflates **66** by using iodosobenzene **76**, triflic acid and a terminal alkyne, whereby the *anti*-addition of *in situ* generated PhIO·TfOH to the triple bond occurred.^{128,129} The addition of benzenesulfinic acid to the alkyne moiety in **24** was also performed, analogously to the chemistry of the discussed above selenium-based alkynylation reagent, to afford **66**.¹³⁰

Especially Arif paid much attention to the synthesis of vinyliodonium triflates **66b-v** *via* Diels-Alder reactions (Scheme 27).¹³¹ The reaction of **24** as a dienophile with a diene was conducted under mild conditions and afforded more than 20 examples in moderate to good yield. Remarkably, dicationic salt **66v** was synthesized from its parent diiodoniumacetylene salt.



Scheme 27: Diels-Alder reactions of **24** with dienes affording alkenyliodonium triflates **66b–66v**. All Diels-Alder products have been synthesized with every residue R^1 depicted in the top right corner (5 examples each).

The property of alkenyliodonium salts as Michael acceptors has attracted much attention over past three decades, and a number of protocols demonstrating their synthetic utility as vinylicating reagents have been established.

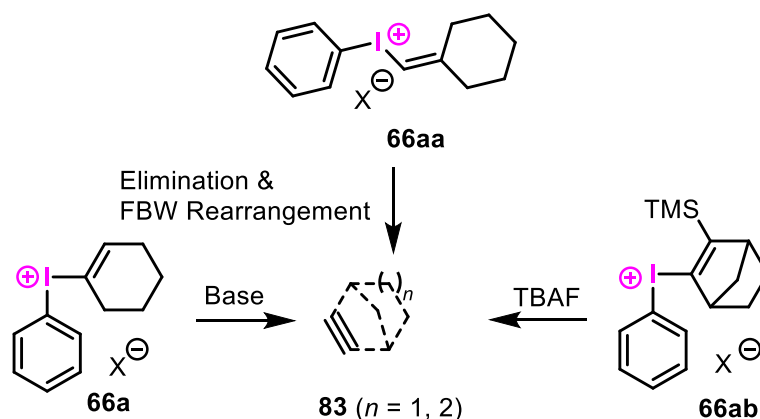


Scheme 28: I) to IV) Synthetic utility of vinyl iodonium salts **66** as alkenylating reagents.

In 1985, Fujita synthesized **66a** and performed a variety of different coupling reactions with this compound (Scheme 28, I).¹³² Gilmann cuprates [LiCuMe_2 , $\text{LiCu}(n\text{-Bu})_2$] and $\text{KCu}(\text{CN})_2$ appeared to be appropriate carbon nucleophiles for the vinylation. The nitration was conducted by utilizing a mixture of CuSO_4 and NaNO_2 . Thiolation and halogenation was done by nucleophilic attack of their corresponding anions. At last, the cyclohexenylester was obtained using palladium catalysis under carbon monoxide atmosphere.

Xu and Huang used Grignard reagents in the presence of CuI and achieved the resultant direct C–C coupling, although with a narrow substrate scope of *E*-alkenes **79** (Scheme 28, II).¹²⁵ Masaki *et al.* utilized tetrabutylammonium halides as halogen sources towards the formation of **80** (Scheme 28, III).¹³⁰ Galton's work from 1965 included the alkenylation of indan-1,3-dione (**81**), although only two examples were reported in this publication without detailed characterization (Scheme 28, IV).²⁸

Additionally, Fujita and Yoshioka demonstrated that vinylidonium salts can be used as aryne precursors (Scheme 29).^{133,134}

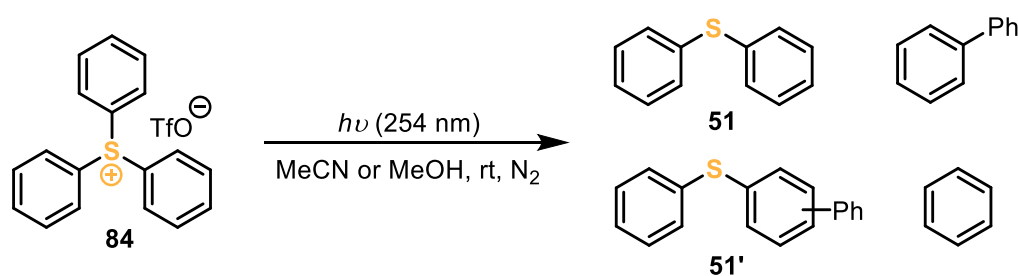


Scheme 29: Synthetic strategies towards aryne formation starting from alkenyliodonium salts **66a**, **66aa** or **66ab**. The first of three options to synthesize arynes **83** from phenyliodonium salt **66a** is the treatment with a base which causes a rapid elimination of iodobenzene and affords aryne **83**. Secondly, in the salt **66aa** with a geminal to PhI group α -proton the latter can be abstracted under basic conditions. This leads to the elimination of iodobenzene and formation of the corresponding vinylcarbene, which undergoes the rapid Fritsch-Buttenberg-Wiechell (FBW) rearrangement accompanied with a ring expansion to a seven membered ring and furnishing aryne **83**. Lastly, β -silylsubstituted iodonium salt **66ab** produces the aryne upon fluoride-induced elimination.

1.4. C(sp²)-Substituted Sulfonium Salts: Aryl substituents

S-(aryl)sulfonium salts are established as industrially useful compounds. Especially triarylsulfonium salts excel in their photosensitivity and are mostly used as photoinitiators for cationic polymerization and as acid generators.¹³⁵ Furthermore, these salts found applications in photolithography, coatings, seals, inks, and as adhesives.^{1,136–139}

The inherent photosensitivity of arylsulfonium salts also attracted the attention of many chemists and was therefore studied intensively. Whereas direct irradiation with highly energetic ultraviolet light caused fragmentation to various photolysis products (Scheme 30),^{136,140,141} their great potential as single-electron reducing agent^{142,143} was also recognized.



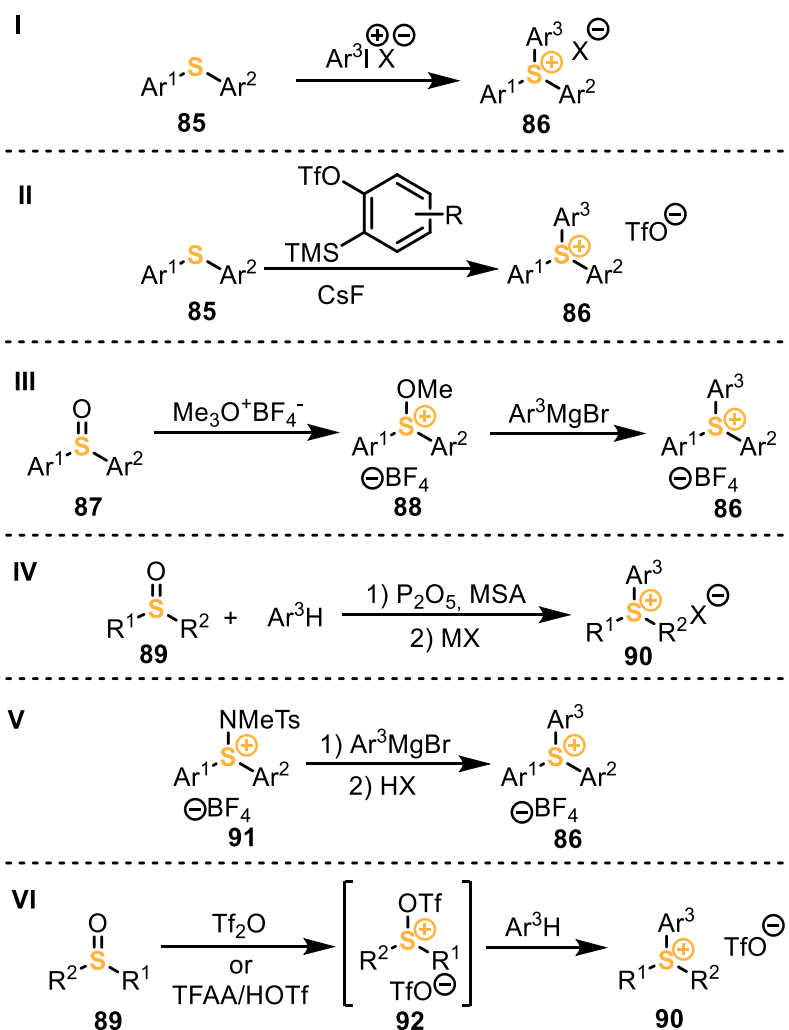
Scheme 30: Photolysis products of triarylsulfonium triflate **84**.

The reactivity of triarylsulfonium salts with alkoxide nucleophiles even assumed the participation of aryl radicals during the course of the nucleophilic aromatic reactions.¹⁴⁴ Since the one-electron reduction of arylsulfonium salts can be performed utilizing photosensitizer,¹⁴⁵ the establishment of these salts in organic chemistry, especially in photoredox catalysis, followed rapidly.^{141,146,147}

In addition to their usefulness in photocatalysis, the employment of arylsulfonium salts in transition metal-catalyzed transformations, where classical coupling partners like (pseudo)halides were replaced by sulfonium salts, was demonstrated as well.¹¹⁵ These more sophisticated transformations, catalyzed both photochemically and by transition metals, have not been sufficiently developed,^{2,141} despite the fact that they have been known for more than two decades.

1.4.1. Synthesis of S-(Aryl) Sulfonium Salts

Various synthetic strategies towards arylsulfonium salts have been reported and are shown in Scheme 31.



Scheme 31: I) to VI) Synthetic strategies towards S-(aryl) sulfonium salts **86**, **90**.

Lam reported on the synthesis of triarylsulfonium salts *via* arylation of arylsulfides with aryliodonium salts (Scheme 31, I).¹⁴⁸ This synthetic method included harsh conditions: without using a copper catalyst, temperatures over 200 °C were required, and this made this approach not convenient. However, the authors demonstrated its applicability not only to arylsulfides, but also to arylselenides. With this method specified sulfonium salts which had no demands of regioselectivity could be prepared.

Peng and coworkers focused their efforts on the arylation of diarylsulfides with *in situ* generated arynes (Scheme 31, II).^{149,150} This method was applicable to diarylselenides as well and could be performed in gram scale without significantly diminished yield.

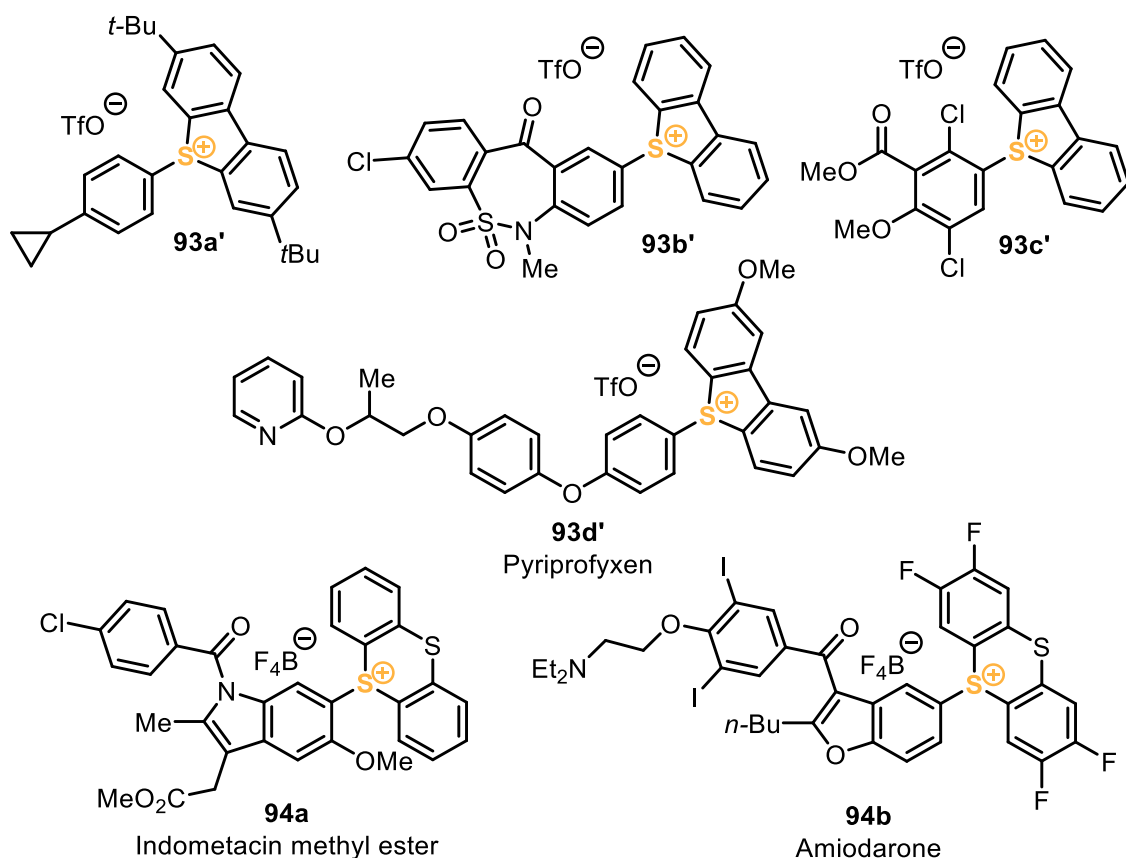
Another reliable synthetic route was the alkylation of sulfoxide **87** with a Meerwein salt and successive treatment with a Grignard reagent (Scheme 31, **III**).^{3,151} The structural diversity of the products which can be obtained was broad but with the typical functional group limitations due to Grignard chemistry. The choice of activators was restricted not only to Meerwein salts, since trimethylsilyl triflate¹⁵² and trimethylsilyl chloride¹⁵³ efficiently served to the same purpose as well.

An alternative approach was the activation of a sulfoxide by the mixture of P₂O₅ and methanesulfonic acid followed by a subsequent counteranion exchange (Scheme 31, **IV**).¹⁵⁴ The reaction was carried out under mild conditions, and the salts were obtained as either hexafluoroarsenates, -phosphates or -antimonates.

It was also shown by Rumpf that the reaction of sulfinimines **91** with Grignard reagents followed the same synthetic pathway as its isoelectronic analog **88** (Scheme 31, **V**).¹⁵⁵ However, since the authors focused on the subsequent chemistry, only one example as triarylsulfonium salt was isolated

Just recently, Tf₂O by Alcarazo¹⁵⁶ and the mixture of TFAA and HOTf by Ritter¹⁵⁷ were introduced both as efficient activators, transforming a large substrate scope into more complex sulfonium salts (Scheme 31, **VI**). The synthesis and applications of S-(aryl)dibenzothiophenium triflates is a part of this thesis and will be discussed in detail in Chapter 3.4.

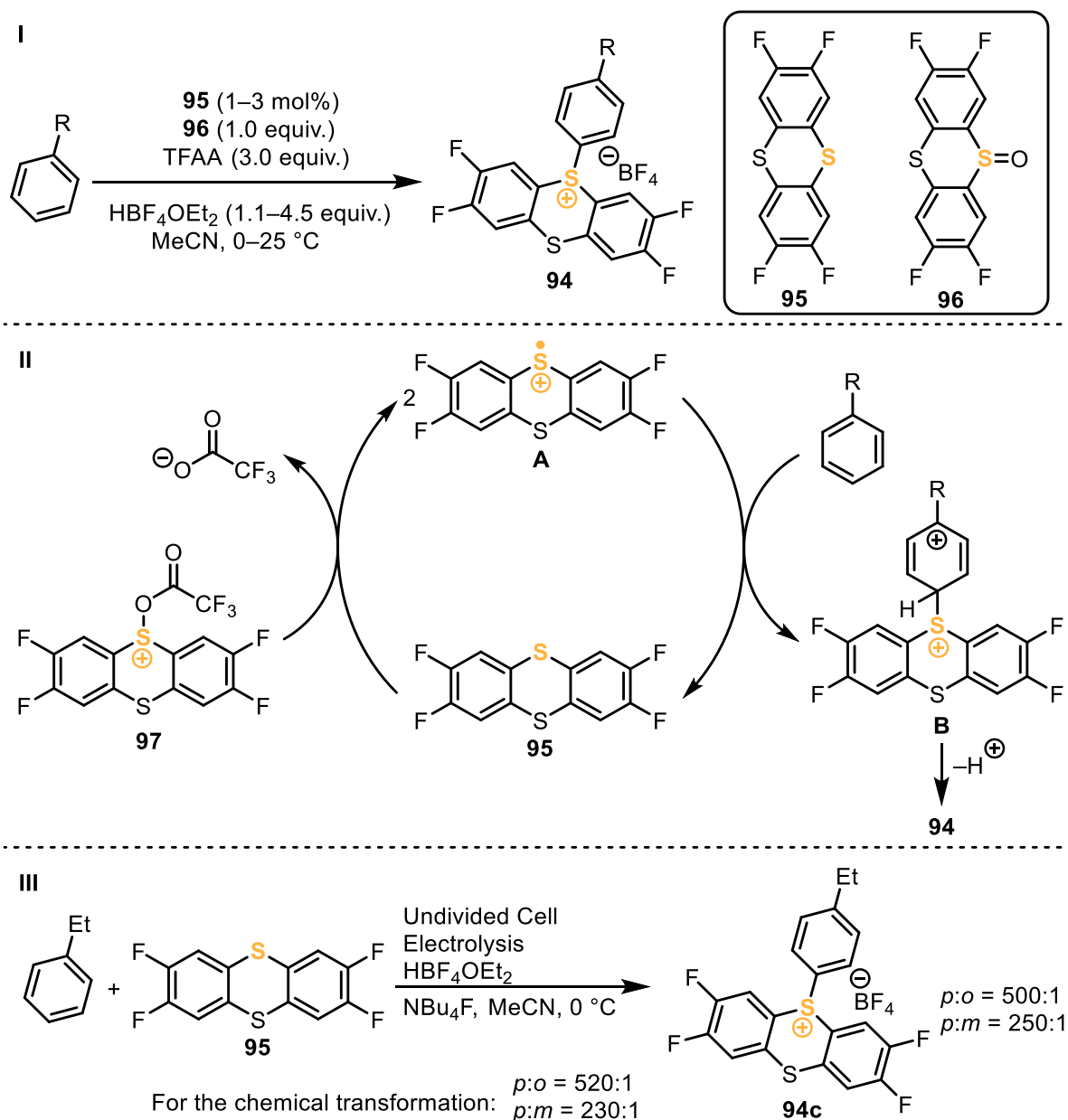
Selected examples for the regioselective sulfenylation are shown in Scheme 32.



Scheme 32: Selected examples for the regioselective sulfenylation, as presented by Ritter *et al.*^{157–159}

Both methods, independently developed by Alcarazo and Ritter, opened a resourceful field of aromatic transition metal-free C–H activation.^{156–159} After activation of the corresponding sulfoxide with an anhydride, the reaction with a non-functionalized arene occurs under mild conditions. Preferably the most electron-rich position of the arene is activated *via* electrophilic aromatic substitution, although site-selectivities occur occasionally by a small percentage.¹⁶⁰ The functional group tolerance of the protocols is broad, ranging from cyclopropyl(alkyl)-, halogenide-, heterocyclic-, ether-, ester-, keto-, amide-, sulfonamide- and even over amine-functionalities (**93a'–94b**). The substrate range in general covers electron-poor arenes like 1,2-dichlorobenzene over those of moderate electron-richness (benzofuran) (see Chapter 3.4.1). Substrates too poor in electrons do simply not react with the activated sulfoxide, whereas too electron-rich ones will undergo a single electron transfer as a side reaction (see Chapter 3.4.1). It has to be noted that the electronic range of the aromatic substrates strongly depends on the structure of the sulfenylation agent, since these provide different electronic properties themselves (see Chapter 1.4.3, Figure 6).

The research group of Ritter developed a method for the highly selective thianthrenation (Scheme 33).¹⁵⁹



Scheme 33: I) General method for the tetrafluorothianthrenation (TFT) of a generic arene; II) Proposed radical mechanism; III) Mechanistic experiment, electrolysis towards **94**.¹⁵⁹

Additionally to the arene, catalytic amounts of **96**, one equivalent of the TFT-sulfoxide **95** and a mixture of TFAA and $\text{HBF}_4\cdot\text{OEt}_2$ was added to afford sulfonium salts **94** under mild conditions (Scheme 33, I). The authors proposed a mechanism for this specific transformation involving a radical step (Scheme 33, II). A disproportionation of activated sulfonium **97** with TFT **95** generated two equivalents of radical cation **A**. A second electron transfer through the reaction with the generic arene delivered dicationic species **B** and regenerated TFT **95**. Under abstraction of a proton, intermediate **B** afforded sulfonium salt **94** by rearomatization.

Ritter and coworkers detected an EPR-signal for radical cation **A** and concluded that this reaction could be conducted by electrolysis in an undivided cell (Scheme 33, **III**). TFT-Salt **94c** could be obtained, and the regioselectivity of the sulfenylation was determined. With a *p*:*o*-ratio of 500:1 and a *p*:*m*-ratio of 250:1, the observations were comparable to those for the same chemical transformation (*p*:*o*-ratio of 520:1, *p*:*m*-ratio of 230:1).

1.4.2. Structure of *S*-(Aryl) Sulfonium Salts

The X-ray structure of **93b** in the solid state is depicted in Figure 5 and discussed as representative for the complete set of *S*-(aryl)sulfonium salts, as all exhibited similar structural features.¹⁵⁶

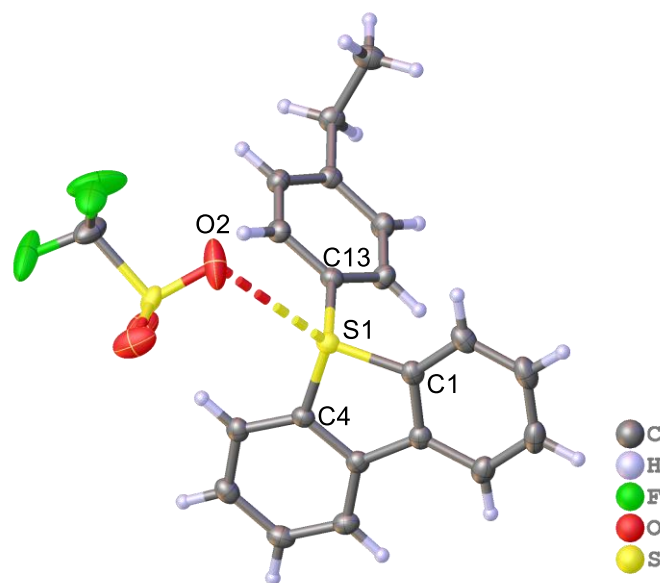


Figure 5: X-ray structure of **93b** in the solid state. Anisotropic displacement shown at 50% probability level. Disorder of the triflate anion (80:20) was omitted for clarity. Selected bond lengths [Å] and angles [°]: S1–C13 1.7038(15), S1–C1 1.7733(16), S1–C4 1.7810(15), S1–O2 3.251(3), C1–S1–O2 138.5, C4–S1–O2 119.0.¹⁵⁶

Again, as expected the sulfur center adopts a pyramidal geometry while the sum of angles around S1 being 300°. The S1–O2 contact is present in this structure with a bond length of 3.251(3) Å which is longer than the one of *S*-(alkynyl)sulfonium salt **5f**. This fact can be traced back to the phenyl group which has a higher steric demand than an alkyne.¹⁵⁶

No additional hydrogen or chalcogen bond could be observed. Since the triflate does not lie in the apical array but in the trigonal plane, the C–S1–O bond angles of 119.0° and 138.5° were observed.

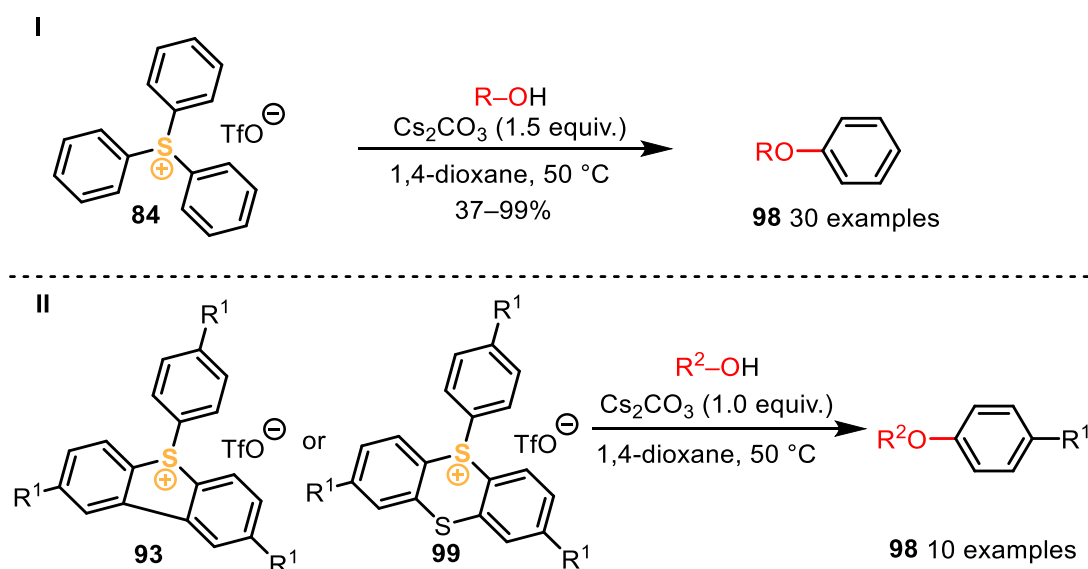
A dimeric arrangement in the solid state of compound **93b** was not found here. The triflate anion is disordered (80:20), which by itself already indicates that it is not tightly fixed in position. Since the triflate-sulfonium chalcogenic bond usually is strongly directed and prefers a 180° angle in respect to the C–S bond, this interaction cannot be very strong. Therefore, a monomeric structure seems to be a plausible consequence.

1.4.3. Reactivity of S-(Aryl) Sulfonium Salts

The reactivities of S-(aryl)sulfonium salts can be divided into three main categories: transition metal-free nucleophilic aromatic substitutions, transition metal-catalyzed transformations and photoredox catalysis.

1.4.3.1. Transition Metal-Free Transformations

Zhang *et al.* demonstrated the formation of ethers by utilizing strong alkoxide nucleophiles for nucleophilic aromatic substitution in triarylsulfonium salts **84** and **99** (Scheme 34).^{161a}

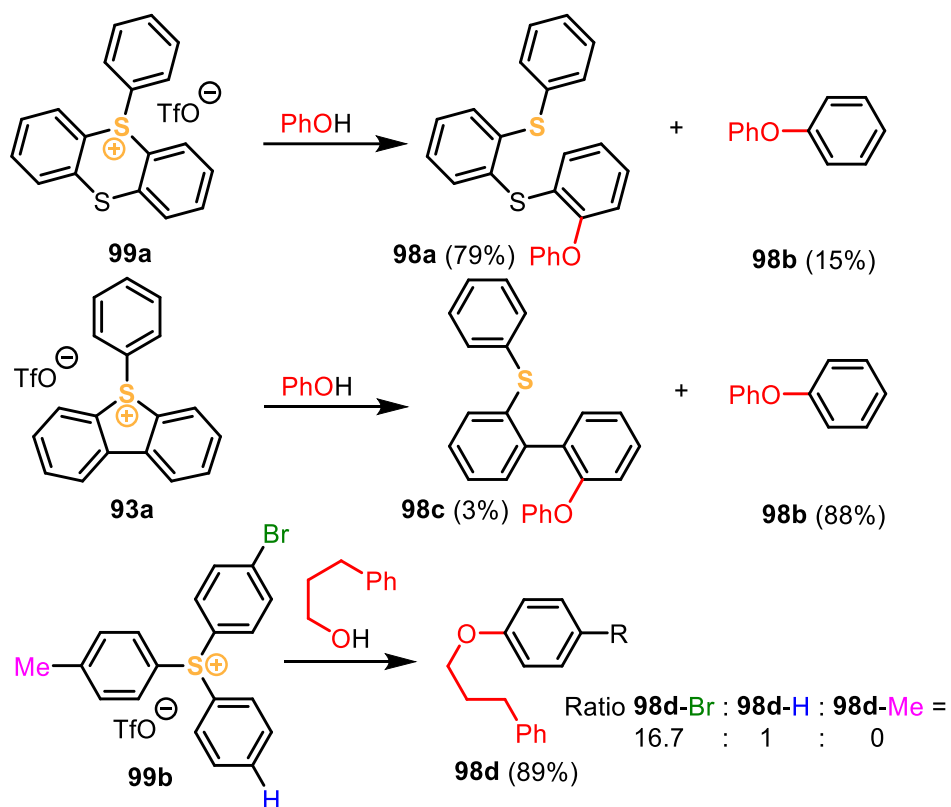


Scheme 34: Ethers from formation via triarylsulfonium salts. I) General method; II) Alternative sulfonium salts.^{161a}

30 ethers were synthesized by phenylation of a set of alcohols (Scheme 34, I & II). Moreover, if salts of triarylsulfonium **99** with different aryl substituents were used, then for each substituent a different reactivity was observed (Scheme 35).

Starting from S-(phenyl)thiantrenium triflate **99a**, the formation of **98a** in 79% yield could be observed along with 15% of diphenyl ether (**98b**). The very similar 5-(phenyl)dibenzothiophenium triflate **93a** delivered phenylated **98b** (88%) as the main product and almost no ring-opened compound **98c**. The authors stated that the reason of the different reactivity remains unclear.

However, treatment of triarylsulfonium salt **99b**, bearing three different aryl substituents (electron-rich, -neutral and -poor), with an alkoxide afforded 89% of **98d** (Scheme 35). As explained by the authors, the alkoxide entered the nucleophilic substitution reaction preferably on the most electron-poor arene center; therefore, a ratio of 16.7 : 1 : 0 for the arene moieties substituted with a bromide, hydrogen and methyl, respectively, was observed.

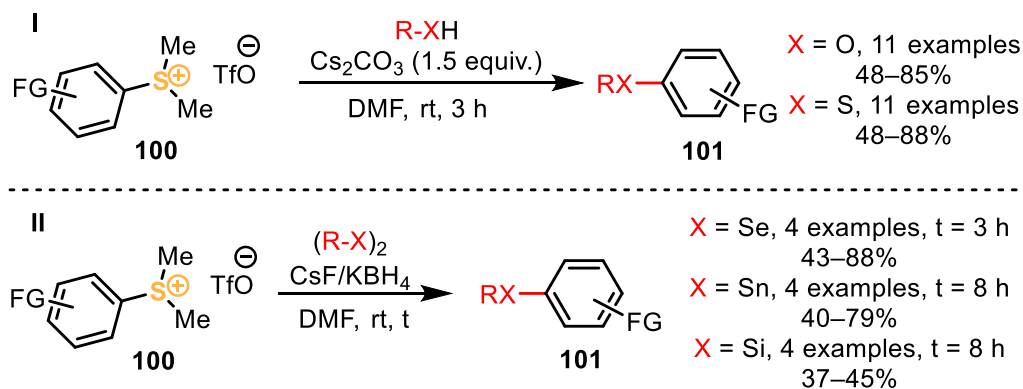


Scheme 35: Three selected examples for the aryl ether formation.^{161a}

Several authors suggest up to three types of mechanisms for this transformation: S_NAr mechanism^{162,163}, the formation of an aryne intermediate¹⁶⁴ and a radical process¹⁶⁵.

Control experiments revealed no diminished yield by using a radical trap which suggests a non-radical mechanism. Additionally, the authors stated that they exclude an aryne intermediate for the base-mediated *O*-arylation of alcohols. Lastly, it has to be mentioned that small amounts of benzene and benzaldehyde were observed by HPLC analysis. This hints towards side reactivity which is a Swern-type oxidation *via* formation of the alkoxyulfoniumion, formed by the sulfonium salt and the direct attack of the alkoxide to the sulfur center, under basic conditions (e. g. **99b** to **98d**).¹⁶¹

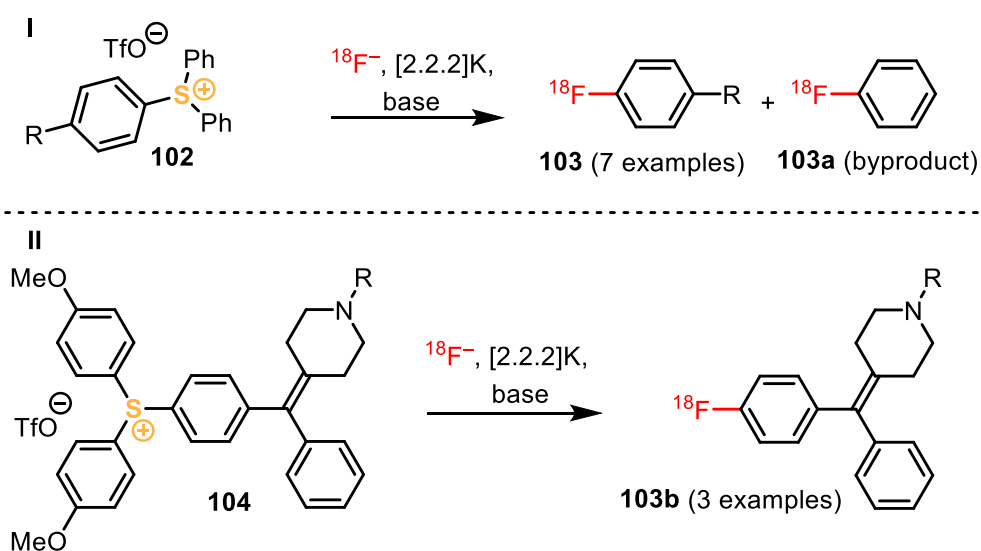
Zhang and coworkers used very similar conditions not only for the *O*-arylation of alcohols but extended this methodology towards *S*-, *Se*-, *Sn*- and *Si*-arylation (Scheme 36).¹⁶⁶



Scheme 36: I) Conditions for the formation of ethers & thioethers; II) Conditions for the selenylation, stannylation and silylation, as reported by Zhang.¹⁶⁶

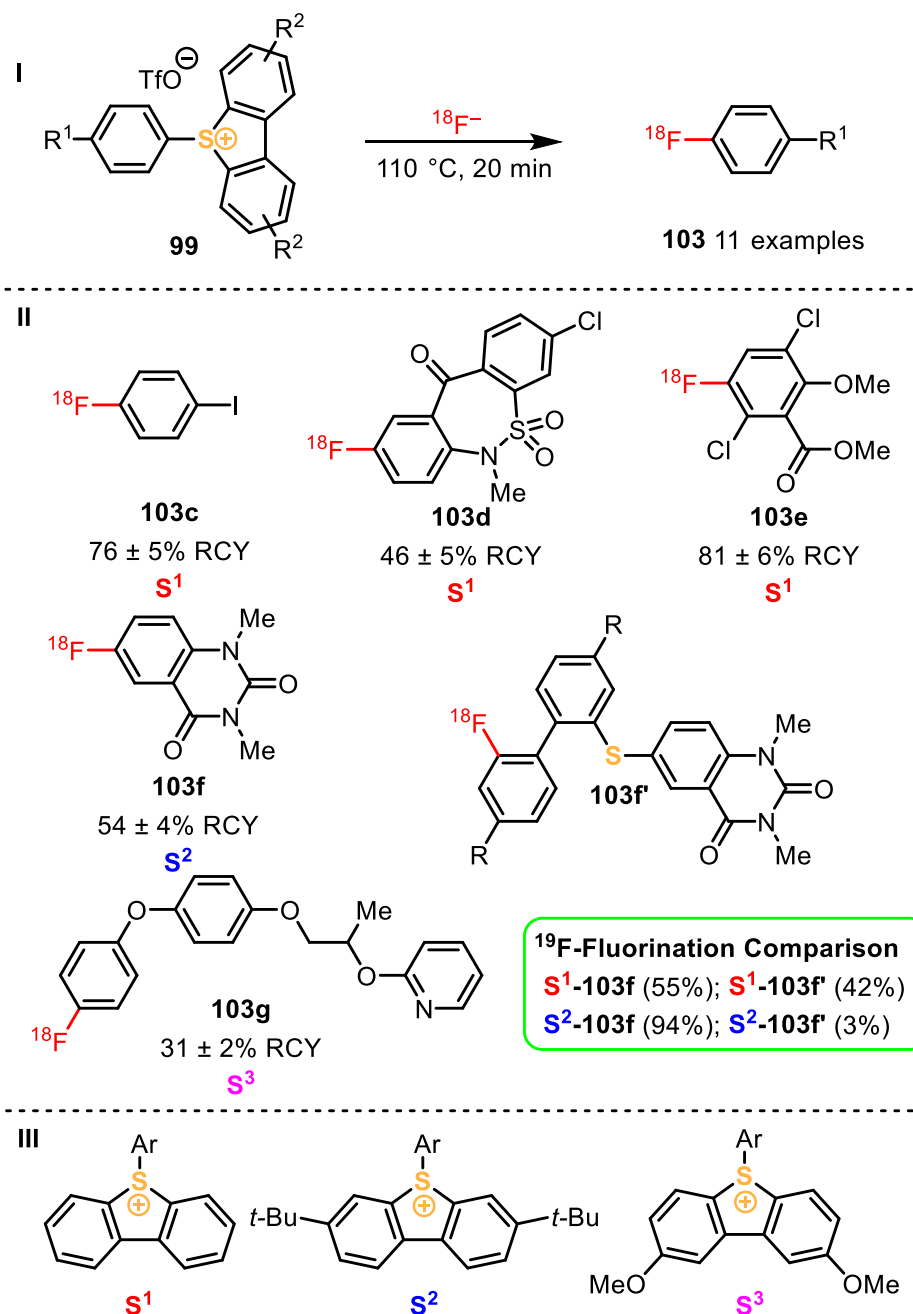
In this protocol the sulfonium salt contained only one aryl substituent; therefore, dimethylsulfide acts as a leaving group. The *O*- and *S*-arylation was done directly by reacting an alkoxide and thiolate with the arylsulfonium salt, respectively, whereas for the selenylation, stannylation and silylation the corresponding dielemental precursor was used.

Another field of interest is the fluorination, even more specific the radio labelling by ¹⁸F-incorporation.^{167,168} ¹⁸F-containing molecules have medical application as PET (positron-emission-tomography) tracers; therefore, selective and mild incorporation of ¹⁸F-fluoride is highly desired. *S*-(Aryl)sulfonium salts turned out to be excellent reaction partners in the direct fluorination of aromatic compounds (Scheme 37).



Scheme 37: Fluorination *via* nucleophilic aromatic substitution in arylsulfonium salts.^{167,168}

However, these methods were applied to a rather narrow substrate scope and additionally side-product **103a** was formed with acyclic sulfonium salt **102** (Scheme 37, I). Ritter combined an efficient side-selective sulfenylation with the late-stage ^{18}F -fluorination (Scheme 38).¹⁵⁷



Scheme 38: I) Methodology for the fluorination; II) Selected examples, RCY = decay-corrected radio chemical yield; III) Parent dibenzothiophene-backbones used for the former sulfenylation. Sulfenylation proceeds with the corresponding sulfoxide and either Tf₂O in DCM or TFAA/HOTf in MeCN.¹⁵⁷

This strategy involved a regioselective sulfenylation with different dibenzothiophene derivatives and successive ^{18}F -fluorination. Temperature of 110 °C was used, and the reaction was stopped after 20 min (Scheme 38, I). The formation of side-products was not reported, and an extract of the substrate scope shown in Scheme 38, II. The sulfenylation was conducted

with three different dibenzothiophene backbones (Scheme 38, III). Compound **103c** was obtained in good yield, and iodine substituent remained unchanged during the reaction. Sulfonamides, ketones (**103d**) and ester functionalities (**103e**) were also tolerated.

Examples **103f** and **103g** show the fluorinated products derived from different dibenzothiophene derivatives (S^2 & S^3). The authors stated the fluorination (S_NAr) will take place at the most electron deficient arene. Hence, S^3 will provide two electron-rich positions which are unlikely to be attacked by a fluoride anion, and the fluorination should take place at the desired exocyclic aryl group. However, S^3 -oxide (S^3O) proves to be less efficient in the sulfenylation step than the more electron-poor S^1 -oxide (S^1O) and therefore cannot be used for the sulfenylation of less electron-rich arenes.

The authors concluded that the choice of the sulfoxide is individual for each arene since the sulfoxide should be adequately electron-poor to sufficiently activate C–H in the arene but electron-rich enough to be highly selective in the fluorination step.

To exemplify this statement, both parent sulfonium salts S^1 -**103f** and S^2 -**103f** were synthesized in satisfactory yields. Nevertheless, the ^{19}F -fluorination yielded 94% of **103f** in the case of S^2 -**103f**, while S^1 -**103f** gave only 55% of **103f** and 42% of **103f'** as side-product (Scheme 38, II).

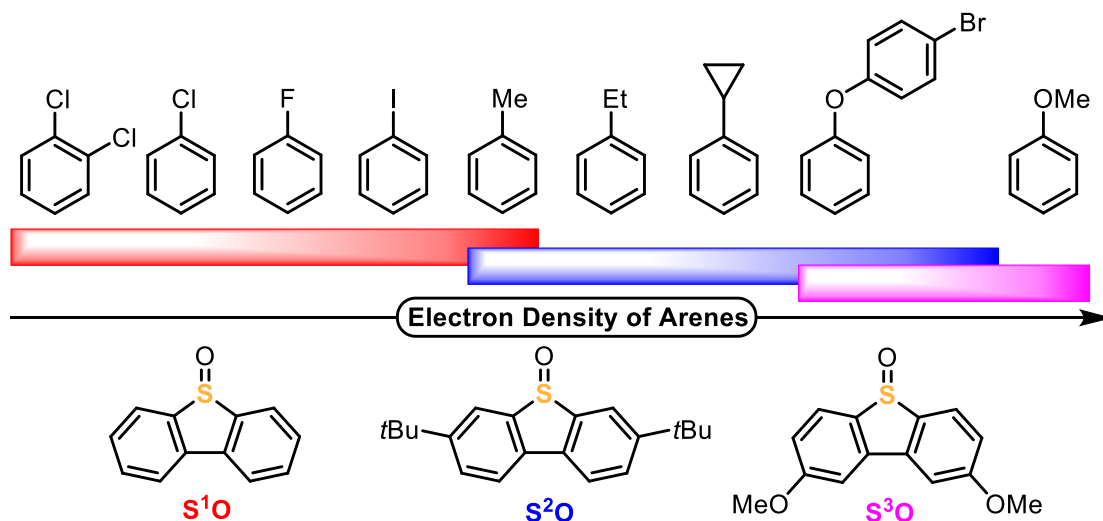


Figure 6: Electronic map of arenes (left: electron-poor to right: electron-rich) for the applicability of the dibenzothiophene scaffolds S^1O , S^2O & S^3O in sulfenylation reactions with arenes.¹⁵⁷

Figure 6 shows the three dibenzothiophene oxides S^1O , S^2O and S^3O (colors S^1O = red; S^2O = blue; S^3O = violet) and their match to arenes in terms of electron density which is underlined with a bar in their corresponding color (can be found in the supporting information of ¹⁵⁷). With this evaluation in hand, theoretically the match of dibenzothiophene oxides with arenes

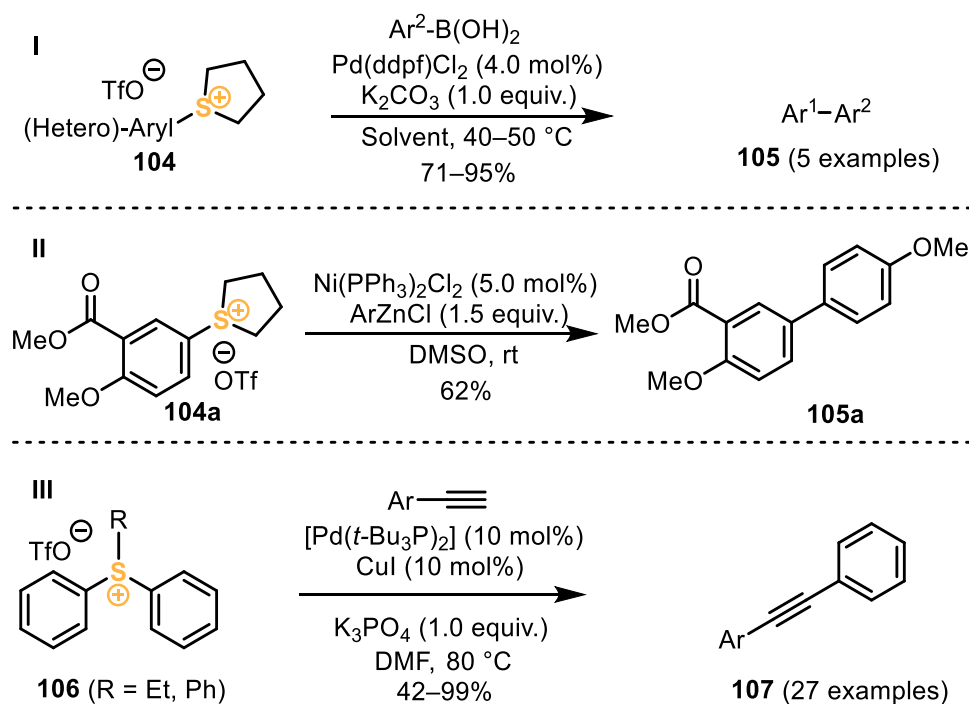
could be predicted. It has to be noted that the reaction with arenes less electron-rich than 1,2-dichlorobenzene is neither efficient nor selective.

1.4.3.2. Transition Metal-Catalyzed Transformations

Liebeskind reported on the transition metal-catalyzed Suzuki coupling with sulfonium salts as (pseudo)halide reactants in the late 20th century (Scheme 39, I).¹¹⁵ In addition, the same reactivity could be found under Stille and Negishi coupling conditions, either palladium- or nickel-catalyzed. The authors especially used tetrahydrothiophene as sulfonium motif to ensure the selective aryl coupling.

One example of an aryl-aryl coupling under nickel catalysis was performed by Procter. Again, tetrahydrothiophene was used as an efficient sulfonium coupling partner for the mild Negishi coupling (Scheme 39, II).¹⁰⁰

The versatile applicability of *S*-(aryl)sulfonium salts also includes Sonogashira couplings, as showed by Zhang and coworkers (Scheme 39, III).¹⁶⁹



Scheme 39: Nickel- or palladium-catalyzed C–C couplings; I) by Liebeskind; II) Negishi coupling by Procter; III) Sonogashira coupling according to Zhang.

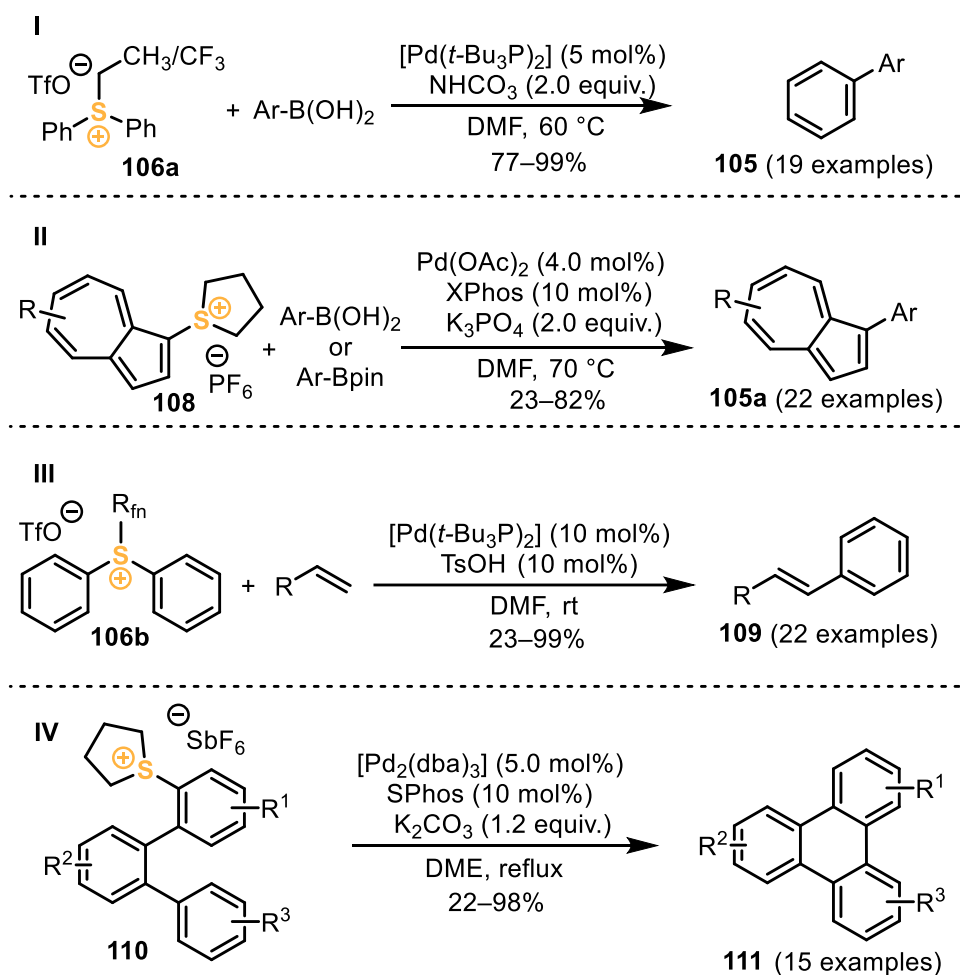
The research group of Zhang also developed a Suzuki coupling protocol, again with an arylboronic acid and an arylsulfonium salt (Scheme 40, I). Moreover, they investigated the effect of different substituents on the diarylsulfonium salt **106**. Amongst all examples, the sulfonium salts which contain either an ethyl- or a trifluoroethyl-group performed best under the

otherwise equal conditions and therefore were used to synthesize 19 products in good yield.¹⁷⁰

Lewis demonstrated the functionalization of azulene derivatives by sulfenylation, whereas sulfonium salts **108** were obtained as hexafluorophosphates. The coupling with **108** under Suzuki coupling conditions yielded a variety of azulene compounds **105a** (Scheme 40, II).¹⁷¹

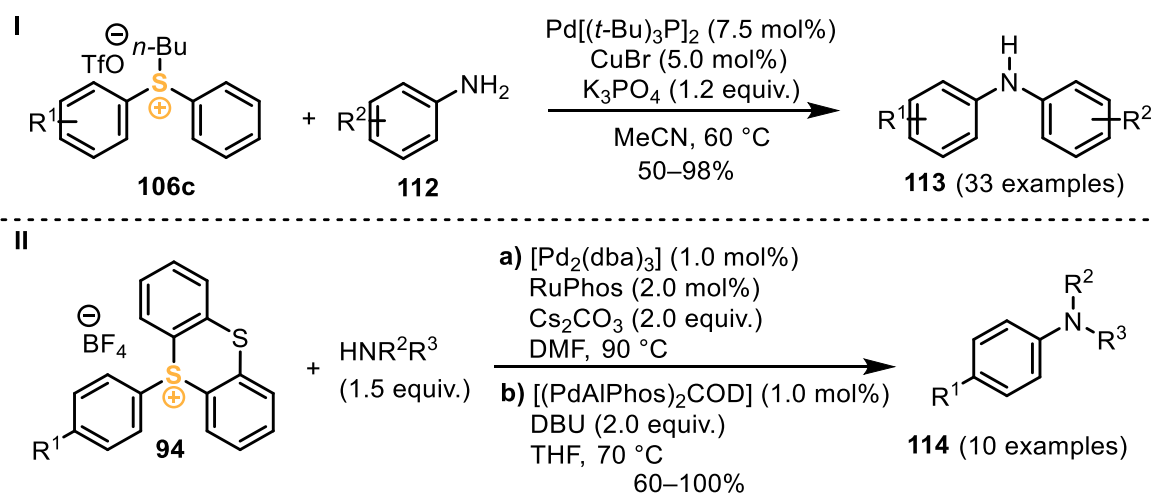
Heck-Reactions were also performed by Zhang *et al.* In this study a diarylsulfonium salt with a perfluorinated alkyl substituent was chosen to couple styrene derivatives under mild conditions (Scheme 40, III).¹⁷²

Yorimitsu used a coupling strategy *via* palladium-catalyzed intramolecular C–H activation starting from tetrahydrothiophenium salts **110**. After the oxidative addition to the C–S bond, an intramolecular aryl-aryl coupling occurred forming a six-membered ring system. This route was used to synthesize 15 compounds of type **111** with different substitution patterns (Scheme 40, IV).¹⁷³



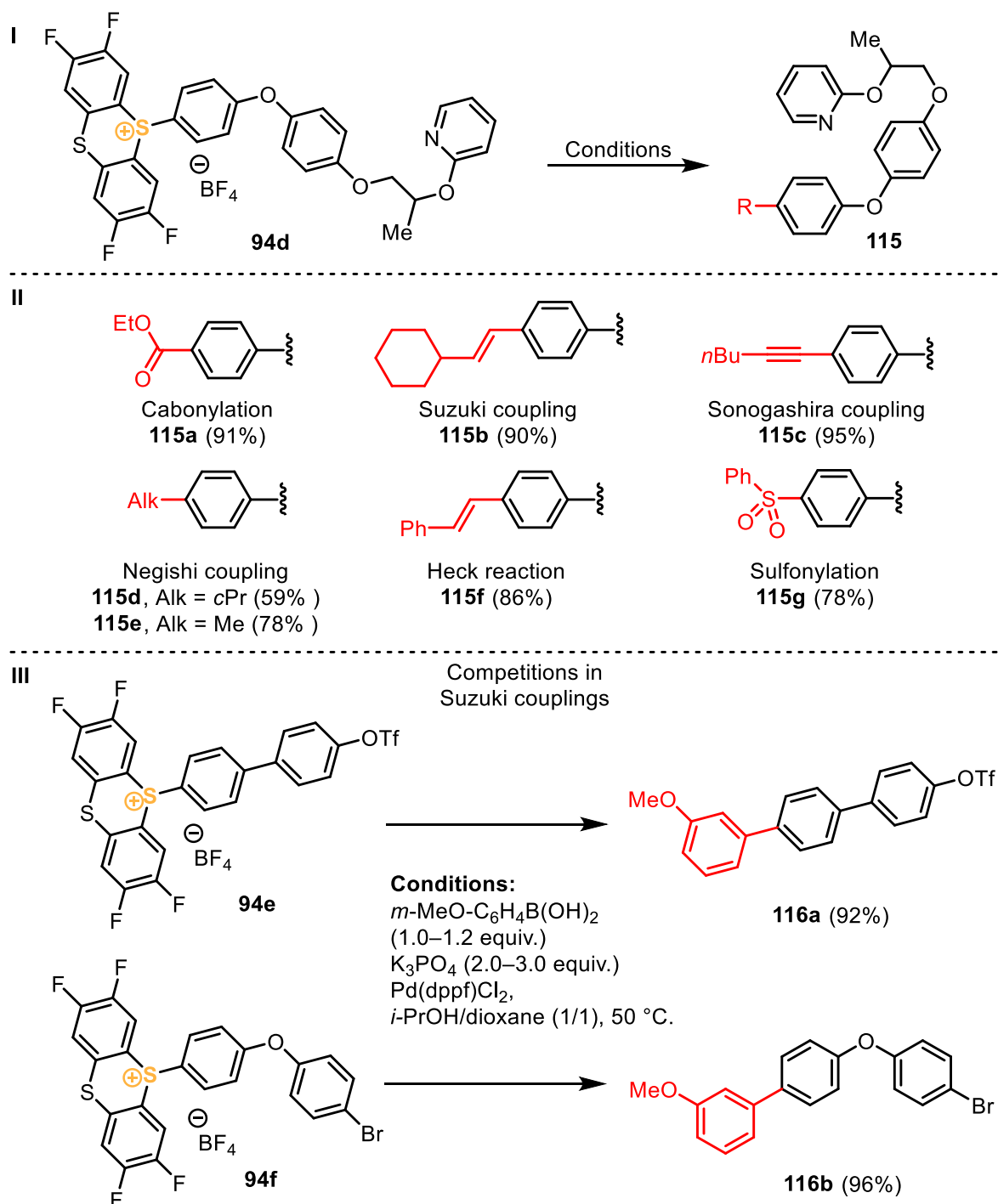
Scheme 40: I) Suzuki coupling reported by Zhang; II) Arylation of azulene by Suzuki coupling, as reported by Lewis; III) Heck reaction according to Zhang; IV) Pd-catalyzed intramolecular C–H arylation reported by Osuka.

Starting from diarylsulfonium salt **106c**, Zhang realized the Ullmann-type C–N coupling reactions (Scheme 41, I). With cooperative palladium/copper catalyst, 33 compounds of type **113** were prepared in moderate to good yields.¹⁶



Scheme 41: I) C-N Ullmann-type coupling reported by Zhang; II) Buchwald-Hartwig-type amination elaborated by Ritter.

Ritter demonstrated the use of thianthrene sulfonium salts in Buchwald-Hartwig-type couplings (Scheme 41, II).¹⁷⁴



Scheme 42: I) Generic scheme for the products of coupling reactions; II) Coupling reaction products; III) Competition reactions of the TFT-moiety vs. (pseudo)halides in Suzuki-type coupling reactions.

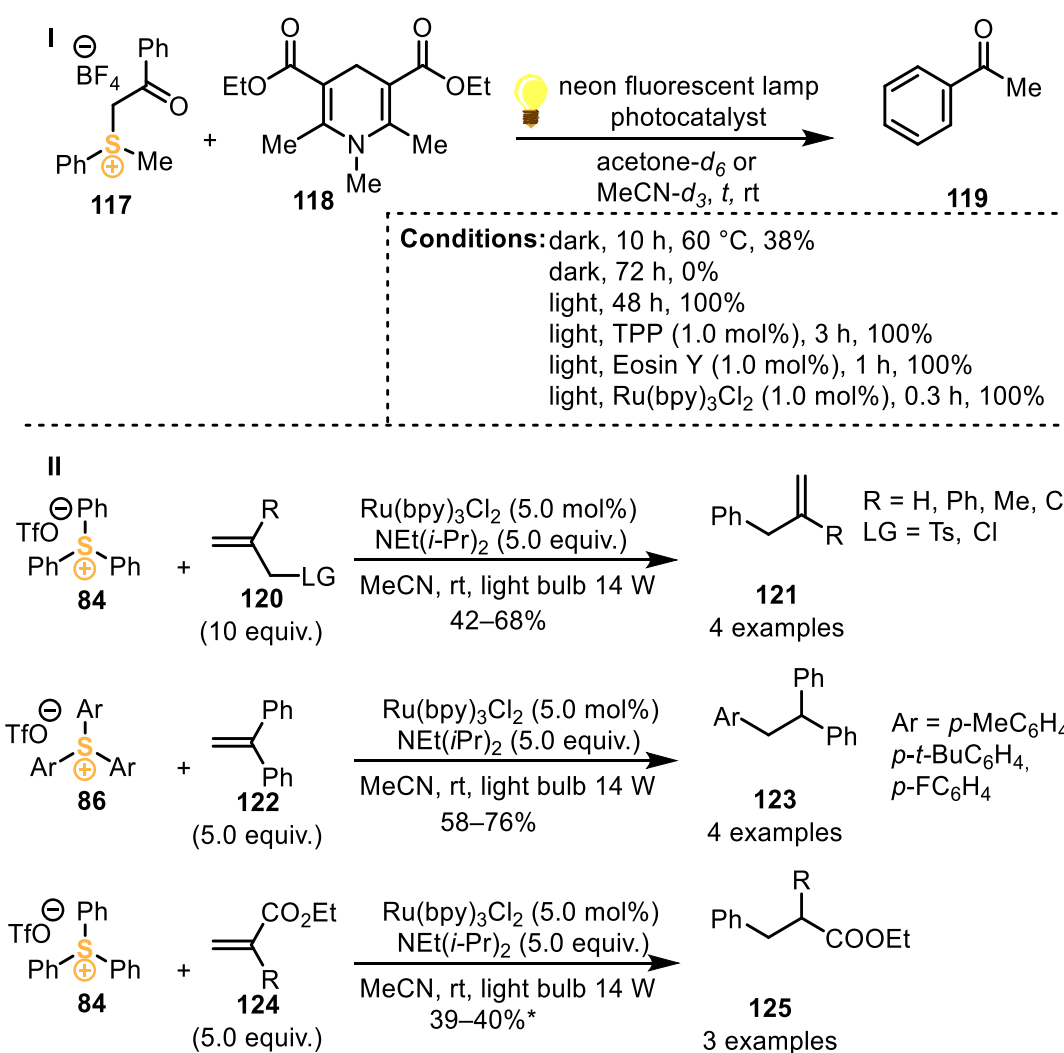
Ritter developed protocols for the synthesis of TFT-sulfonium salts **94** and for arylations with **94** (Scheme 42, I). These salts proved to be efficient in various metal-catalyzed transformations. Starting from sulfonium salt **94d**, a carbonylation (**115a**), Suzuki- (**115b**), Sonogashira- (**115c**), Negishi- (**115d** & **115e**), Heck-type (**115f**) and a sulfenylation (**115g**) reactions could be performed (Scheme 42, II). Scheme 42, III shows the competition reaction

between the TFT-moiety, a triflate and a bromide in the same molecule in a Suzuki cross-coupling. Interestingly, in both cases over 90% of **116a** and **116b** could be isolated in this reaction, hinting towards a huge difference in terms of reactivity for the corresponding (pseudo)halide compared to the TFT-unit. The higher reactivity of the TFT-unit offers orthogonality in chemoselective palladium-catalyzed coupling reactions.¹⁵⁹

Structurally similar iodine^{III} reagents are not suitable for transition metal-catalyzed coupling reactions since the leaving group would be aryl iodide, which itself undergoes oxidative additions under the conditions applied. In contrast, the advantage of sulfonium salts over iodine^{III} reagents is the property of sulfides as side-products to be inert in the presence of transition metals like palladium.²

1.4.3.3. Photochemical Transformations

In 1978, Kellogg and coworkers investigated the reduction of sulfonium salts **117** (Scheme 43, I) promoted by light.^{175,176} Hantzsch ester **118** was used as a hydrogen donor, while the reactants were exposed to the light of a neon fluorescent lamp. If the reaction mixture was solely stirred under the absence of light, acetophenone **119** was obtained in 0 and 38% yield at ambient temperature/72 h or at 60 °C/10 h, respectively. Exposing the reaction mixture to the light drastically increased the yield and shortened the reaction times. Thus, complete conversion of the reactants could be achieved within 20 min by utilizing [Ru(bpy)₃]Cl₂ as a photocatalyst. It was suggested that a single electron transfer, which causes the reduction of the C–S bond, took place. This example represents the very early work on modern photoredox catalysis.

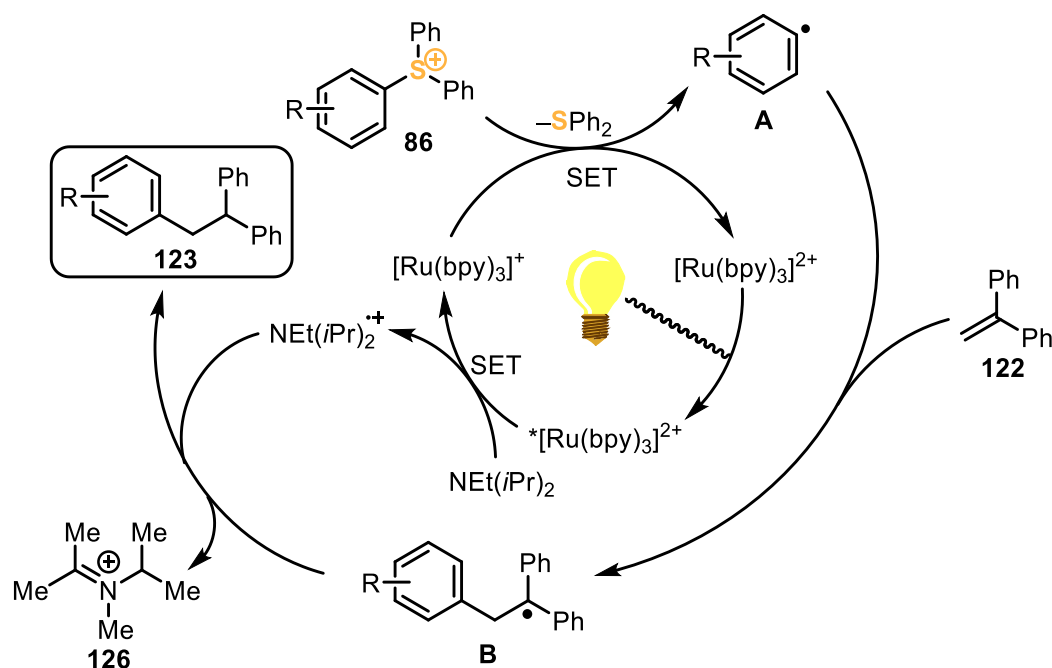


Scheme 43: I) Pioneering work on photoredox catalysis published by Kellogg *et al.*; TPP = *meso*-tetraphenylporphine; II) Photoredox catalysis with aryl sulfonium salts and ethylene derivatives as radical traps reported by Fensterbank, Goddard & Ollivier. *Obtained in 53–60% as a mixture with the 2-phenylacrylate derivative.

Ollivier *et al.* presented related work which involved photocatalytic hydroarylation with sulfonium salts induced with the visible light.¹⁴⁶ The resulting aryl radicals are trapped by ethylene derivatives **120**, 1,1-diphenylethylene **122** or ethylacrylates **124**, which are used in excess, and yielded a scope of **121**, **123** and **125**, respectively (Scheme 43, II).

In this study the effect of the counteranion of the sulfonium salts on the yield was investigated. Triflates, tetrafluoroborates and hexafluorophosphates gave comparable reaction outcomes, whereas transformations with bromides resulted in lower yield. On the contrary, the differences in the electronic densities of aryl substituents on the sulfonium salt or of the substrate itself have only little effect on the product yield.

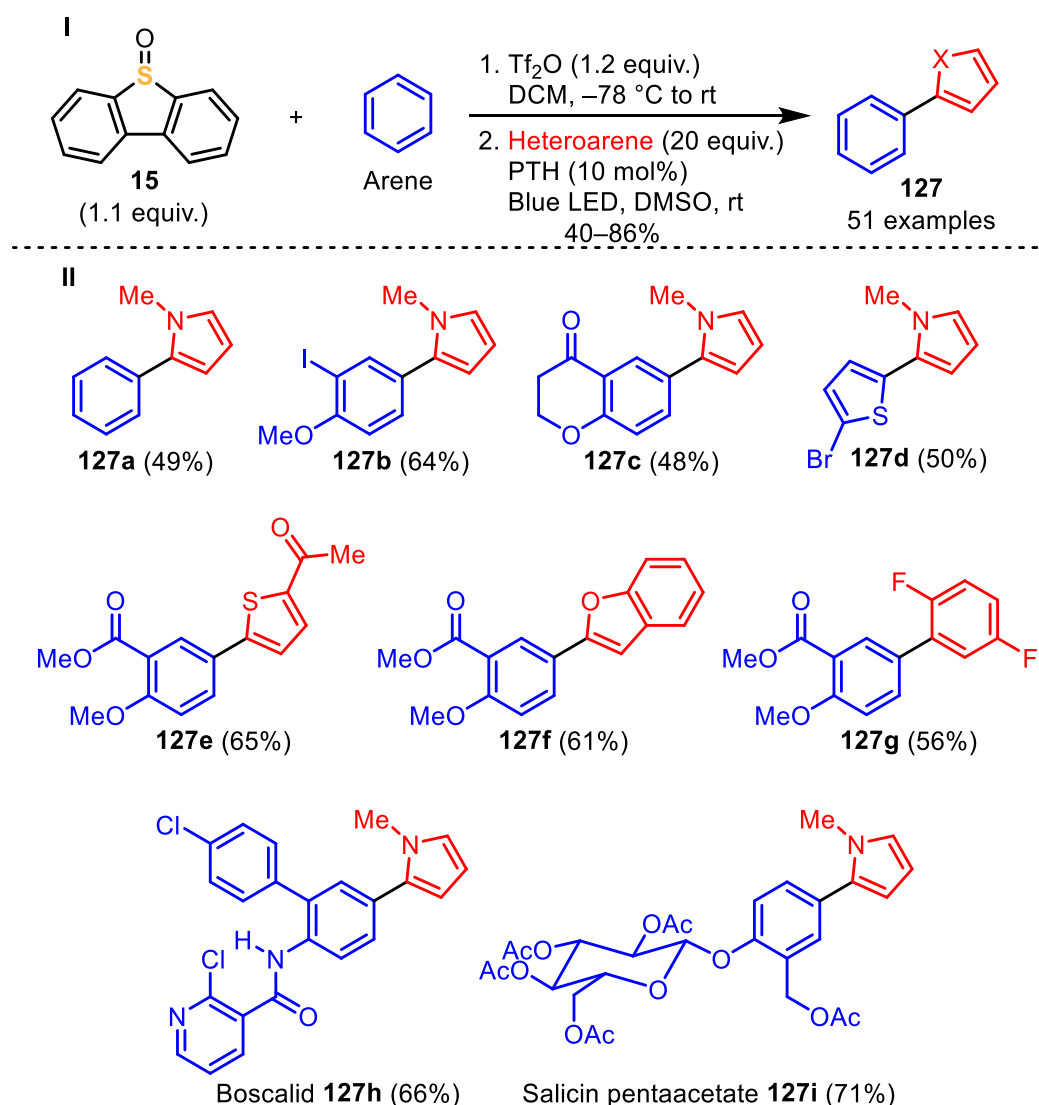
The authors proposed a mechanism of this transformation which is depicted in Scheme 44.



Scheme 44: Proposed mechanism for the photocatalytic transformation of **86** into **123**.

A single electron transfer to the triarylsulfonium salt **86** releases diphenyl sulfide and arylradical **A**, while $[Ru]^I$ is oxidized to $[Ru]^{II}$. In this example 1,1-diphenylethylene **122** acts as the radical acceptor; after radical addition of **A** to **122** and formation of the C–C bond, the stabilized radical intermediate **B** is formed. Irradiation of $[Ru]^{II}$ with light results in the excited $[Ru]^{II}$ -state, which oxidizes diisopropyl amine in the cocatalytic cycle. Finally, **B** formally abstracts a hydrogen atom from the radical cation of the Hünig's base and delivers the desired product **123**.

Just recently, Procter *et al.* published a metal-free C–H/C–H coupling strategy of non-functionalized arenes which is again enabled by an interrupted Pummerer sequence and followed up by photoredox catalysis (Scheme 45, I).¹⁵ The sulfonium salts are generated *in situ* and subsequently subjected to photocatalytic conditions. In this case, the amine is not required as a co-reducing agent. Scheme 45, II presents an extract of the vast and versatile scope of this transformation.

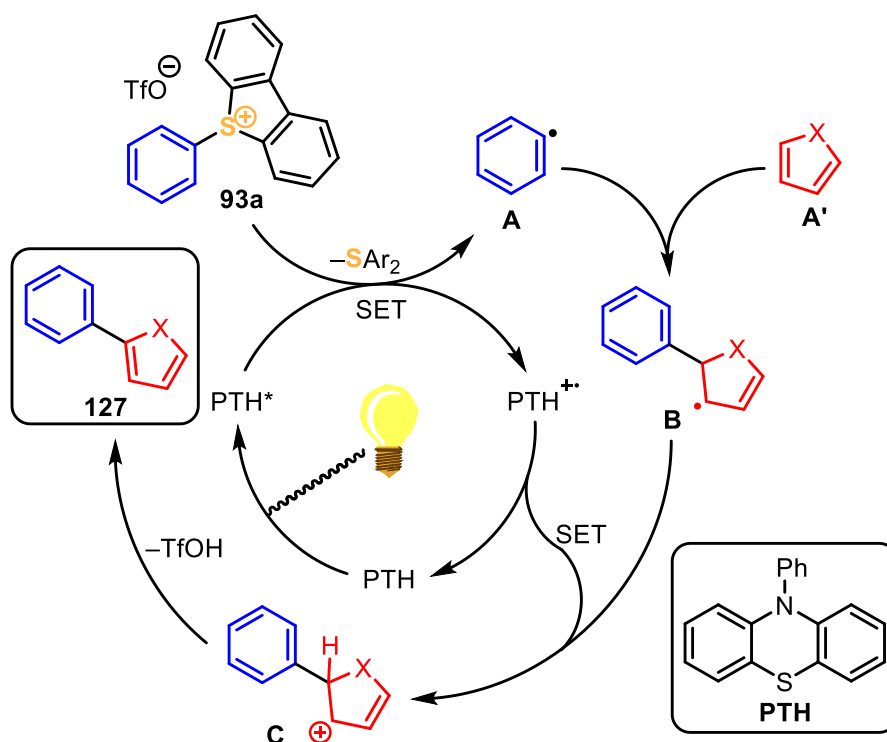


Scheme 45: Selected examples of the C–H/C–H coupling of arenes via the interrupted Pummerer protocol followed by photoredox catalysis.

With this one-pot protocol, a variety of arenes with sufficiently high electron density was functionalized. Among them iodides, ketones, heterocycles like thiophenes as sulfonium salts etc. were tolerated (**127a-127d**). Moreover, changing the coupling partner to thiophenes, benzofuran or 1,4-difluorobenzene yielded the corresponding products at least in good yields, considering the potential regioselectivity issues (**127e-127f**). Procter also provided the late-

stage C–H-functionalization of the bioactive molecules boscalid **127h** and salicin pentaacetate **127i** in 66 and 71% yield, respectively.

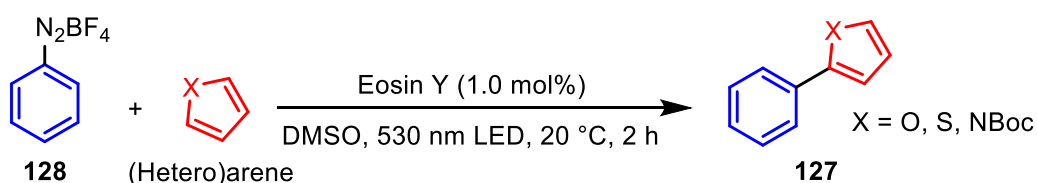
The proposed mechanism of this transformation is shown in Scheme 46.



Scheme 46: Mechanism of the photochemical transformation proposed by Procter; PTH: 10-phenylphenothiazine.

5-(Phenyl)dibenzothiophenium triflate (**93a**) is reduced by the excited state of the photocatalyst; according to the mechanism discussed above in Scheme 44, dibenzothiophene is released under the formation of phenyl radical **A**. The heterocyclic arene **A'** forms a C–C bond with the radical **A** which results in formation of intermediate **B**. A SET between the cationic PTH species and **B** occurs, and cationic intermediate **C** is obtained. Rearomatization of **C** affords the final product **127**.

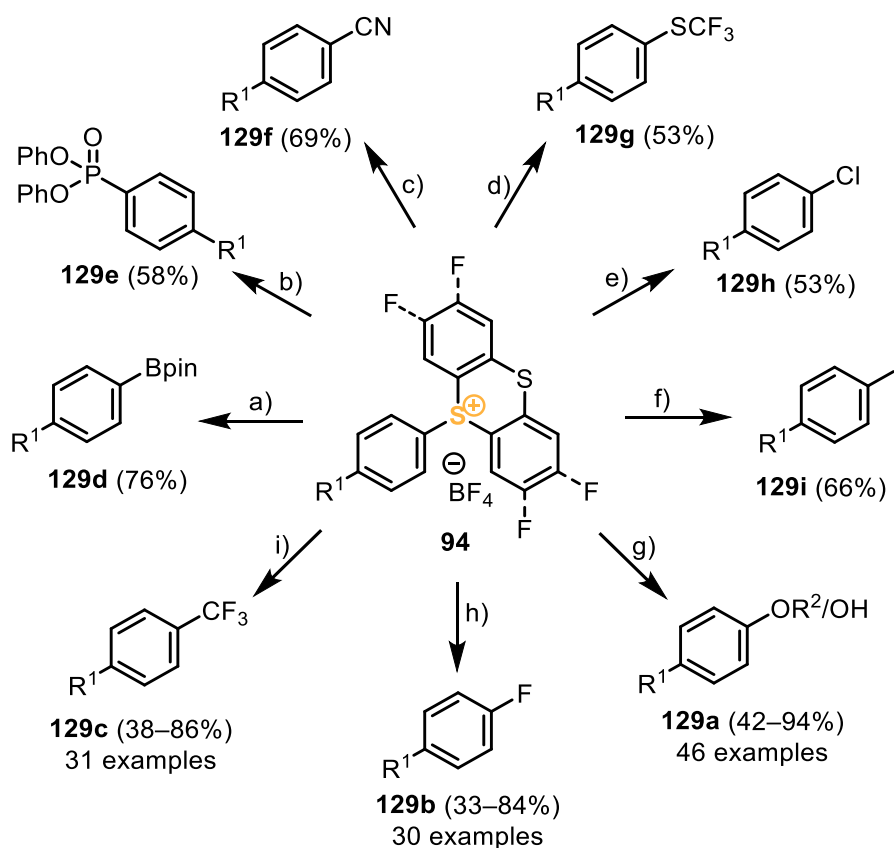
König has shown that the reactivities of diazonium salts **128** in the presence of a photocatalyst and of a radical acceptor in the presence of visible light are very similar to those of sulfonium salts (Scheme 47).¹⁷⁷



Scheme 47: Method for the photoinduced biaryl coupling presented by König.

However, the main disadvantage of this method is the need to obtain diazonium salts, which requires the initial presence of an amino group. The latter can be converted to diazonium salt by the Knoevenagel diazotization method.¹⁷⁸

With the help of photochemical approach Ritter demonstrated such versatile transformations of thianthrenium salts **94** like oxygenation¹⁷⁹, trifluoromethylation¹⁵⁸ and fluorination¹⁸⁰ (**129a-129c**) (Scheme 48).



Scheme 48: Photochemical transformations applying the thianthrenium salts **94**, as elaborated by Ritter. Conditions: a) B₂pin₂ (2.5 equiv.), pyridine (5.0 equiv.), LED; b) P(OPh)₃ (5.0 equiv.), pyridine (4.9 equiv.), NaI (20 mol%), LED; c) NBu₄CN (2.5 equiv.), Cu(MeCN)₄BF₄ (1.2 equiv.), LED; d) NMe₄SCF₃ (1.1 equiv.), Cu(MeCN)₄BF₄ (1.0 equiv.), LED; e) CuCl (2.0 equiv.), NBu₄Cl (2.5 equiv.), LED; f) LiI (10 equiv.), Cu(MeCN)₄BF₄ (1.0 equiv.), MeCN/DMSO (3/2), LED; g) ROH (2.0 equiv.), CuTC (1.0 equiv.), Na₂CO₃ (1.0 equiv.), 3 Å MS, MeCN, then **94** (1.0 equiv.), [Ir[dF(CF₃)ppy]₂(dtbpy)PF₆] (1 mol%), Blue LED or **94** (1.0 equiv.), [Ir[dF(CF₃)ppy]₂(dtbpy)PF₆] (1 mol%), dimethylglyoxime (10 mol%), Cu₂O (0.8 equiv.), MeCN/H₂O (10/3), Blue LED; h) [Ir[dF(CF₃)ppy]₂(dtbpy)PF₆] (1 mol%), Cu(MeCN)₄BF₄ (1.5 equiv.), CsF (1.2 equiv.), Acetone, Blue LED; i) CuSCN (1.5 equiv.), CsF (2.0 equiv.), TMSCF₃ (1.5 equiv.), DMF, then **94** (0.2–0.3 mmol), Ru(bipy)₃(PF₆)₂ (2.0 mol%), MeCN, blue LED.

Moreover, (pseudo)halogenation (**129g-129i**), cyanation phosphorylation and borylations¹⁸¹ of **94** were possible as well (**129d-129f**).¹⁵⁹

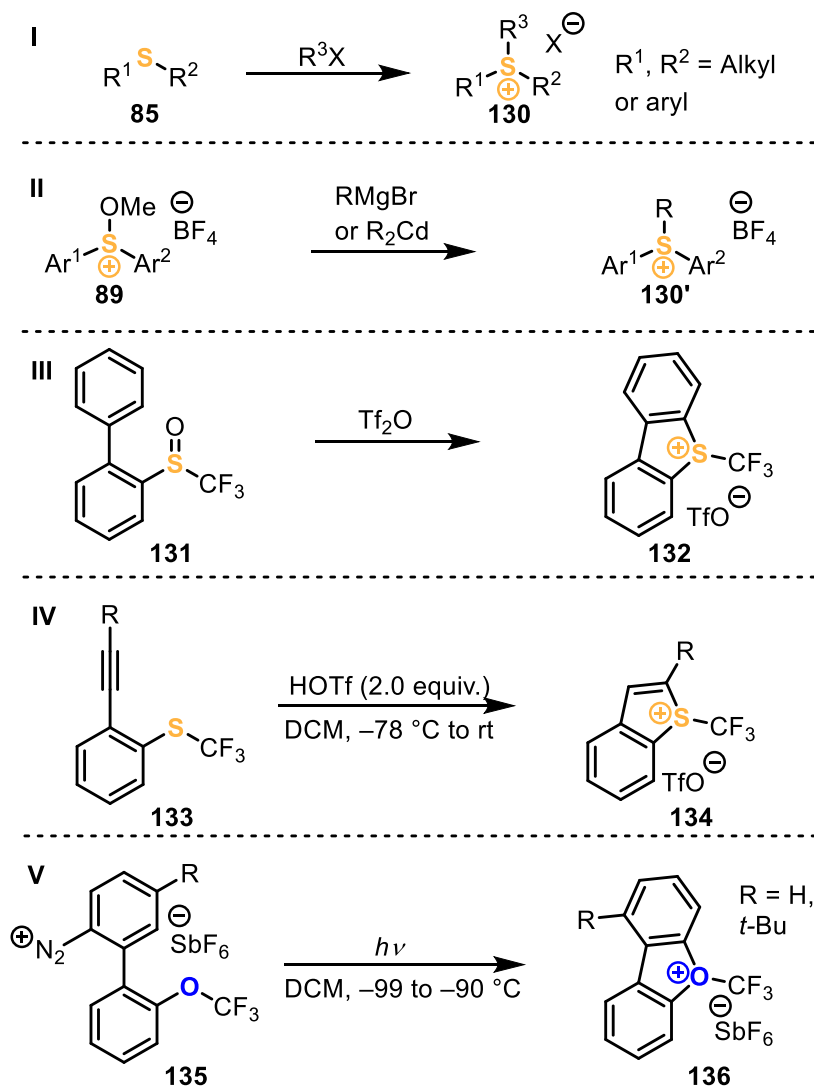
Lastly, the reaction was also performed in the presence of aryl iodides. The thianthrenium moiety proved to be superior in terms of reactivity in this particular competition.

1.5. C(sp³)-Substituted Sulfonium Salts

Since C(sp³)-substituted sulfonium salts play only a minor role in this thesis, the synthetic routes towards this class of compounds and its applications will be only briefly discussed.

1.5.1. Synthesis of S-(Alkyl) Sulfonium Salts

The most general chemical transformations towards S-(alkyl)sulfonium salts are shown in Scheme 49.

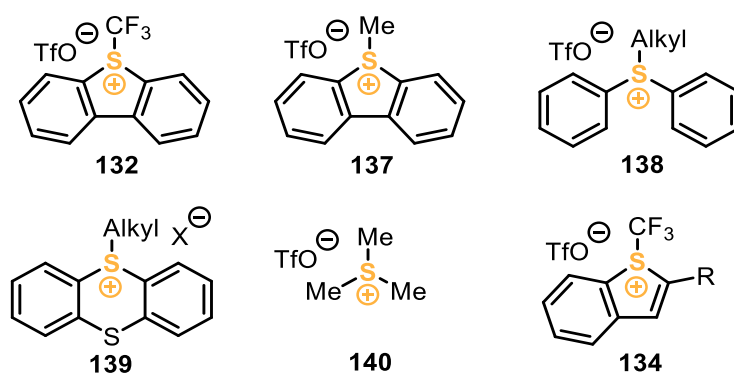


Scheme 49: Formation of S-(alkyl)sulfonium salts I) By S_N-substitution; II) Using Grignard or organocadmium reagents; III) *Via* intramolecular sulfenylation; IV) *Via* acid-induced cyclization; V) Oxonium analog of the Umemoto reagent derived from diazonium salt **135**.

A simplest method for the preparation of S-(alkyl)sulfonium salts **130** is the direct alkylation of the corresponding sulfide **85** with an alkyl iodide or triflate (Scheme 49, I).^{182–184} AgBF₄ or NaClO₄ are commonly used for the subsequent counterion exchange, yielding the salts **130**

either as tetrafluoroborates or perchlorates. Alternatively, alkoxy-substituted sulfonium salt **89** can be reacted with either Grignard or organocadmium reagents to generate **130'** (Scheme 49, II).¹⁸⁵ Treatment of *o*-substituted biaryl sulfoxide **131** with triflic anhydride causes an intramolecular sulfenylation reaction towards **132** (Scheme 49, III).^{186–189} This method is well-known for the synthesis of Umemoto's reagent **132**, which cannot be obtained by straightforward alkylation of the sulfide. Additionally, the acid-induced cyclization strategy of (*o*-ethynylaryl)-substituted sulfides **133** was demonstrated as well (Scheme 49, IV).¹⁹⁰ Lastly, **136**, the oxygen analog of Umemoto's reagent, can also be synthesized, although its handling is quite inconvenient since these compounds are only stable at low temperatures below -90 °C (Scheme 49, V).⁵

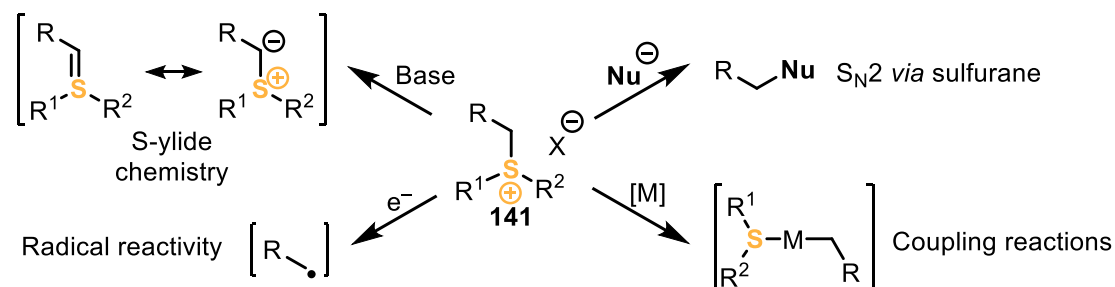
A small collection of *S*-(alkyl)sulfonium salts shown in Scheme 50 was synthesized by Tsuchida¹⁹¹, Shine¹⁹² and Shibata.¹⁹⁰



Scheme 50: Six examples of *S*-(alkyl)sulfonium salts.

1.5.2. Reactivity of S-(Alkyl) Sulfonium Salts

As shown in Scheme 51, S-(alkyl)sulfonium salts can be used in four reactivity modes.



Scheme 51: General reactivity of S-(alkyl)sulfonium salts **141**.

The salts **141** can be converted into an ylide by using a base. The main properties of ylides were already discussed in Chapter 1.3.^{6–8} Ylides are well-established reagents used in organo-, transition metal-, Lewis-acid- and photocatalysis. In general, these compounds are easily accessible, bench-stable and with the mentioned above Johnson-Corey-Chaykovsky reaction even became textbook chemistry.^{193–195}

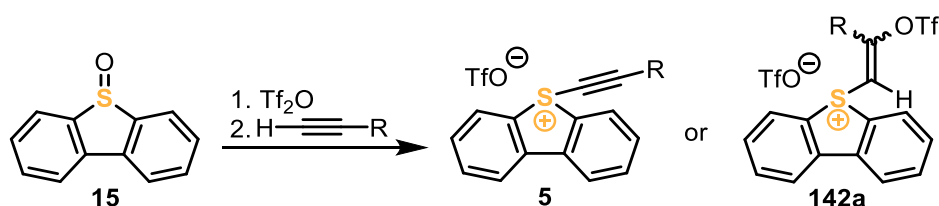
Compounds **141** can also be used for the alkylation of nucleophiles, as shown in the work of Shine¹⁹² and Kamigata¹⁹⁶. Phenols, amines, enolates or thiolates can be used as nucleophiles, whereas the reaction mechanism is dictated by the nucleophile's properties. For hard nucleophiles the reaction pathway suggests the participation of a sulfurane intermediate, which undergoes ligand coupling to furnish the final product (see also a comparable mechanism in Chapter 1.3.3.). For soft nucleophiles a simple S_N2 reaction is proposed.

Yorimitsu used S-(alkyl)sulfonium salts as a potent alkyl radical sources, which can generate radicals under mild photocatalytic conditions.¹² An example which includes the C(sp³)–C(sp³) bond formation employing an iridium-nickel dual photochemical catalytic system and involving a single electron transfer was presented by Novák *et al.*¹⁹⁷

Lastly, the transition metal-catalyzed alkylation of arenes has been explored. For this purpose, palladium catalysis enhanced by the assistance of a copper catalyst proved itself as a powerful tool for the *ortho*-directed trifluoromethylation¹⁹⁸ and methylation.¹⁹⁹ The reaction pathway remains still unclear; both Pd⁰/Pd^{II} and Pd^{II}/Pd^{IV} catalytic cycles have been proposed.

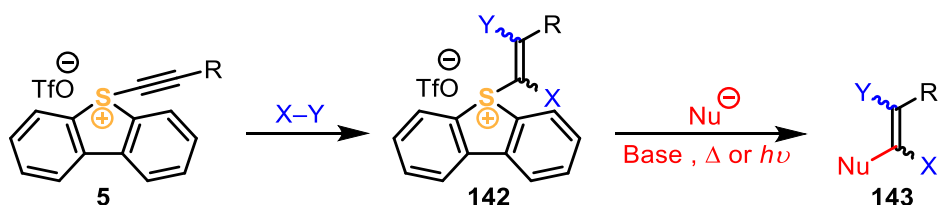
2. Project Aim

Alcarazo *et al.* reported on the synthesis of *S*-(alkynyl)sulfonium salts by the reaction of TMS-capped acetylenes and the bistriflate-activated dibenzothiophene-5-oxide **15**.^{11,23} The direct synthetic approach from terminal alkynes to *S*-(alkynyl)sulfonium salts has never been reported. According to Novák, aryl(trifloxyalkenyl)iodonium triflates were selectively obtained starting from (diacetoxyiodo)benzene and a terminal alkyne.²⁰⁰ With specially focused experiments the aforementioned possible pathway towards *S*-(alkynyl)sulfonium salts shall be unraveled and the reaction products identified (Scheme 52).



Scheme 52: Generic reaction scheme towards *S*-(alkynyl)dibenzothiophenium triflates **5**.

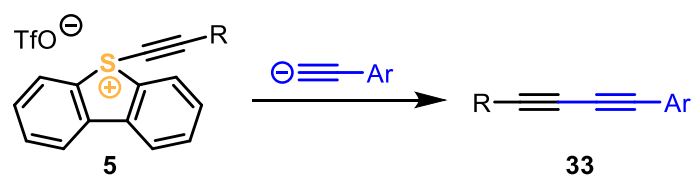
Addition reactions to their parenting alkyne reagents based either on selenium^{25,117,122} or iodine^{127,130} have been reported. Stang also studied the addition of dienes to various iodonium alkynyl triflates *via* Diels-Alder reactions.¹³¹ Therefore, it is of high interest if these addition reactions can be performed on *S*-(alkynyl)dibenzothiophenium triflates **5** (Scheme 53).



Scheme 53: Addition reactions of *S*-(alkynyl)dibenzothiophenium triflates **5** and subsequent Michael-type transformations.

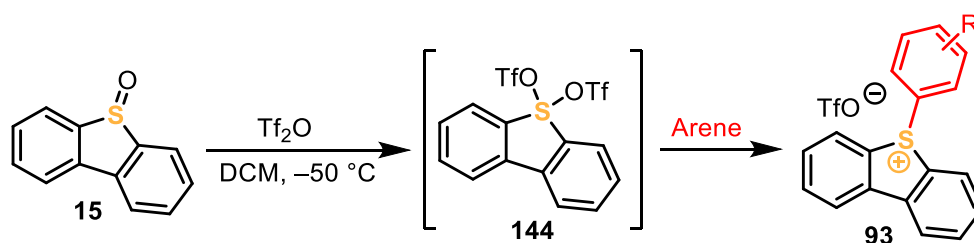
In addition, the ability of structurally related (alkenyl)selenonium and (alkenyl)iodonium salts to undergo Michael-type reactions was demonstrated before.^{28,118–121} To expand the synthetic potential of **5** and to fill the gap in our knowledge, it is also necessary to test the capacity of *S*-(alkenyl)dibenzothiophenium triflates **142** to perform Michael reactions as well (Scheme 53). Following the work of Procter, it will be investigated if these salts undergo C(sp²)-C_{Ar}yl coupling reactions under photocatalytic conditions.¹⁵

Waser found the alkynyliodonium salts to be feasible reaction partners in combination with acetylides for a transition metal-free Cadiot-Chodkiewicz coupling.⁶⁸ Since *S*-(alkynyl)dibenzothiophenium triflates **5** showed similar reactivity to their iodine-based analogues, the reaction with acetylides towards diynes **33** will be investigated (Scheme 54).



Scheme 54: Simplified reaction of an acetylide with alkylation reagent **5**.

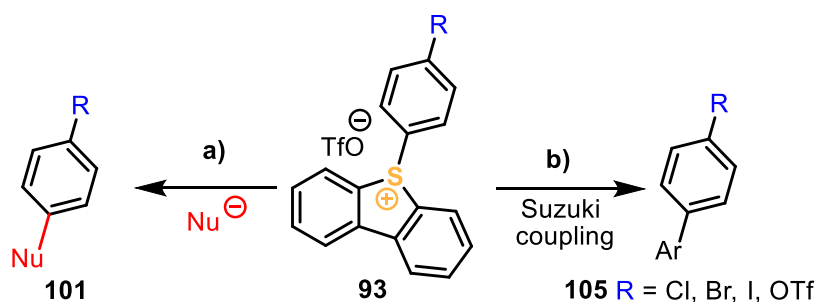
Previously, Procter¹⁷¹ and Ritter^{157,159} independently established protocols for the preparation of *S*-(aryl)sulfonium salts from their parent sulfoxides by activation with either Tf₂O or TFAA. Combined with the recent findings of Alcarazo¹¹, the feasibility of this concept with dibenzothiophene oxide **15** will be tested focusing on the limitations caused by the electronic properties of the arene moieties (Scheme 55).



Scheme 55: Synthesis of *S*-(aryl)dibenzothiophenium triflates **93**.

Moreover, the generally accepted mechanism for the sulfenylation of arenes with TFT is associated with a radical process.¹⁵⁹ It will be investigated in detail whether this also applies to the reaction shown in Scheme 55.

The ability of *S*-(aryl)sulfonium salts to undergo *ipso*-substitutions have previously been reported.^{161a} However, the authors only had limited access to triarylsulfonium salts with two substituents being connected to each other. Therefore, the potential of *ipso*-substitutions with *S*-(aryl)dibenzothiophenium triflates **93** will be explored in this thesis (Scheme 56, a).



Scheme 56: a) *ipso*-Substitution of **93** with nucleophiles; b) Chemoselective Suzuki coupling with **93**.

Ritter showed that chemoselective cross-coupling reactions with TFT salts is possible and yielded desired products in high yields and without affecting concurring (pseudo)halides.¹⁵⁹

In this thesis the chemoselectivity in *S*-(aryl)dibenzothiophenium salts **93** will be investigated in Suzuki couplings. Moreover, it is of high interest to explore their limitations in terms of Pd catalyst loading and reaction temperatures (Scheme 56, **b**). These experiments will provide information about the relative reactivity of dibenzothiophenium salts in comparison to common (pseudo)halides in palladium catalysis.

3. Results and Discussion

3.1. Synthesis & Applications of (Z)-Vinyl-Dibenzothiophenium Triflates

3.1.1. Alternative Approach towards S-(Alkynyl)dibenzothiophenium Triflates

Up to date the synthesis of 5-(alkynyl)dibenzochalcogenium triflates is restricted to TMS-protected alkynes.^{11,23,25} To make the synthesis towards the corresponding salts more atom economic, terminal alkynes were envisaged as substitutes (Figure 7).

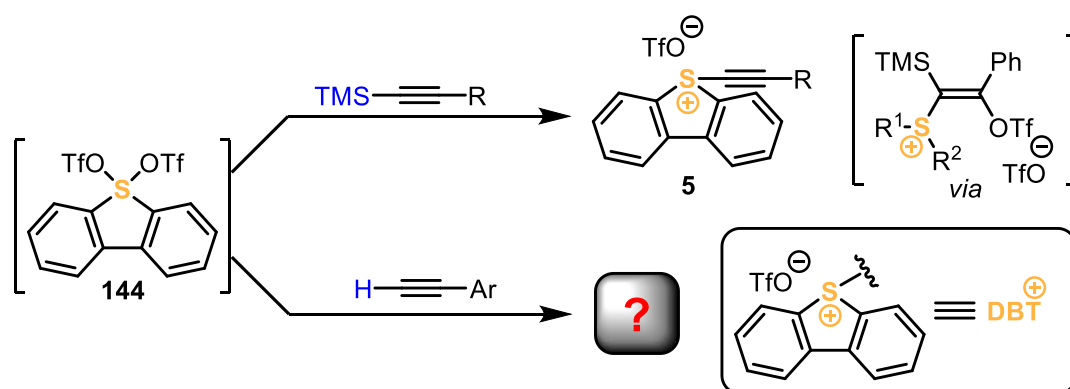
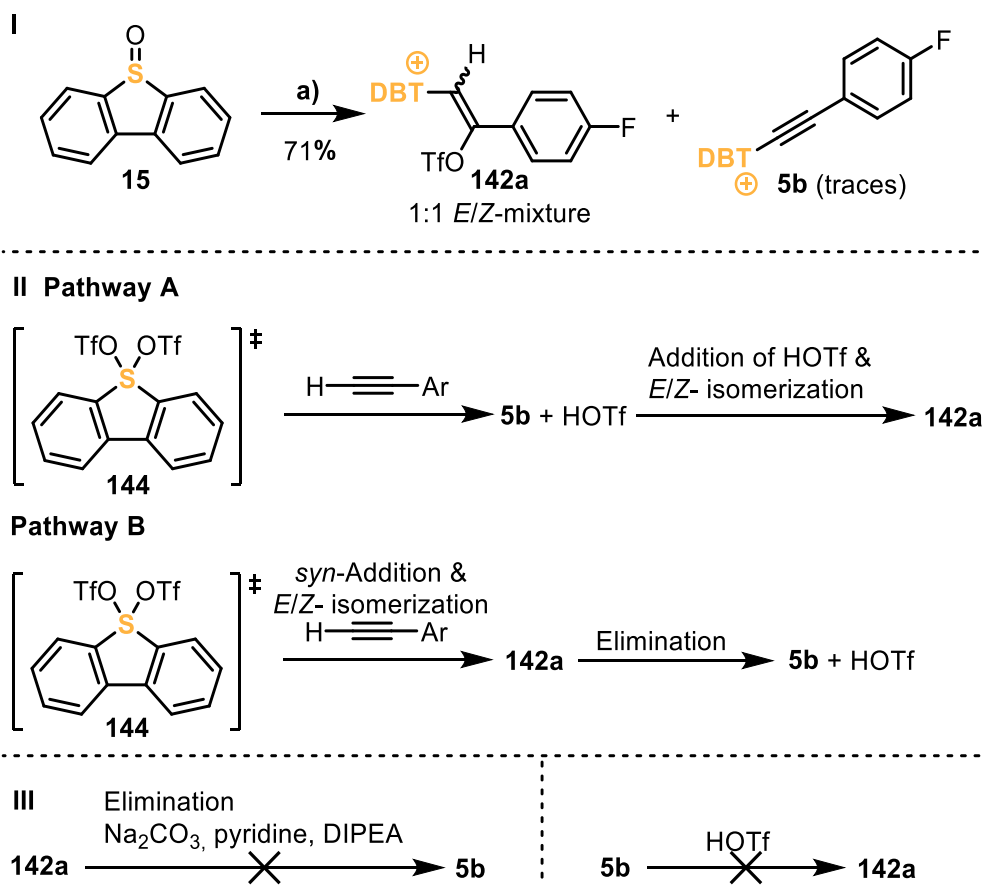


Figure 7: General synthetic method towards 5-(alkynyl)dibenzothiophenium triflates **5** with TMS-protected alkynes & terminal alkynes. Dibenzothiophenium triflate will be abbreviated with DBT⁺ in reaction schemes.

In mechanistic rationalizations reported in the literature, the *syn*-addition of **144** to the triple bond is proposed as an intermediate step.²² After the addition, TMSOTf is rapidly released since this intermediate is unstable, and the desired product **5** is formed. Substitution of TMS-protected alkynes with a terminal one would change the leaving group to triflic acid. It is unclear if the trimethylsilyl group plays a crucial role during the reaction to form the desired alkynyl sulfonium salts or not.

According to Alcarazo, the reaction of **15** with the TMS-capped 1-ethynyl-4-fluorobenzene delivered the *S*-(alkynyl)sulfonium salt in good yield.¹¹ It was envisioned that 1-ethynyl-4-fluorobenzene as a terminal alkyne would show similar reactivity. Especially this alkyne was chosen since tracking of the fluorine distribution with ¹⁹F NMR allows identification of fluorine-containing species. Surprisingly, the salt **142a** was formed as the main product in good yield of 71% and identified as a 1:1 mixture of *E/Z*-isomers (Scheme 57, I).

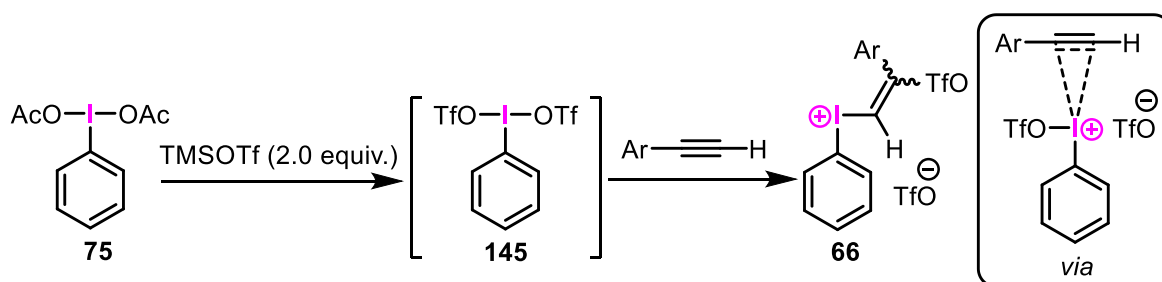


Scheme 57: Reagents and conditions: a) 1. HOTf (0.5 equiv.), Tf₂O (1.2 equiv.), then *p*-F-C₆H₄-acetylene (1.2 equiv.), DCM, -50 °C → rt, 16 h.

MS analysis and ¹⁹F NMR spectra confirmed the presence of **142a**, although **5b** was also found as traces. Therefore, it can be assumed, that either **5b** formed first and the released equivalent of HOTf added to the triple bond, or **142a** is indeed an intermediate formed by a *syn*-addition of bis-triflate adduct **144**, which later undergoes an elimination reaction towards **5b** (Scheme 57, II). Treatment of **142a** with different types of bases (Na₂CO₃, pyridine, and DIPEA) did not result in formation of **5b** (Scheme 57, III). Other bases or reaction conditions were not tested since too nucleophilic bases would decompose **5b**. The reaction from **5b** towards **142a** with stoichiometric amounts of triflic acid did not result in the desired addition reaction either (Scheme 57, III).

In case of using TMS-alkynes, the addition reaction did not happen since solely TMS-OTf appears to be inert towards addition reactions in this system. According to the literature reports, the addition of TMS-OTf to triple bonds under Lewis acid catalysis is possible, whereas formally HOTf acts as an addition partner to the triple bond. The triflic acid is generated *in situ* by hydrolysis of TMS-OTf with water.²⁰¹

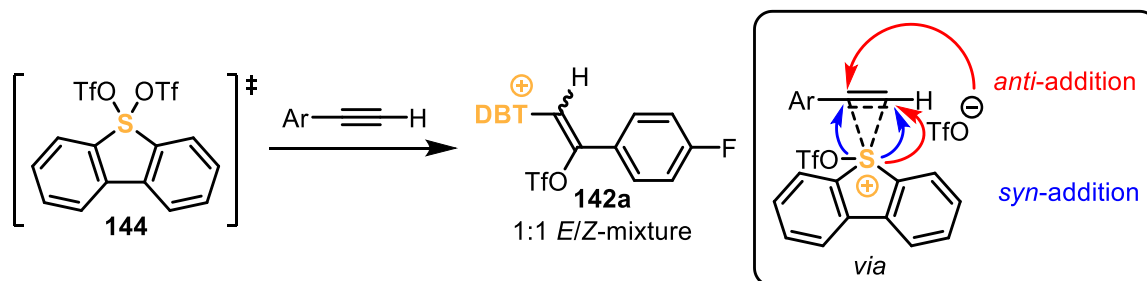
Novák investigated a closely related reaction involving the synthesis of aryl(trifloxyalkenyl)iodonium triflates from (diacetoxyiodo)benzene, a terminal alkyne and TMS-OTf as a triflate source (Scheme 58).²⁰⁰



Scheme 58: Reaction towards aryl(trifloxyalkenyl)iodonium triflates **66** presented by Novák.

The authors frequently observed formation of the mixture of *E*- and *Z*-isomers whereas the *E*-configuration predominated. Using DFT calculations they found a low energy gap between both isomers. The separation of both isomers by crystallization was not successful. However, the authors did not mention the formation of an alkynyl iodonium triflate as intermediate and rather suggested a transition state formed by the coordination of the iodine^{III}-center to the acetylenic bond.

Taking Novák's results into account, a similar transition state can be formulated which includes the coordination of the sulfur-center to the alkyne (Scheme 59).



Scheme 59: Alternative pathway towards **142a** rationalized on the base of Novák.²⁰⁰

A *syn*-addition (Scheme 59, blue arrows) or the *anti*-addition (Scheme 59, red arrow) from the depicted transition state can be formulated. Both reaction pathways lead to the formation of another product; the *syn*-addition to the *Z*-isomer and the nucleophilic attack to the *E*-isomer.

A 1:1 mixture of both isomers leads to the fact that both reaction pathways coexist and occur equally likely. The formation of **5b** occurs *via* an elimination reaction.

In conclusion, the rationalization shown in Scheme 59 is the most plausible explanation towards the formation of **142a**. The fact that small amounts of **5b** could be observed means, that it is possible to generate this reagent *via* this method in principle. However, the window for the appropriate reaction conditions towards **5b** are rather narrow and require precise determination and operation. Therefore, using TMS-capped alkynes to synthesize *S*-(alkynyl)dibenzothiophenium triflates is the most reliable method in this regard.

Two decades ago the formation of β -functionalized (*Z*)-vinylsulfones *via* the formation of β -sulfonylselenonium salts were described (see Chapter 1.3.4).^{25,117,121} The selenonium salts could be isolated and crystallized as either triflates or tetrafluoroborates, although the *Z*-isomer was formed exclusively. The general structural motif in **142** is similar to those obtained in the former described reaction (Figure 8).

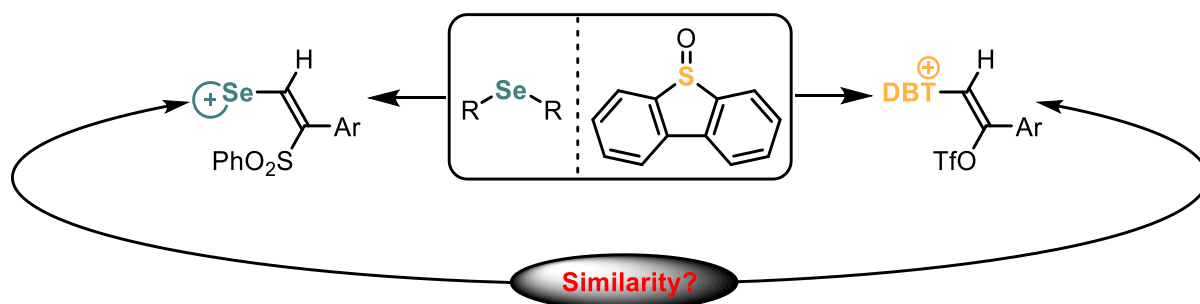
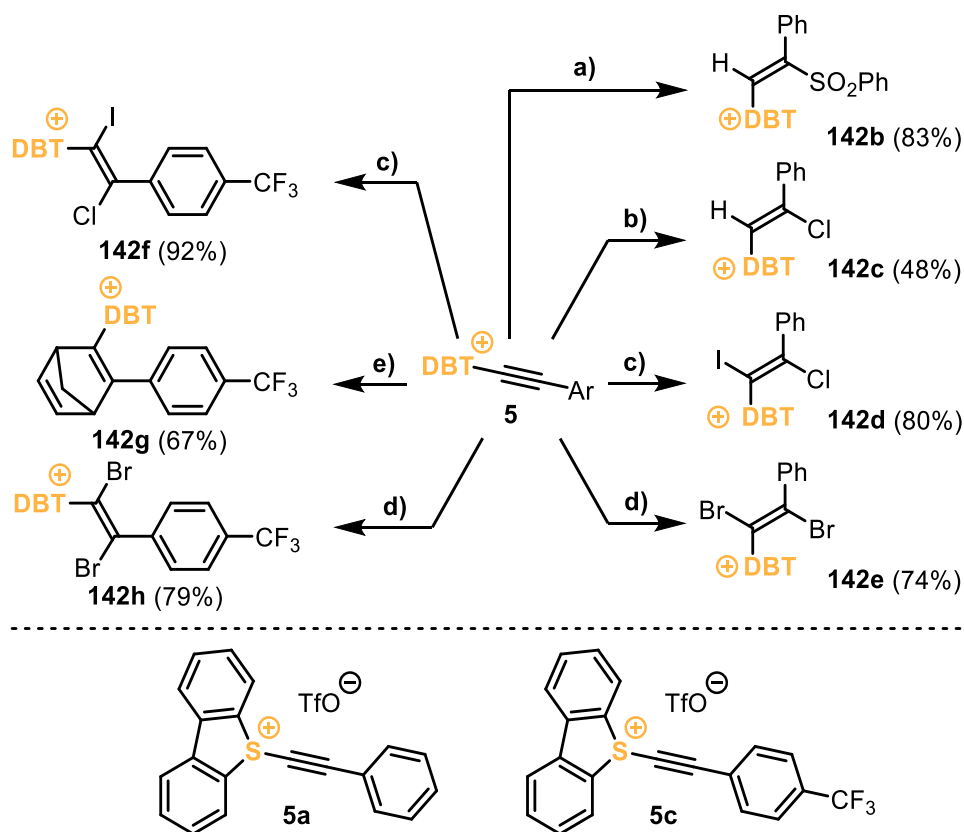


Figure 8: Similarity of previously published β -sulfonylselenonium salts and β -trifluorsulfonyldibenzothiophenium salts.

With this preliminary results and related literature reports in hand, other addition reactions towards *S*-(alkynyl)dibenzothiophenium triflates were performed.

3.1.2. Addition Reactions of *S*-(Alkynyl)dibenzothiophenium Triflates

The addition reaction of phenylsulfinic acid to the triple bond of **5** occurs *via* a simple *anti*-addition reaction mechanism.¹¹⁷ Therefore, other reagents known to undergo similar reactivity in the presence of alkynes like acids, halogens and dienes (Diels-Alder reactions) were tested. Similar addition reactions were done with iodine^{III}-based alkynylation reagents before.²⁰²



Scheme 60: Reactivity of the salts **5**. Reagents and conditions: a) PhSO₂H (1.0 equiv.) DCM/*t*-BuOH, rt, 12 h; b) 2 M HCl in Et₂O (1.5 equiv.), DCM/*t*-BuOH, rt, 12 h; c) I-Cl (1.2 equiv.), DCM, rt, 12 h; d) Br₂ (1.0 equiv.), DCM, rt, 12 h; e) Cyclopentadiene (5.0 equiv.), MeCN, 100 °C, MW, 2 h.

When phenylsulfonic acid was added to *S*-(alkynyl)sulfonium salt **5a** under protic conditions, compound **142b** was obtained in 83% yield in gram scale (Scheme 60). Interestingly, the reaction was not proceeding without *tert*-butanol as an external proton source in addition to PhSO₂H. The addition of hydrochloric acid was conducted successfully yielding 48% of **142c**. Halogens like iodo monochloride and bromine gave products **142d** & **142e** in 80 and 74% yield, respectively.

The same reaction conditions were applied to more electron poor **5c** and gave **142f** and **142h** in high yields. Additionally, **5c** could be converted easily to **142g** with excess of cyclopentadiene in 100 °C *via* typical Diels-Alder reaction conditions.

3.1.2.1. Structure of *S*-(Alkenyl)dibenzothiophenium Triflates **142b** & **142f**

Structure of the salt **142b** in the crystal is shown in Figure 9.

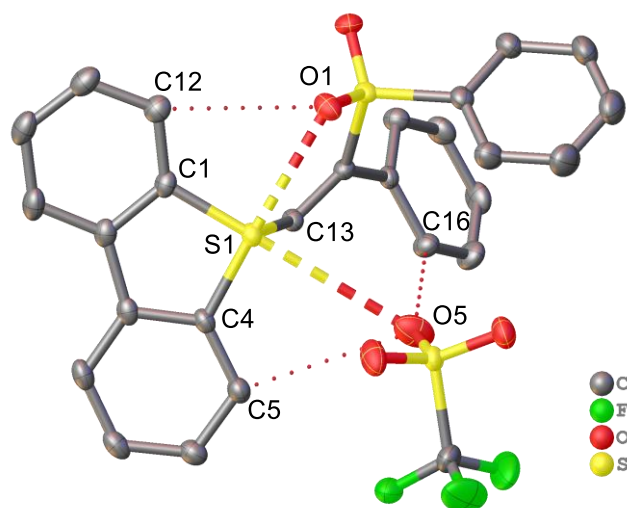


Figure 9: X-Ray structure of **142b** in the solid state. Anisotropic displacement shown at 50% probability level. Hydrogen atoms were omitted for clarity. Selected bond lengths [Å] and angles [°]: S1–C1 1.7923(12), S1–C4 1.7836(12), S1–C13 1.7947(12), S1–O1 2.6801(10), S1–O5 3.428(5), O1–C12 3.0674(16), O5–C5 3.325(5), O5–C16 3.231(4), C4–S1–O1 176.7, C1–S1–O5 172.0.

The structure of **142b** in the solid-state shows two chalcogen contacts to the sulfonium center, whereas the bond distance of the intermolecular contact O1–S1 is significantly shorter than O5–S1 (triflate contact) with S1–O1 of 2.6801(10) Å. The strongly interacting oxygen atom of the sulfonium moiety O1 lies in a colinear bond angle in C4–S1–O1 of 176.7, which is only slightly distorted. One intramolecular hydrogen bond between O1 and H12 could be observed. The rather weakly interacting triflate anion shows two additional hydrogen bonds to the *ortho*-aryl protons of C5 and C16. Surprisingly, no interactions from the hydrogen atom of C13 were present which differs much to the observations of the solid-state structures of other vinylsulfonium salts (see Chapter 1.3.2). Additionally, a sum of angles around S1 with 297.5° was measured and tends to stronger pyramidalization compared to other vinylsulfonium salts. No dimeric structural motif could be observed in the crystal structure of **142b**. The strong interactions of the sulfonium center indicate low electron density at the sulfur atom. Therefore, it is likely that this compound will undergo a vinylation reaction in the presence of nucleophiles *via* the mechanisms discussed in Chapter 1.3.4 (selenonium analog). The crystal structure of the salt **142f** is presented in Figure 10 and will be discussed representatively as typical for structures **142d**, **142e** and **142h** as well.

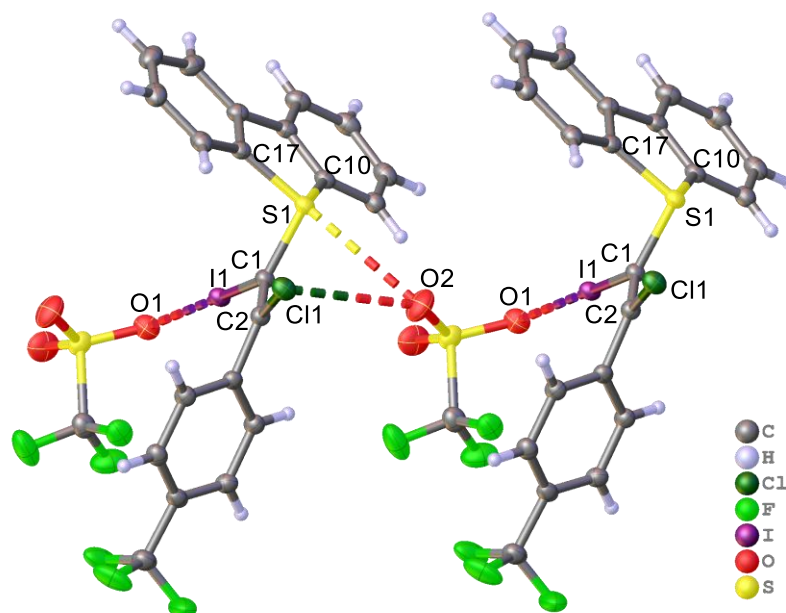
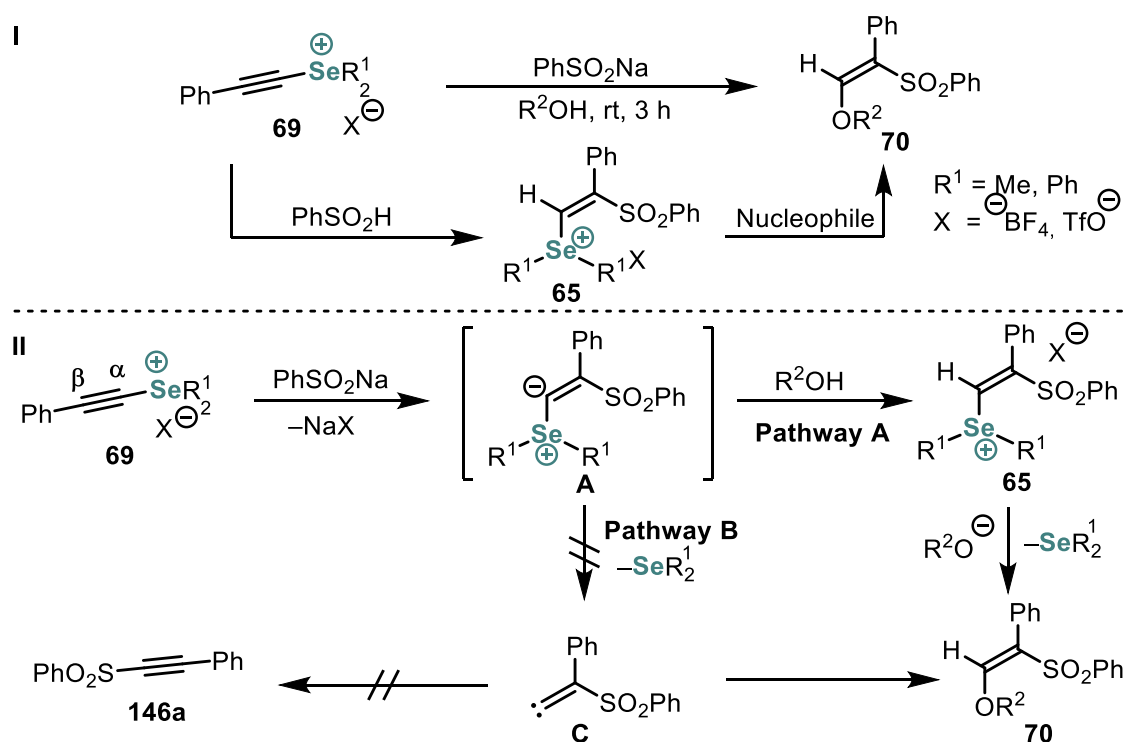


Figure 10: X-Ray structure of **142f** in the solid state. Anisotropic displacement shown at 50% probability level. Selected bond lengths [Å] and angles [°]: S1–C1 1.7866(10), S1–C10 1.7761(10), S1–C17 1.7831(11), S1–O2 3.3742(13), O2–Cl1 3.2082(12), I1–O1 2.8310(9), C17–S1–O2 159.6, C1–I1–O1 173.6, C2–Cl1–O2 79.6.

In the solid-state structure of **142f** displayed a strong tendency of halogen bonding. The triflate anion is the bridging link between the halogenides connected to the vinyl moiety (O1–I1 and O2–Cl1). The halogenide-triflate interactions are quite strong, and the distances are shorter than their corresponding sum of van-der-Waals-radii, especially O1–I1 (vdW-radius_{O-I} = 3.50 Å).²⁰³ This results in a weakened interaction of the triflate anion to the sulfonium moiety, as indicated by slightly longer bonding distance between S1 and O2 than the corresponding sum of van-der-Waals radii.

3.1.3. Michael-Type Reaction of Vinylsulfonium Salt **142b**

As mentioned in Chapter 1.3.4, Muraoka used the higher analogs of **142b** as Michael acceptors.¹²⁰ Starting from Se-alkynylated selenonium salts **69**, the authors found the facile conversion of **69** into (*Z*)- β -(alkoxyvinyl)sulfones **70** (Scheme 61, I). This transformation could be performed in one step by adding **69** to PhSO₂Na and stirring in an alcoholic solvent. It was also possible to realize an addition reaction of PhSO₂H onto **69** to generate **65**. Upon treatment of this salt with nucleophiles such as alkoxides, **70** could be prepared as well.

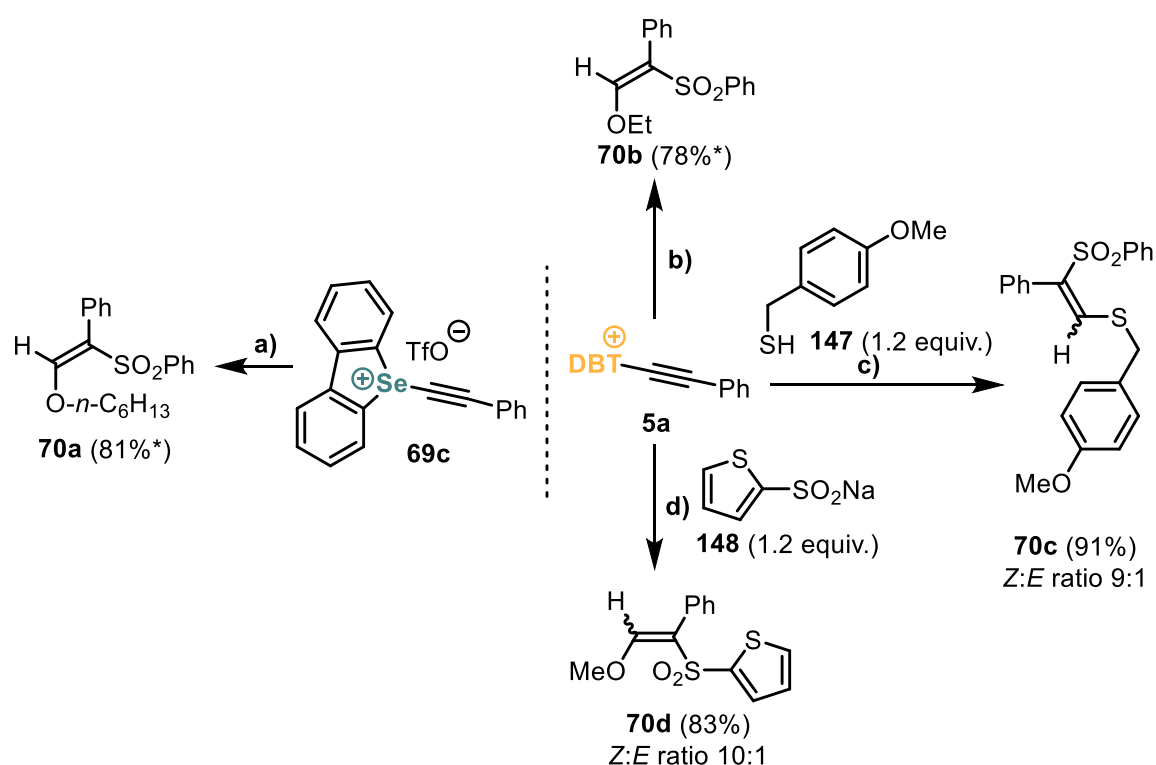


Scheme 61: I) General reaction conditions for the transformation to **70**; II) Pathway **A** and Pathway **B** leading to the formation of either product **146a** or **70**, respectively.¹²⁰

Mechanistically this transformation was described as an addition of the sulfinate salt (Scheme 61, II). Zwitterionic intermediate **A** is formed and could potentially undergo two reaction pathways. According to Pathway **A**, the alkenyl anion **A** can be protonated due to the presence of a protic solvent forming β -sulfonylselenium salt **65**. Successive attack of a nucleophile (alkoxide in this case) to the α -carbon forms the desired product **70**. Pathway **B** includes the elimination of the neutral dialkylselenide. The vinyl carbene **C** is formed, which results in either 1,2-migration of the phenyl or the sulfone to form product **146a** *via* insertion in the O–H bond of the alcohol. However, as formation of **146a** was never observed, which decreases the likelihood for Pathway **B** to be operative.

With this information in hand, we have tested if *S*-(alkynyl)dibenzoselenophenium triflate **69c** undergoes the same reaction pathway as its analogues. Compound **69c** was synthesized by well-known previously reported procedures.^{25,204}

Employing the reaction conditions similar to indicated in Muraoka's work,¹²⁰ product **70a** was isolated in 81% yield [Scheme 62, **a**], and comparable to observed by Kataoka reactivity and kinetics properties were detected. Then *S*-(alkynyl)dibenzoselenophene triflate **69c** was replaced by less toxic *S*-(alkynyl)dibenzothiophene triflate **5a**, which presumably should possess similar reactivity.²⁰⁵ The reaction was carried out in ethanol instead of hexanol [Scheme 62, **b**]. Product **70b** was obtained in comparable to the product **70a** yield.

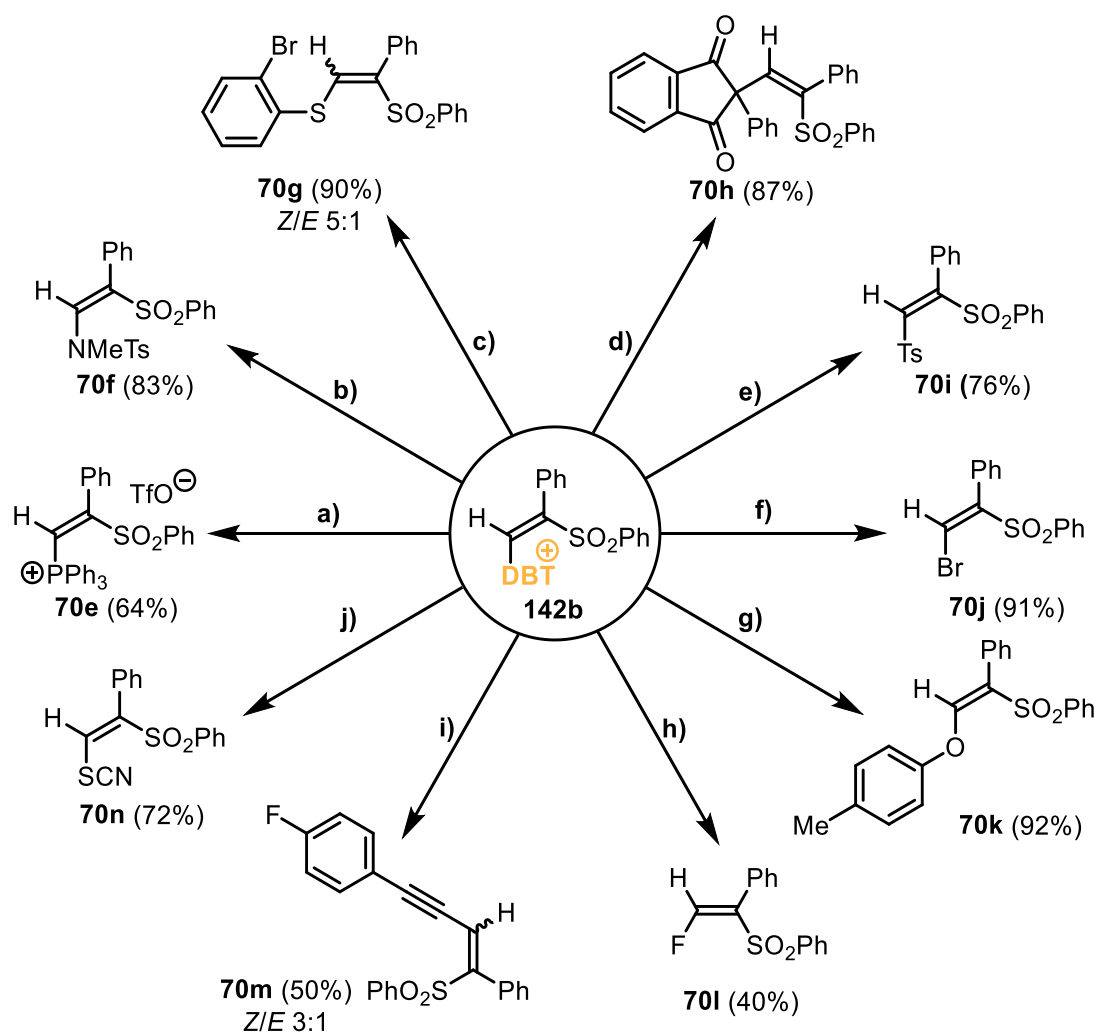


Scheme 62: Comparison of reactivity of the salts **69c** and **5a**. Reagents and conditions: a) PhSO₂Na (1.1 equiv.), 1-hexanol, rt, 1 h; b) PhSO₂Na (1.1 equiv.), EtOH, rt, 1 h; c) PhSO₂Na (1.2 equiv.), MeCN, rt, 1 h; d) DCM:MeOH, rt, 1 h. * The compound was not characterized but H-NMR and MS confirmed the structure of the product.

It was also investigated if alcohol can be replaced by another solvent with acidic properties. Utilizing thiol **147** resulted in excellent yield of the sulfide **70c** [(Scheme 62, **c**)]. Surprisingly, **70c** was obtained as a diastereomeric mixture with a *Z*:*E*-ratio of 9:1.

With sodium thiophene-2-sulfinate (**148**) alkyne **5a** gave the expected product **70d** in good yield [Scheme 62, **d**]. A *Z*:*E*-ratio of 10:1 was observed as well, and the *Z*-isomer could be isolated. Configuration of the major *Z* diastereomer of **70d** was confirmed by NOE experiments.

In Chapter 3.1.2 the successful synthesis of **142b** was described. With this reagent in hand, it was tested if nucleophiles can attack the sp^2 -hybridized α -carbon in **142b** and replace dibenzothiophene. The scope of different nucleophiles is shown in Scheme 63, whereas one salt **142b** was used as a representative example for this compound class.

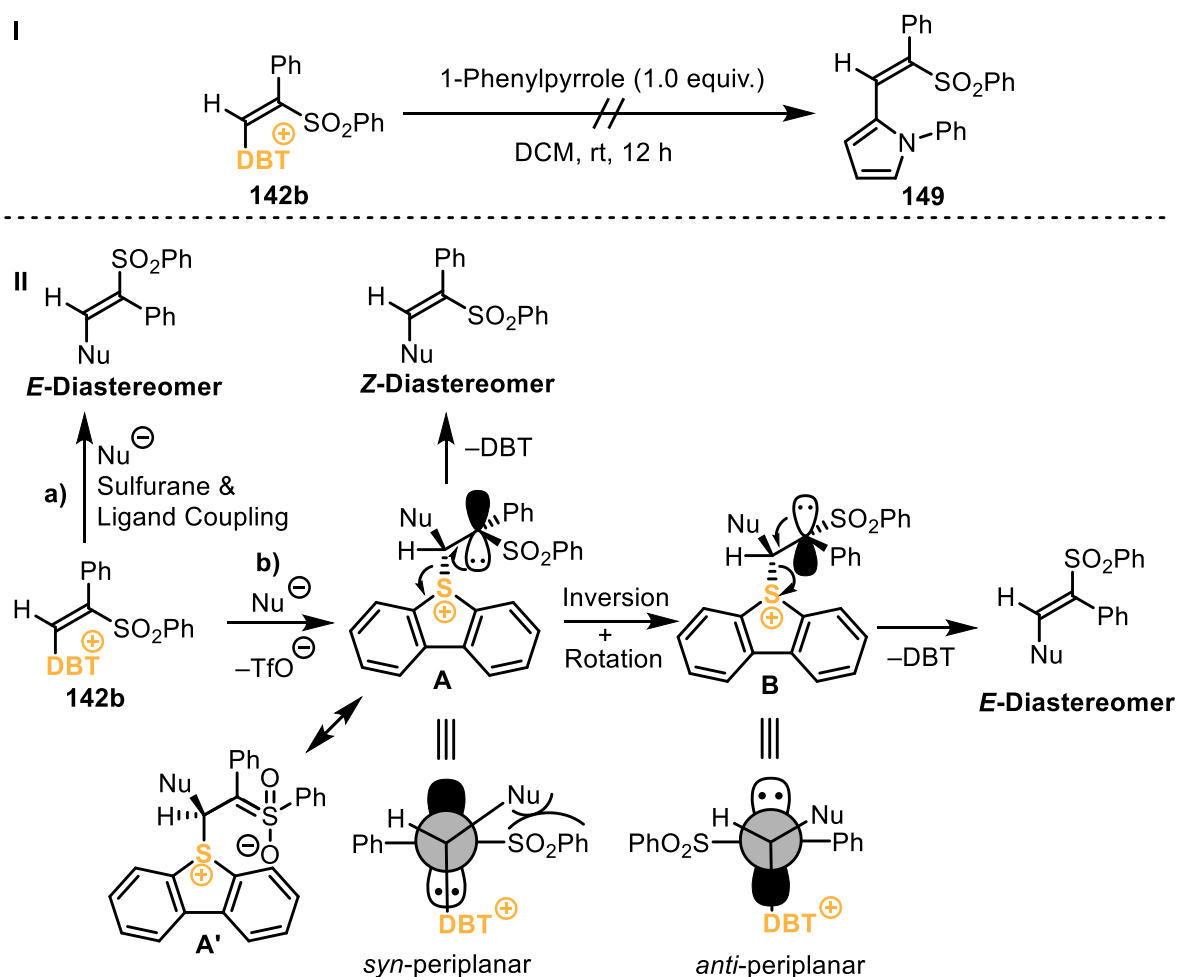


Scheme 63: Different nucleophiles converting **142b** into β -functionalized (Z)-alkynylsulfones. Reagents and conditions: a) PPh_3 (1.2 equiv.), DCM, rt, 12 h; b) $MeNHTs$ (1.2 equiv.), Cs_2CO_3 (1.2 equiv.), DCM, rt, 12 h; c) *o*-Br-thiophenol (1.0 equiv.), Cs_2CO_3 (1.0 equiv.), DCM, rt, 12 h; d) 1,3-Diketone (1.0 equiv.), Cs_2CO_3 (1.0 equiv.), DCM, rt, 12 h; e) $TsNa$ (1.0 equiv.), DCM:*t*-BuOH, rt, 12 h; f) $n-Bu_4NBr$ (1.0 equiv.), DCM, rt, 12 h; g) *p*-Cresol (1.0 equiv.), Cs_2CO_3 (1.0 equiv.), DCM, rt, 12 h; h) KF (1.2 equiv.), DCM/*t*-BuOH, rt, 12 h; i) $LiHMDS$ (1.0 equiv.), 1-ethynyl-4-fluorobenzene (1.0 equiv.), DCM, $-78^\circ C \rightarrow$ rt, 15 min; j) $NaSCN$ (1.1 equiv.), DCM/*t*-BuOH, rt, 12 h.

Triphenylphosphine gave phosphonium salt **70e** in acceptable yield. Thiolates, sulfonamides and 1,3-diketones under basic conditions gave **70g**, **70f** and **70h** in 90, 83 and 87% yield, respectively. Compound **70g** was obtained as a 5:1 mixture of *Z/E* isomers which could not be separated, whereas **70h** was isolated as the single *Z* isomer in 87% yield. Also, tosylsulfonic sodium salt and a bromide from $n-Bu_4NBr$ afforded the expected products **70i** and **70j**,

respectively, in satisfactory yields. Fluoride as a much weaker nucleophile than bromide was tested as well, and the desired product **70l** was isolated in only 40% yield. *para*-Cresol converted **142b** into **70k** in 92% yield without isomerization. 1-Ethynyl-4-fluorobenzene was deprotonated with LiHMDS at -78°C and reacted with **142b** to give **70m** in 50% yield as a 3:1 *Z/E* mixture of diastereomers. The pseudohalide thiocyanate yielded **70n** in 72%.

It was investigated if electron-rich aromatic molecules can act as nucleophiles as well (Scheme 64, I). As 1-phenylpyrrole was found to be an efficient nucleophile in electrophilic cyanation²⁴, it was tested again in reaction with the salt **142b**. However, the desired product **149** could not be detected in the reaction mixture. Based on this result it was assumed that the electron-rich aromatic systems cannot be alkenylated by **142b**.



Scheme 64: I) Attempted reaction of **142b** with 1-phenylpyrrole as a nucleophile. II) Mechanistic explanation of *E/Z*-isomerization during the nucleophilic attack.

As indicated above, in several cases the formation of both diastereomers, *E* and *Z*, was observed. In Scheme 64, II two operative mechanisms are proposed. Pathway a) describes the attack of the nucleophile to the sulfur center, forming the corresponding sulfurane

intermediate which then delivers exclusively the *E*-Diastereomer *via* ligand coupling (see also Chapter 1.3.3).

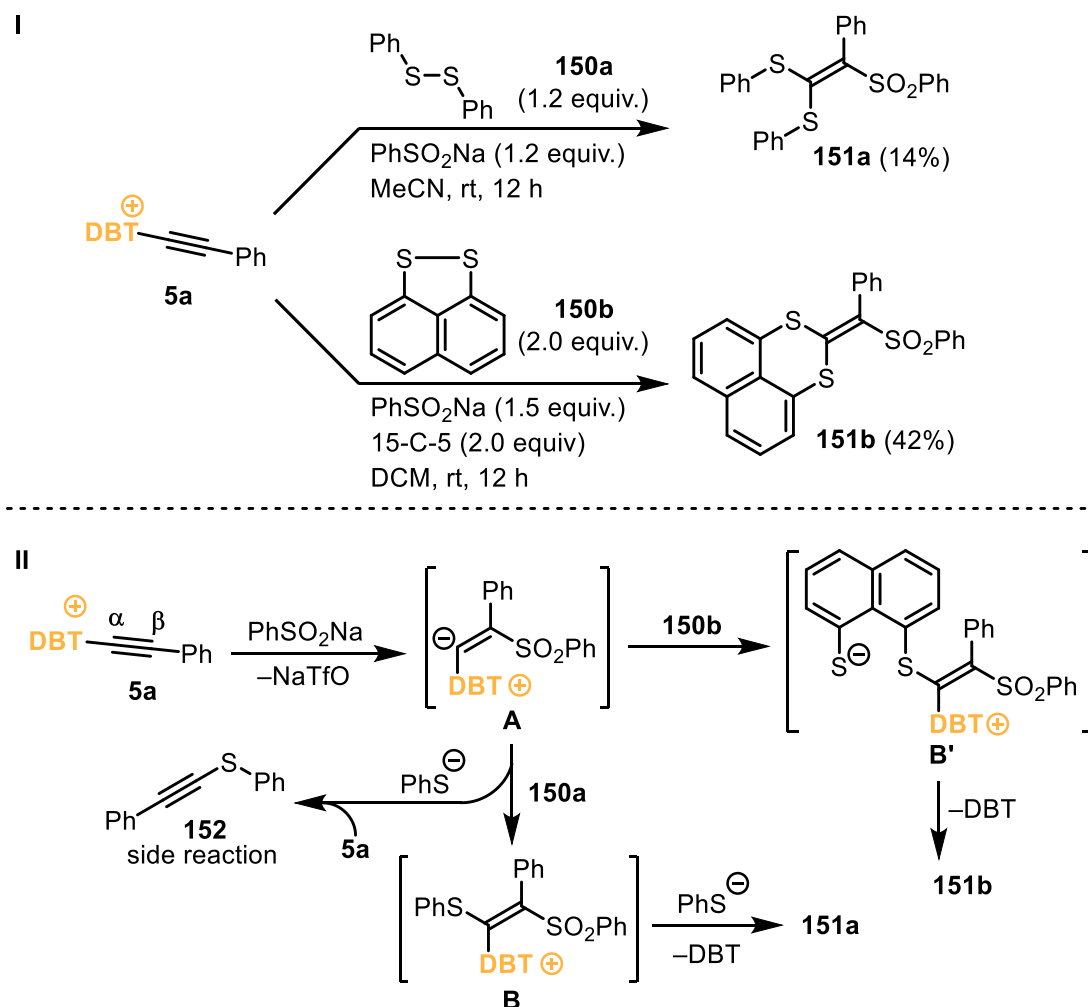
In Pathway **b**) the mechanistic rationalization towards this phenomenon is proposed assuming *syn*-elimination in the intermediate carbanions as a key step. *trans*-Elimination should result in predominant formation of the *E*-product, as conformation leading to the *E*-isomer is less sterically hindered.

After the nucleophilic attack, the initially formed intermediate **A** possesses an appropriate conformation to produce the main *Z*-diastereomer immediately *via syn*-elimination. However, if the steric demands of the nucleophile causes a steric clash, intermediate **A** can undergo an inversion of configuration at the carbanionic center affording, after turning along the C-C axis, a new conformation **B**, in which the steric clash is minimized.^{206a,b} The *syn*-elimination in **B** affords the *E*-diastereomer, and a mixture of two isomers will occur.

It cannot be excluded, that the intermediates can additionally be stabilized by Coulomb's forces as in **A'** as well as secondary 1,2-interactions between the nucleophile and the sulfone may take part upon the isomerization.

3.1.3.1. Reactions with Disulfides

The concept of the one-pot reaction described by Muraoka is reported with different proton-donating nucleophiles.¹²⁰ In the literature the insertion of the alkenyl moiety into an unpolarized bond is not reported (see Chapter 3.1.3 for comparison). Therefore, it was tested if disulfides are appropriate reaction partners for this transformation (Scheme 65).



Scheme 65: I) Reaction conditions towards formation of **151a** and **151b**; II) Proposed mechanism towards generation of **151a** and **151b**.

The reaction conditions applied to **5a** with diphenyl disulfide **150a** as geminal addition partner were similar as for the common nucleophiles such as alkoxides (Scheme 65, I). The reaction was sluggish and yielded low amounts of desired product **151a**.

Another cyclic disulfide **150b** was used instead, and **151b** could be isolated in 42% yield. In this reaction 15-Crown-5 was utilized to dissolve the sulfinate salt in DCM.

Expectedly, the reaction was slower since a non-polarized bond must be broken by alkenyl anion **A** (Scheme 65, II). When diphenyldisulfide is used as a reaction partner, the released

phenylthiolate appears to be potent for electrophilic alkylation and consumes starting material **5a** to form **152**.¹¹ Compound **152** was detected by mass spectrometry; its formation was clearly a reason for the low yield of **151a**.

The attack of alkenyl anion **A** to the cyclic disulfide **150b** results in zwitterionic species **B'**. The local high concentration of the nucleophile facilitates C–S bond formation towards vinylsulfide **151b** under abstraction of dibenzothiophene.

The connectivity in **151b** could be confirmed by X-ray crystallography; the structure of **151b** in the crystal is shown in Figure 11.

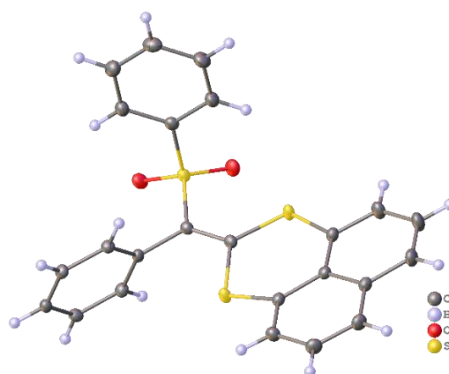


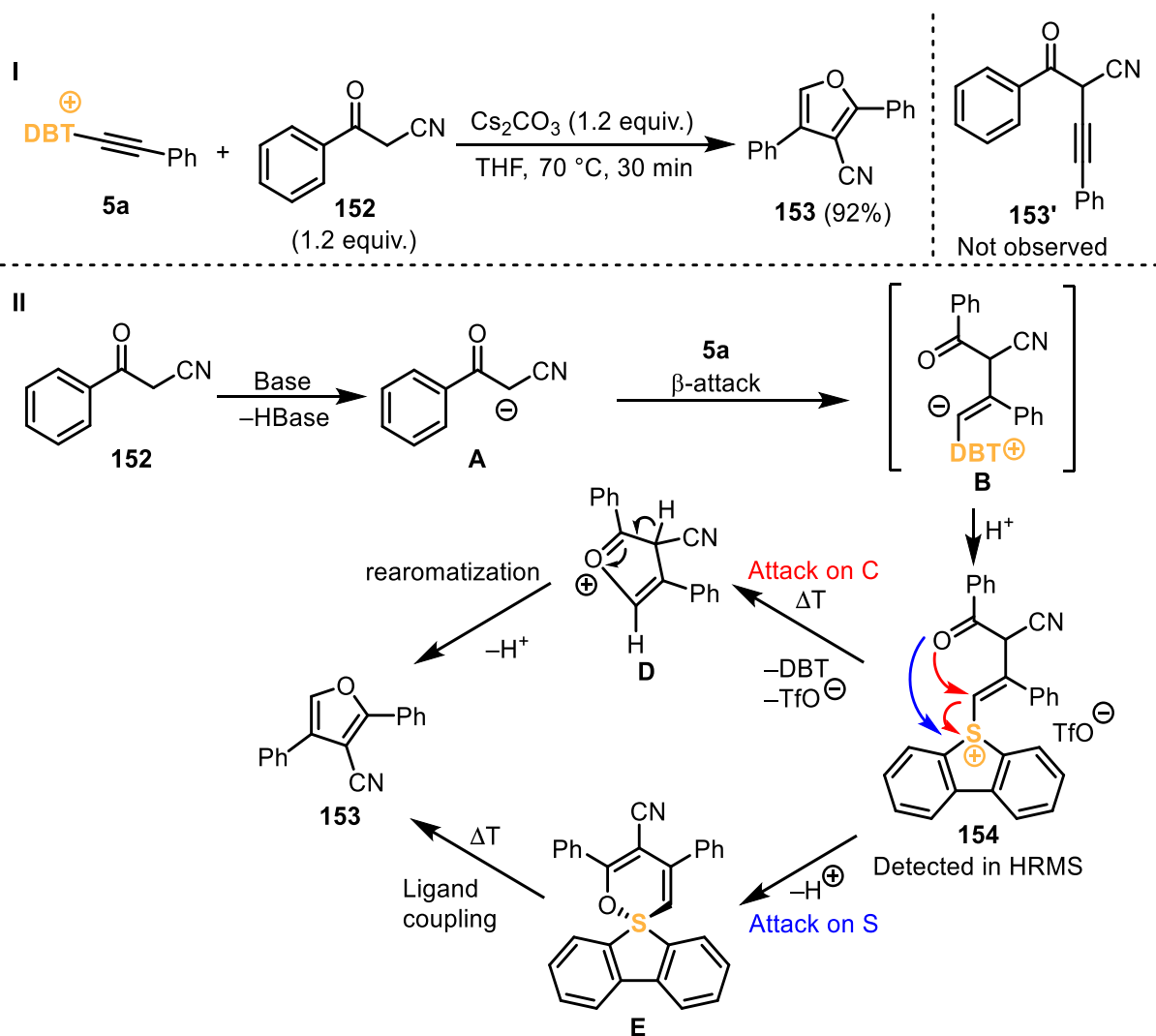
Figure 11: X-Ray structure of **151b** in the solid state. Anisotropic displacement shown at 50% probability level.

The structural motif of a vinylsulfide moiety is known in the literature albeit this compound class can be described as quite exotic.^{207,208}

3.1.3.2. Reaction with Benzoylacetonitrile

Based on the results obtained with phenylsulfonic acid salts and the work of Alcarazo, our efforts were focused on reaction of alkylation reagent **5a** and benzoyl acetonitrile **152**.¹¹ Especially, the phenylacetylation of **152** gave inconsistent results compared to other examples in this publication, and the reaction was therefore declared as affording an indistinct complex mixture of products.

With more insight to the structural product diversity the experiment was repeated, whereas alkylation product **153'** was not in focus (Scheme 66, I). Furan **153** could be detected as exclusive product in the reaction of benzoyl acetonitrile with reagent **5a**. Under elevated temperature and basic conditions, **153** was obtained in excellent yield in a short reaction time. The reaction was also performed at room temperature; however, as expected, the consumption of starting material was not complete after 12 hours.



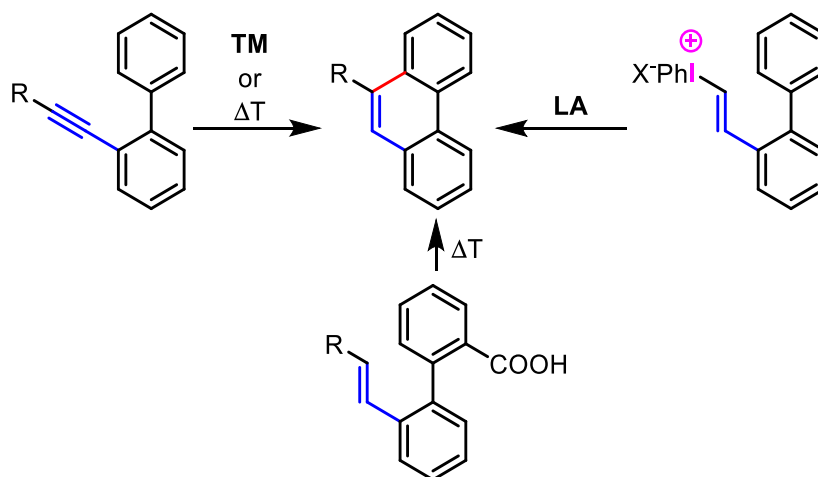
Scheme 66: Attempted alkylation of benzoyl acetonitrile with the salt **5a**. **I**) Reaction conditions; **II**) Mechanism towards the formation of 2,3,4-trisubstituted furan **153**.

The mechanism of the reaction is visualized in Scheme 66. First, deprotonation of the acidic proton in methylene moiety of benzoyl acetonitrile **152** can occur. Then a nucleophilic β -attack of **A** furnished the intermediate **B**. Protonation of **B** resulted in alkenylsulfonium salt **154**, which could be detected in HRMS. Upon heating the oxygen atom can attack either the α -carbon, eliminating dibenzothiophene and forming the furan scaffold **D**. Last, rearomatization occurred under abstraction of a proton to form **153**. Alternatively, the attack can also proceed at the sulfur which results in the formation of sulfurane **E**. From there **153** can be obtained by a thermal induced ligand coupling. Related selenurane analogs of **E** have been reported and even were isolated although these compounds decompose easily to furane scaffolds related to **153**.²⁰⁹ **E** could never be isolated since the compound seems to be unstable.

This result is very similar to those reported by Fujita, who used iodine^{III}-based alkynylation reagents.²¹⁰

3.1.4. Phenanthrene Synthesis *via* Photochemical Cyclization of Vinylsulfonium Salts

As phenanthrenes can be cleaved in many positions retrosynthetically, the synthetic tools for the preparation of these compounds is rather broad. Most of these transformations rely on transition metal catalysis applying palladium-²¹¹, platinum-²¹² or ruthenium-based catalysts²¹³, or thermal induction for either the construction of the whole phenanthrene scaffold or the final cyclization step from the parent alkyne.^{214,215} (Scheme 67).



Scheme 67: Cyclizations towards a generic phenanthrene.

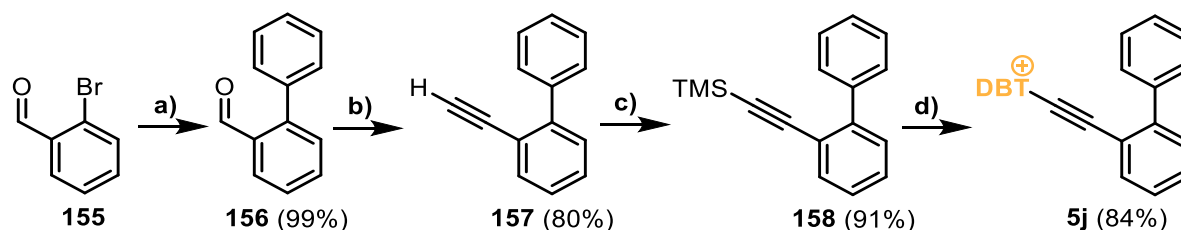
Another synthetic strategy involved *ortho*-vinylated biphenyls which can be transformed *in situ* into their hypervalent vinyl iodine reagent and cyclized with a Lewis acid (Scheme 67).²¹⁶ Alternatively, a decarboxylation reactions of *ortho*-carboxylic acids also undergo cyclizations towards phenanthrenes.²¹⁷

However, these transformations either depend on transition metal catalysis or harsh reaction conditions which limit the tolerance of functional groups.

Up to now a synthetic route from *S*-(alkynyl)sulfonium salts is not reported. This prompted us to perform the synthesis of an *ortho*-biphenyl-substituted *S*-(alkynyl)sulfonium salt with the purpose of their subsequent cyclization.

3.1.4.1. Synthesis of *S*-(Alkynyl)sulfonium Salt **5j**

The synthetic route to sulfonium salt **5j** in four steps and 61% overall yield is shown in Scheme 68.



Scheme 68: Synthesis of the sulfonium salt **5j**. Reagents and conditions: I) a) PhB(OH)_2 (1.2 equiv.), K_3PO_4 (2.0 equiv.), $\text{Pd(PPh}_3)_2\text{Cl}_2$ (5.0 mol%), DMSO, 80 °C, 12 h;²¹⁸ b) Ohira-Bestmann-Reagent (1.2 equiv.), K_2CO_3 (2.0 equiv.), MeOH, rt, 12 h;⁸² c) *n*-BuLi (1.0 equiv.), TMSCl (1.0 equiv.), THF, -78 °C \rightarrow rt, 12 h;²³ d) DBTO (1.0 equiv.), Tf_2O (1.0 equiv.), -50 °C \rightarrow rt, 1 h.²³

Besides the reaction conditions in the caption of Scheme 68, all these transformations were known and described in the literature. Starting from virtually quantitative Suzuki cross-coupling with 2-bromobenzaldehyde (**155**), the obtained biphenyl-2-aldehyde (**156**) was easily converted to alkyne **157** with the Ohira-Bestmann-reagent, then successively treated with *n*-BuLi and TMSCl to afford TMS-capped alkyne **158** in good yield. At last, compound **5j** was synthesized according to the indicated literature procedure in good yield, even on gram scale.

3.1.4.2. Structure of *S*-(Alkynyl)dibenzothiophenium Triflate **5j**

The structure of **5j** in the solid state is shown in Figure 12.

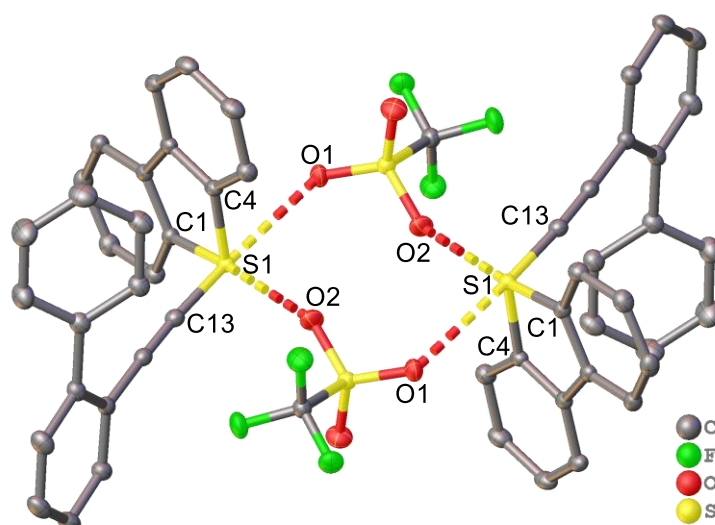
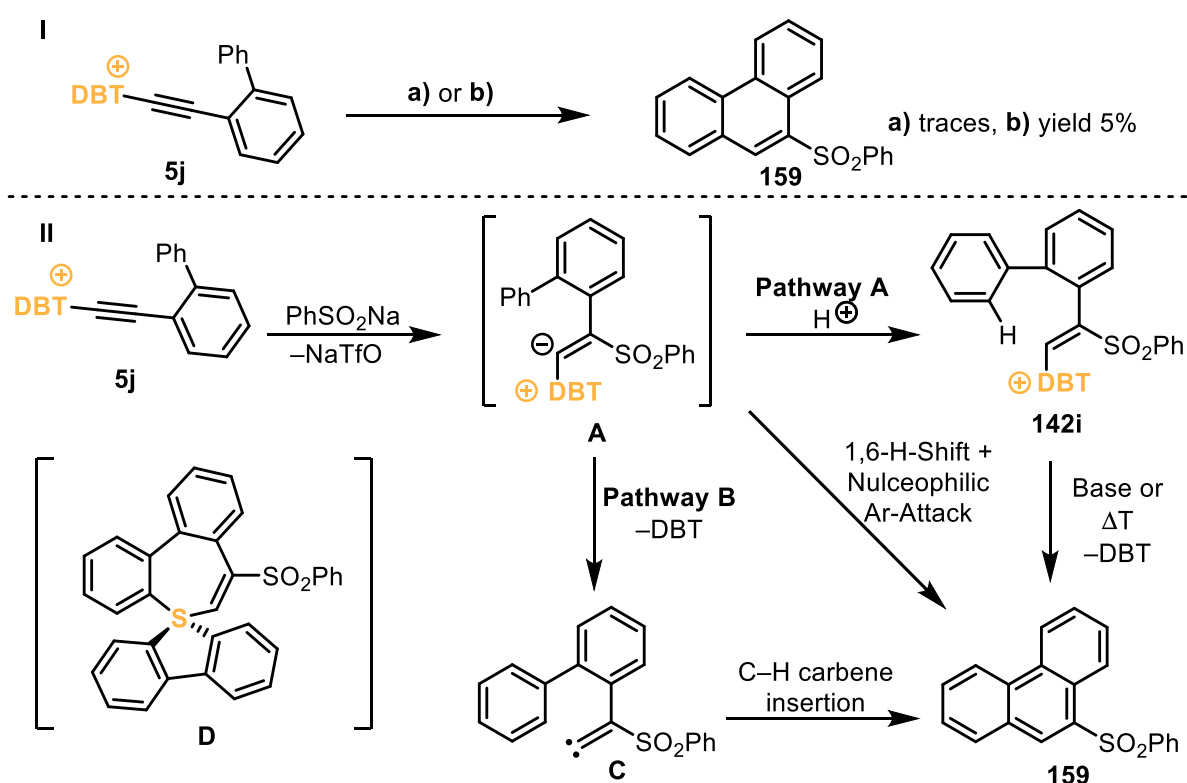


Figure 12: X-Ray structure of **5j** in the solid state. Anisotropic displacement shown at 50% probability level. Hydrogen atoms were omitted for clarity. Selected bond lengths [Å] and angles [°]: S1–C1 1.7878(10), S1–C4 1.7886(10), S1–C13 1.6966(10), S1–O1 2.8287(8), S1–O2 2.9297(9), C1–S1–O2 175.7, C13–S1–O1 174.9.

The salt **5j** demonstrated the typical dimer formation in the solid state. This phenomenon was previously observed in the whole family of *S*-(alkynyl)sulfonium salts and discussed above. The bond distance of S1–O1 with 1.6966 Å is comparable to those in other *S*-(alkynyl)sulfonium salts. Two observed chalcogen bonds differ only slightly; both are shorter than the sum of van-der-Waals radii for a S–O bond. This indicates strong Lewis acidity at the sulfur center, and similar behavior like of the known *S*-(alkynyl)sulfonium salts in the presence of nucleophiles can be expected.¹¹

3.1.4.3. Photochemical Cyclization of Vinylsulfonium Salts

With the salt **5j** being synthesized, multiple strategies for the cyclization towards the phenanthrene scaffold were attempted. It was envisioned to obtain **159** upon exposure of **5j** to elevated temperatures or by treatment with sodium phenylsulfinate under aprotic conditions (Scheme 69, I). Unfortunately, only traces of **159** could be detected after prolonged heating in MeCN, while applying reaction condition **b**) merely led to 5% of the desired product **159**.



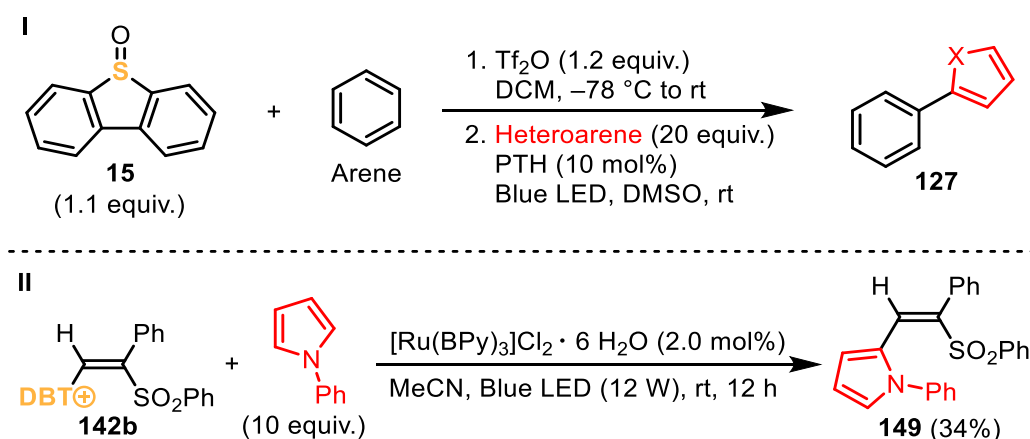
Scheme 69: I) Attempted cyclizations of the salt **5j**. Reagents and conditions: a) MeCN, 100°C, 16 h. b) PhSO₂Na (1.5 equiv.), 15-C-5 (2.0 equiv.), DCM, rt, 12 h. II) Proposed reaction pathways towards **159**.

The mechanistic consideration of the cyclization step for condition **b**) is depicted in Scheme 69, II. S-(Alkynyl)sulfonium salt **5j** enters an addition reaction furnishing zwitterionic alkenylsulfonium structure **A**. Vinyl carbene intermediate **C**, which could potentially be formed from **A**, undergoes a rapid C-H bond insertion to form **159** (Pathway B). Alternatively, intermediate **142i** could first be generated by protonation of **A** (Pathway A). Either elevated temperatures or a base could transform **142i** into **159**. It should also be noted that **A** can be converted into **159** directly via a 1,6-hydrogen shift and successive nucleophilic aromatic attack to the α -carbon. If intermediate **D** as key step is considered for pathway A, a seven

membered sulfurane is formed which should be energetically unfavorable. The high energetic barrier of **D** would explain the low yields in this reaction under the given conditions.

With the superior goal for an intramolecular cyclization reaction, a closer look to photocatalytic protocols was taken. As alkenylsulfonium salt **142i** can be synthesized and isolated, it might be reactive upon single electron reduction, and the cyclization could be done by a radical attack.

The research group of Procter developed a method for transition metal-free aryl-aryl coupling, which exploits the straightforward *in situ* formation of *S*-(aryl)dibenzothiophenium triflates and their proneness to undergo mild photocatalytic transformations (Scheme 70, I).¹⁵ In this reaction an excess of trapping reagent was used, whereas PTH served as an efficient photocatalyst.



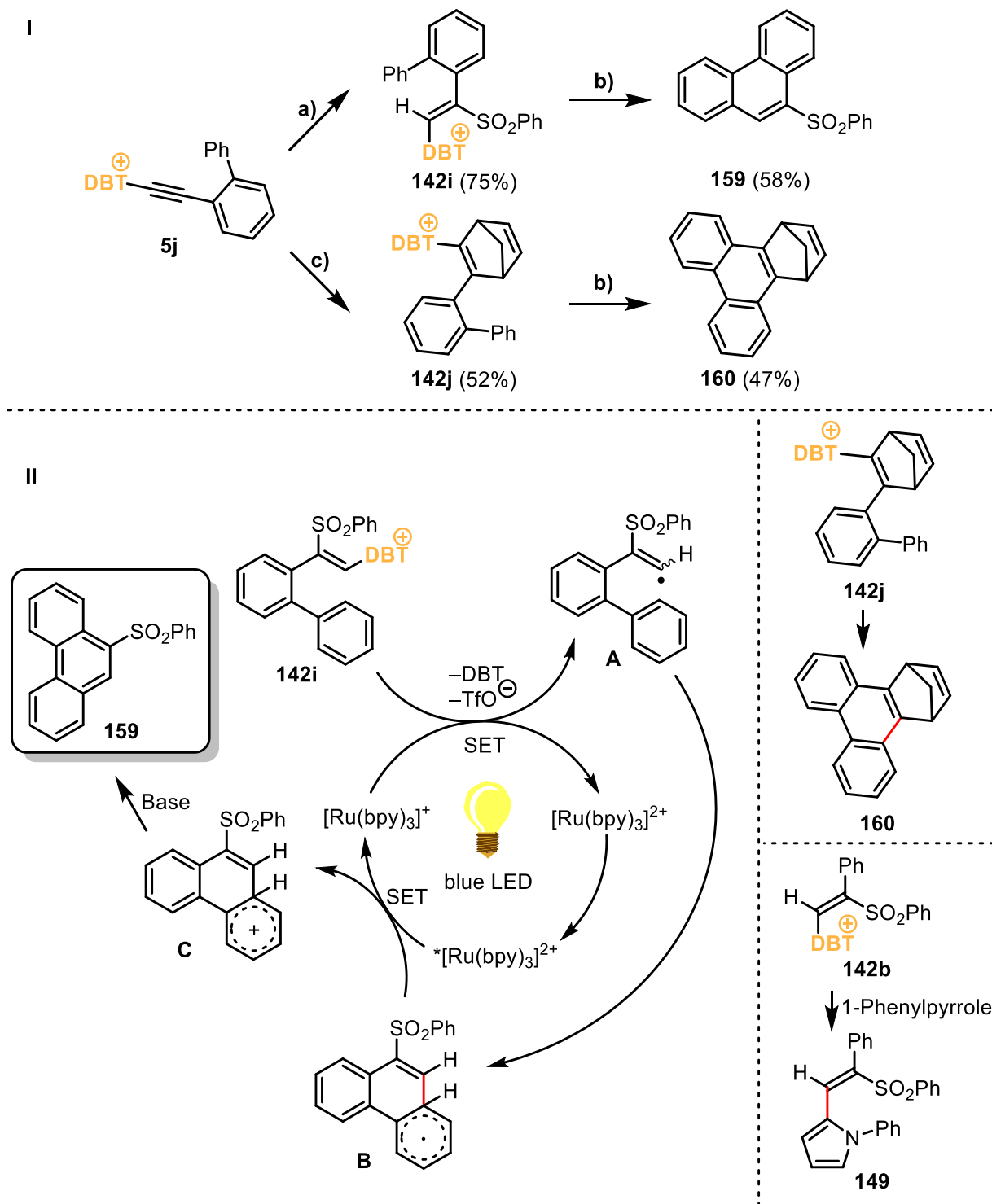
Scheme 70: I) Reaction conditions developed by Procter; II) Modified reaction conditions applied to sulfonium salt **142b**.

In Procter's transformation an aryl-aryl coupling has been done. This is not desired result in the case of cyclization of **159**, since not aryl, but a vinyl radical would be generated after single electron transfer.

Upon applying modified reaction conditions to vinylsulfonium salt **142b** with an excess of 1-phenylpyrrole as a trapping reagent, alkenylpyrrole **149** was obtained in 34% yield (Scheme 70, II). The result of this test reaction seemed to be promising for potential cyclization of *ortho*-biphenylvinylsulfonium salts.

Based on the result previously discussed in Chapter 3.1.2, an addition reactions to *S*-(alkynyl)sulfonium salt **5j** have been performed (Scheme 71, I). The reaction of **5j** with phenylsulfinic acid yielded the salt **142i** in 75% yield. Then the latter was exposed to photocatalytic conditions and yielded 58% of phenanthrene derivative **159** *via* an

intramolecular radical cyclization. Additionally, **5j** could be converted to **142j** by a Diels-Alder reaction with cyclopentadiene. The salt **142j** showed the same reactivity by applying photocatalysis and yielded hydrocarbon **160** in 47% yield.



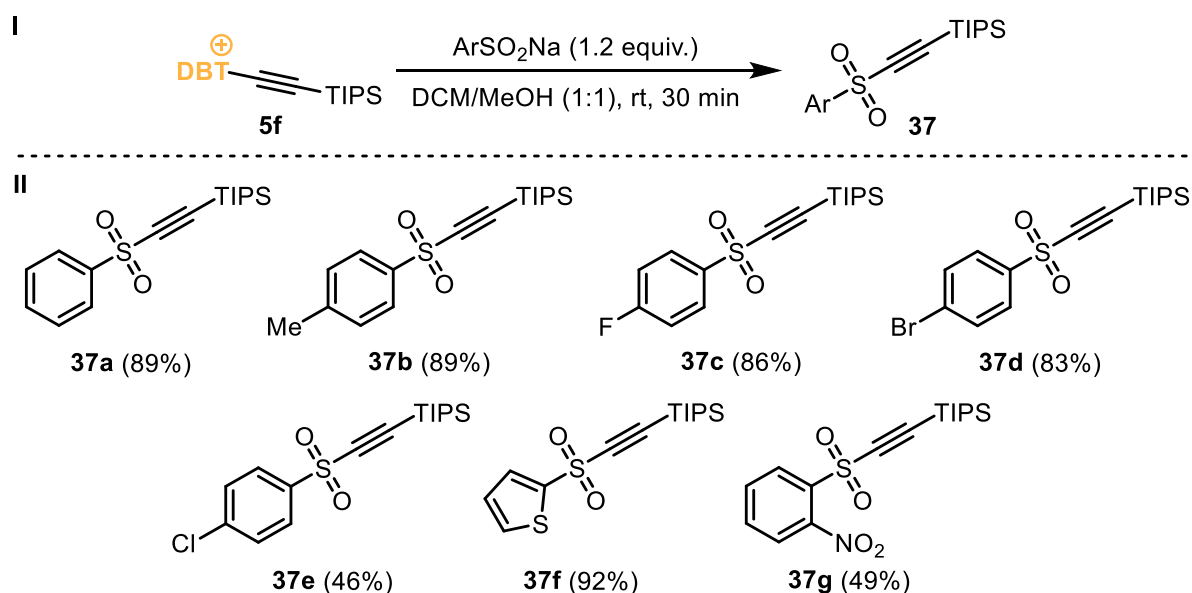
Scheme 71: I) Reagents and conditions: a) PhSO_2H (2.0 equiv.), $\text{DCM}/t\text{-BuOH}$, rt, 12 h; b) Cs_2CO_3 (1.1 equiv.), $[\text{Ru}(\text{BPY})_3]\text{Cl}_2 \times 6 \text{H}_2\text{O}$ (2.0 mol%), MeCN , Blue LED (28 W), rt, 16 h.; c) Cyclopentadiene (5.0 equiv.), MeCN , MW, 100°C , 3 h. II) Mechanistic proposal towards **159**, **160** and **149**.

A mechanistic rationalizations derived from the mechanism of Procter's transformation¹⁵ are shown in Scheme 71, II. Tris(bipyridine)ruthenium(II) chloride is known to be excited by blue light (ca. 460 nm). The ruthenium^I species can reduce **159** upon releasing dibenzothiophene to form alkenyl radical **A**. The latter undergoes rapid intramolecular cyclization towards intermediate **B** forming the C–C bond. The excited ruthenium^{II} species takes the electron from **B** affording the cationic intermediate **C**. After deprotonation and rearomatization, the final product **159** is formed.

The mechanism for converting **142j** to **160** and **142b** to **149** is analogous. The yield of **149** is lower (34%) since this transformation is not intra- but intermolecular. Additionally, the radical attack could also occur in 3-position of the pyrrole or at the phenyl group. Multifunctionalization of 1-phenylpyrrole, which would explain the low yield of the compound **149**, is also possible. However, **149** was the only isolated product.

3.2. Alkynylsulfone Synthesis

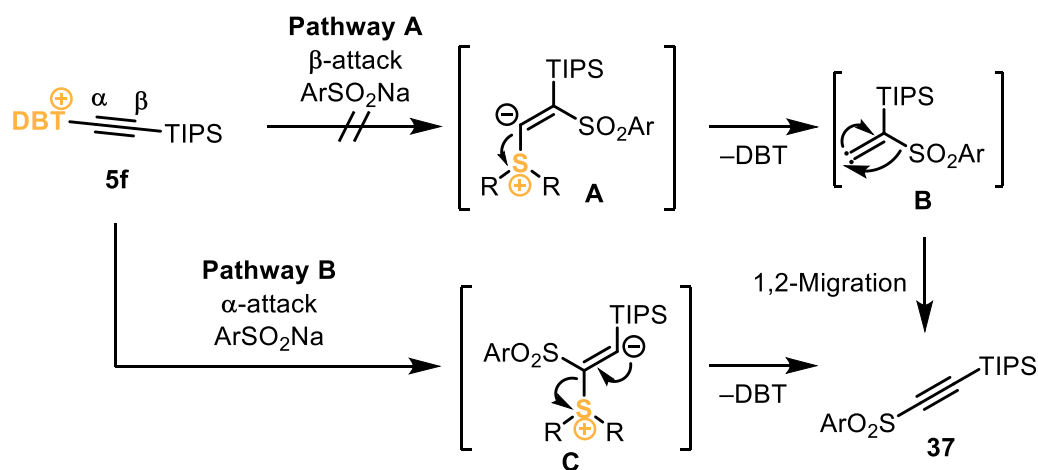
In Chapter 3.1.3 the reactions of sodium arylsulfonates with *S*-(alkynyl)dibenzothiophenium triflates were explored extensively. In accordance with previous findings by Alcarazo *et al.*, these salts consistently underwent a β -attack on the alkyne moiety, whereas the triisopropylsilyl-substituted alkylation reagent **5f** was exclusively attacked by nucleophiles in α -position.¹¹ Therefore, the reactive behavior of aryl sulfonates in the presence of **5f** was investigated (Scheme 72, I).



Scheme 72: Preparation of alkynylsulfones **37**: I) Reaction conditions; II) Scope of sodium sulfonates with the transfer reagent **5f**.

A 1:1 mixture of DCM and methanol had to be used because of the low solubility of sodium arylsulfonate in aprotic organic solvents. Unexpectedly, product **37a** was obtained in excellent yield within a short reaction time. Other sodium sulfonates were also tested, and the scope of the reaction is shown in Scheme 72, II. A methyl group as in the sulfonate **37b** had no influence on the yield of the reaction. As shown in examples **37c**, **37d** and **37e**, halogens were also tolerated in this transformation, although **37e** was obtained in moderate yield of 46%. This could be explained by the electron-withdrawing nature of the chlorine substituent, which reduced the nucleophilicity of the sulfonate. The same effect was observed for *o*-nitrosubstituted sulfonate, as the product **37g** was obtained in moderate yield. On the other hand, utilizing a sulfonate salt with an electron-rich heterocyclic moiety furnished **37f** in excellent yield, again indicating a correlation between the yield of the desired 1-triisopropyl-2-sulfonylacetylen and electron density on the utilized sulfonate salt.

A mechanism for this transformation is described in Scheme 73. Two potential pathways can be formulated towards generation of the desired product **37**. Pathway A consists of a β -attack of the nucleophile forming intermediate **A**. Intermediate **A** could eliminate dibenzothiophene to form the alkenylcarbene **B**, which forms the product **37** via a 1,2-migration of the TIPS group. However, based on the work of Alcarazo *et al.*, a β -attack on **5f** can be ruled out due to steric bulkiness of the TIPS substituent.¹¹ Additionally, in none of the investigated examples insertion products of the vinyl carbene were detected as a byproduct.



Scheme 73: Proposed reaction pathways **A** & **B** towards alkynylsulfones **37**.

In the case of an α -attack of the sulfinate sulfonium salt **C** should be formed. The latter rapidly decomposed to the desired product **37** via elimination of dibenzothiophene. However, **C** (or protonated **C**) was never detected by mass spectrometry (for more detailed mechanistic explanation see Chapter 1.2.3).

The connectivity in alkynylsulfonium salt **37e** was confirmed by X-ray crystallography; its structure in the solid state is shown in Figure 13.

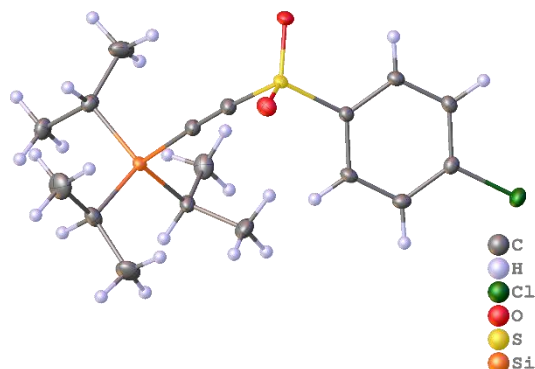
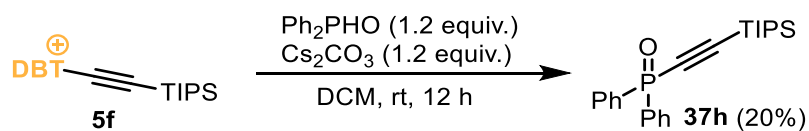


Figure 13: X-Ray structure of **37e** in the solid state. Anisotropic displacement shown at 50% probability level.

Additionally, diphenylphosphine oxide was considered to be an appropriate nucleophile for alkylation since it is structurally similar to arylsulfonic salts (Scheme 74).



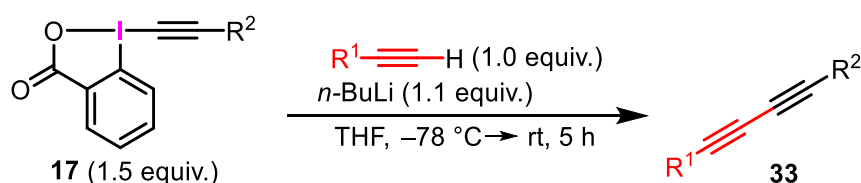
Scheme 74: Reaction of diphenylphosphine oxide with **5f**.

However, when **5f** was subjected to the conditions shown in Scheme 74 under basic conditions, the reaction afforded only 20% of **37h**. This transformation was not further investigated.

3.3. Diyne Synthesis

Based on the previous work of Alcarazo *et al.*, new nucleophiles in a similar reactive fashion were tested.¹¹ The research group of Waser investigated the transition metal-free coupling of terminal alkynes with hypervalent iodine-based alkynylating reagents **17** (Scheme 75).⁵³ Their approach was the deprotonation of the alkyne with *n*-BuLi at $-78\text{ }^{\circ}\text{C}$ in THF followed by adding the alkynylation reagent. While stirring over several hours, the reaction mixture was allowed to warm up to rt and afforded hetero-coupled diyne **33**.

Waser chose exactly 1.5 equivalents of alkynylation reagent and 1.1 equivalents of *n*-BuLi to suppress formation of homocoupling products, which is an ubiquitous side reaction in this transformation. In some cases, this undesired side reaction still occurred. The authors stated that the presence of polar or silyl groups in the terminal alkyne reduces the reactivity and increases the amounts of homocoupling products. Therefore, this transformation is most suitable for electron-neutral alkynes.

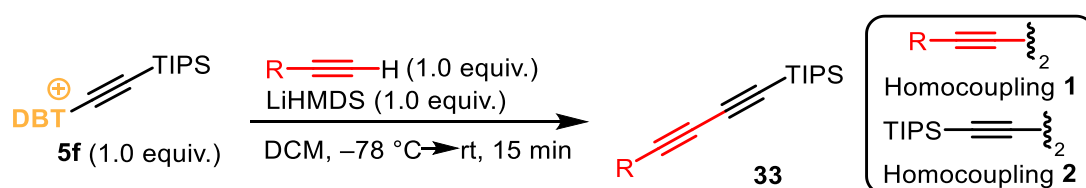


Scheme 75: Reaction conditions for the alkyne-alkyne coupling, as reported by Waser.⁵³

Since hypervalent iodine^{III}-based alkynylation reagents **17** and *S*-(alkynyl)dibenzothiophenium triflates **5** have many parallels in terms of reactivity, it was obvious to investigate the alkyne-alkyne coupling with sulfonium salt **5** as well.

As dichloromethane was required as a solvent to ensure the solubility of the sulfonium salts, even at low temperatures, lithium hexamethyldisilazane appeared to be a base of choice since it is basic enough and does not react with dichloromethane.

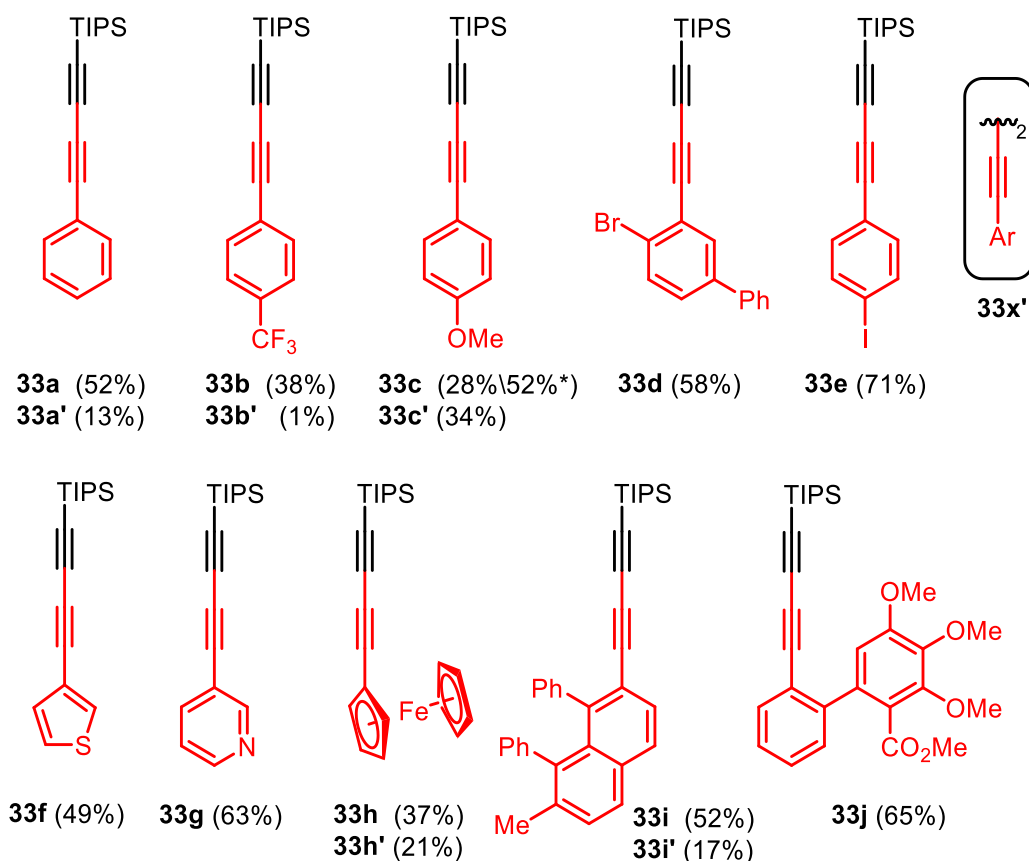
Exactly one equivalent of the alkyne, base and transfer reagent **5f** was utilized under chosen conditions (Scheme 76).



Scheme 76: Reaction conditions for the alkyne-alkyne coupling with the transfer reagent **5f**.

Altering the ratio of either one of the reactants caused formation of more undesired homocoupling products. In a few examples homocoupling side products could be isolated. Replacing LiHMDS with *n*-BuLi and DCM with THF resulted in worse yields.

A set of diynes was synthesized under the given conditions, and their scope is shown in Scheme 77. First of all, it should be mentioned that there was no obvious direct correlation between the electronic densities on the substrates and the efficacy of homocoupling. The occurrence of the side products seems to be individual to each example.



Scheme 77: Scope and limitations for the diyne formation; yields of homocoupling products are shown below those of the heterocoupling products and marked with an apostrophe (generic homocoupled product: 33x'). *1.0 equiv. of CuCN was used to suppress homocoupling formation.²¹⁹

Starting with electroneutral phenylacetylene, diyne **33a** was obtained in 52% yield. Additionally, 13% of diphenyl diacetylene **33a'** could be isolated as a homocoupling product. Compound **33b** was obtained in 38% yield and accompanied with only small amounts of **33b'**. *para*-Methoxy-substituted **33c** as an electron-rich product was isolated in 28% yield, whereas **33c'** was formed as a major product (34% yield). However, utilizing one equivalent of CuCN allowed to increase the yield of **33c** to 52% and suppressed homocoupling completely.²¹⁹ Isolation of **33d** and **33e** demonstrated the compatibility of this method with halogenated arylacetylenes. Moreover, heterocyclic substrates **33f** and **33g** were also tolerated without

occurrence of homocoupling. Ferrocenylacetylene yielded almost equal amounts of hetero- (**33h**) and homocoupling (**33h'**) products. More sophisticated alkynes gave **33i** and **33j** in acceptable yields. In these couplings the ester groups remain intact (**33j**), whereas homocoupling product **33i'** was isolated in considerable amounts.

The connectivity in **33i'** and **33j** was confirmed by X-ray crystallography; their structures in solid state are shown in Figure 14.

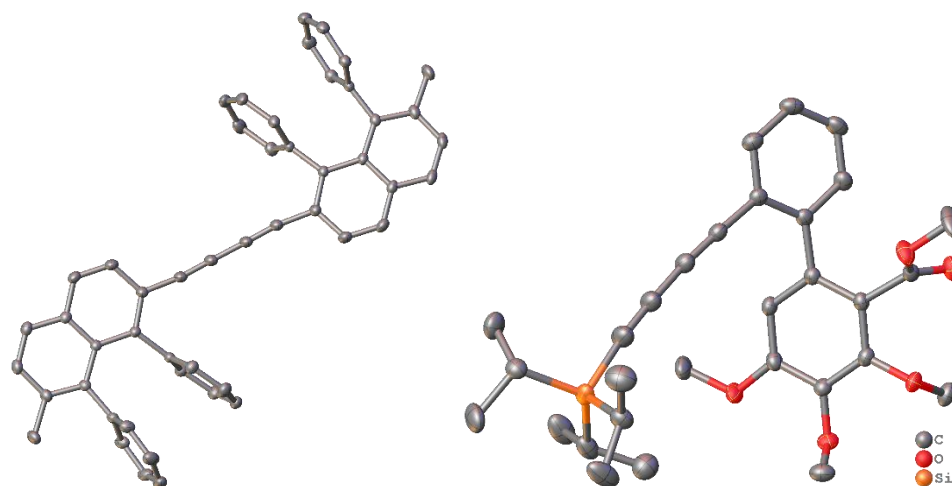
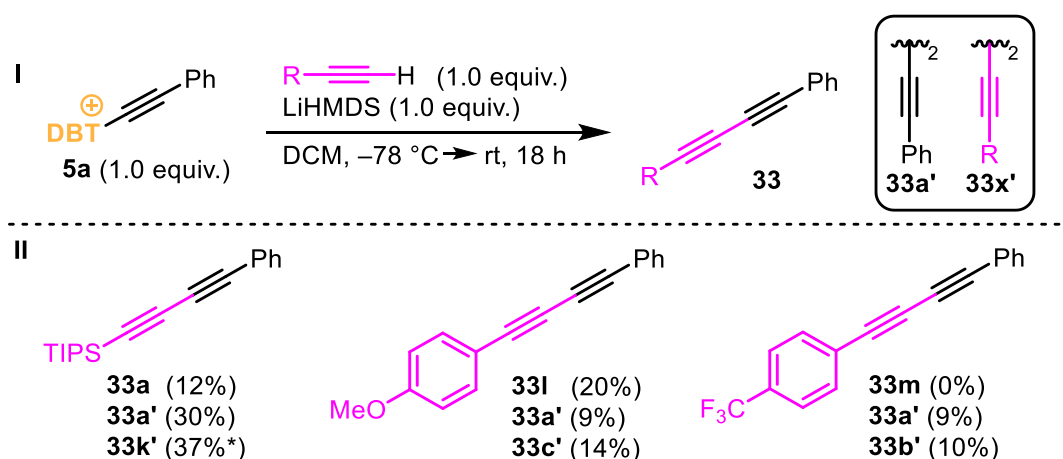


Figure 14: X-Ray structures of **33i'** & **33j** in the solid state. Anisotropic displacement shown at 50% probability level. Hydrogen atoms were omitted for clarity.

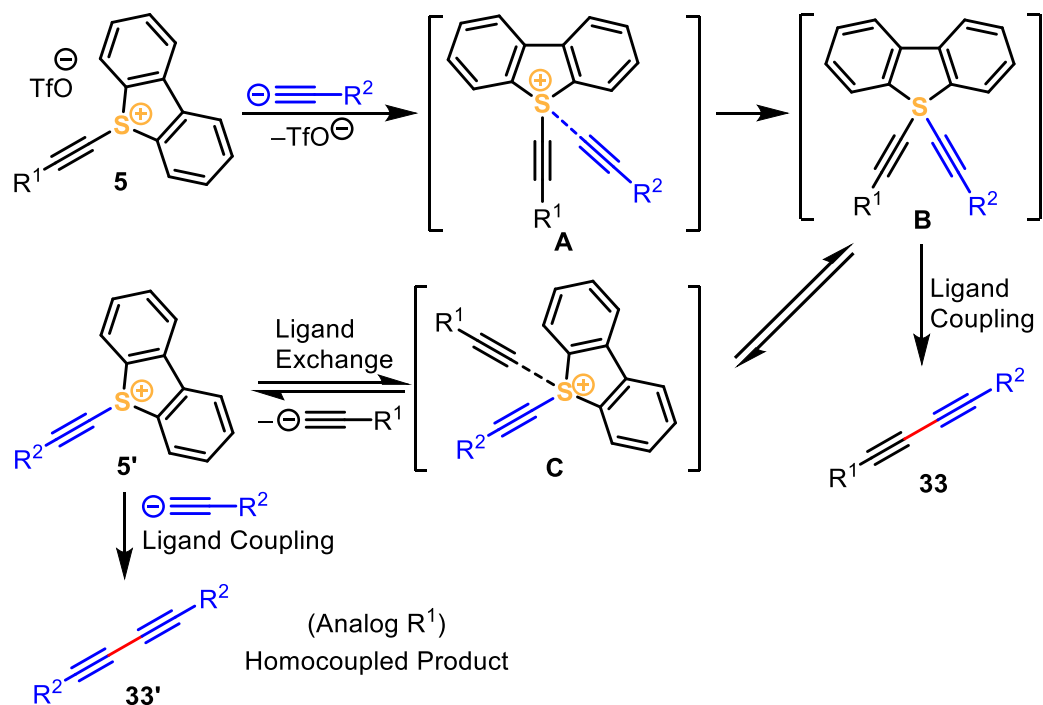
Additionally, alkynylation reagent **5a** was examined for the diyne formation, as presented in Scheme 76. Here, the same reaction conditions were applied, with the exception of the reaction time. The latter had to be lengthened to 18 h, since the reaction proceeds much more slowly compared to the analogous reaction with **5f**.



Scheme 78: I) General method for the diyne formation from **5a**; II) Isolated products **33a**, **33l** & **33m** synthesized by this method (with homocoupling products **33a'**–**c'**,**k'**). *Product was not isolated, yield determined by ^1H NMR.

Reagent **5a** is likely to be more prone to follow the homocoupling pathway (Scheme 78). Only 12% of **33a** and significant amounts of homocoupled products **33a'** and **33k'** were isolated. Diyne **33l** was also obtained in rather low yield, as well as the corresponding side products **33a'** and **33c'**. Lastly, the coupling of **5a** with *para*-trifluoromethyl-substituted alkyne afforded solely the homocoupling products **33a'** and **33b'**. The reaction was not further investigated due to disappointing initial results.

The mechanistic proposal is depicted in Scheme 79 (see also Chapter 1.2.3).



Scheme 79: Mechanistic proposal towards diene formation with the transfer reagents **5**.

The mechanistic rationalization is similar to those proposed by Alcarazo *et al.* (Scheme 79).¹¹ At first, generic *S*-(alkynyl)sulfonium salt **5** is attacked by an acetylide forming intermediate **A**, in which the acetylide is coordinated with the sulfur center. Afterwards a C–S bond between the sulfur and the acetylenic carbanion is formed and sulfurane **B** is obtained. After elimination of dibenzothiophene from **B** the ligand coupling furnished the desired heterocoupled diene **33**.

This mechanism however does not explain the occurrence of homocoupling products. Therefore, the second reaction pathway from **B** is proposed, in which **B** is in equilibrium with intermediate **C**. The dissociation of acetylenic ligand $R^1C\equiv C^-$ in **C** leads to formation of *S*-(alkynyl)sulfonium salt **5'** upon release of the ligand. Attack of the second equivalent of $R^2C\equiv C^-$ on **5'** will deliver the homocoupled product **33'** by the same mechanism.

The exact role of the *in situ* generated copper acetylides to suppress the homocoupling formation is speculative and remains unclear.²¹⁹

3.4. Synthesis & Reactivity of *S*-(Aryl)dibenzothiophenium Triflates

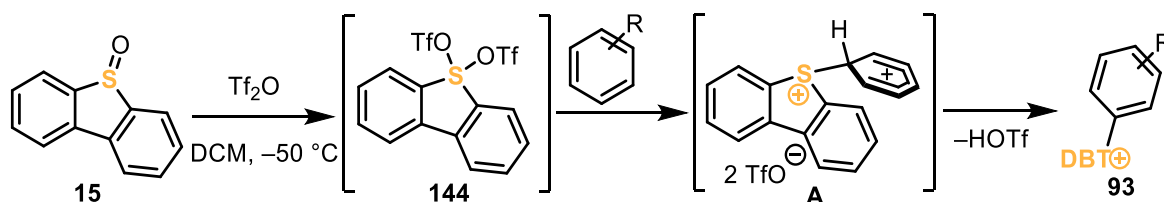
Triarylsulfonium salts are known since half a decade and their potential in organic chemistry is still not exhausted.^{220,221} In this thesis a family of *S*-(aryl)dibenzothiophenium triflates was synthesized, characterized and used in *ipso*-substitutions and Suzuki couplings. Moreover, mechanistic insights towards the formation of these salts were gained.

The research group of Ritter developed a strongly related protocol for the synthesis of *S*-(aryl)dibenzothiophenium triflates independently at the same time. Therefore, some of the following content overlaps with the work of Ritter and coworkers.^{156,157}

3.4.1. Synthesis of *S*-(Aryl)dibenzothiophenium Triflates

The well-established method by Alcarazo including the activation of dibenzothiophene **15** with Tf₂O has been associated with the synthesis of *S*-(alkynyl)- or *S*-(cyano)dibenzothiophenium triflates so far.^{11,23,24} The potential for the sulfenylation of aromatic compounds has been realized and exploited in this thesis. Preliminary results disclosed the rapid and selective formation of *para*-sulfenylated ethylbenzene after exposure of **144** with the aforementioned arene.

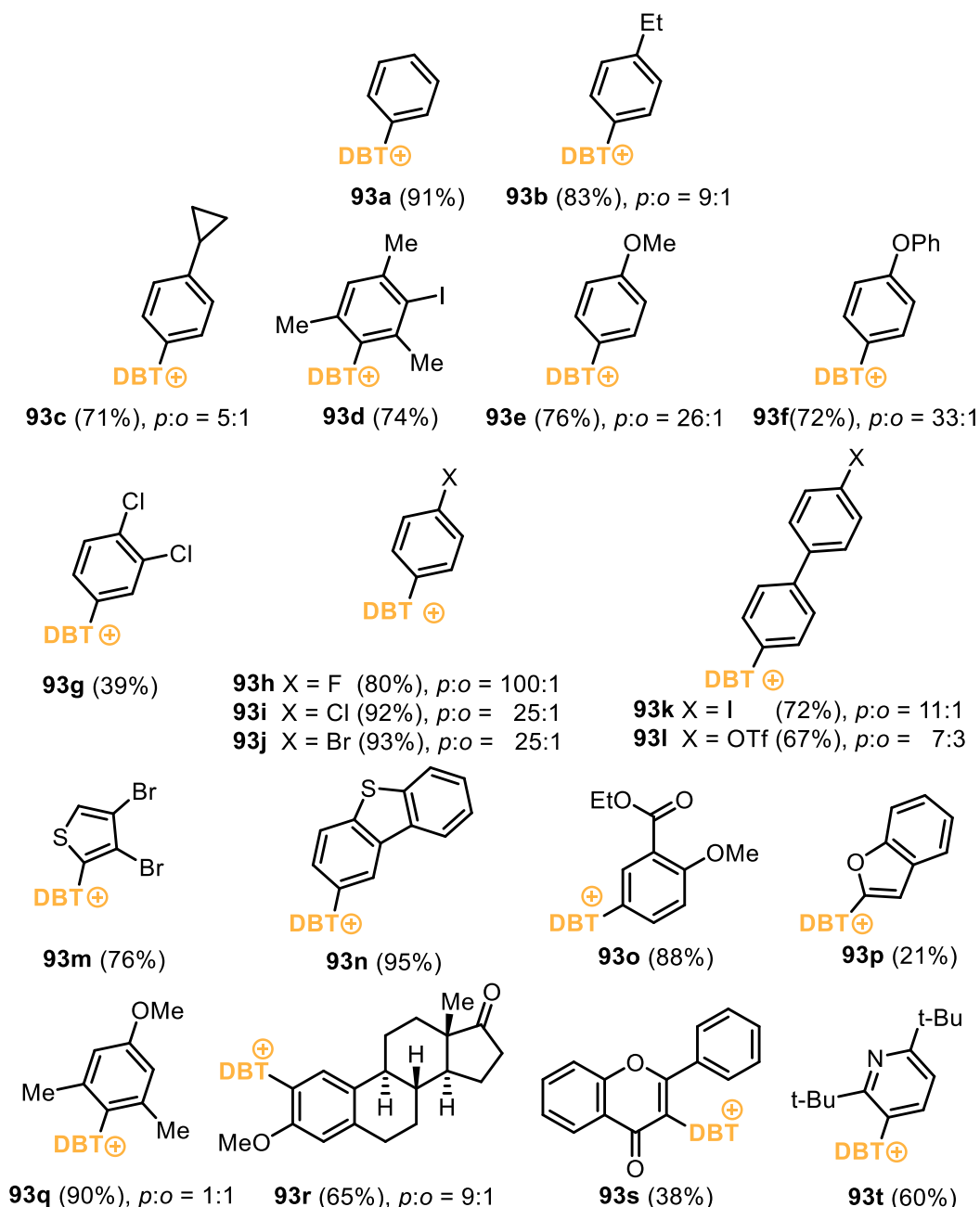
Therefore, the scope and limitations of the synthesis of *S*-(aryl)sulfonium salts **93** from electron-rich arenes were explored (Scheme 80).



Scheme 80: General reaction conditions to the formation of aryl sulfonium salts **93**.

As usually the reaction was carried out at $-50\text{ }^{\circ}\text{C}$, which avoids the decomposition of intermediate **144**. In the presence of a sufficiently electron-rich aromatic system, an electrophilic aromatic substitution reaction occurs smoothly, preferably in *para* position respect to the most electron-rich substituent. The resulting *S*-(aryl)dibenzothiophenium triflates are air stable, even survive aqueous workups without noticeable decomposition,

which makes them very convenient in handling. The scope of *S*-(aryl)dibenzothiophenium triflates is shown in Scheme 81.

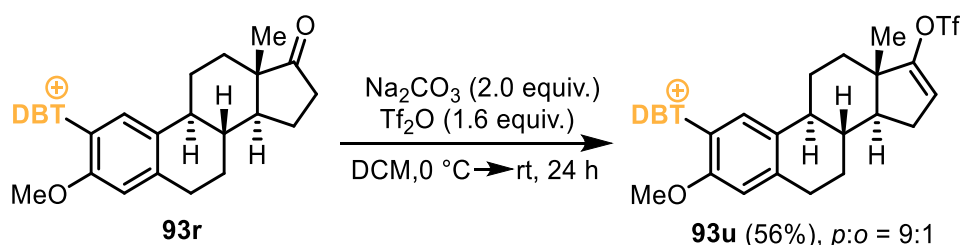


Scheme 81: Scope and limitations towards *S*-(aryl)dibenzothiophenium triflates **93**.

Starting from electro-neutral benzene, **93a** was obtained in 91% yield. An additional ethyl group directed the electrophile in *para*- and *ortho*-position (9:1) in product **93b**, which was isolated in 83% yield. In **93c** a *para/ortho*-ratio of 5:1 was observed. This cannot be explained by the steric factors, as a cyclopropyl group provides greater steric bulk than the ethyl group,^{206c} but should be attributed to the special property of a cyclopropyl to exhibit *o*-orientation due to its very special electronic properties.^{206d} Compound **93d** was obtained in

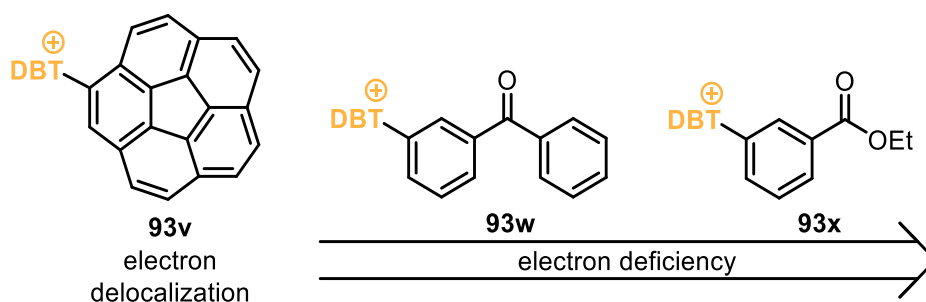
good yield as well, demonstrating that *ortho*-disubstitution in the sulfonium aryl did not inhibit the transformation. Using anisole gave product **93e** in good yield with a *para/ortho*-ratio of 26:1. This indicated that the regioselectivity is controlled not only sterically but also electronically. An even better *para*-selectivity was observed in the product **93f**. 1,2-Dichlorobenzene was functionalized to form **93g**, although in moderate yield. Halogenated benzene rings yielded **93h** to **93j** smoothly with an excellent *para* selectivity. *para*-iodo- and *para*-triflate-substituted biphenyl yielded **93h** and **93i** in 72 and 67% yield, respectively. Heterocyclic 3,4-dibromothiophene was converted into **93m** in 76% yield. The reaction with dibenzothiophene occurred almost quantitatively and afforded 95% of **93n**. Arylsulfonium salt **93o** was obtained in 88% yield. This example shows once more the electronic effect of a methoxy group, which tolerates electron-withdrawing groups like an ester. Benzofuran was functionalized in 2-position furnishing **93p** in a yield of 21%. Product **93q** was obtained as a mixture of 1:1 ratio in regards of regioselectivity. Methoxylated estrone was converted into **93r** in 65% yield, also forming a *para-ortho* mixture in a 9:1 ratio. Flavone could also be functionalized at the double bond yielding 38% of **93s**. Surprisingly, sterically demanding 2,6-di-*tert*-butylpyridine was rather efficiently converted to **93t**. Exclusively the *ortho*-position in respect to the *tert*-butyl group was functionalized in acceptable yield of 60%.

Upon the synthesis of **93r**, small amounts of compound **93u** were detected in HRMS (Scheme 82). Therefore, it was investigated whether **93u** could be intentionally synthesized by simple enolization and triflation of **93r**. This transformation was conducted in the presence of the dibenzothiophene moiety without essential decomposition and yielded **93u** in moderate yield. The *para/ortho*-ratio still remained 9:1.



Scheme 82: Post-synthetic modification of **93r** to **93u**.

Apart from the products presented in Scheme 81, other starting materials were tested as well. Three additional examples are shown in Scheme 83.



Scheme 83: Reaction with miscellaneous substrates.

Corannulene was functionalized, and crude ^1H NMR and HRMS could confirm the presence of the desired compound **93v**. However, the dimer **93n** was also formed, and these two monocationic salts could not be separated by column chromatography. All attempts to perform a selective crystallization for the characterization of the sulfonium salt failed, although a not well-defined crystal structure of sulfenylated **93v** could be obtained (see Experimental part 5). Multiple attempts of altering temperature or reaction time did not lead to selective formation of **93v**. It is assumed, that the delocalization of the electron density provided by the annulated aromatic system prevents the selective formation of the sulfonium salt.

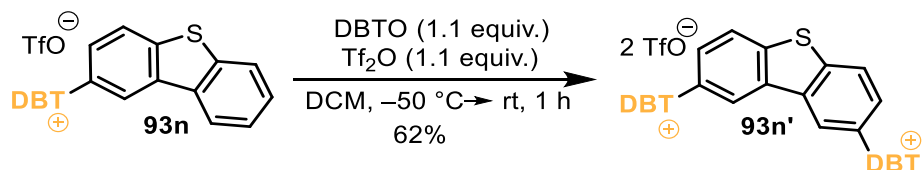
To evaluate the lower limit of electron-poor arenes in this reaction, acetophenone was chosen as an electron-deficient substrate. Here the same problem was encountered. The two sulfonium salts **93w** and **93n** were formed and could be separated neither by column chromatography nor by crystallization. This experience is in accordance with the results of Ritter.¹⁵⁷ In Chapter 1.4.3.1 the match of the dibenzothiophene oxides with different arenes is described. According to the authors, a less electron-rich than 1,2-dichlorobenzene arene cannot be sulfenylated efficiently, which is the case here.

More electron-poor benzoate did not form the corresponding sulfonium salt **93x** at all. Exclusively starting material could be reisolated, and a mixture of different sulfonium salts was obtained (for the detailed description see Chapter 3.4.5).

The limitation of this reaction is connected to the electronic nature of the reaction center in the aryl substrate. Hence, no further electron poor substrates were tested.

As depicted in Scheme 81, the sulfenylation to **93n** proceeded well. Occasionally, the formation of dicationic salt **93n'** could be observed in some sulfenylation reactions of arenes as a byproduct additionally to **93n** (explanation for the formation of dibenzothiophene see in Chapter 3.4.5). Albeit the separation of **93n'** from the monocationic salts by column

chromatography or crystallization was always successful, this observation led to the idea of the premeditated synthesis of **93n'** by the sulfenylation of sulfonium salt **93n** (Scheme 84).

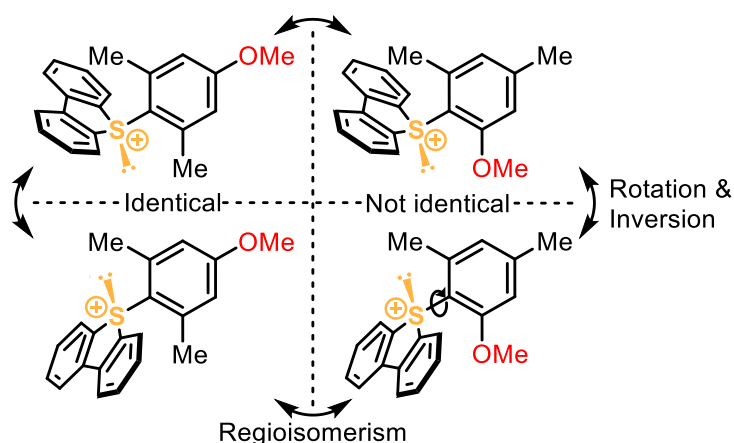


Scheme 84: Synthesis of dication **93n'** from monocation **93n**.

The reaction afforded 62% of desired compound **93n'**. In conclusion this result represents the limitations of suitable arenes for this reaction. The arene should be at least as electron-rich than dibenzothiophene (and **93n**). In the reactions where **93n** is not formed as a side product the reaction towards **93n'** can obviously not occur and will not diminish the yield of the targeted sulfonium salt.

The product **93q** was isolated as a 1:1 mixture of *para-ortho* regioisomers (Scheme 81). In fact, 3 isomers are present in this example.

Due to the high inversion/rotation barrier of the sulfonium salt, the *ortho*-positions are not equivalent and constitute distinguishable isomers (Scheme 85). In the case where the reaction took place at the *para*-position in respect to the methoxy group, either rotation around the C–S axis or inversion of the sulfonium moiety lead to the identical molecule. However, for the *ortho*-substitution both operations result in a second *ortho*-substituted isomer. In this particular example inversion and rotation forming the same product. The three isomers were obtained as a mixture and could not be separated neither by column chromatography nor crystallization.



Scheme 85: All isomers of the salt **93q**. The triflate anions were omitted for simplification.

Compound **93d** also shows two signal sets in the ^1H NMR spectrum caused by the high rotation/inversion barrier of the *ortho*-disubstituted sulfonium moiety.

Temperature-dependent ^1H NMR experiments enabled the determination of the rotation/inversion barrier of **93d**. Rotation/inversion rate constant k was calculated using Formula (1), with the average line broadening $\Delta\vartheta_{1/2}$ for $T_1 = 25\text{ }^\circ\text{C}$ and $T_2 = 120\text{ }^\circ$. The barrier ΔG of compound **93d** was then calculated by Formula (2), with the R being the universal gas constant.

$$k = \pi \cdot \Delta\vartheta_{1/2} \quad (1)$$

$$\Delta G = RT \left[23,76 - \ln \left(\frac{k}{T} \right) \right] = 82.34 \frac{\text{kJ}}{\text{mol}} \quad (2)$$

With typical values for inversion barriers of triarylsulfonium salts being 23.9–31.0 kcal · mol⁻¹, the energetic barrier with 19.6 kcal · mol⁻¹ for **93d** is lower than average.^{2,3} For *S*-aryl trisubstituted sulfonium salts no data for the value range for the rotational barrier is available. This large deviation leads to a high probability that the calculated value can be assigned to the rotational barrier.

3.4.2. Structure of *S*-(Aryl)dibenzothiophenium Triflates **93o** & **93m**

The crystal structure of **93o** is depicted in Figure 15. Arylsulfonium salt **93o** adopts a dimeric structure analog to those observed in most structures of *S*-(alkynyl)sulfonium salts in the solid state (see Chapter 1.2.2). Two chalcogen interactions between two triflate anions and two sulfonium centers can be observed, whereas one of them is by far shorter than the other. The sulfonium salt **93b**, which crystal structure is presented and discussed above in Chapter 1.4.2, possesses a monomeric structure in the solid state. This differs from the structure of **93o** fundamentally.

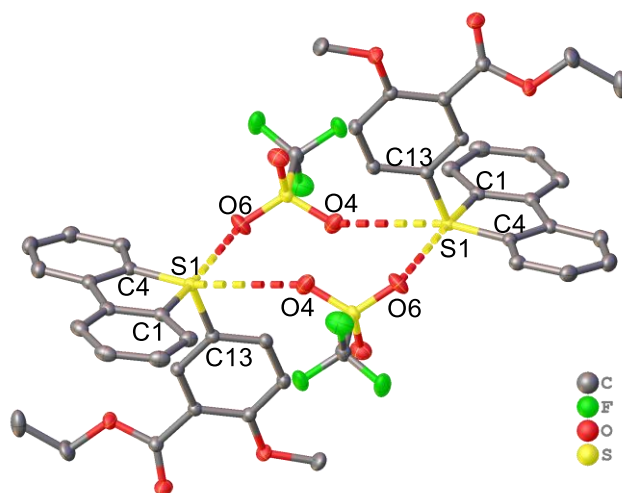


Figure 15: X-Ray structure of **93o** in the solid state. Anisotropic displacement shown at 50% probability level. Hydrogen atoms were omitted for clarity. Selected bond lengths [Å] and angles [°]: S1–C1 1.7789(10), S1–C4 1.7791(9), S1–C13 1.7762(9), S1–O3 3.5321(12), S1–O6 2.9904(13), C1–S1–O6 174.6, C4–S1–O4 163.3.

The structure of **93m** in the solid state shows additional interactions to the usual ones associated with sulfonium salts (Figure 16).

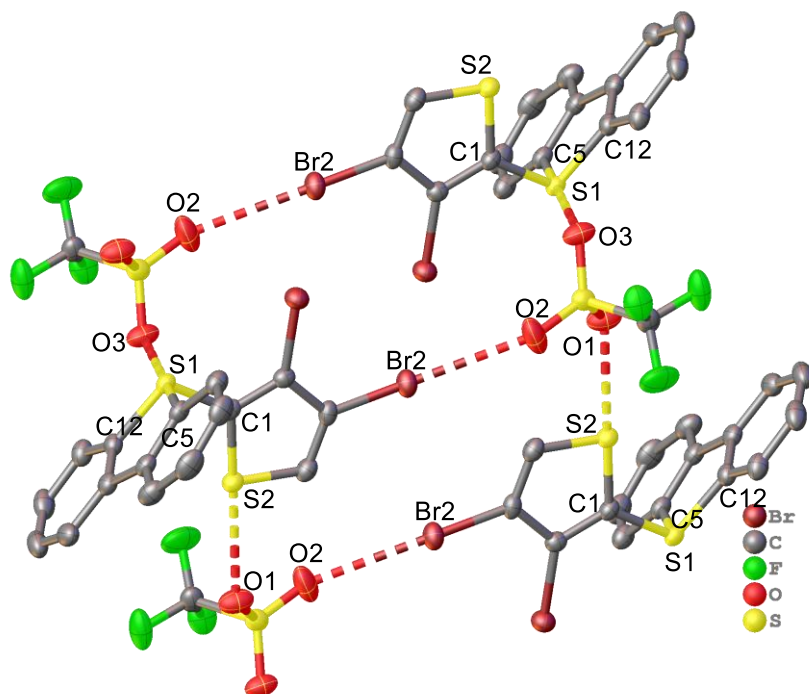


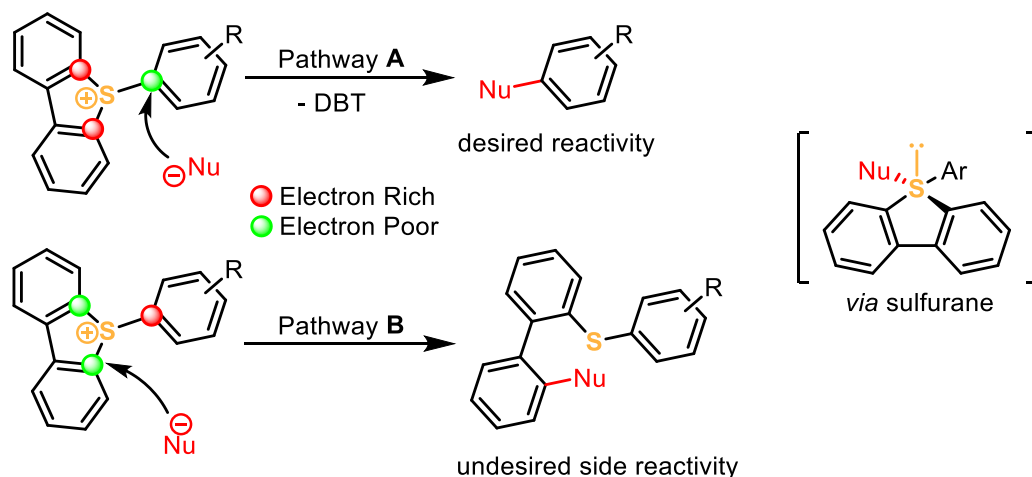
Figure 16: X-Ray structure of **93m** in the solid state. Anisotropic displacement shown at 50% probability level. Hydrogen atoms were omitted for clarity. Selected bond lengths [Å] and angles [°]: S1–C1 1.763(3), S1–C5 1.785(3), S1–C12 1.784(3), S2–C1 1.718 (3), S1–O3 3.057(2), S2–O1 2.775(3), Br2–O2 2.978(3), C5–S1–O3 179.7, C1–S2–O1 177.3.

The presence of the halogenated thiophene moiety enables halogen interactions between Br2 and O2 from the triflate anion which are much shorter than the sum of the corresponding van-

der-Waals radii. Similar interactions have been described in the solid-state structures shown in Chapter 3.1.2.1. Additionally, a strong triflate contact to the thiophene sulfur is present (S2–O2 2.775 Å) which is even shorter than the triflate contact to the sulfonium center (S1–O3 3.057 Å). The aforementioned interactions cause a polymeric structure of **93m** in the solid state.

3.4.3. Nucleophilic Aromatic Substitution of *S*-(Aryl)sulfonium Triflates

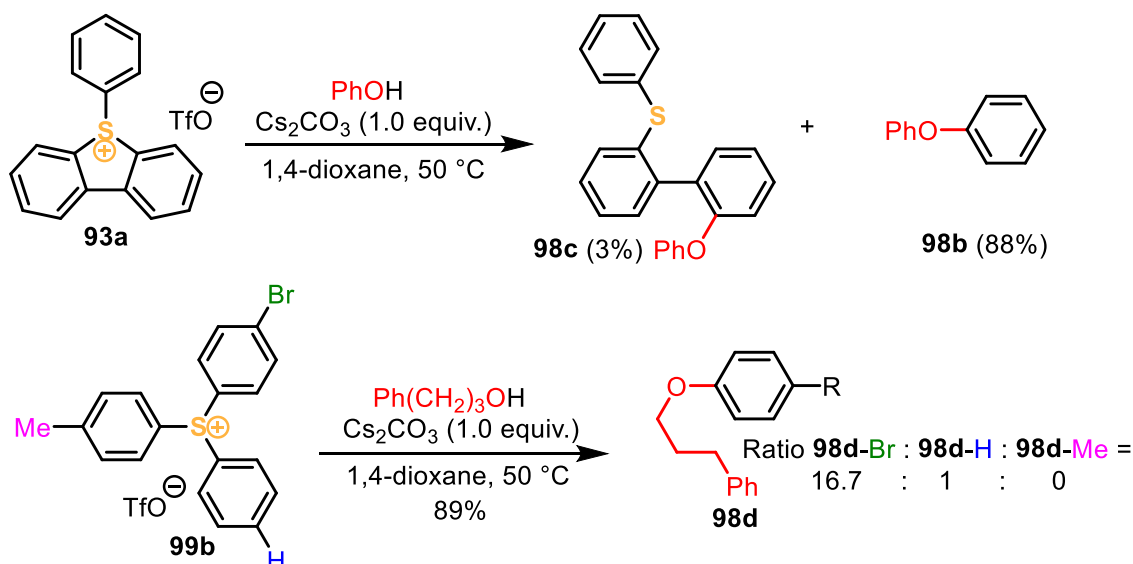
With the set of *S*-(aryl)sulfonium salts in hand, the reactivity towards nucleophiles was tested. A nucleophilic aromatic substitution in explicitly the exocyclic aryl position was envisioned (Scheme 86, Pathway A).



Scheme 86: Potential reactivity of *S*-(aryl)dibenzothiophenium triflates in the presence of nucleophiles. Triflate anions were omitted for simplification.

Dibenzothiophene will be then released to form a covalent bond between the nucleophile and the aryl group. Depending on the nature of the sulfonium salt and the nucleophile, the undesired reaction products produced along pathway B can also be observed. Mechanistically it is proposed that the reaction undergoes the formation of a sulfurane, which then forms the product upon a ligand coupling.^{103,157}

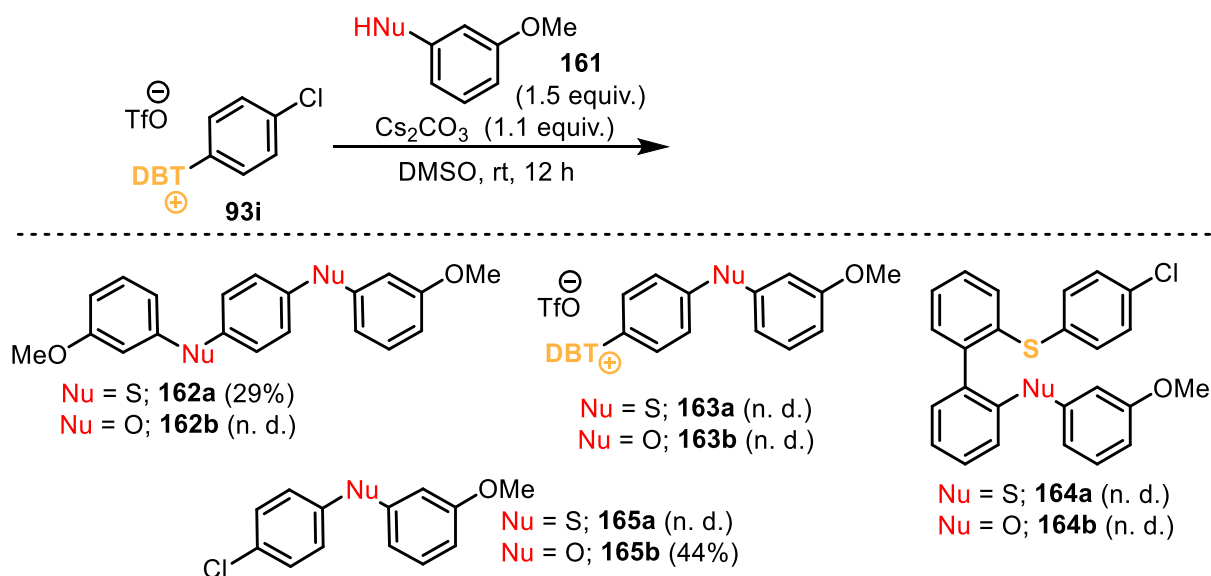
Similar transformations with arylsulfonium salts have been reported before. Scheme 87 shows the strongly related work of Zhang *et al.* which deals with the *O*-arylation under basic conditions.^{161a}



Scheme 87: Base-mediated *O*-arylation with arylsulfonium salts **93a**, **99b**.^{161a}

The transformation from **93a** is of special interest since this salt structurally represents the family of the salts presented in Scheme 81, and undesired **98c** is only observed as a minor product. Additionally, the authors evaluated the electronic influence of the aryl substituents of the arylsulfonium salt. The authors explained the transformation of **99b** as a result of synchronous nucleophilic substitution on the most electron-poor aryl center.

Following the work of Zhang *et al.*, *para*-chloro-substituted compound **93i** was tested as an appropriate dibenzothiophenium salt. Obviously, the electron-withdrawing effect of chlorine should have facilitated the *ipso*-substitution on the sulfonium salt (Scheme 88).



Scheme 88: Reaction of the salt **93i** with phenol and thiophenol under basic condition.

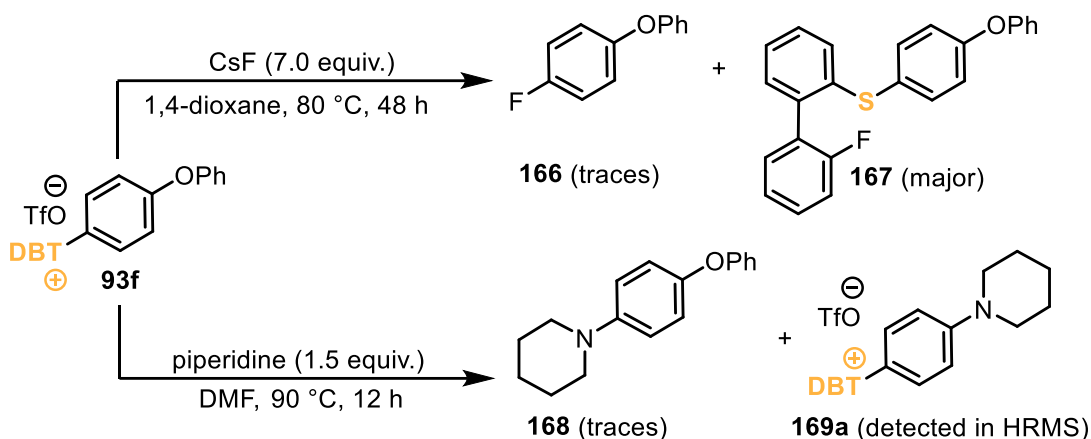
3-Methoxythiophenol (**161a**) and 3-methoxyphenol (**161b**) were used as nucleophiles, and cesium carbonate served as a base. The reaction mixtures were stirred for 12 hours at room temperature. In the first reaction, product **162a** was isolated in 29% yield; however, it remained unclear if its predecessors **163** or **165** were formed first and successively underwent the second *ipso*-substitution. Raising the reaction temperature to 100 °C did not lead to a higher yield of **162a**.

Under identical reaction conditions, reaction with 3-methoxyphenol resulted in 44% of **165b**. No other reaction product could be identified in the reaction mixture. Moreover, none of the additional reaction products could be isolated even when the reaction temperature was raised to 100 °C, while the traces of **162b**, **163b** and **164b** could be detected in HRMS. This result shows that the first nucleophilic attack is more likely to take place at the sulfonium moiety.

The use of other phenols under the same conditions did not result in formation of the corresponding ethers, although these compounds could be detected in HRMS. Because of the unpromising results the reaction conditions were changed, and another sulfonium salt was tested in these nucleophilic aromatic substitution reactions. Nevertheless, it should be mentioned that these results are in accordance with those of Zhang *et al.*. In both cases the most electron poor aromatic position underwent *ipso*-substitution with the nucleophile. Additionally, products from the endocyclic nucleophilic attack could not be observed.

The newly selected substrate should be easily available in gram scale and should have as few *ortho*-substituted impurity as possible. Moreover, the salt must not have substituents which are able to undergo *ipso*-substitutions being themselves the leaving group in this reaction. The sulfonium salt of choice was **93f** (with proportion *p:o* = 33:1), and fluorination and amination reactions were attempted instead of ether and thioether formations (Scheme 89).

Analogously to the *ipso*-fluorination procedure described by Ritter (detailed discussion see in Chapter 1.4.3.1),¹⁵⁷ compound **93f** was treated with an excess of cesium fluoride in 1,4-dioxane at 80 °C over two days. Formation of compound **167** as the main product could be observed, whereas **166** was only detected as traces by GC–MS. This result is in accordance with those of Ritter *et al.*, since the electron density in *para* position to the phenoxy substituent was too high to provide an exocyclic attack of the nucleophile.

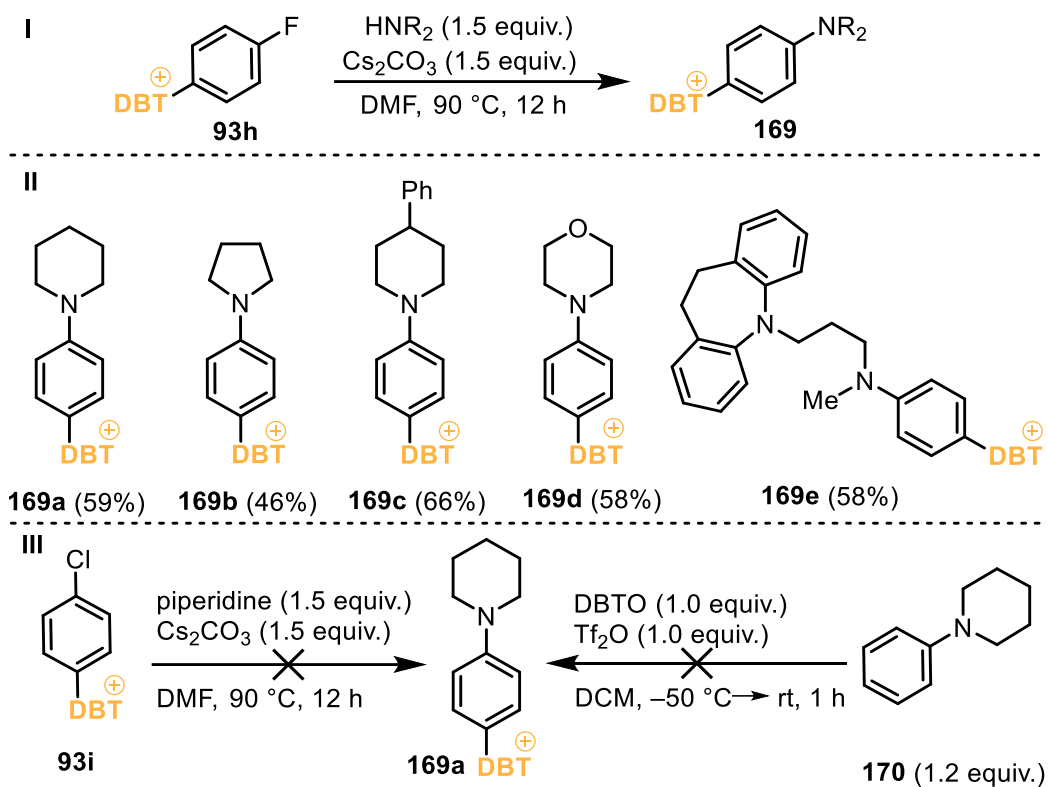


Scheme 89: Attempted fluorination and amination of the salt **93f**.

Just recently Zhang *et al.* published a procedure for transition metal-free *N*-arylation by triarylsulfonium salts.²²² Based on their closely related results, an *ipso*-amination was envisioned (Scheme 89). Unfortunately, only traces of **168** were observed but significant amounts of **169a** could be detected in HRMS.

This observation led to the idea to use the salt **93h** instead of **93f** since it is known that a fluoride anion is a good leaving group in an electron-poor aromatic environment. For example, 1-fluoro-2,4-dinitrobenzene, also known as Sanger's reagent, is used for the selective reaction of free amino groups in terminal amino acids.²²³ Using the good leaving group properties of the fluoride of **93f** the sulfonium salt **169a** was synthesized intentionally which is not accessible in another synthetic way.

Similar reaction conditions than shown in Scheme 89 were applied to **93h**, and product **169a** was isolated in 59% yield. A small scope for the aniline derivatives is presented in Scheme 90, I & II.

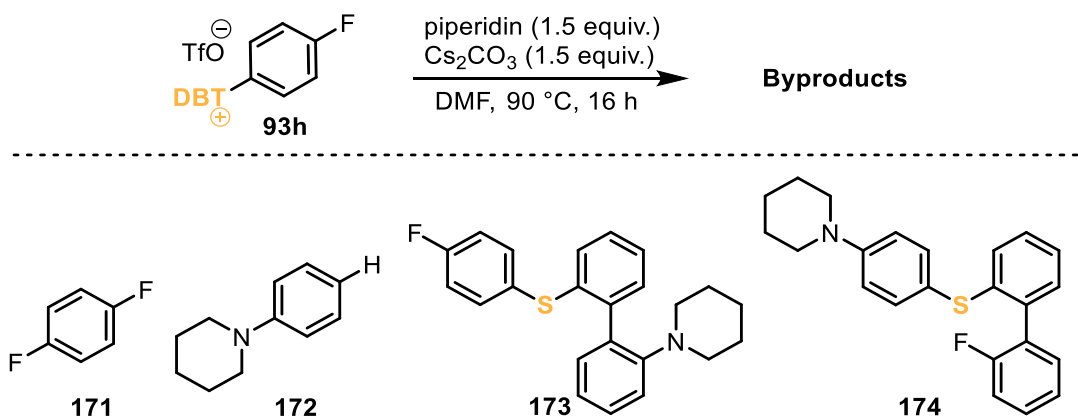


Scheme 90: Scope of the transformations towards anilines **169a–169e**.

The reaction is common for secondary amines. The aniline derivatives **169a–169e** were obtained in yields ranging from 46 to 66%.

Moreover, it was investigated if **169a** can be obtained by *ipso*-substitution from **93i** (Scheme 90, **III**). The presence of the desired sulfonium salt could not be confirmed. Another way to prepare **169a** would obviously be the sulfonylation starting from parent arene **170**, but again the formation of **169a** could not be detected. This observation was confirmed by mechanistic experiments (see Chapter 3.4.5 for detailed explanation), which reveal that too electron-rich aromatic substrates undergo radical pathways instead of electrophilic aromatic substitution reactions.

In every example a significant amount of the starting material was lost during the reaction. Therefore, the side products were qualitatively investigated *via* HRMS; the results are depicted in Scheme 91.



Scheme 91: Side products of the nucleophilic aromatic substitution in aryl fluoride with a secondary amine.

A fluoride ion is released after the nucleophilic attack. As shown in Scheme 89, fluoride is a suitable nucleophile for aromatic substitutions. This explains the formation of side products **171** and **173**. Moreover, the endocyclic side reactivity at the dibenzothiophene moiety takes place, as can be demonstrated by formation of the products **173** and **174**. The desulfination product of **93h**, aniline **172**, was identified as well. All of these side reactions withdrew a significant portion of starting material and diminish the yields of **169a–169e**.

3.4.3.1. Structure of *S*-(Aryl)dibenzothiophenium Triflates **169c** & **169d**

Structures of **169c** and **169d** in the solid state are shown in Figure 17.

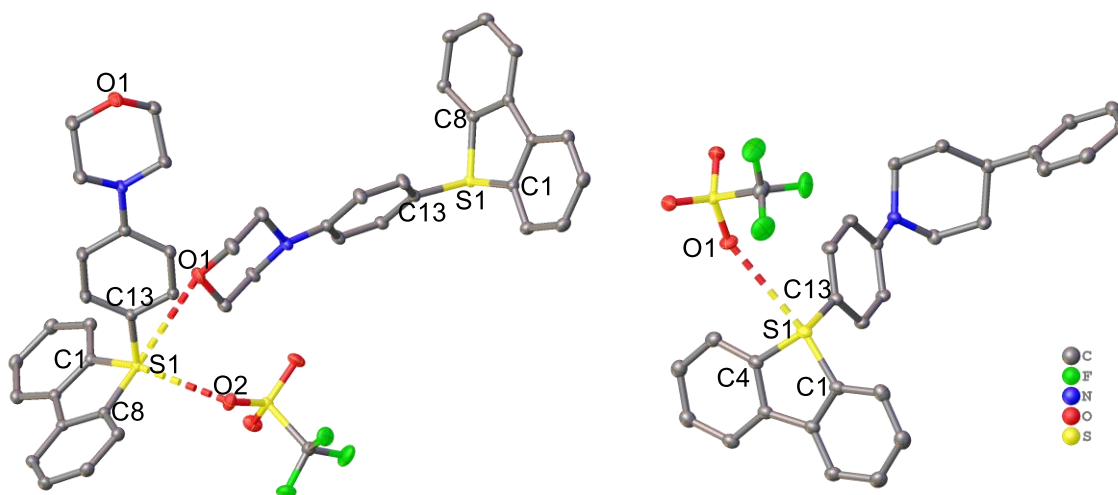


Figure 17: X-Ray structure of the salts **169d** (left) & **169c** (right) in the solid state. Anisotropic displacement shown at 50% probability level. Hydrogen atoms were omitted for clarity. **169d**, selected bond lengths [Å] and angles [°]: S1–C1 1.7785(9), S1–C8 1.7830(9), S1–C13 1.7592(10), S1–O1 3.4837(8), S1–O2 3.100(9), C8–S1–O1 177.3, C1–S1–O2 161.0. **169c**, selected bond lengths [Å] and angles [°]: S1–C1 1.7827(10), S1–C4 1.7846(10), S1–C13 1.7647(9), S1–O1 3.2189(7), C1–S1–O1 163.5.

The salt **169d** adopts a trigonal-bipyramidal geometry around the sulfur center, as expected for a sulfonium salt. Two chalcogen bonds are present, whereas the triflate-sulfonium

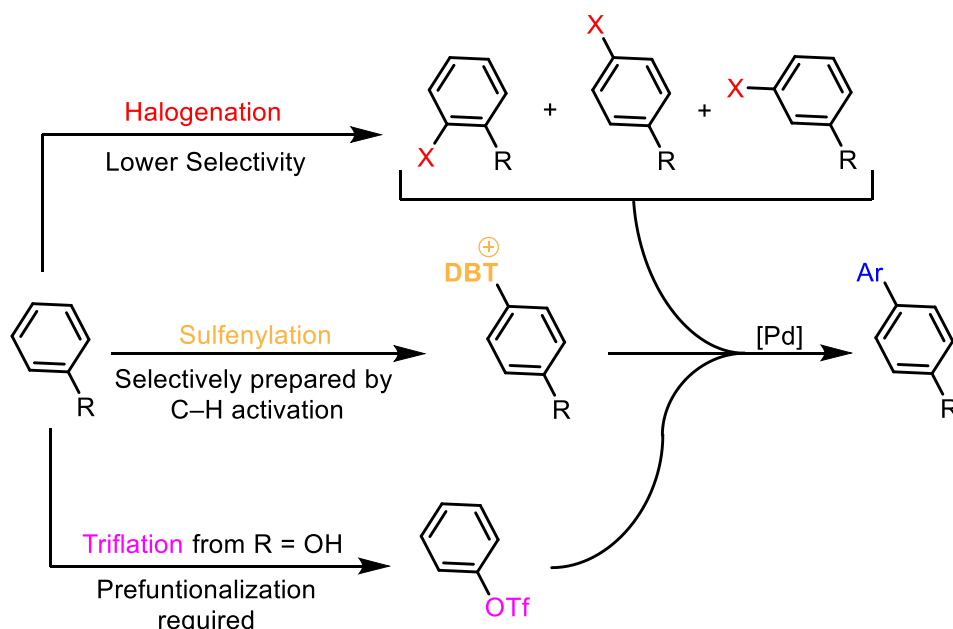
interaction is stronger with the distance of S1–O2 being slightly shorter than the sum of the van-der-Waals radii of the corresponding elements. The second chalcogen interaction is the very weak coordination from the oxygen of the morpholine unit, although it lies in an almost ideal colinear array with C8–S1–O1 being 177.3°.

The rather weak interactions with the sulfonium center indicate moderate Lewis acidity of the sulfur. Therefore, it is no surprise that the sulfonium center does not suffer from the attack of nucleophiles extensively albeit the applied harsh reaction conditions for its synthesis.

The solid-state structure of **169c** shows no unusual features since it crystallizes in a monomeric structure in solid-state and shows no additional interactions. Again, the triflate-sulfonium contact with 3.2189(7) Å being comparatively weak underlines the observation of low susceptibility towards nucleophilic attacks at the sulfur center.

3.4.4. Palladium Catalysis with *S*-(Aryl)sulfonium Triflates

In a classical Suzuki couplings either halogenated²²⁴ or triflated²²⁵ arenes are commonly used. However, the direct selective halogenation of aromatic compounds still remains a challenge up to date (Scheme 92).^{226,227} Triflation of an aromatic substance requires the presence of an OH group in the molecule, and therefore prefunctionalization is needed.²²⁸ It is also known that arylsulfonium salts can serve the same purpose as halides or triflates in Suzuki couplings.¹¹⁵ With the sulfenylation method which is related to the work of Ritter and discussed in Chapter 1.4.1, a selective cross-coupling reaction starting from unfunctionalized arenes is possible in a two-step protocol.^{156,157}



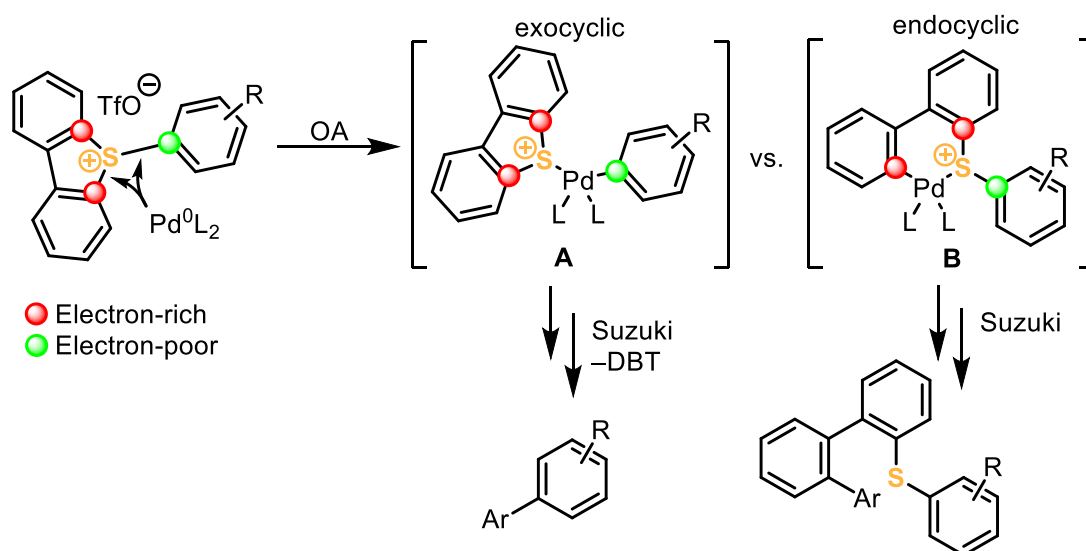
Scheme 92: General halogenation, sulfenylation and triflation strategy.

The utilization of arylsulfonium salts as excellent cross-coupling partners was reported already in the literature (see Chapter 1.4.3.2). However, *S*-(aryl)dibenzothiophenium triflates were not used in transition metal catalysis up to now.

A *S*-(aryl)dibenzothiophenium triflate possesses three *S*-C_{Ar_{yl}} bonds where the palladium center can oxidatively insert (Scheme 93). Statistically the two endocyclic bonds are favored over the exocyclic one with a ratio 2:1. Depending upon the insertion position, different reaction products will be formed. To prevent this, either arylsulfonium salts with the same aryl substituents or with two alkyl groups are used (see Chapter 1.4.3.2). Some transition metal-catalyzed reactions require basic conditions which might convert alkylsulfonium salts into ylides and cause undesired side reactions (see Chapter 1.3).

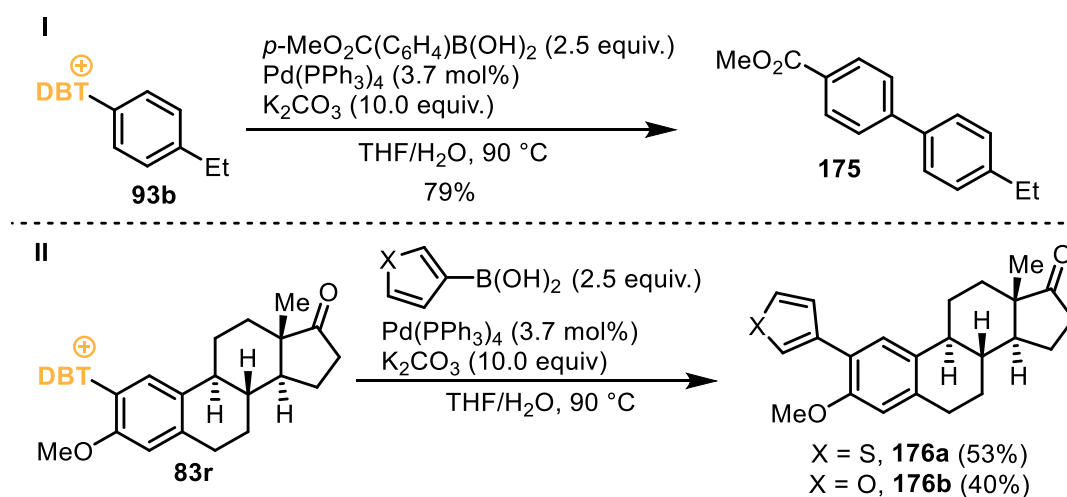
Furthermore, the oxidative addition will most likely take place at the most electron-deficient *S*-C_{Ar_{yl}} bond.²²⁹ The aim of this transformation is the selective coupling of the exocyclic aryl group **A**. If the exocyclic aryl group is more electron-rich than the dibenzothiophenium backbone, palladium species **B** is formed more likely, and the undesired thioether scaffold will be obtained as a byproduct.

The research group of Ritter solved this issue with the thianthrenation of arenes. Here the endocyclic bond of the thianthrenium salt remained unaffected by the transition metal since the second sulfur atom makes the thianthrene backbone more electron-rich compared to the dibenzothiophenium systems.^{159,174}



Scheme 93: Palladium intermediates **A** and **B** towards different reaction products.

With the aforementioned considerations taken into account, a modified procedure from Kotha *et al.* was used for Suzuki-type couplings with *S*-(aryl)sulfonium salts (Scheme 94).²³⁰

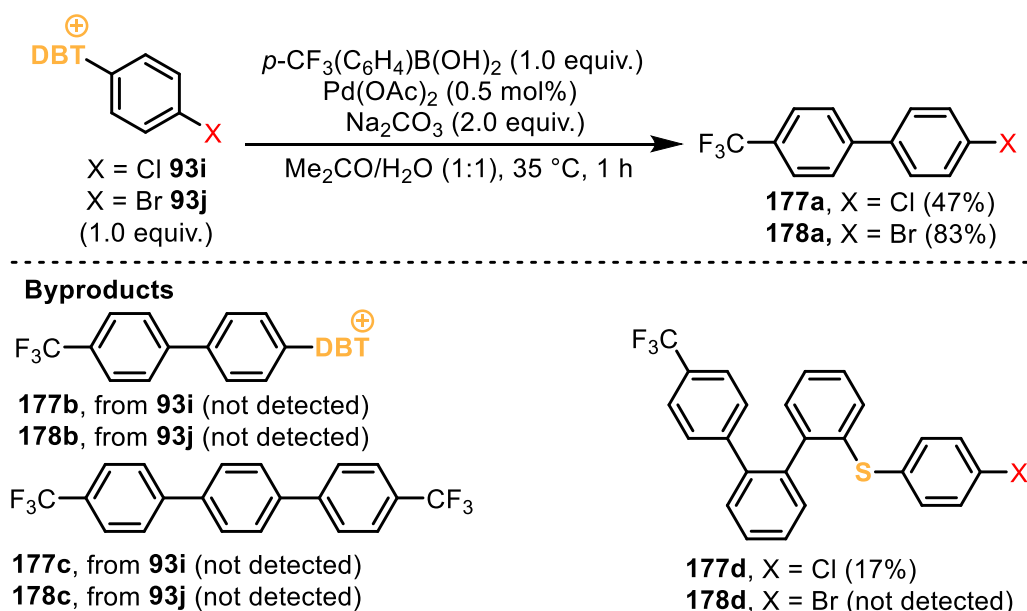


Scheme 94: Initial results for the Suzuki couplings with *S*-(aryl)dibenzothiophenium triflates.

The initial results for Suzuki reactions were quite promising. The salt **93b** was chosen as a simple example and coupled with an electron-poor boronic acid. Compound **175** was obtained in a yield of 79% as the only reaction product (Scheme 94, I). The same reaction was conducted with estrone derivative **93r** as a more complex example (Scheme 94, II). Usually electron-poor boronic acids facilitate Suzuki-Miyaura couplings (SMC) since their boronate species are more stabilized.²³¹ Under the same reaction conditions reactions with electron-richer boronic acids afforded **176a** and **176b** in moderate yields without any side-products.

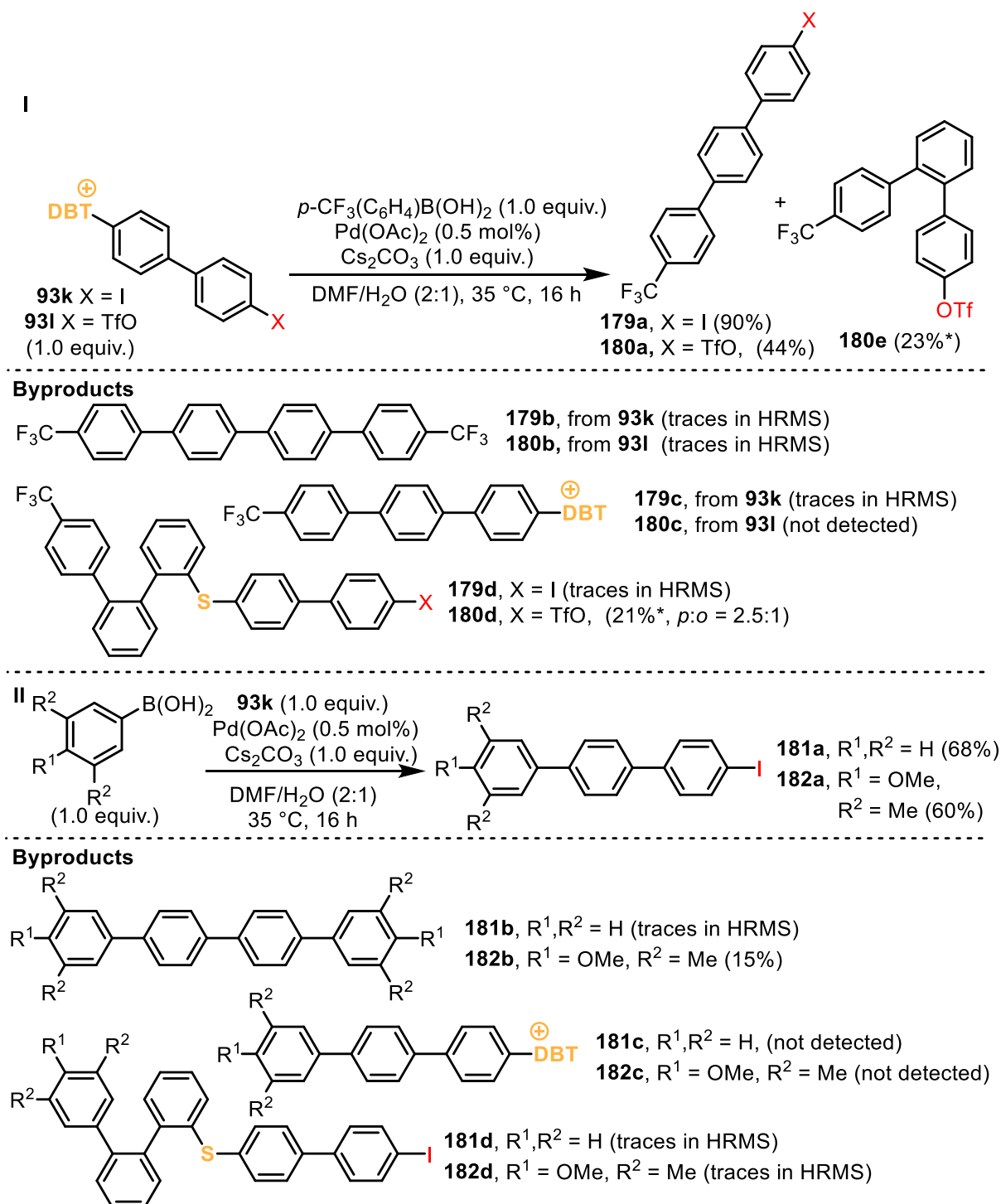
With these initial results in hand, the limitations of the SMC with *S*-(aryl)dibenzothiophenium triflates were explored. A Suzuki protocol with low catalyst loading and mild reaction

conditions was targeted.²³² Furthermore, the limitations of the reaction in presence of an additional (pseudo)halogenide were determined. Arylsulfonium salts **93i** to **93l** were chosen as having a (pseudo)halide and a sulfonium moiety in one molecule. This resulted in a competition of the sulfonium salts versus the (pseudo)halide in the SMC reactions. If exactly one equivalent of the boronic acid and the sulfonium salt was used, the relative reactivity of dibenzothiophenium triflates comparatively to different (pseudo)halides can be estimated by the ratio of the reaction products. As previously described (Scheme 93), four reaction products could be the outcome in this reaction (Scheme 95).



Scheme 95: Reaction conditions for the competitive SMC reactions: sulfonium vs. Cl & Br.

In this reaction 0.5 mol% of $\text{Pd}(\text{OAc})_2$ at 35°C was used. To ensure the solubility of the sulfonium salts at this temperature, the reaction was conducted in a mixture of water and acetone. Chloro-substituted compound **93i** yielded 47% of **177a** and 17% of **177d** after only one hour. The formation of **177b** or **177c** could not be observed, which means 64% of the consumed sulfonium moiety totally. The results obtained with **93j** were better by far, as desired product **178a** was obtained in 83% yield without the formation of side products.



Scheme 96: I) Reaction conditions for the competitive SMC reactions: sulfonium vs. I & TfO. (*could be identified and quantified by ^1H NMR but not separated from other reaction products and not characterized). II) SMC with other boronic acids.

Aryl iodides and triflates are known to be the most reactive coupling partners in Suzuki cross-coupling reactions.²³³ Therefore, the direct competition of a dibenzothiophenium moiety with iodides and triflates would be highly interesting (Scheme 96). Compounds **93k** and **93l** were used under similar conditions as shown in Scheme 95, whereas DMF was used instead of acetone and the reaction time was elongated to 16 h. The advantage of both sulfonium salts

is that both substituents are connected to individual aryl rings which minimize the electronic influence on both substituents *vice versa*. Salt **93k** was converted to **179a** in excellent yield of 91% (Scheme 96, I). Only traces of **179b**, **179c** and **179d** were detected.

Aryl triflate **93l** however delivered inferior results with 44% of product **180a**. Since **93l** is a 7:3 mixture of *para-ortho* isomers by itself, 23% of *ortho-180a* should be present but cannot be isolated and characterized. Product **180c** could not be detected in this case, but significant amounts of side product **180d** (*p:o* = 2.5:1), which unfortunately was inseparable from the *ortho-180a*, was obtained in 21% yield,

The reaction with **93k** was repeated while altering the boronic acid to electroneutral phenylboronic acid (Scheme 96, II). The desired product **181a** was isolated as the main product in 68% yield, and traces of **181b** and **181d** could be detected.

Continuing with an electron-rich boronic acid, product **182a** was isolated again as the main product (60% yield). However, activation of both sides, the iodide and sulfonium salt, did occur as well. By-product **182b** was isolated in 15% yield, and additionally traces of **182d** could be observed.

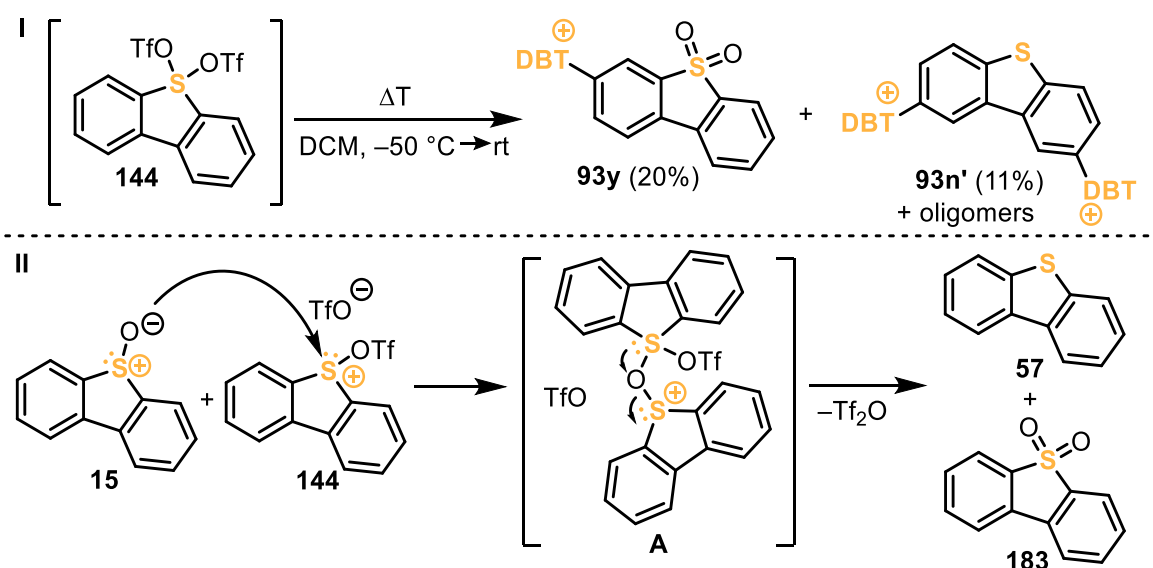
Overall, it can be summarized that dibenzothiophenium salts possess a superior reactivity in comparison to (pseudo)halides, even higher than of iodides and triflates. The chemoselectivity for Suzuki couplings is not only dependent on the aryl substitution pattern, but also on the nature of the boronic acids. Electron-poor boronic acids outperform electron-rich ones in terms of selectivity. Other catalysts and solvent mixtures were not tested. Lower temperatures could potentially enhance chemoselectivity as well. Ritter reported similar results with TFT-functionalized arenes which undergo highly chemoselective SMC reactions in the presence of bromides and triflates (see Chapter 1.4.3.2).

3.4.5. Mechanistic investigation: Preparation of *S*-(Aryl)dibenzothiophenium Triflates

Besides the exploration of scope and limitations for *S*-(aryl)dibenzothiophenium triflates and their applications, a deeper insight into the reaction mechanism towards these sulfonium salts was undertaken. The reaction towards arylsulfonium salts from parenting arenes with non-appropriate electron density shows the formation of side products. According to Ritter *et al.*, a less electron-rich arene than 1,2-dichlorobenzene results in an inefficient arylsulfonium salt

formation, whereas benzofuran defines the upper limit of electron-richness for this reaction.^{2,156,157}

Conducting the sulfenylation with electron-poor examples, the arenes were reisolated and a mixture of byproducts was obtained. Therefore, it was speculated that the electron-poor arenes did not take part in the reaction at all and bistriflate adduct **144** underwent thermally induced side reactions. The attention was focused on **144** which is an orange suspension at – 50 °C. When exposing **144** to elevated temperatures (up to room temperature), the suspension disappeared irreversible affording a yellow solution, and multiple compounds are formed (Scheme 97).



Scheme 97: I) Thermal decomposition of **144**; II) Proposed mechanism towards **57** & **183**.

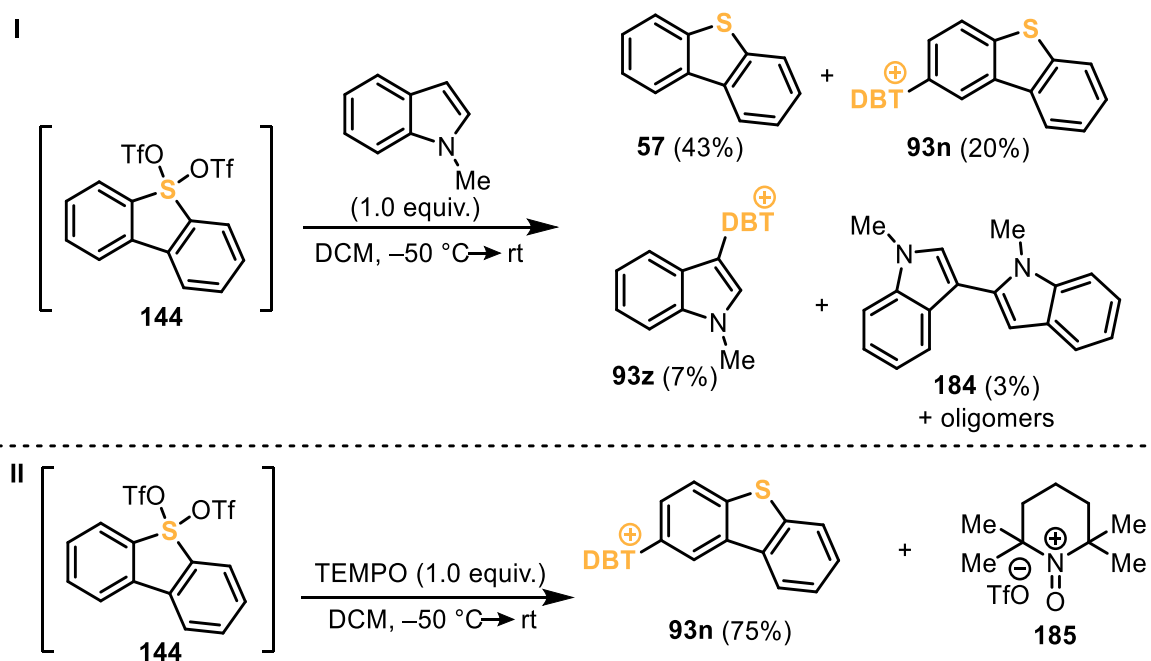
The salt **93y** was isolated in 20% yield along with 11% of **93n'** (Scheme 97, I). Additionally, oligomeric structures related to **93n** bearing up to four positive charges could be observed in HRMS.

The formation of sulfone **93y** suggests that a triflic anhydride induced disproportionation reaction between two dibenzothiophene oxide units, resulting in one equivalent of **57** and **183** (Scheme 97, II). These compounds then undergo the *S*-arylation reaction in the presence of remaining **144**.

The activation of **93y** at the *meta*-position supports the theory that the *S*-arylation reaction follows an electrophilic aromatic substitution mechanism. All EPR monitorings throughout decomposition of **144** did not show any EPR activity; therefore, a radical mechanism towards the formation of *S*-(aryl)dibenzothiophenium triflates is less likely.¹⁵⁹ As an electron-rich

aromatic system, dibenzothiophene **57** is further transformed into **93n'** at the *para*-positions in respect to the sulfur and then into other oligomeric polycationic structures derived from **93n'** via the same mechanism.

Furthermore, the reaction of 1-methylindole was thoroughly investigated. This reactant exceeds the aforementioned upper limitations of the *S*-arylation of **144**, since it is more electron rich than benzofuran (Scheme 98).



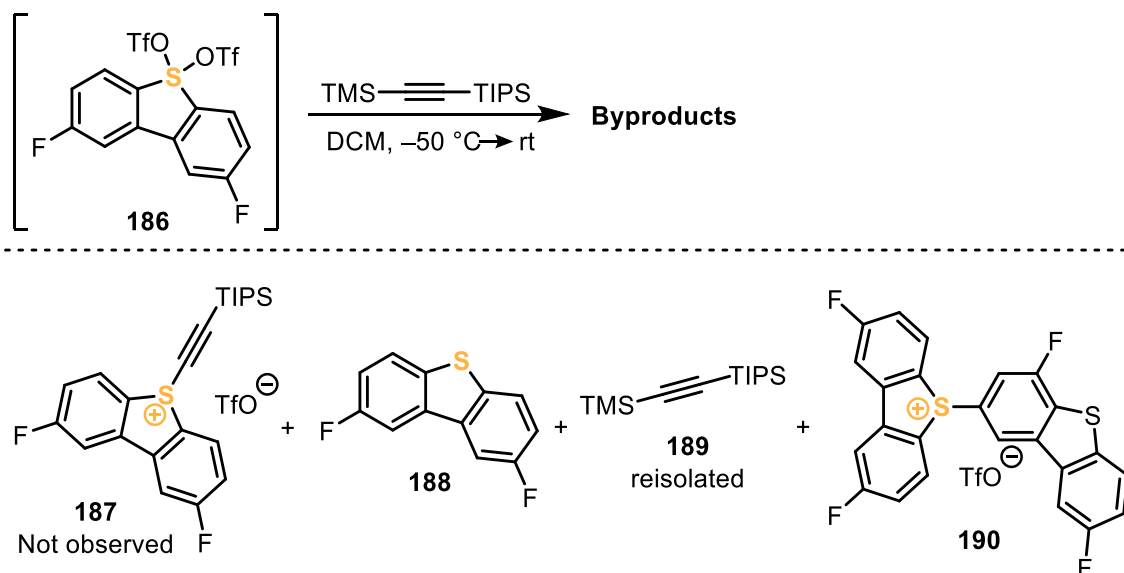
Scheme 98: I) Reactivity of **144** in the presence of electron-rich arenes beyond the limitation gap of benzofuran. II) Reaction of **144** with TEMPO.

Besides formation of **93n** and dibenzothiophene **57**, the sulfenylation took place in the 3-position of the indole and yielded **93z** in 7% (Scheme 98, I; characterization of **93z** can be found in ¹⁵⁶). As an electron-rich aromatic compound, the indole is able to dimerize under abstraction of an electron. Therefore, **184** is formed in small amounts including oligomeric structures derived from **184**.

To confirm that a SET reaction with **144** is possible, **144** was treated with TEMPO (Scheme 98, II). Indeed, product **93n** (75% yield) as well as oxoammonium triflate **185** were isolated from the reaction mixture.

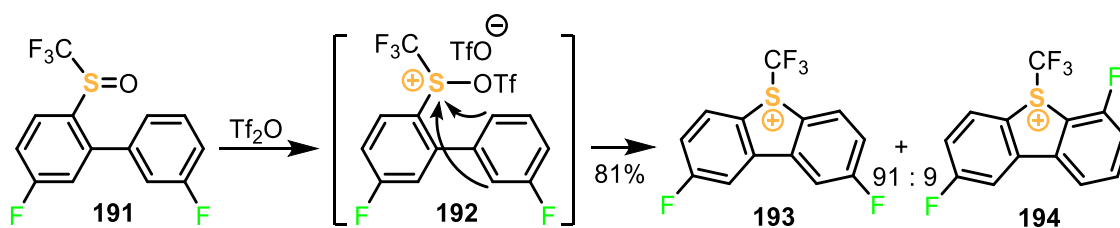
Originally, it was envisioned that the reaction of difluorosubstituted dibenzothiophene oxide derived from **188** with triflic anhydride as activator yields *S*-(alkynyl)sulfonium salt **187** (Scheme 99). However, the desired compound could not be obtained, albeit large amounts of

188 and **189** were reisolated. Additionally, small amounts of **190** were crystallized from the reaction mixture, and its structure was determined by X-ray crystallography.



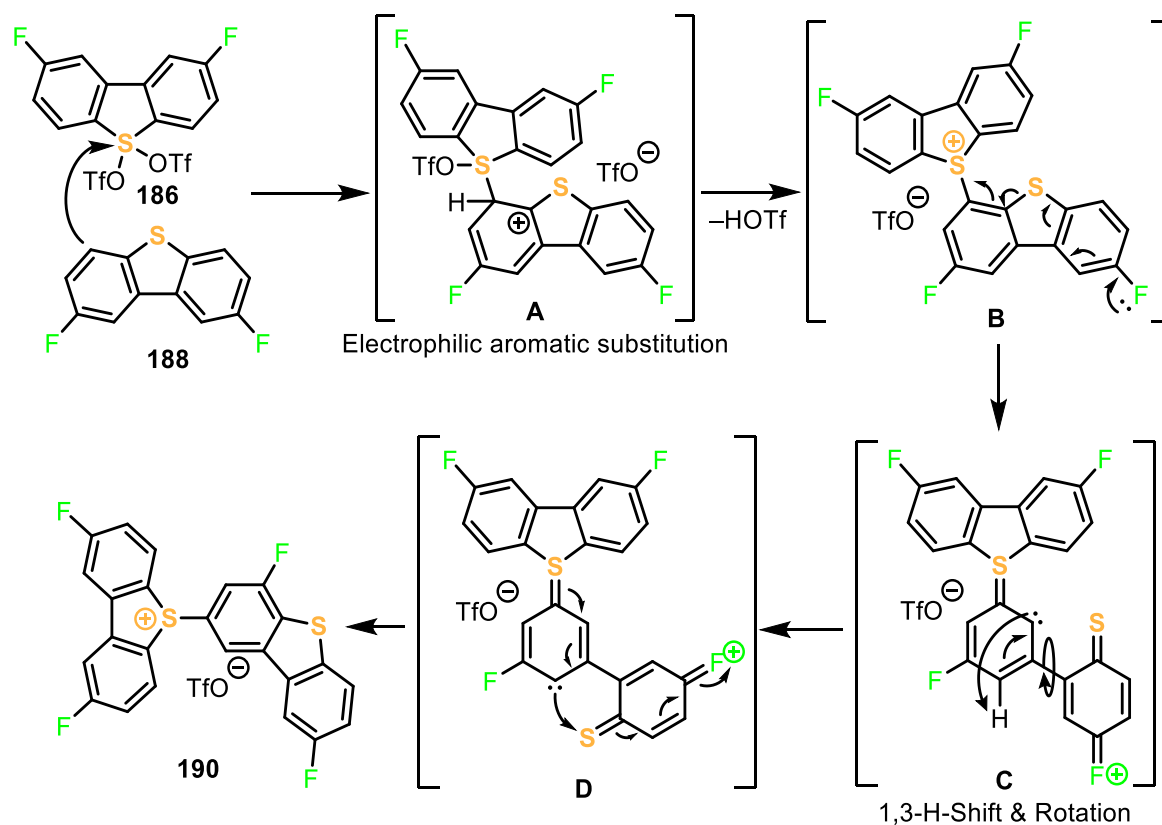
Scheme 99: Reaction outcome from **186** with TMS-capped TIPS-acetylene.

Remarkably, one of the fluoride substituents in **190** changed the position from *para* to *ortho* in respect to the sulfur. Umemoto *et al.* observed a similar structural motif in the synthesis of fluoride-decorated *S*-(trifluoromethyl)dibenzothiophenium triflates (Scheme 100) although the isomer formation has a different origin than in the case of **190**.²³⁴ The authors proposed a mechanism starting from **192** which involved two possible attacks from both *ortho*-positions of the aromatic system which form the five membered heterocycles **193** and **194**.



Scheme 100: Transformation of sulfoxide **191** towards **193** and **194**, as reported by Umemoto.

With this information in hand, a mechanistic rationalization towards the formation of **190** is proposed and presented in Scheme 101.



Scheme 101: Proposed mechanism towards **190**. Compound **188** is formed *via* the disproportionation reaction analogously to **57**.

Ditriflate **186**, as the activated electrophilic intermediate from the parent sulfoxide, reacts with **188** towards intermediate **A** which is formed by the disproportionation reaction described in Scheme 97. Intermediate **A** then releases one equivalent of triflic acid by rearomatization and delivers sulfonium salt **B**. The positive mesomeric effect of the fluoride causes a C–S bond cleavage and generates intermediate **C**. This non-cyclic intermediate underwent rotation of the aromatic group, and intermediate **D** is formed after the hydrogen 1,3-shift. Cyclization in **D** accompanied by aromatization with *ortho*-migration of the C–S bond afforded *S*-(aryl)sulfonium salt **190**.

3.4.5.1. Structure of *S*-(Aryl)-2,7-difluorodibenzothiophenium Triflate **190**

The structure of **190** in the solid state is shown in Figure 18.

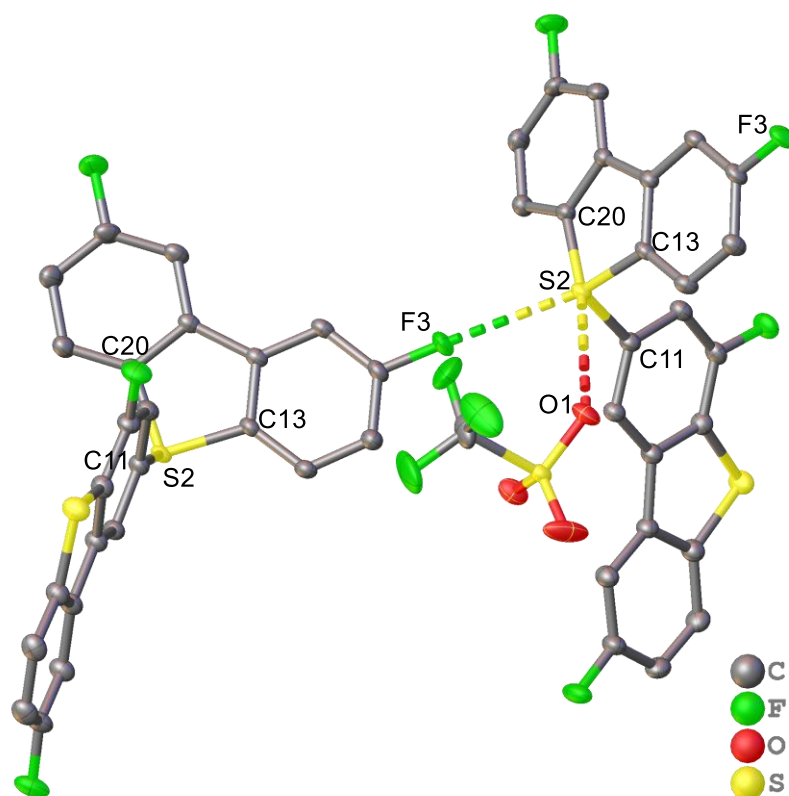
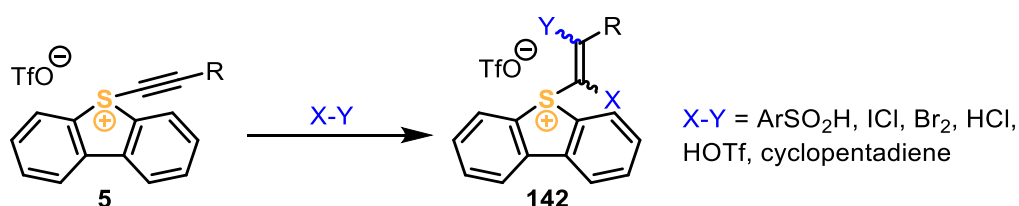


Figure 18: X-Ray structure of **190** in the solid state. Anisotropic displacement shown at 50% probability level. Hydrogen atoms were omitted for clarity. Selected bond lengths [Å] and angles [°]: S2–C11 1.7856(14), S2–C13 1.7834(14), S2–C20 1.7840(15), S2–F3 3.1509 (13), S2–O1 3.2386(14), C13–S2–F3 166.0, C20–S2–O1 164.9.

Compound **190** shows two interactions emanating from the sulfonium unit. The distance between the triflate and the sulfur (S2–O1) is slightly shorter than the sum of the van-der-Waals radii of the corresponding elements and this interaction is therefore weak compared to those observed in other dibenzothiophenium triflates. Surprisingly, the aromatic fluoride interacts with the sulfonium center with a bond distance of F3–S2 [3.1509(13) Å] which is shorter than the sum of their van der Waals-radii. This sulfonium salt forms a polymeric structure in the solid state over the S2–F3 interaction.

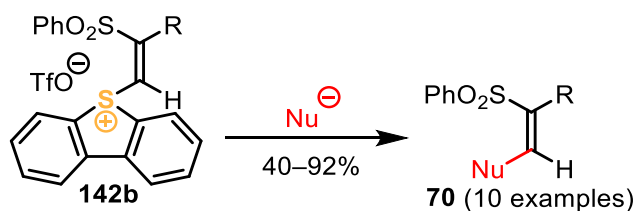
4. Summary

The content of this thesis focused on the general syntheses and applications *S*-substituted alkynyl-, alkenyl- and arylidibenzothiophenium triflates. Inspired by previous results from Alcarazo *et al.*, we investigated the problem if *S*-(alkynyl)dibenzothiophenium triflates can be generated by utilizing terminal alkynes instead of TMS-capped alkynes, as described in well-established protocols.^{11,23} The resultant alkenylsulfonium salt indicates the addition reaction of triflic acid to *S*-(alkynyl)dibenzothiophenium triflate (Scheme 102). This observation led to the idea to perform addition reactions of halogens, acids and Diels-Alder cycloadditions of dienes to the triple bond of *S*-(alkynyl)dibenzothiophenium triflates **5** with the goal to obtain the corresponding alkenylsulfonium salts **142** (Scheme 102).



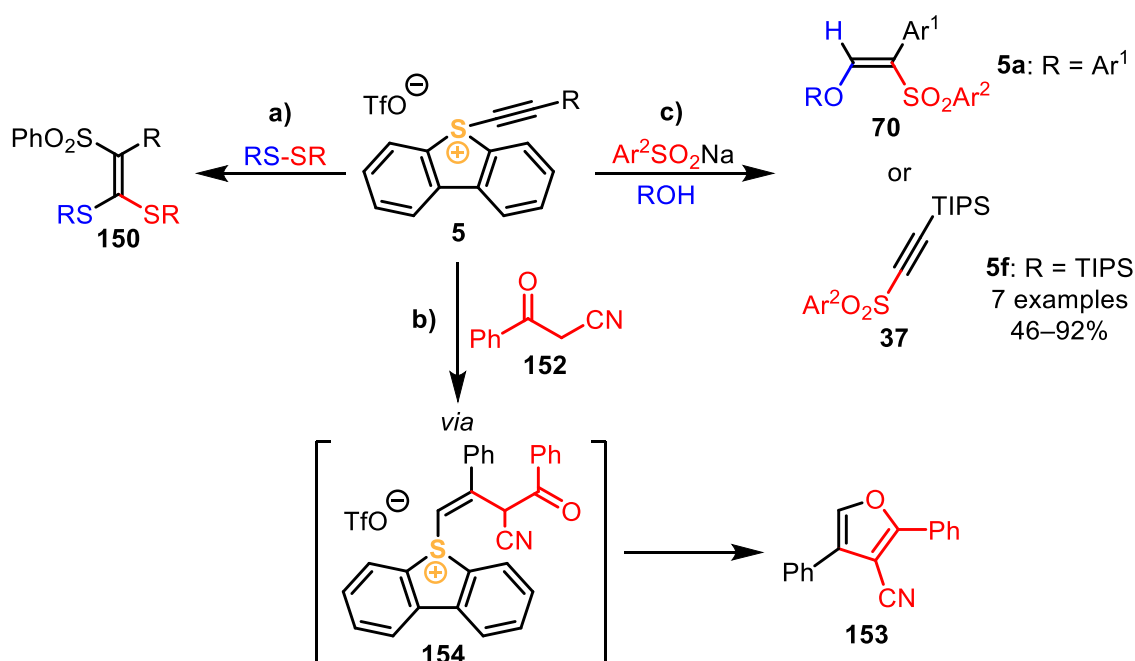
Scheme 102: Addition reactions of *S*-(alkynyl)dibenzothiophenium triflates **5**.

With the successfully synthesized alkenylsulfonium reagents in hand, their abilities as potential Michael-acceptors were tested (Scheme 103).



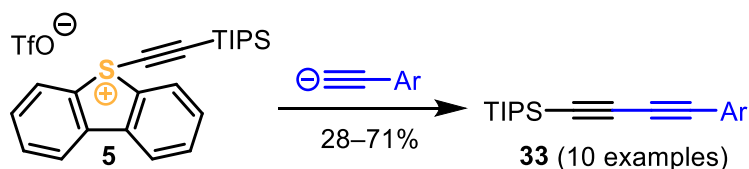
Scheme 103: Michael-type reaction of a generic nucleophile and alkenylsulfonium salts **142b**.

In addition to conventional Michael-type reactions, the reaction of disulfides as Michael-acceptors was also investigated in a one-pot protocol under aprotic conditions (Scheme 104, **a**). The reaction of benzoyl acetonitrile as a nucleophile with *S*-(phenylacetylene)dibenzothiophenium triflate (**5a**) revealed the formation of a furan scaffold *via* an *S*-(alkenyl)dibenzothiophenium triflate intermediate, which could be observed in HRMS (Scheme 104, **b**). These findings are in accordance with prior mechanistic proposals by Alcarazo *et al.*¹¹, which were further supported by the investigation of the chemical behavior of arylsulfonic acid sodium salts in the presence of alkynylation reagents **5a** and **5f** (Scheme 104, **c**).



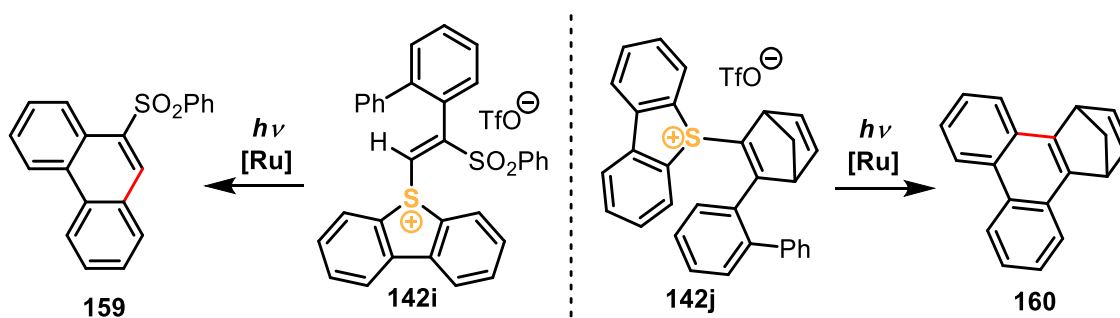
Scheme 104: Reactions of *S*-(alkynyl)sulfonium salts **5** with: a) disulfides, b) sodium arylsulfonates or c) benzoylacetonitrile **152**.

To expand the scope of nucleophiles presented by Alcarazo *et al.*¹¹, a closer look to the diyne formation with acetylides and sulfonium salt **5f** was given. A versatile scope of diynes was demonstrated (Scheme 105).



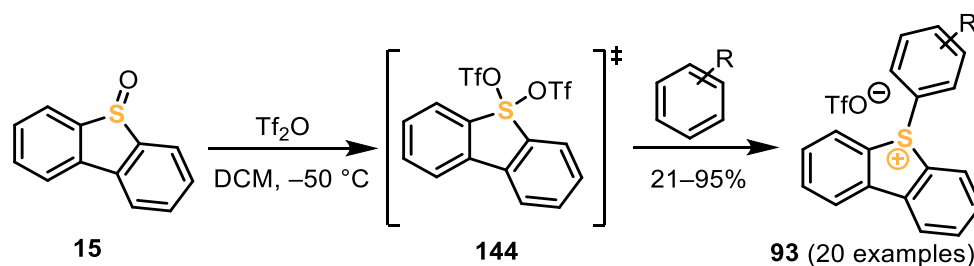
Scheme 105: Simplified reaction of an acetylide with alkylation reagent **5**.

Additionally, it was shown that alkenylsulfonium salts are potent vinyl radical generators under photocatalytic conditions, and with specially designed *S*-(alkenyl)sulfonium salts photocatalytic phenanthrene synthesis was successful (Scheme 106).



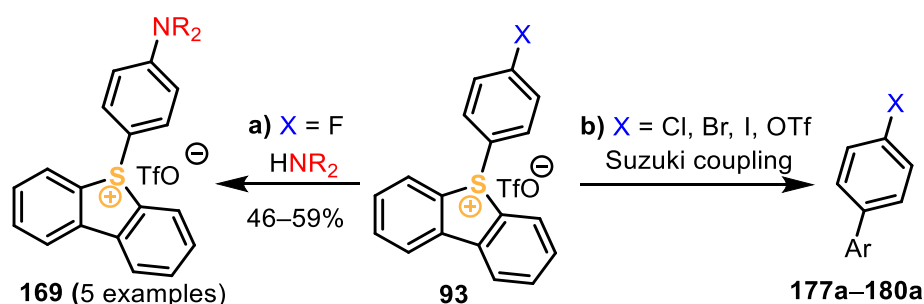
Scheme 106: Photocatalytic formation of phenanthrenes **159** and **160** starting from **142i** and **142j**, respectively.

A synthetic protocol for the preparation of *S*-(aryl)dibenzothiophenium salts **93** starting from inexpensive dibenzothiophene *S*-oxide and simple arenes *via* the *in situ* formation of dibenzothiophenium bistriflate **144** was elaborated (Scheme 107).¹⁵⁶



Scheme 107: Synthesis of *S*-(aryl)dibenzothiophenium triflates **93**.

The scope of the method regarding the nature of the arene was evaluated, intermediates along the reaction sequence have been trapped, and side-reactions identified. Interpretation of these findings enabled a deeper insight into the reaction mechanism for the formation of the desired molecules. Moreover, the X-ray structures of a complete set of these salts were reported and their reactivities studied. *ipso*-Substitution on the fluorobenzene sulfonium salt with *N*-nucleophiles was investigated opening a new synthetic approach to aniline-derivatized sulfonium salts (Scheme 108, **a**). In addition, chemoselective Suzuki coupling with low Pd-catalyst loading under mild conditions was observed with the dibenzothiophenium moiety in the presence of iodides and triflates (Scheme 108, **b**).



Scheme 108: a) *ipso*-Substitution in **93h** with secondary amines; b) Chemoselective Suzuki coupling.

5. Experimental Part

All anhydrous solvents were obtained from a solvent purification system MBSPS7 from M.Braun Intergas-Systeme GmbH. All reactions were carried out under nitrogen atmosphere unless other way stated. IR: JASCO FT-4100 spectrometer, wavenumbers in cm^{-1} . Microwave: Biotage Initiator. MS (EI): Finnigan MAT 8200 (70 eV), ESIMS: Finnigan MAT 95, accurate mass determinations: Bruker APEX III FT-MS (7 T magnet). GC-MS: Reactions were monitored by GC-MS on Agilent Technologies 7820A gas chromatography system coupled with an Agilent Technologies 5977 E MSD EI-MS detector.

NMR: Spectra were recorded on a Bruker AV 500, 400 or DPX 300; ^1H and ^{13}C chemical shifts (δ) are given in ppm using the residual solvent signals and were converted to the TMS scale; coupling constants (J) in Hz. All flash chromatography was performed using a Biotage One automated column chromatography system on CHROMABOND[®] Flash BT 15g (or 25g) SiOH 40-63 μm from Macherey-Nagel. Thin layer chromatography (TLC) analysis was performed using POLYGRAM[®] SIL G/UV₂₅₄ TLC plates from Macherey-Nagel; visualization by UV irradiation and/or phosphomolybdic acid staining. All commercially available compounds (Acros, ABCR, Alfa Aesar, Aldrich, Fluorochem, TCI) were used as received.

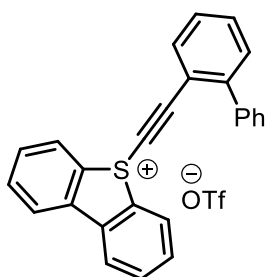
All not-commercially available known compounds were either synthesized according to literature procedures or their analytical data compared to the indicated literature.

Crystal structure analysis: Data collection was performed on a Bruker D8 Venture four-circle-diffractometer from Bruker AXS GmbH; used detector: Photon II from Bruker AXS GmbH; used X-ray sources: microfocus $1\mu\text{S}$ Cu/Mo from Incoatec GmbH with mirror optics HELIOS and single-hole collimator from Bruker AXS GmbH.

Used programs: APEX3 Suite (v2017.3-0) and therein integrated programs SAINT (Integration) und SADABS (Absorption correction) from Bruker AXS GmbH; structure solution was done with SHELXT, refinement with SHELXS₂; OLEX2 was used for data finalization.

5-([1,1'-Biphenyl]-2-ylethynyl)-5*H*-dibenzo[*b,d*]thiophen-5-ium

Trifluoromethanesulfonate (5j):

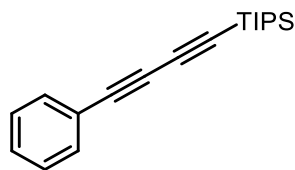


A Schlenk flask was charged with a stirring bar and dibenzo[*b,d*]thiophen oxide (1.0 g, 4.99 mmol, 1.0 equiv.). The reaction vessel was purged with nitrogen and anhydrous DCM (40 mL) was added. The reaction mixture was cooled down to $-50\text{ }^{\circ}\text{C}$ and stirred for 5 min. Tf_2O (0.91 mL, 4.99 mmol, 1.0 equiv.) was added dropwise and the resulting orange suspension was stirred for 10 minutes. Afterwards ([1,1'-biphenyl]-2-ylethynyl)trimethylsilane (1.25 g, 5.99 mmol, 1.2 equiv.) was added in one portion and the reaction mixture was warmed up to room temperature over 15 min. The solvent was evaporated to a small fraction, the crude compound precipitated with diethyl ether (25 mL) and successively washed with diethyl ether (2 x 25 mL). After drying in *vacuo* the compound was obtained as a yellow solid (2.14 g, 4.19 mmol, 84% yield). $^1\text{H NMR}$ (400 MHz, CD_3CN): δ = 8.27 – 8.22 (m, 4H), 7.95 (td, J = 7.6, 1.0 Hz, 2H), 7.81 – 7.74 (m, 3H), 7.68 – 7.63 (m, 1H), 7.49 – 7.45 (m, 2H), 7.30 – 7.25 (m, 3H), 7.18 – 7.13 (m, 2H) ppm. $^{13}\text{C NMR}$ (101 MHz, CD_3CN): δ = 147.3, 140.1, 139.4, 135.9, 135.5, 134.1, 133.1, 131.3, 130.9, 129.6, 129.32, 129.30, 128.92, 128.90, 125.7, 122.1 (q, $^1J_{\text{C-F}}$ = 322 Hz), 116.9, 106.1 ppm. IR (ATR): $\tilde{\nu}$ = 3088, 2177, 1447, 1274, 1253, 1224, 1159, 1028, 758, 638 cm^{-1} . HRMS (ESI) *calcd* for $\text{C}_{26}\text{H}_{17}\text{S}^+$ [M-OTf] $^+$ m/z : 361.1046; found: 361.1045.

General Procedure for the Synthesis of Compounds 33a-33m

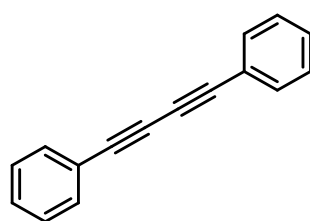
The corresponding terminal alkyne (0.2 mmol) was dissolved in anhydrous DCM (2 mL, 0.1 M) under inert atmosphere. LiHMDS (0.2 mL of 1 M solution in THF, 0.2 mmol, 1.0 equiv.) was added at $-78\text{ }^{\circ}\text{C}$ under stirring. The reaction mixture was allowed to warm up to $0\text{ }^{\circ}\text{C}$ and stirred for 5 min. Successively it was cooled back to $-78\text{ }^{\circ}\text{C}$, and the transfer reagent **5f** (103 mg, 0.2 mmol, 1.0 equiv.) was added in one portion. The reaction mixture was warmed up to room temperature and stirred for an additional 10 min. The reaction was quenched with water and extracted with EtOAc (3 x 5 mL). After drying over Na_2SO_4 the solvent was evaporated. The product was isolated by column chromatography (pentane) or HPLC.

Triisopropyl(phenylbuta-1,3-diyne-1-yl)silane (33a):



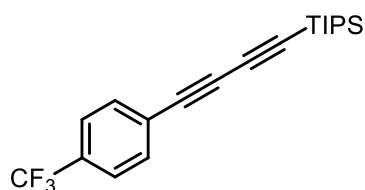
Diyne **33a** was obtained as a colorless oil in 52% yield. $^1\text{H NMR}$ (300 MHz, CDCl_3): $\delta = 7.54 - 7.49$ (m, 2H), $7.39 - 7.28$ (m, 3H), 1.12 (s, 21H) ppm. $^{13}\text{C NMR}$ (75 MHz, CDCl_3): $\delta = 132.8, 129.4, 128.5, 121.7, 89.6, 88.0, 75.7, 74.8, 18.7, 11.5$ ppm. **IR** (neat): $\tilde{\nu} = 2943, 2865, 2202, 2101, 1459, 1017, 879, 755, 677, 602$ cm^{-1} . **HRMS** (EI) *calcd for* $\text{C}_{19}\text{H}_{26}\text{Si}^+$ $[\text{M}]^+$ m/z : 282.1798; found: 282.1788. Analytical data are identical to the previously reported ones.⁵¹

1,4-Diphenylbuta-1,3-diyne (33a'):



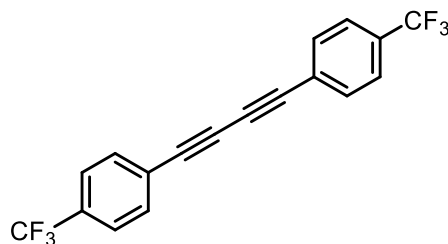
Was isolated as a homocoupling by-product of **33a** and obtained as colorless needles in 13% yield. $^1\text{H NMR}$ (300 MHz, CDCl_3) $\delta = 7.54$ (dd, $J = 7.5, 1.9$ Hz, 2H), 7.35 (d, $J = 7.2$ Hz, 3H). $^{13}\text{C NMR}$ (75 MHz, CDCl_3): $\delta = 132.5, 129.2, 128.4, 121.8, 81.6, 76.6$ ppm. **HRMS** (EI) *calcd for* $\text{C}_{16}\text{H}_{10}^+$ $[\text{M}]^+$ m/z : 202.0777; found: 202.0781. Analytical data corresponds to those reported in literature.²³⁵

Triisopropyl{[4-(trifluoromethyl)phenyl]buta-1,3-diyne-1-yl}silane (33b):



Was obtained as a colorless oil in 38% yield. $^1\text{H NMR}$ (300 MHz, CDCl_3): $\delta = 7.64 - 7.55$ (m, 4H), 1.12 (m, 21H) ppm. $^{19}\text{F NMR}$ (282 MHz, CDCl_3): $\delta = -63.0$ ppm. $^{13}\text{C NMR}$ (125 MHz, CDCl_3): $\delta = 133.0, 131.1, 125.7, 125.5$ (q, $^3J_{\text{C-F}} = 3.9$ Hz), $122.1, 89.9, 89.1, 77.0, 74.0, 18.7, 11.4$ ppm. **IR** (neat): $\tilde{\nu} = 2945, 2865, 2103, 1612, 1462, 1316, 1126, 1064, 841, 594$ cm^{-1} . **HRMS** (EI) *calcd for* $\text{C}_{20}\text{H}_{25}\text{F}_3\text{Si}^+$ $[\text{M}]^+$ m/z : 350.1672; found: 350.1675. The compound was reported in literature although its analytical data is not provided.²³⁶

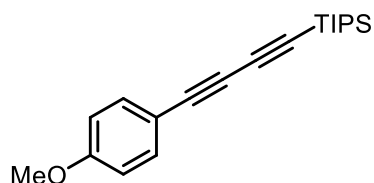
1,4-Bis[4-(trifluoromethyl)phenyl]buta-1,3-diyne (33b'):



Was isolated as a homocoupling by-product of **33b** & **33n** (see Chapter 3.3) and obtained as colorless crystals in 1% yield. $^1\text{H NMR}$ (300 MHz, CDCl_3): $\delta = 7.71 - 7.53$ (m, 8H) ppm. $^{19}\text{F NMR}$ (282 MHz, CDCl_3): $\delta = -63.0$ ppm. $^{13}\text{C NMR}$ (75 MHz, CDCl_3): $\delta = 133.0, 131.1$ (q, $^2J_{\text{C-F}} = 34.1$ Hz), 125.6 (q, $^3J_{\text{C-F}} = 3.8$ Hz), 125.4 (q, $^4J_{\text{C-F}} = 1.5$ Hz), 123.6 (q, $^1J_{\text{C-F}} = 256$ Hz), $81.1, 75.8$. **HRMS** (EI)

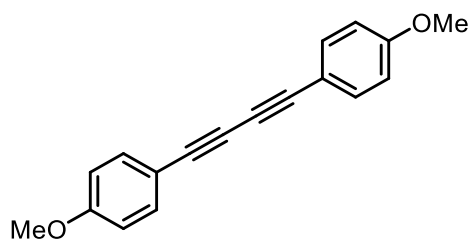
calcd for C₁₈H₈F₆⁺ [M]⁺ *m/z*: 338.0525; found: 350.0533. Analytical data corresponds to those reported in the literature.²³⁷

Triisopropyl[(4-methoxyphenyl)buta-1,3-diyn-1-yl]silane (33c):



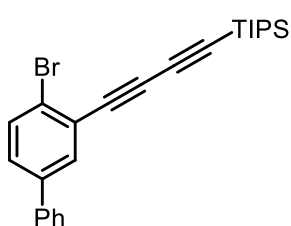
Was obtained as a yellow oil in 28% yield (*cf.* 52% with 1.0 equiv. of CuCN according to the literature procedure²¹⁹). ¹H NMR (300 MHz, CDCl₃): δ = 7.48 – 7.41 (m, 2H), 6.86 – 6.81 (m, 2H), 3.81 (s, 3H), 1.11 (s, 21H) ppm. ¹³C NMR (75 MHz, CDCl₃): δ = 160.5, 134.5, 114.3, 113.6, 89.9, 87.2, 75.9, 73.7, 55.5, 18.7, 11.5 ppm. IR (neat): $\tilde{\nu}$ = 2943, 2862, 2199, 2098, 1502, 1298, 1249, 1171, 830, 671 cm⁻¹. HRMS (EI) *calcd for* C₂₀H₂₈OSi⁺ [M]⁺ *m/z*: 312.1903; found: 312.1904. Analytical data corresponds to those reported in the literature.²³⁸

1,4-Bis(4-methoxyphenyl)buta-1,3-diyne (33c'):



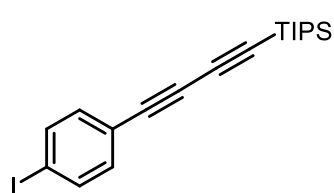
Was isolated as a homocoupling by-product of **33c** & **33m** and obtained as colorless needles in 34% yield. ¹H NMR (300 MHz, CDCl₃): δ = 7.46 (d, *J* = 8.9 Hz, 4H), 6.85 (d, *J* = 8.9 Hz, 4H), 3.82 (s, 6H) ppm. ¹³C NMR (75 MHz, CDCl₃): δ = 160.2, 134.0, 114.1, 114.0, 81.2, 72.9, 55.4 ppm. HRMS (EI) *calcd for* C₁₈H₁₄O₂⁺ [M]⁺ *m/z*: 262.0988; found: 262.0989. Analytical data corresponds to those reported in the literature.²³⁵

{(4-Bromo-[1,1'-biphenyl]-3-yl)buta-1,3-diyn-1-yl}triisopropylsilane (33d):



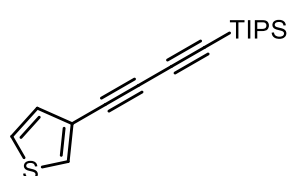
Was obtained as a colorless oil in 58% yield. ¹H NMR (300 MHz, CDCl₃): δ = 7.77 (d, *J* = 2.2 Hz, 1H), 7.63 (d, *J* = 8.4 Hz, 1H), 7.56 – 7.51 (m, 2H), 7.47 – 7.37 (m, 4H), 1.13 (s, 21H) ppm. ¹³C NMR (75 MHz, CDCl₃): δ = 140.5, 139.0, 133.4, 133.0, 129.1, 129.1, 128.2, 127.0, 125.1, 124.5, 90.1, 89.3, 79.0, 73.8, 18.7, 11.5 ppm. IR (neat): $\tilde{\nu}$ = 2940, 2862, 2098, 1464, 1238, 1014, 882, 760, 695, 607 cm⁻¹. HRMS (EI) *calcd for* C₂₅H₂₉BrSi⁺ [M]⁺ *m/z*: 436.1216; found: 436.1219.

[(4-Iodophenyl)buta-1,3-diyn-1-yl]triisopropylsilane (33e):



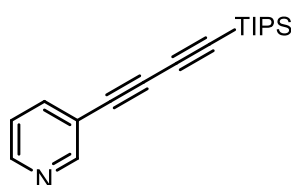
Was obtained as a slightly yellow oil in 71% yield. $^1\text{H NMR}$ (300 MHz, CDCl_3): δ = 7.66 (d, J = 8.6 Hz, 2H), 7.22 (d, J = 8.7 Hz, 2H), 1.11 (s, 21H) ppm. $^{13}\text{C NMR}$ (125 MHz, CDCl_3): δ = 137.8, 134.1, 121.2, 95.7, 89.4, 89.1, 76.2, 74.7, 18.7, 11.4 ppm. **IR** (neat): $\tilde{\nu}$ = 2943, 2865, 2204, 2101, 1462, 1002, 879, 815, 656, 601 cm^{-1} . **HRMS** (EI) *calcd for* $\text{C}_{19}\text{H}_{25}\text{I}\text{Si}^+$ $[\text{M}]^+$ m/z : 408.0765; found: 408.0761.

Triisopropyl(thiophen-3-ylbuta-1,3-diyn-1-yl)silane (33f):



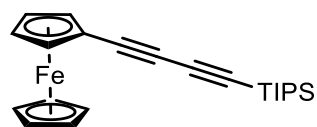
Was obtained as a slightly brown oil in 49% yield. $^1\text{H NMR}$ (300 MHz, CDCl_3) δ = 7.58 (d, J = 4.0 Hz, 1H), 7.26 (dd, J = 4.9, 3.1 Hz, 1H), 7.15 (d, J = 6.1 Hz, 1H), 1.11 (s, 21H). $^{13}\text{C NMR}$ (125 MHz, CDCl_3): δ = 131.7, 130.4, 125.7, 120.8, 89.6, 87.9, 74.5, 70.9, 18.7, 11.5 ppm. **IR** (neat): $\tilde{\nu}$ = 3112, 2940, 2862, 2199, 2101, 1459, 994, 861, 778, 659 cm^{-1} . **HRMS** (EI) *calcd for* $\text{C}_{17}\text{H}_{24}\text{SSi}^+$ $[\text{M}]^+$ m/z : 288.1363; found: 288.1374.

3-[(Triisopropylsilyl)buta-1,3-diyn-1-yl]pyridine (33g):



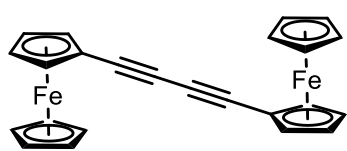
Was obtained as a yellow oil in 63% yield. $^1\text{H NMR}$ (300 MHz, CDCl_3): δ = 8.73 (s, 1H), 8.56 (d, J = 4.2 Hz, 1H), 7.78 (d, J = 7.9 Hz, 1H), 7.29 – 7.22 (m, 1H), 1.11 (s, 21H). $^{13}\text{C NMR}$ (125 MHz, CDCl_3): δ = 153.5, 149.3, 139.6, 123.1, 119.2, 89.9, 89.0, 78.0, 72.2, 18.7, 11.4 ppm. **IR** (neat): $\tilde{\nu}$ = 2940, 2862, 2204, 2106, 1462, 1404, 996, 882, 659, 602 cm^{-1} . **HRMS** (EI) *calcd for* $\text{C}_{18}\text{H}_{25}\text{NSi}^+$ $[\text{M}]^+$ m/z : 283.1751; found: 283.1750.

(Ferrocenylbuta-1,3-diyn-1-yl)triisopropylsilane (33h):



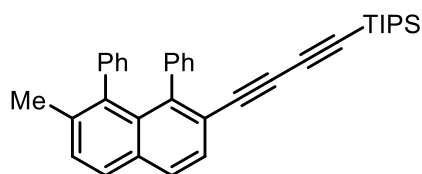
Was obtained as red crystals in 37% yield. $^1\text{H NMR}$ (300 MHz, CDCl_3): δ = 4.50 (q, J = 1.6 Hz, 2H), 4.27 – 4.22 (m, 7H), 1.11 (m, 21H) ppm. $^{13}\text{C NMR}$ (75 MHz, CDCl_3): δ = 90.3, 84.8, 76.0, 72.3, 71.1, 70.2, 69.3, 62.9, 18.6, 11.4 ppm. **IR** (ATR): $\tilde{\nu}$ = 2943, 2865, 2360, 2202, 1462, 996, 884, 820, 659 cm^{-1} . **HRMS** (ESI) *calcd for* $\text{C}_{23}\text{H}_{31}\text{FeSi}^+$ $[\text{M}+\text{H}]^+$ m/z : 391.1539; found: 391.1530. Analytical data corresponds to those reported in the literature.²³⁹

1,4-Diferrocenylbuta-1,3-diyne (33h')



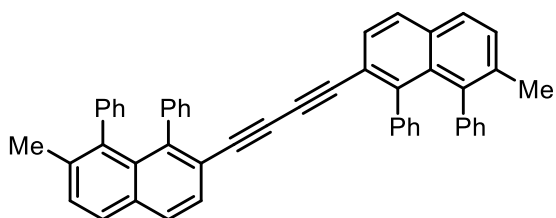
Was isolated as a homocoupling by-product of **33i**. and obtained as red crystals in 21% yield. $^1\text{H NMR}$ (300 MHz, CDCl_3): $\delta = 4.51$ (t, $J = 1.8$ Hz, 4H), 4.26 (d, $J = 6.0$ Hz, 14H) ppm. $^{13}\text{C NMR}$ (75 MHz, CDCl_3): $\delta = 79.2, 72.3, 71.1, 70.3, 69.4, 63.8$ ppm. IR (ATR): $\tilde{\nu} = 2955, 2926, 2865, 2360, 2342, 1732, 1462, 856, 841, 666$ cm^{-1} . HRMS (ESI) *calcd for* $\text{C}_{24}\text{H}_{18}\text{Fe}_2^+$ $[\text{M}]^+$ m/z : 418.0102; found: 418.0100. Analytical data corresponds to those reported in the literature.²⁴⁰

Triisopropyl[(7-methyl-1,8-diphenylnaphthalen-2-yl)buta-1,3-diyn-1-yl]silane (33i):



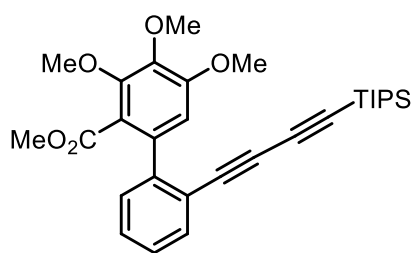
Was obtained as a white solid in 40% yield. $^1\text{H NMR}$ (300 MHz, CDCl_3): $\delta = 7.79$ (d, $J = 8.5$ Hz, 2H), 7.53 (d, $J = 9.6$ Hz, 1H), 7.43 (d, $J = 8.3$ Hz, 1H), 6.92 (d, $J = 4.4$ Hz, 6H), 6.78 (d, $J = 4.9$ Hz, 2H), 6.69 (d, $J = 5.3$ Hz, 2H), 1.99 (s, 3H), 1.02 (s, 21H) ppm. $^{13}\text{C NMR}$ (125 MHz, CDCl_3): $\delta = 145.9, 141.2, 141.0, 139.2, 136.7, 133.2, 131.1, 130.6, 130.6, 129.8, 128.0, 127.79, 127.77, 127.3, 126.9, 126.0, 125.7, 121.7, 89.7, 88.2, 78.5, 76.1, 21.6, 18.5, 11.3$ ppm. IR (ATR): $\tilde{\nu} = 2925, 2851, 2360, 2339, 1735, 1646, 1464, 1173, 1036, 697$ cm^{-1} . HRMS (EI) *calcd for* $\text{C}_{36}\text{H}_{38}\text{Si}^+$ $[\text{M}]^+$ m/z : 498.2737; found: 498.2754.

1,4-Bis(7-methyl-1,8-diphenylnaphthalen-2-yl)buta-1,3-diyne (33i')



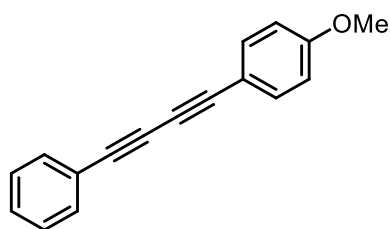
Was isolated as a homocoupling by-product of **33j** and obtained as a white solid in 17% yield. $^1\text{H NMR}$ (300 MHz, CDCl_3): $\delta = 7.74$ (t, $J = 8.3$ Hz, 4H), 7.40 (dd, $J = 8.3, 6.1$ Hz, 4H), 6.94 – 6.81 (m, 12H), 6.70 – 6.60 (m, 8H), 1.96 (s, 6H) ppm. $^{13}\text{C NMR}$ (125 MHz, CDCl_3): $\delta = 145.0, 141.2, 140.9, 139.2, 136.6, 133.0, 131.1, 130.6, 130.4, 129.6, 127.9, 127.7, 127.3, 126.8, 125.9, 125.6, 122.2, 82.4, 77.9, 21.6$ ppm. IR (ATR): $\tilde{\nu} = 3056, 2945, 2865, 2362, 2336, 2199, 2093, 1463, 696, 681$ cm^{-1} . HRMS (ESI) *calcd for* $\text{C}_{50}\text{H}_{35}^+$ $[\text{M}+\text{H}]^+$ m/z : 635.2733; found: 635.2730.

Methyl 3,4,5-Trimethoxy-2'-[(triisopropylsilyl)buta-1,3-diyne-1-yl]-[1,1'-biphenyl]-2-carboxylate (33j):



Was obtained as white crystals in 65% yield. $^1\text{H NMR}$ (300 MHz, CDCl_3): δ = 7.59 (d, J = 9.3 Hz, 1H), 7.38 – 7.25 (m, 3H), 6.86 (s, 1H), 3.97 (s, 3H), 3.92 (s, 3H), 3.91 (s, 3H), 3.58 (s, 3H), 1.07 (s, 21H) ppm. $^{13}\text{C NMR}$ (75 MHz, CDCl_3): δ = 167.5, 154.1, 151.8, 143.8, 141.9, 134.4, 134.1, 129.3, 129.0, 127.6, 121.6, 120.6, 110.4, 89.7, 88.6, 78.3, 74.7, 62.2, 61.1, 56.3, 52.1, 18.7, 11.4 ppm. **IR** (ATR): $\tilde{\nu}$ = 2943, 2688, 2361, 2340, 1733, 1459, 1113, 1030, 878, 756 cm^{-1} . **HRMS** (ESI) *calcd* for $\text{C}_{30}\text{H}_{39}\text{O}_5\text{Si}^+$ $[\text{M}+\text{H}]^+$ m/z : 507.2561; found: 507.2558.

1-Methoxy-4-(phenylbuta-1,3-diyne-1-yl)benzene (33l):

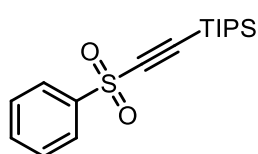


Was obtained as a white solid in 20% yield. $^1\text{H NMR}$ (300 MHz, CDCl_3): δ = 7.56 – 7.44 (m, 4H), 7.34 (d, J = 6.6 Hz, 3H), 6.86 (d, J = 8.8 Hz, 2H), 3.83 (s, 3H) ppm. $^{13}\text{C NMR}$ (75 MHz, CDCl_3): δ = 160.5, 134.3, 132.6, 129.2, 128.6, 122.2, 114.3, 113.9, 82.0, 81.2, 74.3, 72.7, 55.5 ppm. **IR** (ATR): $\tilde{\nu}$ = 2940, 2865, 2199, 2092, 1511, 1246, 1139, 1022, 882, 669 cm^{-1} . **HRMS** (EI) *calcd* for $\text{C}_{17}\text{H}_{12}\text{O}^+$ $[\text{M}]^+$ m/z : 232.0883; found: 232.0889. Analytical data corresponds to those reported in the literature.²⁴¹

General Procedure for the synthesis of Compounds 37a-37h

Transfer reagent **5f** (103 mg, 0.2 mmol, 1 equiv.) and the corresponding sulfinate (0.24 mmol, 1.2 equiv.) were dissolved in DCM (5 mL), and the reaction mixture was stirred for 30 min at ambient temperature on air. The reaction was monitored by TLC. Upon completion of the reaction, pentane (5 mL) was added, and the reaction mixture was transferred directly to a pre-wetted column (hexanes). The pure product was obtained by column chromatography (hexanes).

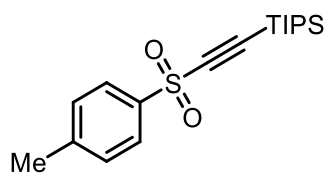
Triisopropyl[(phenylsulfonyl)ethynyl]silane (37a):



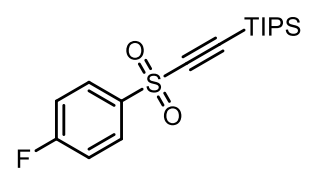
Was obtained as a colorless oil in 89% yield. $^1\text{H NMR}$ (300 MHz, CDCl_3): δ = 8.05 – 8.00 (m, 2H), 7.67 (t, J = 7.4 Hz, 1H), 7.57 (t, J = 7.5 Hz, 2H), 1.16 – 1.00 (m, 21H) ppm. $^{13}\text{C NMR}$ (75 MHz, CDCl_3): δ = 142.3, 134.2,

129.4, 127.3, 101.1, 100.8, 18.5, 11.0 ppm. **IR** (neat): $\tilde{\nu}$ = 2946, 2865, 2360, 2119, 1738, 1335, 1159, 784, 681, 570 cm^{-1} . **HRMS** (EI) *calcd for* $\text{C}_{17}\text{H}_{26}\text{O}_2\text{SSi}^+$ $[\text{M}]^+$ m/z : 322.1417; found: 322.1422. Analytical data corresponds to those reported in the literature.⁵⁸

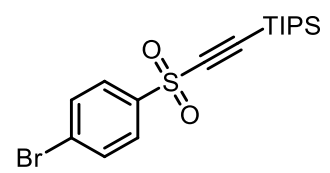
Triisopropyl(tosylethynyl)silane (37b):

 Was obtained as a white solid in 89% yield. **¹H NMR** (400 MHz, CDCl_3): 7.88 (d, J = 8.9 Hz, 2H), 7.35 (d, J = 9.3 Hz, 2H), 2.45 (s, 3H), 1.13 – 1.00 (m, 21H) ppm. **¹³C NMR** (101 MHz, CDCl_3): δ = 145.3, 139.3, 130.0, 127.4, 101.0, 100.2, 21.8, 18.4, 11.0 ppm. **IR** (ATR): $\tilde{\nu}$ = 2942, 2867, 2118, 1461, 1333, 1159, 1084, 771, 670, 545 cm^{-1} . **HRMS** (ESI) *calcd for* $\text{C}_{18}\text{H}_{28}\text{NaO}_2\text{SSi}^+$ $[\text{M}+\text{Na}]^+$ m/z : 359.1472; found: 359.1470. Analytical data corresponds to those reported in the literature.⁵⁸

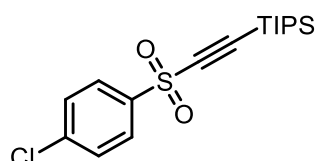
{[(4-Fluorophenyl)sulfonyl]ethynyl}triisopropylsilane (37c):

 Was obtained as a colorless oil in 86% yield. **¹H NMR** (400 MHz, CDCl_3): δ = 8.03 (dd, J = 9.1, 5.0 Hz, 2H), 7.28 – 7.21 (m, 2H), 1.12 – 1.01 (m, 21H) ppm. **¹⁹F NMR** (376 MHz, CDCl_3): δ = -102.45 ppm. **¹³C NMR** (101 MHz, CDCl_3): δ = 167.1 (d, J = 257.5 Hz), 138.3 (d, J = 3.3 Hz), 130.3 (d, J = 9.9 Hz), 116.8 (d, J = 22.8 Hz), 101.3, 100.6, 18.4, 11.0 ppm. **IR** (neat): $\tilde{\nu}$ = 2947, 2864, 2360, 2118, 1592, 1341, 1151, 777, 670, 545 cm^{-1} . **HRMS** (ESI) *calcd for* $\text{C}_{17}\text{H}_{25}\text{FNaO}_2\text{SSi}^+$ $[\text{M}+\text{Na}]^+$ m/z : 363.1221; found: 363.1221. Analytical data corresponds to those reported in the literature.⁵⁸

{[(4-Bromophenyl)sulfonyl]ethynyl}triisopropylsilane (37d):

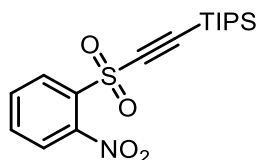
 Was obtained as a white solid in 83% yield. **¹H NMR** (400 MHz, CDCl_3) δ = 7.87 (d, J = 8.8 Hz, 2H), 7.71 (d, J = 8.8 Hz, 2H), 1.13 – 1.01 (m, 21H) ppm. **¹³C NMR** (101 MHz, CDCl_3): δ = 141.2, 132.7, 129.6, 128.9, 101.8, 100.3, 18.5, 11.0 ppm. **IR** (ATR): $\tilde{\nu}$ = 2945, 2867, 2360, 2337, 2121, 1571, 1464, 1338, 1159, 788 cm^{-1} . **HRMS** (ESI) *calcd for* $\text{C}_{17}\text{H}_{29}\text{BrNO}_2\text{SSi}^+$ $[\text{M}+\text{NH}_4]^+$ m/z : 418.0866; found: 418.0864. Analytical data corresponds to those reported in the literature.⁵⁸

{[(4-Chlorophenyl)sulfonyl]ethynyl}triisopropylsilane (37e):

 Was obtained as a white solid in 46% yield. **¹H NMR** (400 MHz, CDCl_3): δ = 7.94 (d, J = 8.9 Hz, 2H), 7.54 (d, J = 8.9 Hz, 2H), 1.13 – 1.01 (m, 21H) ppm. **¹³C NMR** (101 MHz, CDCl_3): δ = 141.0, 140.7,

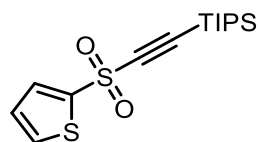
129.7, 128.8, 101.7, 100.4, 18.4, 11.0 ppm. **IR** (ATR): $\tilde{\nu}$ = 2947, 2867, 1734, 1458, 1341, 1165, 1030, 791, 681, 670 cm^{-1} . **HRMS** (ESI) *calcd for* $\text{C}_{17}\text{H}_{25}\text{ClNaO}_2\text{SSi}^+$ $[\text{M}+\text{Na}]^+$ m/z : 379.0925; found: 379.0920. Analytical data corresponds to those reported in the literature.⁵⁸

Triisopropyl[[(2-nitrophenyl)sulfonyl]ethynyl]silane (37f):



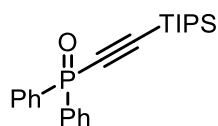
Was obtained as an orange solid in 49% yield. **¹H NMR** (400 MHz, CDCl_3) δ = 8.33 – 8.26 (m, 1H), 7.99 – 7.92 (m, 1H), 7.87 – 7.79 (m, 2H), 1.20 – 1.06 (m, 21H) ppm. **¹³C NMR** (101 MHz, CDCl_3): δ = 148.3, 135.4, 135.2, 133.1, 131.0, 125.5, 102.6, 99.3, 18.5, 11.1 ppm. **IR** (ATR): $\tilde{\nu}$ = 2948, 2867, 2360, 2340, 2124, 1542, 1336, 1159, 803, 575 cm^{-1} . **HRMS** (ESI) *calcd for* $\text{C}_{17}\text{H}_{26}\text{NO}_4\text{SSi}^+$ $[\text{M}+\text{H}]^+$ m/z : 368.1346; found: 368.1342.

Triisopropyl[(thiophen-2-ylsulfonyl)ethynyl]silane (37g):



Was obtained as a white solid in 92% yield. **¹H NMR** (400 MHz, CDCl_3): δ = 7.80 (dd, J = 3.8, 1.4 Hz, 1H), 7.75 (dd, J = 5.0, 1.4 Hz, 1H), 7.14 (dd, J = 5.0, 3.8 Hz, 1H), 1.14 – 1.02 (m, 21H) ppm. **¹³C NMR** (101 MHz, CDCl_3): δ = 143.3, 134.9, 134.2, 127.9, 100.9, 100.8, 18.4, 11.0 ppm. **IR** (ATR): $\tilde{\nu}$ = 2121, 1461, 1402, 1341, 1153, 1012, 884, 785, 670, 574 cm^{-1} . **HRMS** (ESI) *calcd for* $\text{C}_{15}\text{H}_{25}\text{O}_2\text{S}_2\text{Si}^+$ $[\text{M}+\text{H}]^+$ m/z : 329.1060; found: 329.1063. Analytical data corresponds to those reported in the literature.⁵⁴

Diphenyl[(triisopropylsilyl)ethynyl]phosphine Oxide (37h):

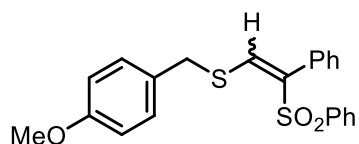


The transfer reagent **5f** (103 mg, 0.2 mmol, 1 equiv.), diphenylphosphine oxide (48.5 mg, 0.24 mmol, 1.2 equiv.) and Cs_2CO_3 (78.2 mg, 0.24 mmol, 1.2 equiv.) was dissolved in DCM (5 mL), and the reaction mixture was stirred for 30 min at ambient temperature on air with TLC monitoring. Upon completion of the reaction, pentane (5 mL) was added, and the reaction mixture was transferred directly to a pre-wetted column (hexanes). The pure product was obtained by column chromatography (hexanes). Compound **37i** was obtained as a white solid in 20% yield. **¹H NMR** (400 MHz, CDCl_3): δ = 7.89 – 7.79 (m, 4H), 7.52 (dd, J = 7.4, 1.7 Hz, 2H), 7.46 (ddd, J = 8.5, 6.5, 3.3 Hz, 4H), 1.20 – 1.07 (m, 21H) ppm. **³¹P NMR** (162 MHz, CDCl_3): δ = 6.9 ppm. **¹³C NMR** (101 MHz, CDCl_3): δ = 133.4 (d, J = 120.4 Hz), 132.6 (d, J = 3.6 Hz), 131.0 (d, J = 11.1 Hz), 128.7 (d, J = 13.4 Hz), 113.5 (d, J = 19.0 Hz), 101.3 (d, J = 151.9 Hz), 18.6, 11.2 ppm. **HRMS** (ESI) *calcd for* $\text{C}_{23}\text{H}_{32}\text{OPSi}^+$

[M+H]⁺ *m/z*: 383.1955; found: 383.1956. Analytical data corresponds to those reported in the literature.³⁵

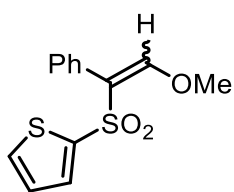
(*E/Z*)-(4-Methoxybenzyl)[2-phenyl-2-(phenylsulfonyl)vinyl]sulfane

(70c):



The transfer reagent **5a** (87 mg, 0.2 mmol, 1 equiv.), the corresponding thiol **147** (37 mg, 0.24 mmol, 1.2 equiv.) and the corresponding sulfinate PhSO₂Na (39.4 mg, 0.24 mmol, 1.2 equiv.) were dissolved in MeCN (3 mL), and the reaction mixture was stirred at room temperature for 1 h on air with TLC monitoring. Upon completion of the reaction, pentane (5 mL) was added, and the reaction mixture was transferred directly to a pre-wetted column (hexanes). The pure product was obtained by column chromatography (hexanes). Sulfane **70c** was obtained as a yellow solid in 91% yield [mixture of *E/Z* isomers (1:9)]. ¹H NMR (400 MHz, CDCl₃): δ = 7.70 (d, *J* = 8.3 Hz, 2H), 7.51 (t, *J* = 7.4 Hz, 1H), 7.38 (d, *J* = 8.3 Hz, 2H), 7.25 – 7.19 (m, 5H), 7.11 (d, *J* = 6.8 Hz, 2H), 6.95 (s, 1H), 6.83 (d, *J* = 8.7 Hz, 2H), 3.94 (s, 2H), 3.78 (s, 3H) ppm. ¹³C NMR (101 MHz, CDCl₃): δ = 159.3, 144.4, 140.7, 135.0, 134.9, 133.4, 130.3, 129.9, 128.8, 128.7, 128.5, 128.3, 127.6, 114.4, 55.5, 39.8 ppm. IR (ATR): $\tilde{\nu}$ = 2971, 2360, 2340, 1739, 1512, 1364, 1301, 1231, 1143, 667 cm⁻¹. HRMS (ESI) *calcd for* C₂₂H₂₀NaO₃S₂⁺ [M+Na]⁺ *m/z*: 419.0746; found: 419.0739.

(*E/Z*)-2-[(2-Methoxy-1-phenylvinyl)sulfonyl]thiophene (70d):

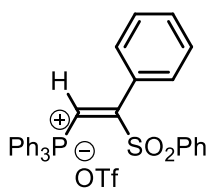


The transfer reagent **5a** (87 mg, 0.2 mmol, 1 equiv.) and sodium thiophene-2-sulfinate (**148**, 40.8 mg, 0.24 mmol, 1.2 equiv.) were dissolved in a mixture of DCM (1.5 mL) and MeOH (1.5 mL), and the reaction mixture was stirred at room temperature for 1 h on air. The reaction was monitored by TLC. Upon completion of the reaction, pentane (5 mL) was added, and the reaction mixture was transferred directly to a pre-wetted column (hexanes). The pure product was obtained by column chromatography (gradient hexanes → hexanes/EtOAc 1:1). Thiophene **70d** was obtained as a white solid in 83% yield [mixture *E/Z* isomers (1:9)]. Analytical data of the *Z*-isomer: ¹H NMR (400 MHz, CDCl₃): δ = δ 7.60 (t, *J* = 4.0 Hz, 2H), 7.32 (dt, *J* = 8.5, 3.7 Hz, 5H), 7.05 (dd, *J* = 4.9, 3.8 Hz, 1H), 6.55 (s, 1H), 3.93 (s, 3H) ppm. ¹³C NMR (101 MHz, CDCl₃): δ = 156.3, 143.8, 133.1, 132.9, 131.6, 131.1, 128.7, 128.4, 127.2, 122.1, 62.9

ppm. IR (ATR): $\tilde{\nu}$ = 1699, 1311, 1224, 1132, 1039, 1014, 720, 694, 670 cm^{-1} . HRMS (ESI) *calcd* for $\text{C}_{13}\text{H}_{13}\text{O}_3\text{S}_2^+$ $[\text{M}+\text{H}]^+$ m/z : 281.0301; found: 281.0305.

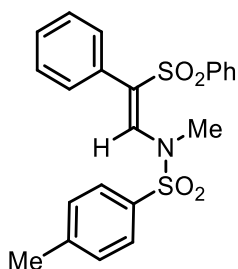
(Z)-Triphenyl[2-phenyl-2-(phenylsulfonyl)vinyl]phosphonium

Trifluoromethanesulfonate (70e)



A Schlenk flask equipped with a stirring bar was charged with the salt **142b** (115.3 mg, 0.2 mmol, 1 equiv.) and triphenylphosphine (63 mg, 0.24 mmol, 1.2 equiv.). The reactants were dissolved in DCM (2 mL). The reaction mixture was stirred at room temperature for 12 h. The solvent was evaporated to a minimum volume, and diethyl ether (10 mL) was added to precipitate the salt. The latter was filtered off, washed once more with diethyl ether (10 mL) and dried in vacuo. The salt **70e** was obtained as a white solid in 64% yield. $^1\text{H NMR}$ (400 MHz, CD_3CN): δ = 8.54 (d, J = 8.6 Hz, 2H), 8.31 (d, J = 7.9 Hz, 2H), 7.98 (t, J = 7.7 Hz, 2H), 7.95 – 7.88 (m, 5H), 7.87 – 7.82 (m, 2H), 7.77 (d, J = 7.5 Hz, 3H), 7.64 – 7.59 (m, 3H), 7.46 – 7.38 (m, 2H), 7.31 (d, J = 4.6 Hz, 4H), 6.85 (s, 1H) ppm. $^{31}\text{P NMR}$ (162 MHz, CD_3CN): δ = 16 ppm. $^{13}\text{C NMR}$ (101 MHz, CD_3CN): δ = 166.5, (d, $^2J_{\text{P-C}}$ = 3.6 Hz), 157.3, 141.0, 136.8, 135.8, 135.7 (d, $^4J_{\text{P-C}}$ = 3.2 Hz), 135.0 (d, $^1J_{\text{P-C}}$ = 10.8 Hz), 134.6 (d, $^4J_{\text{P-C}}$ = 10.7 Hz), 132.9, 132.4, 131.7, 131.3 (d, $^1J_{\text{P-C}}$ = 13.3 Hz), 131.0 (d, $^2J_{\text{P-C}}$ = 13.5 Hz), 130.8, 130.2, 130.2, 129.7 (d, $^2J_{\text{P-C}}$ = 13.7 Hz), 129.6 (d, $^2J_{\text{P-C}}$ = 14.0 Hz), 127.9, 125.3, 122.1 (q, $^1J_{\text{C-F}}$ = 321 Hz), 122.0 (d, $^1J_{\text{P-C}}$ = 93.7 Hz), 121.3 ppm. IR (ATR): $\tilde{\nu}$ = 3730, 3628, 2266, 1648, 1255, 1148, 1029, 686, 636, 515 cm^{-1} . HRMS (ESI) *calcd* for $\text{C}_{32}\text{H}_{26}\text{O}_2\text{PS}^+$ $[\text{M}-\text{OTf}]^+$ m/z : 505.1386; found: 505.1385.

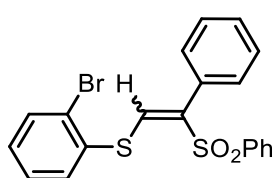
(Z)-N,4-dimethyl-N-[2-phenyl-2-(phenylsulfonyl)vinyl]benzenesulfonamide (70f):



A mixture of the salt **142b** (115.3 mg, 0.2 mmol, 1.0 equiv.), Cs_2CO_3 (78.2 mg, 0.24 mmol, 1.2 equiv.) and *N*,4-dimethylbenzenesulfonamide (44.5 mg, 0.24 mmol, 1.2 equiv.) in DCM (2 mL) was stirred at room temperature for 12 h under ambient atmosphere with TLC monitoring, then directly transferred to a pre-wetted column (hexanes). The pure product was obtained by column chromatography (gradient hexanes \rightarrow hexanes:EtOAc 1:1).

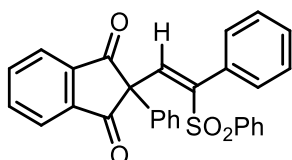
Sulfonamide **70f** was obtained as an off-white solid in 83% yield. $^1\text{H NMR}$ (400 MHz, CDCl_3): δ = 8.38 (s, 1H), 7.74 (d, J = 8.3 Hz, 2H), 7.56 – 7.47 (m, 3H), 7.40 – 7.33 (m, 4H), 7.28 (d, J = 7.5 Hz, 1H), 7.16 (t, J = 7.9 Hz, 2H), 6.93 (d, J = 8.3 Hz, 2H), 2.47 (s, 3H), 2.46 (s, 3H) ppm. $^{13}\text{C NMR}$ (101 MHz, CD_3CN): δ = 145.3, 139.8, 136.7, 134.2, 133.0, 132.5, 130.4, 129.5, 129.3, 128.8, 128.3, 128.0, 127.5, 122.2, 34.8, 21.8 ppm. IR (ATR): $\tilde{\nu}$ = 1630, 1357, 1287, 1170, 1141, 1082, 978, 943, 688, 545 cm^{-1} . HRMS (ESI) *calcd* for $\text{C}_{22}\text{H}_{22}\text{NNaO}_4\text{S}_2^+$ $[\text{M}+\text{Na}]^+$ m/z : 450.0804; found: 450.0794.

(*E/Z*)-(2-Bromophenyl)[2-phenyl-2-(phenylsulfonyl)vinyl]sulfane (**70g**):



A mixture of the salt **142b** (115.3 mg, 0.2 mmol, 1.0 equiv.), Cs_2CO_3 (65.2 mg, 0.2 mmol, 1.0 equiv.) and 2-bromobenzenethiol (37.8 mg, 0.2 mmol, 1.0 equiv.) in DCM (2 mL) was stirred at room temperature for 12 h under ambient atmosphere with TLC monitoring, then directly transferred to a pre-wetted column (hexanes). The pure product was obtained by column chromatography (gradient hexanes \rightarrow hexanes:EtOAc 1:1). Sulfane **70g** was obtained as a white solid in 90% yield [mixture of *Z/E* isomers (5:1)]. $^1\text{H NMR}$ (400 MHz, CDCl_3): δ = 7.85 (dd, J = 8.4, 1.2 Hz, 2H), 7.67 – 7.61 (dt J = 1.4, 8.0 Hz, 2H), 7.59 – 7.52 (m, 1H), 7.47 – 7.42 (m, 2H), 7.41 – 7.26 (m, 4H), 7.26 – 7.19 (m, 3H), 6.98 (s, 1H) ppm. $^{13}\text{C NMR}$ (101 MHz, CDCl_3): δ = 144.7, 140.4, 136.3, 135.7, 134.4, 134.3, 134.0, 133.6, 130.6, 130.3, 130.0, 129.0, 128.8, 128.44, 128.39, 127.8 ppm. IR (ATR): $\tilde{\nu}$ = 3728, 3626, 1737, 1557, 1447, 1306, 1146, 1084, 753, 664 cm^{-1} . HRMS (ESI) *calcd* for $\text{C}_{20}\text{H}_{16}\text{O}_2\text{S}_2^+$ $[\text{M}+\text{H}]^+$ m/z : 430.9770; found: 430.9769.

(*Z*)-2-Phenyl-2-[2-phenyl-2-(phenylsulfonyl)vinyl]-1*H*-indene-1,3(2*H*)-dione (**70h**):

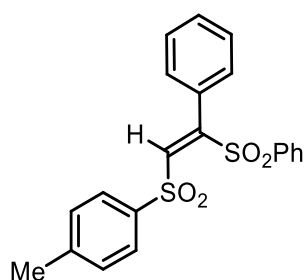


A mixture of the salt **142b** (115.3 mg, 0.2 mmol, 1.0 equiv.), Cs_2CO_3 (65.2 mg, 0.2 mmol, 1.0 equiv.) and indandione (29.2 mg, 0.2 mmol, 1.0 equiv.) in DCM (2 mL) was stirred at room temperature for 12 h under ambient atmosphere with TLC monitoring, then directly transferred to a pre-wetted column (hexanes). The pure product was obtained by column chromatography (gradient hexanes \rightarrow hexanes:EtOAc 4:1). Compound **70h** was obtained as an orange oil in 87% yield. $^1\text{H NMR}$ (400 MHz, CDCl_3): δ = 7.90 (s, 1H), 7.53 (t, J = 7.2 Hz, 2H), 7.49 – 7.45 (m, 2H), 7.45 – 7.29 (m, 12H), 7.27 – 7.23 (m, 2H), 7.16 (d, J = 7.2 Hz, 1H) ppm. ^{13}C

NMR (101 MHz, CDCl₃): δ = 192.8, 168.2, 150.7, 139.1, 138.4, 133.51, 133.45, 130.8, 130.6, 130.6, 129.6, 129.6 (2 ¹³C-Signals overlapping), 128.9, 128.8, 128.6, 128.5, 128.4, 128.3, 128.1, 127.5, 122.8, 119.4, 116.9 ppm (4 more ¹³C-Signals than expected, Ph at tertiary carbon has no rotational freedom). **IR** (neat): $\tilde{\nu}$ = 3725, 3626, 1715, 1378, 1308, 1204, 1146, 1082, 689, 646 cm⁻¹. **HRMS** (ESI) *calcd for* C₂₉H₂₀NaO₄S⁺ [M+Na]⁺ *m/z*: 487.0975; found: 487.0975.

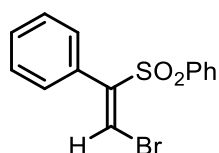
(Z)-1-Methyl-4-[[2-phenyl-2-(phenylsulfonyl)vinyl]sulfonyl]benzene

(70i):



Compound **142b** (115.3 mg, 0.2 mmol, 1.0 equiv.) and sodium *p*-tolylsulfinate (35.6 mg, 0.2 mmol, 1.0 equiv.) were dissolved in DCM/*t*-BuOH (2 mL/few drops). The reaction mixture was stirred at room temperature for 12 h under ambient atmosphere with TLC monitoring, then directly transferred to a pre-wetted column (hexanes). The pure product was obtained by column chromatography (gradient hexanes → hexanes:EtOAc 1:1). Compound **70i** was obtained as a colorless oil in 76% yield. **¹H NMR** (400 MHz, CDCl₃): δ = 7.98 (d, *J* = 8.3 Hz, 2H), 7.75 (d, *J* = 8.3 Hz, 2H), 7.58 (t, *J* = 7.5 Hz, 1H), 7.47 – 7.32 (m, 5H), 7.29 – 7.24 (m, 2H), 7.22 – 7.18 (m, 2H), 6.87 (s, 1H), 2.47 (s, 3H) ppm. **¹³C NMR** (101 MHz, CDCl₃): δ = 151.9, 145.3, 141.4, 138.6, 138.4, 134.4, 132.7, 130.4, 129.9, 129.8, 129.4, 129.1, 128.6, 128.5, 21.9 ppm. **IR** (neat): $\tilde{\nu}$ = 3060, 3011, 1595, 1325, 1148, 1079, 907, 726, 670, 563 cm⁻¹. **HRMS** (ESI) *calcd for* C₂₁H₁₉O₄S₂⁺ [M+H]⁺ *m/z*: 399.0719; found: 399.0704.

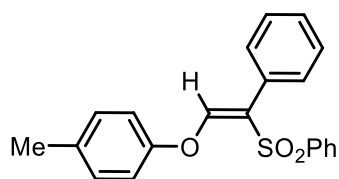
(Z)-[2-Bromo-1-(phenylsulfonyl)vinyl]benzene (70j)



The salt **142b** (115.3 mg, 0.2 mmol, 1.0 equiv.) and NEt₄Br (0.2 mmol, 1.0 equiv.) were dissolved in DCM (2 mL). The reaction mixture was stirred at room temperature for 12 h under ambient atmosphere and with TLC monitoring, then directly transferred to a pre-wetted column (hexanes). The pure product was obtained by column chromatography (gradient hexanes → hexanes:EtOAc 8:2). Compound **70j** was obtained as a colorless oil in 91% yield. **¹H NMR** (400 MHz, CDCl₃): δ = 7.84 – 7.79 (m, 2H), 7.60 (ddt, *J* = 7.9, 7.0, 1.2 Hz, 1H), 7.49 – 7.44 (m, 2H), 7.41 – 7.36 (m, 1H), 7.34 – 7.29 (m, 2H), 7.25 – 7.21 (m, 2H), 7.01 (s, 1H) ppm. **¹³C NMR** (101 MHz, CDCl₃): δ = 147.7, 139.8, 134.2, 133.9, 130.0, 129.7, 129.0, 129.0 (2 ¹³C-Signals overlapping), 128.4, 117.4 ppm. **IR** (neat): $\tilde{\nu}$ = 1576, 1445, 1319, 1146, 1082, 836, 718, 686, 533, 512 cm⁻¹. **HRMS** (ESI) *calcd for*

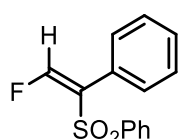
$C_{14}H_{11}BrNaO_2S^+$ $[M+Na]^+$ m/z : 344.9555; found: 344.9553. Analytical data corresponds to those reported in the literature.¹²⁰

(Z)-1-Methyl-4-[[2-phenyl-2-(phenylsulfonyl)vinyl]oxy]benzene (70k):



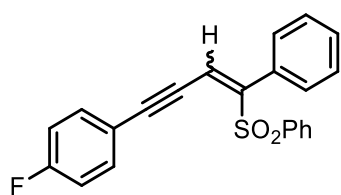
A mixture of the salt **142b** (115.3 mg, 0.2 mmol, 1.0 equiv.), CS_2CO_3 (65.2 mg, 0.2 mmol, 1.0 equiv.) and *p*-cresol (21.6 mg, 0.2 mmol, 1.0 equiv.) was stirred in DCM (2 mL) at room temperature for 12 h under ambient atmosphere and with TLC monitoring. The reaction mixture was directly transferred to a pre-wetted column (hexanes). The pure product was obtained by column chromatography (gradient hexanes \rightarrow hexanes:EtOAc 1:1). Compound **70k** was obtained as a white solid in 92% yield. 1H NMR (400 MHz, $CDCl_3$): δ = 7.98 (dd, J = 8.4, 1.3 Hz, 2H), 7.61 – 7.56 (m, 1H), 7.52 – 7.46 (m, 2H), 7.43 – 7.36 (m, 5H), 7.11 (d, J = 8.1 Hz, 2H), 6.90 (s, 1H), 6.83 (d, J = 8.6 Hz, 2H), 2.31 (s, 3H) ppm. ^{13}C NMR (101 MHz, $CDCl_3$): δ = 154.4, 150.3, 142.5, 134.9, 133.1, 131.3, 131.0, 130.4, 129.0, 128.8, 128.5, 128.1, 125.9, 117.2, 20.8 ppm. IR (ATR): $\tilde{\nu}$ = 3080, 2923, 1632, 1600, 1504, 1224, 1141, 726, 686, 574 cm^{-1} . HRMS (ESI) *calcd* for $C_{21}H_{18}NaO_3S^+$ $[M+Na]^+$ m/z : 373.0869; found: 373.0863.

(Z)-[2-Fluoro-1-(phenylsulfonyl)vinyl]benzene (70l):



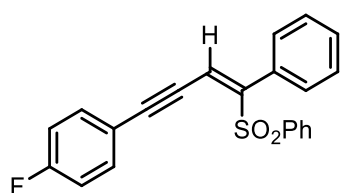
KF (13.9 mg, 0.24 mmol, 1.2 equiv.) was dissolved in a mixture of DCM (1 mL) and *t*-BuOH (1 mL), and compound **142b** (115.3 mg, 0.2 mmol, 1 equiv.) was added in one portion. The reaction mixture was stirred for 12 h at room temperature under ambient atmosphere, then directly transferred to a pre-wetted column (hexanes). The pure product was obtained by column chromatography (gradient hexanes \rightarrow hexanes:EtOAc 4:1). Compound **70l** was obtained as a white solid in 40% yield. 1H NMR (400 MHz, $CDCl_3$): δ = 7.84 (d, J = 7.5 Hz, 2H), 7.62 (t, J = 7.5 Hz, 1H), 7.50 (t, J = 7.8 Hz, 2H), 7.41 (d, J = 7.3 Hz, 1H), 7.35 (t, J = 7.4 Hz, 2H), 7.29 – 7.25 (m, 2H), 6.83 (d, J = 78.5 Hz, 1H) ppm. ^{19}F NMR (376 MHz, $CDCl_3$): δ = -101.96 (d, J = 78.6 Hz) ppm. ^{13}C NMR (101 MHz, $CDCl_3$): δ = 152.8 (d, $^1J_{C-F}$ = 292.7 Hz), 140.8, 133.9, 131.0 (d, $^2J_{C-F}$ = 3.2 Hz), 130.2, 130.2, 129.9, 129.2, 128.7, 128.1 (d, $^3J_{C-F}$ = 1.1 Hz) ppm. IR (neat): $\tilde{\nu}$ = 3728, 3628, 1648, 1325, 1180, 1135, 1079, 732, 667, 553 cm^{-1} . HRMS (ESI) *calcd* for $C_{14}H_{12}FO_2S^+$ $[M+H]^+$ m/z : 263.0537; found: 263.0538.

(Z/E)-1-Fluoro-4-[4-phenyl-4-(phenylsulfonyl)but-3-en-1-yn-1-yl]benzene (70m and 70m')



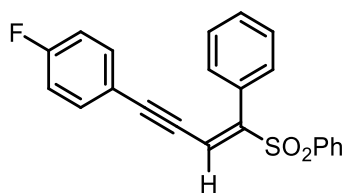
To the solution of 1-ethynyl-4-fluorobenzene (24.1 mg, 0.2 mmol, 1.0 equiv.) in DCM (2 mL) was added LiHMDS (0.2 mL of a 1 M solution in THF; 0.2 mmol, 1.0 equiv.) added. The reaction mixture was stirred 10 min at room temperature under nitrogen atmosphere. Compound **142b** (115.3 mg, 0.2 mmol, 1 equiv.) was added in one portion, and the reaction mixture was stirred for an additional 12 h at room temperature, then directly transferred to a pre-wetted column (hexanes). The pure product was obtained by column chromatography (gradient hexanes → hexanes:EtOAc 4:1). Compound **70m** was obtained as a white solid in 50% yield [mixture of *Z/E* isomers **70m** & **70m'** (3:1)].

(Z)-1-Fluoro-4-[4-phenyl-4-(phenylsulfonyl)but-3-en-1-yn-1-yl]benzene (70m):



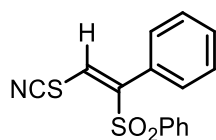
¹H NMR (400 MHz, CDCl₃): 7.83 (dd, *J* = 8.4, 1.2 Hz, 2H), 7.62 – 7.57 (m, 2H), 7.57 – 7.52 (m, 1H), 7.42 (t, *J* = 7.6 Hz, 2H), 7.38 – 7.31 (m, 5H), 7.09 (t, *J* = 8.7 Hz, 2H), 6.43 (s, 1H) ppm. **¹⁹F NMR** (377 MHz, CDCl₃) δ = -108.40 ppm. **¹³C NMR** (101 MHz, CDCl₃): δ = 163.4 (d, ¹*J*_{C-F} = 253 Hz), 150.5, 140.6, 134.4 (d, ³*J*_{C-F} = 8.9 Hz), 134.3, 133.6, 129.8, 129.6, 129.0, 128.4, 128.2, 120.4, 118.7 (d, ⁴*J*_{C-F} = 3.7 Hz), 116.1 (d, ²*J*_{C-F} = 22.3 Hz), 103.2, 84.9 ppm. **IR** (neat): $\tilde{\nu}$ = 3733, 3626, 2191, 1504, 1317, 1226, 1151, 838, 764, 667 cm⁻¹. **HRMS** (ESI) *calcd* for C₂₂H₁₆FO₂S⁺ [M+H]⁺ *m/z*: 363.0850; found: 363.0847.

(E)-1-Fluoro-4-[4-phenyl-4-(phenylsulfonyl)but-3-en-1-yn-1-yl]benzene (70m')



¹H NMR (400 MHz, CDCl₃): δ = 7.66 (dd, *J* = 8.4, 1.2 Hz, 2H), 7.53 (t, *J* = 7.5 Hz, 1H), 7.40 (t, *J* = 7.8 Hz, 2H), 7.37 – 7.29 (m, 5H), 7.26 (s, 1H), 7.18 (dd, *J* = 8.9, 5.4 Hz, 2H), 6.95 (t, *J* = 8.7 Hz, 2H) ppm. **¹⁹F NMR** (377 MHz, CDCl₃): δ = -108.31 ppm. **¹³C NMR** (101 MHz, CDCl₃): δ = 163.3 (d, ¹*J*_{C-F} = 252 Hz), 150.9, 138.8, 134.2 (d, ³*J*_{C-F} = 8.7 Hz), 133.6, 130.9, 130.3, 129.6, 129.0, 128.6, 128.2, 120.1, 118.1 (d, ⁴*J*_{C-F} = 3.6 Hz), 116.0 (d, ²*J*_{C-F} = 22.2 Hz), 100.8, 84.5 ppm. **IR** (neat): $\tilde{\nu}$ = 3735, 3628, 2198, 1306, 1143, 836, 686, 667, 592 cm⁻¹. **HRMS** (ESI) *calcd* for C₂₂H₁₆FO₂S⁺ [M+H]⁺ *m/z*: 363.0850; found: 363.0845.

(Z)-[(1-Phenyl-2-thiocyanatovinyl)sulfonyl]benzene (70n):

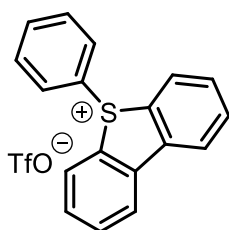


To the stirred solution of NaSCN (19.5 mg, 0.24 mmol, 1.2 equiv.) in a mixture of DCM (1 mL) and *t*-BuOH (1 mL), the salt **142b** (115.3 mg, 0.2 mmol, 1 equiv.) was added in one portion. The reaction mixture was stirred at room temperature for 12 min under ambient atmosphere, then directly transferred to a pre-wetted column (hexanes). The pure product was obtained by column chromatography (gradient hexanes → hexanes:EtOAc 4:1). Compound **70n** was obtained as a white solid in 72% yield. **¹H NMR** (400 MHz, CDCl₃): δ = 7.65 (dd, *J* = 8.4, 1.2 Hz, 2H), 7.60 (t, *J* = 7.5 Hz, 1H), 7.47 – 7.42 (m, 2H), 7.37 (t, *J* = 7.4 Hz, 1H), 7.29 (t, *J* = 7.6 Hz, 2H), 7.22 – 7.18 (m, 2H), 6.99 (s, 1H) ppm. **¹³C NMR** (101 MHz, CDCl₃): δ = 142.5, 138.1, 134.6, 131.7, 131.2, 130.2, 129.5, 129.4, 128.8, 128.1, 111.9 ppm. **IR** (neat): $\tilde{\nu}$ = 3030, 1737, 1367, 1306, 1210, 1146, 1084, 753, 684, 651 cm⁻¹. **HRMS** (ESI) *calcd for* C₁₅H₁₁NNaO₂S₂⁺ [M+Na]⁺ *m/z*: 324.0123; found: 324.0122.

General Procedure for the Synthesis of Compounds 93a-93t

Reliable up to 5 mmol scale: Triflic anhydride (1.1 equiv.) was added to a suspension of dibenzo[*b,d*]thiophene 5-oxide (**15**) in dry DCM (9 mL/mmol) maintaining the temperature between –60 °C and –50 °C. The reaction mixture was stirred for 20 min at this temperature, followed by the addition of the respective aromatic substrate, then slowly warmed up to –20 °C over a period of 15 hours. After this, the reaction mixture was allowed to warm up to RT, and the solvent was evaporated *in vacuo* to afford crude **93a-93t**, which were washed with dry Et₂O (2 × 10 mL/mmol) to obtain the desired products as solids. Further purification was achieved by column chromatography on silica gel with DCM/MeOH (100/3) or DCM/acetone (10/1) as an eluent. Usually a quartett around 122 ppm (Triflate-CF₃) in **¹³C NMR** can be found in all examples. If it is not listed amongst the signals, the sample was too diluted, and the signals disappeared in the noise.

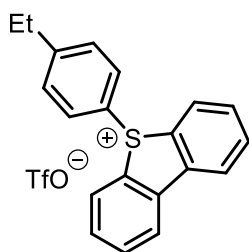
5-Phenyl-5*H*-dibenzo[*b,d*]thiophen-5-ium Trifluoromethanesulfonate (93a):



The salt **93a** was obtained as a pale-yellow solid in 91% yield. **¹H NMR** (300 MHz, CD₃CN): δ = 8.35 (dd, *J* = 7.9, 0.7 Hz, 2H), 8.08 (d, *J* = 8.1 Hz, 2H), 7.95 (td, *J* = 7.7, 1.0 Hz, 2H), 7.78 – 7.69 (m, 3H), 7.63 – 7.56 (m, 4H) ppm. **¹³C NMR** (75 MHz, CD₃CN) δ = 140.5, 136.2, 135.5, 132.9, 132.7, 132.6, 131.5,

128.9, 127.9, 125.6 ppm. IR (ATR): = 3088, 2358, 2337, 1448, 1258, 1225, 1155, 1030, 755, 635 cm^{-1} . HRMS (+ESI) *calcd for* $\text{C}_{18}\text{H}_{13}\text{S}^+$ [M-OTf] $^+$ *m/z*: 261.0733; found: 261.0734.

5-(4-Ethylphenyl)-5*H*-dibenzo[*b,d*]thiophen-5-ium Trifluoromethanesulfonate (93b):

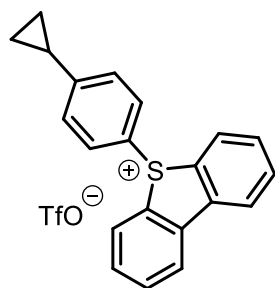


The salt **93b** was obtained as a white solid in 83% yield (*o/p* ratio, 1/9).

$^1\text{H NMR}$ (400 MHz, CD_3CN): δ = 8.34 (ddd, J = 7.9, 1.2, 0.6 Hz, 2H), 8.07 (ddd, J = 8.1, 1.0, 0.6 Hz, 2H), 7.95 – 7.89 (m, 2H), 7.70 (ddd, J = 8.1, 7.5, 1.2 Hz, 2H), 7.52 – 7.47 (m, 2H), 7.44 – 7.39 (m, 2H), 2.66 (q, J = 7.6 Hz, 2H), 1.15 (t, J = 7.6 Hz, 3H) ppm. $^{13}\text{C NMR}$ (101 MHz, CD_3CN): δ = 153.7,

140.2, 135.3, 133.1, 132.5, 132.0, 131.5, 128.7, 125.4, 124.1, 122.0 (q, $^1J_{\text{C-F}}$ = 321 Hz) 29.2, 15.2 ppm. IR (ATR): = 3083, 2360, 2339, 1448, 1261, 1157, 1025, 830, 763, 633 cm^{-1} . HRMS (+ESI) *calcd for* $\text{C}_{20}\text{H}_{17}\text{S}^+$ [M-OTf] $^+$ *m/z*: 298.1046 found: 298.0145. **Mp** = 178.7 $^\circ\text{C}$.

5-(4-Cyclopropylphenyl)-5*H*-dibenzo[*b,d*]thiophen-5-ium Trifluoromethanesulfonate (93c):

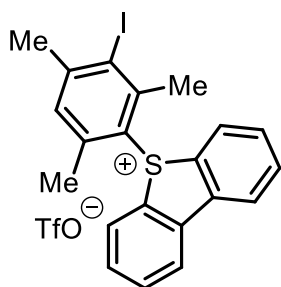


The salt **93c** was obtained as a white solid in 71% yield (*o/p* ratio 1:5).

$^1\text{H NMR}$ (400 MHz, CD_2Cl_2): δ = 8.24 (ddd, J = 7.9, 1.2, 0.6 Hz, 2H), 8.06 – 8.03 (m, 2H), 7.93 – 7.88 (m, 2H), 7.68 (ddd, J = 8.1, 7.5, 1.2 Hz, 2H), 7.49 – 7.44 (m, 2H), 7.22 – 7.18 (m, 2H), 1.93 (tt, J = 8.3, 4.9 Hz, 1H), 1.14 – 1.08 (m, 2H), 0.79 – 0.72 (m, 2H) ppm. $^{13}\text{C NMR}$ (101 MHz, CD_2Cl_2): δ = 154.6, 139.5, 135.0, 132.5, 132.3, 131.2, 129.1, 128.7,

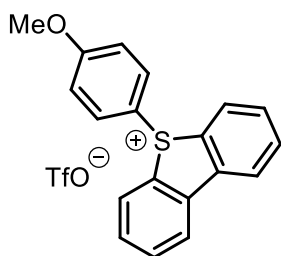
124.8, 121.3 (q, $^1J_{\text{C-F}}$ = 322 Hz), 121.5, 11.8, 10.8 ppm. IR (ATR): = 3088, 2363, 1591, 1485, 1448, 1264, 1157, 1028, 763, 635 cm^{-1} . HRMS (+ESI) *calcd for* $\text{C}_{21}\text{H}_{17}\text{S}^+$ [M-OTf] $^+$ *m/z*: 301.1046; found: 301.1057. **Mp** = 148.8 $^\circ\text{C}$.

5-(3-Iodo-2,4,6-trimethylphenyl)-5*H*-dibenzo[*b,d*]thiophen-5-ium Trifluoromethanesulfonate (93d):



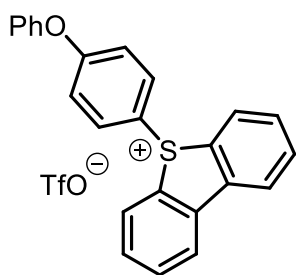
The salt **93d** was obtained as a brown solid in 74% yield; in the solution exist as a 1:1 mixture of rotamers. $^1\text{H NMR}$ (300 MHz, CDCl_3): δ = 8.25 (d, J = 7.8 Hz, 2H), 8.07 (t, J = 7.6 Hz, 2H), 7.89 (t, J = 7.6 Hz, 2H), 7.72 (ddd, J = 10.1, 5.6, 2.7 Hz, 2H), 7.41/6.96 (s, 1H), 3.41/3.11 (s, 3H), 2.55/2.52 (s, 3H), 1.51/1.19 (s, 3H) ppm. $^{13}\text{C NMR}$ (75 MHz, CDCl_3): δ = 152.7, 152.6, 150.2, 147.7, 145.4, 142.1, 139.4, 139.2, 134.8, 134.7, 134.1, 132.6, 132.4, 132.3, 129.3, 128.9, 128.37, 128.33, 125.0, 124.9, 123.5, 117.4, 111.2, 109.6, 31.6, 31.4, 31.0, 25.6, 23.0, 17.9 ppm. **IR** (ATR): = 3086, 2360, 2337, 1448, 1256, 1225, 1157, 1030, 763, 635 cm^{-1} . **HRMS** (+ESI) *calcd for* $\text{C}_{21}\text{H}_{18}\text{I}\text{S}^+$ [$\text{M}-\text{OTf}$] $^+$ m/z : 429.0168; found: 429.0168. **Mp** = 216.2 $^\circ\text{C}$.

5-(4-Methoxyphenyl)-5*H*-dibenzo[*b,d*]thiophen-5-ium Trifluoromethanesulfonate (93e):



The salt **93e** was obtained as a pale pink solid in 76% yield (*o/p* ratio 1:25). $^1\text{H NMR}$ (300 MHz, CDCl_3): δ = 8.22 – 8.18 (m, 2H), 8.06 (d, J = 7.8 Hz, 2H), 7.83 (td, J = 7.6, 1.0 Hz, 2H), 7.63 – 7.52 (m, 4H), 7.00 – 6.94 (m, 2H), 3.82 (s, 3H) ppm. $^{13}\text{C NMR}$ (101 MHz, CDCl_3): δ = 165.1, 138.7, 134.4, 133.3, 132.6, 131.8, 128.4, 124.3, 121.0 (q, $^1J_{\text{C-F}}$ = 320 Hz), 117.3, 114.5, 56.2 ppm. **IR** (ATR): = 3090, 2358, 2337, 1591, 1493, 1261, 1157, 1030, 763, 637 cm^{-1} . **HRMS** (+ESI) *calcd for* $\text{C}_{19}\text{H}_{15}\text{OS}^+$ [$\text{M}-\text{OTf}$] $^+$ m/z : 291.0838; found: 291.0838. **Mp** = 165.0 $^\circ\text{C}$.

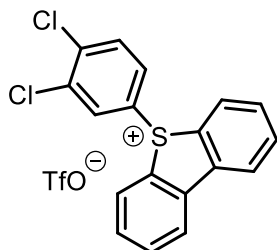
5-(4-Phenoxyphenyl)-5*H*-dibenzo[*b,d*]thiophen-5-ium Trifluoromethanesulfonate (93f):



The salt **93f** was obtained as a white solid in 72% yield (*o/p* ratio 1:33). $^1\text{H NMR}$ (400 MHz, CD_3CN): δ = 8.33 (ddd, J = 7.9, 1.2, 0.6 Hz, 2H), 8.06 (ddd, J = 8.1, 1.0, 0.6 Hz, 2H), 7.94 (ddd, J = 7.9, 7.5, 1.1 Hz, 2H), 7.73 (ddd, J = 8.1, 7.5, 1.2 Hz, 2H), 7.55 – 7.49 (m, 2H), 7.49 – 7.41 (m, 2H), 7.32 – 7.25 (m, 1H), 7.11 – 7.02 (m, 4H) ppm. $^{13}\text{C NMR}$ (101 MHz, CD_3CN): δ = 164.7, 155.2, 140.2, 135.4, 134.2, 133.5, 132.6, 131.4, 128.7, 126.7, 125.5, 122.1 (q, $^1J_{\text{C-F}}$ = 320 Hz), 121.5, 120.5, 118.6, ppm. **IR** (ATR): = 3090, 2360, 2339, 1579,

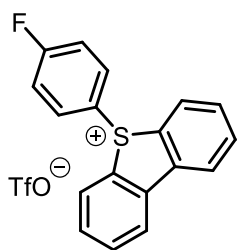
1485, 1251, 1171, 1025, 763, 637 cm^{-1} . **HRMS** (+ESI) *calcd* for $\text{C}_{24}\text{H}_{17}\text{OS}^+$ $[\text{M}-\text{OTf}]^+$ m/z : 353.0995; found: 353.0999. **Mp** = 172.2 $^{\circ}\text{C}$.

5-(3,4-Dichlorophenyl)-5*H*-dibenzo[*b,d*]thiophen-5-ium Trifluoromethanesulfonate (93g):



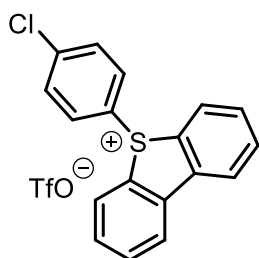
The salt **93g** was obtained as an orange solid in 39% yield. **$^1\text{H NMR}$** (300 MHz, CD_3CN): δ = 8.35 (dd, J = 7.9, 1.1 Hz, 2H), 8.09 (d, J = 8.7 Hz, 2H), 8.01 – 7.93 (m, 2H), 7.82 (d, J = 2.4 Hz, 1H), 7.77 – 7.68 (m, 3H), 7.41 (dd, J = 8.7, 2.4 Hz, 1H) ppm. **$^{13}\text{C NMR}$** (75 MHz, CD_3CN): δ = 140.6, 139.0, 135.8, 134.3, 133.3, 132.8, 132.1, 130.8, 129.2, 127.4, 125.8, 124.8 ppm. **IR** (ATR): = 3088, 2358, 2337, 1456, 1376, 1258, 1160, 1025, 757, 637 cm^{-1} . **HRMS** (+ESI) *calcd* for $\text{C}_{18}\text{H}_{11}\text{Cl}_2\text{S}^+$ $[\text{M}-\text{OTf}]^+$ m/z : 328.9953; found: 328.9955. **Mp** = 131.7 $^{\circ}\text{C}$.

5-(4-Fluorophenyl)-5*H*-dibenzo[*b,d*]thiophen-5-ium Trifluoromethanesulfonate (93h):



The salt **93h** was obtained as a white solid in 80% yield (*o/p* ratio > 1:100). **$^1\text{H NMR}$** (400 MHz, CD_3CN): δ = 8.35 (ddd, J = 7.8, 1.2, 0.6 Hz, 2H), 8.08 (ddd, J = 8.1, 1.0, 0.6 Hz, 2H), 7.95 (td, J = 7.7, 1.1 Hz, 2H), 7.73 (ddd, J = 8.1, 7.5, 1.2 Hz, 2H), 7.68 – 7.61 (m, 2H), 7.37 – 7.29 (m, 2H) ppm. **$^{13}\text{C NMR}$** (101 MHz, CD_3CN): δ = 167.3 (d, J = 257 Hz), 140.3, 135.5, 134.7 (d, J = 9.5 Hz), 133.0, 132.7, 128.9, 125.6, 122.9 (d, J = 3.4 Hz), 122.0 (q, $^1J_{\text{C-F}}$ = 321 Hz), 119.8 ppm. **$^{19}\text{F NMR}$** (376 MHz, CD_3CN): δ = -79.3, -102.8 ppm. **IR** (ATR): = 3096, 2365, 2342, 1586, 1488, 1264, 1163, 1025, 763, 637 cm^{-1} . **HRMS** (+ESI) *calcd* for $\text{C}_{18}\text{H}_{12}\text{FS}^+$ $[\text{M}-\text{OTf}]^+$ m/z : 279.0638; found: 279.0638. **Mp** = 171.5 $^{\circ}\text{C}$.

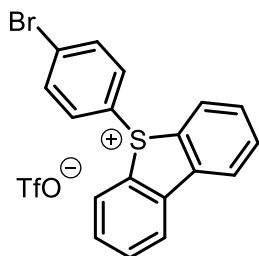
5-(4-Chlorophenyl)-5*H*-dibenzo[*b,d*]thiophen-5-ium Trifluoromethanesulfonate (93i):



The salt **93i** was obtained as a pale-yellow solid in 92% yield (*o/p* ratio 1:25). **$^1\text{H NMR}$** (400 MHz, CD_3CN) δ = 8.34 (ddd, J = 7.9, 1.2, 0.5 Hz, 2H), 8.10 (ddd, J = 8.1, 1.0, 0.6 Hz, 2H), 7.97 – 7.92 (m, 2H), 7.72 (ddd, J = 8.1, 7.4, 1.2 Hz, 2H), 7.57 (s, 4H) ppm. **$^{13}\text{C NMR}$** (101 MHz, CD_3CN) δ = 142.1, 140.3, 135.5, 133.1, 132.6, 132.5, 129.0, 126.3, 125.5, 122.0 (q, $^1J_{\text{C-F}}$ =

320 Hz) ppm. **IR** (ATR): = 3086, 2926, 1709, 1571, 1448, 1251, 1152, 1022, 760, 630 cm^{-1} . **HRMS** (+ESI) *calcd for* $\text{C}_{18}\text{H}_{12}\text{ClS}^+$ $[\text{M}-\text{OTf}]^+$ m/z : 295.0343; found: 295.0343. **Mp** = 188.8 $^{\circ}\text{C}$.

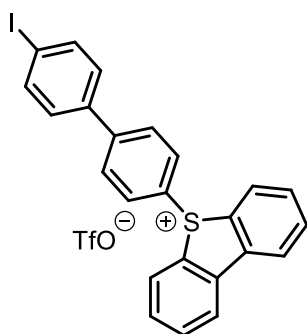
5-(4-Bromophenyl)-5*H*-dibenzo[*b,d*]thiophen-5-ium Trifluoromethanesulfonate (93j):



The salt **93j** was obtained as a pale-yellow solid in 93% yield (*o/p* ratio 1:26). **^1H NMR** (400 MHz, CD_3CN): δ = 8.34 (ddd, J = 7.9, 1.3, 0.6 Hz, 2H), 8.14 (dt, J = 8.1, 0.8 Hz, 2H), 7.94 (td, J = 7.7, 1.1 Hz, 2H), 7.76 – 7.69 (m, 4H), 7.55 – 7.47 (m, 2H) ppm. **^{13}C NMR** (101 MHz, CD_3CN): δ = 140.4, 135.5, 133.1, 132.6, 132.6, 130.6, 129.1, 127.3, 125.5, 121.8 (q, $^1J_{\text{C-F}}$ =

320 Hz) ppm. **IR** (ATR): = 3066, 3000, 2360, 1442, 1382, 1248, 1025, 997, 756, 630 cm^{-1} . **HRMS** (+ESI) *calcd for* $\text{C}_{18}\text{H}_{12}\text{BrS}^+$ $[\text{M}-\text{OTf}]^+$ m/z : 338.9838; found: 338.9838. **Mp** = 204.8 $^{\circ}\text{C}$.

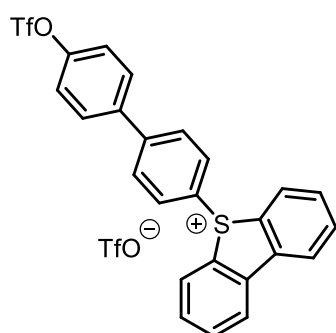
5-(4'-Iodo-[1,1'-biphenyl]-4-yl)-5*H*-dibenzo[*b,d*]thiophen-5-ium Tri-fluoromethanesulfonate (93k):



The salt **93k** was obtained as a beige solid in 72% yield (*o/p* ratio 1:11). **^1H NMR** (400 MHz, CD_3CN): δ = 8.36 (ddd, J = 8.0, 1.3, 0.6 Hz, 2H), 8.10 (ddd, J = 8.1, 1.1, 0.6 Hz, 2H), 7.96 (td, J = 7.7, 1.0 Hz, 2H), 7.88 – 7.78 (m, 4H), 7.74 (ddd, J = 8.0, 7.5, 1.2 Hz, 2H), 7.66 – 7.61 (m, 2H), 7.43 – 7.38 (m, 2H) ppm. **^{13}C NMR** (101 MHz, CD_3CN): δ = 147.3, 140.4, 139.2, 138.5, 135.5, 132.9, 132.7, 132.1, 130.6, 130.2,

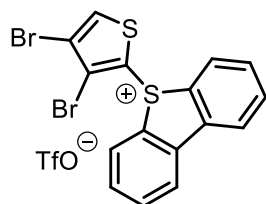
128.9, 126.4, 125.6, 122.1 (q, $^1J_{\text{C-F}}$ = 320 Hz), 95.9 ppm. **IR** (ATR): = 3086, 2363, 2339, 1261, 1225, 1160, 1030, 1002, 760, 637 cm^{-1} . **HRMS** (+ESI) *calcd for* $\text{C}_{24}\text{H}_{16}\text{IS}^+$ $[\text{M}-\text{OTf}]^+$ m/z : 463.0012; found: 463.0012. **Mp** = 241.4 $^{\circ}\text{C}$.

5-(4'-{[(Trifluoromethyl)sulfonyl]oxy}-[1,1'-biphenyl]-4-yl)-5H-dibenzo[*b,d*]thiophen-5-ium Trifluoromethanesulfonate (93l):



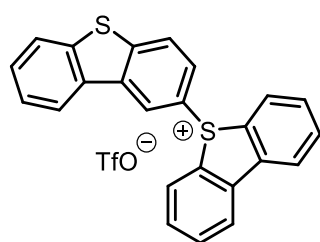
The salt **93l** was obtained as a pale-yellow solid in 67% yield (*o/p* ratio 3:7). Analytical NMR data of the major regioisomer. **¹H NMR** (400 MHz, CD₃CN): δ = 7.94 (dd, *J* = 7.9, 1.2 Hz, 2H), 7.72 – 7.68 (m, 2H), 7.53 (td, *J* = 7.5, 1.0 Hz, 2H), 7.41 – 7.37 (m, 2H), 7.35 – 7.29 (m, 4H), 7.26 – 7.22 (m, 2H), 7.07 – 7.03 (m, 2H) ppm. **¹⁹F NMR** (282 MHz, CD₃CN): –73.8, –79.2 ppm. **¹³C NMR** (101 MHz, CD₃CN): δ = 151.1, 146.5, 139.7, 136.4, 135.6, 132.8, 132.3, 132.1, 131.1, 130.7, 129.0, 127.2, 125.7, 123.21, 122.1 (q, ¹*J*_{C-F} = 320 Hz), 119.7 (q, ¹*J*_{C-F} = 320 Hz) ppm. **IR** (ATR): $\tilde{\nu}$ = 2361, 1730, 1589, 1260, 1143, 1084, 1028, 753, 635, 518 cm⁻¹. **HRMS** (+ESI) *calcd for* C₂₅H₁₆F₃O₃S₂⁺ [M–OTf]⁺ *m/z*: 485.0488; found: 485.0495.

5-(3,4-Dibromothiophen-2-yl)-5H-dibenzo[*b,d*]thiophen-5-ium Trifluoromethanesulfonate (93m):



The salt **93m** was obtained as a yellow solid in 76% yield. **¹H NMR** (500 MHz, CD₃CN): δ = 8.33 (dd, *J* = 7.8, 1.2 Hz, 2H), 8.21 – 8.18 (m, 2H), 8.05 (s, 1H), 8.00 (td, *J* = 7.7, 1.0 Hz, 2H), 7.78 (ddd, *J* = 8.5, 7.6, 1.2 Hz, 2H) ppm. **¹³C NMR** (126 MHz, CD₃CN): δ = 140.3, 136.3, 136.1, 133.0, 131.7, 129.3, 128.6, 125.8, 122.1 (q, ¹*J*_{C-F} = 322 Hz), 121.6, 117.2 ppm. **IR** (ATR): = 3086, 2360, 1709, 1448, 1258, 1223, 1157, 1033, 755, 633 cm⁻¹. **HRMS** (+ESI) *calcd for* C₁₆H₉Br₂S₂⁺ [M–OTf]⁺ *m/z*: 424.8486; found: 424.8486. **Mp** = 268.0 °C.

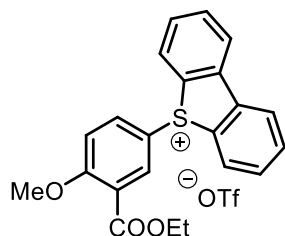
[2,5'-Bidibenzo[*b,d*]thiophen]-5'-ium Trifluoromethanesulfonate (93n):



The salt **93n** was obtained as a white solid in 95% yield. **¹H NMR** (300 MHz, CD₃CN): δ = 8.76 (d, *J* = 2.0 Hz, 1H), 8.38 (d, *J* = 7.9 Hz, 2H), 8.34 – 8.29 (m, 1H), 8.09 (t, *J* = 8.2 Hz, 3H), 8.03 – 7.93 (m, 3H), 7.72 (t, *J* = 7.8 Hz, 2H), 7.66 – 7.57 (m, 2H), 7.27 (dd, *J* = 8.7, 2.0 Hz, 1H) ppm. **¹³C NMR** (75 MHz, CD₃CN): δ = 147.4, 141.0, 140.4, 138.2, 135.5, 134.6, 133.3, 132.7, 129.8, 129.0, 127.3, 127.2, 126.8, 126.7, 125.7, 124.2, 123.5, 122.5

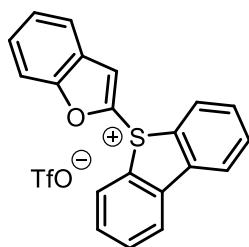
ppm. **IR** (ATR): $\tilde{\nu}$ = 3091, 2364, 1707, 1255, 1221, 1153, 1025, 761, 638, 518 cm^{-1} . **HRMS** (+ESI) *calcd for* $\text{C}_{24}\text{H}_{15}\text{S}_2^+$ $[\text{M}]^+$ m/z : 367.0610; found: 367.0597.

5-[3-(Ethoxycarbonyl)-4-methoxyphenyl]-5*H*-dibenzo[*b,d*]thiophen-5-ium Trifluoromethanesulfonate (93o):



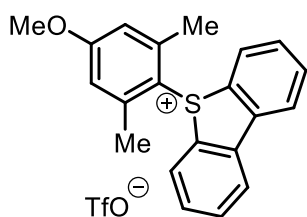
The salt **93o** was obtained as a yellow solid in 88% yield. **$^1\text{H NMR}$** (400 MHz, CD_3CN): δ = 8.34 (d, J = 8.5 Hz, 2H), 8.07 (d, J = 8.5 Hz, 2H), 7.97 – 7.91 (m, 3H), 7.74 – 7.69 (m, 2H), 7.57 (dd, J = 9.1, 2.7 Hz, 1H), 7.22 (d, J = 9.2 Hz, 1H), 4.26 (q, J = 7.1 Hz, 2H), 3.89 (s, 3H), 1.28 (t, J = 7.1 Hz, 3H) ppm. **$^{13}\text{C NMR}$** (101 MHz, CD_3CN): δ = 164.8, 164.4, 140.2, 136.4, 135.5, 135.1, 133.3, 132.7, 128.9, 125.6, 124.6, 122.1 (q, $^1J_{\text{C-F}}$ = 321 Hz), 116.7, 116.3, 62.6, 57.7, 14.4 ppm. **IR** (ATR): $\tilde{\nu}$ = 2361, 1730, 1589, 1260, 1143, 1084, 1028, 753, 635, 518 cm^{-1} . **HRMS** (+ESI) *calcd for* $\text{C}_{22}\text{H}_{19}\text{O}_3\text{S}^+$ $[\text{M}-\text{OTf}]^+$ m/z : 363.1049; found: 363.1054.

5-(Benzofuran-2-yl)-5*H*-dibenzo[*b,d*]thiophen-5-ium Trifluoromethane-sulfonate (93p):



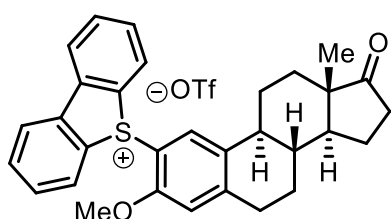
The salt **93p** was obtained as a beige solid in 21% yield. **$^1\text{H NMR}$** (400 MHz, CD_3CN): δ = 8.40 – 8.35 (m, 3H), 8.18 – 8.12 (m, 2H), 7.98 (td, J = 7.7, 1.0 Hz, 2H), 7.87 (ddd, J = 7.9, 1.4, 0.7 Hz, 1H), 7.74 (ddd, J = 8.2, 7.5, 1.2 Hz, 2H), 7.51 (ddd, J = 8.6, 7.3, 1.4 Hz, 1H), 7.43 (ddd, J = 8.2, 7.3, 1.0 Hz, 1H), 7.30 (dq, J = 8.5, 0.9 Hz, 1H) ppm. **$^{13}\text{C NMR}$** (101 MHz, CD_3CN): δ = 158.7, 140.8, 135.9, 133.1, 132.7, 130.8, 129.7, 129.2, 127.3, 126.2, 126.1, 125.6, 124.4, 122.1 (q, $^1J_{\text{C-F}}$ = 320 Hz), 112.9 ppm. **IR** (ATR): = 3090, 2922, 1714, 1611, 1443, 1260, 1159, 1029, 762, 636 cm^{-1} . **HRMS** (+ESI) *calcd for* $\text{C}_{20}\text{H}_{13}\text{OS}^+$ $[\text{M}-\text{OTf}]^+$ m/z : 301.0682; found: 301.0685. **Mp** = 146.0 $^\circ\text{C}$.

5-(4-Methoxy-2,6-dimethylphenyl)-5*H*-dibenzo[*b,d*]thiophen-5-ium Trifluoromethanesulfonate (93q):



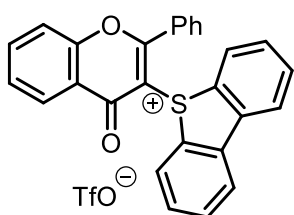
The salt **93q** was obtained as an orange solid in 72% yield (*o/p* ratio 1:1). **¹H NMR** (300 MHz, CD₃CN): δ = 8.35 (d, *J* = 8.4 Hz, 2H), 8.01 (d, *J* = 8.1 Hz, 2H), 7.97 (d, *J* = 7.6 Hz, 2H), 7.75 (td, *J* = 7.8, 1.2 Hz, 2H), 7.10 (d, *J* = 2.9 Hz, 1H), 6.73 (d, *J* = 2.9 Hz, 1H), 3.86 (s, 3H), 3.03 (s, 3H), 1.22 (s, 3H) ppm. **¹³C NMR** (75 MHz, CD₃CN): δ = 166.3, 150.9, 146.5, 139.9, 134.9, 132.4, 128.1, 126.5, 125.4, 119.7, 118.3, 117.0, 113.9, 56.9, 22.5, 17.9 ppm. **IR** (ATR): = 3085, 1578, 1448, 1323, 1262, 1222, 1159, 1029, 762, 636 cm⁻¹. **HRMS** (+ESI) *calcd* for C₂₁H₁₉OS⁺ [M-OTf]⁺ *m/z*: 319.1151; found: 319.1151. **Mp** = 141.0 °C.

5-[(8*R*,9*S*,13*S*,14*S*)-3-Methoxy-13-methyl-17-oxo-7,8,9,11,12,13,14,15,16,17-decahydro-6*H*-cyclopenta[*a*]phenanthren-2-yl]-5*H*-dibenzo[*b,d*]thiophen-5-ium Trifluoromethanesulfonate (93r):



The salt **93r** was obtained as a beige solid in 65% yield (*o/p* ratio 1:9). **¹H NMR** (400 MHz, CD₂Cl₂): δ = 8.25 (d, *J* = 7.9 Hz, 2H), 8.06 – 8.00 (m, 2H), 7.94 – 7.87 (m, 2H), 7.75 – 7.68 (m, 2H), 7.08 (s, 1H), 6.90 (s, 1H), 3.81 (s, 3H), 3.03 – 2.90 (m, 2H), 2.44 (dd, *J* = 18.3, 8.8 Hz, 1H), 2.21 – 1.90 (m, 5H), 1.83 – 1.73 (m, 3H), 1.64 – 1.29 (m, 4H), 0.83 (s, 3H) ppm. **¹³C NMR** (101 MHz, CD₂Cl₂): δ = 220.1, 157.7, 149.2, 140.0, 139.9, 136.5, 134.8, 134.8, 132.0, 128.3, 128.2, 124.7, 114.7, 57.5, 50.6, 48.1, 44.1, 37.9, 36.2, 31.8, 30.6, 26.2, 25.9, 21.9, 14.1 ppm. **IR** (ATR): $\tilde{\nu}$ = 2923, 2361, 1731, 1255, 1146, 1028, 758, 635, 571, 512 cm⁻¹. **HRMS** (+ESI) *calcd* for C₃₁H₃₁O₂S⁺ [M-OTf]⁺ *m/z*: 467.2039; found: 467.2039.

5-(4-Oxo-2-phenyl-4*H*-chromen-3-yl)-5*H*-dibenzo[*b,d*]thiophen-5-ium Trifluoromethanesulfonate (93s)

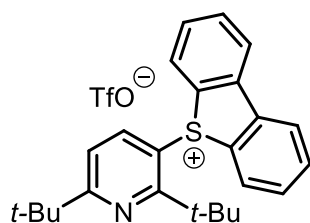


The salt **93s** was obtained as a beige solid in 36% yield. **¹H NMR** (400 MHz, CD₃CN): δ = 8.33 (dd, *J* = 7.8, 1.2 Hz, 2H), 8.10 (dt, *J* = 8.0, 0.8 Hz, 4H), 7.94 – 7.76 (m, 8H), 7.71 (ddd, *J* = 8.5, 7.5, 1.2 Hz, 2H), 7.52 (ddd, *J* = 8.1, 7.1, 1.0 Hz, 1H) ppm. **¹³C NMR** (101 MHz, CD₃CN): δ = 178.3, 172.1, 156.6, 141.3, 137.4, 134.8, 134.7, 131.8, 131.3, 130.4, 130.4, 128.9, 128.6, 128.0,

126.3, 124.9, 123.5, 121.9 (q, $^1J_{C-F} = 321$ Hz), 119.8, 105.4 ppm. **IR** (ATR): = 3085, 1707, 1655, 1532, 1363, 1260, 1151, 1029, 759, 634 cm^{-1} . **HRMS** (+ESI) *calcd for* $\text{C}_{27}\text{H}_{17}\text{O}_2\text{S}^+$ [M-OTf] $^+$ *m/z*: 405.0944; found: 405.0964. **Mp** = 191.6 °C.

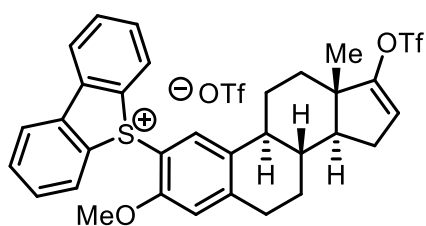
5-(2,6-di-*tert*-Butylpyridin-3-yl)-5*H*-dibenzo[*b,d*]thiophen-5-ium

Trifluoromethanesulfonate (93t):



The salt **93t** was obtained as a white solid in 60% yield. $^1\text{H NMR}$ (400 MHz, CD_3CN): $\delta = 8.39$ (d, $J = 7.9$ Hz, 2H), 7.98 (t, $J = 7.7$ Hz, 2H), 7.93 (d, $J = 8.1$ Hz, 2H), 7.73 (t, $J = 7.8$ Hz, 2H), 7.21 (d, $J = 8.6$ Hz, 1H), 6.89 (d, $J = 8.6$ Hz, 1H), 1.86 (s, 9H), 1.31 (s, 9H) ppm. $^{13}\text{C NMR}$ (101 MHz, CD_3CN): $\delta = 175.3, 170.5, 140.4, 140.3, 135.7, 133.4, 132.9, 128.5, 126.0, 121.6, 118.5, 41.3, 39.4, 32.3, 29.9$ ppm. **IR** (ATR): $\tilde{\nu} = 2955, 2923, 2361, 2335, 1568, 1255, 1151, 1028, 761, 635$ cm^{-1} . **HRMS** (+ESI) *calcd for* $\text{C}_{25}\text{H}_{28}\text{NS}^+$ [M-OTf] $^+$ *m/z*: 374.1937; found: 374.1937.

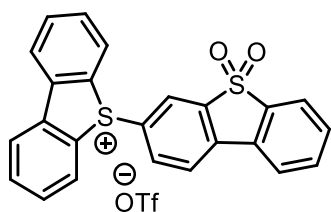
5-[(8*R*,9*S*,13*S*,14*S*)-3-Methoxy-13-methyl-17-[(trifluoromethyl)sulfonyl]oxy}-7,8,9,11,12,13,14,15-octahydro-6*H*-cyclopenta[*a*]phenanthren-2-yl)-5*H*-dibenzo[*b,d*]thiophen-5-ium Trifluoromethanesulfonate (93u):



The salt **93r** (704 mg, 1.14 mmol, 1.0 equiv.) and Na_2CO_3 (241.6 mg, 2.28 mmol, 2.0 equiv.) were suspended in DCM, and Tf_2O (515.8 mg, 307 μL , 1.83 mmol, 1.6 equiv.) was added at 0 °C. The reaction mixture was stirred for 24 h at this temperature, and subsequently the reaction was quenched with water. The aqueous phase was extracted with DCM (3 \times), the combined organic phases were dried over MgSO_4 and concentrated *in vacuo*. The desired compound was obtained as a beige solid (476 mg, 0.64 mmol, 56%) after column chromatography (DCM/MeOH, 95:5). The salt **93u** was obtained as a beige solid in 56% yield (*o/p* ratio 1:9). $^1\text{H NMR}$ (400 MHz, CD_3CN): $\delta = 8.31$ (dt, $J = 7.7, 1.7$ Hz, 2H), 8.05 (dt, $J = 8.3, 1.5$ Hz, 2H), 7.94 – 7.89 (m, 2H), 7.72 (ddd, $J = 7.8, 6.2, 1.6$ Hz, 2H), 7.10 – 6.97 (m, 2H), 5.67 (dd, $J = 3.3, 1.7$ Hz, 1H), 3.75 (d, $J = 1.5$ Hz, 3H), 2.93 (h, $J = 4.3$ Hz, 3H), 2.35 – 2.20 (m, 2H), 2.14 – 1.97 (m, 2H), 1.78 – 1.68 (m, 2H), 1.60 – 1.49 (m, 2H), 1.45 – 1.30 (m, 2H), 0.94 (s, 3H) ppm. $^{13}\text{C NMR}$ (75 MHz, CD_3CN): $\delta = 159.9, 157.9, 149.2, 140.7,$

140.6, 136.3, 135.0, 135.0, 134.3, 132.2, 131.3, 131.0, 128.5, 128.5, 125.2, 125.2, 116.6, 115.3, 109.8, 57.6, 54.1, 45.8, 44.4, 36.6, 33.2, 30.3, 28.8, 26.5, 26.0, 15.6 ppm. ^{19}F NMR (377 MHz, CD_3CN): $\delta = -74.6, -79.3$ ppm. IR (ATR): = 2935, 2864, 2358, 1598, 1420, 1262, 1222, 1146, 1029, 636 cm^{-1} . HRMS (+ESI) *calcd for* $\text{C}_{32}\text{H}_{30}\text{F}_3\text{O}_4\text{S}_2^+$ [M-OTf] $^+$ m/z 599.1532; found: 599.1532. Mp = 229.7 °C.

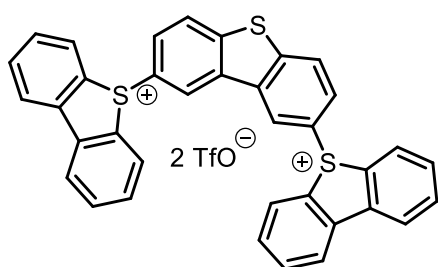
(3,5'-Bidibenzo[*b,d*]thiophen)-5'-ium 5,5-Dioxide Trifluoromethanesulfonate (93y):



The reaction was carried out according to the general procedure without the addition of an aromatic substrate. Dibenzo[*b,d*]thiophene 5-oxide (**15**) (300 mg, 1.50 mmol, 1.0 equiv.) was dissolved in DCM (12 mL), and Tf_2O (465.3 mg, 277 μL , 1.65 mmol, 1.1 equiv.) was added at -60 °C. The reaction mixture was then allowed to warm up to RT over the period of four hours. The crude product was purified by column chromatography using a gradient of DCM/MeOH (95:5 \rightarrow 90:10), whereupon compound **93n'** (45 mg, 80 μmol , 11%) was isolated as an off-white solid and compound **93y** (81 mg, 147 μmol , 20%) was isolated as a beige solid. ^1H NMR (400 MHz, CD_3CN) $\delta = 8.36$ (ddd, $J = 7.9, 1.3, 0.5$ Hz, 2H), 8.18 – 8.11 (m, 4H), 8.06 – 8.03 (m, 1H), 7.98 (ddd, $J = 7.9, 7.5, 1.0$ Hz, 2H), 7.88 (ddd, $J = 7.7, 1.2, 0.6$ Hz, 1H), 7.84 (dd, $J = 8.4, 1.9$ Hz, 1H), 7.79 (td, $J = 7.6, 1.2$ Hz, 1H), 7.77 – 7.69 (m, 3H) ppm. ^{13}C NMR (101 MHz, CD_3CN) $\delta = 207.5, 140.7, 138.8, 138.5, 137.4, 135.8, 135.8, 133.8, 132.8, 132.2, 130.0, 129.8, 129.2, 126.4, 125.8, 125.7, 124.9, 123.0, 122.1$ (q, $^1J_{\text{C-F}} = 320$ Hz) ppm. IR (ATR): = 3085, 2926, 1592, 1443, 1255, 1228, 1162, 1026, 765, 641 cm^{-1} . HRMS (+ESI) *calcd for* $\text{C}_{24}\text{H}_{15}\text{O}_2\text{S}_2^+$ [M-OTf] $^+$ m/z : 399.0508; found: 399.0510.

(5,2':8',5''-Terdibenzo[*b,d*]thiophenes)-5,5''-dium

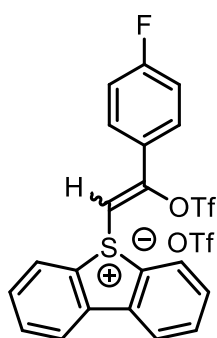
Trifluoromethanesulfonate (93n')



To a stirred solution of dibenzo[*b,d*]thiophene 5-oxide (**15**) (200.3 mg, 1.0 mmol, 1.0 equiv.) in DCM (10 mL), trifluoromethanesulfonic anhydride (282.1 mg, 168 μL , 1.0 mmol, 1.0 equiv.) was added in one portion at -50 °C under the atmosphere of N_2 . The reaction mixture was stirred for 15 min under the indicated temperature. Successively, the salt **93n** (516.6 mg, 1.0

mmol, 1.0 equiv.) was added as a solid in one portion, the mixture was stirred vigorously for 30 minutes and warmed up to room temperature during additional 30 min. The clear solution was transferred into a round-bottom flask, and the solvent was evaporated to a minimal volume. Then diethyl ether (150 mL) was added to the residue, and the dicationic salt precipitated. Analytically pure **93n'** was obtained by washing the precipitate with DCM (2 × 10 mL) as a beige solid in 62% yield. ¹H NMR (400 MHz, CD₃CN): δ = 8.80 (d, *J* = 2.0 Hz, 2H), 8.41 (dd, *J* = 7.9, 1.2 Hz, 4H), 8.15 (d, *J* = 8.7 Hz, 2H), 8.11 (dt, *J* = 8.1, 0.8 Hz, 4H), 7.99 (td, *J* = 7.7, 1.0 Hz, 4H), 7.73 (ddd, *J* = 8.5, 7.5, 1.2 Hz, 4H), 7.43 (dd, *J* = 8.7, 2.0 Hz, 2H) ppm. ¹³C NMR (101 MHz, CD₃CN): δ = 147.9, 140.5, 136.4, 135.6, 133.0, 132.7, 129.0, 128.5, 127.8, 127.6, 125.7, 124.3 ppm. IR (ATR): = 2908, 2360, 2335, 1273, 1255, 1156, 1031, 765, 636, 538 cm⁻¹. HRMS (+ESI) *calcd for* C₃₆H₂₂S₃²⁺ [M–2OTf]²⁺ *m/z*: 275.0436; found: 275.0440.

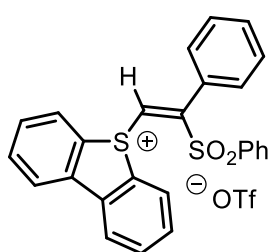
(*E/Z*)-5-[2-(4-Fluorophenyl)-2-[(trifluoromethyl)sulfonyl]oxy]vinyl]-5H-dibenzo[*b,d*]thiophen-5-ium Trifluoromethanesulfonate (**142a**):



A Schlenk flask, equipped with a stirring bar and charged with dibenzothiophene oxide **15** (200 mg, 1.0 mmol, 1.0 equiv.), was evacuated, filled with nitrogen, and the solid was dissolved in DCM (4 mL). The solution was cooled down to –50 °C, then HOTf (50 μL, 0.5 mmol, 0.5 equiv.) and successively Tf₂O (338.6 mg, 201.5 μL, 1.2 mmol, 1.2 equiv.) were added. The solution remained almost colorless; no orange suspension was formed. (*p*-fluorophenyl)acetylene (144.2 mg, 1.2 mmol, 1.2 equiv.) was added, the reaction mixture was warmed up and stirred at room temperature for 16 h. The solvent was removed under reduced pressure and the residue solidified with diethyl ether (10 mL) in the ultrasonic bath. After washing an additional time with diethyl ether (10 mL), the solvent was removed applying a filtration cannula. The residual solid was dried in vacuum affording compound **142a** as an off-white solid in 71% yield [mixture of *E/Z* isomers (1:1)]. ¹H NMR (400 MHz, CD₃CN): δ = 8.35 (d, *J* = 8.6 Hz) and 8.32 (d, *J* = 7.9 Hz (2H)); 8.26 (dt, *J* = 8.1, 0.9 Hz) and 8.23 (dt, *J* = 8.1, 0.8 Hz) (2H); 8.04 – 7.96 (m, 7H), 7.81 (t, *J* = 8.2 Hz, 4H), 7.76 (dd, *J* = 9.1, 5.1 Hz, 2H), 7.52 (t, *J* = 8.8 Hz) and 7.30 (t, *J* = 8.8 Hz) (2H); 6.70 (s) and 6.62 (s) (1H) ppm. ¹⁹F NMR (376 MHz, CD₃CN): δ = –72.6, –73.9, –79.3, –104.6, –104.8 ppm. ¹³C NMR (101 MHz, CDCl₃): δ = 166.9 (d, ¹*J*_{C–F} = 255.6 Hz), 166.8 (d, ¹*J*_{C–F} = 254.8 Hz), 163.9, 161.9, 141.2, 141.0, 137.2, 137.1, 136.1, 136.1, 134.1, 134.0, 133.1, 132.8 (d, ²*J*_{C–F} = 8.9 Hz), 131.7, 131.6, 130.1, 129.8, 129.5 (d, ²*J*_{C–F} = 11.6

Hz), 129.1, 126.7 (d, $^3J_{C-F} = 3.1$ Hz), 125.7, 125.7, 125.7, 125.1 (d, $^3J_{C-F} = 3.3$ Hz), 121.0, 120.8, 118.1, 118.8, 117.7, 112.5, 108.7 (d, $^4J_{C-F} = 1.7$ Hz) ppm. **IR** (ATR): $\tilde{\nu} = 3734, 3626, 1600, 1426, 1218, 1127, 1025, 765, 633, 512$ cm $^{-1}$. **HRMS** (ESI) *calcd for* C $_{31}$ H $_{13}$ F $_4$ O $_3$ S $_2^+$ [M-OTf] $^+$ *m/z*: 453.0237; found: 453.0235.

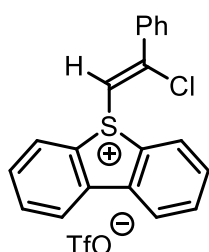
(Z)-5-[2-Phenyl-2-(phenylsulfonyl)vinyl]-5H-dibenzo[*b,d*]thiophen-5-ium Trifluoromethanesulfonate (142b):



A Schlenk flask was equipped with a stirring bar and charged with sulfonium salt **5a** (1.01 g, 2.32 mmol, 1 equiv.) and phenylsulfinic acid (330 mg, 2.32 mmol, 1 equiv.). The reactants were dissolved in a mixture of DCM (10 mL) and *t*-BuOH (1 mL). The reaction mixture was stirred at room temperature for 12 h. The solvents were evaporated to a minimum volume, and diethyl ether (50 mL) was added to precipitate the salt. The latter was filtered off, washed once more with diethyl ether (30 mL) and dried in vacuo affording product **142b** as a beige solid (1.1 g, 1.93 mmol, 83%). **$^1\text{H NMR}$** (400 MHz, CD $_3$ CN) $\delta = 8.52$ (d, $J = 8.2$ Hz, 2H), 8.31 (d, $J = 7.8$ Hz, 2H), 7.98 (t, $J = 7.7$ Hz, 2H), 7.93 (d, $J = 8.5$ Hz, 2H), 7.87 – 7.83 (m, 2H), 7.79 (t, $J = 7.5$ Hz, 1H), 7.64 – 7.59 (m, 2H), 7.43 (t, $J = 8.7$ Hz, 1H), 7.34 – 7.29 (m, 4H), 6.84 (s, 1H) ppm. **$^{13}\text{C NMR}$** (101 MHz, CD $_3$ CN): $\delta = 157.5, 141.1, 136.9, 136.3, 135.8, 132.9, 132.5, 131.7, 130.9, 130.6, 130.30, 130.28, 129.8, 129.6, 127.9, 125.4, 122.1$ (q, $^1J_{C-F} = 321$ Hz) ppm. **IR** (ATR): $\tilde{\nu} = 2360, 2337, 1447, 1309, 1253, 1224, 1148, 1028, 759, 635$ cm $^{-1}$. **HRMS** (ESI) *calcd for* C $_{26}$ H $_{19}$ O $_2$ S $_2^+$ [M-OTf] $^+$ *m/z*: 427.0821; found: 427.0821.

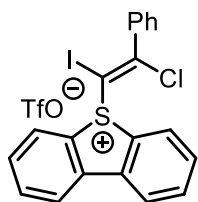
(Z)-5-(2-Chloro-2-phenylvinyl)-5H-dibenzo[*b,d*]thiophen-5-ium Trifluoromethanesulfonate (142c):

The salt **5a** (102 mg, 235 μ mol, 1.0 equiv.) was dissolved in DCM (2 mL), and HCl (0.18 mL of a 2 M solution in Et $_2$ O; 360 μ mol, 1.53 equiv.) was added. The reaction was mixture stirred at room temperature for 12 h under the atmosphere of nitrogen. The solvent was removed under reduced pressure, and the residue was solidified by sonication with diethyl ether (10 mL) in the ultrasonic bath. After repeated washing with diethyl ether (10 mL), the solvent was removed using a filtration cannula and the solid dried in vacuum. The salt **142c** was obtained as a white foam in 48% yield. **$^1\text{H NMR}$** (400 MHz, CD $_3$ CN): $\delta = 8.32$ (d, $J = 8.6$ Hz,



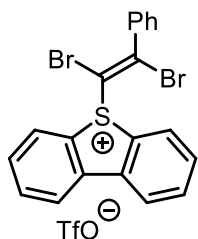
2H), 8.27 (d, $J = 8.1$ Hz, 2H), 7.97 (t, $J = 8.2$ Hz, 2H), 7.79 (t, $J = 7.2$ Hz, 2H), 7.76 – 7.73 (m, 2H), 7.61 – 7.57 (m, 1H), 7.52 – 7.47 (m, 2H), 6.84 (s, 1H) ppm. $^{13}\text{C NMR}$ (101 MHz, CDCl_3): $\delta = 156.4, 141.0, 135.6, 134.3, 134.0, 132.6, 130.7, 130.2, 129.3, 128.7, 125.4, 122.1$ (q, $^1J_{\text{C-F}} = 322$ Hz), 113.7 ppm. **IR** (ATR): $\tilde{\nu} = 1702, 1557, 1445, 1253, 1221, 1151, 1028, 924, 753, 635$ cm^{-1} . **HRMS** (ESI) *calcd for* $\text{C}_{20}\text{H}_{14}\text{ClS}^+ [\text{M-OTf}]^+$ m/z : 321.0499; found: 321.0494.

(*E*)-5-(2-Chloro-1-iodo-2-phenylvinyl)-5*H*-dibenzo[*b,d*]thiophen-5-ium Trifluoromethanesulfonate (142d):



The salt **5a** (102 mg, 235 μmol , 1 equiv.) was dissolved in DCM (2 mL) and iodine monochloride (45.8 mg, 282 μmol , 1.2 equiv.) was added. The reaction mixture was stirred at room temperature for 12 h under the atmosphere of nitrogen. The solvent was removed under reduced pressure, and the residue was solidified by sonication with diethyl ether (10 mL) in the ultrasonic bath. After repeated washing with diethyl ether (10 mL), the solvent was removed using a filtration cannula and the solid dried in vacuum. The salt **142d** was obtained as a white solid in 80% yield. $^1\text{H NMR}$ (400 MHz, CD_3CN): $\delta = 8.32$ (dd, $J = 8.1, 1.5$ Hz, 2H), 8.28 (dd, $J = 8.1, 1.6$ Hz, 2H), 8.07 – 8.02 (m, 2H), 7.87 – 7.81 (m, 2H), 7.62 (dd, $J = 8.0, 1.7$ Hz, 2H), 7.59 – 7.51 (m, 3H) ppm. $^{13}\text{C NMR}$ (101 MHz, CDCl_3): $\delta = 155.5, 141.8, 139.1, 136.5, 132.9, 132.9$ (^{13}C -signals overlapping), 130.9, 130.0, 129.8, 129.6, 125.6, 122.1 (q, $^1J_{\text{C-F}} = 321$ Hz), 84.0 ppm. **IR** (ATR): $\tilde{\nu} = 3086, 2360, 2268, 1253, 1221, 1156, 1025, 758, 673, 638$ cm^{-1} . **HRMS** (ESI) *calcd for* $\text{C}_{20}\text{H}_{13}\text{ClIS}^+ [\text{M-OTf}]^+$ m/z : 446.9466; found: 446.9466.

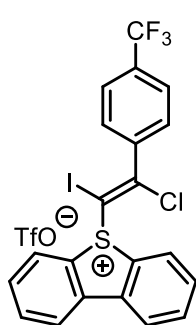
(*E*)-5-(1,2-Dibromo-2-phenylvinyl)-5*H*-dibenzo[*b,d*]thiophen-5-ium Trifluoromethanesulfonate (142e):



The salt **5a** (102 mg, 235 μmol , 1.0 equiv.) was dissolved in DCM (2 mL), and bromine (37.6 mg, 12 μL , 235 μmol , 1.0 equiv.) was added. The reaction mixture was stirred at room temperature for 12 h under the atmosphere of nitrogen. The solvent was removed under reduced pressure, and the residue was solidified by sonication with diethyl ether (10 mL) in the ultrasonic bath. After repeated washing with diethyl ether (10 mL), the solvent was removed using a filtration cannula and the solid dried in vacuum. The salt **142e** was obtained as a yellow solid in 74% yield. $^1\text{H NMR}$ (400 MHz, CD_3CN): $\delta = 8.38$ (d, $J = 8.1$ Hz, 2H), 8.31 (d, $J = 8.6$ Hz, 2H), 8.01 (t, J

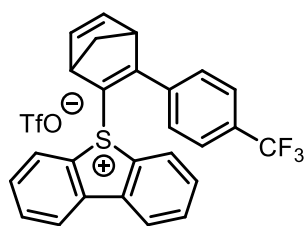
= 7.7 Hz, 2H), 7.83 (t, J = 8.4 Hz, 2H), 7.58 (dd, J = 7.4, 2.3 Hz, 2H), 7.54 – 7.47 (m, 3H) ppm. ^{13}C NMR (101 MHz, CDCl_3): δ = 144.4, 141.9, 138.7, 136.6, 132.8, 132.6, 129.9, 129.8, 129.5, 129.3, 125.6, 122.1 (q, $^1J_{\text{C-F}}$ = 322 Hz), 108.2 ppm. IR (ATR): $\tilde{\nu}$ = 1445, 1258, 1224, 1156, 1025, 758, 697, 670, 635, 518 cm^{-1} . HRMS (ESI) *calcd for* $\text{C}_{20}\text{H}_{13}\text{Br}_2\text{S}^+$ [M–OTf] $^+$ m/z : 442.9099; found: 442.9100.

(E)-5-{2-Chloro-1-iodo-2-[4-(trifluoromethyl)phenyl]vinyl}-5H-dibenzo[*b,d*]thiophen-5-ium Trifluoromethanesulfonate (142f):



To the stirred solution of the salt **5c** (754 mg, 1.5 mmol, 1 equiv.) in DCM (10 mL) iodo monochloride (268 mg, 1.65 mmol, 1.1 equiv.) was added in one portion. After a short period, precipitation of the solid from DCM was observed. The reaction mixture was stirred at room temperature for an additional 12 h under ambient atmosphere. The solvent was removed under reduced pressure and the residue solidified by sonication with *n*-hexane (100 mL) in the ultrasonic bath. After repeated washing with *n*-hexane (100 mL), the solvent was removed using either a filtration cannula or by decantation. The residual solid was dried in vacuum affording the salt **142f** as a yellow solid in 92% yield. ^1H NMR [400 MHz, $(\text{CD}_3)_2\text{CO}$]: δ = 8.58 (d, J = 8.1 Hz, 2H), 8.54 (d, J = 7.8 Hz, 2H), 8.12 (t, J = 8.1 Hz, 2H), 7.93 (s, 6H) ppm. ^{19}F NMR [377 MHz, $(\text{CD}_3)_2\text{CO}$]: δ = –63.6, –78.8 ppm. ^{13}C NMR [101 MHz, $(\text{CD}_3)_2\text{CO}$]: δ = 152.3, 143.2 (q, $^4J_{\text{C-F}}$ = 1.3 Hz), 141.9, 136.4, 132.8, 131.5, 130.9, 130.5, 130.0, 126.9 (q, $^3J_{\text{C-F}}$ = 3.6 Hz), 125.6, 124.6 (q, $^1J_{\text{C-F}}$ = 272.6 Hz), 122.3 (q, $^1J_{\text{C-F}}$ = 322.3 Hz), 87.6 ppm. IR (ATR): $\tilde{\nu}$ = 3730, 3628, 1739, 1325, 1242, 1165, 1023, 670, 633, 512 cm^{-1} . HRMS (ESI) *calcd for* $\text{C}_{21}\text{H}_{12}\text{ClF}_3\text{S}^+$ [M–OTf] $^+$ m/z : 514.9340; found: 514.9344.

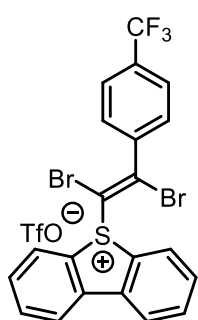
5-{3-[4-(Trifluoromethyl)phenyl]bicyclo[2.2.1]hepta-2,5-dien-2-yl}-5H-dibenzo[*b,d*]thiophen-5-ium Trifluoromethanesulfonate (142g):



The salt **5c** (200 mg, 0.40 mmol, 1.0 equiv.) was dissolved in MeCN (2 mL, not anhydrous), and freshly prepared cyclopentadiene (168.2 μL , 132.2 mg, 2.0 mmol, 5 equiv.) was added in one portion. The reaction mixture was heated in a sealed microwave vial under microwave irradiation at 100 $^\circ\text{C}$ for 2 h under ambient atmosphere, and the solution turns dark green. The product was solidified by sonication with *n*-hexane (20

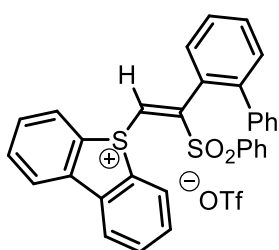
mL) in the ultrasonic bath. After washing with a second portion of *n*-hexane (20 mL), the solvent was removed either applying a filtration cannula or by decantation. The residual solid was dried in vacuum affording the salt **142g** as a pale green solid in 67% yield. ¹H NMR (400 MHz, CD₃CN): δ = 8.38 (dd, *J* = 8.2, 4.0 Hz, 2H), 8.30 (d, *J* = 8.6 Hz, 1H), 8.03 – 7.94 (m, 6H), 7.87 – 7.82 (m, 1H), 7.71 – 7.60 (m, 2H), 6.97 – 6.92 (m, 1H), 6.24 – 6.20 (m, 1H), 4.25 (s, 1H), 2.77 (s, 1H), 2.22 – 2.15 (m, 1H), 1.99 – 1.96 (m, 1H) ppm. ¹⁹F NMR (377 MHz, CD₃CN): δ = –63.3, –79.3 ppm. ¹³C NMR (101 MHz, CD₃CN): δ = 178.7, 143.3, 141.3, 141.2, 140.9, 136.6 (q, ⁴*J*_{C-F} = 1.3 Hz), 135.6, 135.5, 132.9 (q, ²*J*_{C-F} = 32.8 Hz), 132.68, 131.9, 131.3, 129.8, 129.44, 129.42, 129.42 (2 ¹³C-signals overlapping), 129.0, 127.4, 127.1 (q, ³*J*_{C-F} = 3.8 Hz), 126.0, 125.6, 125.1 (q, ¹*J*_{C-F} = 272.0 Hz), 122.1 (q, ¹*J*_{C-F} = 320.2 Hz), 71.6, 60.0, 52.2 ppm (19 ¹³C-Signals expected, 26 detected because of the hindered rotation of the DBT-unit). IR (ATR): $\tilde{\nu}$ = 3091, 2950, 1710, 1325, 1258, 1159, 1121, 1068, 1028, 635 cm⁻¹. HRMS (ESI) *calcd for* C₂₆H₁₈F₃S⁺ [M–OTf]⁺ *m/z*: 419.1076; found: 419.1079.

(*E*)-5-{1,2-Dibromo-2-[4-(trifluoromethyl)phenyl]vinyl}-5*H*-dibenzo[*b,d*]thiophen-5-ium Trifluoromethanesulfonate (142h):



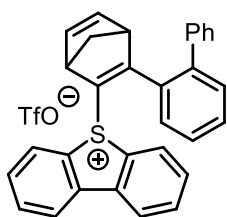
The salt **5c** (115.6 mg, 230 μmol, 1.0 equiv.) was dissolved in DCM (2 mL), and bromine (36.8 mg, 11.8 μL, 0.23 mmol, 1.0 equiv.) was added in one portion. The reaction mixture was stirred at room temperature for 1 h under ambient atmosphere. The solvent was removed under reduced pressure, and the residue was solidified by sonication with diethyl ether (10 mL) in the ultrasonic bath. After repeated washing with diethyl ether (10 mL) and pentane (10 mL), the solvents were removed applying either a filtration cannula or by decantation, and the residual solid was dried in vacuum furnishing the salt **142f** as a white solid in 79% yield. ¹H NMR (400 MHz, CD₃CN): δ = 8.37 (d, *J* = 7.7 Hz, 2H), 8.31 (dd, *J* = 8.1, 0.9 Hz, 2H), 8.03 (td, *J* = 7.7, 1.0 Hz, 2H), 7.86 – 7.80 (m, 4H), 7.76 – 7.71 (m, 2H) ppm. ¹⁹F NMR (377 MHz, CD₃CN): δ = –63.7, 79.3 ppm. ¹³C NMR (101 MHz, CDCl₃): δ = 142.5, 142.1, 142.1, 136.8, 133.3, 133.0, 130.2, 130.0, 129.1, 127.1 (q, ³*J*_{C-F} = 3.8 Hz, CF₃), 125.9, 125.7, 122.1 (q, ¹*J*_{C-F} = 321 Hz), 110.5 ppm. IR (ATR): $\tilde{\nu}$ = 3730, 1325, 1255, 1224, 1159, 1130, 1063, 1028, 761, 635 cm⁻¹. HRMS (ESI) *calcd for* C₂₁H₁₂Br₂F₃S⁺ [M–OTf]⁺ *m/z*: 512.8953; found: 512.8964.

(Z)-5-{2-([1,1'-Biphenyl]-2-yl)-2-(phenylsulfonyl)vinyl}-5H-dibenzo-
[b,d]thiophen-5-ium Trifluoromethanesulfonate (142i):



A Schlenk flask was equipped with a stirring bar and charged with the salt **5j** (944.5 mg, 1.85 mmol, 1.0 equiv.) and phenylsulfinic acid (526 mg, 3.70 mmol, 2.0 equiv.). The reactants were dissolved in a mixture of DCM (15 mL) and *t*-BuOH (2 mL). After stirring the reaction mixture at room temperature for 12 h, the solvents were evaporated to a minimal volume, diethyl ether (50 mL) was added to precipitate the salt. The latter was filtered off, washed once more with diethyl ether (30 mL) and dried in vacuo affording the salt **142i** as a pale yellow in 75% yield. $^1\text{H NMR}$ (400 MHz, CD_3CN): δ = 8.26 (d, J = 7.9 Hz, 2H), 8.06 (d, J = 8.1 Hz, 2H), 7.98 – 7.90 (m, 3H), 7.86 (d, J = 7.4 Hz, 2H), 7.79 – 7.75 (m, 2H), 7.74 – 7.69 (m, 2H), 7.49 (t, J = 7.6 Hz, 1H), 7.36 (t, J = 7.7 Hz, 1H), 7.27 – 7.19 (m, 3H), 7.03 (t, J = 7.8 Hz, 2H), 6.58 (d, J = 9.5 Hz, 2H), 6.52 (s, 1H) ppm. $^{13}\text{C NMR}$ (101 MHz, CD_3CN): δ = 157.2, 143.8, 140.9, 139.8, 137.3, 136.2, 135.8, 132.9, 132.2, 131.9, 131.3, 130.9, 130.8, 130.6, 130.1, 129.9, 129.5, 129.2, 128.7, 128.6, 128.4, 125.4, 122.1 (q, $^1J_{\text{C-F}}$ = 321 Hz) ppm. IR (ATR): $\tilde{\nu}$ = 3735, 3626, 3064, 3014, 1445, 1255, 1148, 1025, 635 cm^{-1} . HRMS (ESI) *calcd for* $\text{C}_{32}\text{H}_{23}\text{O}_2\text{S}^+$ [M-OTf] $^+$ m/z : 503.1134; found: 503.1137.

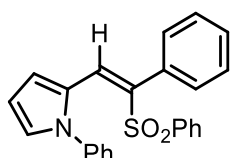
5-{3-([1,1'-Biphenyl]-2-yl)bicyclo[2.2.1]hepta-2,5-dien-2-yl}-5H-
dibenzo[b,d]thiophen-5-ium Trifluoromethanesulfonate (142j):



The salt **5j** (204 mg, 0.4 mmol, 1.0 equiv.) was dissolved in MeCN (2 mL, not anhydrous), and freshly prepared cyclopentadiene (168.2 μL , 132.2 mg, 2.0 mmol, 5.0 equiv.) was added in one portion. The reaction mixture was heated in a sealed microwave vial at 100 $^\circ\text{C}$ for 3 h in a microwave under ambient atmosphere, and the solution turned brown. The reaction mixture was solidified by sonication with Et_2O (30 mL) in the ultrasonic bath. After repeated washing with Et_2O (30 mL), the solvent was removed applying either a filtration cannula or by decantation, and the solid was dried in vacuum furnishing the product **142j** as a dark brown solid in 52% yield. $^1\text{H NMR}$ (400 MHz, CD_3CN): δ = 8.29 (t, J = 9.4 Hz, 2H), 7.95 – 7.88 (m, 2H), 7.71 (d, J = 8.7 Hz, 1H), 7.68 – 7.63 (m, 3H), 7.62 – 7.60 (m, 1H), 7.60 – 7.55 (m, 3H), 7.54 – 7.49 (m, 3H), 7.26 (d, J = 8.0 Hz, 2H), 6.56 – 6.51 (m, 1H), 6.06 – 6.02 (m, 1H), 3.84 – 3.79 (m, 1H), 2.57 –

2.52 (m, 1H), 2.08 – 2.05 (m, 1H), 1.86 – 1.83 (m, 1H) ppm. ^{13}C NMR (101 MHz, CD_3CN): δ = 142.2, 141.7, 141.5, 141.1, 140.7, 135.4, 135.3, 132.5, 132.4, 132.1, 131.8, 131.7, 131.1, 130.0, 129.8, 129.6, 129.3, 129.2, 129.0, 128.8, 128.4, 128.0, 125.9, 125.5, 122.1 (q, $^1J_{\text{C-F}}$ = 322 Hz), 72.0, 61.2, 51.1 ppm. IR (ATR): $\tilde{\nu}$ = 3730, 3628, 3594, 1539, 1260, 1151, 1028, 755, 673, 651 cm^{-1} . HRMS (ESI) *calcd* for $\text{C}_{31}\text{H}_{23}\text{S}^+$ [M-OtF] $^+$ m/z : 427.1515; found: 427.1518.

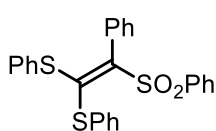
(Z)-1-Phenyl-2-[2-phenyl-2-(phenylsulfonyl)vinyl]-1H-pyrrole (149)



A microwave tube was equipped with a stirring bar and charged with the salt **142b** (115.3 mg, 200 μmol , 1.0 equiv.), *N*-phenylpyrrole (286.4 mg, 2.0 mmol, 10 equiv.) and $[\text{Ru}(\text{BPy})_3\text{Cl}_2 \times 6 \text{H}_2\text{O}]$ (3 mg, 6.2 μmol , 3.1 mol%).

The tube was closed and flushed three times with nitrogen. MeCN (2 mL) was added, and the solution was degassed for 2 min. The reaction mixture was exposed to Blue LED light irradiation (28 W) for 16 h. Afterwards the reaction mixture was directly transferred to a pre-wetted column (hexanes). The pure product **149** was obtained by column chromatography (gradient hexanes \rightarrow hexanes:EtOAc 4:1) as a white solid in 34% yield. ^1H NMR (400 MHz, CDCl_3): δ = 7.71 (s, 1H), 7.59 – 7.48 (m, 6H), 7.40 – 7.32 (m, 7H), 7.03 (dd, J = 8.1, 1.2 Hz, 2H), 6.95 – 6.92 (m, 1H), 6.10 – 6.04 (m, 1H), 5.56 (d, J = 5.4 Hz, 1H) ppm. ^{13}C NMR (101 MHz, CDCl_3): δ = 139.6, 138.6, 135.4, 133.0, 132.2, 131.0, 130.1, 129.8, 129.2, 129.2 (^{13}C -signals overlapping), 128.8, 128.53, 128.49, 127.2, 126.9, 126.7, 115.0, 110.7 ppm. IR (ATR): $\tilde{\nu}$ = 3733, 3628, 1616, 1498, 1447, 1301, 1146, 1082, 694, 603 cm^{-1} . HRMS (ESI) *calcd* for $\text{C}_{24}\text{H}_{20}\text{NO}_2\text{S}^+$ [M+H] $^+$ m/z : 386.1209; found: 386.1202.

[2-Phenyl-2-(phenylsulfonyl)ethene-1,1-diyl]bis(phenylsulfane) (151a):



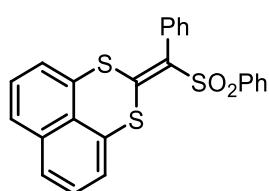
The transfer reagent **5a** (87.0 mg, 0.20 mmol, 1.0 equiv.), diphenyl disulfide (**150a**, 52.4 mg, 0.24 mmol, 1.2 equiv.) and sodium phenylsulfinate (49.2 mg, 0.24 mmol, 1.2 equiv.) were dissolved in MeCN (3 mL). The reaction

mixture was stirred at room temperature under an atmosphere of nitrogen with TLC monitoring. Upon completion of the reaction (12 h), pentane (5 mL) was added, and the reaction mixture was transferred directly to a pre-wetted column (hexanes). The pure product **151a** was obtained by column chromatography (gradient hexanes \rightarrow hexanes:EtOAc 8:2) as a white solid in 14% yield. ^1H NMR (400 MHz, CDCl_3): δ = 7.99 (d, J = 8.0 Hz, 2H), 7.58 (t, J = 7.4 Hz, 1H), 7.46 (t, J = 7.8 Hz, 2H), 7.41 – 7.37 (m, 3H), 7.30 (d, J = 9.6 Hz, 2H), 7.17 (t, J = 8.6 Hz,

2H), 7.08 – 7.01 (m, 4H), 6.81 (d, $J = 7.9$ Hz, 2H), 6.66 (d, $J = 8.0$ Hz, 2H) ppm. $^{13}\text{C NMR}$ (101 MHz, CDCl_3): $\delta = 151.2, 144.0, 141.5, 135.1, 133.3, 133.1, 132.3, 132.2, 131.7, 130.8, 130.1, 129.3, 128.82, 128.75, 128.52, 128.47, 128.2, 128.1$ ppm. IR (ATR): $\tilde{\nu} = 2274, 1868, 1752, 1696, 1539, 1212, 1148, 684, 670, 651$ cm^{-1} . HRMS (ESI) *calcd for* $\text{C}_{26}\text{H}_{20}\text{NaO}_2\text{S}_3^+$ $[\text{M}+\text{Na}]^+$ m/z : 483.0518; found: 483.0514.

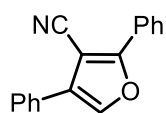
2-[Phenyl(phenylsulfonyl)methylene]naphtho[1,8-de][1,3]dithiine

(151b):



The transfer reagent **5a** (87.0 mg, 0.20 mmol, 1.0 equiv.), the corresponding disulfide **150b** (76.1 mg, 0.4 mmol, 2.0 equiv.), 15-C-5 (0.09 mL, 4 mmol, 2.0 equiv.) and sodium phenylsulfinate (49.2 mg, 0.3 mmol, 1.5 equiv.) were dissolved in DCM (3 mL). The reaction mixture was stirred at room temperature under an atmosphere of atmosphere with TLC monitoring. Upon completion of the reaction (12 h), pentane (5 mL) was added, and the reaction mixture was transferred directly to a prewetted column (hexanes). The pure product **151b** was obtained by column chromatography (gradient hexanes \rightarrow hexanes:EtOAc 8:2) as a white solid in 42% yield. $^1\text{H NMR}$ (400 MHz, CDCl_3): $\delta = 7.83$ (dd, $J = 8.4, 1.2$ Hz, 2H), 7.63 (d, $J = 8.1$ Hz, 1H), 7.61 – 7.55 (m, 2H), 7.50 (d, $J = 6.2$ Hz, 1H), 7.48 – 7.35 (m, 6H), 7.30 – 7.26 (m, 1H), 7.10 (dd, $J = 11.3, 7.2$ Hz, 3H) ppm. $^{13}\text{C NMR}$ (101 MHz, CDCl_3): $\delta = 143.3, 140.7, 134.3, 133.5, 133.1, 131.8, 130.8, 129.6, 128.9, 128.8, 128.3, 128.2, 128.1, 127.5, 127.4, 126.7, 126.4, 124.1, 123.3, 122.7$ ppm. IR (ATR): $\tilde{\nu} = 1557, 1506, 1314, 1207, 1146, 1082, 684, 667, 651, 577$ cm^{-1} . HRMS (ESI) *calcd for* $\text{C}_{24}\text{H}_{17}\text{O}_2\text{S}_3^+$ $[\text{M}+\text{H}]^+$ m/z : 433.0385; found: 433.0388.

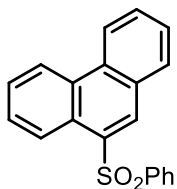
2,4-Diphenylfuran-3-carbonitrile (153):



A mixture of the transfer reagent **5a** (87.0 mg, 0.2 mmol, 1.0 equiv.), Cs_2CO_3 (78.2 mg, 0.24 mmol, 1.2 equiv.) and benzoylacetonitrile (**152**, 30.2 μL , 34.8 mg, 0.24 mmol, 1.2 equiv.) in THF (2 mL) was stirred at 70 $^\circ\text{C}$ for 30 min under ambient atmosphere. The reaction was monitored by TLC. The reaction mixture was directly transferred to a pre-wetted column (hexanes). The pure product **153** was obtained by column chromatography (gradient hexanes \rightarrow hexanes:EtOAc 95:5) as a yellow solid in 92% yield. $^1\text{H NMR}$ (400 MHz, CDCl_3): $\delta = 8.06$ (dd, $J = 8.3, 1.4$ Hz, 2H), 7.67 – 7.63 (m, 3H), 7.54 – 7.44 (m, 5H), 7.41 (t, $J = 7.3$ Hz, 1H) ppm. $^{13}\text{C NMR}$ (101 MHz, CDCl_3): $\delta = 161.3, 138.5, 130.5, 129.4,$

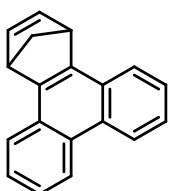
129.24, 129.23, 129.0, 128.7, 128.2, 127.2, 125.7, 115.2, 91.8 ppm. IR (ATR): $\tilde{\nu}$ = 2223, 1782, 1547, 1491, 1447, 1200, 1068, 916, 767, 688 cm^{-1} . HRMS (ESI) *calcd for* $\text{C}_{17}\text{H}_{12}\text{NO}^+$ $[\text{M}+\text{H}]^+$ m/z : 246.0913; found: 246.0911. Analytical data are identical to the previously reported ones.²⁰⁹

9-(Phenylsulfonyl)phenanthrene (159):



A microwave vial equipped with a stirring bar was charged with **142i** (130.5 mg, 0.2 mmol, 1.0 equiv.), Cs_2CO_3 (71.7 mg, 0.22 mmol, 1.1 equiv.) and $[\text{Ru}(\text{BPy})_3]\text{Cl}_2 \times 6 \text{H}_2\text{O}$ (3 mg, 4.0 μmol , 2.0 mol%). The vial was purged three times with nitrogen and sealed. After adding degassed MeCN (2 mL) and degassing once more for two min, the reaction mixture was exposed to blue LED light irradiation (28W) at room temperature for 16 h, then transferred directly to a pre-wetted column (hexanes). The pure product **159** was obtained by column chromatography (gradient hexanes \rightarrow hexanes:EtOAc 8:2) as a pale-yellow solid in 58% yield. $^1\text{H NMR}$ (400 MHz, CDCl_3): δ = 8.92 (s, 1H), 8.74 – 8.67 (m, 2H), 8.63 (d, J = 9.0 Hz, 1H), 8.11 (d, J = 8.5 Hz, 1H), 8.00 (d, J = 7.3 Hz, 2H), 7.83 (t, J = 8.4 Hz, 1H), 7.73 (t, J = 7.1 Hz, 1H), 7.68 (t, J = 7.0 Hz, 1H), 7.62 – 7.58 (m, 1H), 7.53 (t, J = 7.3 Hz, 1H), 7.47 (t, J = 7.4 Hz, 2H) ppm. $^{13}\text{C NMR}$ (101 MHz, CDCl_3): δ = 141.7, 134.3, 133.2, 133.1, 132.9, 131.4, 130.9, 130.2, 129.4, 129.2, 127.8, 127.7, 127.5, 127.5 (2 ^{13}C -signals overlapping), 126.1, 125.5, 123.4, 122.9 ppm. IR (ATR): $\tilde{\nu}$ = 1447, 1322, 1151, 1082, 791, 753, 734, 686, 649, 566 cm^{-1} . HRMS (ESI) *calcd for* $\text{C}_{20}\text{H}_{14}\text{NaO}_2\text{S}^+$ $[\text{M}+\text{Na}]^+$ m/z : 341.0607; found: 341.0608. Analytical data are identical to the previously reported ones.²¹¹

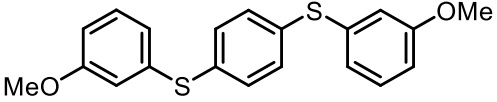
1,4-Dihydro-1,4-methanotriphenylene (160):



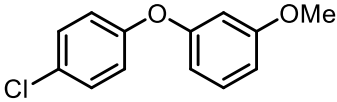
A microwave vial equipped with a stirring bar was charged with the salt **142j** (115.3 mg, 0.2 mmol, 1.0 equiv.), Cs_2CO_3 (71.7 mg, 0.22 mmol, 1.1 equiv.) and $[\text{Ru}(\text{BPy})_3]\text{Cl}_2 \times 6 \text{H}_2\text{O}$ (3 mg, 4.0 μmol , 2.0 mol%), purged three times with nitrogen and sealed. After adding degassed MeCN (2 mL) and degassing once more for two min, the reaction mixture was exposed to blue LED light irradiation (28W) at room temperature for 16 h, then transferred directly to a pre-wetted column (hexanes). The pure product **160** was obtained by column chromatography (gradient hexanes \rightarrow hexanes:DCM 8:2) as a white solid in 47% yield. $^1\text{H NMR}$ (400 MHz, CDCl_3): δ = 8.73 (d, J = 8.1 Hz, 2H), 8.06 (d, J = 7.6 Hz, 2H), 7.66 – 7.56 (m, 4H), 7.02 (s, 2H), 4.63 (s, 2H), 2.55 (d, J = 6.6 Hz, 1H), 2.46 (d, J = 6.6 Hz, 1H) ppm. $^{13}\text{C NMR}$ (101 MHz, CDCl_3): δ = 147.9, 143.8, 129.0, 128.7,

126.5, 125.3, 123.6, 123.5, 72.5, 49.2 ppm. IR (ATR): $\tilde{\nu}$ = 3060, 2980, 2928, 2862, 1506, 1298, 753, 720, 670, 660 cm^{-1} . HRMS (GCMS) *calcd for* $\text{C}_{19}\text{H}_{14}^+$ $[\text{M}]^+$ m/z : 242.1090; found: 242.1090. Analytical data are identical to the previously reported ones.²⁴²

1,4-Bis[(3-methoxyphenyl)thio]benzene (162a):

 To the stirred mixture of Cs_2CO_3 (90 mg, 0.275 mmol, 1.1 equiv.) and compound **93i** (111 mg, 0.25 mmol, 1.0 equiv.) in DMSO (1.25 mL), 3-methoxythiophenol (**161a**, 53 mg, 0.375 mmol, 1.5 equiv.) was added at RT and under an atmosphere of N_2 . The reaction mixture was then stirred for 12 h; the reaction was quenched by the addition of demineralized water. The aqueous phase was extracted with EtOAc (3×5 mL); the combined organic phases were washed with brine, dried over MgSO_4 and concentrated *in vacuo*. The crude product was purified by column chromatography (gradient hexane/EtOAc, 100:0 \rightarrow 95:5) affording compound **162a** as a white solid in 29% yield. $^1\text{H NMR}$ (400 MHz, CD_3CN): δ = 7.51 – 7.18 (m, 6H), 7.08 – 6.58 (m, 6H), 3.73 (s, 6H) ppm. $^{13}\text{C NMR}$ (101 MHz, CD_3CN): δ = 161.4, 137.3, 135.9, 132.7, 131.5, 124.4, 117.6, 114.4, 56.4 ppm. IR (ATR): $\tilde{\nu}$ = 2934, 1707, 1584, 1471, 1243, 1093, 1034, 850, 776, 682 cm^{-1} . HRMS (ESI) *calcd for* $\text{C}_{20}\text{H}_{18}\text{O}_2\text{S}_2^+$ $[\text{M}]^+$ m/z 354.0748; found: 354.0745. Analytical data are identical to the previously reported ones.²⁴³

1-(4-Chlorophenoxy)-3-methoxybenzene (165b):

 To the stirred mixture of Cs_2CO_3 (91 mg, 0.28 mmol, 1.1 equiv.) and compound **93i** (111 mg, 0.25 mmol, 1.0 equiv.) in DMSO (1.25 mL), 3-methoxyphenol (**161b**, 47 mg, 379 μmol , 1.52 equiv.) was added at RT under an atmosphere of N_2 . The reaction mixture was then stirred for 12 h, the reaction was quenched by the addition of demineralized water. The aqueous phase was extracted with EtOAc (3×5 mL); the combined organic phases were washed with brine, dried over MgSO_4 and concentrated *in vacuo*. The crude product was purified by column chromatography (gradient hexane/EtOAc, 0% \rightarrow 5%) affording compound **165b** as a yellow oil in 44% yield. $^1\text{H NMR}$ (400 MHz, CDCl_3): δ = 7.31 – 7.27 (m, 2H), 7.23 (ddd, J = 8.4, 7.6, 0.9 Hz, 1H), 6.98 – 6.93 (m, 2H), 6.67 (ddd, J = 8.3, 2.2, 1.1 Hz, 1H), 6.59 – 6.55 (m, 2H), 3.78 (s, 3H) ppm. $^{13}\text{C NMR}$ (101 MHz, CDCl_3): δ = 161.2, 158.2, 155.8, 130.4, 129.9, 128.5, 120.4, 111.1, 109.4, 105.1, 55.5 ppm. IR (neat): $\tilde{\nu}$ = 2954, 2837, 1579, 1483, 1265, 1222, 1135, 1092, 1042, 832 cm^{-1} . HRMS (ESI) *calcd*

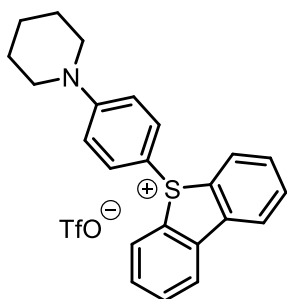
for $C_{13}H_{11}ClO_2^+$ $[M]^+$ m/z 234.0448; found: 235.0529. Analytical data are identical to the previously reported ones.²⁴⁴

General Procedure for the Synthesis of Compounds 169a-169e

The salt **93h** (100 mg, 233 μ mol, 1.00 equiv.) and Cs_2CO_3 (113.7 mg, 349 μ mol, 1.50 equiv.) were suspended in dry DMF (2 mL), and the respective amine (1.50 equiv.) was added. The suspension was then stirred at 90 °C for 12 h. The reaction mixture was allowed to cool down to room temperature, and the reaction was quenched with H_2O . The aqueous phase was extracted with EtOAc (3×10 mL), the combined organic phases were dried over Na_2SO_4 and concentrated under reduced pressure. The crude mixture was then purified by column chromatography (DCM:MeOH, 100:3) to obtain the desired products.

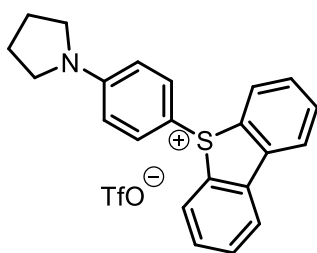
5-[4-(Piperidin-1-yl)phenyl]-5H-dibenzo[*b,d*]thiophen-5-ium

Trifluoromethanesulfonate (169a):



The salt **169a** was obtained as a red foam in 59% yield. 1H NMR (400 MHz, CD_3CN): δ = 8.30 (d, J = 7.8 Hz, 2H), 7.97 (d, J = 8.0 Hz, 2H), 7.90 (t, J = 7.6 Hz, 2H), 7.69 (t, J = 7.7 Hz, 2H), 7.27 (d, J = 9.1 Hz, 2H), 6.94 – 6.89 (m, 2H), 3.40 – 3.35 (m, 4H), 1.65 – 1.53 (m, 6H) ppm. ^{13}C NMR (101 MHz, CD_3CN): δ = 155.9, 139.8, 135.0, 134.6, 133.7, 132.4, 128.4, 125.3, 122.2 (q, $^1J_{C-F}$ = 321 Hz), 116.1, 105.9, 48.7, 25.9, 24.8 ppm. IR (ATR): $\tilde{\nu}$ = 2936, 1704, 1576, 1504, 1239, 1151, 1034, 755, 633, 515 cm^{-1} . HRMS (ESI) *calcd* for $C_{23}H_{22}NS^+$ $[M-OTf]^+$ m/z : 344.1468; found: 344.1467.

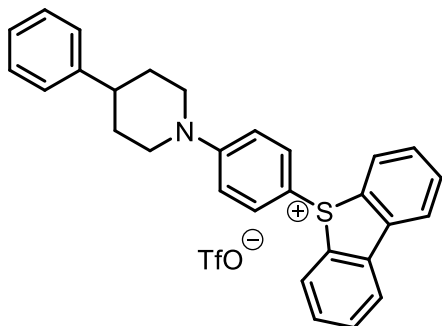
5-[4-(Pyrrolidin-1-yl)phenyl]-5H-dibenzo[*b,d*]thiophen-5-ium Trifluoromethanesulfonate (169b):



The salt **169b** was obtained as a beige foam in 46% yield. 1H NMR (400 MHz, CD_3CN): δ = 8.30 (dd, J = 8.4, 1.2 Hz, 2H), 7.97 – 7.94 (m, 2H), 7.90 (td, J = 7.7, 1.0 Hz, 2H), 7.71 – 7.66 (m, 2H), 7.26 (d, J = 9.3 Hz, 2H), 6.60 (d, J = 9.3 Hz, 2H), 3.31 – 3.25 (m, 4H), 1.99 – 1.95 (m, 4H) ppm. ^{13}C NMR (101 MHz, CD_3CN): δ = 153.1, 139.7, 135.0, 134.9, 133.7, 132.4, 128.3, 125.2, 122.2 (q, $^1J_{C-F}$ = 321 Hz), 114.6, 103.6, 48.6, 26.0 ppm. IR

(ATR): $\tilde{\nu}$ = 2859, 1587, 1509, 1399, 1253, 1151, 1068, 761, 638, 521 cm^{-1} . **HRMS** (ESI) *calcd* for $\text{C}_{22}\text{H}_{20}\text{NS}^+$ [M-OTf]⁺ *m/z*: 330.1311; found: 330.1314.

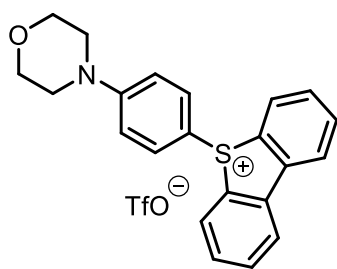
5-[4-(4-Phenylpiperidin-1-yl)phenyl]-5*H*-dibenzo[*b,d*]thiophen-5-ium Trifluoromethanesulfonate (169c):



The salt **169c** was obtained as a red solid in 66% yield. **¹H NMR** (400 MHz, CD_3CN): δ = 8.30 (d, J = 8.5 Hz, 2H), 7.98 (d, J = 8.5 Hz, 2H), 7.94 – 7.85 (m, 3H), 7.70 – 7.64 (m, 2H), 7.30 (d, J = 9.4 Hz, 2H), 7.20 – 7.15 (m, 3H), 6.95 (d, J = 9.5 Hz, 2H), 3.99 (d, J = 13.3 Hz, 2H), 3.02 – 2.93 (m, 2H), 2.32 (s, 1H), 1.83 (d, J = 13.6 Hz, 2H), 1.67 – 1.54 (m, 2H). **¹³C**

NMR (101 MHz, CD_3CN): δ = 155.8, 146.7, 139.8, 135.0, 134.5, 133.7, 132.4, 129.5, 128.4, 127.7, 127.3, 125.3, 122.2 (q, $^1J_{\text{C-F}}$ = 322 Hz), 116.4, 106.7, 48.3, 42.8, 33.4 ppm. **IR** (ATR): $\tilde{\nu}$ = 2928, 1667, 1584, 1506, 1258, 1226, 1156, 1031, 758, 633 cm^{-1} . **HRMS** (ESI) *calcd* for $\text{C}_{29}\text{H}_{26}\text{NS}^+$ [M-OTf]⁺ *m/z*: 420.1781; found: 420.1782.

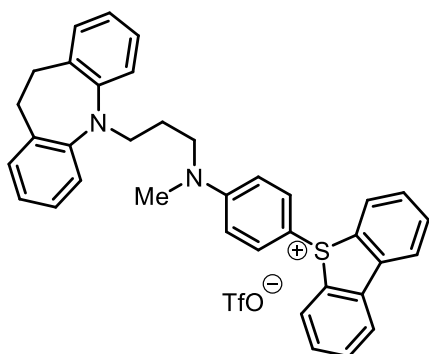
5-(4-Morpholinophenyl)-5*H*-dibenzo[*b,d*]thiophen-5-ium Trifluoromethanesulfonate (169d):



The salt **169d** was obtained as a white solid in 58% yield. **¹H NMR** (400 MHz, CD_3CN): δ = 8.31 (dd, J = 8.0, 1.2 Hz, 2H), 7.99 (dt, J = 8.1, 0.9 Hz, 2H), 7.93 – 7.89 (m, 2H), 7.69 (td, J = 8.1, 1.2 Hz, 2H), 7.34 (d, J = 9.4 Hz, 2H), 6.95 (d, J = 9.4 Hz, 2H), 3.73 – 3.69 (m, 4H), 3.31 – 3.26 (m, 4H) ppm. **¹³C NMR** (101 MHz, CD_3CN): δ = 156.3, 139.9, 135.1, 134.4, 133.6, 132.5, 128.4, 125.3, 122.2 (q, $^1J_{\text{C-F}}$ = 321 Hz), 116.3, 108.9, 66.9, 47.4 ppm. **IR** (ATR): $\tilde{\nu}$ = 2853, 1664, 1589, 1445, 1250, 1156, 1025, 764, 630, 518 cm^{-1} . **HRMS** (ESI) *calcd* for $\text{C}_{22}\text{H}_{20}\text{NOS}^+$ [M-OTf]⁺ *m/z*: 346.1260; found: 346.1264.

5-[4-{{3-(10,11-Dihydro-5H-dibenzo[*b,f*]azepin-5-yl)propyl}(methyl)-amino}phenyl]-5H-dibenzo[*b,d*]thiophen-5-ium

Trifluoromethanesulfo-nate (169e):



The salt **169e** was obtained as a yellow foam in 58% yield.

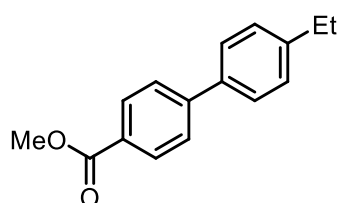
¹H NMR (300 MHz, CD₃CN): δ = 8.31 (d, *J* = 8.3 Hz, 2H), 7.95 – 7.89 (m, 4H), 7.69 (t, *J* = 7.8 Hz, 2H), 7.10 – 7.02 (m, 8H), 6.87 (dd, *J* = 10.1, 5.9 Hz, 2H), 6.46 (d, *J* = 9.4 Hz, 2H), 3.70 (t, *J* = 6.2 Hz, 2H), 3.42 – 3.35 (m, 2H), 3.12 (s, 4H), 2.87 (s, 3H), 1.73 (dt, *J* = 13.7, 6.4 Hz, 2H) ppm. **¹³C NMR** (101 MHz, CD₃CN): δ = 154.5, 149.1, 139.7, 135.2, 134.9,

134.8, 133.3, 132.4, 130.8, 128.3, 127.4, 125.2, 123.8, 122.2 (q, ¹*J*_{C-F} = 322 Hz), 120.8, 114.2, 104.5, 50.6, 47.9, 38.8, 32.7, 25.1 ppm. **IR** (ATR): $\tilde{\nu}$ = 2921, 2360, 1707, 1579, 1363, 1260, 1224, 1148, 1025, 753 cm⁻¹. **HRMS** (ESI) *calcd for* C₃₆H₃₃N₂S⁺ [M-OTf]⁺ *m/z*: 525.2359; found: 525.2362.

General Procedure for the synthesis of Compounds 175, 176a & 176b

Compound **93b** (100.9 mg, 0.23 mmol, 1.0 equiv.), 4-methoxycarbonylphenylboronic acid (103.5 mg, 0.575 mmol, 2.5 equiv.) and Pd(PPh₃)₄ (10 mg, 8.6 μ mol, 3.7 mol%) were dissolved in a mixture of THF (2 mL) and 2 M aqueous K₂CO₃ solution (1 mL). The heterogenous mixture was degassed and subsequently heated under reflux at 90 °C for 16 h under an atmosphere of N₂. The reaction mixture was then diluted with DCM (2 mL) and filtered through a pad of celite. The organic layer was then washed with brine, dried over Na₂SO₄ and concentrated *in vacuo*. The crude product was purified by column chromatography (gradient hexanes/EtOAc, 100:0 \rightarrow 90:10).

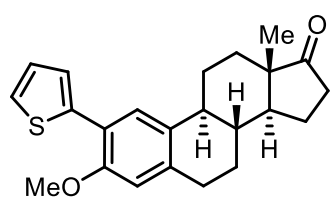
Methyl 4'-Ethyl-[1,1'-biphenyl]-4-carboxylate (175):



Compound **175** was obtained as a white solid in 79% yield. **¹H NMR** (400 MHz, CDCl₃): δ = 8.12 – 8.08 (m, 2H), 7.67 – 7.64 (m, 2H), 7.58 – 7.53 (m, 2H), 7.33 – 7.28 (m, 2H), 3.94 (s, 3H), 2.71 (q, *J* = 7.6 Hz, 2H), 1.29 (t, *J* = 7.6 Hz, 3H) ppm. **¹³C NMR** (101 MHz,

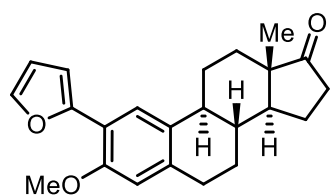
CDCl₃): δ = 167.2, 145.7, 144.6, 137.5, 130.2, 128.7, 128.6, 127.3, 126.9, 52.2, 28.7, 15.7 ppm. **IR** (ATR): $\tilde{\nu}$ = 2965, 1718, 1434, 1361, 1279, 1222, 1110, 829, 765, 527 cm⁻¹. **HRMS** (ESI) *calcd* for C₁₆H₁₇O₂⁺ [M+H]⁺ *m/z*: 241.1223; found: 241.1225. The analytical data were identical to the previously reported ones.²⁴⁵

(8*R*,9*S*,13*S*,14*S*)-3-Methoxy-13-methyl-2-(thiophen-2-yl)-6,7,8,9,11,12,13,14,15,16-decahydro-17*H*-cyclopenta[*a*]phenanthren-17-one
(176a):



Compound **176a** was obtained as a white solid in 53% yield (*o/p* ratio 1:9). **¹H NMR** (400 MHz, CDCl₃): δ = 7.53 (dd, *J* = 3.1, 1.3 Hz, 1H), 7.42 – 7.37 (m, 2H), 7.34 – 7.31 (m, 1H), 6.71 (s, 1H), 3.84 (s, 3H), 2.95 (d, *J* = 10.0 Hz, 2H), 2.55 – 2.43 (m, 2H), 2.34 – 2.26 (m, 1H), 2.20 – 2.02 (m, 3H), 2.00 – 1.94 (m, 1H), 1.67 – 1.47 (m, 6H), 0.92 (s, 3H) ppm. **¹³C NMR** (101 MHz, CDCl₃): δ = 221.0, 154.6, 138.7, 136.8, 132.0, 129.6, 128.7, 127.1, 125.6, 124.7, 124.5, 123.3, 123.0, 122.7, 111.8, 108.7, 56.0, 55.7, 50.6, 50.5, 48.2, 44.5, 44.1, 38.6, 38.0, 36.0, 31.7, 29.8, 28.6, 26.7, 26.3, 26.1, 21.7, 21.7, 14.0, 14.0 ppm. **IR** (ATR): $\tilde{\nu}$ = 2926, 2856, 2360, 2337, 1734, 1710, 1456, 1258, 1034, 788 cm⁻¹. **HRMS** (ESI) *calcd* for C₂₃H₂₆NaO₂S⁺ [M+Na]⁺ *m/z*: 389.1546; found: 389.1550.

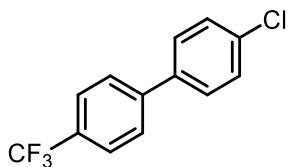
(8*R*,9*S*,13*S*,14*S*)-2-(Furan-2-yl)-3-methoxy-13-methyl-6,7,8,9,11,12,13,14,15,16-decahydro-17*H*-cyclopenta[*a*]phenanthren-17-one
(176b):



Compound **176b** was obtained as a white solid in 40% yield (*o/p* ratio 1:9). **¹H NMR** (400 MHz, CDCl₃): δ = 7.92 (s, 1H), 7.45 (t, *J* = 1.8 Hz, 1H), 7.39 (s, 1H), 6.77 – 6.75 (m, 1H), 6.69 (s, 1H), 3.88 (s, 3H), 2.97 – 2.90 (m, 2H), 2.56 – 2.44 (m, 2H), 2.33 – 2.25 (m, 1H), 2.21 – 1.95 (m, 4H), 1.64 – 1.48 (m, 6H), 0.92 (s, 3H) ppm. **¹³C NMR** (101 MHz, CDCl₃): δ = 221.1, 155.9, 154.7, 142.4, 142.3, 141.4, 141.0, 137.3, 136.2, 132.6, 132.0, 125.6, 125.2, 122.0, 121.2, 119.8, 119.0, 112.8, 111.6, 109.7, 108.6, 55.9, 55.6, 50.6, 50.6, 48.2, 48.1, 44.5, 44.1, 38.6, 38.0, 36.0, 31.8, 29.8, 28.8, 26.7, 26.3, 26.2, 21.7, 14.0 ppm. **IR** (ATR): $\tilde{\nu}$ = 2928, 2862, 2360,

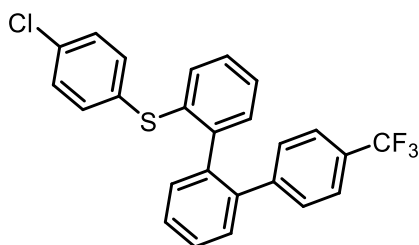
2337, 1737, 1517, 1239, 1049, 873, 791 cm^{-1} . **HRMS** (ESI) *calcd* for $\text{C}_{23}\text{H}_{26}\text{NaO}_3^+$ $[\text{M}+\text{Na}]^+$ m/z : 373.1774; found: 373.1769.

4-Chloro-4'-(trifluoromethyl)-1,1'-biphenyl (177a):



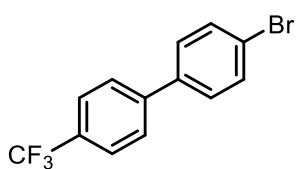
The salt **93i** (0.6 mmol, 1.0 equiv.), *p*-trifluoromethylphenylboronic acid (114.0 mg, 0.6 mmol, 1.0 equiv.), Na_2CO_3 (127.2 mg, 1.2 mmol, 2.0 equiv.) and $[\text{Pd}(\text{OAc})_2]$ (1.12 mg, 5.0 μmol , 0.5 mol%) were dissolved in degassed water/acetone mixture (6.5 mL; 3.5:3). The heterogeneous reaction mixture was vigorously stirred at 35 $^\circ\text{C}$ for 1 h under an atmosphere of N_2 , then diluted with ethylacetate (10 mL) and filtered through a pad of celite. The organic layer was washed with brine, dried over Na_2SO_4 and concentrated *in vacuo*. The crude product was purified by column chromatography (gradient hexanes/EtOAc, 100:0 \rightarrow 90:10). Compound **177a** was obtained as white needles (73.2 mg, 0.26 mmol, 47%). **^1H NMR** (300 MHz, CDCl_3): δ = 7.73 – 7.63 (m, 4H), 7.53 (d, J = 8.6 Hz, 2H), 7.45 (d, J = 8.5 Hz, 2H) ppm. **^{13}C NMR** (75 MHz, CDCl_3): δ = 143.6, 138.3, 134.6, 129.3, 129.3 (2 ^{13}C -signals overlapping), 128.7, 127.4, 127.4 (2 ^{13}C -signals overlapping), 126.0 (q, $^3J_{\text{C-F}}$ = 3.6 Hz) ppm. **^{19}F NMR** (282 MHz, CDCl_3) δ = -63.0 ppm. **IR** (ATR): $\tilde{\nu}$ = 2968, 2360, 2337, 1739, 1592, 1328, 1117, 1071, 817, 744 cm^{-1} . **HRMS** (EI) *calcd* for $\text{C}_{13}\text{H}_8\text{ClF}_3^+$ $[\text{M}]^+$ m/z : 256.0261; found: 256.0259. The analytical data were identical to the previously reported ones.²⁴⁶

(4-Chlorophenyl){4''-(trifluoromethyl)-[1,1':2',1''-terphenyl]-2-yl}sulfane (177d):



Compound **177d** was obtained as a pale-yellow solid as a byproduct of **177a** (46.3 mg, 0.10 mmol, 17%). **^1H NMR** (600 MHz, CD_3CN): δ = 7.52 – 7.48 (m, 3H), 7.46 – 7.42 (m, 2H), 7.34 (d, J = 8.0 Hz, 2H), 7.30 – 7.20 (m, 6H), 7.04 (d, J = 7.3 Hz, 1H), 6.89 (d, J = 8.5 Hz, 2H) ppm. **^{19}F NMR** (565 MHz, CD_3CN) δ = -62.9 ppm. **^{13}C NMR** (151 MHz, CD_3CN): δ = 146.4, 143.2, 140.7, 139.9, 135.5, 135.2, 133.7, 133.3, 132.7, 132.1, 131.9, 131.3, 130.9, 130.2, 129.6, 129.4, 129.1, 129.0, 128.9, 128.7, 128.2, 126.4, 125.53, 125.50 (q, $^3J_{\text{C-F}}$ = 4.0 Hz), 124.6 ppm. **IR** (ATR): $\tilde{\nu}$ = 2971, 2360, 2337, 1739, 1362, 1322, 1215, 1124, 1068, 667 cm^{-1} . **HRMS** (EI) *calcd* for $\text{C}_{25}\text{H}_{16}\text{ClF}_3\text{S}^+$ $[\text{M}]^+$ m/z : 440.0608; found: 440.0607.

4-Bromo-4'-(trifluoromethyl)-1,1'-biphenyl (178a):

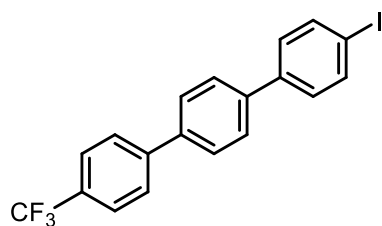


The salt **93j** (1.0 mmol, 1.0 equiv.), *p*-trifluoromethylphenylboronic acid (189.9 mg, 1.0 mmol, 1.0 equiv.), Na₂CO₃ (212 mg, 2.0 mmol, 2.0 equiv.) and [Pd(OAc)₂] (1.12 mg, 5.0 μmol, 0.5 mol%) were dissolved in degassed water/acetone mixture (6.5 mL; 3.5:3). The heterogeneous reaction mixture was vigorously stirred at 35 °C for 1 h under an atmosphere of N₂, then diluted with ethylacetate (10 mL) and filtered through a pad of celite. The organic layer was washed with brine, dried over Na₂SO₄ and concentrated *in vacuo*. The crude product was purified by column chromatography (gradient hexanes/EtOAc, 100:0 → 90:10). Compound **178a** was obtained as white needles (250 mg, 0.83 mmol, 83%). ¹H NMR (300 MHz, CDCl₃) δ = 7.68 (q, *J* = 8.5 Hz, 4H), 7.61 (d, *J* = 8.5 Hz, 2H), 7.46 (d, *J* = 8.5 Hz, 2H) ppm. ¹³C NMR (101 MHz, CDCl₃): δ = 143.6, 138.8, 132.3, 129.7, 129.0, 127.8, 127.4, 126.0 (q, ³J_{C-F} = 3.6 Hz), 122.8 ppm. ¹⁹F NMR (282 MHz, CDCl₃) δ -62.5 ppm. IR (ATR): $\tilde{\nu}$ = 3006, 2361, 1710, 1363, 1325, 1224, 1162, 1121, 1068, 814 cm⁻¹. HRMS (GCMS) *calcd for* C₁₃H₈BrF₃⁺ [M]⁺ *m/z*: 299.9756; found: 299.9756. The analytical data were identical to the previously published ones.²⁴⁷

General Procedure for the Synthesis of Compounds 179a, 180a, 181a, 182a & 182b

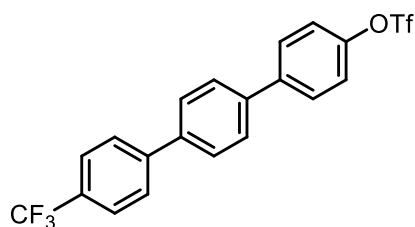
Compounds **93k** or **93l** (0.16 mmol, 1.0 equiv.), *p*-trifluoromethylphenylboronic acid (31.0 mg, 0.16 mmol, 1.0 equiv.) and Cs₂CO₃ (53.2 mg, 0.16 mmol, 1.0 equiv.) were added to the degassed DMF-Pd(OAc)₂ stock solution [0.185 mg/0.8 μmol, 0.5 mol% Pd(OAc)₂ in 0.66 mL DMF]/0.33 mL water (2:1)]. The heterogeneous reaction mixture was vigorously stirred at 35 °C for 16 h under an atmosphere of N₂, then diluted with DCM (10 mL) and filtered through a pad of celite. The organic layer was washed with water and brine, dried over Na₂SO₄ and concentrated *in vacuo*. The crude product was purified by column chromatography (gradient hexanes/EtOAc, 100:0 → 90:20) affording the white solid. Subsequently the latter was recrystallized from the minimal amount of warm CHCl₃. The compound **179a** was not well soluble in CDCl₃.

4-Iodo-4''-(trifluoromethyl)-1,1':4',1''-terphenyl (179a):



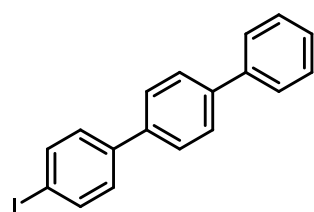
Compound **179a** (62.1 mg, 0.14 mmol, 90%) was obtained as a white solid. $^1\text{H NMR}$ (500 MHz, CDCl_3): $\delta = \delta$ 7.80 (d, $J = 8.5$ Hz, 2H), 7.72 (d, $J = 3.8$ Hz, 4H), 7.67 (d, $J = 3.5$ Hz, 4H), 7.38 (d, $J = 8.6$ Hz, 2H) ppm. $^{13}\text{C NMR}$ (126 MHz, CDCl_3): $\delta = 144.2$, 140.1, 139.2, 138.1, 129.8, 129.5, 129.0, 127.9, 127.6, 127.4, 125.9 (q, $^1J_{\text{C-F}} = 3.6$ Hz), 125.5, 123.3 ppm. $^{19}\text{F NMR}$ (471 MHz, CDCl_3): $\delta -62.4$ ppm. **IR** (ATR): $\tilde{\nu} = 2358, 2339, 1615, 1332, 1163, 1123, 1069, 838, 815, 666$ cm^{-1} . **HRMS** (EI) *calcd for* $\text{C}_{19}\text{H}_{12}\text{F}_3\text{I}^+$ $[\text{M}]^+$ m/z : 423.9930; found: 423.9942.

4''-(Trifluoromethyl)-[1,1':4',1''-terphenyl]-4-yl Trifluoromethanesulfonate (180a):



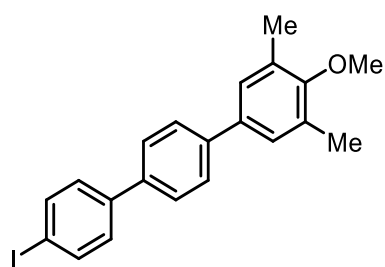
Compound **180a** was obtained as a white solid in (31.4 mg, 0.07 mmol, 44%). $^1\text{H NMR}$ (400 MHz, CDCl_3): $\delta = \delta$ 7.76 – 7.66 (m, 10H), 7.38 (d, $J = 8.8$ Hz, 2H) ppm. $^{19}\text{F NMR}$ (377 MHz, CDCl_3) $\delta = -62.5, -72.8$ ppm. $^{13}\text{C NMR}$ (101 MHz, CDCl_3): $\delta = 149.3, 144.0, 141.0, 139.6, 139.2, 129.8$ (q, $^2J_{\text{C-F}} = 39.2$ Hz), 129.0, 128.0, 127.9, 127.5, 126.0 (q, $^3J_{\text{C-F}} = 3.9$ Hz), 124.5 (q, $^1J_{\text{C-F}} = 272.3$ Hz, CF_3), 122.0, 119.0 (q, $^1J_{\text{C-F}} = 321.3$ Hz, OTf) ppm. **IR** (ATR): $\tilde{\nu} = 3006, 2361, 1710, 1363, 1325, 1224, 1162, 1121, 1068, 814$ cm^{-1} . **HRMS** (EI) *calcd for* $\text{C}_{20}\text{H}_{12}\text{F}_6\text{O}_3\text{S}^+$ $[\text{M}]^+$ m/z : 446.0411; found: 446.0396.

4-Iodo-1,1':4',1''-terphenyl (181a):



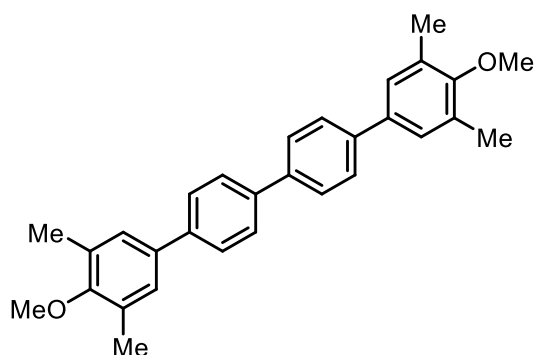
Compound **181a** was obtained as a white solid in (39.8 mg, 0.12 mmol, 68%). $^1\text{H NMR}$ (400 MHz, CDCl_3): $\delta = \delta$ 7.81 – 7.76 (m, 2H), 7.69 – 7.61 (m, 6H), 7.49 – 7.44 (m, 2H), 7.40 – 7.34 (m, 3H) ppm. $^{13}\text{C NMR}$ (101 MHz, CDCl_3): $\delta = 140.8, 140.7, 140.4, 139.1, 138.1, 129.0, 129.0, 127.8, 127.6, 127.4, 127.2, 93.2$ ppm. **IR** (ATR): $\tilde{\nu} = 2360, 2340, 1707, 904, 814, 729, 667, 649, 513, 417$ cm^{-1} . **HRMS** (EI) *calcd for* $\text{C}_{18}\text{H}_{13}\text{I}^+$ $[\text{M}]^+$ m/z : 356.0056; found: 356.0062. The analytical data were identical to the previously reported ones.²⁴⁸

4''-Iodo-4-methoxy-3,5-dimethyl-1,1':4',1''-terphenyl (182a):



Compound **182a** was obtained as a white solid in (40.6 mg, 0.10 mmol, 60%). **¹H NMR** (400 MHz, CDCl₃): = δ 7.77 (d, *J* = 8.5 Hz, 2H), 7.64 – 7.58 (m, 4H), 7.39 – 7.35 (m, 2H), 7.28 (s, 2H), 3.77 (s, 3H), 2.36 (s, 6H) ppm. **¹³C NMR** (101 MHz, CDCl₃): δ = 156.9, 140.5, 140.4, 138.6, 138.0, 136.2, 131.4, 129.0, 127.62, 127.57, 127.2, 93.1, 60.0, 16.4 ppm. **IR** (ATR): $\tilde{\nu}$ = 2360, 2338, 1474, 1242, 1167, 1014, 808, 679, 667, 649 cm⁻¹. **HRMS** (EI) *calcd* for C₂₁H₁₉I O⁺ [M]⁺ *m/z*: 414.0475; found: 414.0470.

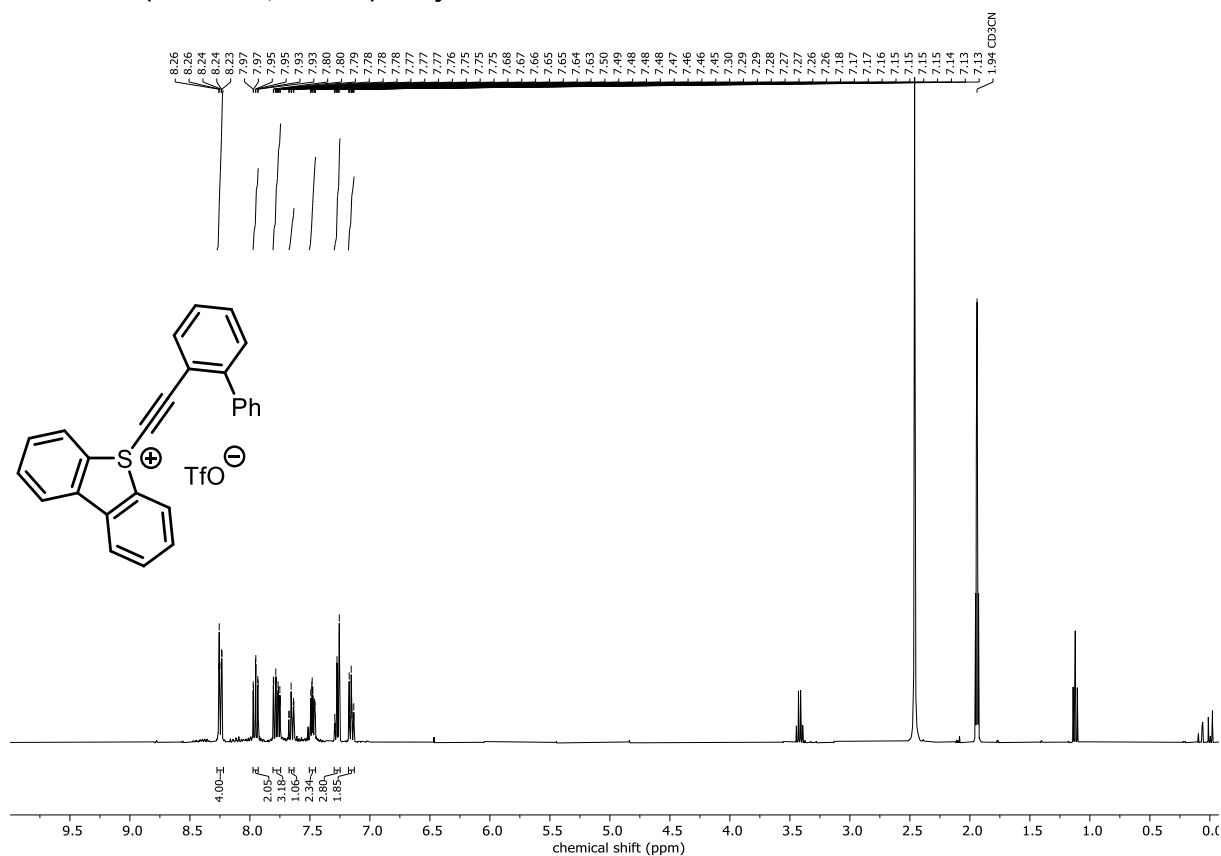
4,4'''-Dimethoxy-3,3''',5,5'''-tetramethyl-1,1':4',1''':4'',1'''-quaterphenyl (182b):



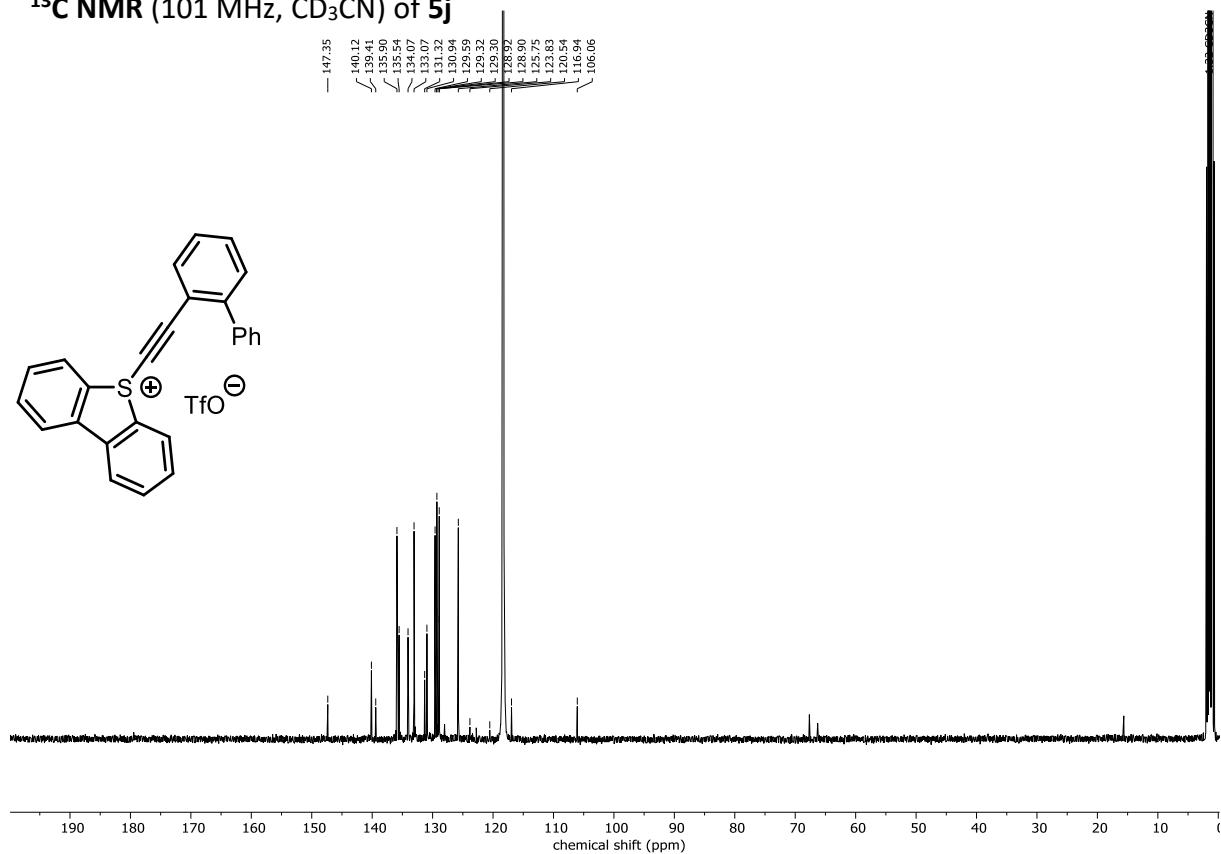
Compound **182a** was obtained as a white solid in (10.5 mg, 0.03 mmol, 15%). **¹H NMR** (300 MHz, CDCl₃): = δ 7.66 (q, *J* = 8.3 Hz, 8H), 7.30 (s, 4H), 3.78 (s, 6H), 2.37 (s, 12H) ppm. **¹³C NMR** (101 MHz, CDCl₃): δ = 156.8, 140.0, 139.4, 136.4, 131.3, 127.6, 127.5, 127.4, 60.0, 16.5 ppm. **IR** (ATR): $\tilde{\nu}$ = 2359, 2338, 1474, 1242, 1162, 1014, 823, 679, 669, 648 cm⁻¹. **HRMS** (EI) *calcd* for C₃₀H₃₀O₂⁺ [M]⁺ *m/z*: 422.2240; found: 422.4435.

NMR Spectra

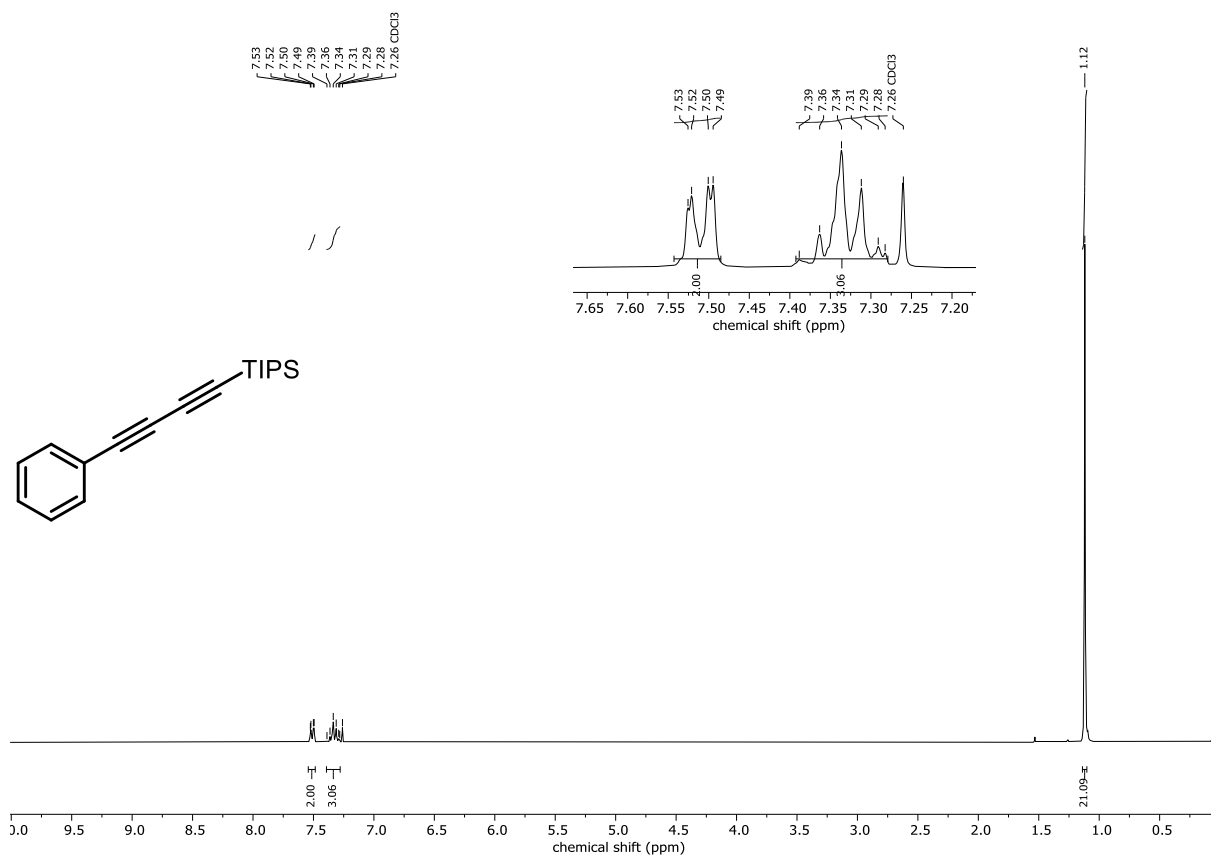
^1H NMR (400 MHz, CD_3CN) of **5j**



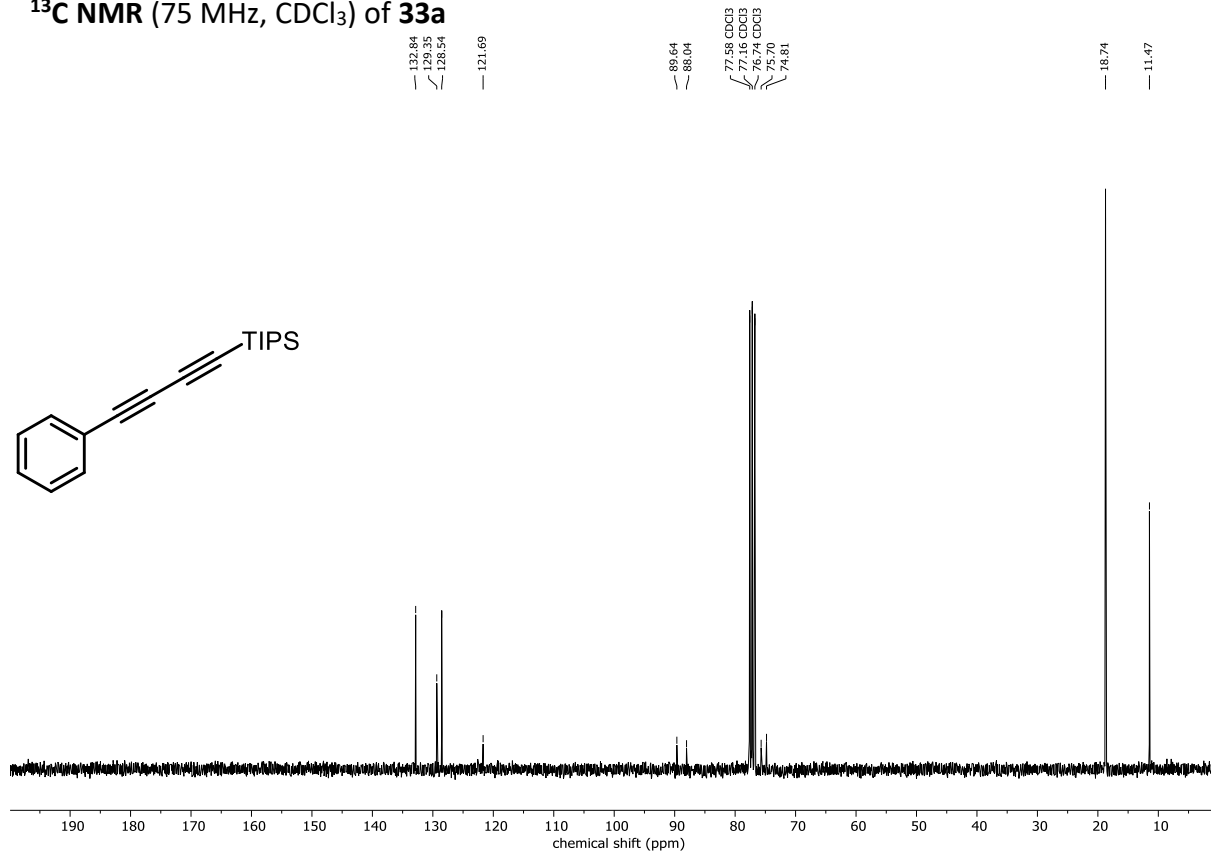
^{13}C NMR (101 MHz, CD_3CN) of **5j**



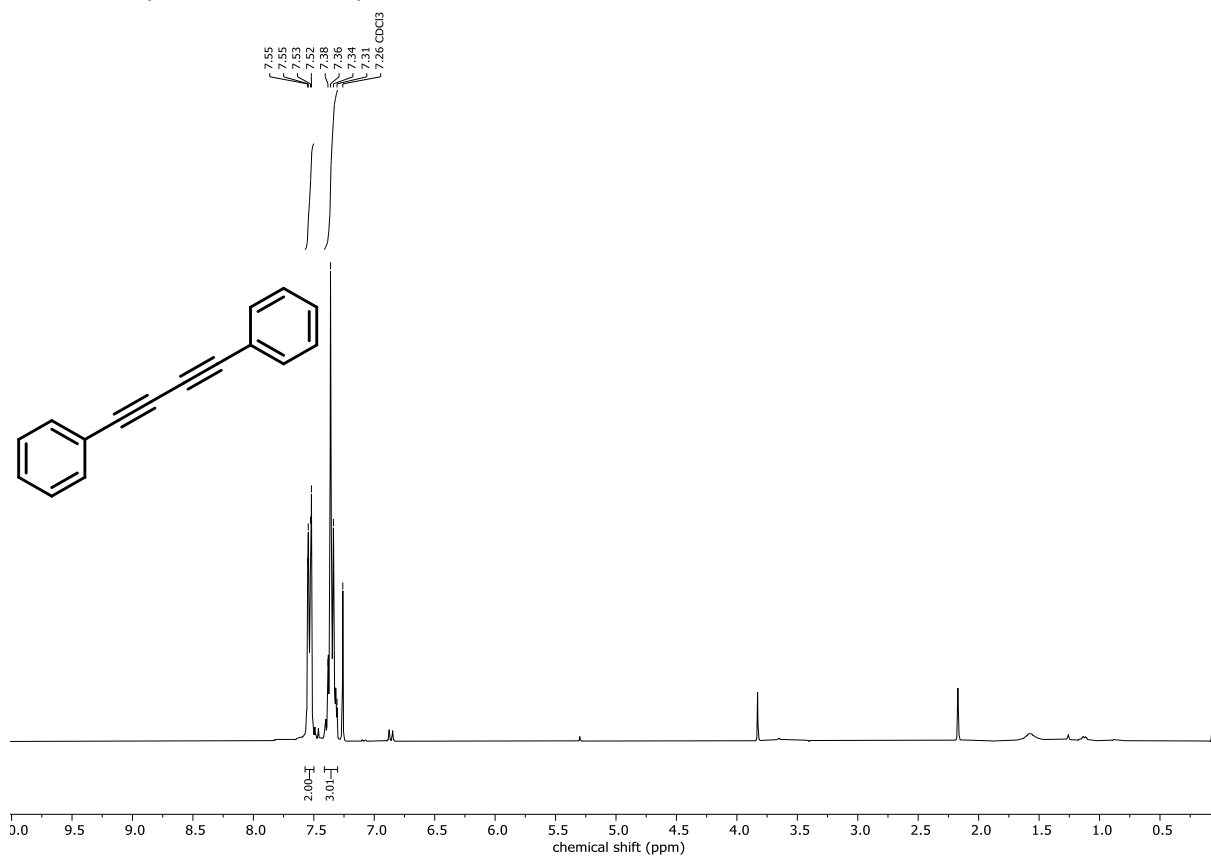
¹H NMR (300 MHz, CDCl₃) of 33a



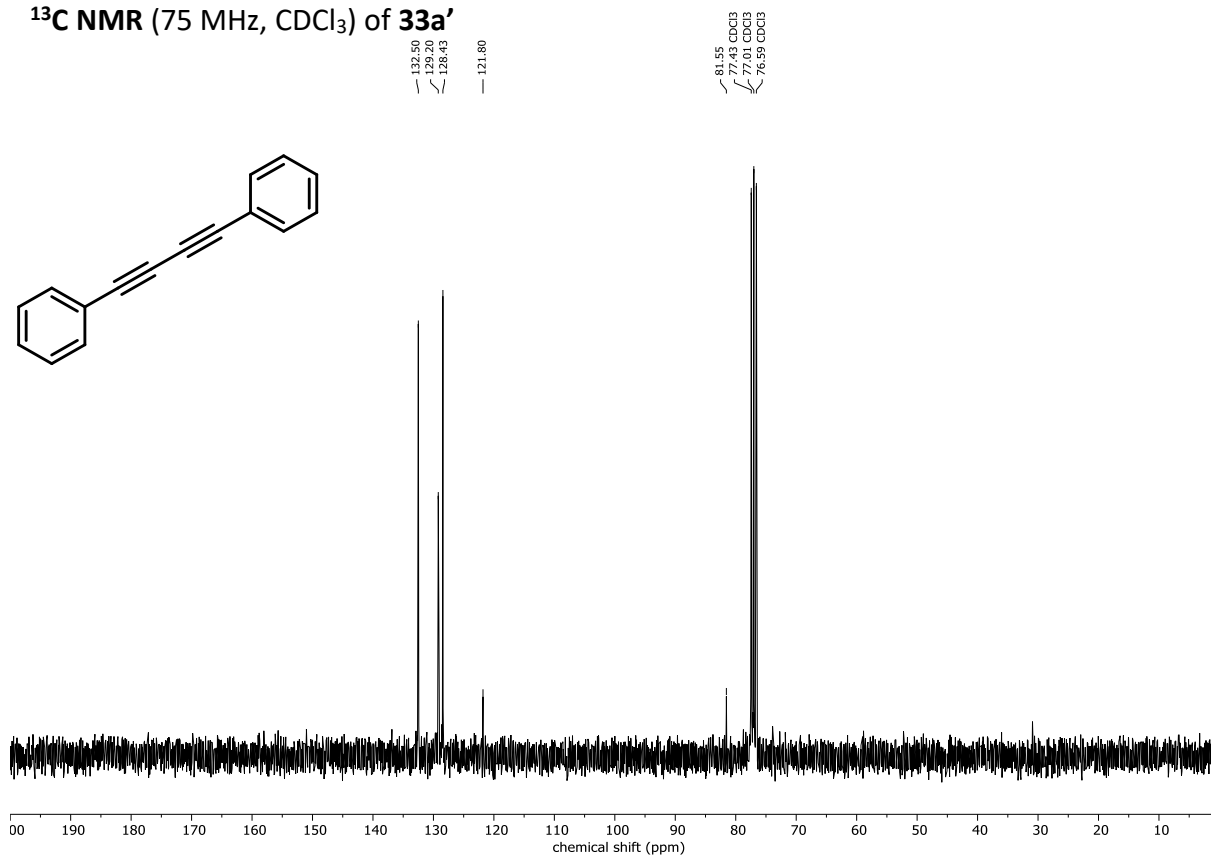
¹³C NMR (75 MHz, CDCl₃) of 33a



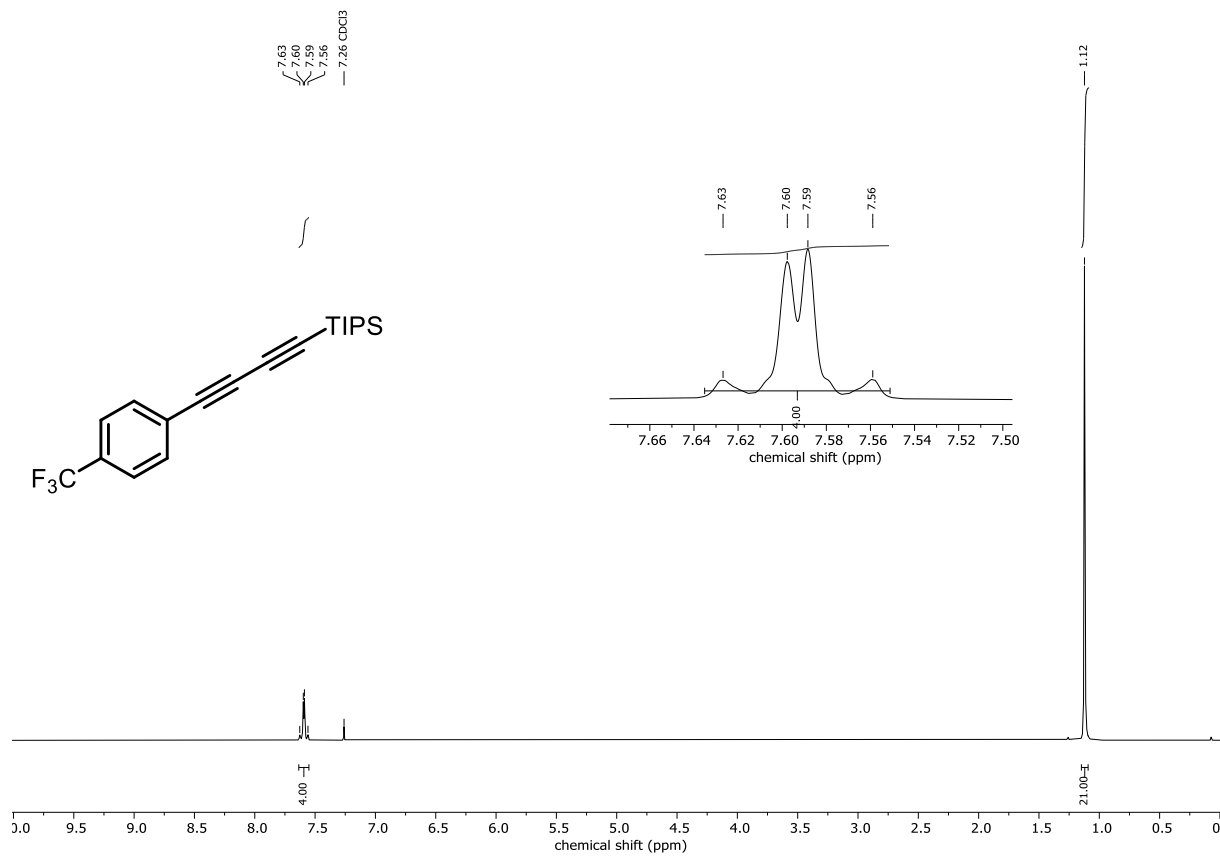
¹H NMR (300 MHz, CDCl₃) of 33a'



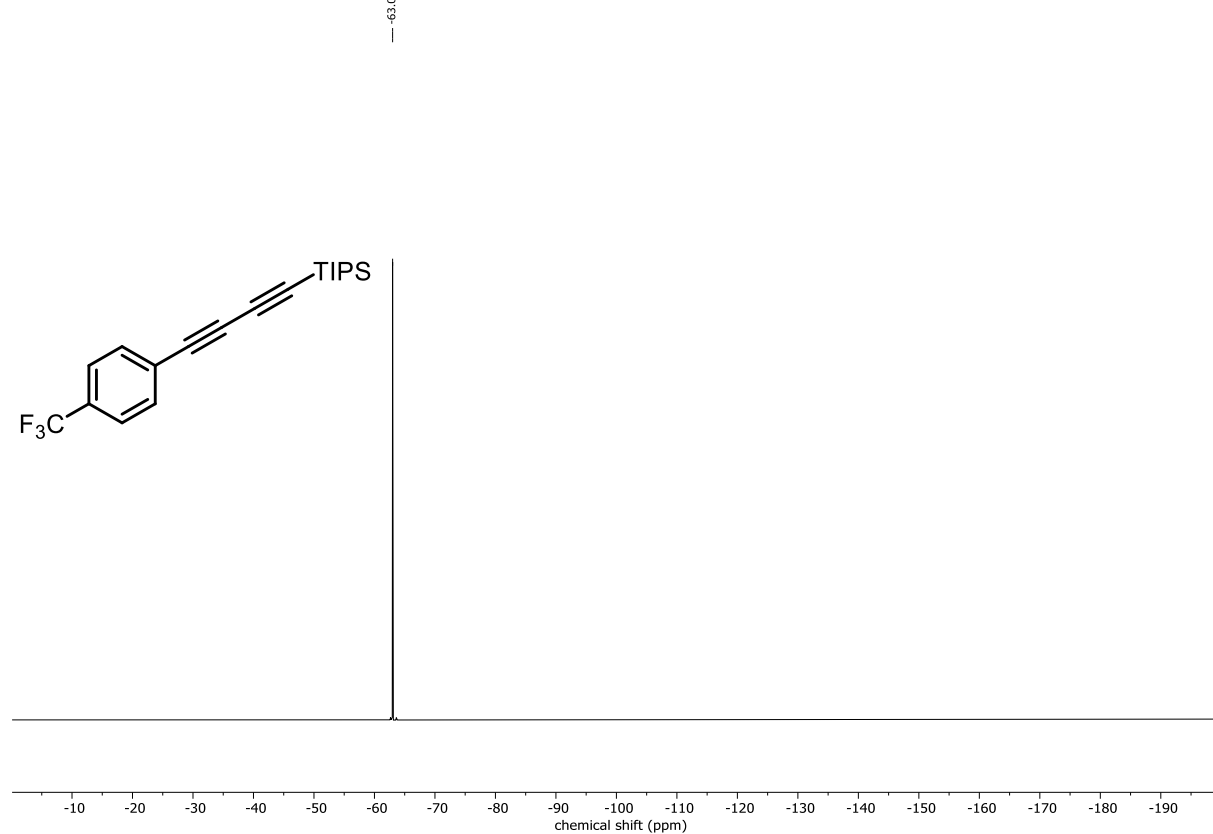
¹³C NMR (75 MHz, CDCl₃) of 33a'



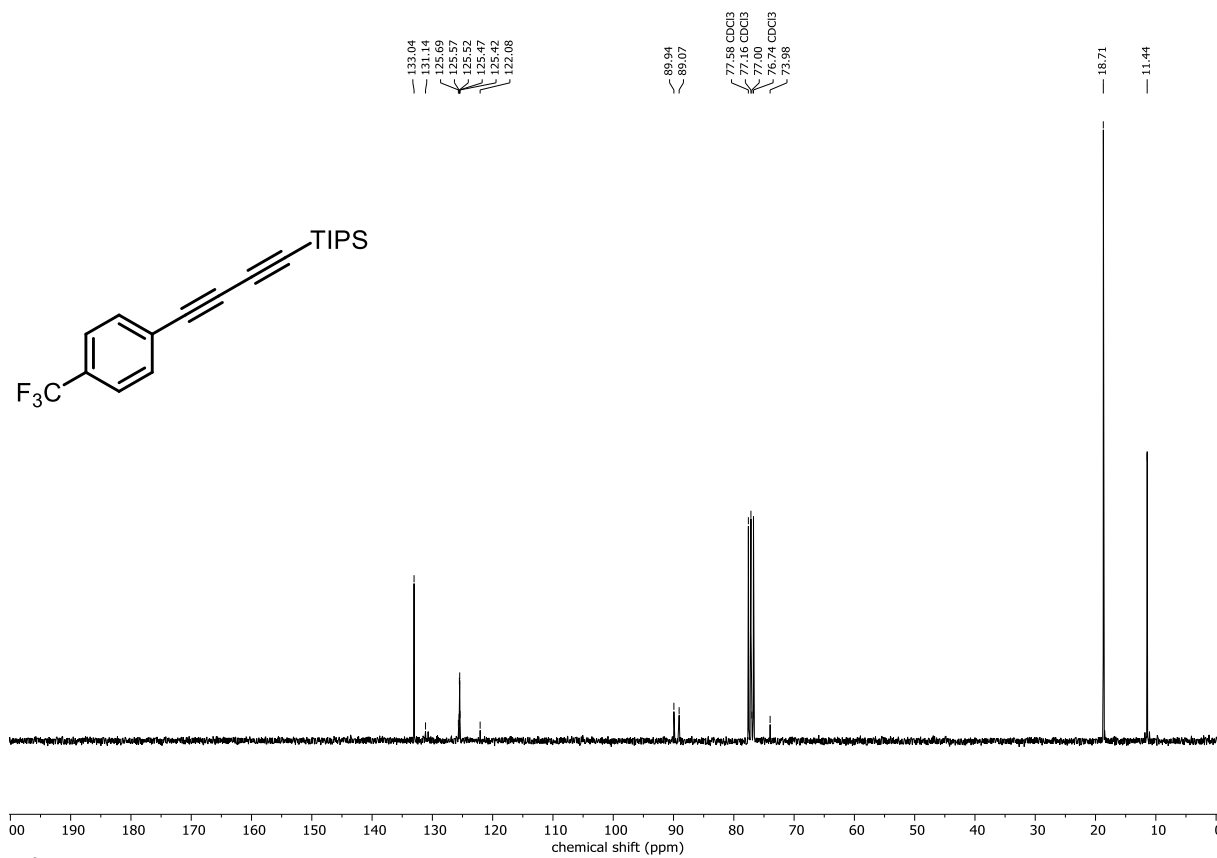
^1H NMR (300 MHz, CDCl_3) of **33b**



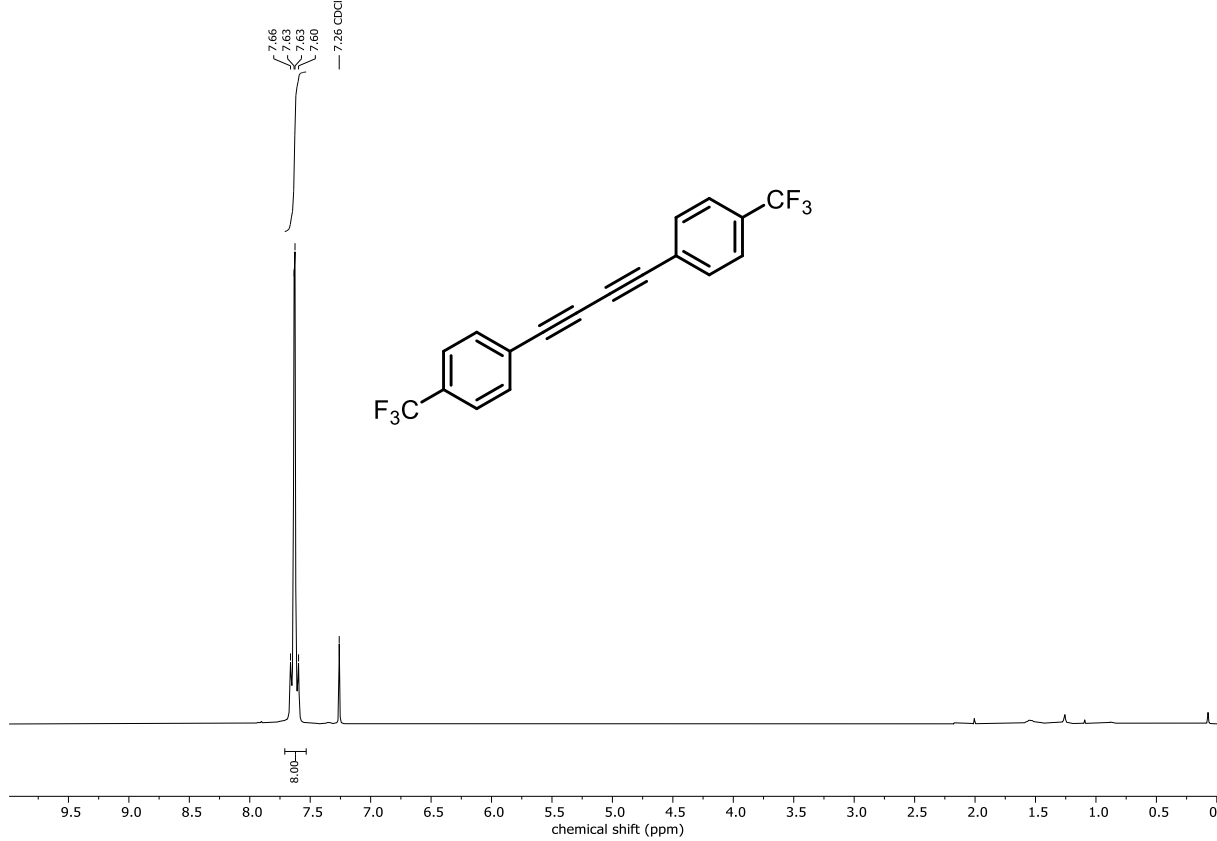
^{19}F NMR (282 MHz, CDCl_3) of **33b**



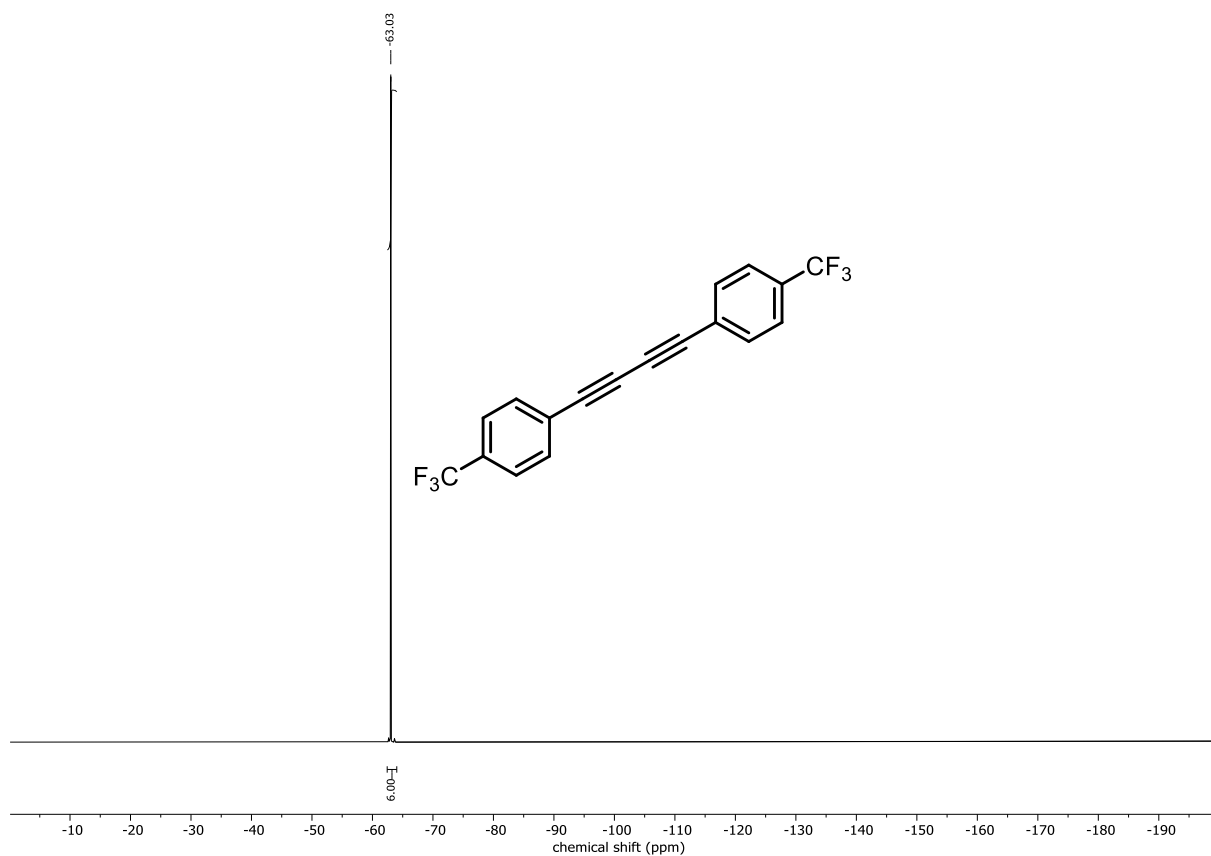
^{13}C NMR (75 MHz, CDCl_3) of **33b**



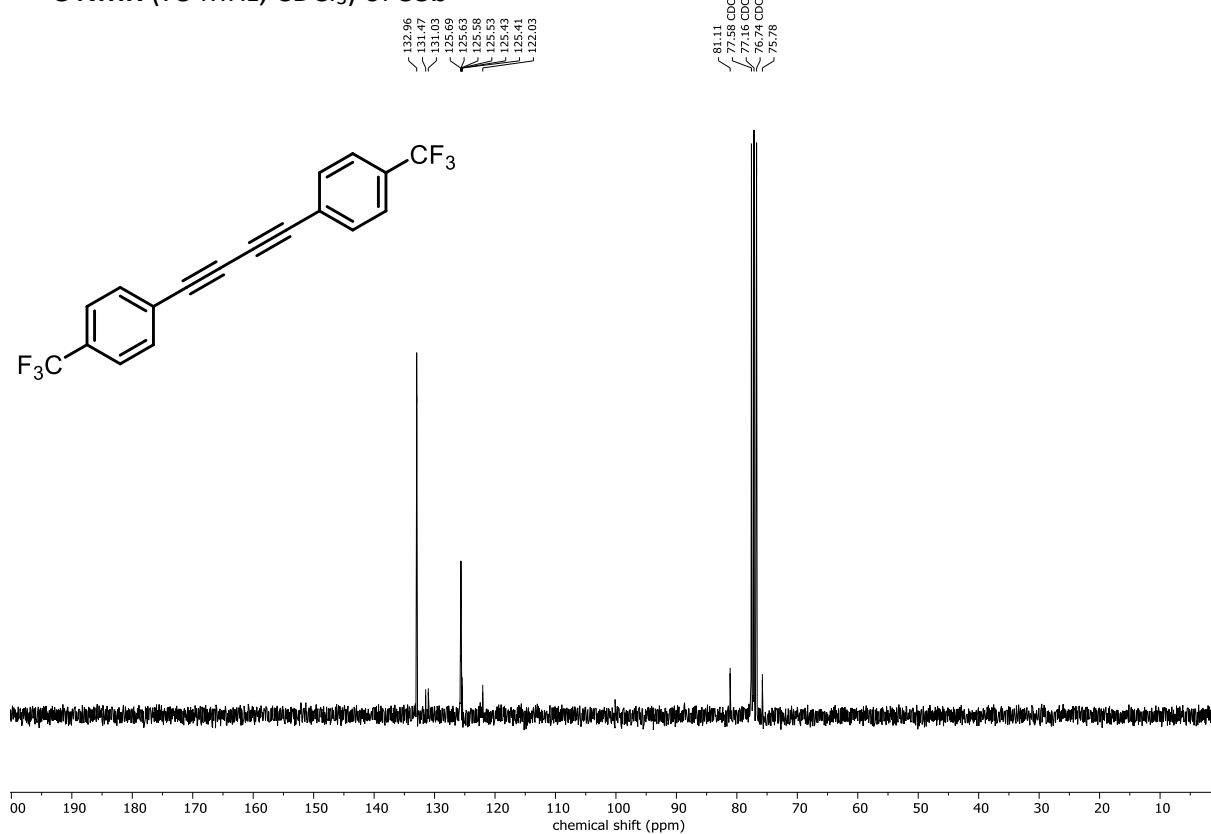
^1H NMR (300 MHz, CDCl_3) of **33b'**



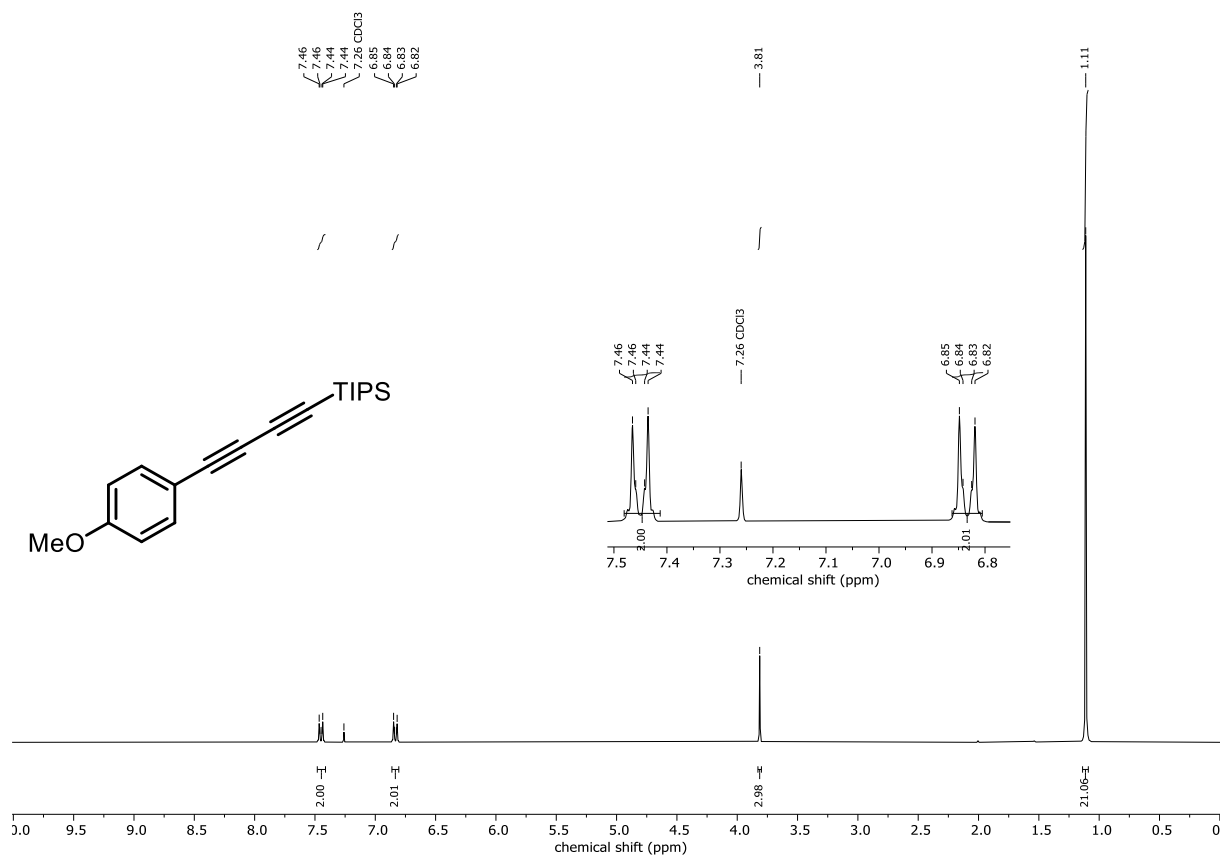
¹⁹F NMR (282 MHz, CDCl₃) of 33b'



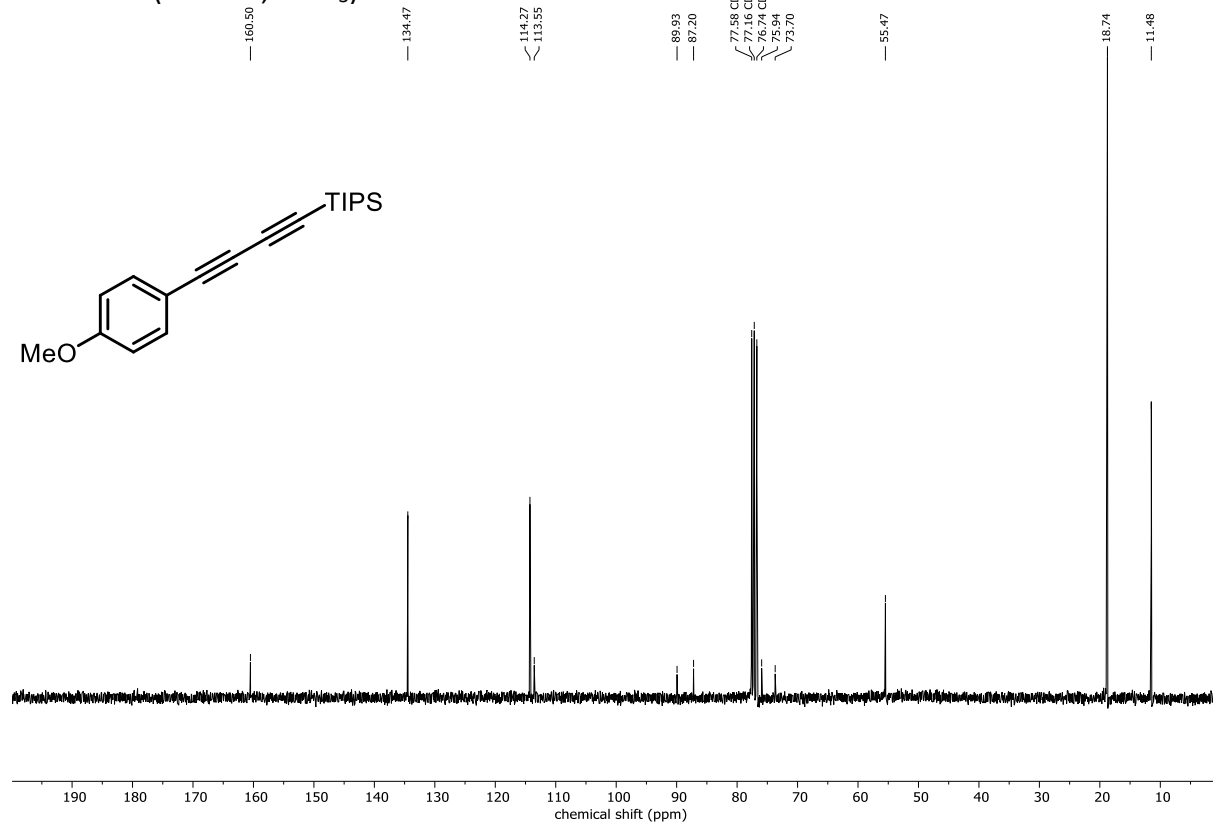
¹³C NMR (75 MHz, CDCl₃) of 33b'



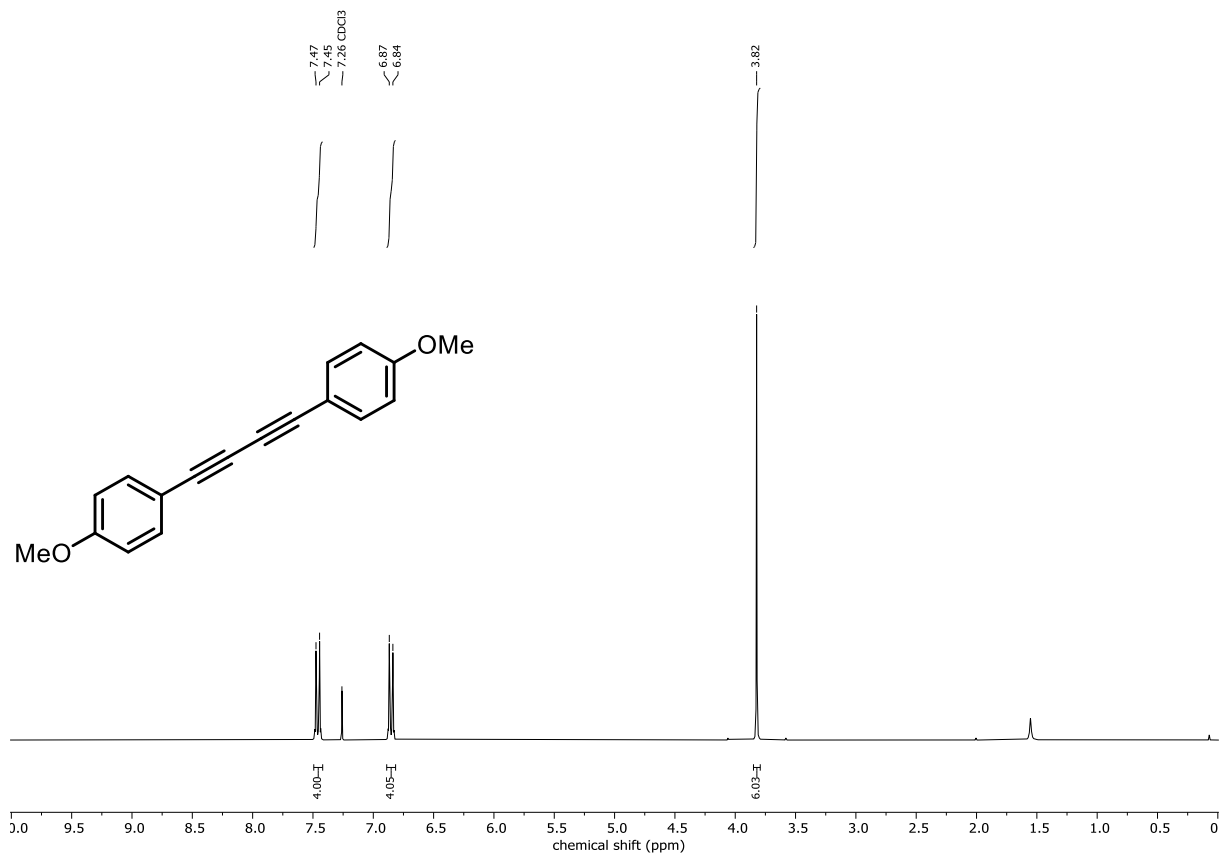
¹H NMR (300 MHz, CDCl₃) of 33c



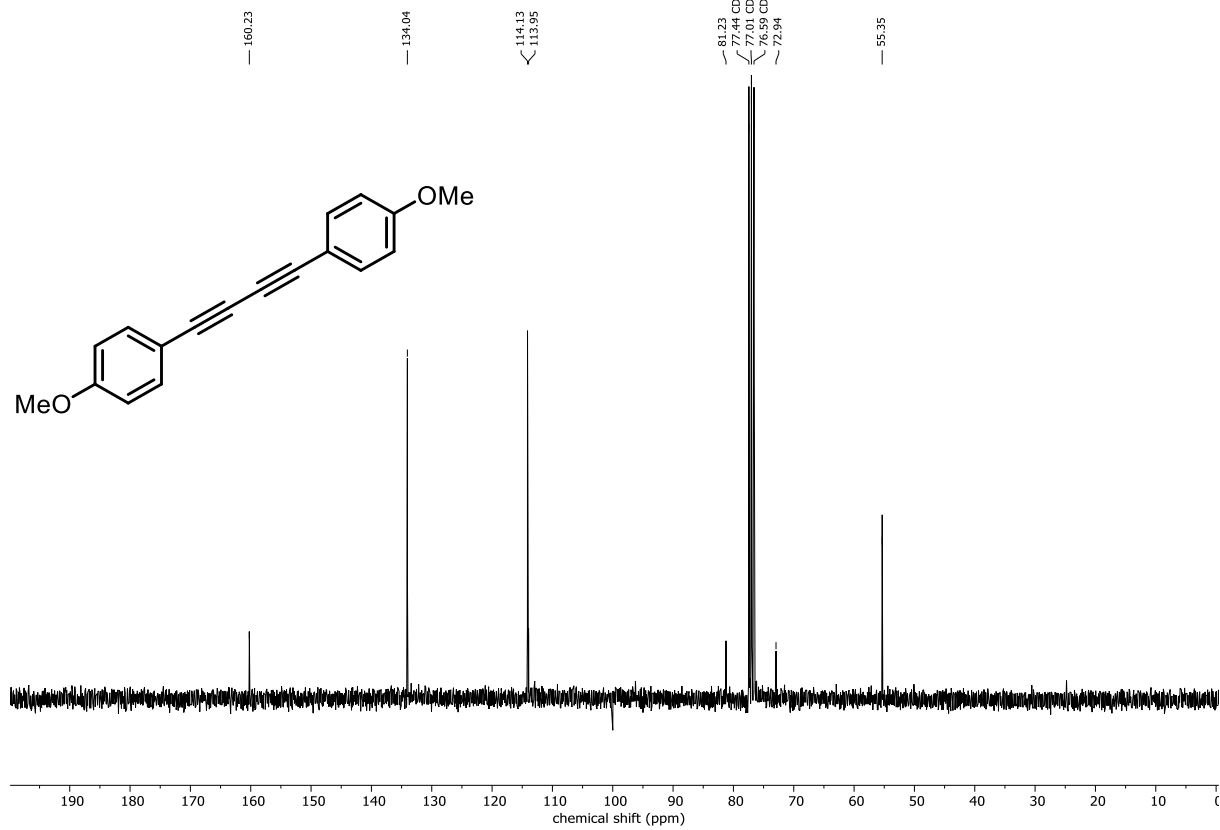
¹³C NMR (75 MHz, CDCl₃) of 33c



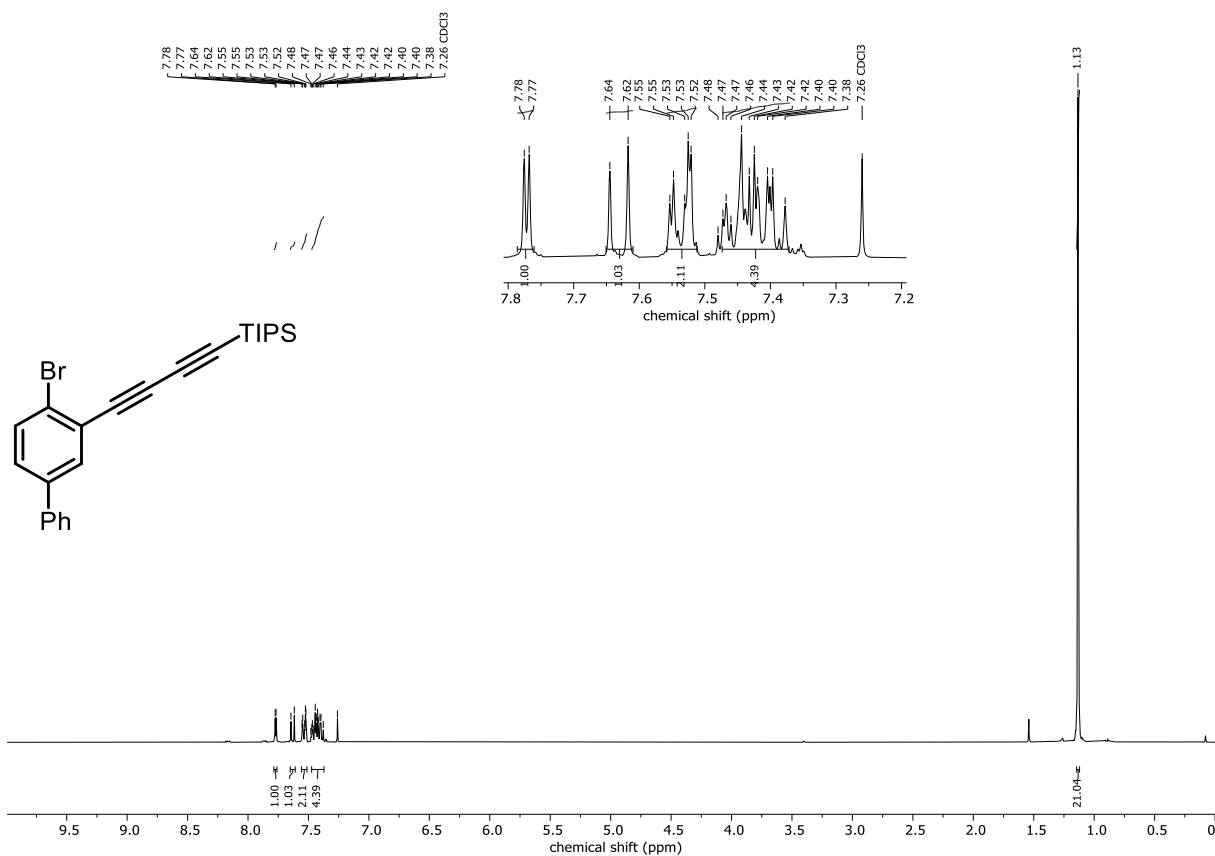
¹H NMR (300 MHz, CDCl₃) of 33c'



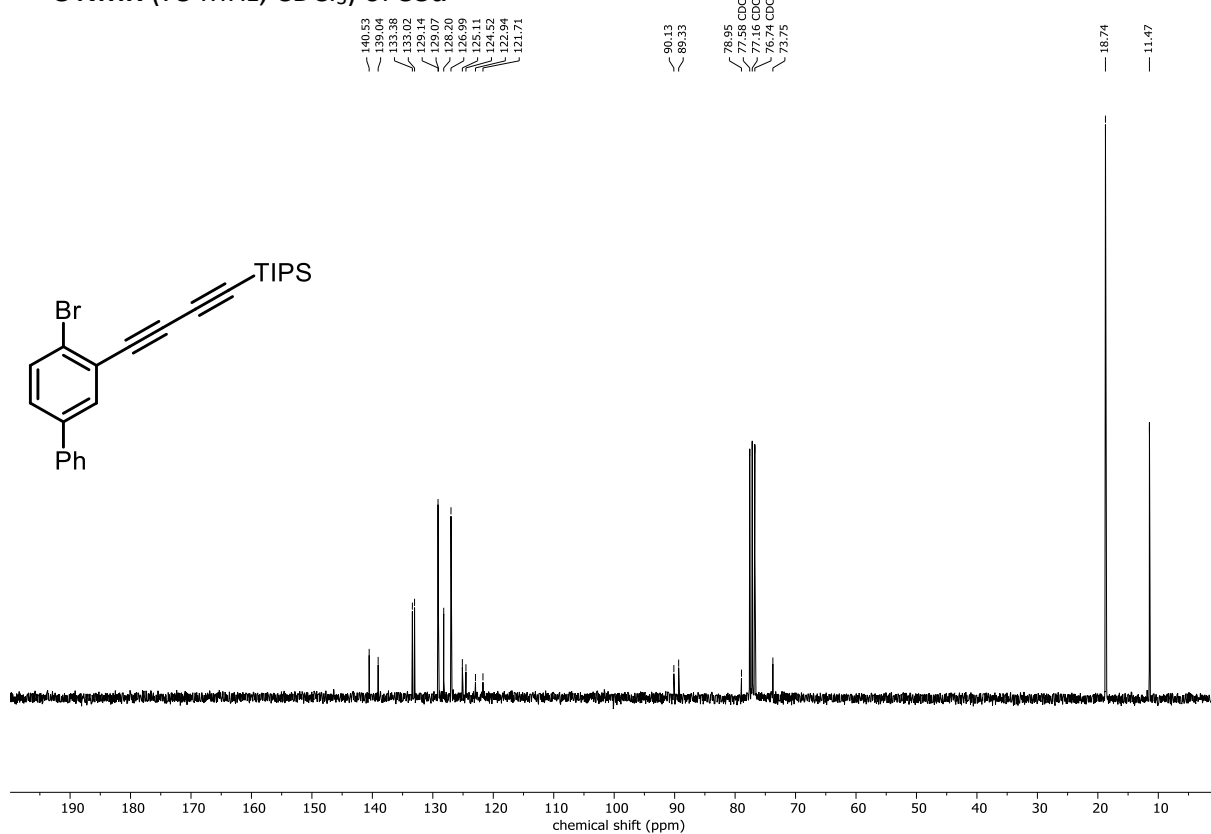
¹³C NMR (75 MHz, CDCl₃) of 33c'



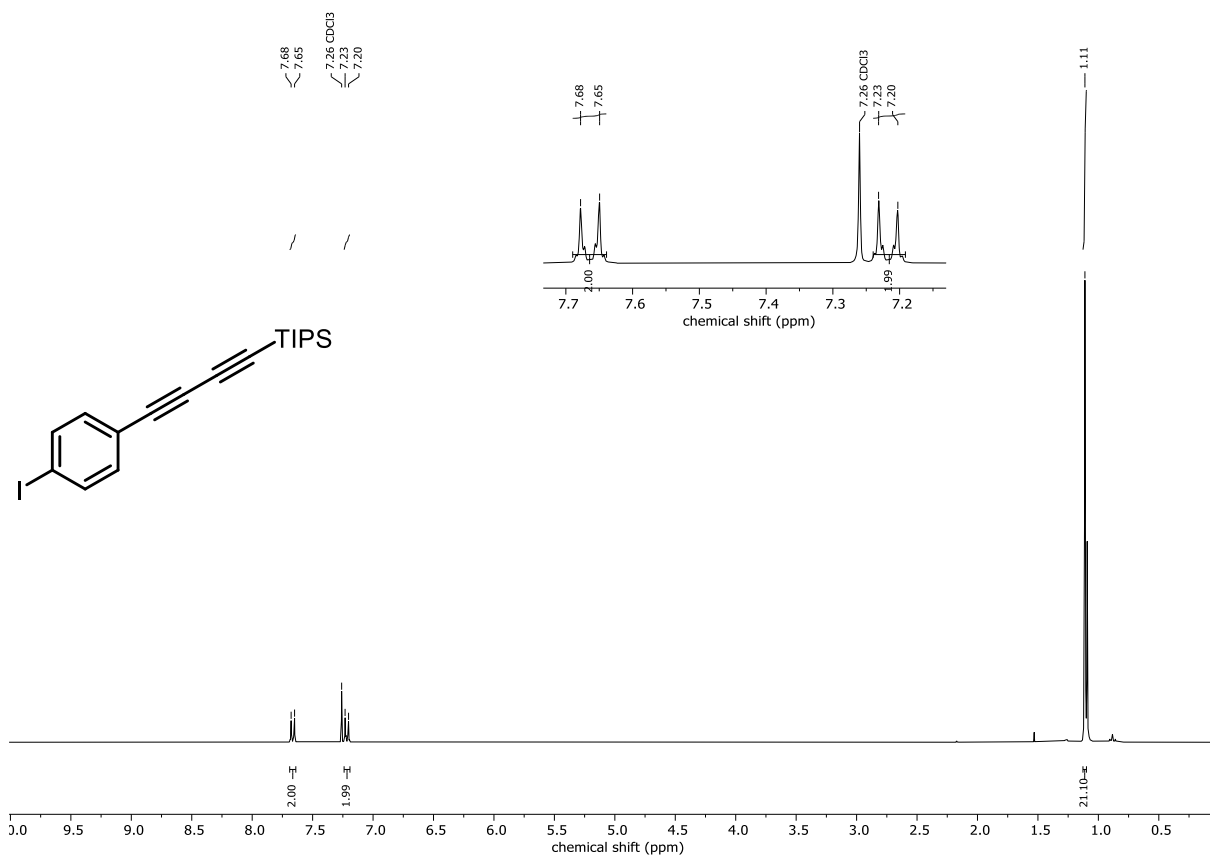
¹H NMR (300 MHz, CDCl₃) of 33d



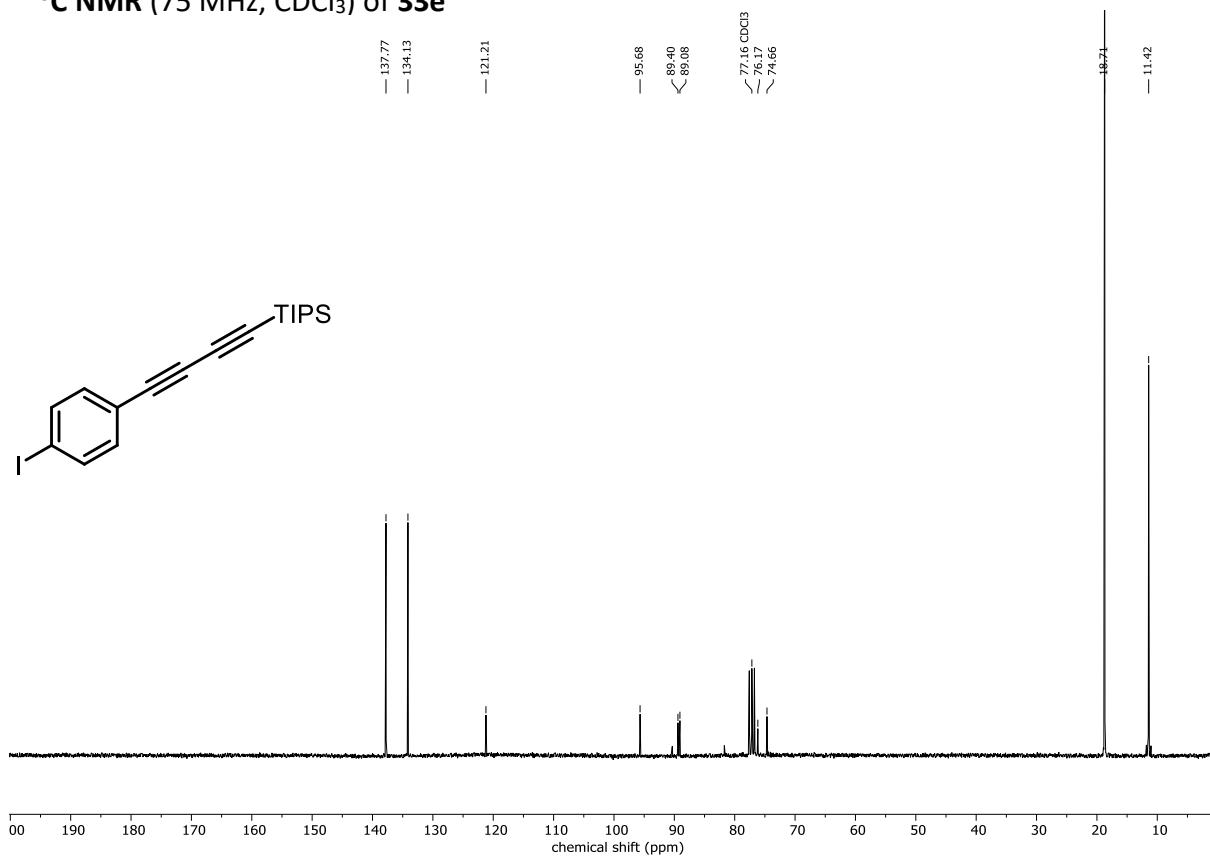
¹³C NMR (75 MHz, CDCl₃) of 33d



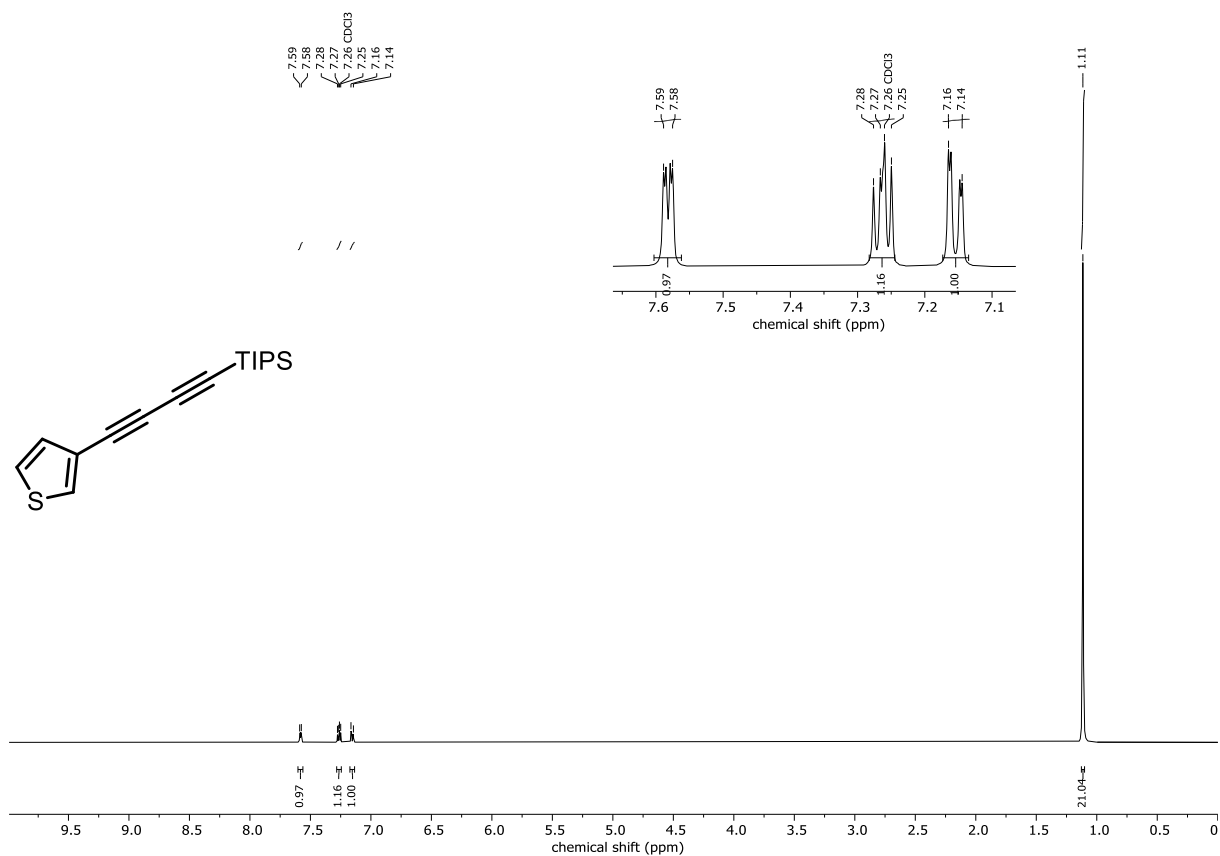
¹H NMR (300 MHz, CDCl₃) of 33e



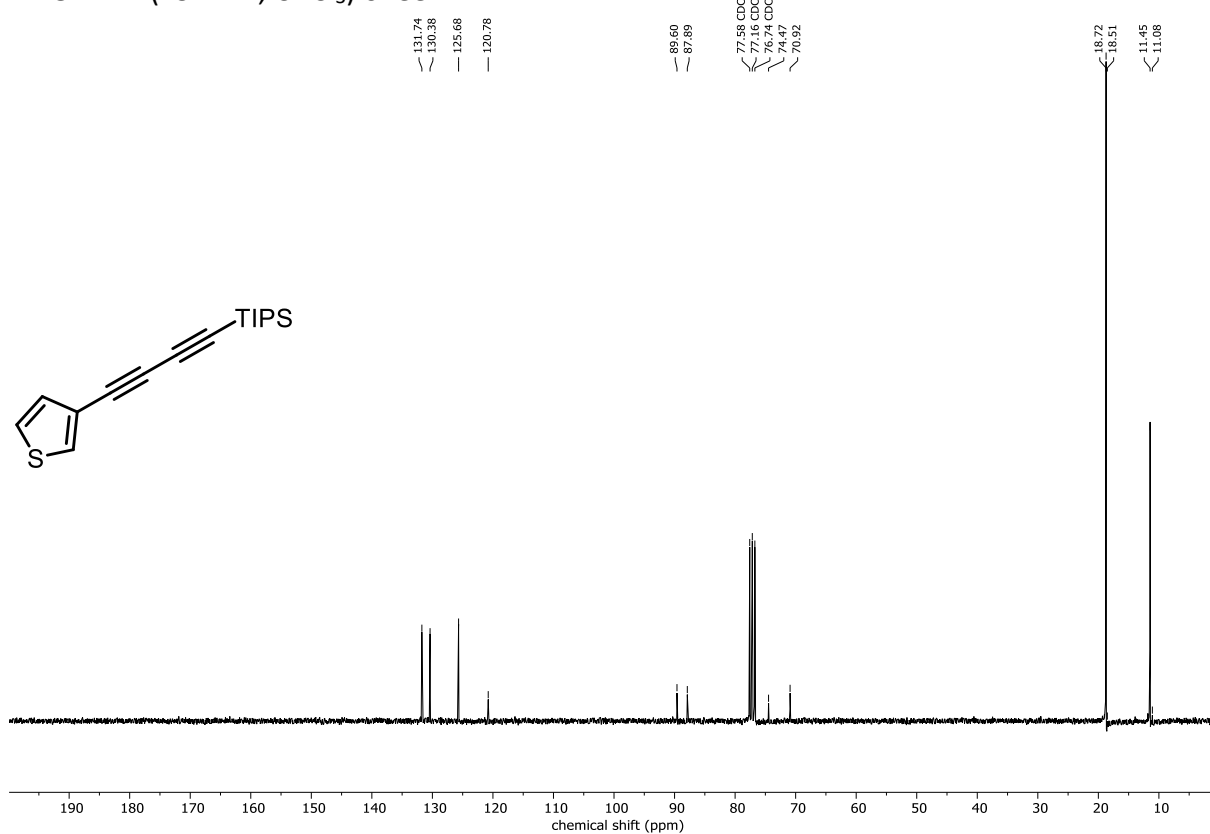
¹³C NMR (75 MHz, CDCl₃) of 33e



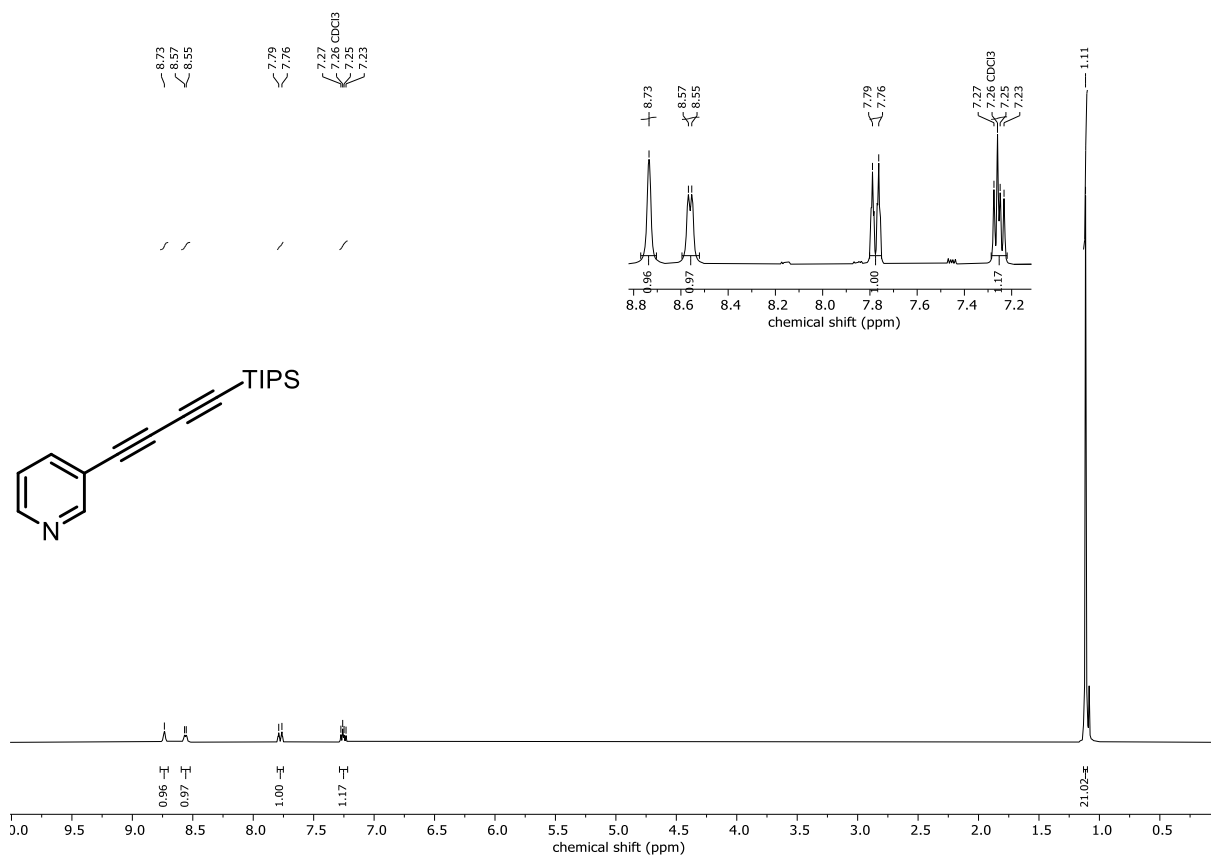
^1H NMR (300 MHz, CDCl_3) of **33f**



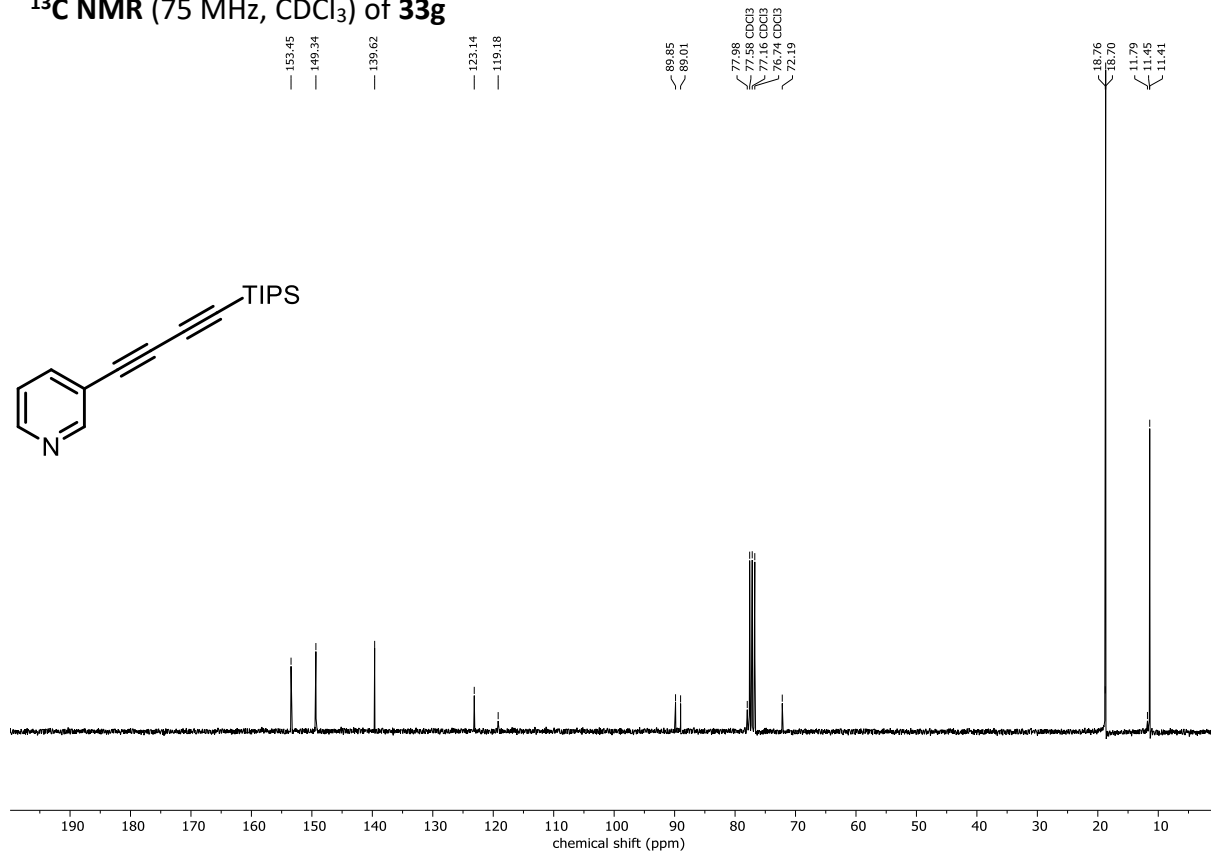
^{13}C NMR (75 MHz, CDCl_3) of **33f**



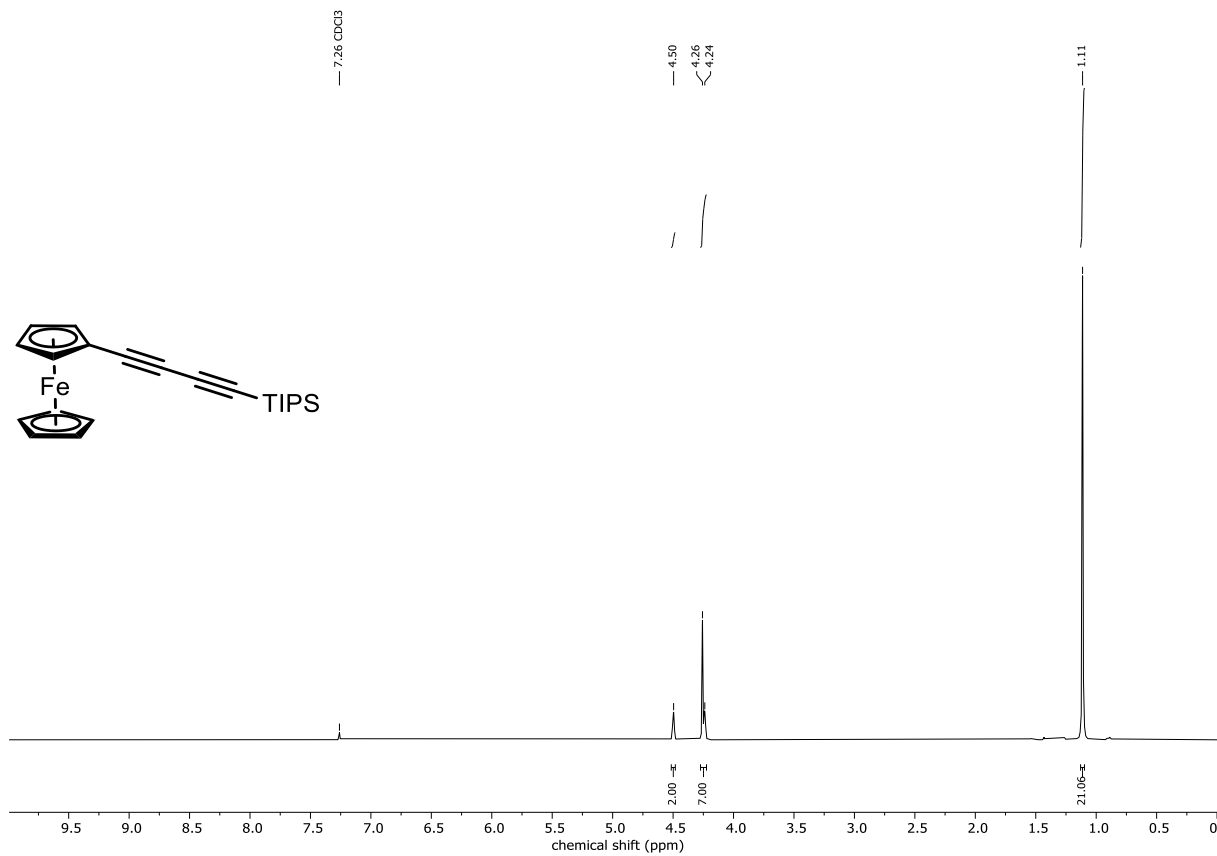
¹H NMR (300 MHz, CDCl₃) of 33g



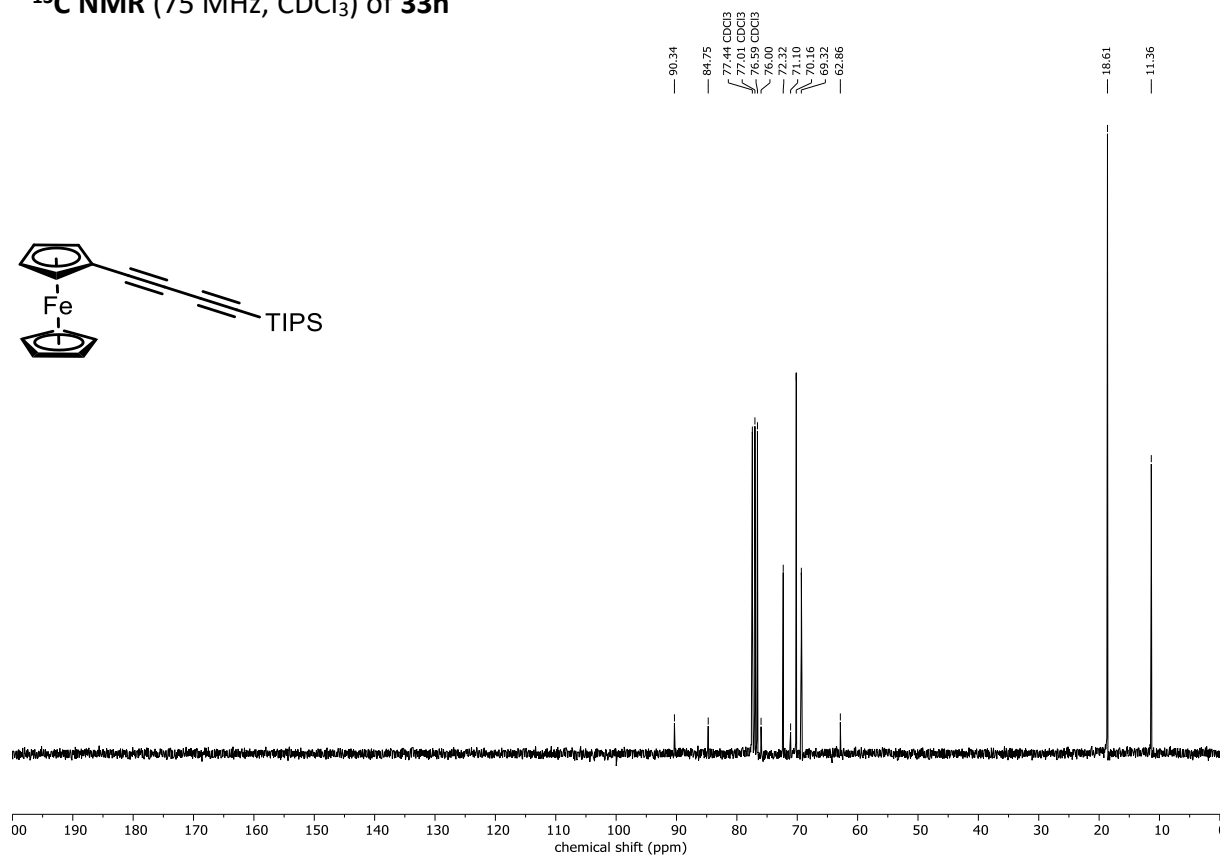
¹³C NMR (75 MHz, CDCl₃) of 33g



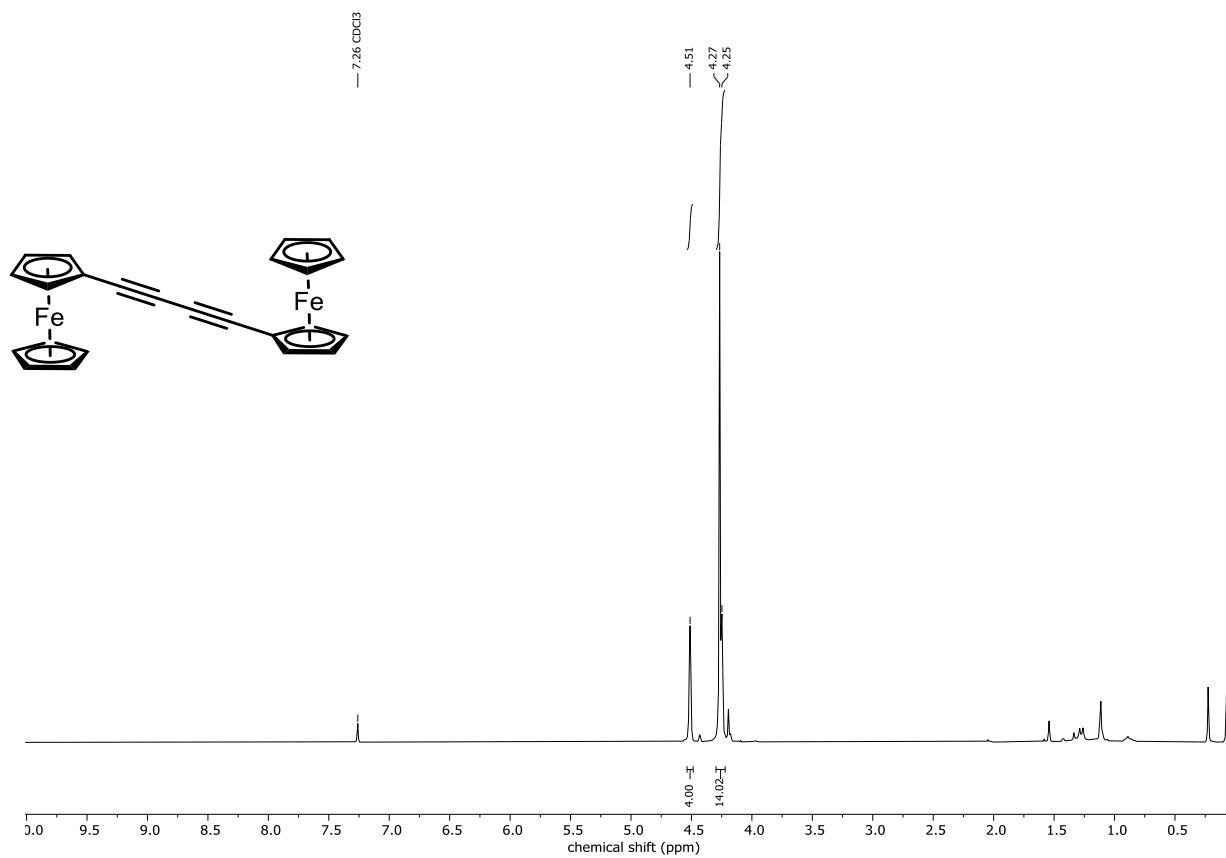
¹H NMR (300 MHz, CDCl₃) of 33h



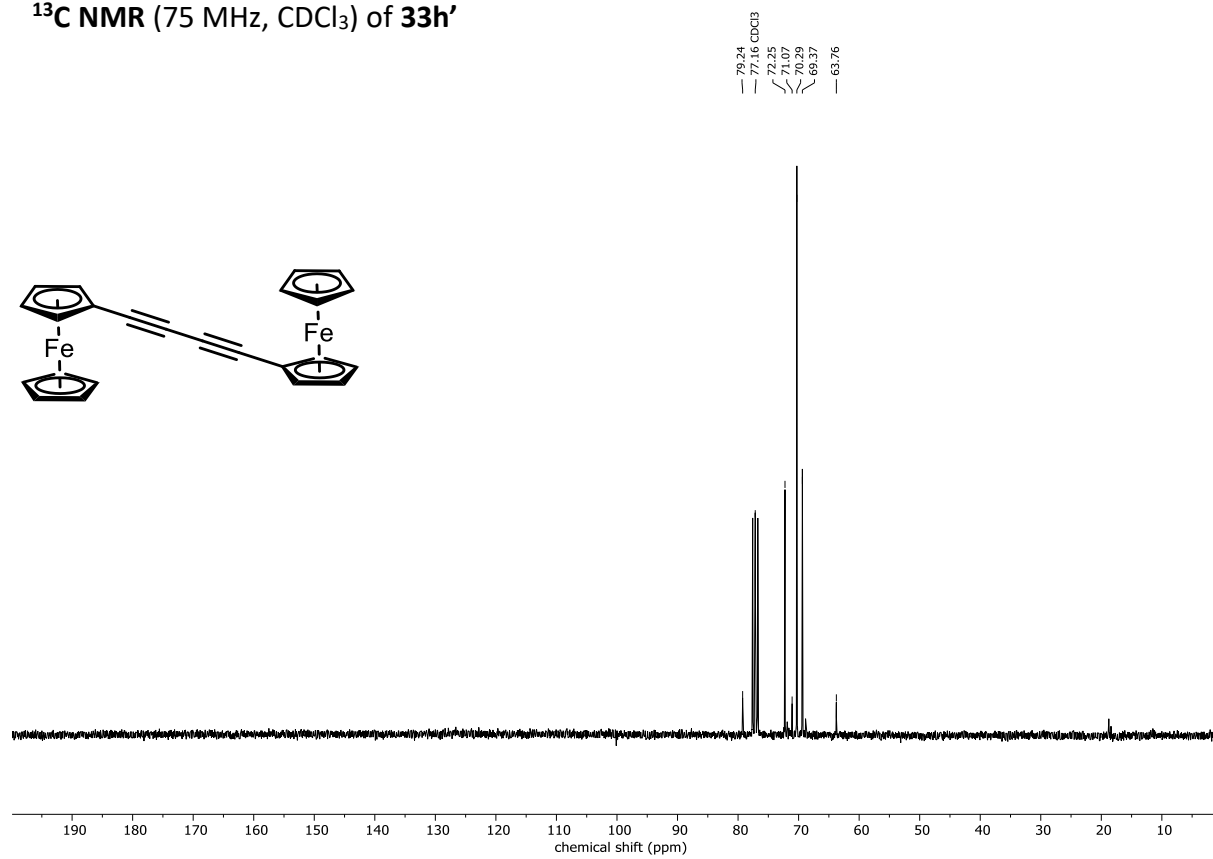
¹³C NMR (75 MHz, CDCl₃) of 33h



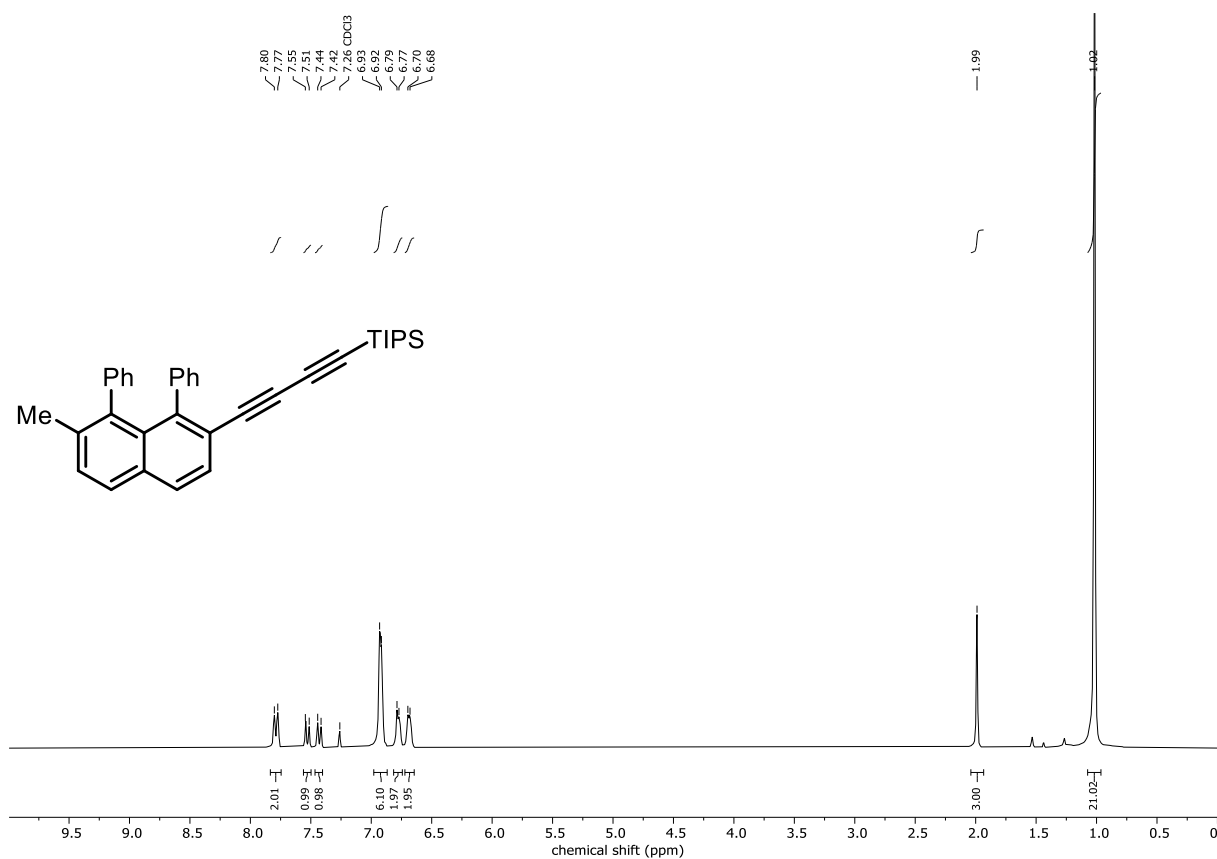
^1H NMR (300 MHz, CDCl_3) of **33h'**



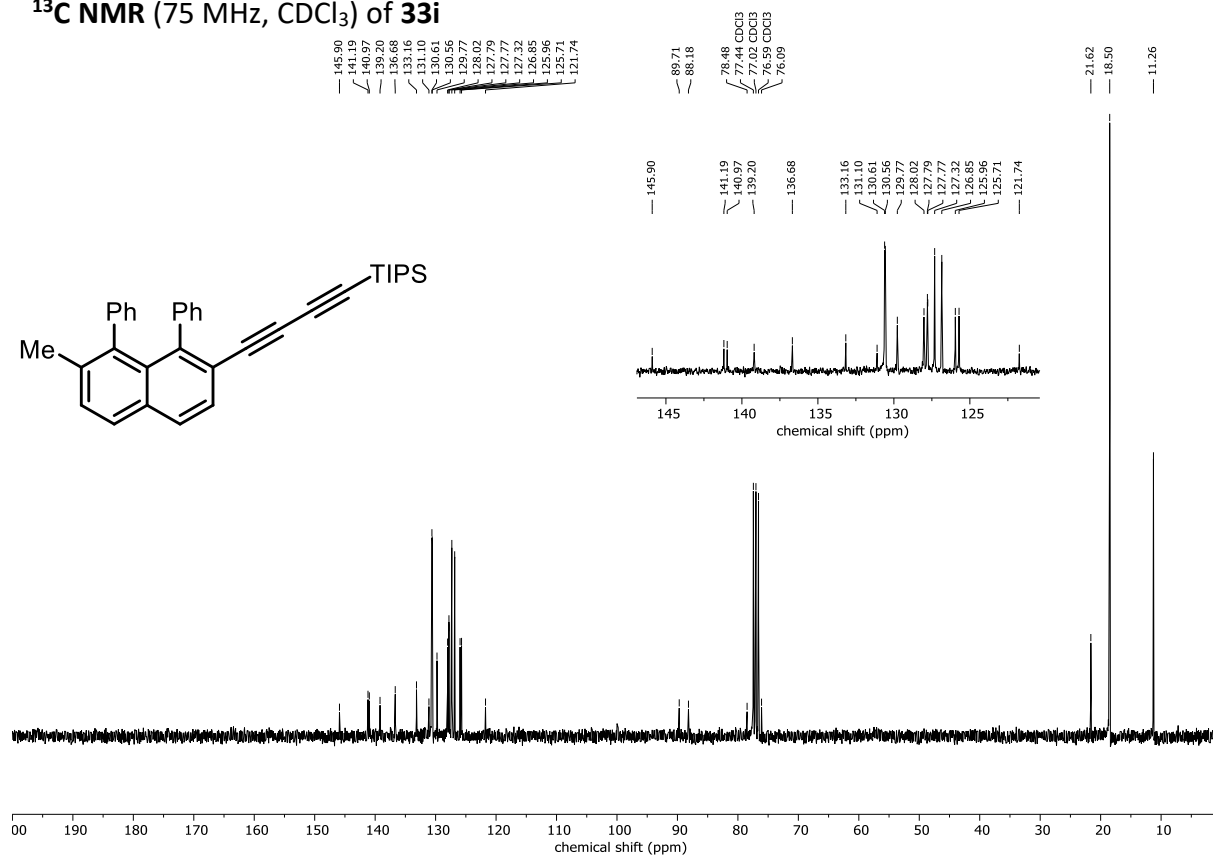
^{13}C NMR (75 MHz, CDCl_3) of **33h'**



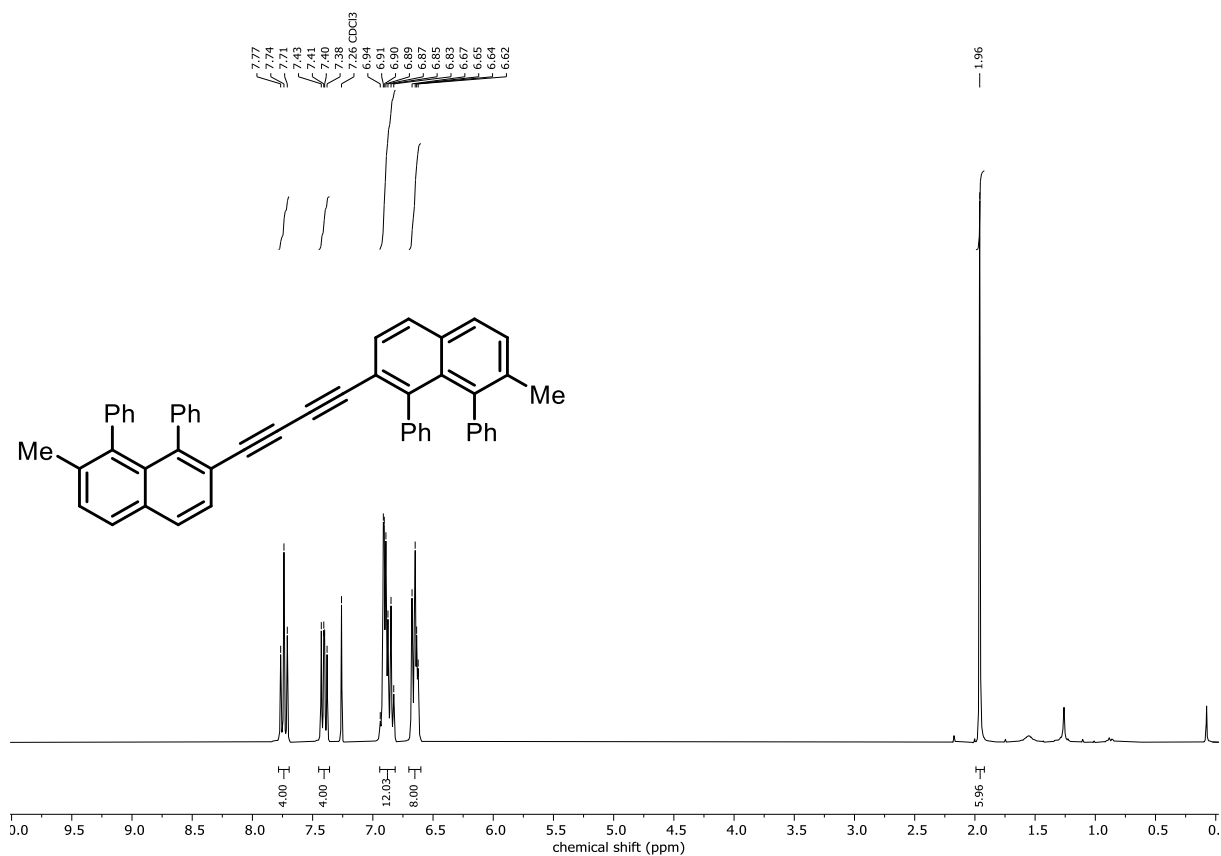
^1H NMR (300 MHz, CDCl_3) of **33i**



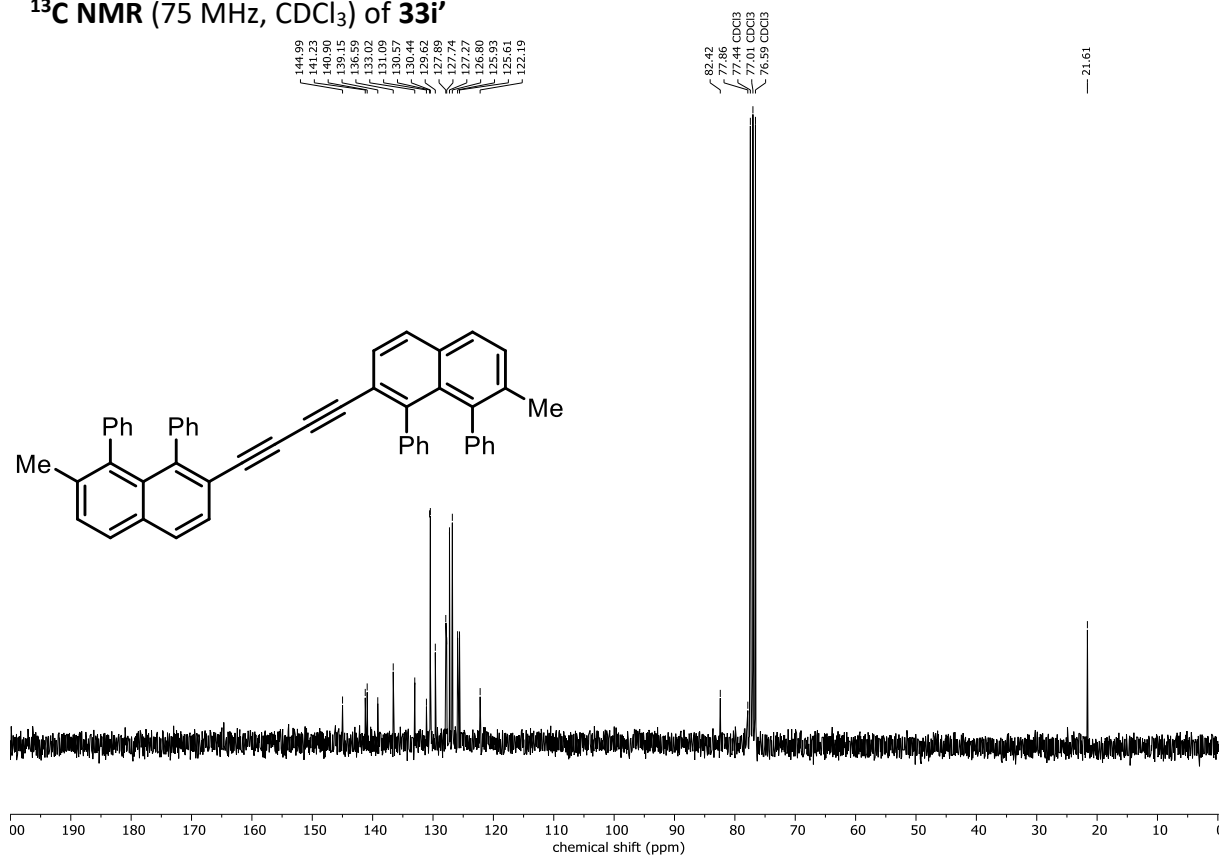
^{13}C NMR (75 MHz, CDCl_3) of **33i**



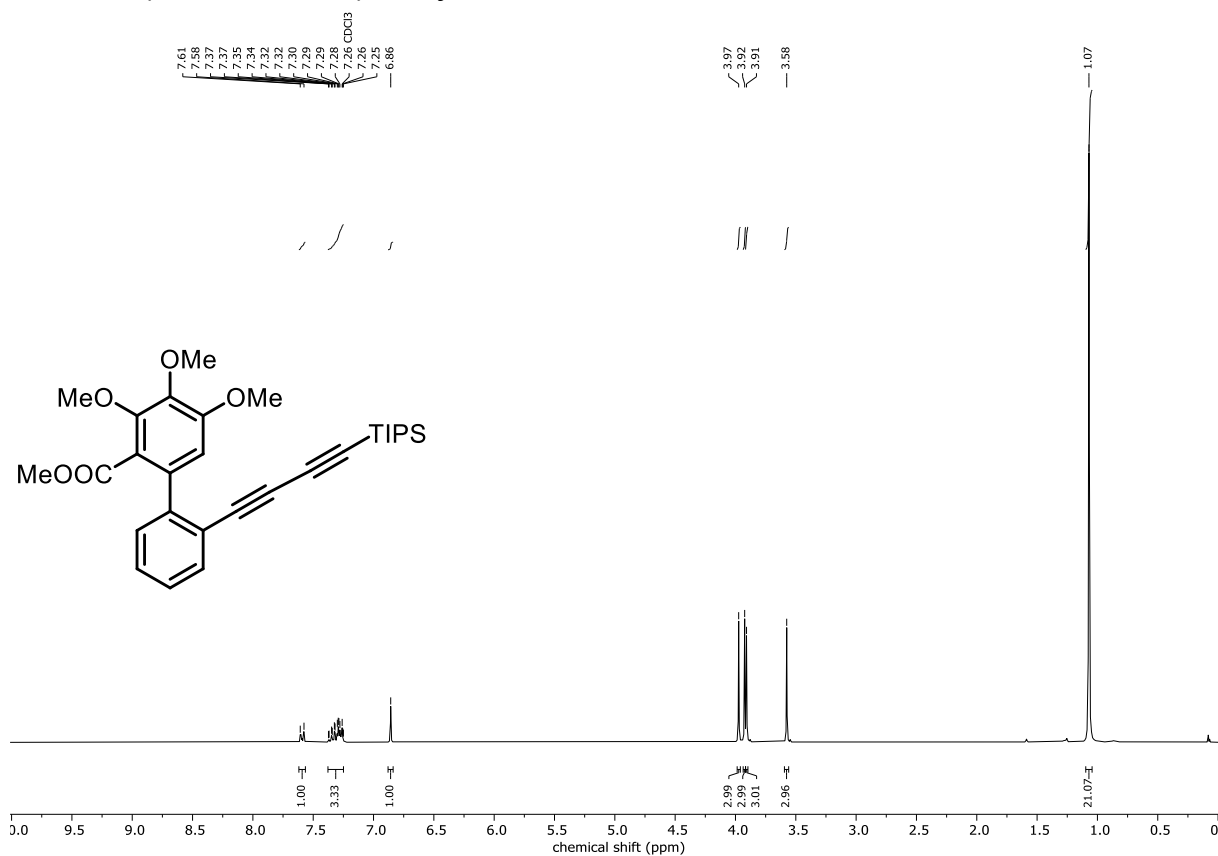
¹H NMR (300 MHz, CDCl₃) of 33i'



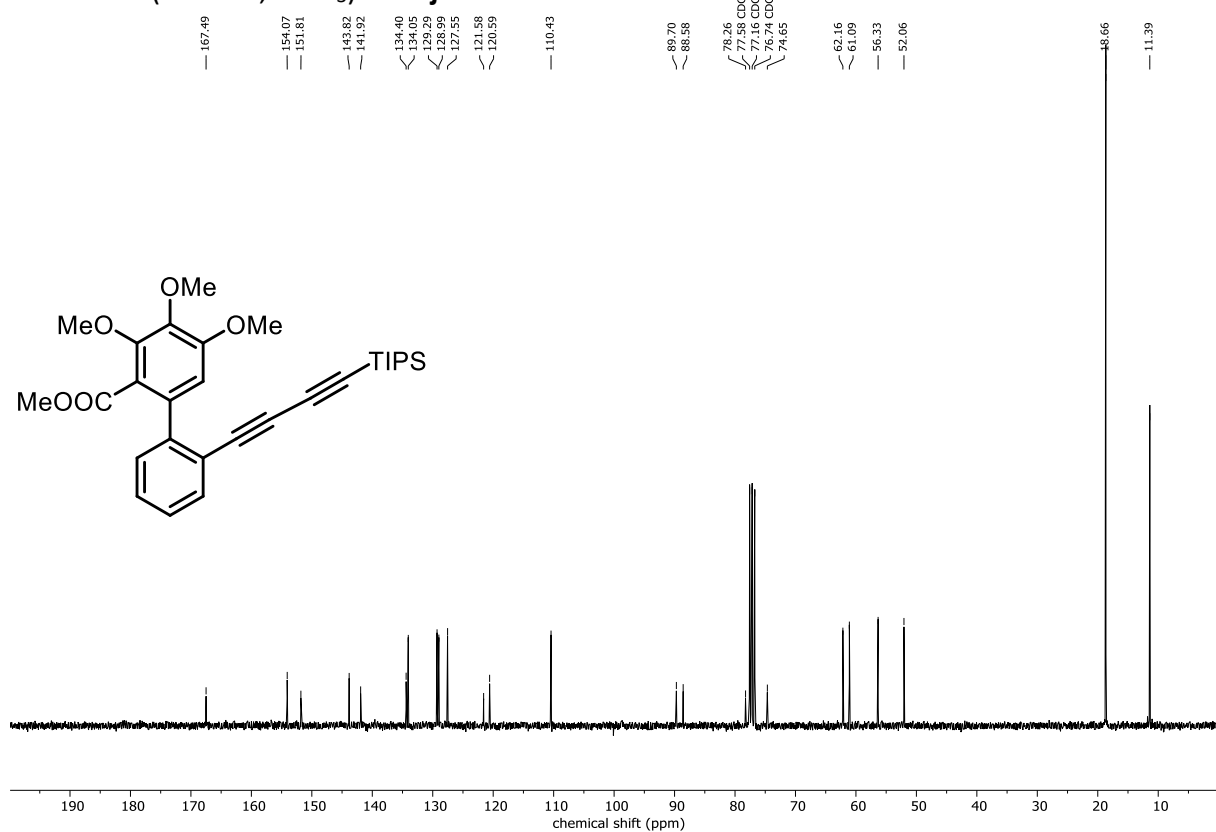
¹³C NMR (75 MHz, CDCl₃) of 33i'



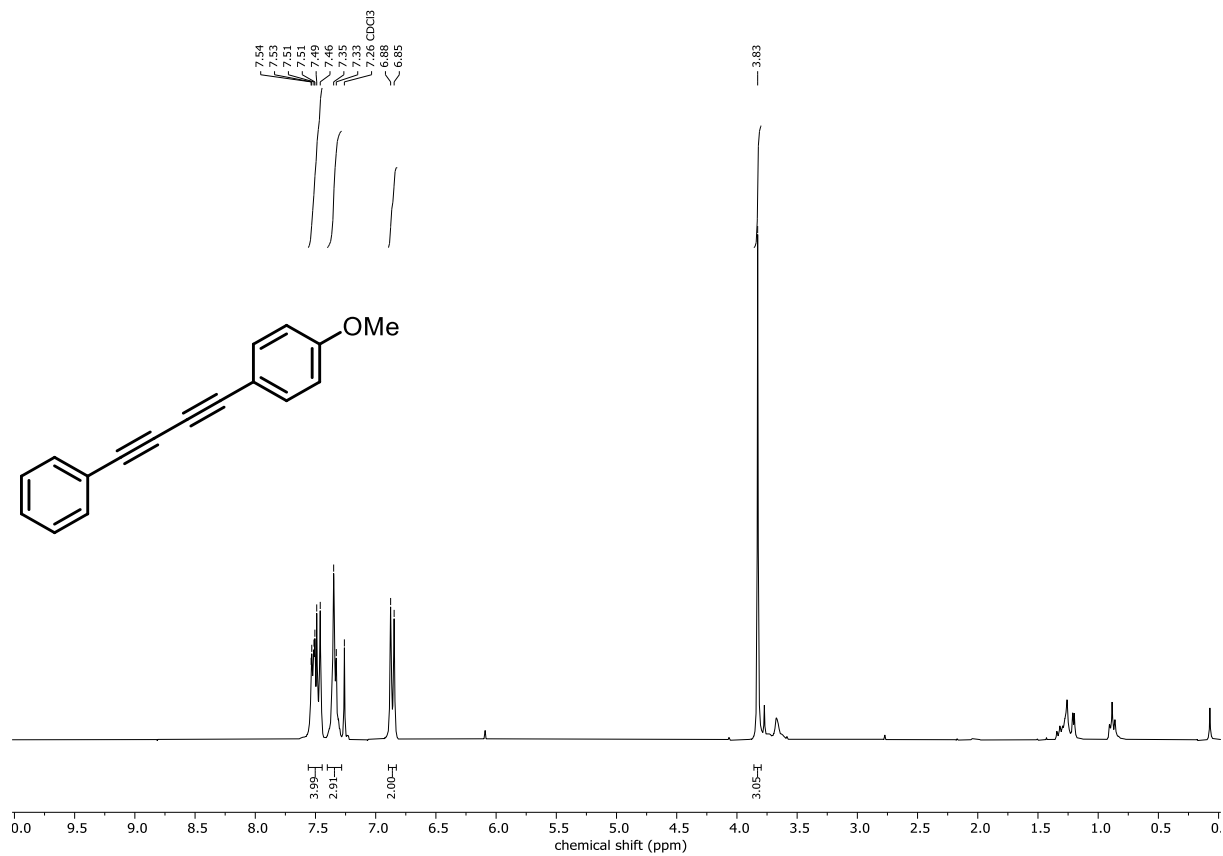
¹H NMR (300 MHz, CDCl₃) of **33j**



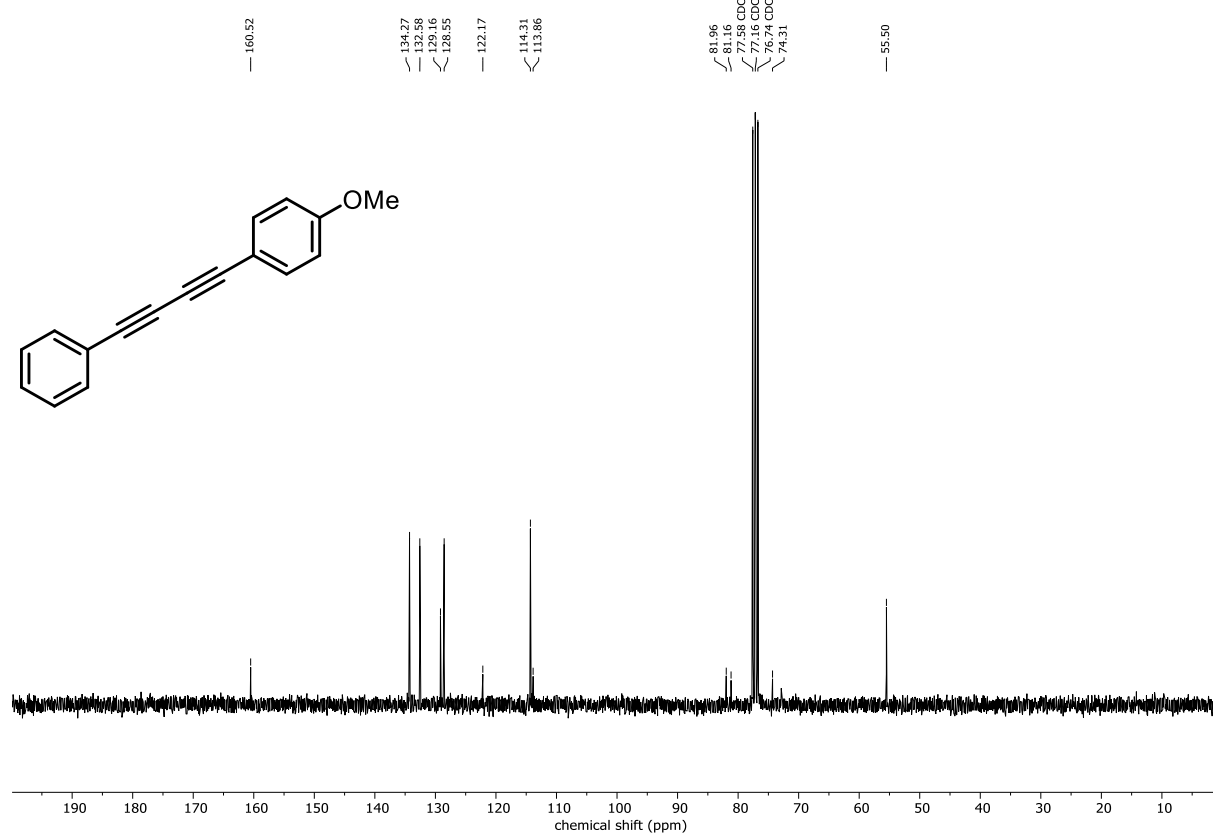
¹³C NMR (75 MHz, CDCl₃) of **33j**



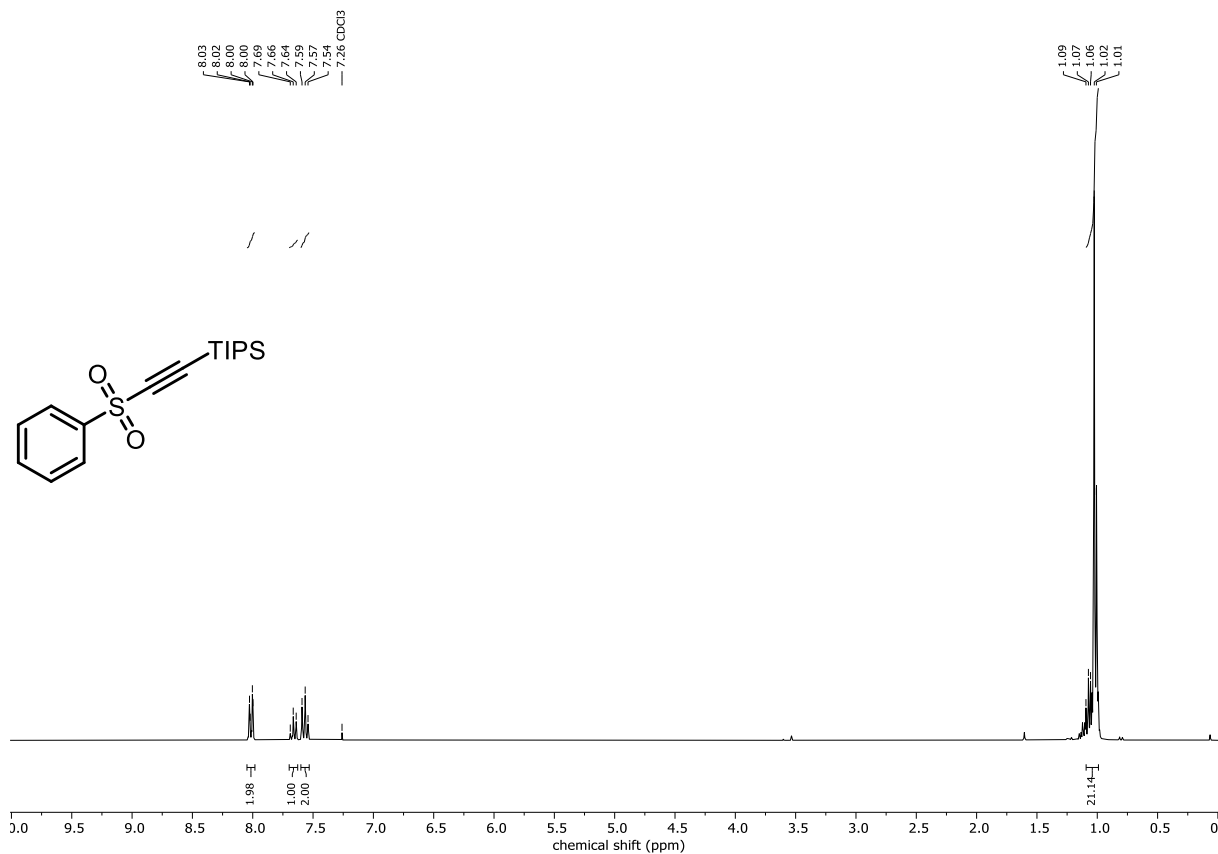
^1H NMR (300 MHz, CDCl_3) of **33I**



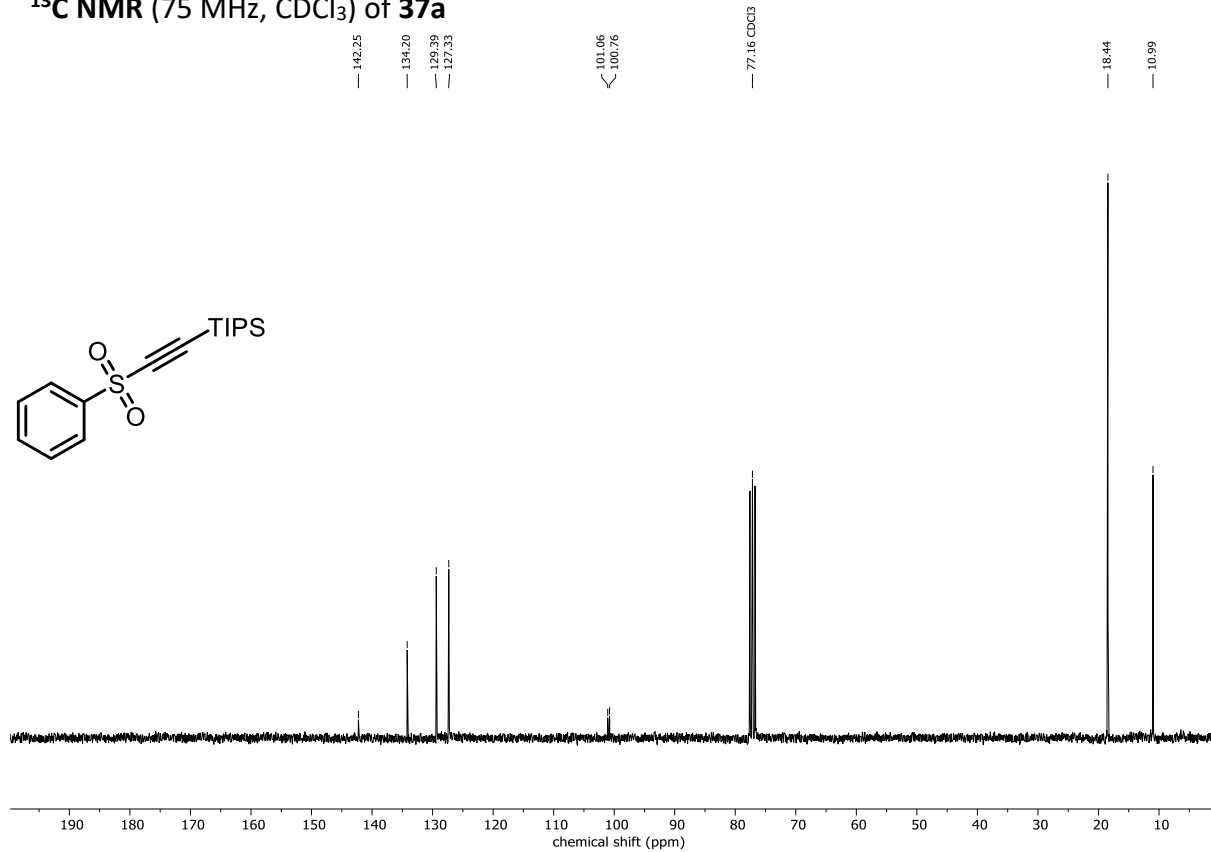
^{13}C NMR (75 MHz, CDCl_3) of **33I**



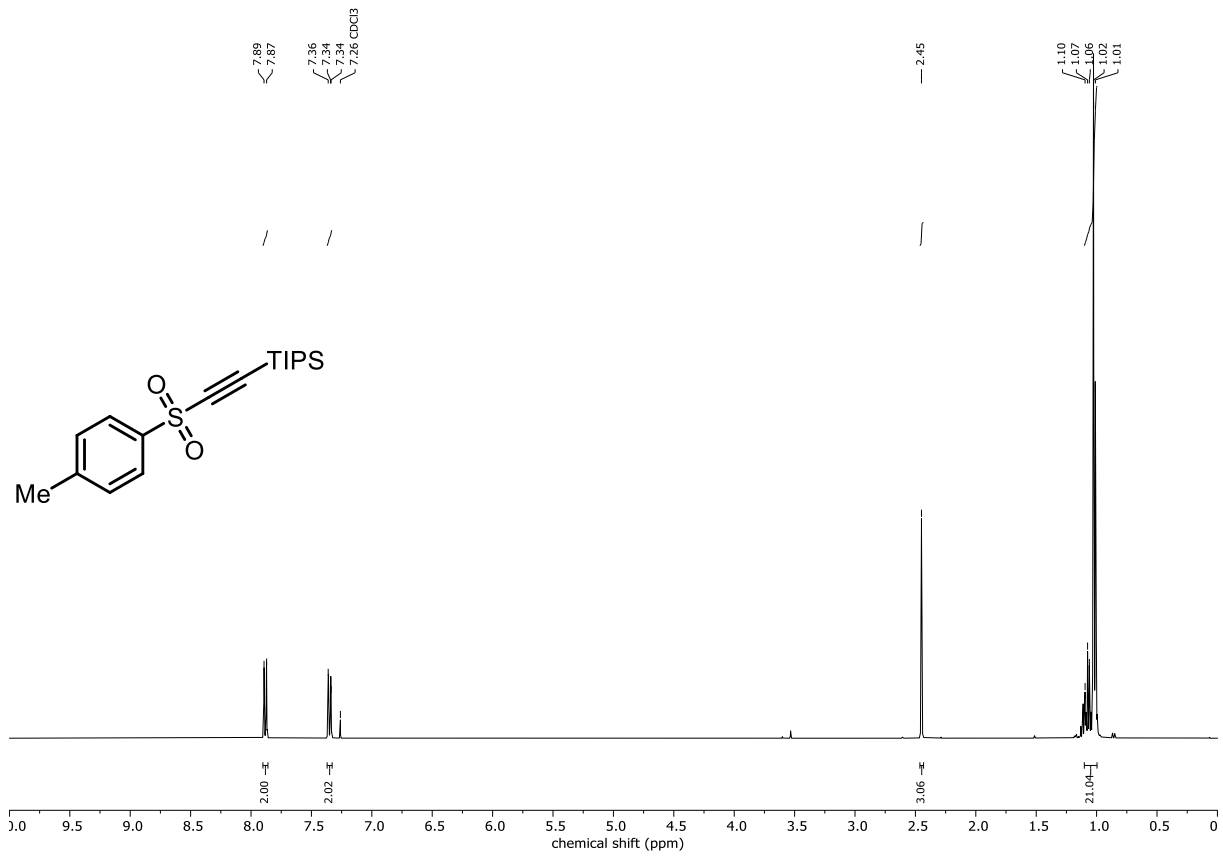
¹H NMR (300 MHz, CDCl₃) of 37a



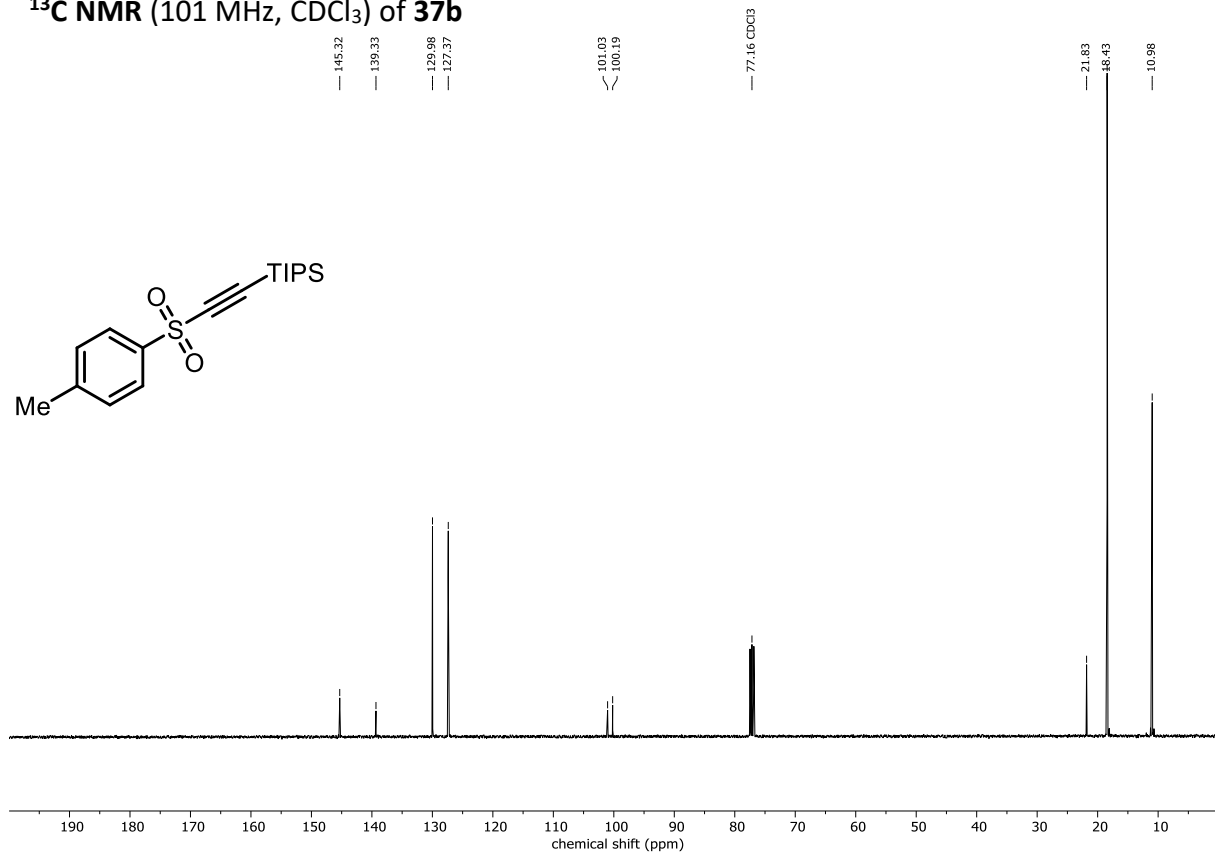
¹³C NMR (75 MHz, CDCl₃) of 37a



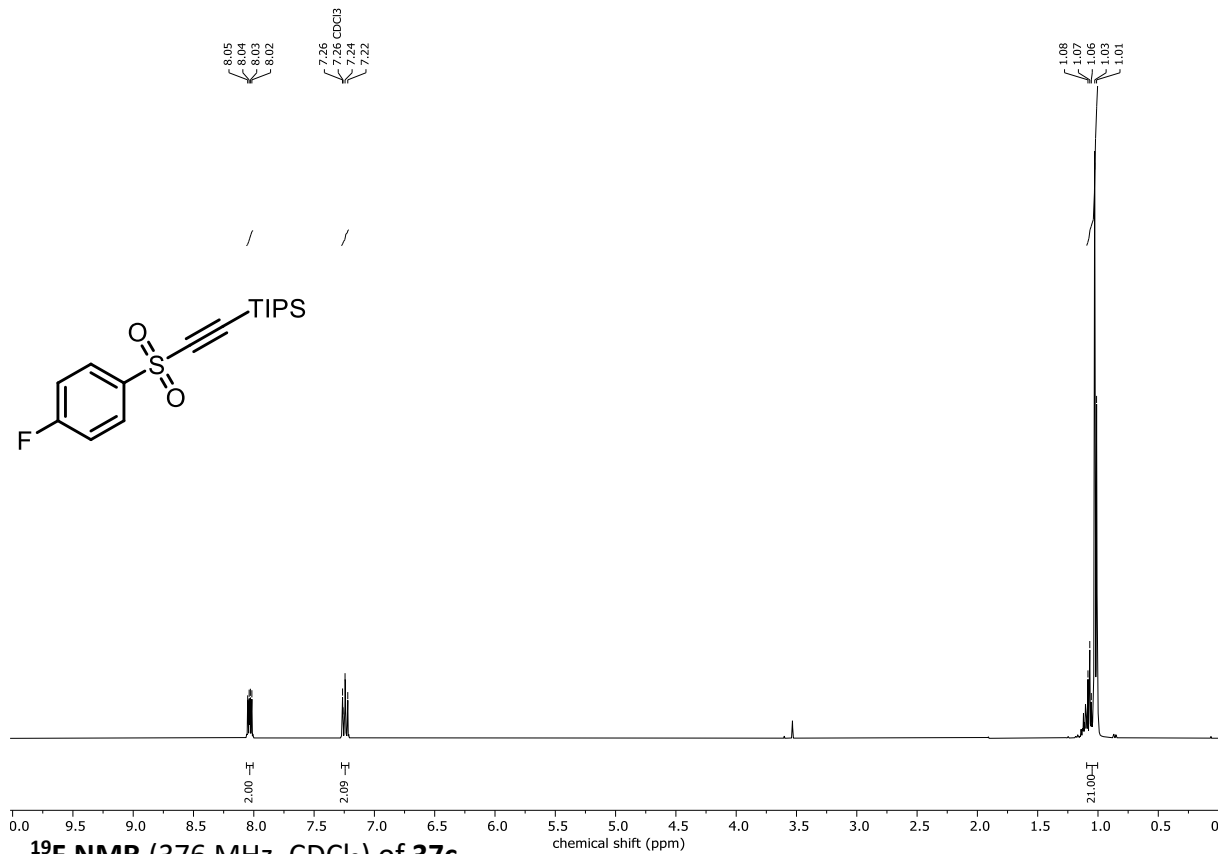
¹H NMR (400 MHz, CDCl₃) of 37b



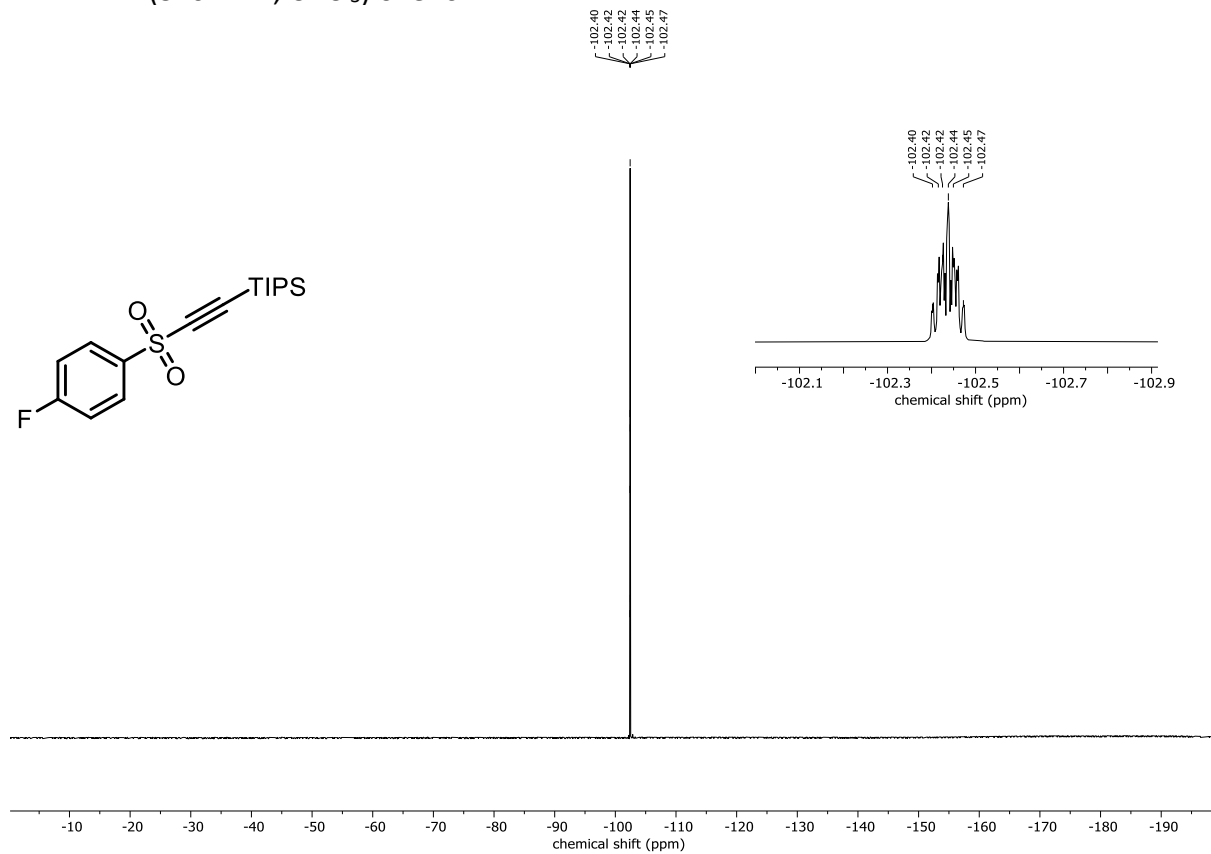
¹³C NMR (101 MHz, CDCl₃) of 37b



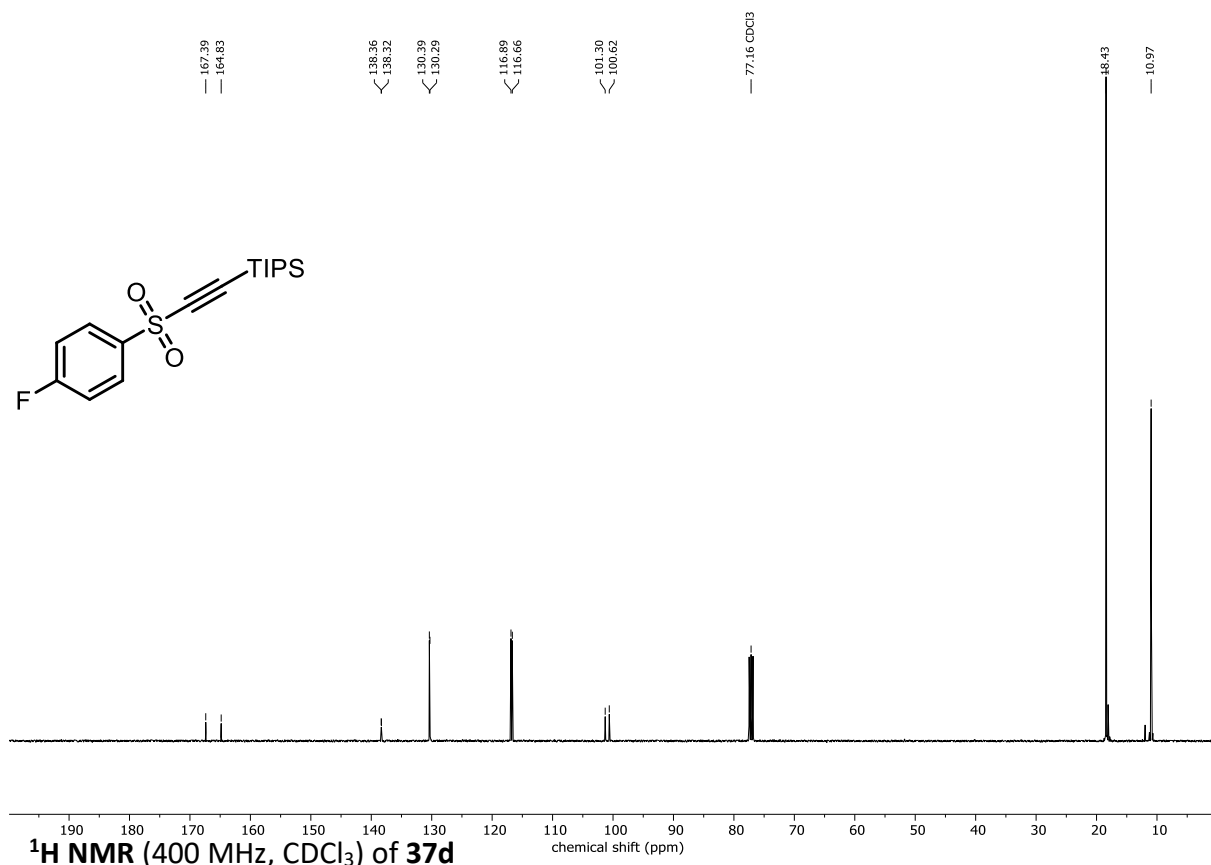
¹H NMR (400 MHz, CDCl₃) of 37c



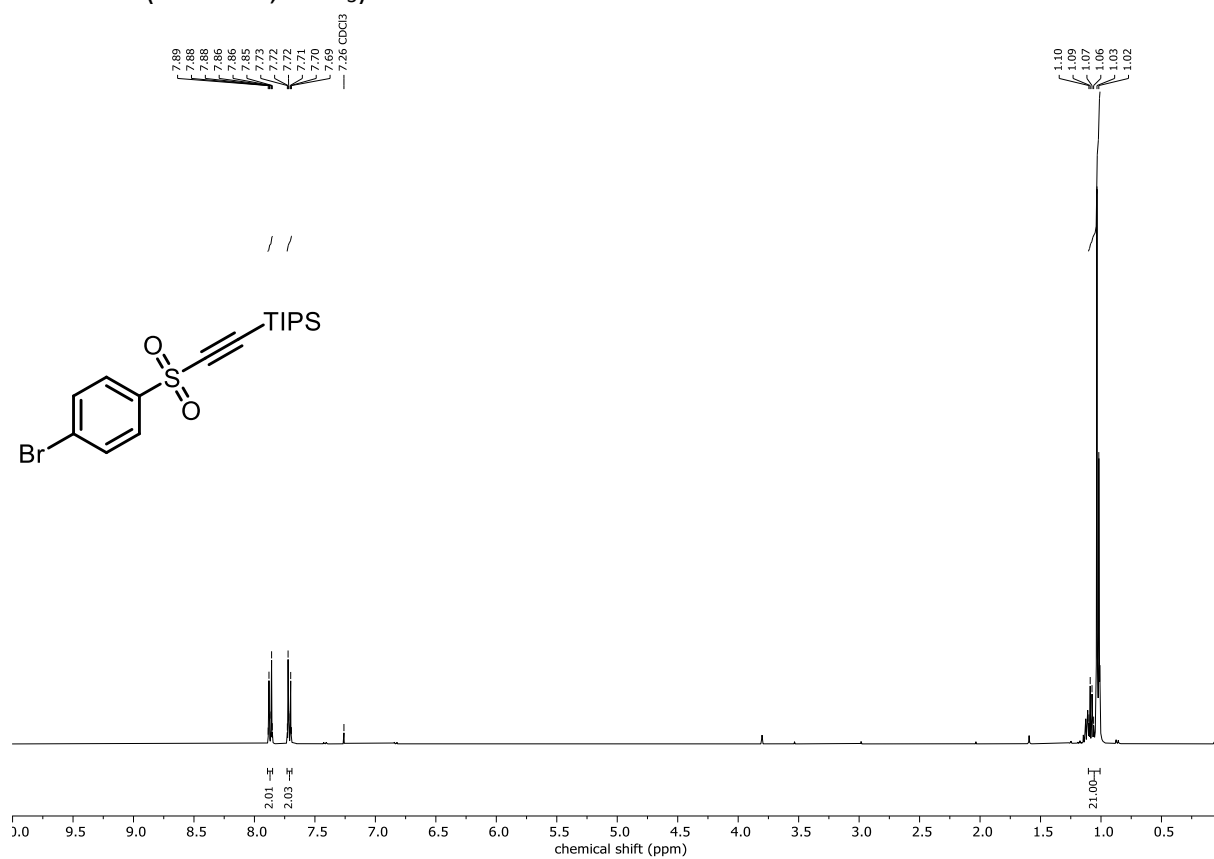
¹⁹F NMR (376 MHz, CDCl₃) of 37c



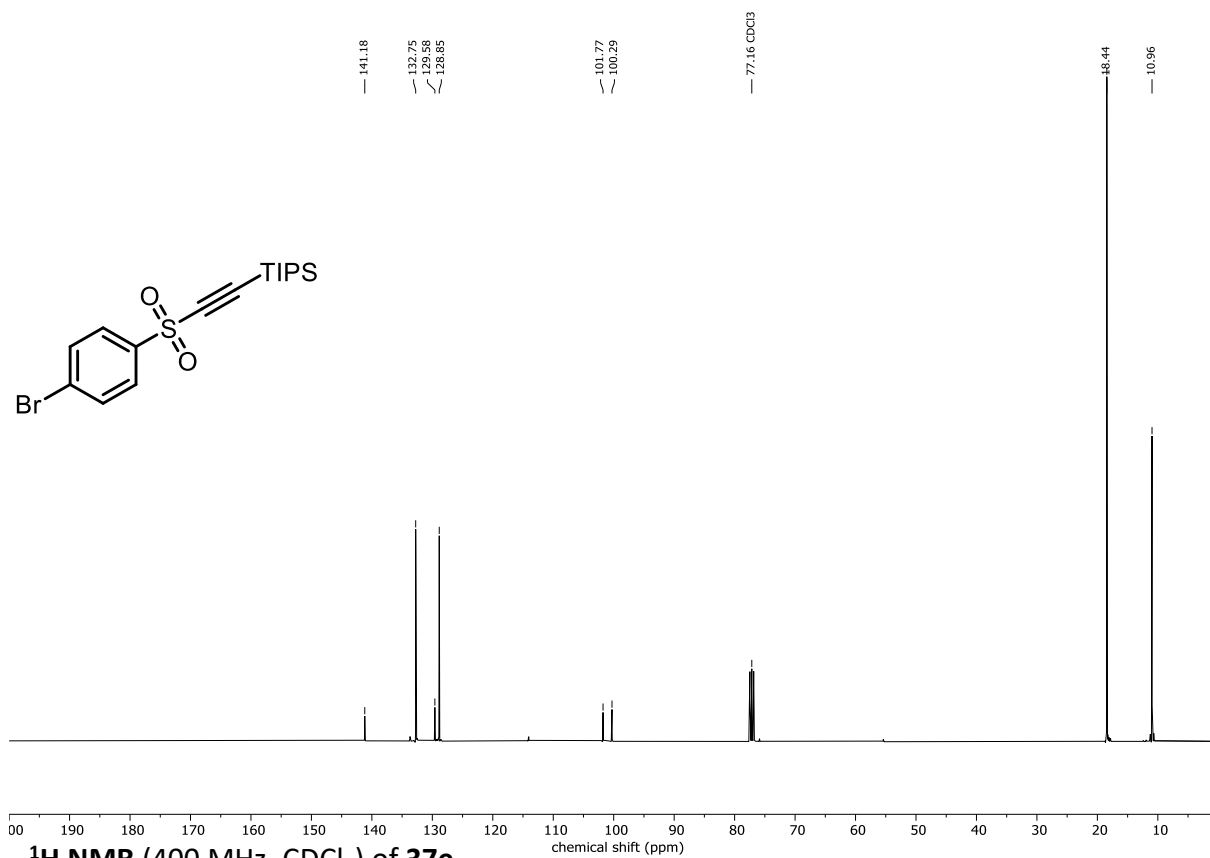
¹³C NMR (101 MHz, CDCl₃) of 37c



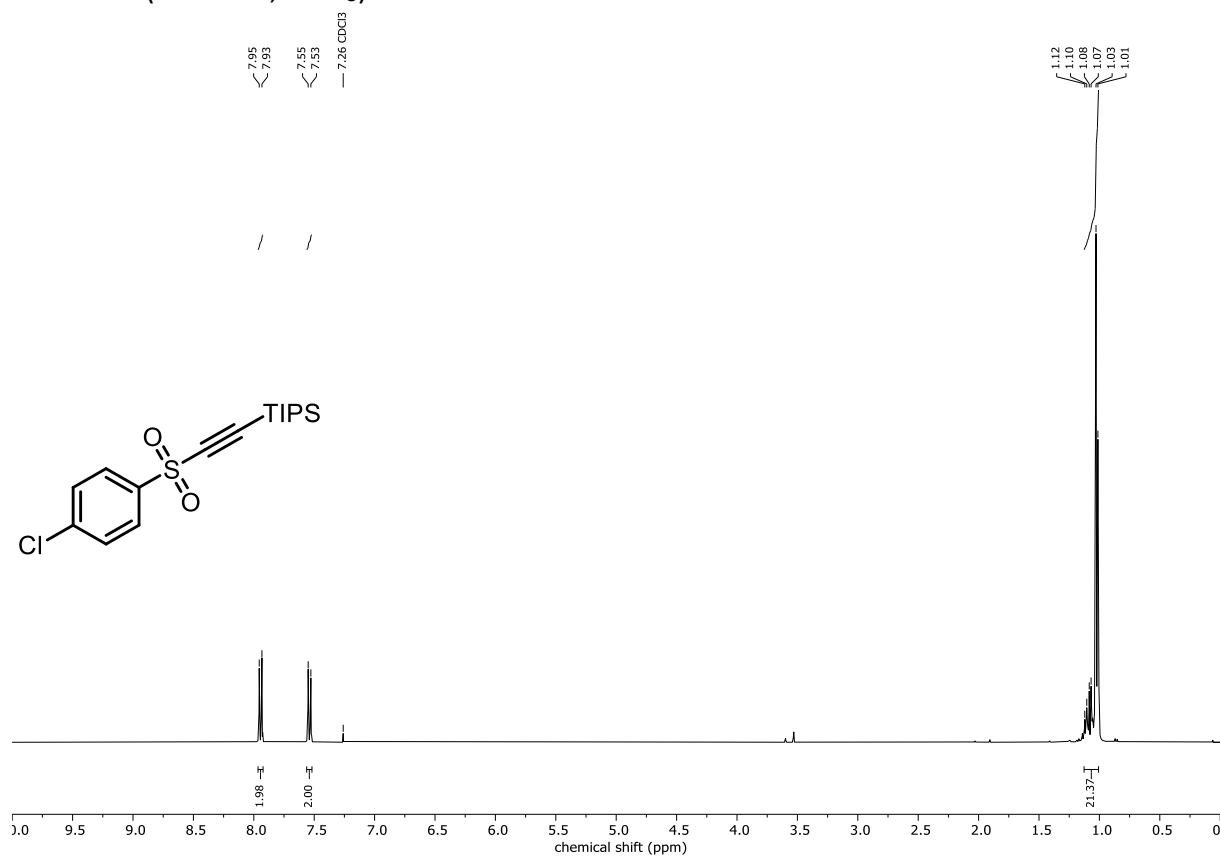
¹H NMR (400 MHz, CDCl₃) of 37d



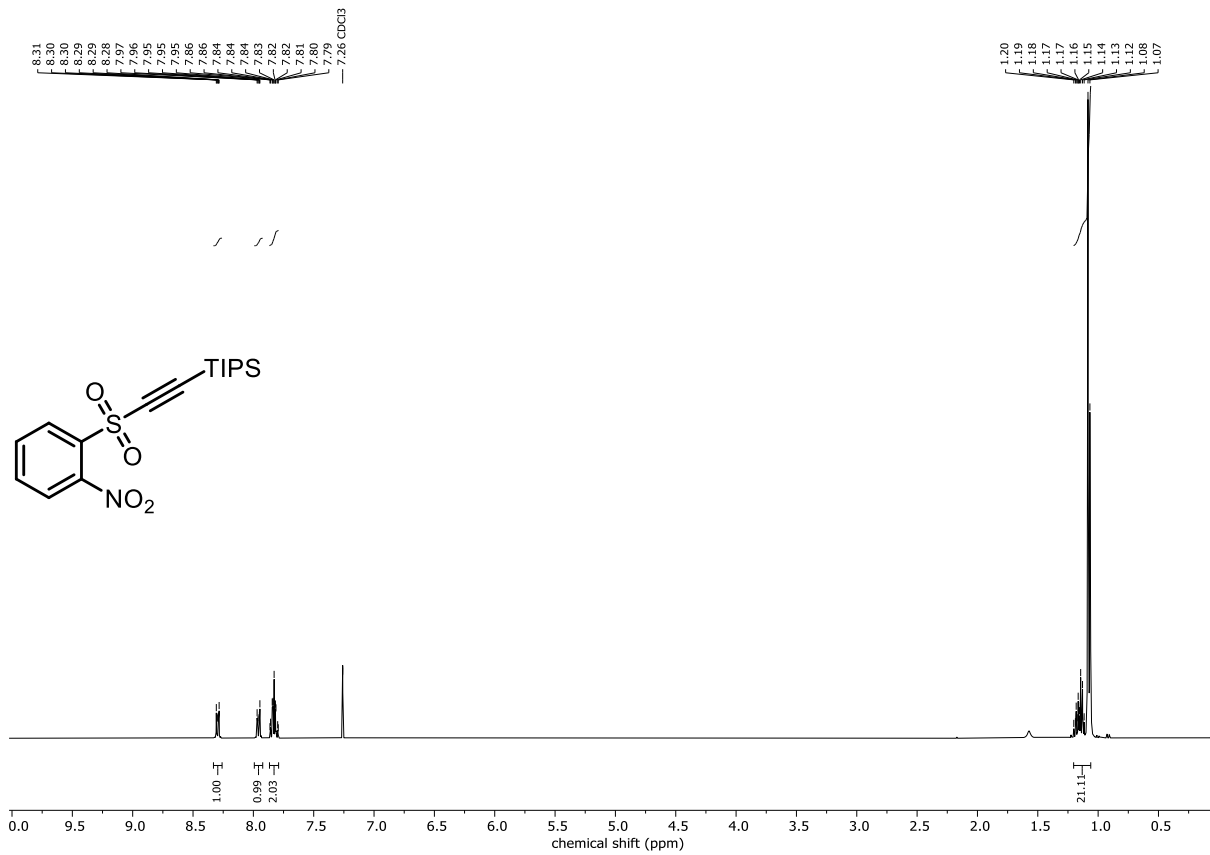
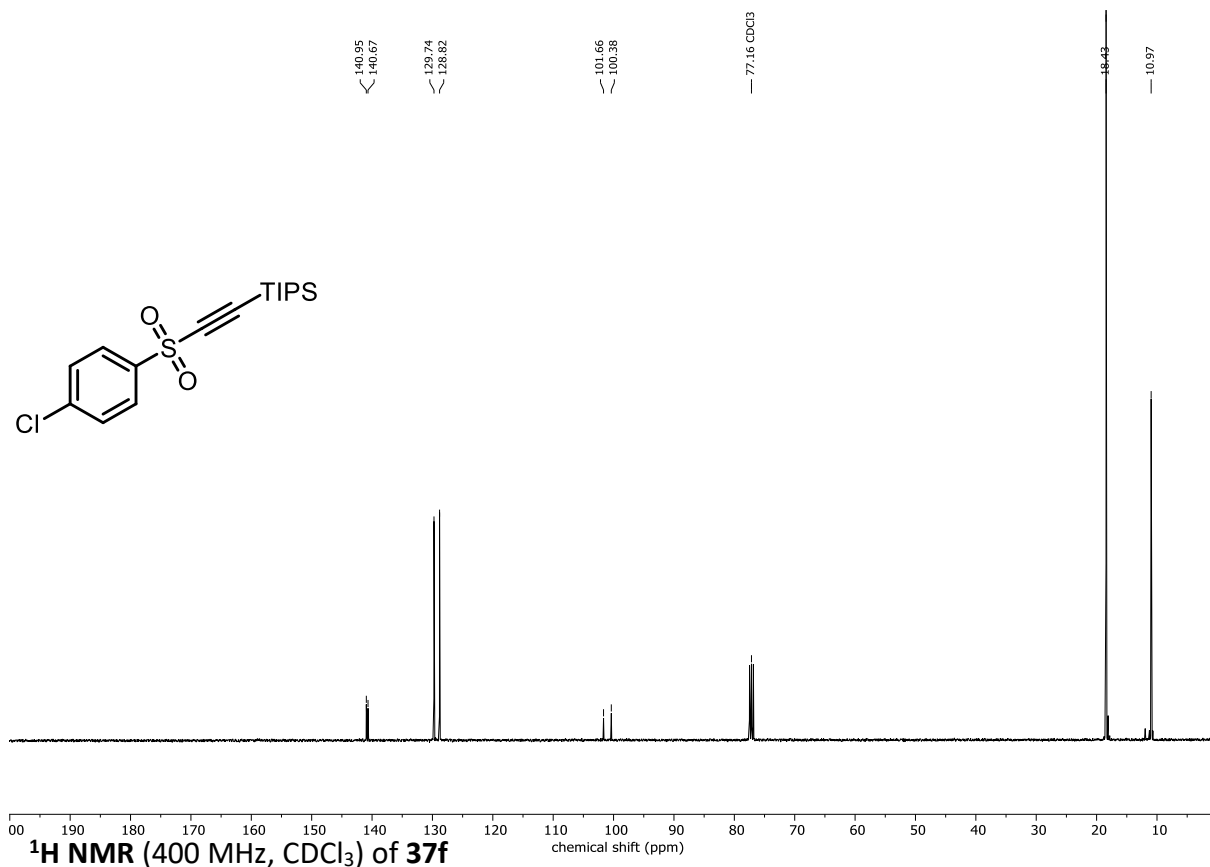
¹³C NMR (101 MHz, CDCl₃) of 37d



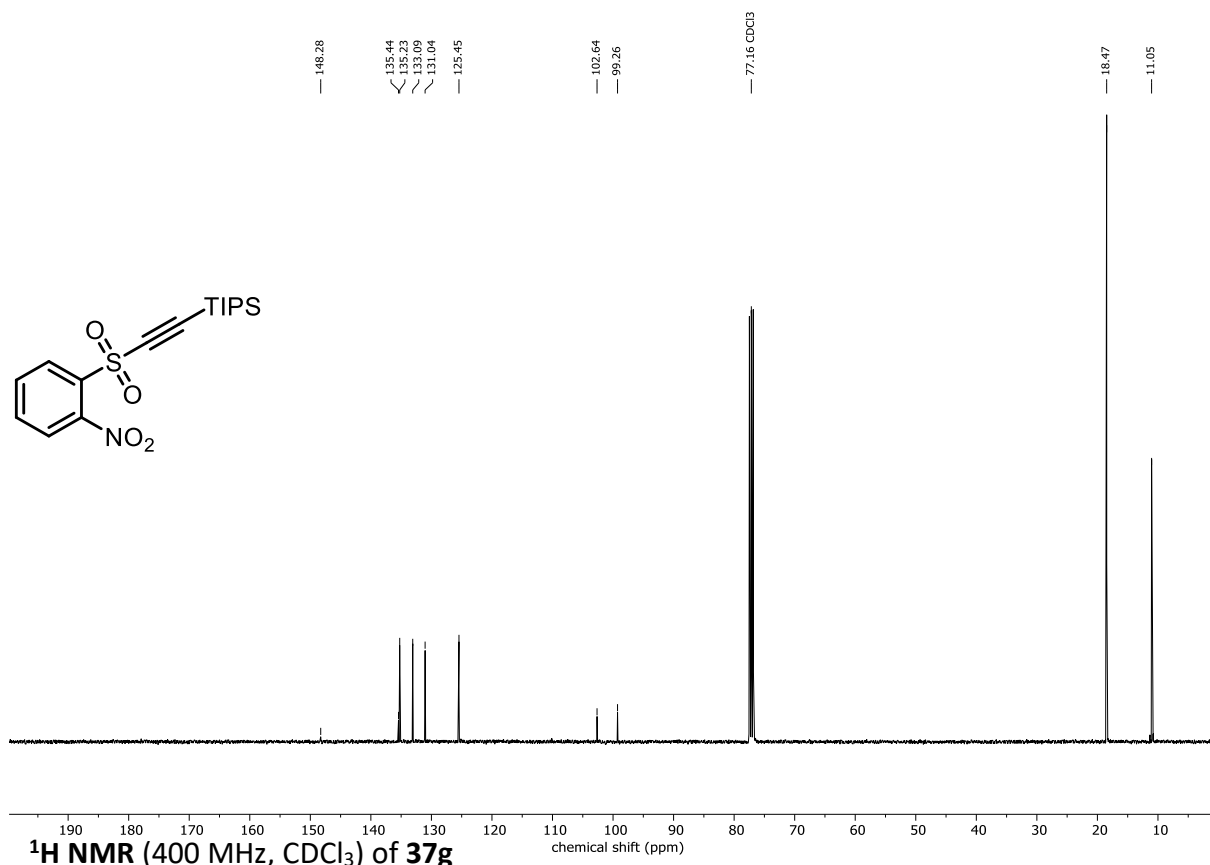
¹H NMR (400 MHz, CDCl₃) of 37e



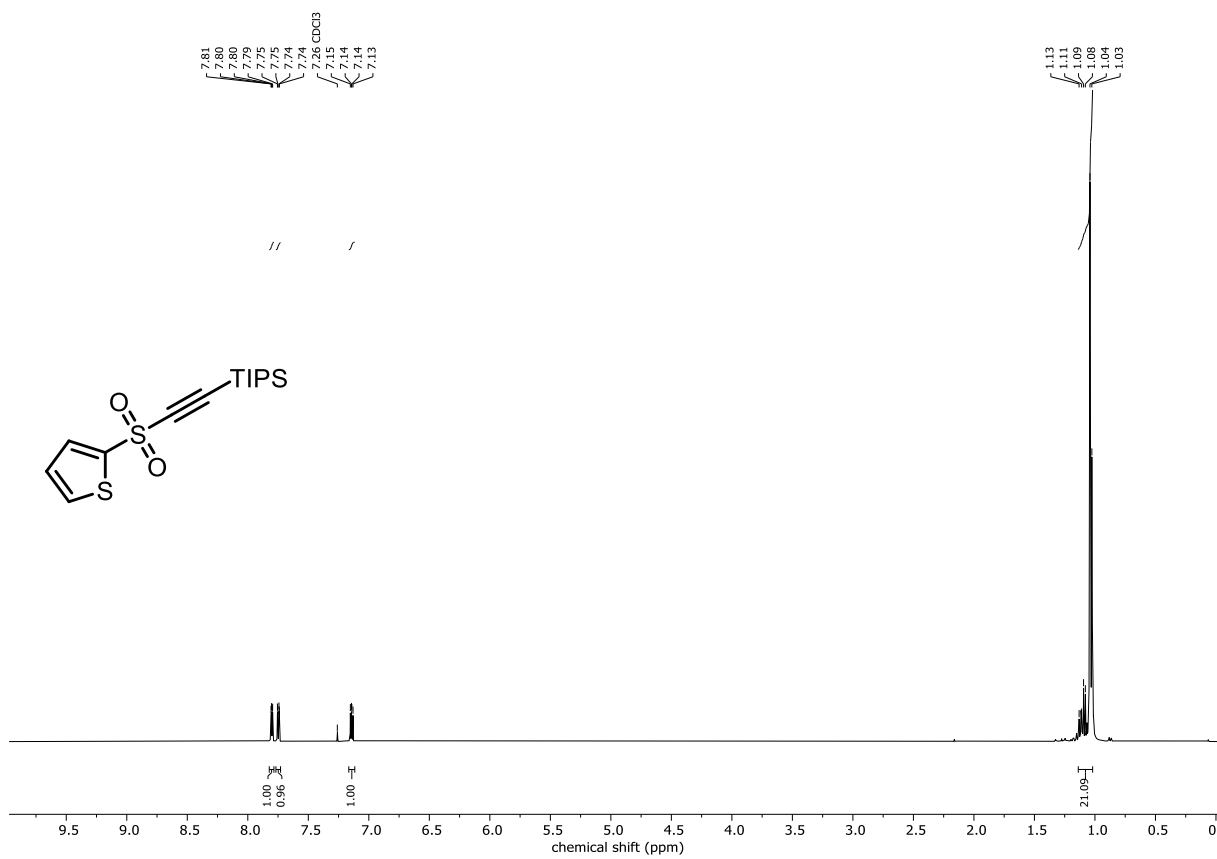
¹³C NMR (101 MHz, CDCl₃) of **37e**



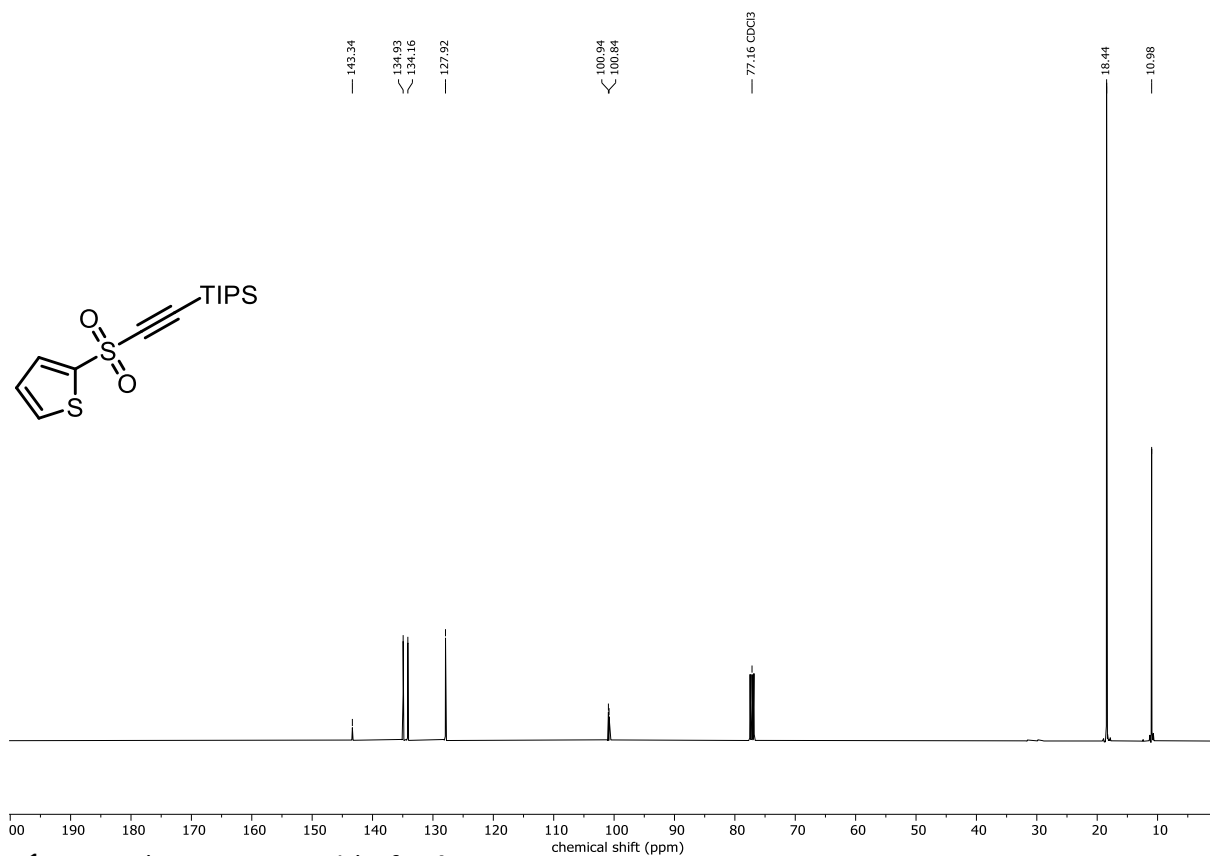
¹³C NMR (101 MHz, CDCl₃) of **37f**



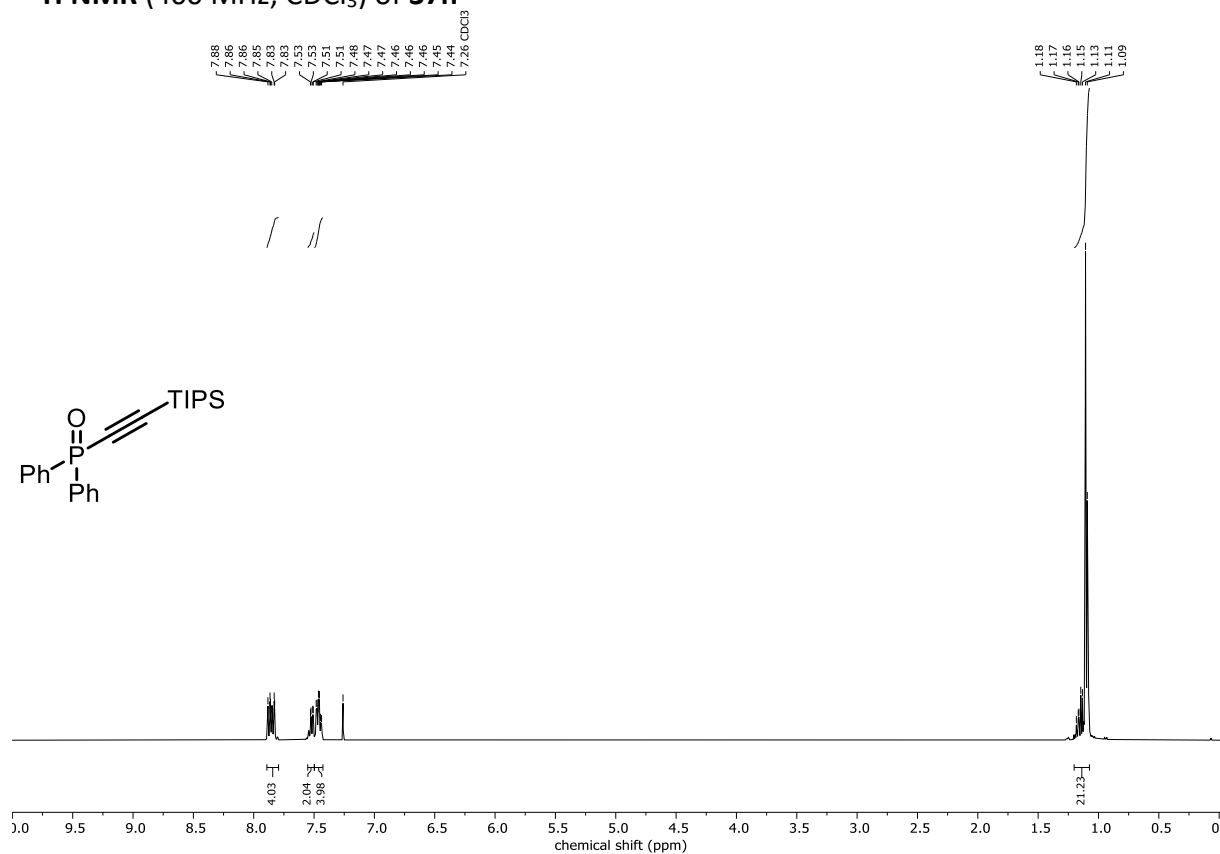
¹H NMR (400 MHz, CDCl₃) of **37g**



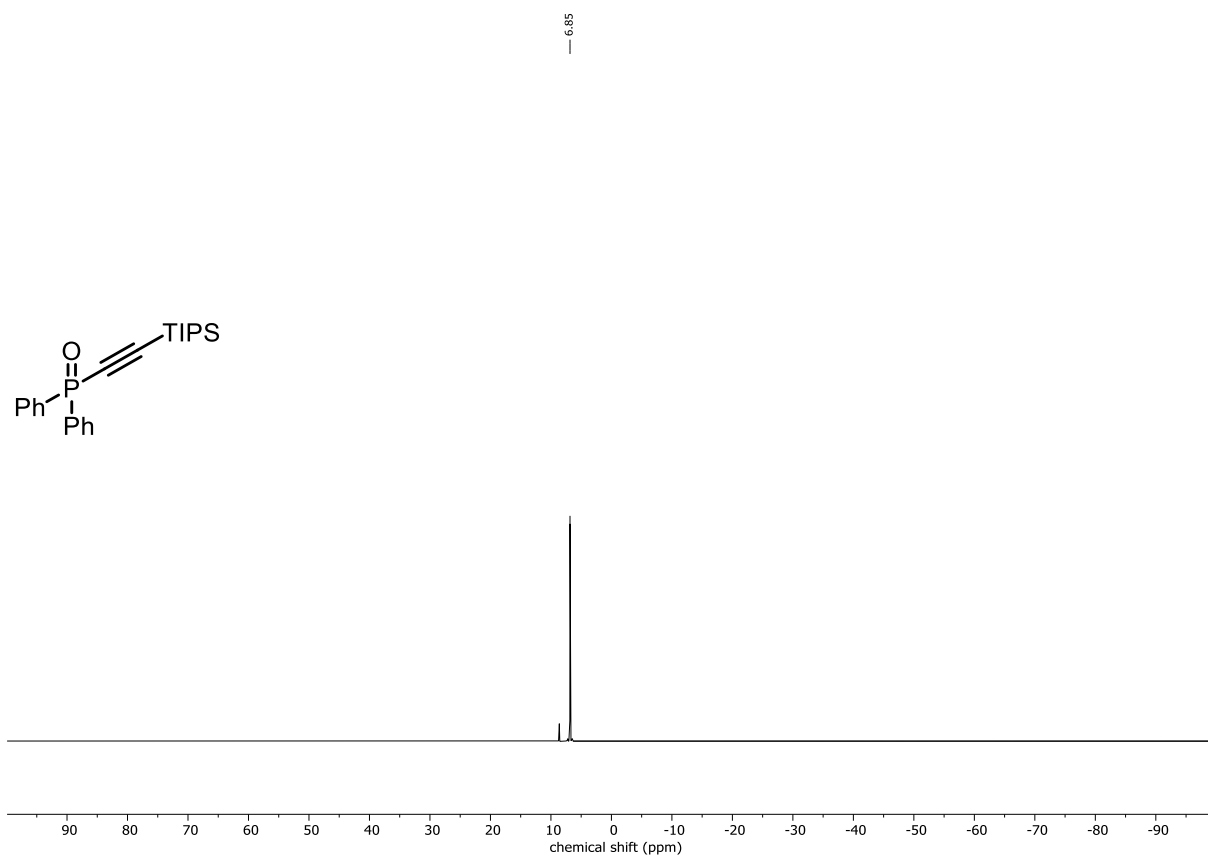
¹³C NMR (101 MHz, CDCl₃) of 37g



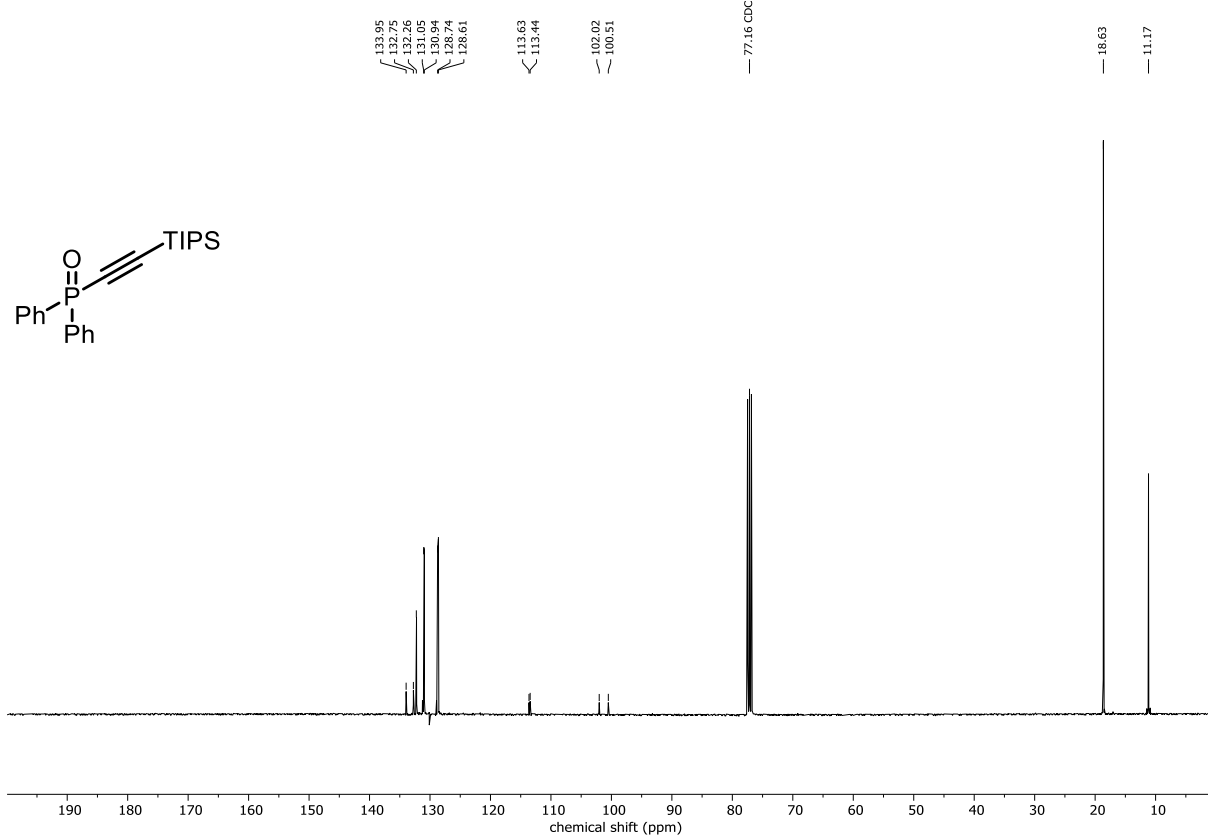
¹H NMR (400 MHz, CDCl₃) of 37h



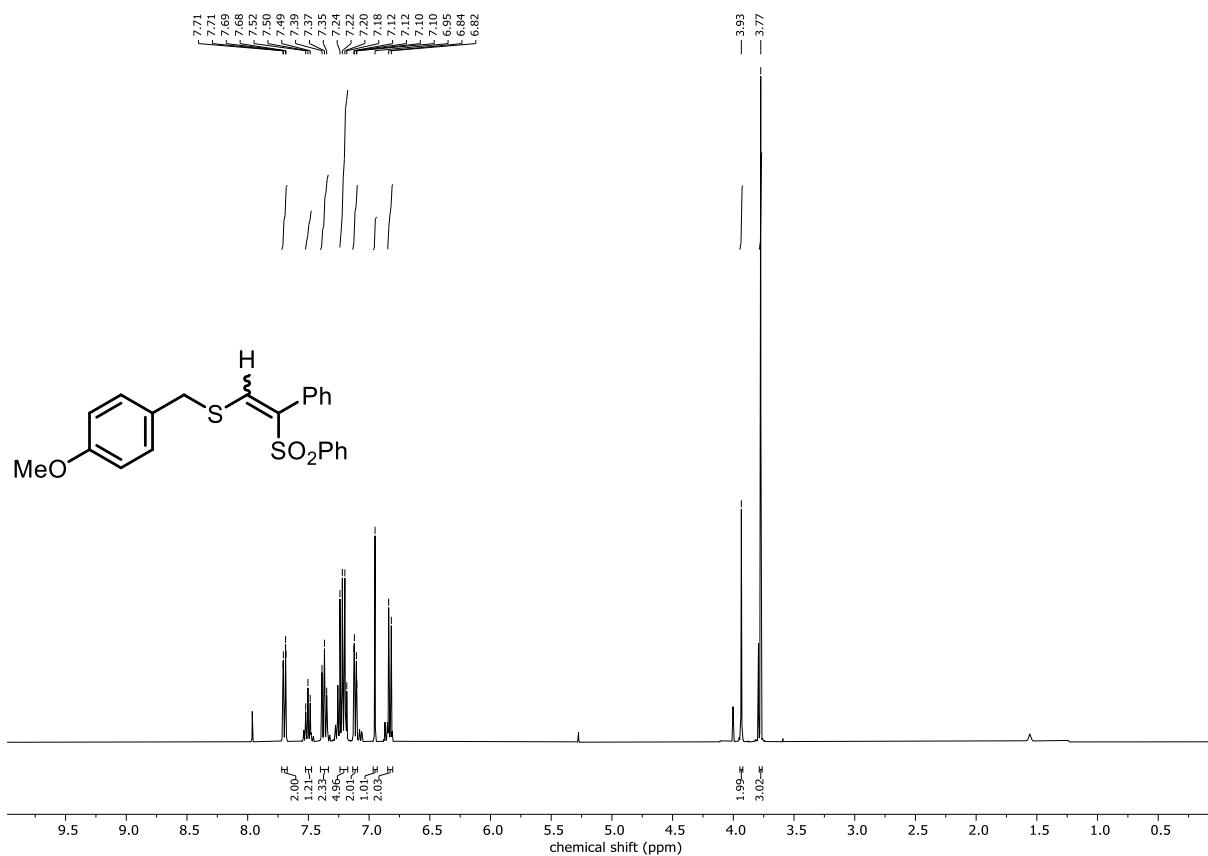
³¹P NMR (162 MHz, CDCl₃) of 37h



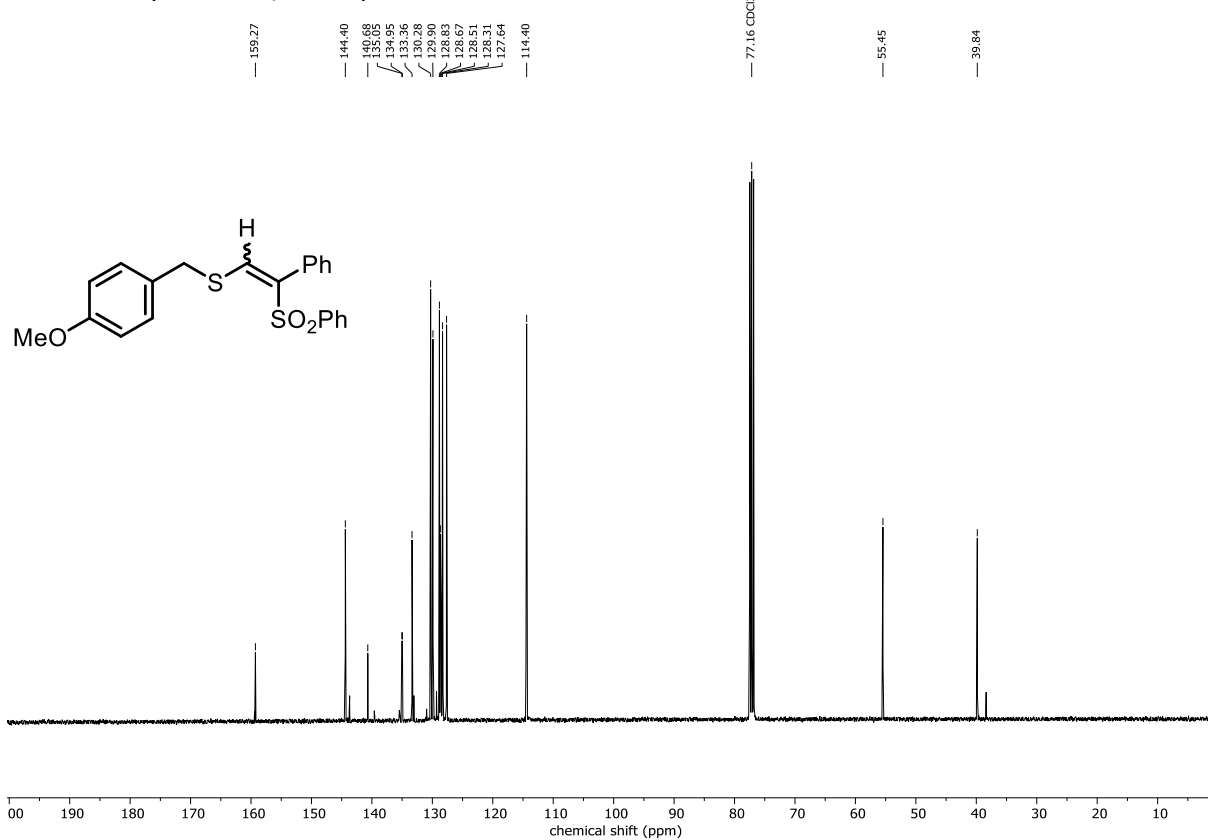
¹³C NMR (101 MHz, CDCl₃) of 37h



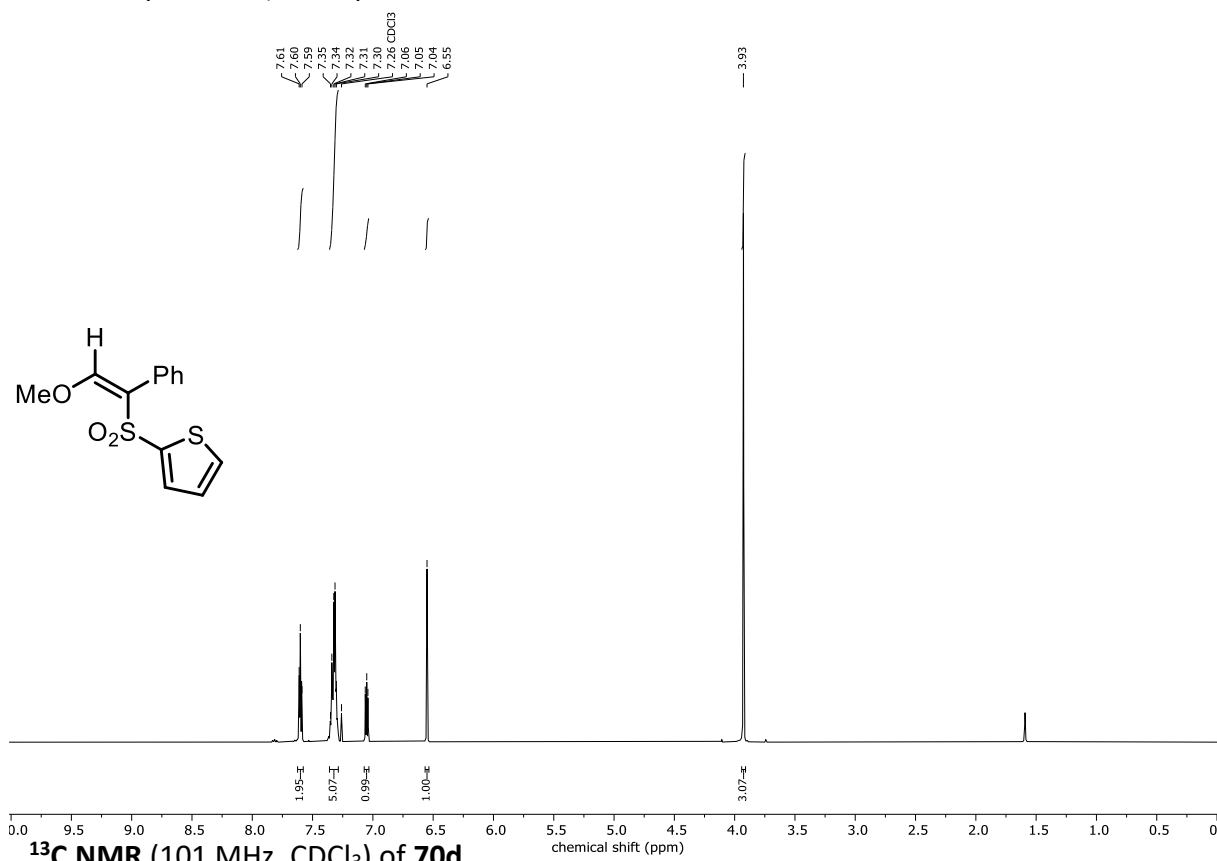
¹H NMR (400 MHz, CDCl₃) of 70c



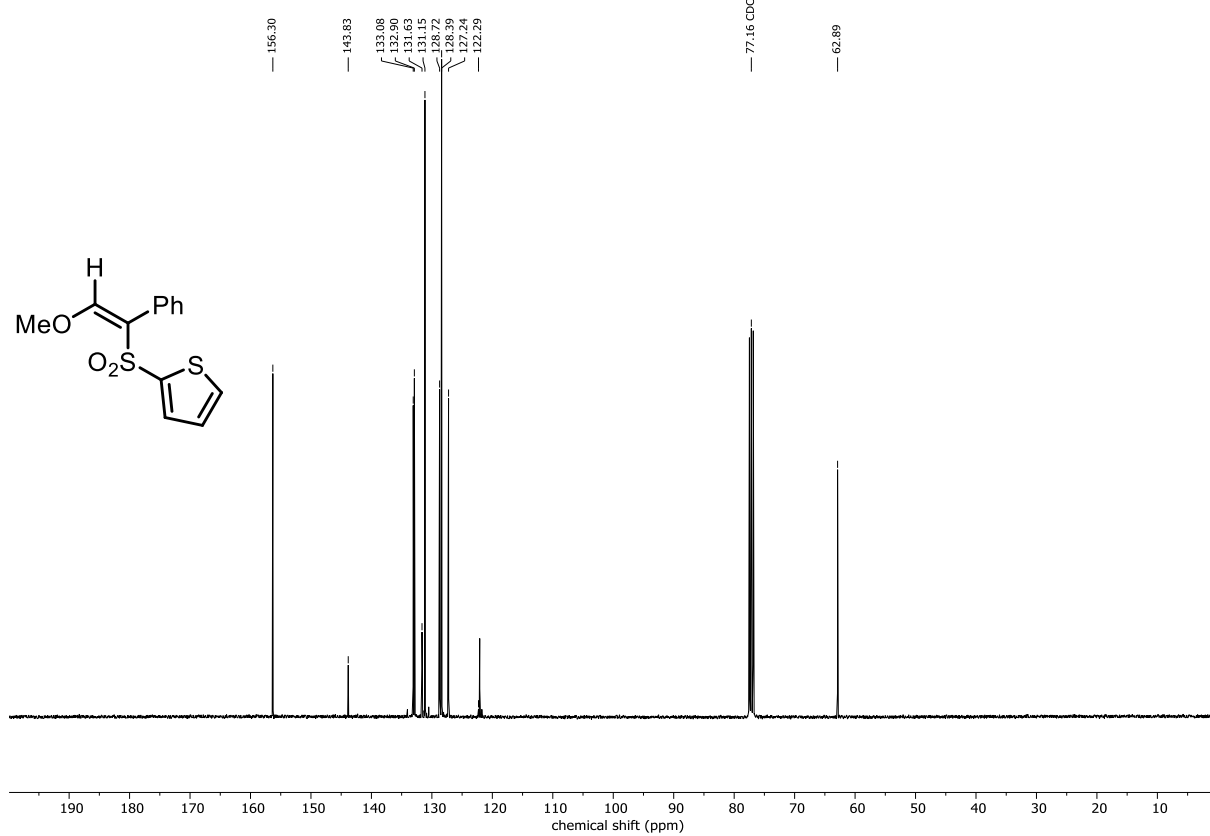
¹³C NMR (101 MHz, CDCl₃) of 70c



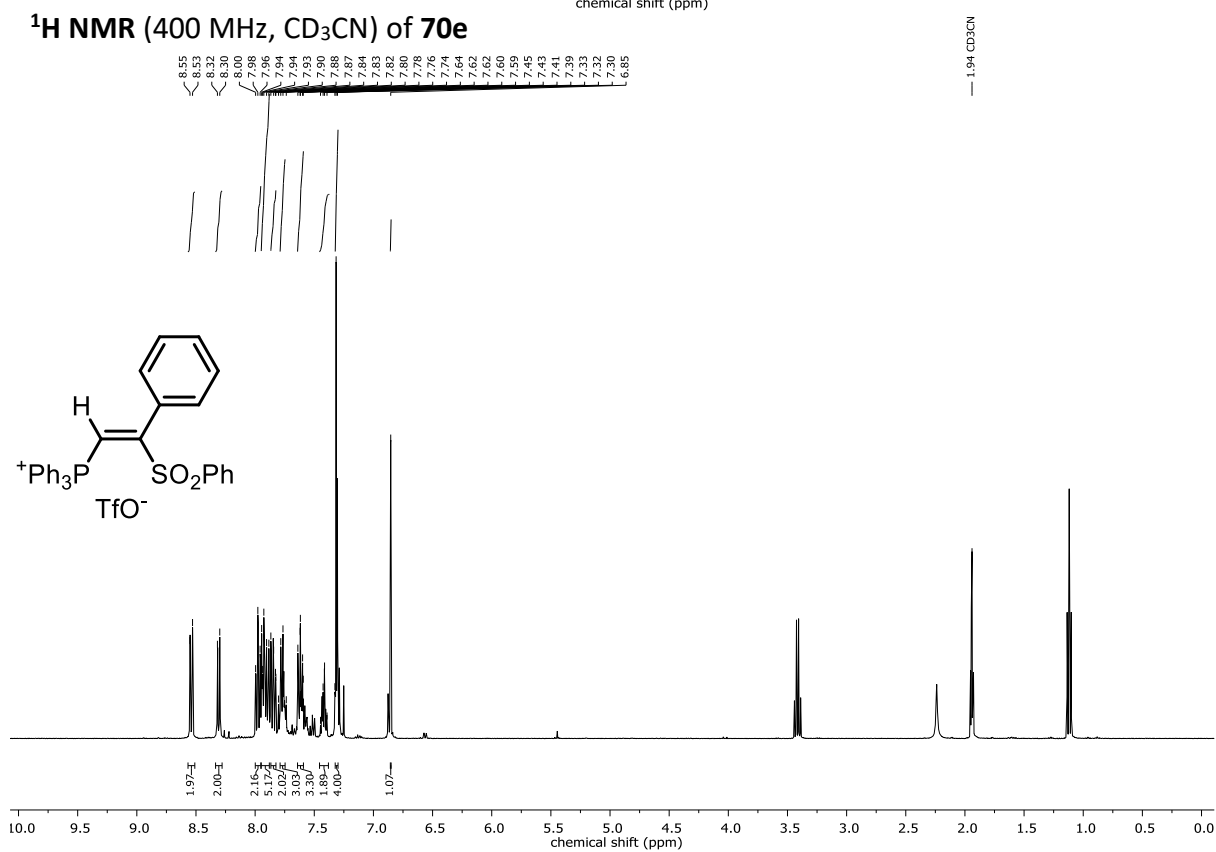
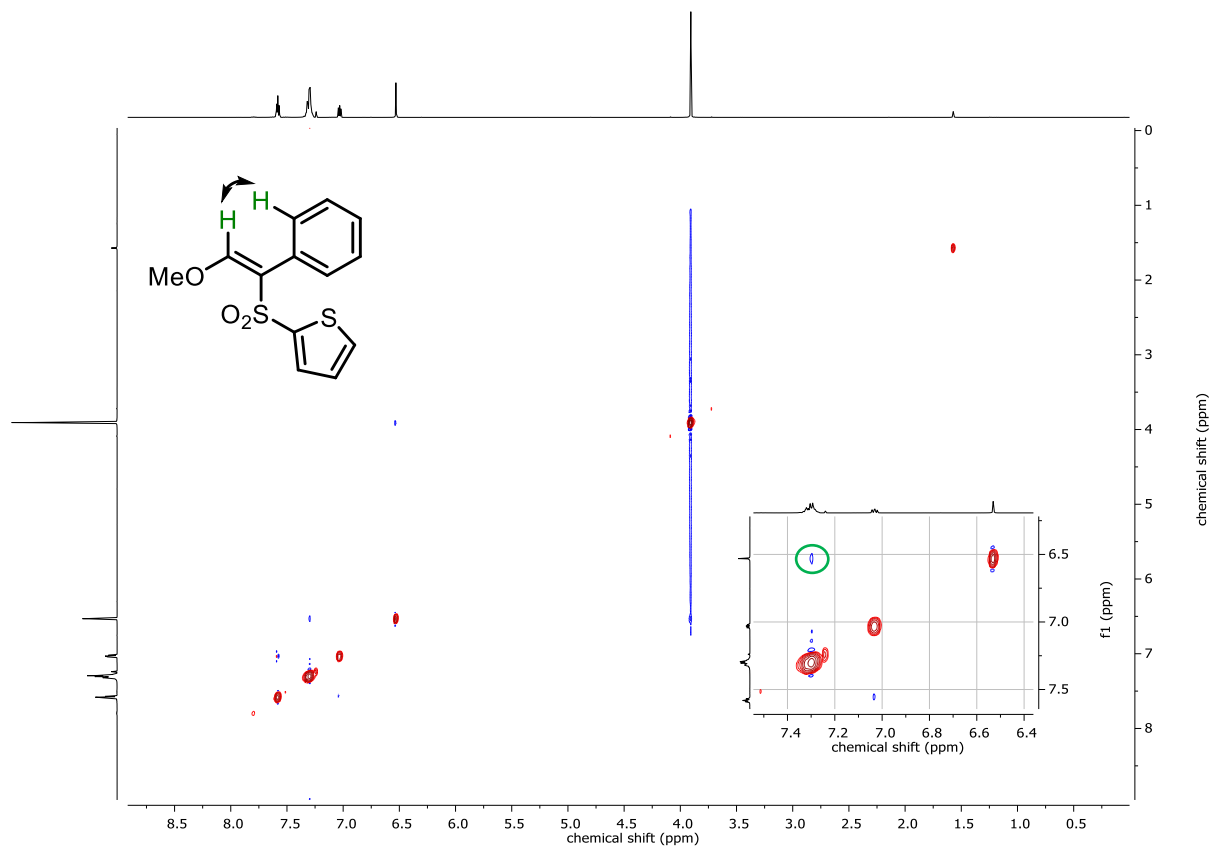
¹H NMR (400 MHz, CDCl₃) of 70d



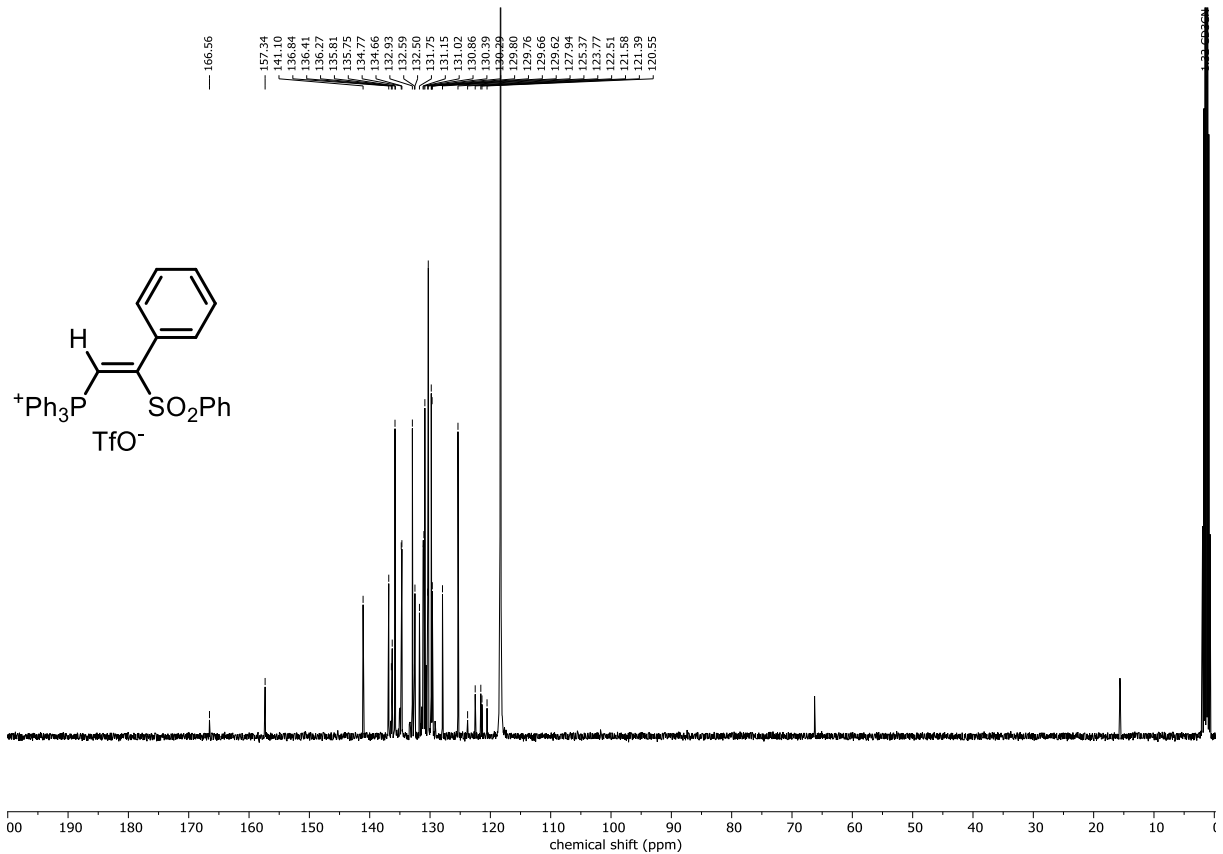
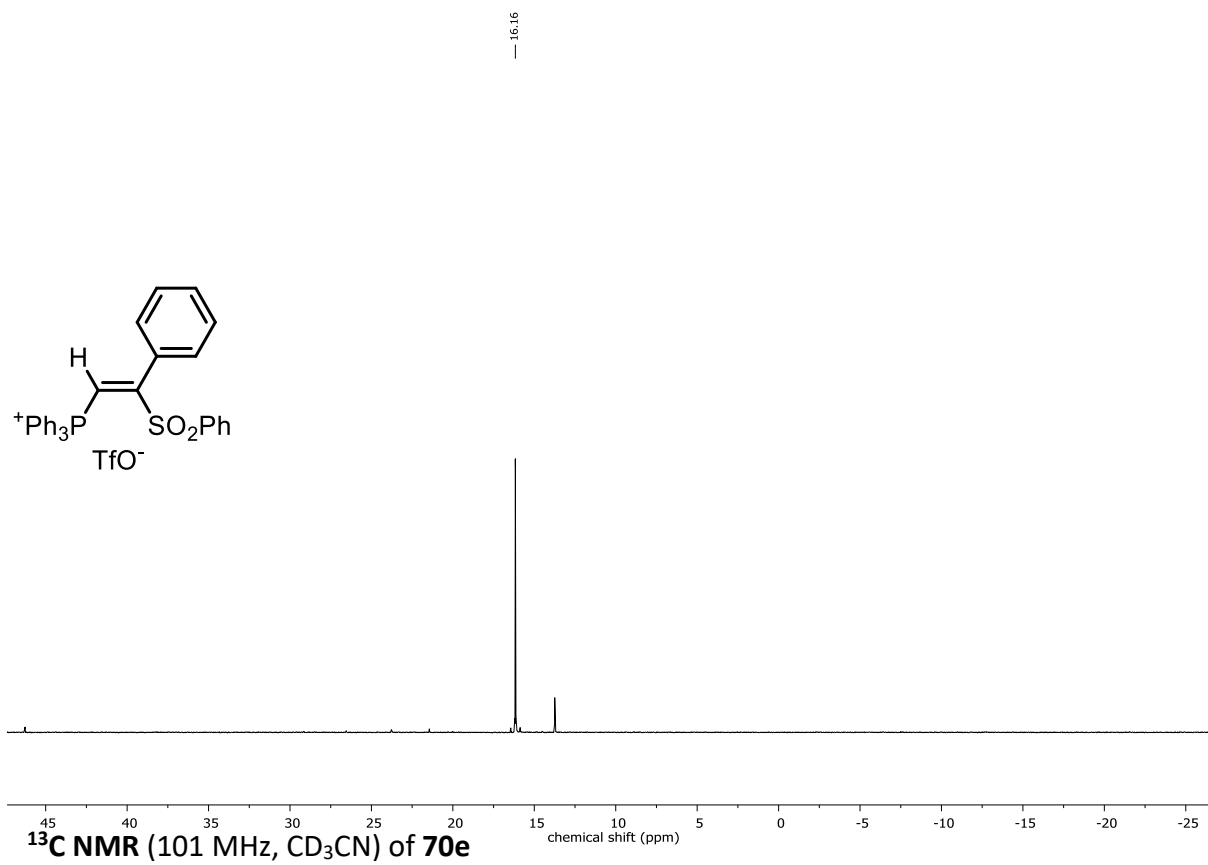
¹³C NMR (101 MHz, CDCl₃) of 70d



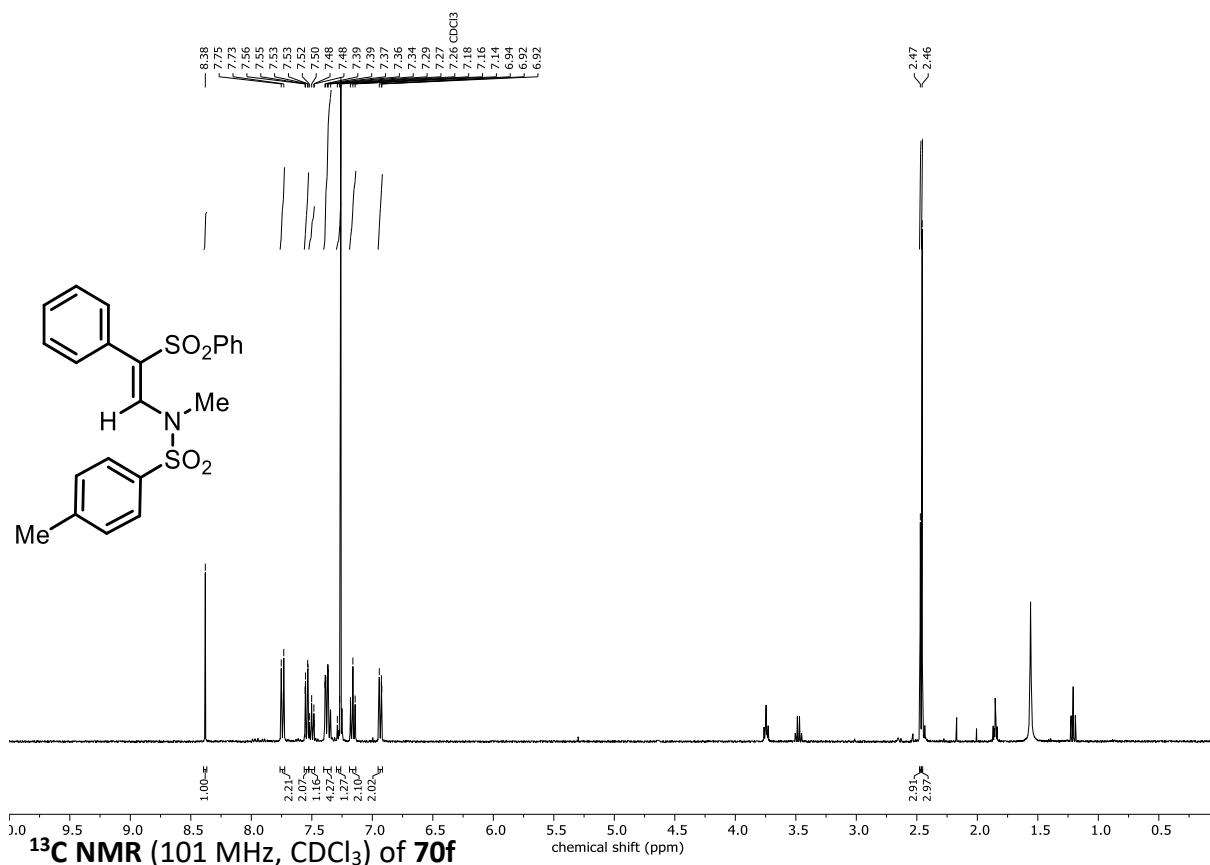
NOE-Experiment of 70d



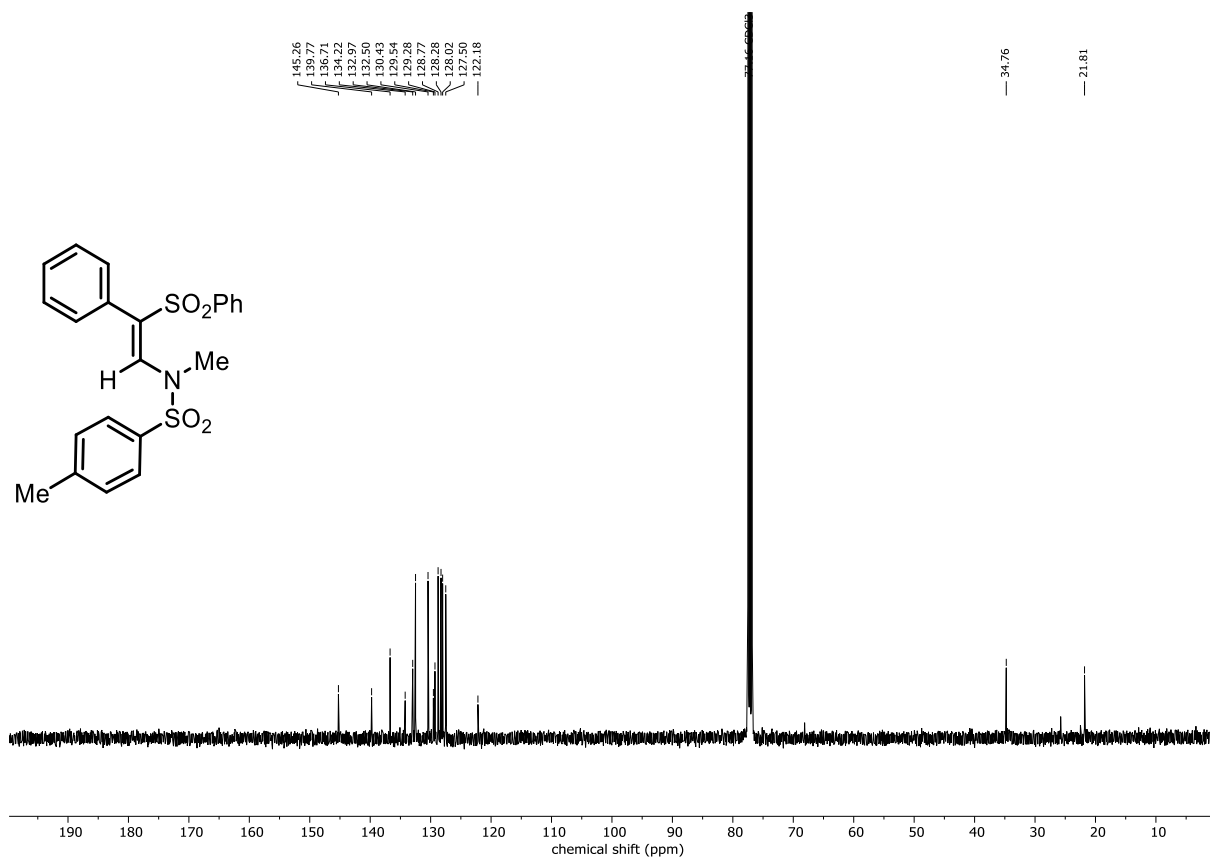
³¹P NMR (162 MHz, CD₃CN) of 70e



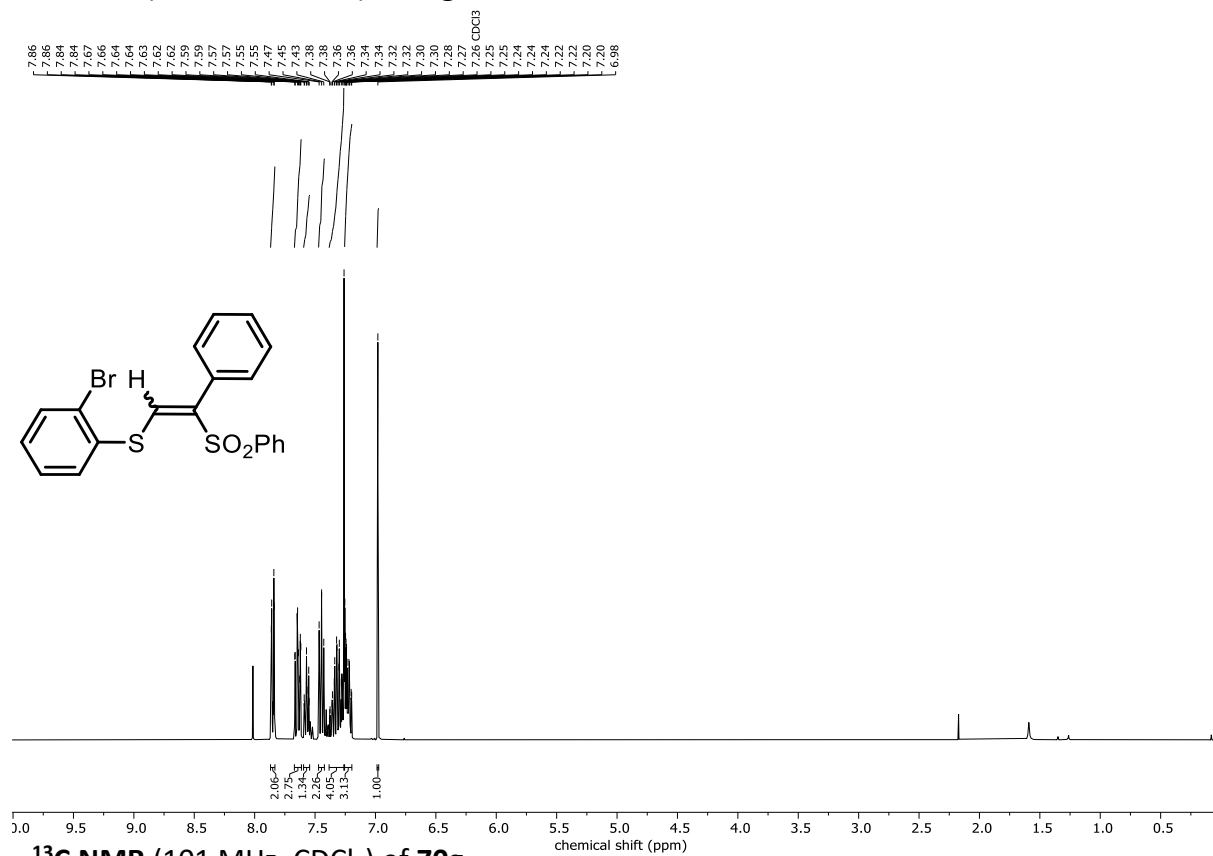
¹H NMR (400 MHz, CDCl₃) of **70f**



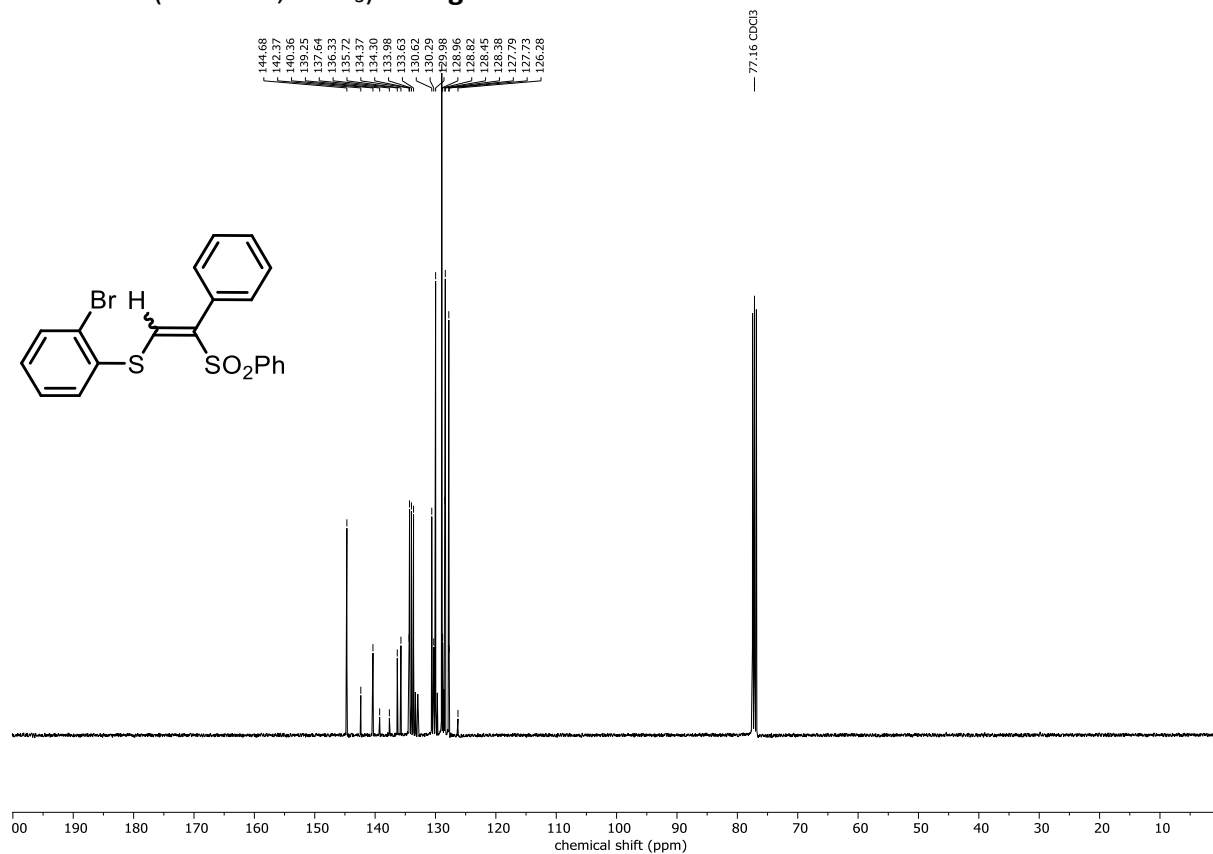
¹³C NMR (101 MHz, CDCl₃) of **70f**



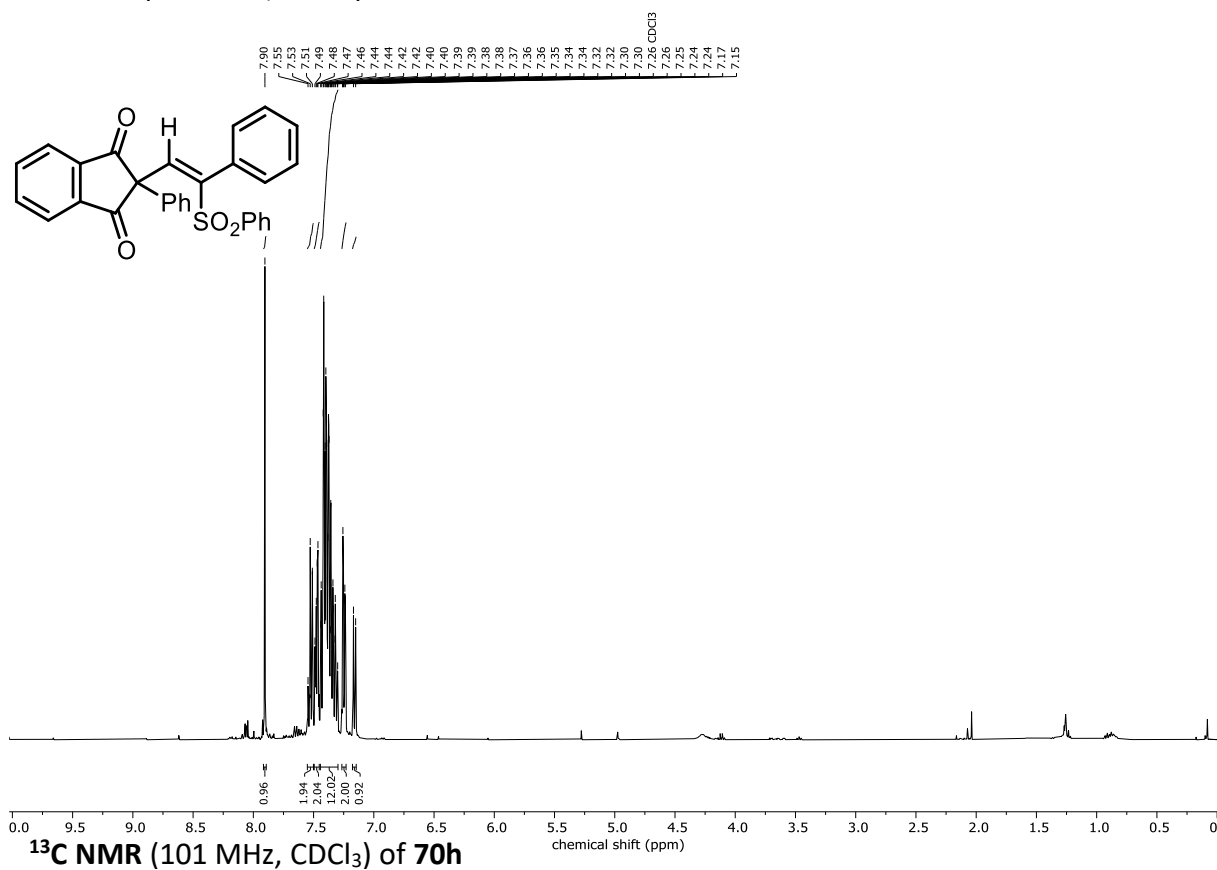
¹H NMR (400 MHz, CDCl₃) of 70g



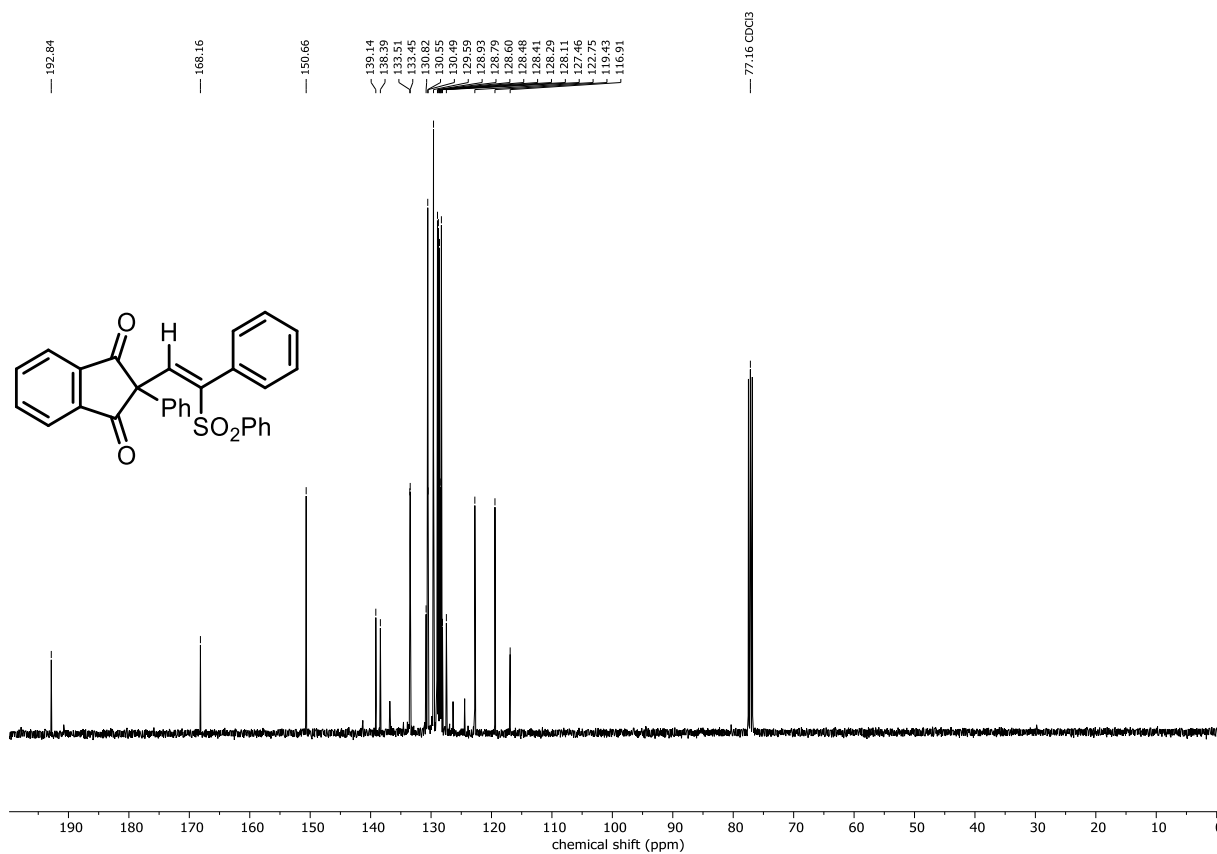
¹³C NMR (101 MHz, CDCl₃) of 70g



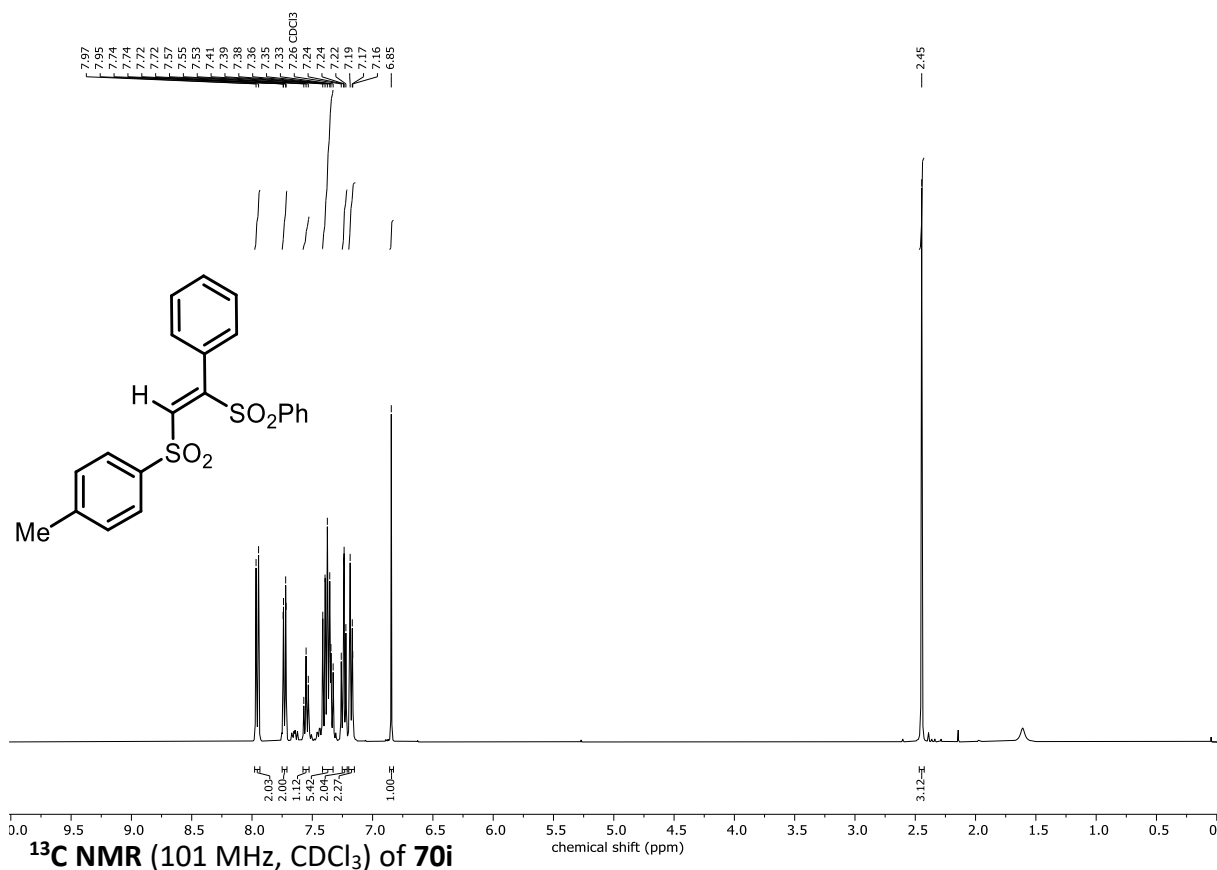
¹H NMR (400 MHz, CDCl₃) of 70h



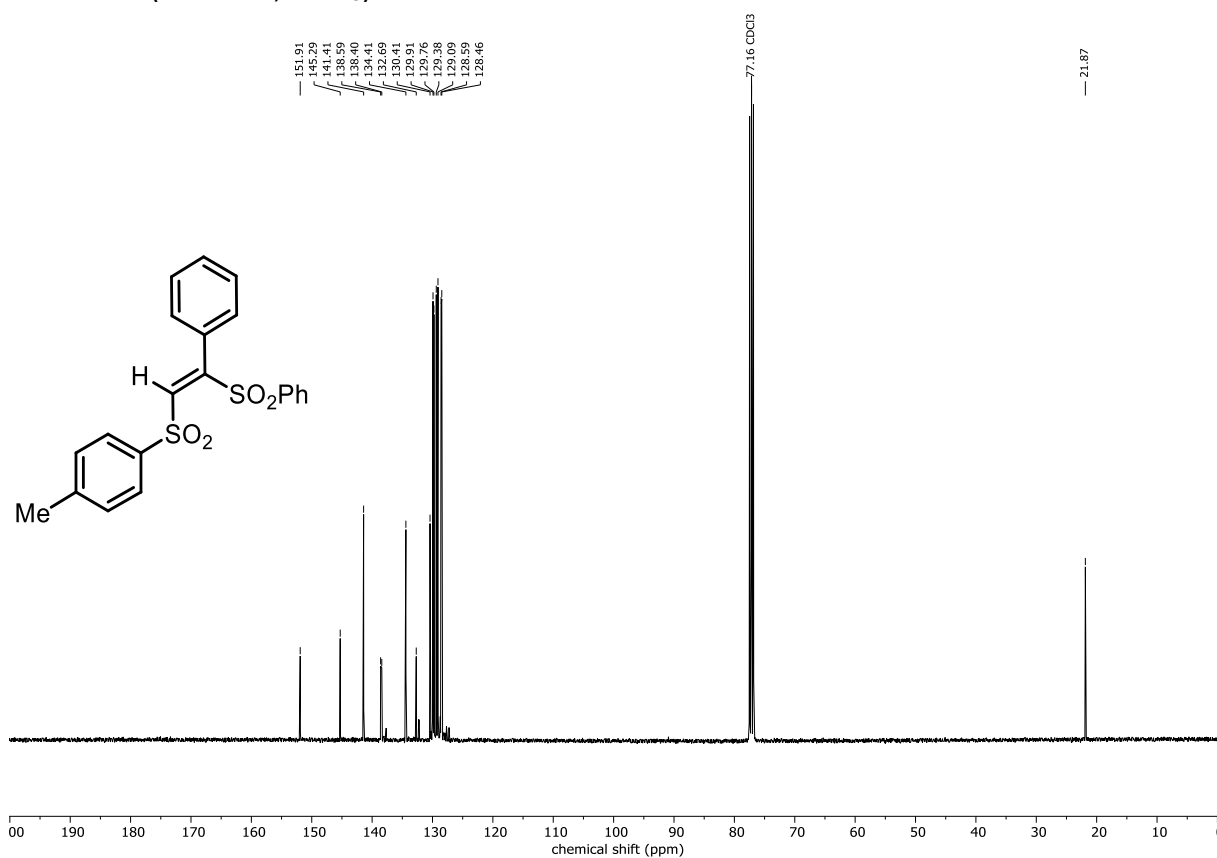
¹³C NMR (101 MHz, CDCl₃) of 70h



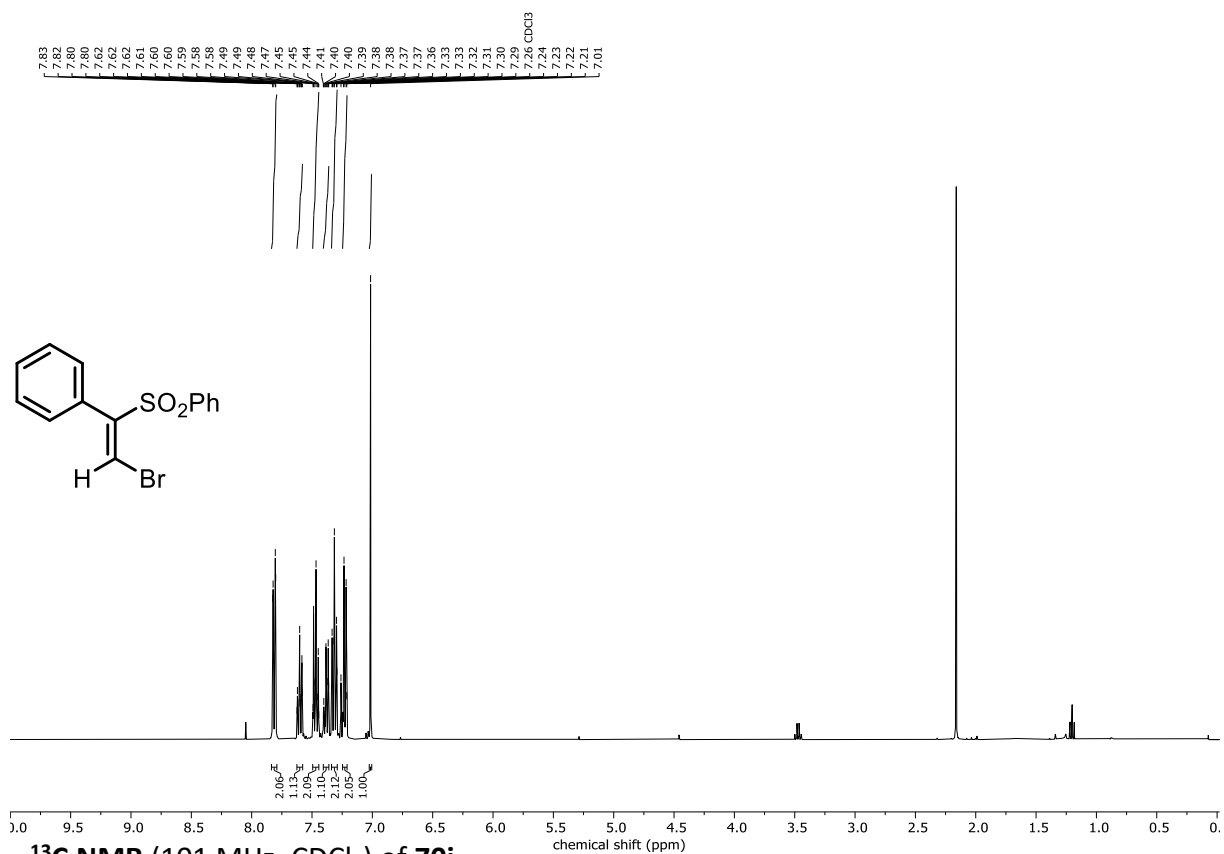
¹H NMR (400 MHz, CDCl₃) of 70i



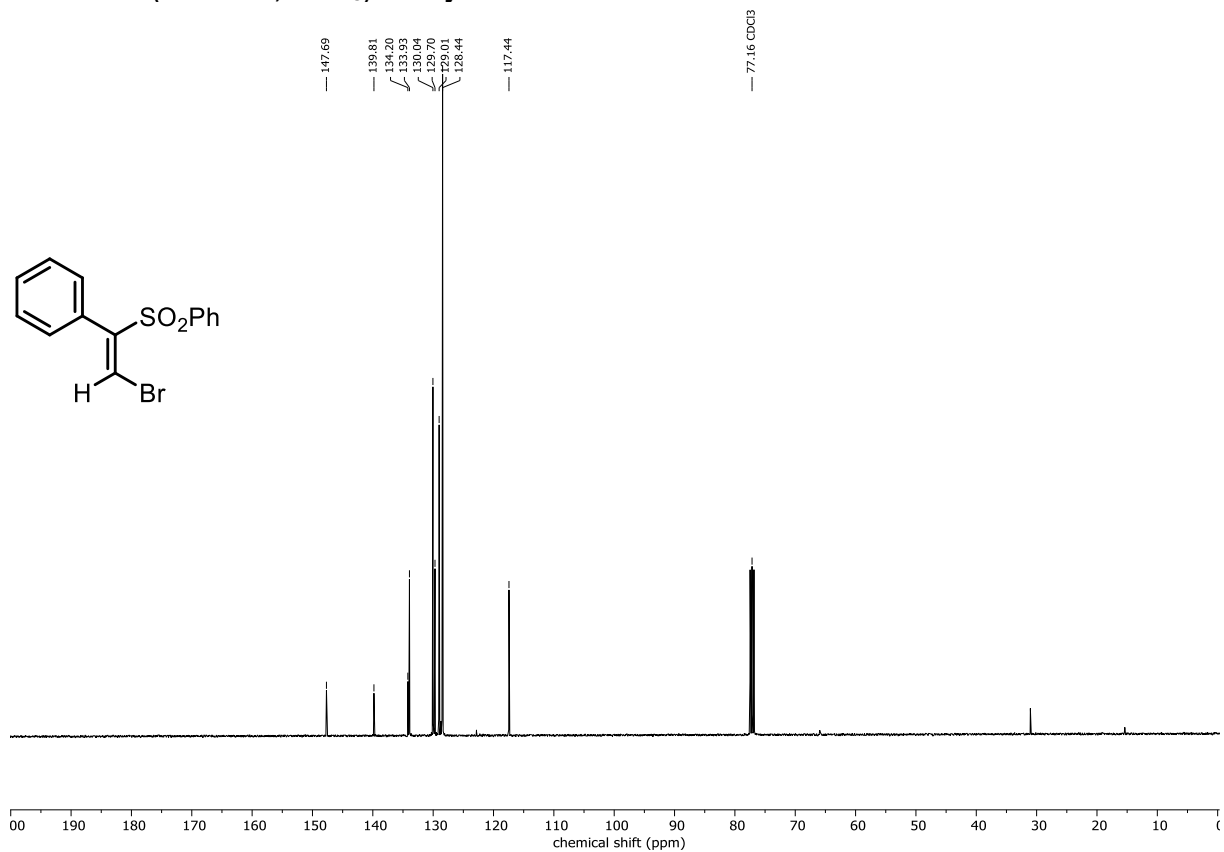
¹³C NMR (101 MHz, CDCl₃) of 70i



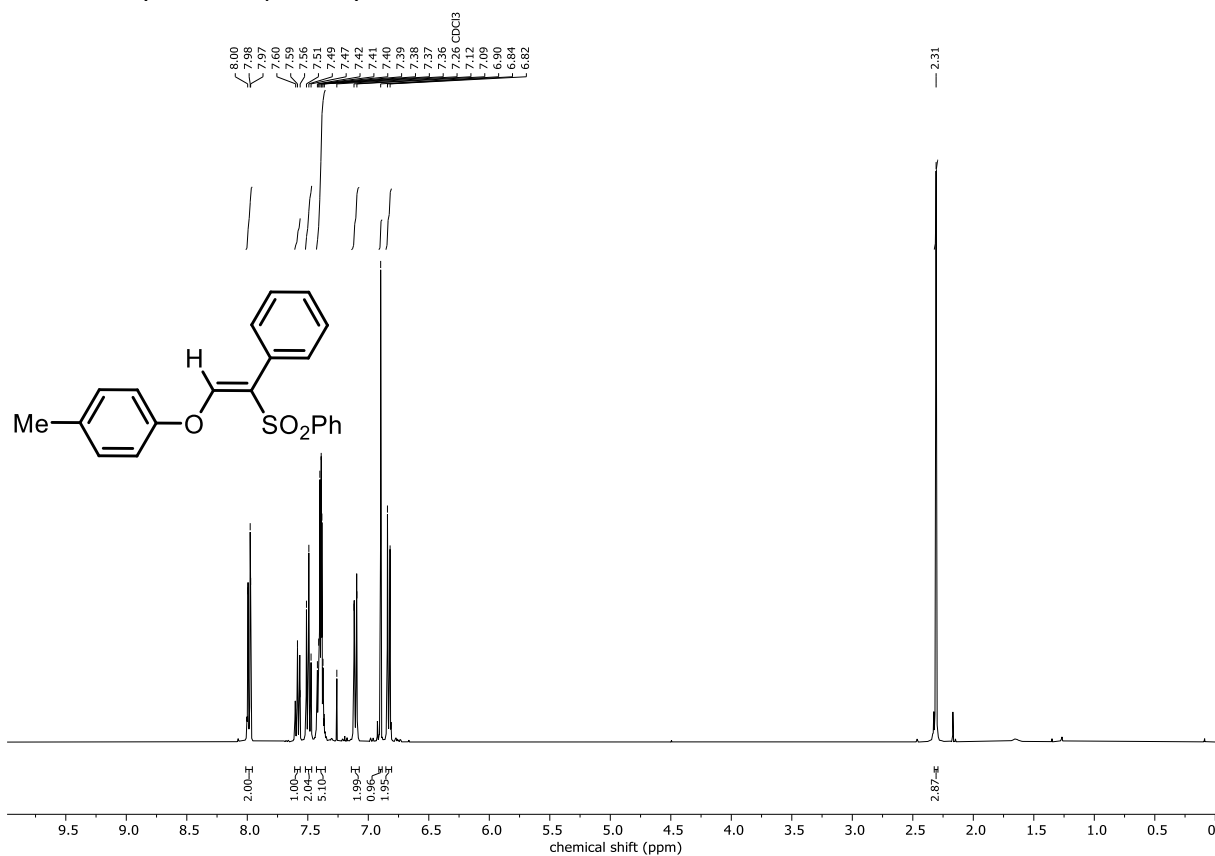
¹H NMR (400 MHz, CDCl₃) of 70j



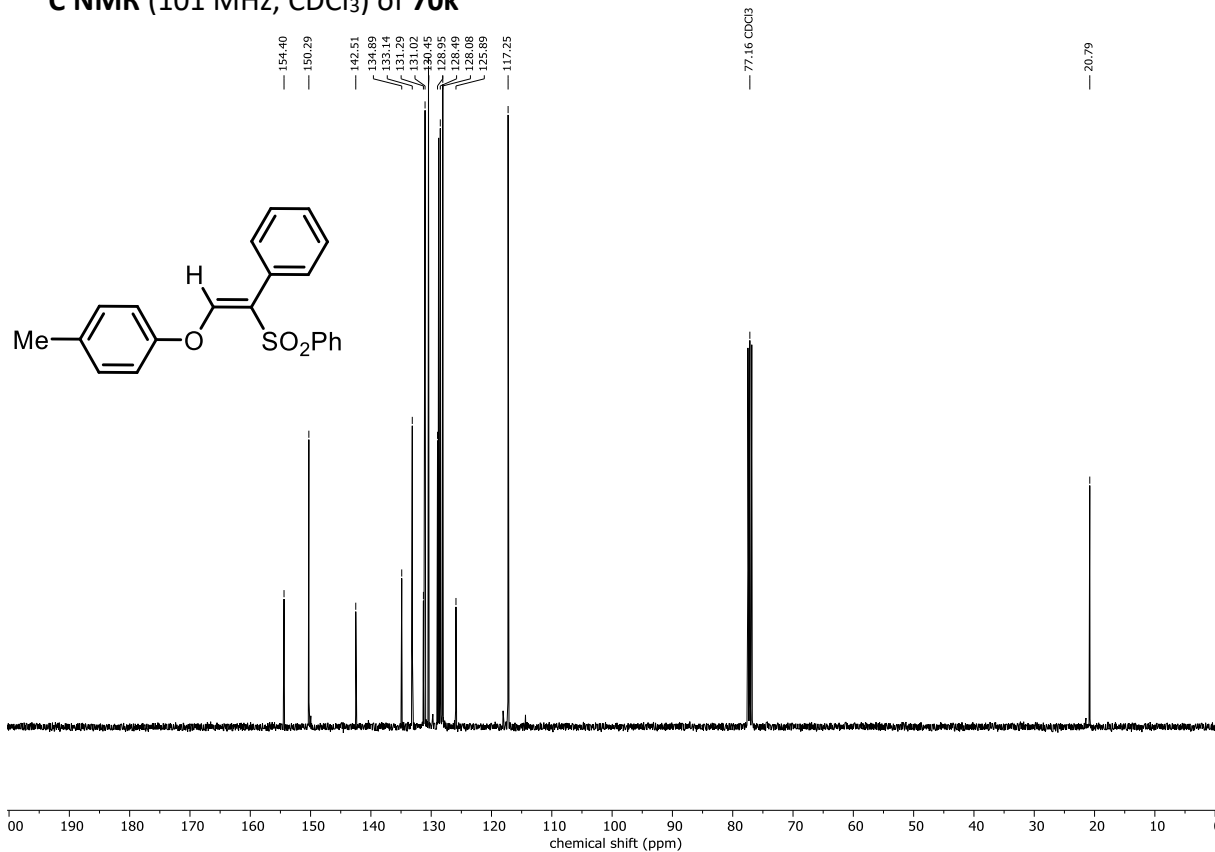
¹³C NMR (101 MHz, CDCl₃) of 70j



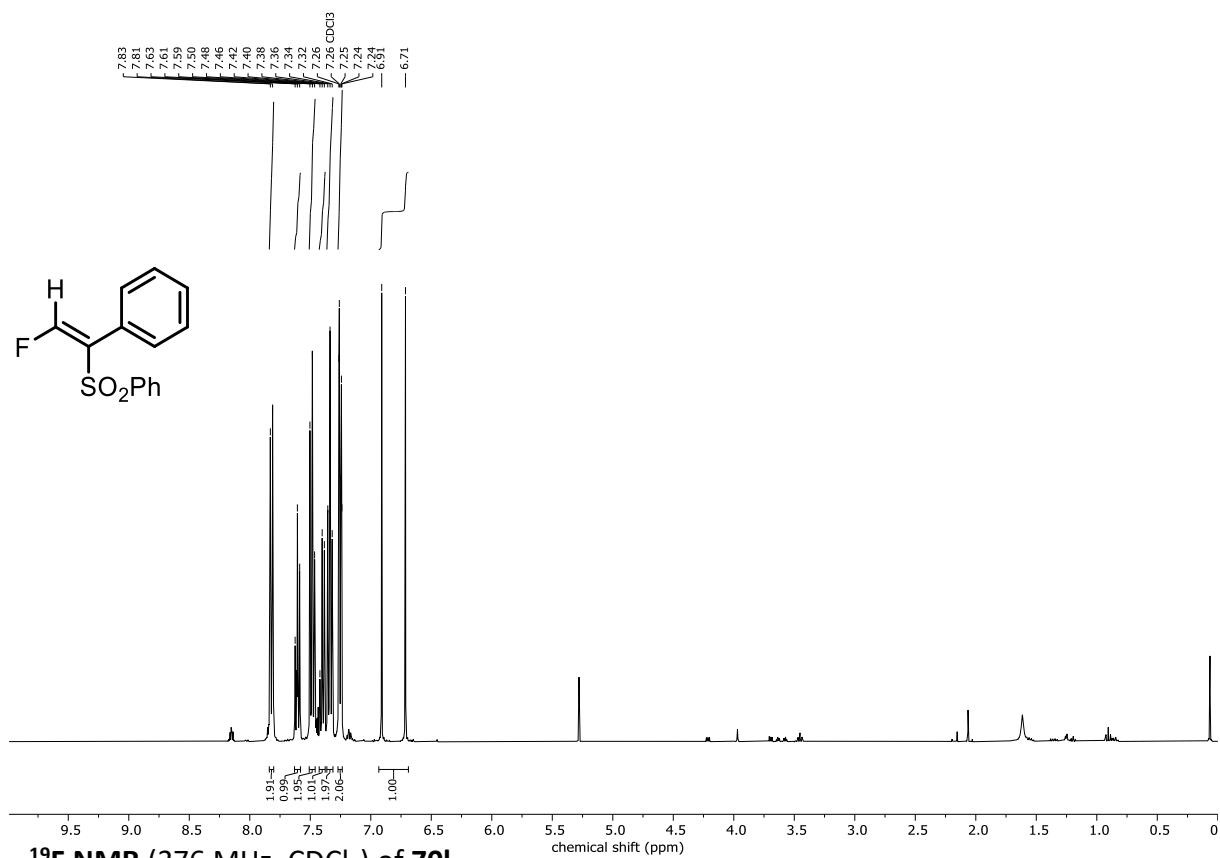
¹H NMR (400 MHz, CDCl₃) of 70k



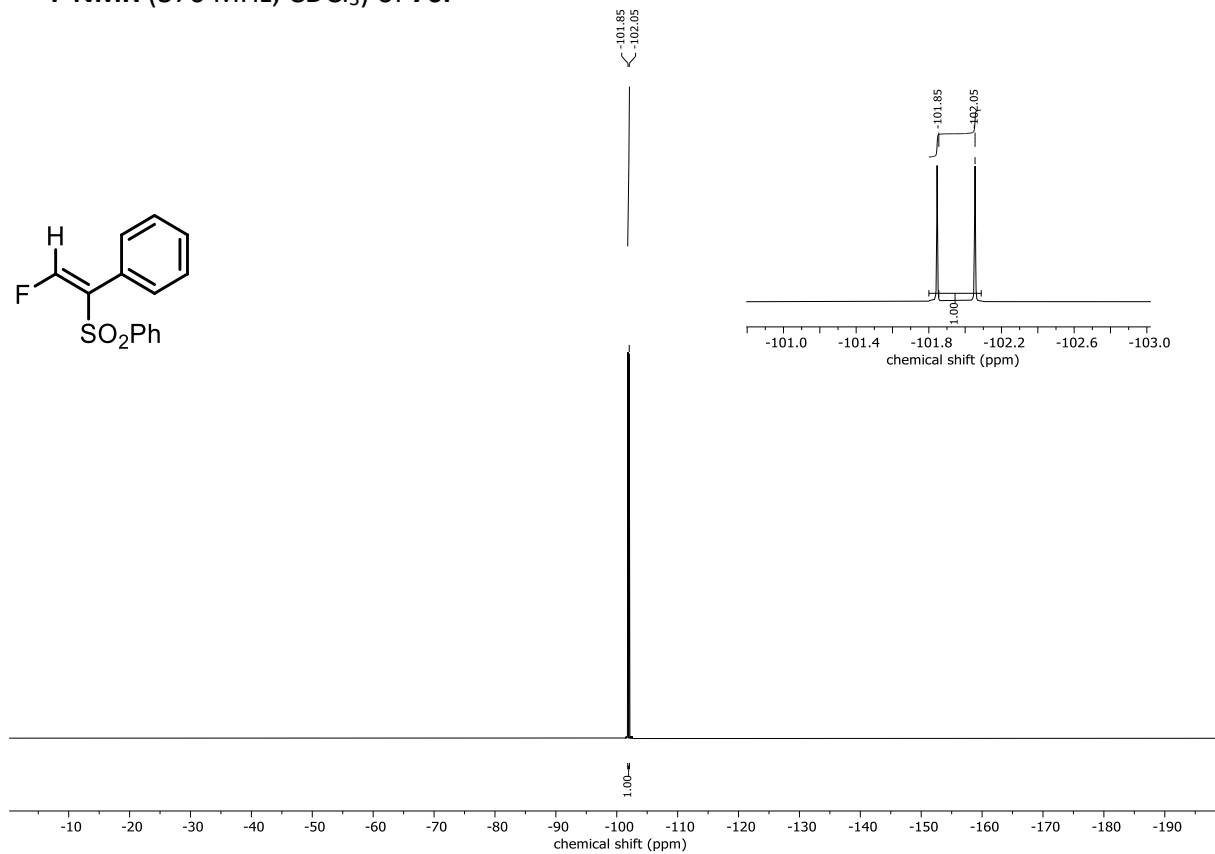
¹³C NMR (101 MHz, CDCl₃) of 70k



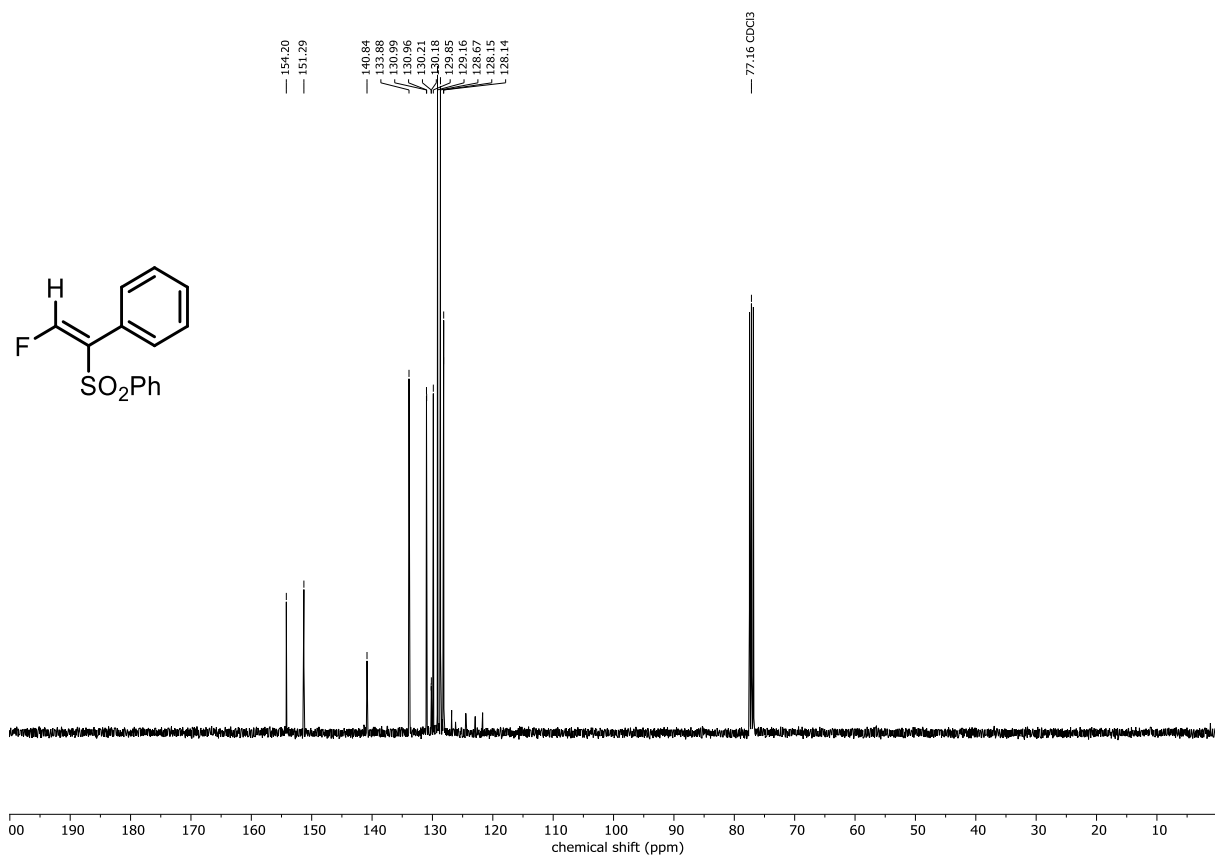
¹H NMR (400 MHz, CDCl₃) of 70I



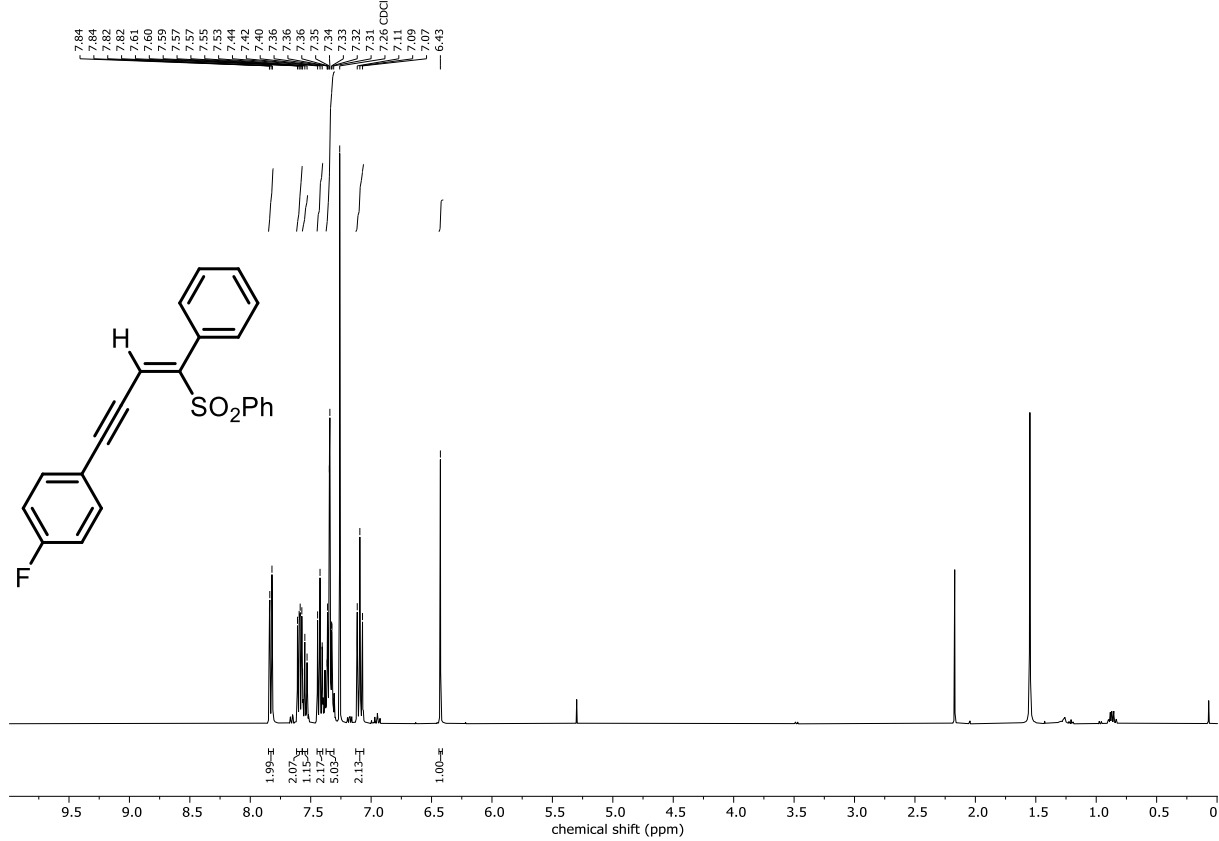
¹⁹F NMR (376 MHz, CDCl₃) of 70I



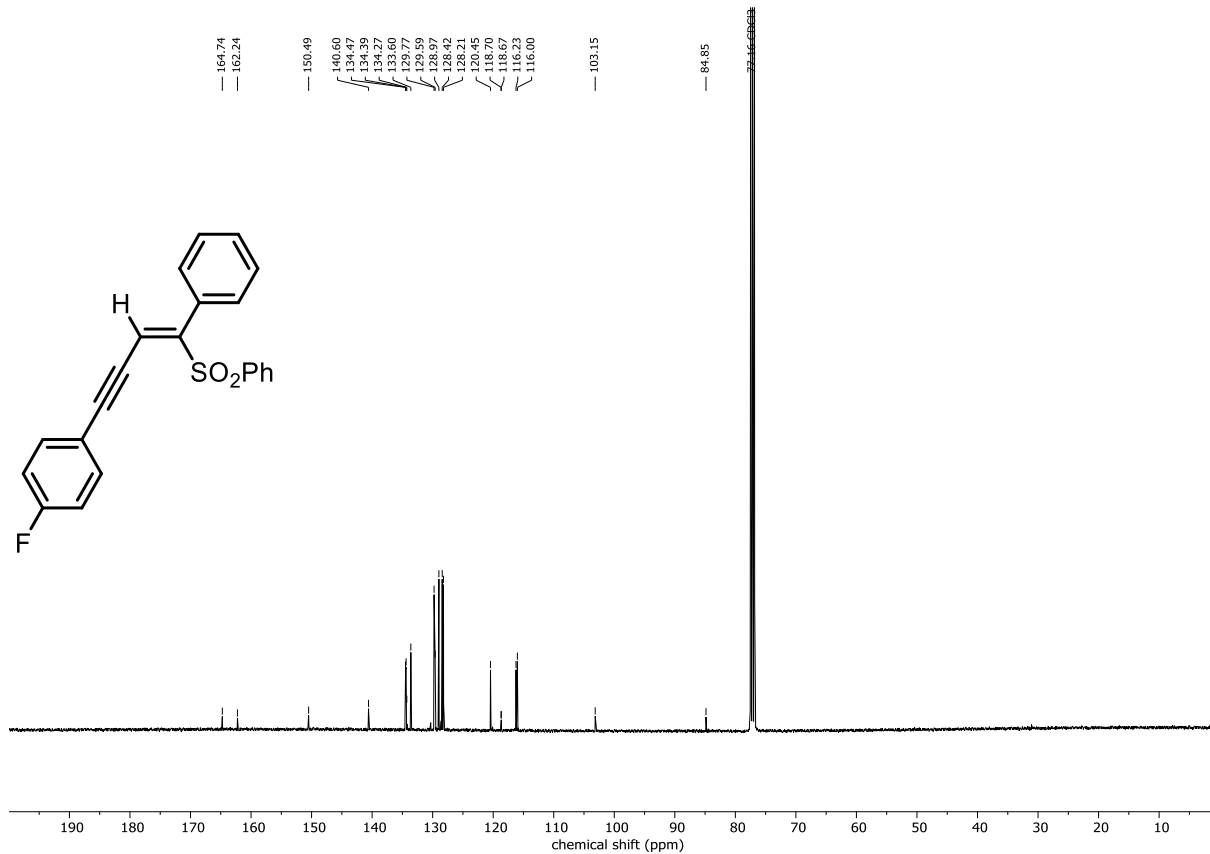
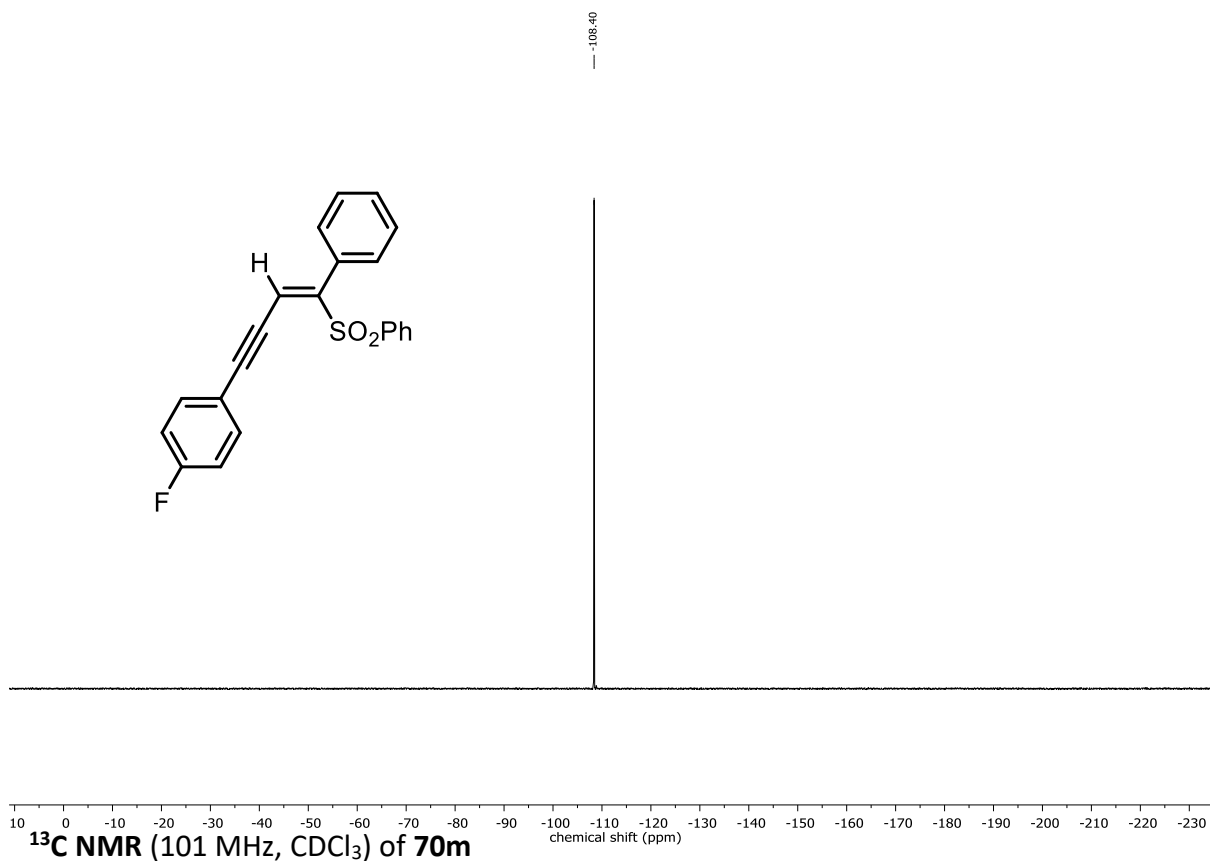
¹³C NMR (101 MHz, CDCl₃) of 70l



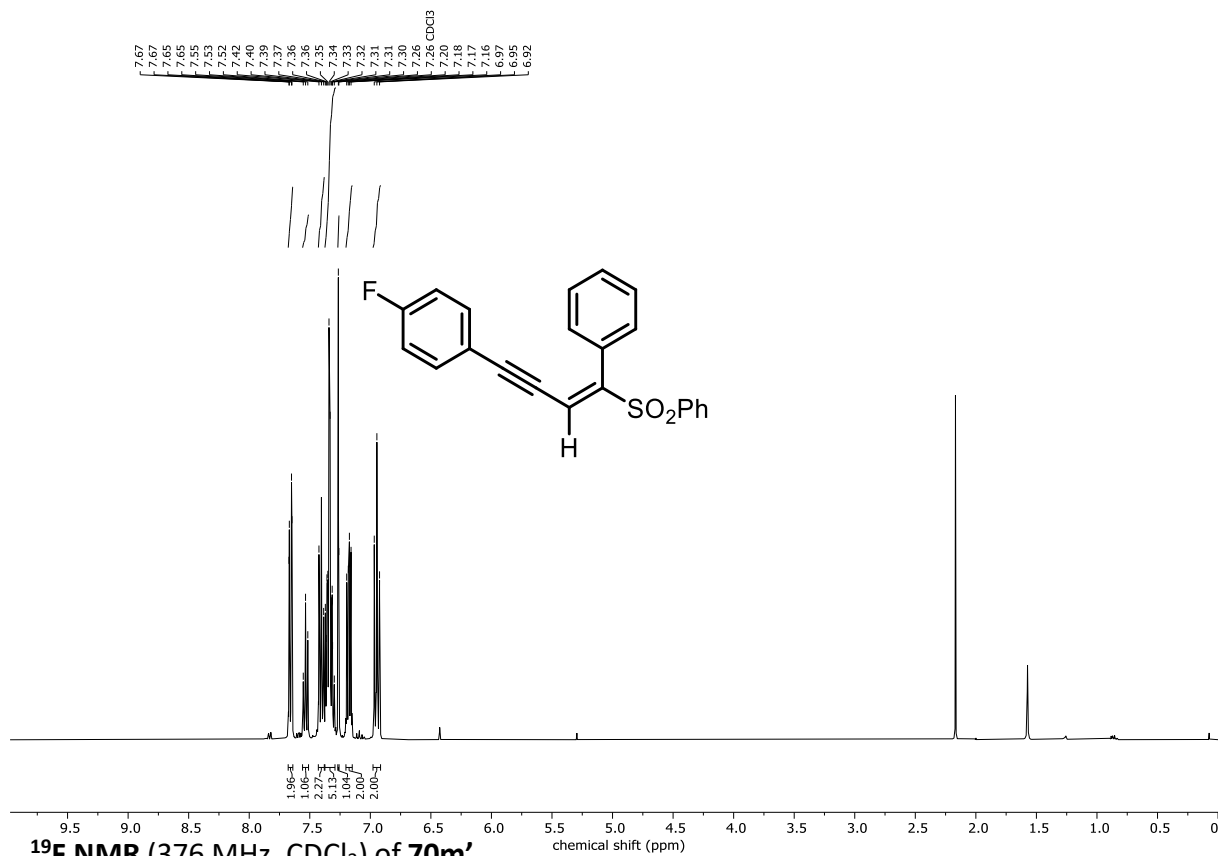
¹H NMR (400 MHz, CDCl₃) of 70m



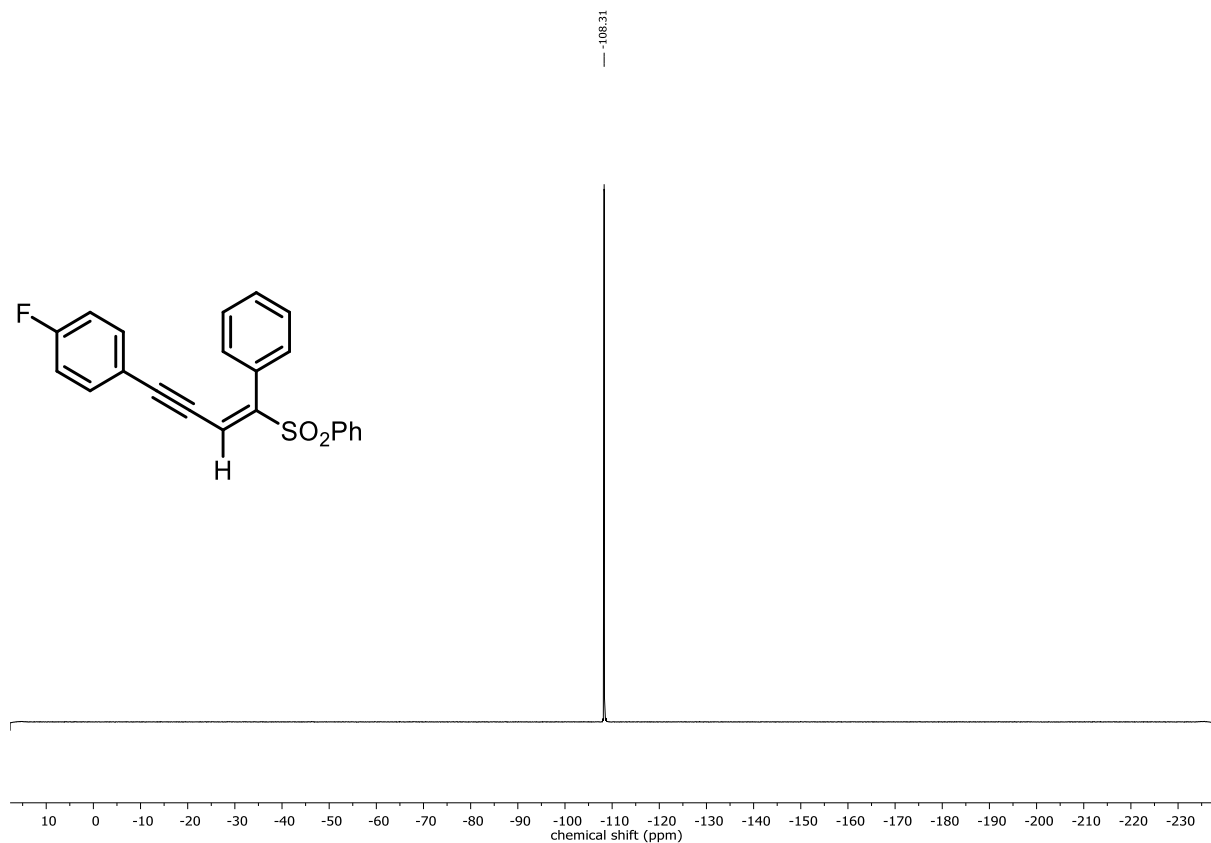
¹⁹F NMR (376 MHz, CDCl₃) of 70m



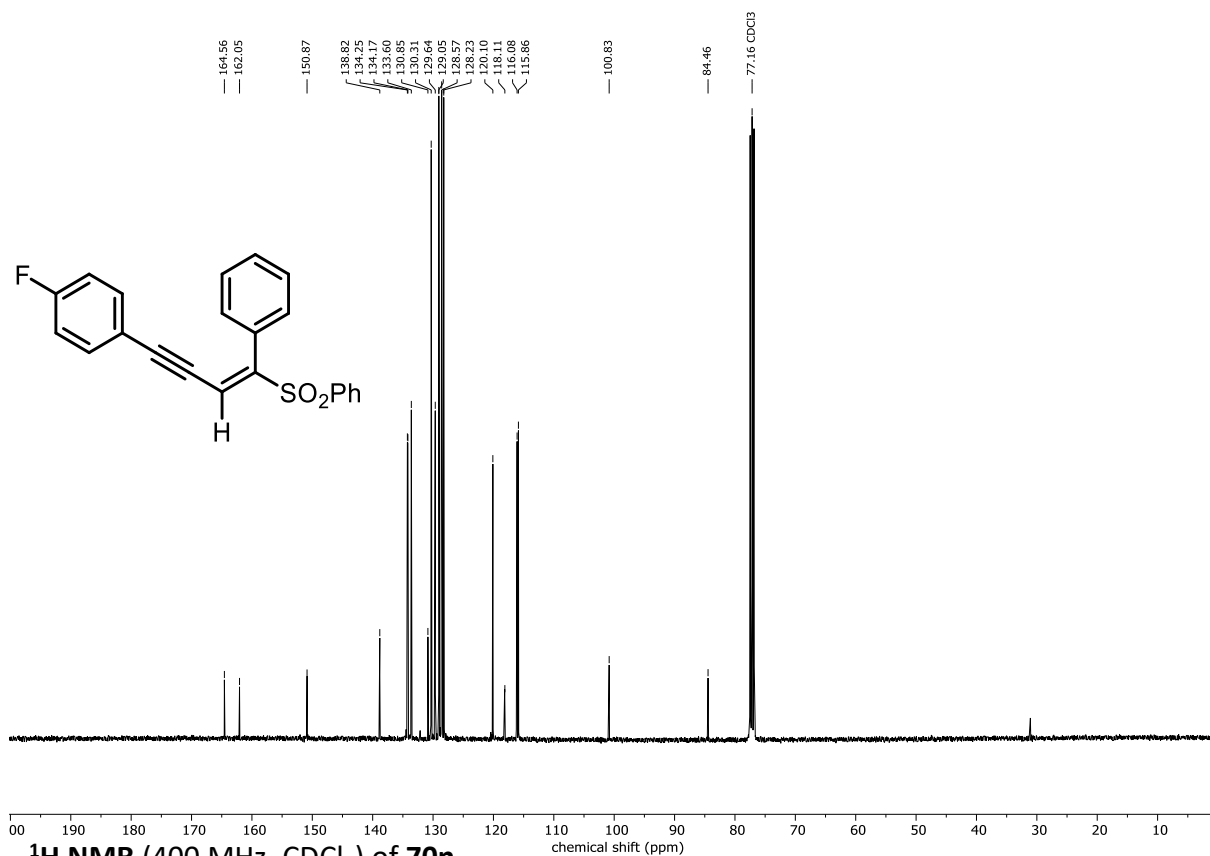
^1H NMR (400 MHz, CDCl_3) of 70m'



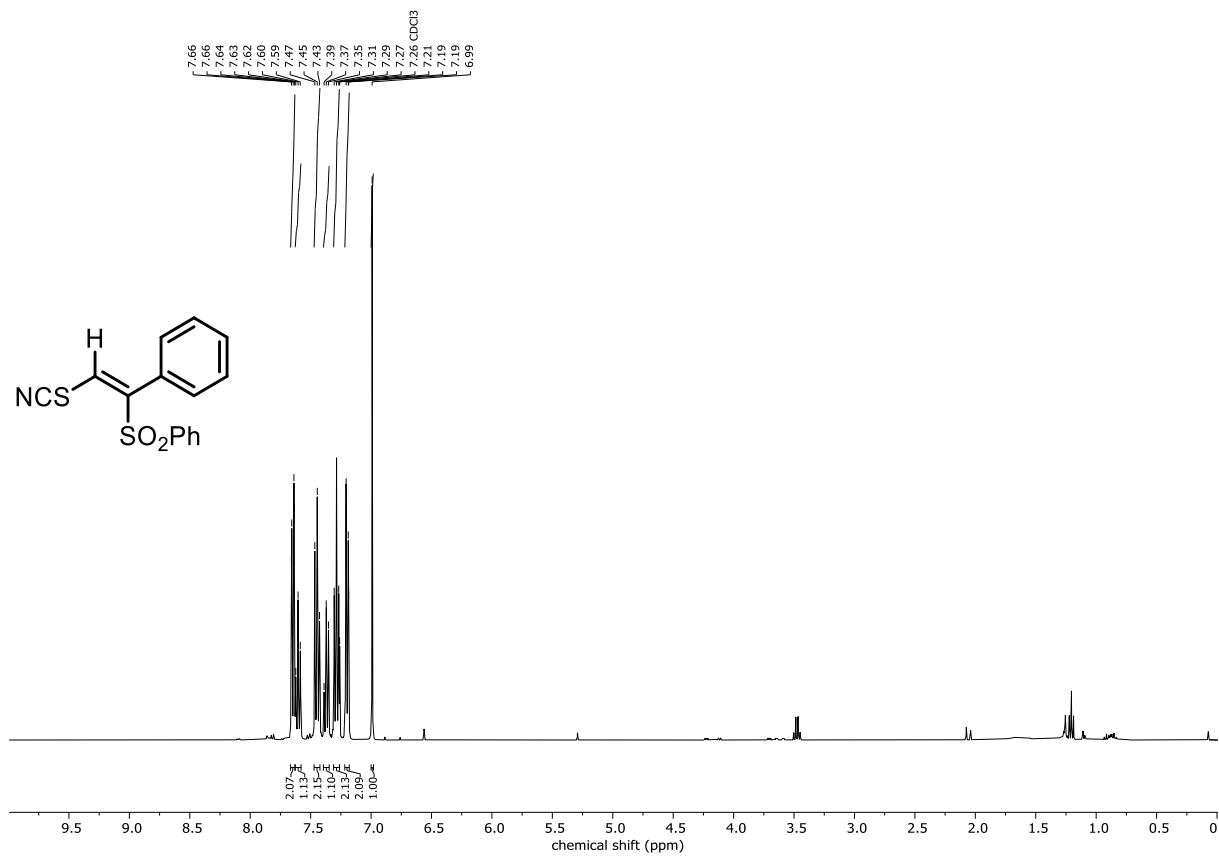
^{19}F NMR (376 MHz, CDCl_3) of 70m'



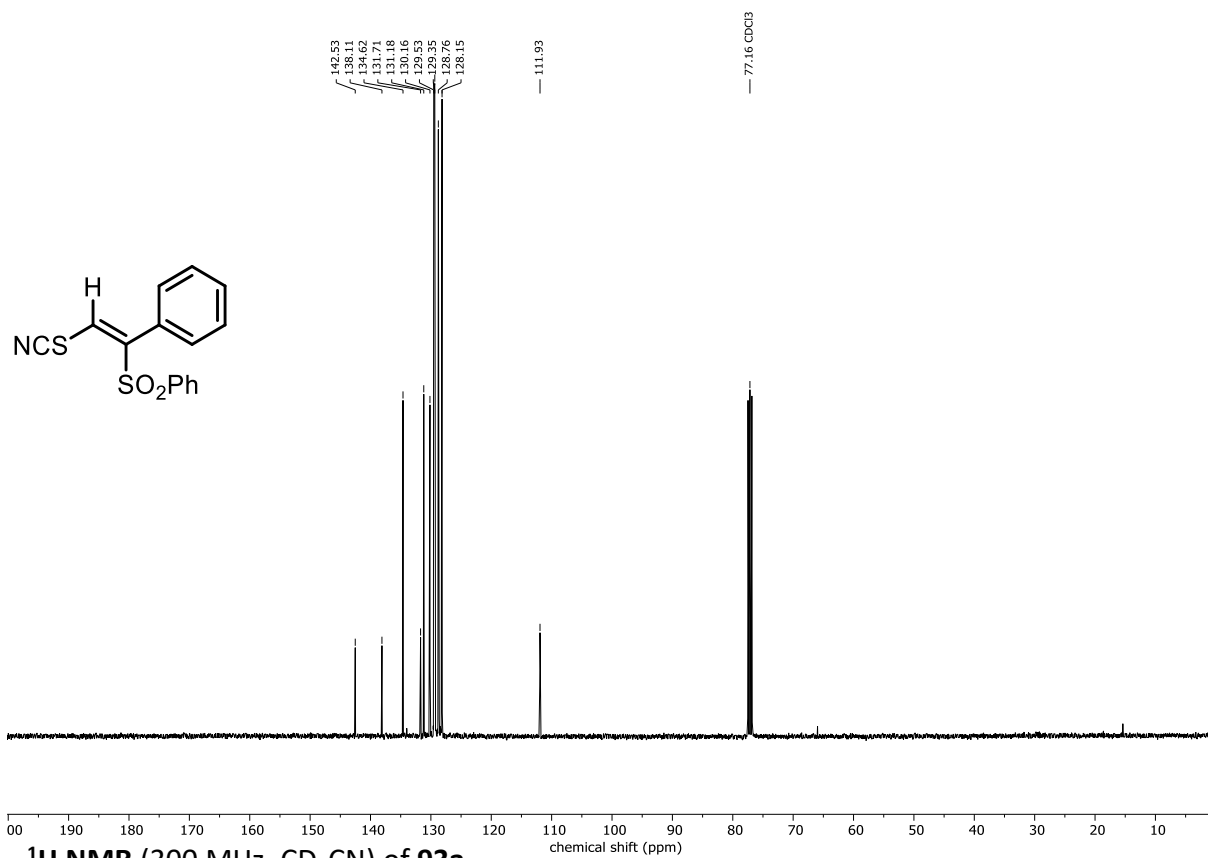
¹³C NMR (101 MHz, CDCl₃) of 70m'



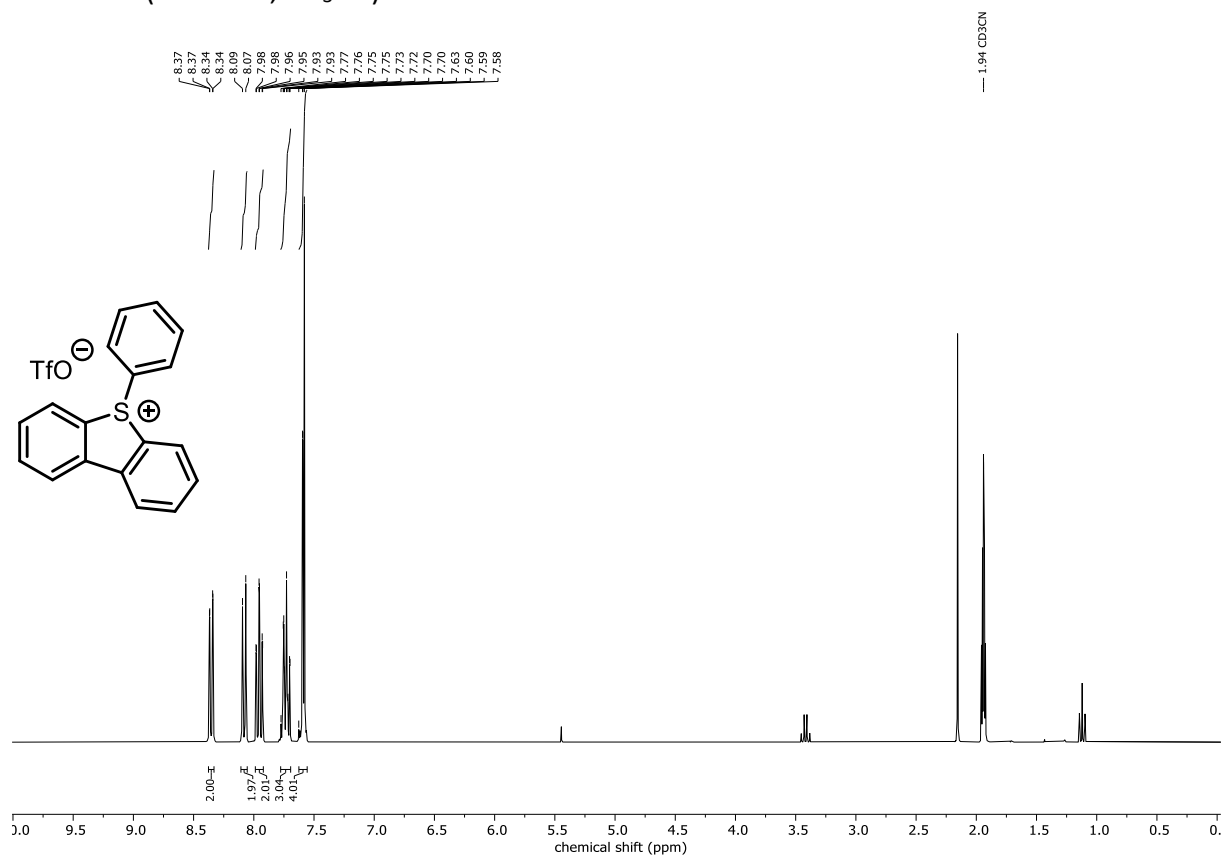
¹H NMR (400 MHz, CDCl₃) of 70n



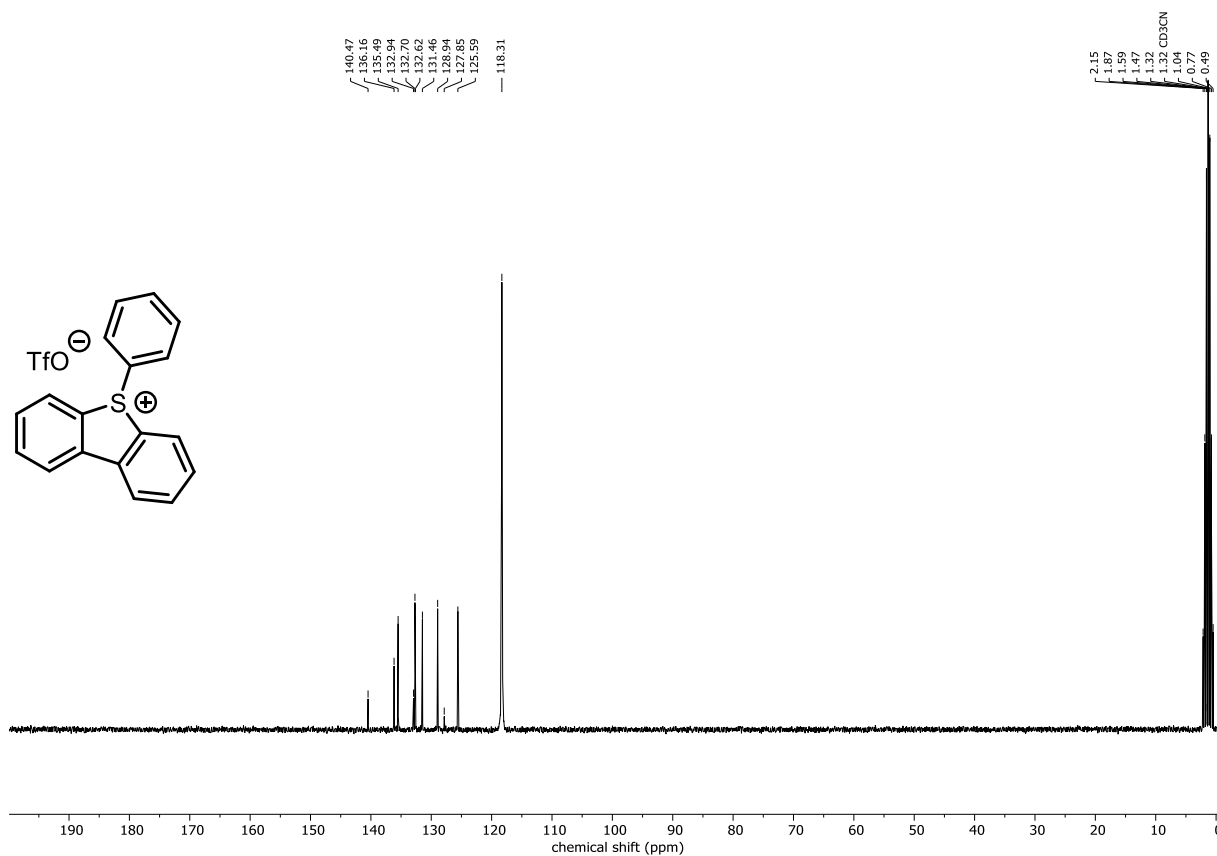
¹³C NMR (101 MHz, CDCl₃) of 70n



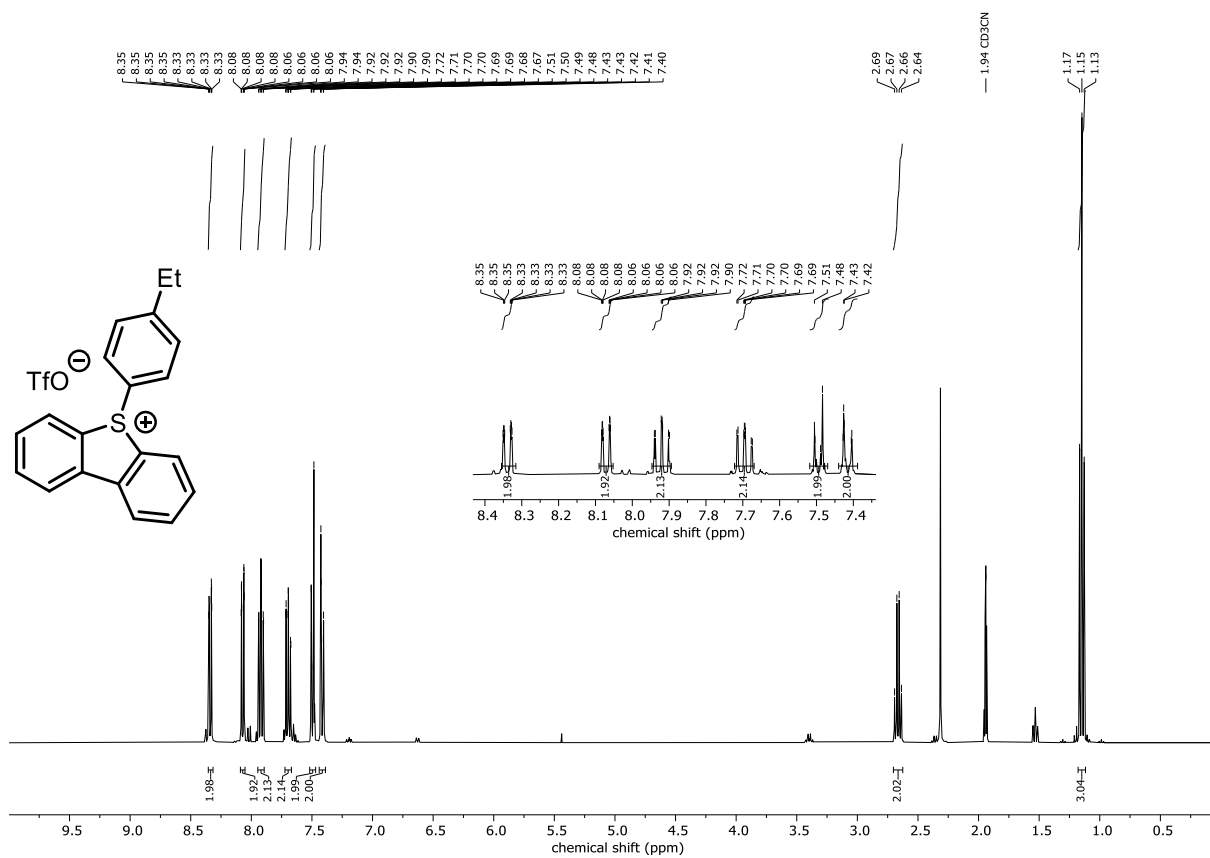
¹H NMR (300 MHz, CD₃CN) of 93a



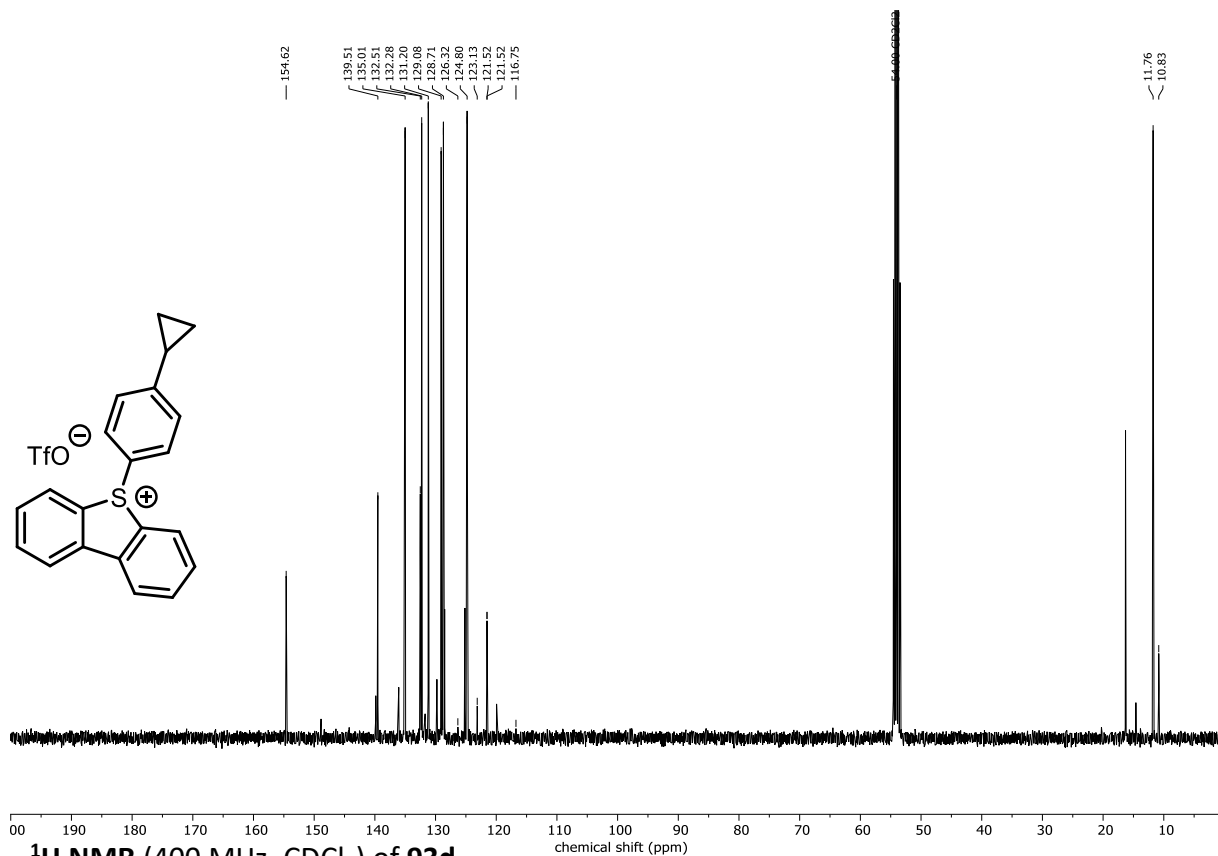
¹³C NMR (75 MHz, CD₃CN) of 93a



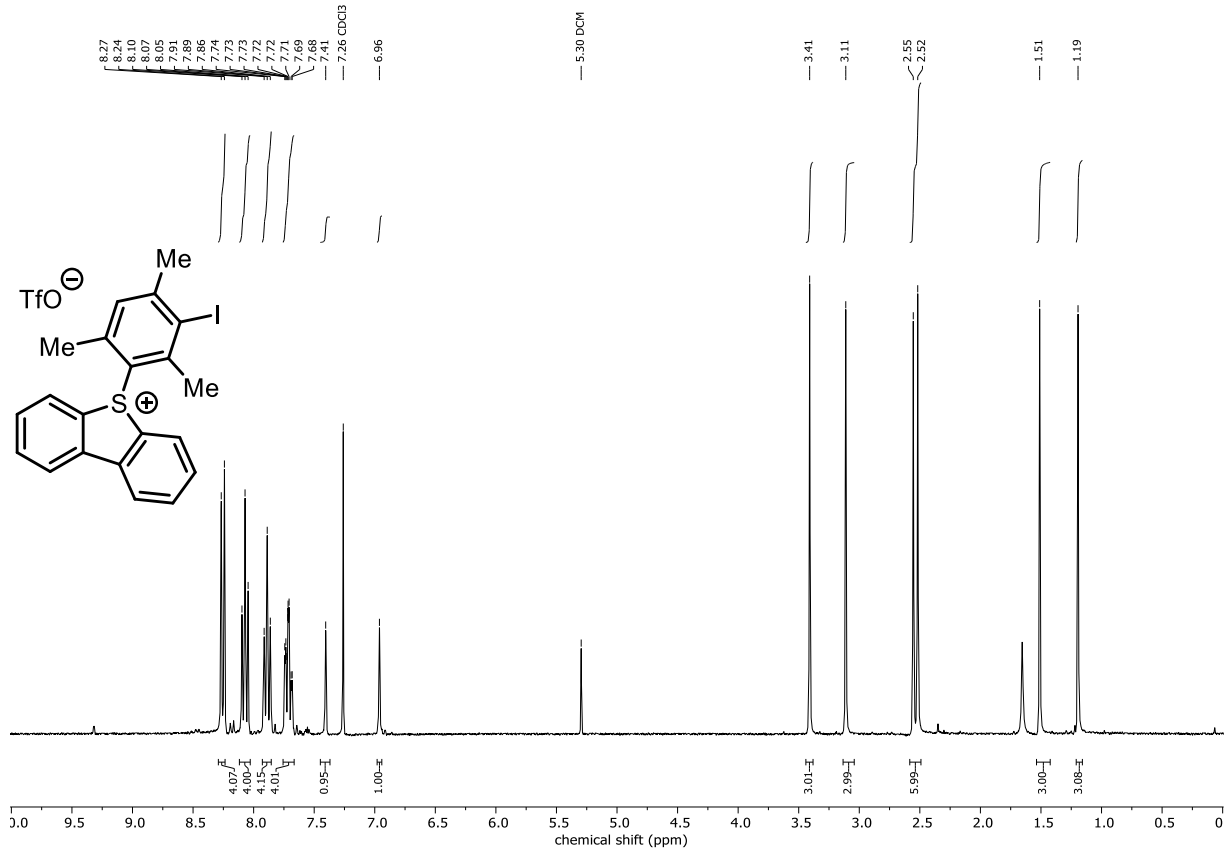
¹H NMR (400 MHz, CD₃CN) of 93b



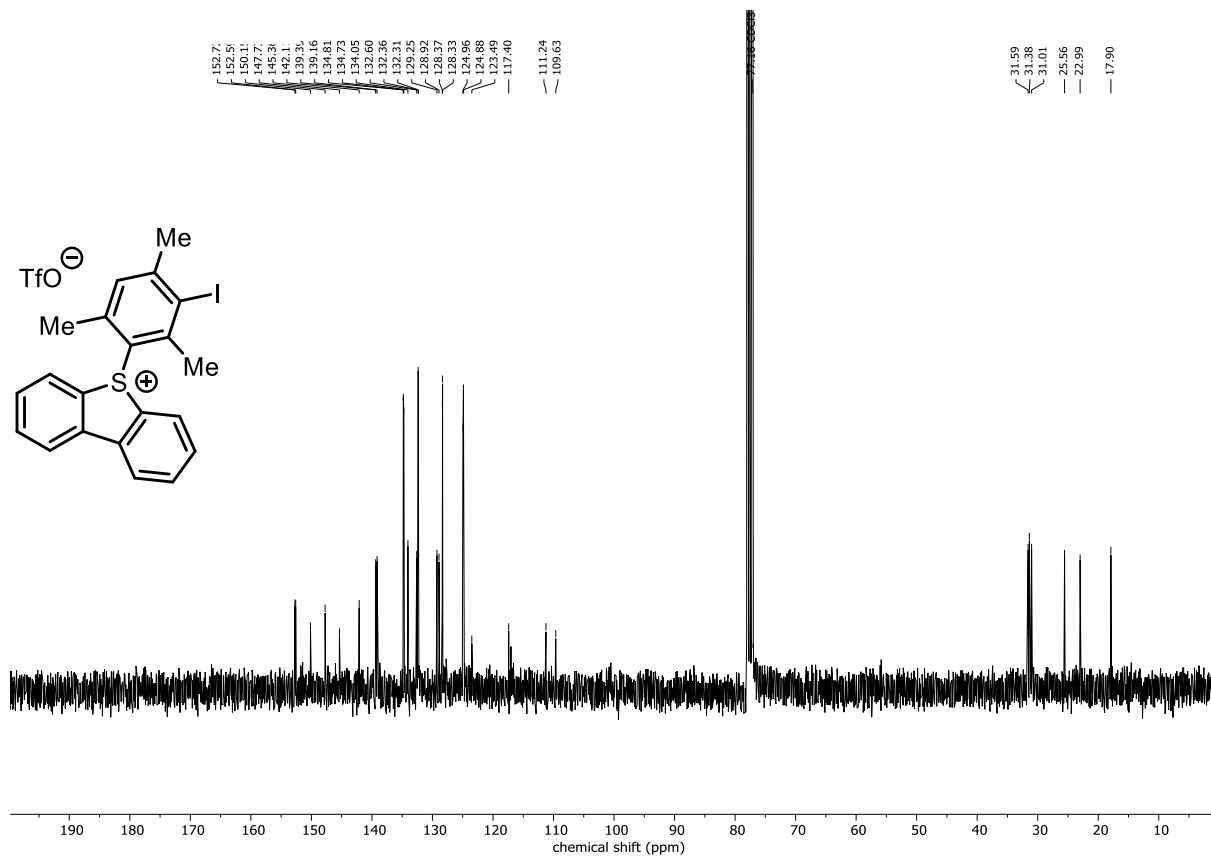
¹³C NMR (101 MHz, CD₂Cl₂) of 93c



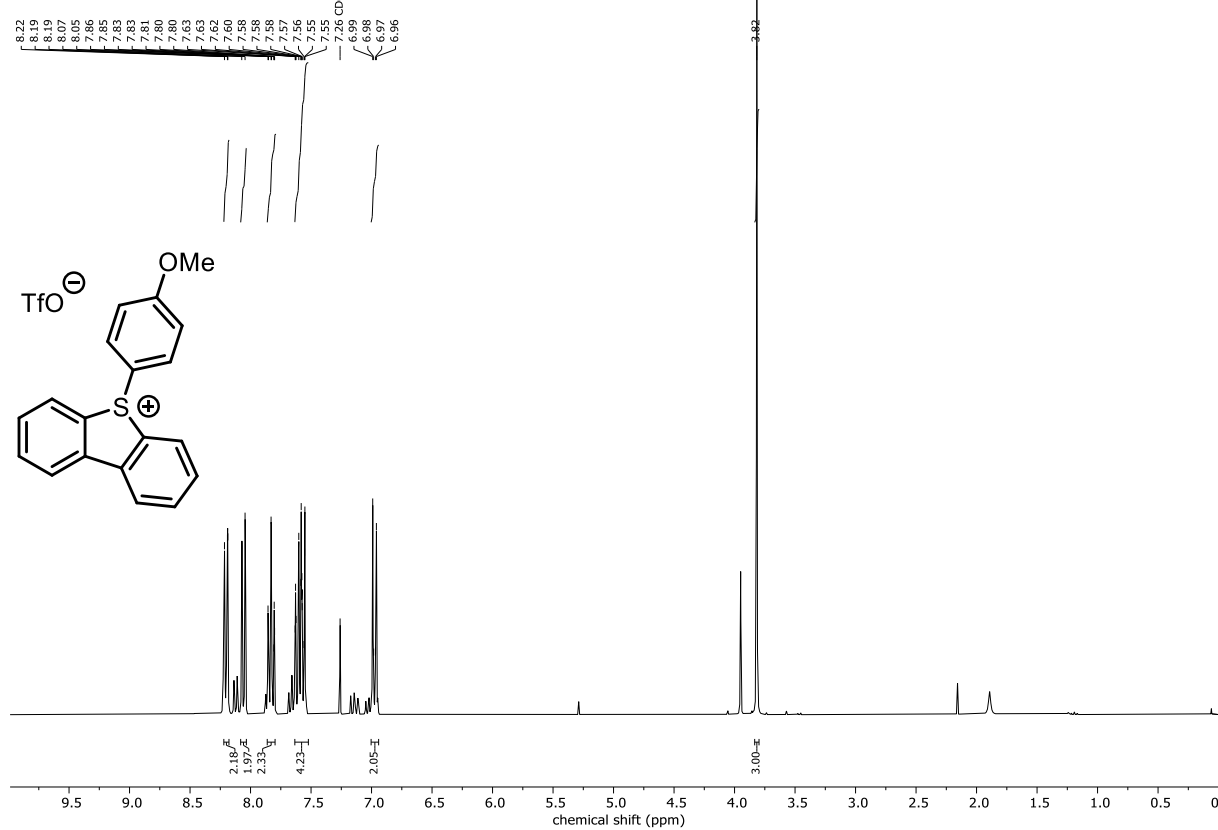
¹H NMR (400 MHz, CDCl₃) of 93d



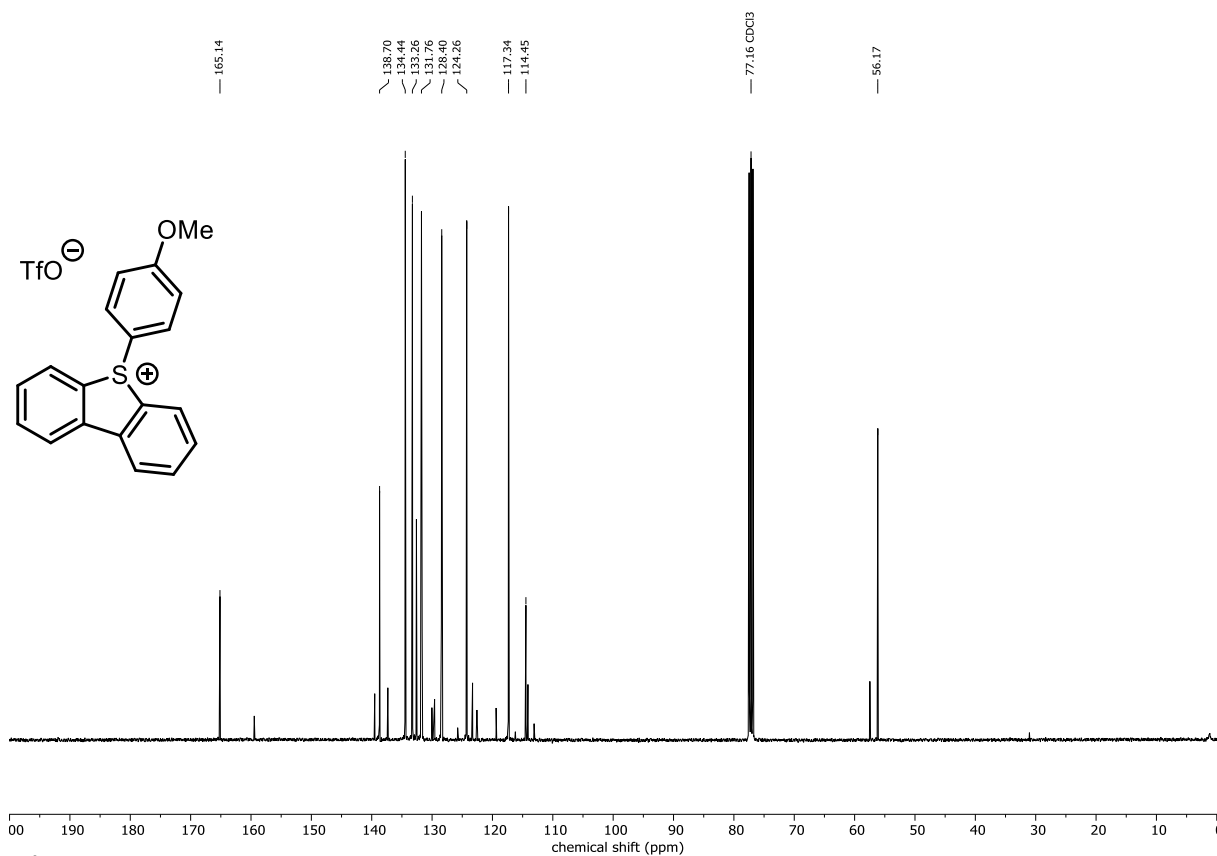
¹³C NMR (101 MHz, CDCl₃) of 93d



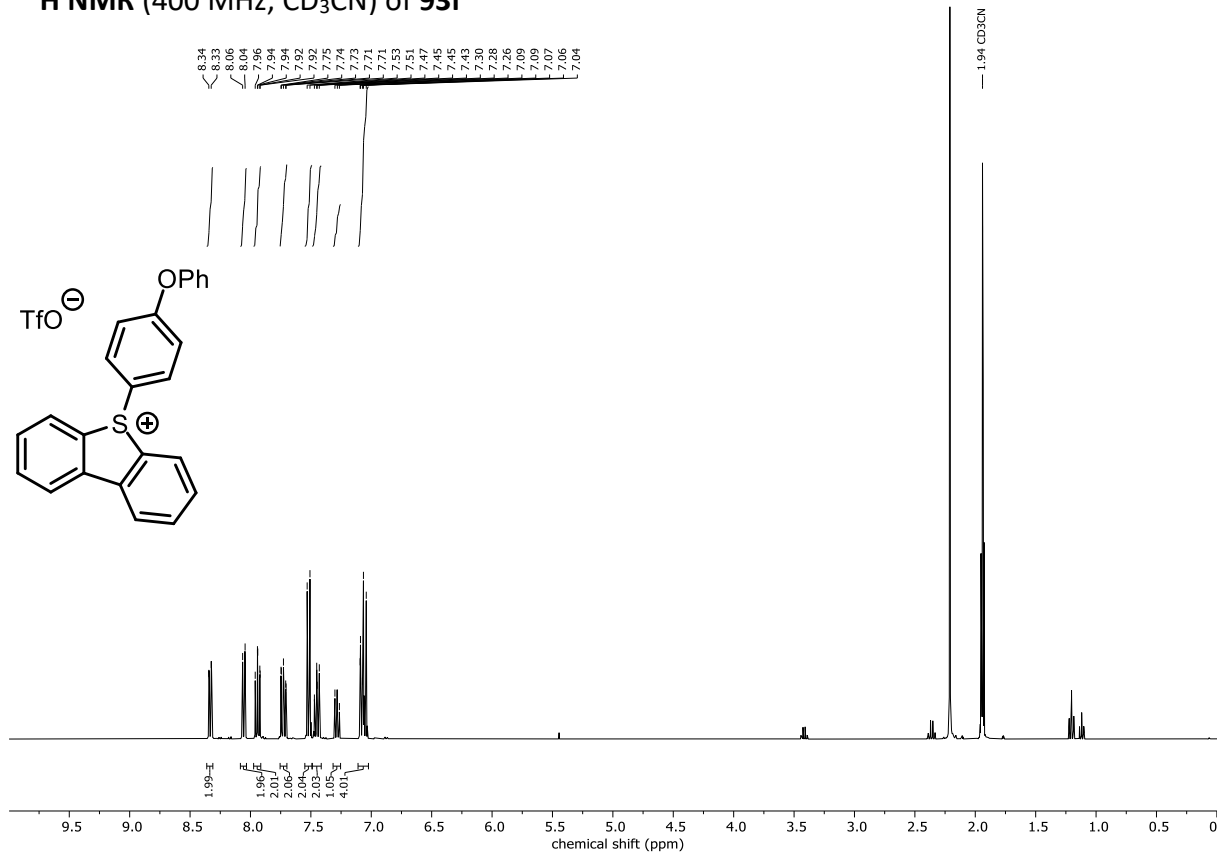
¹H NMR (400 MHz, CDCl₃) of 93e



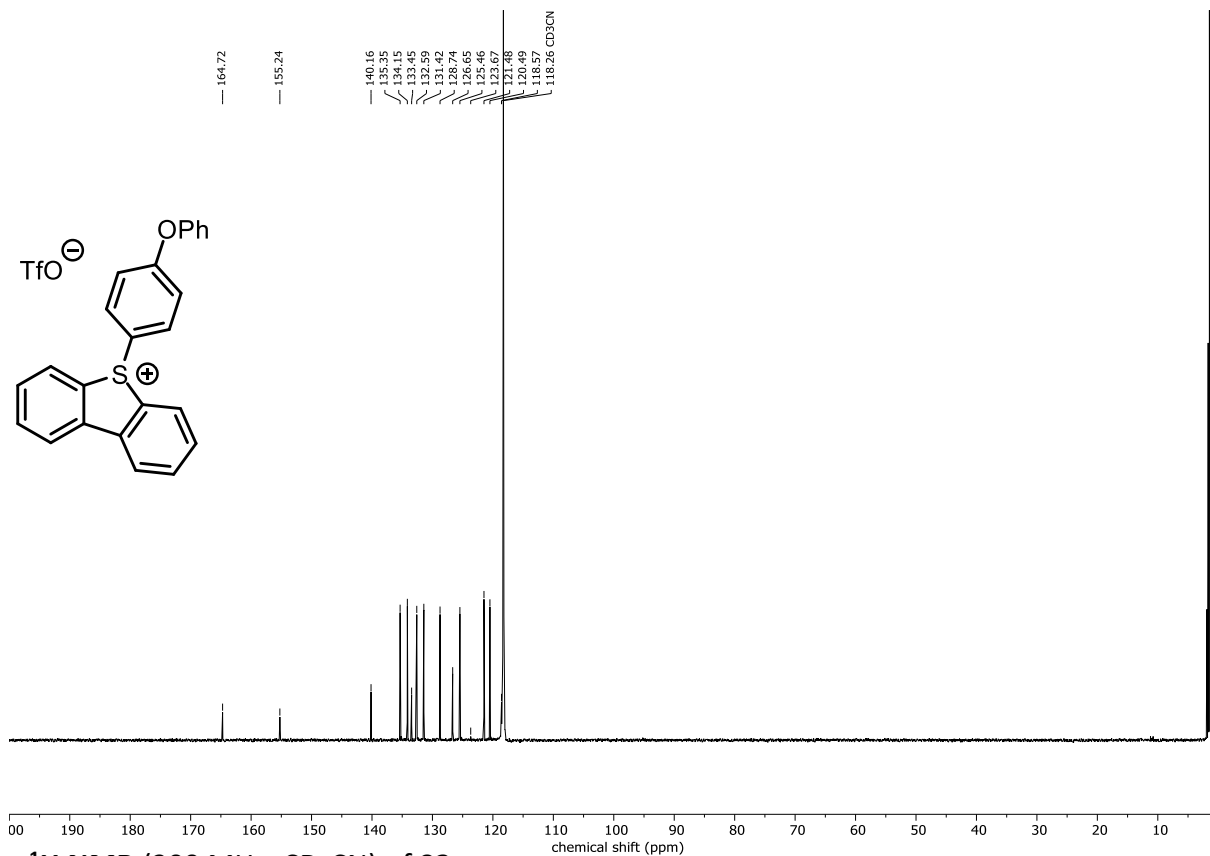
¹³C NMR (101 MHz, CD₃CN) of 93f



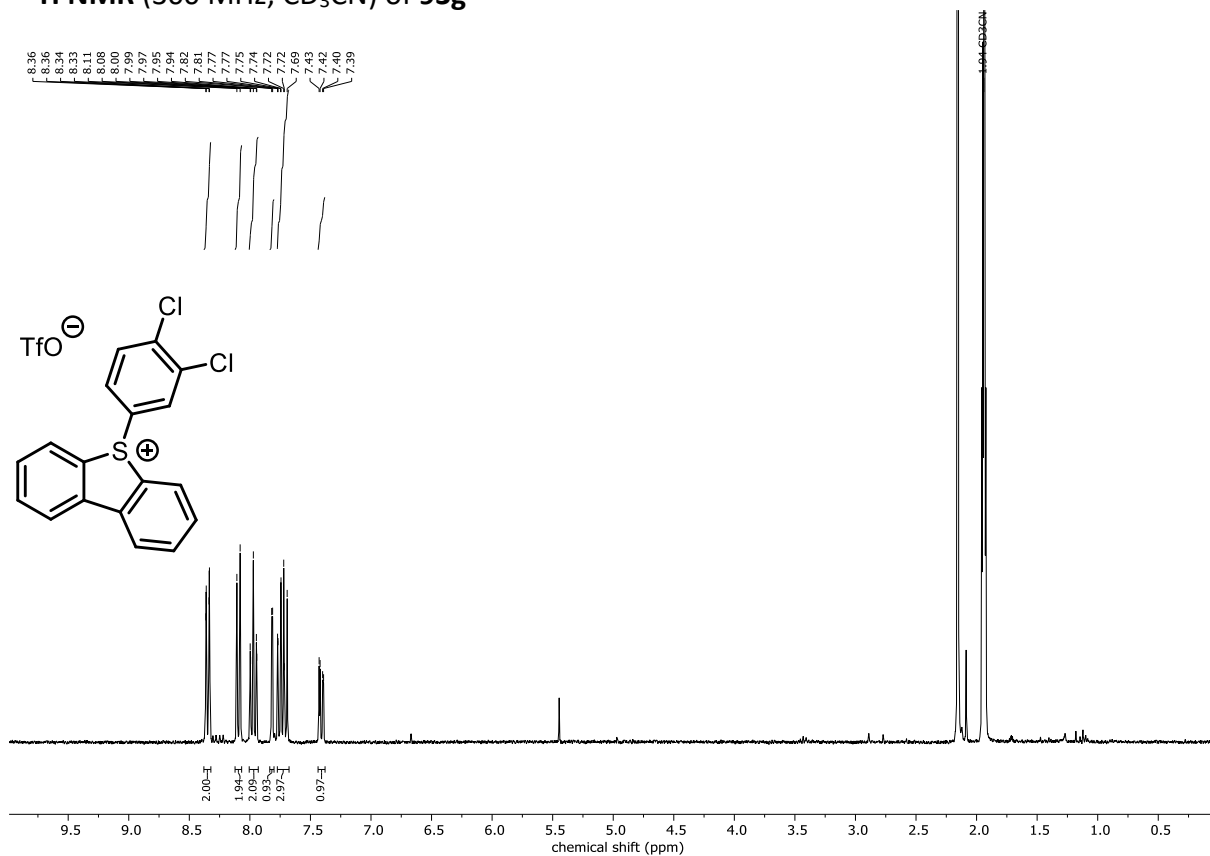
¹H NMR (400 MHz, CD₃CN) of 93f



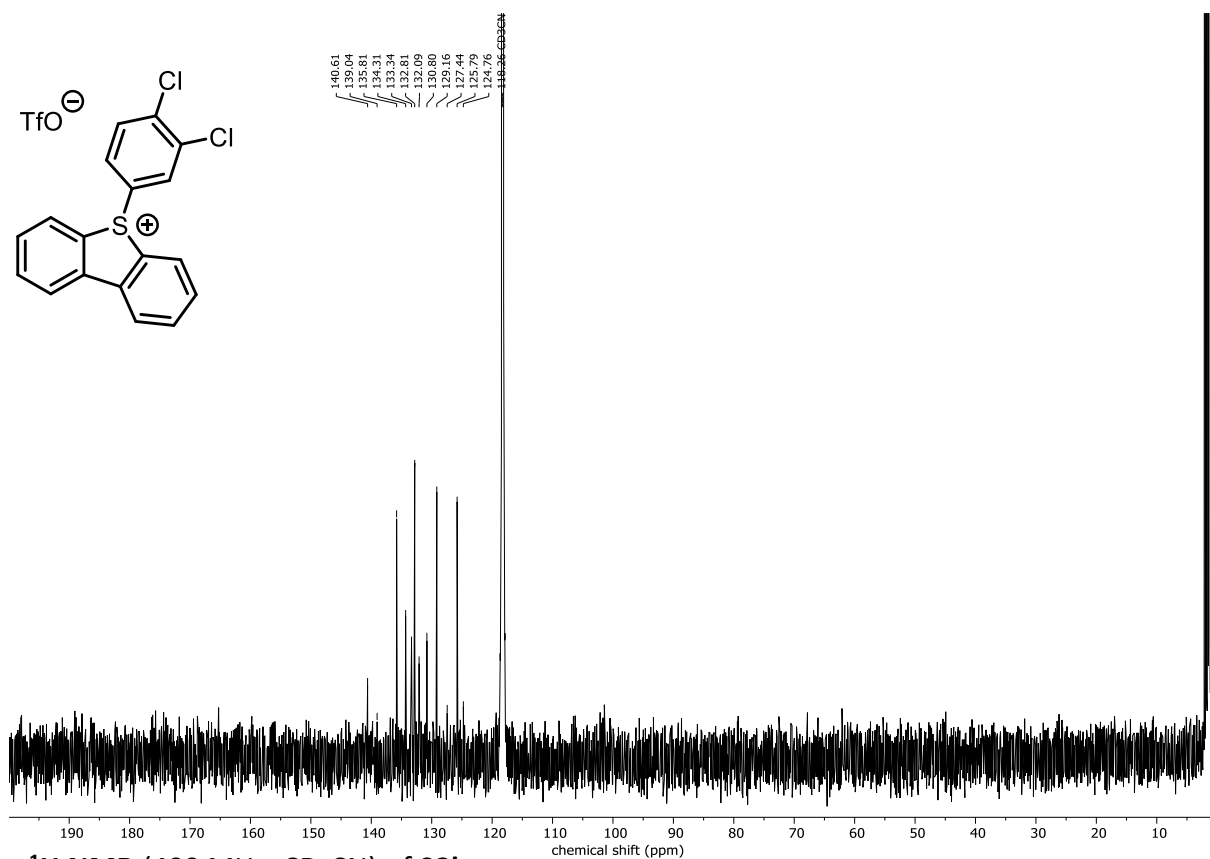
¹³C NMR (101 MHz, CDCl₃) of 93e



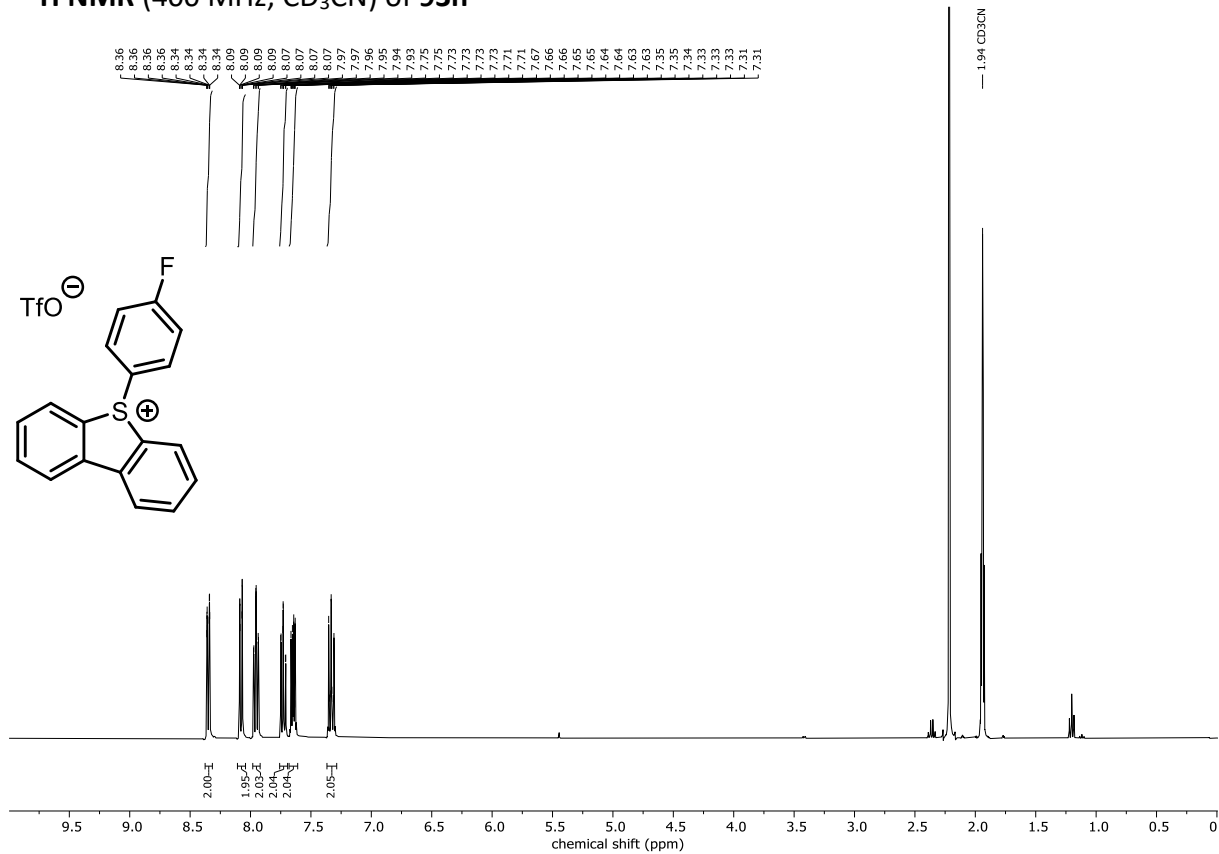
¹H NMR (300 MHz, CD₃CN) of 93g



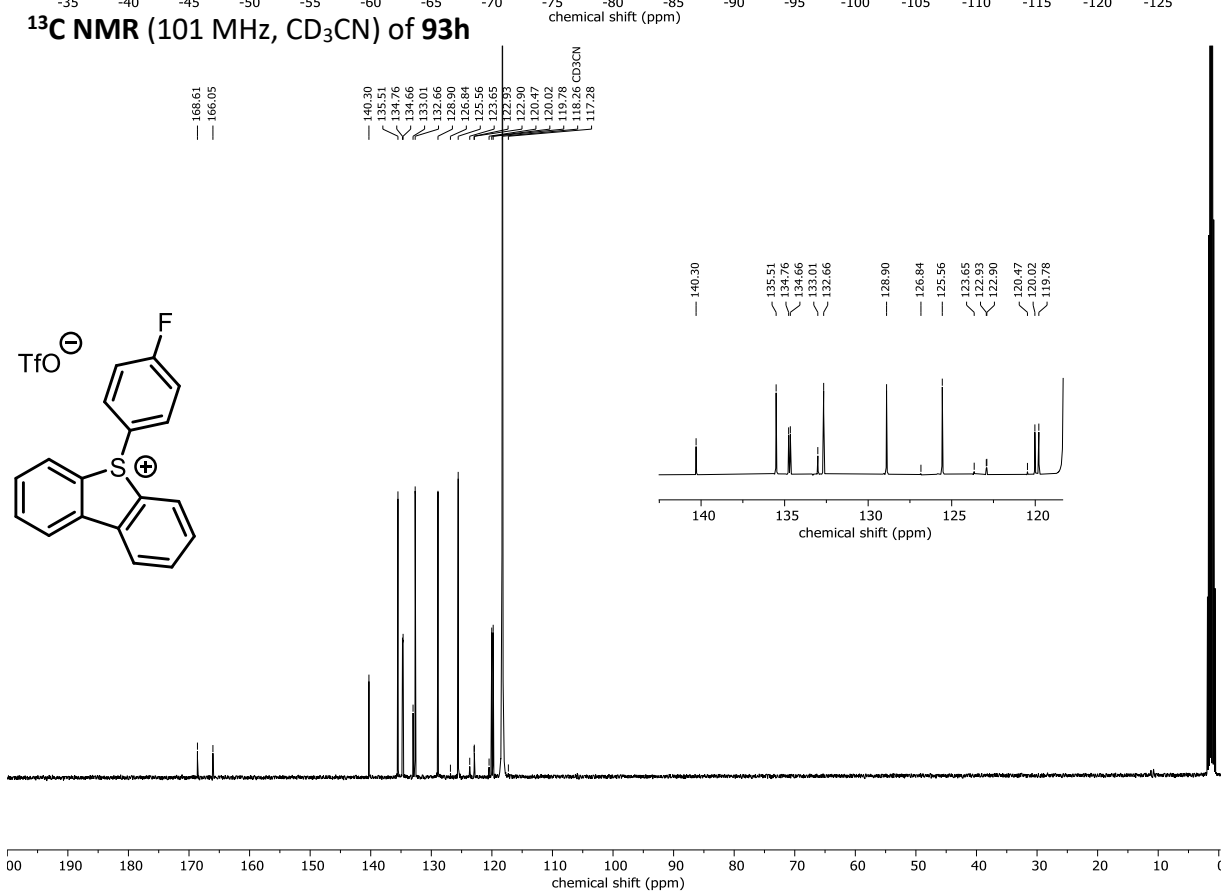
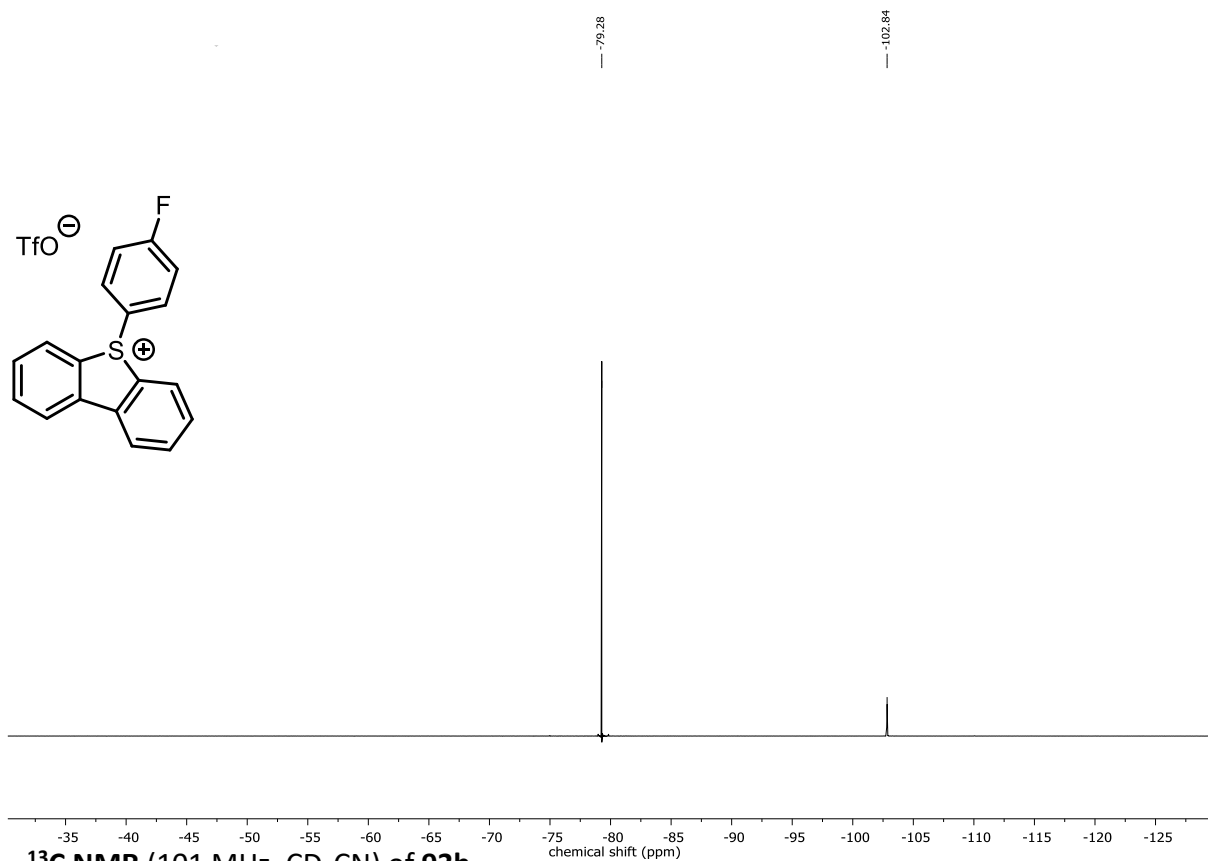
¹³C NMR (75 MHz, CD₃CN) of 93g



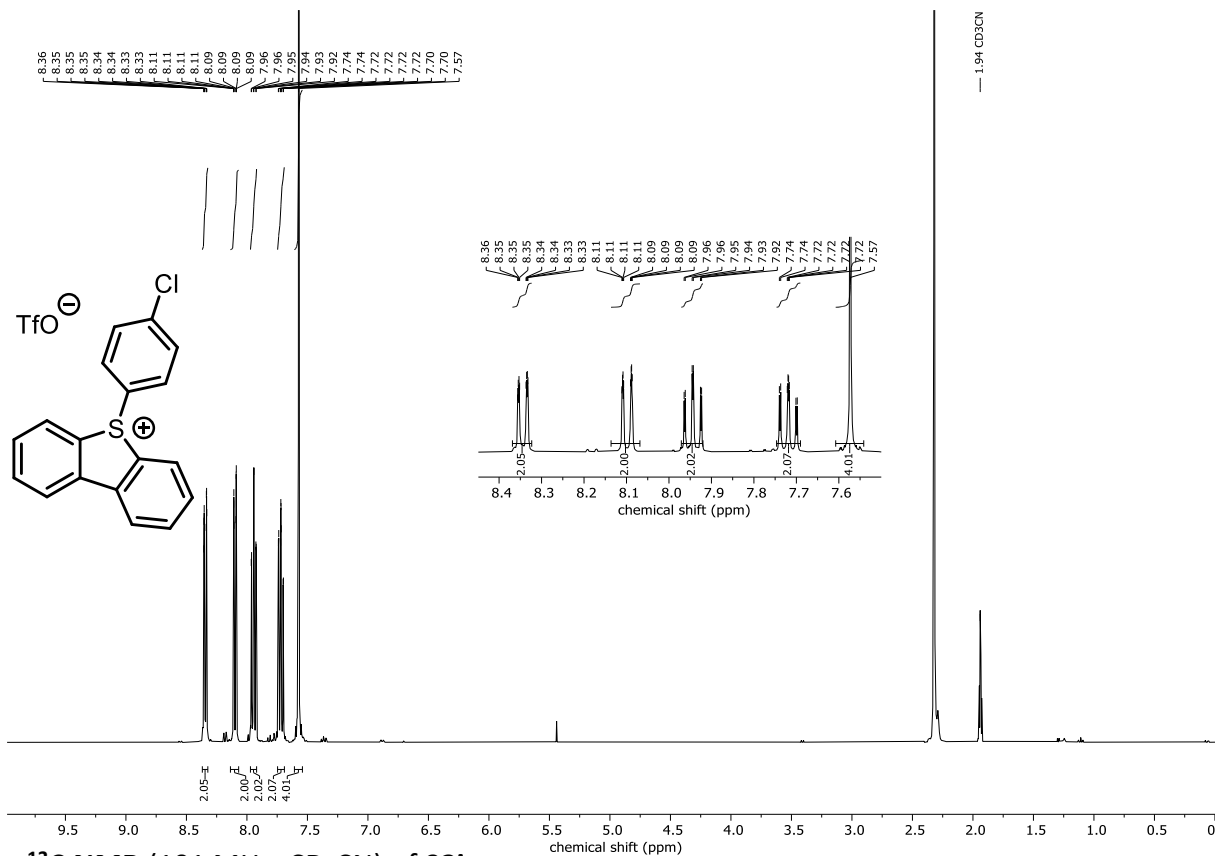
¹H NMR (400 MHz, CD₃CN) of 93h



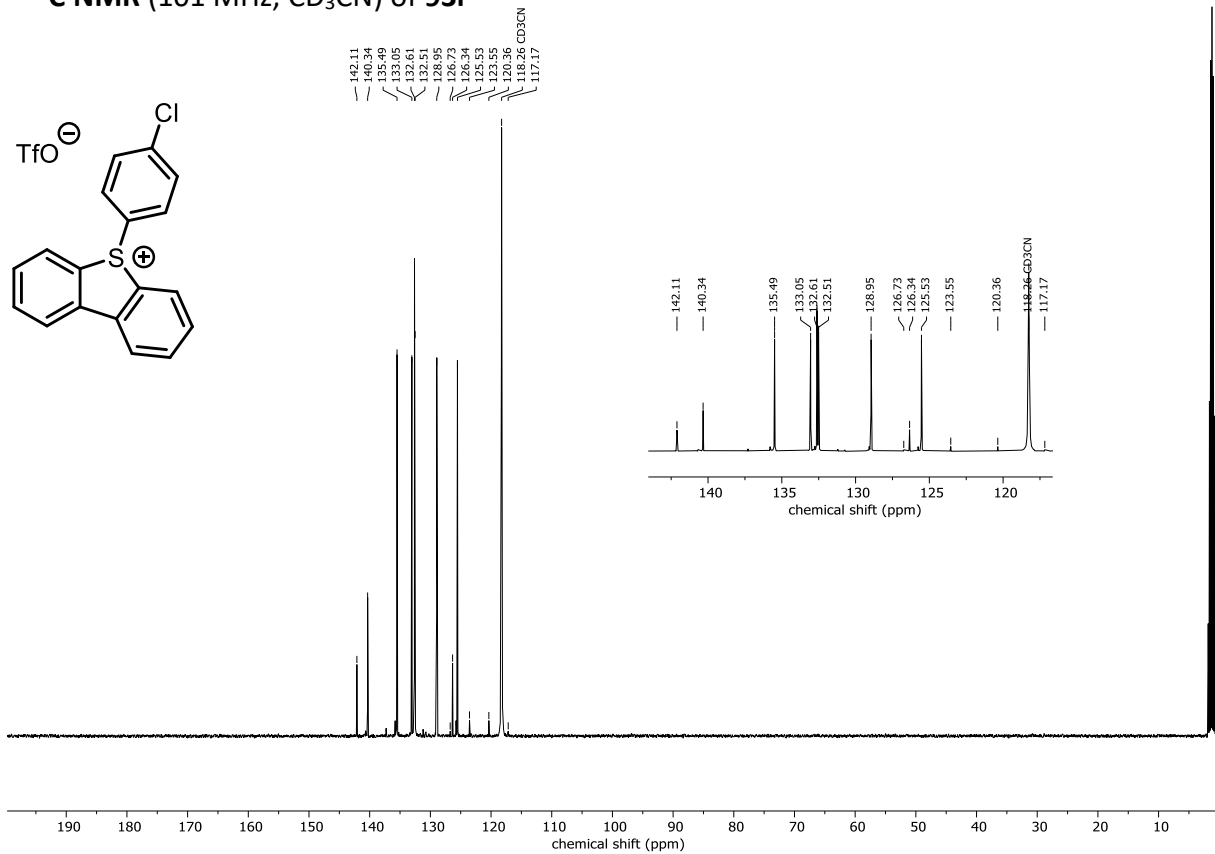
¹⁹F NMR (376 MHz, CD₃CN) of 93h



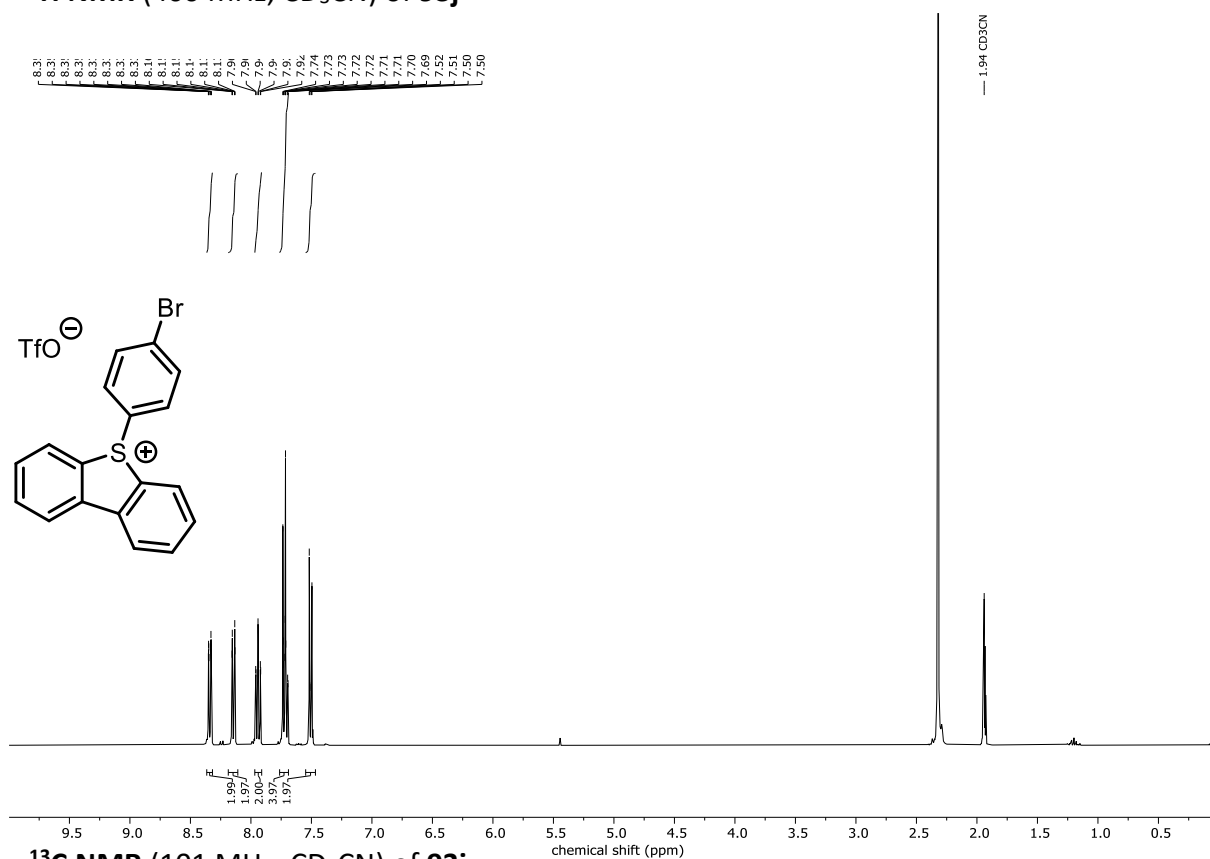
¹H NMR (400 MHz, CD₃CN) of 93i



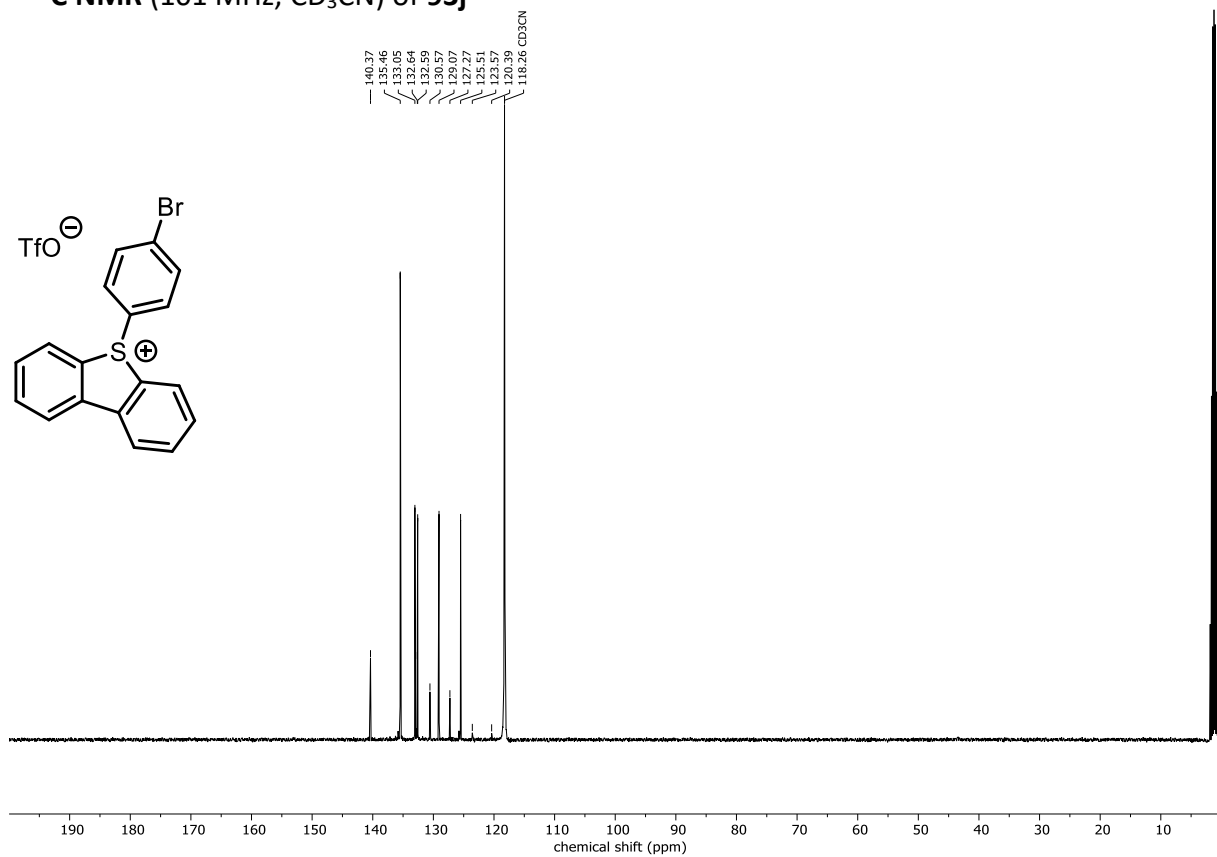
¹³C NMR (101 MHz, CD₃CN) of 93i



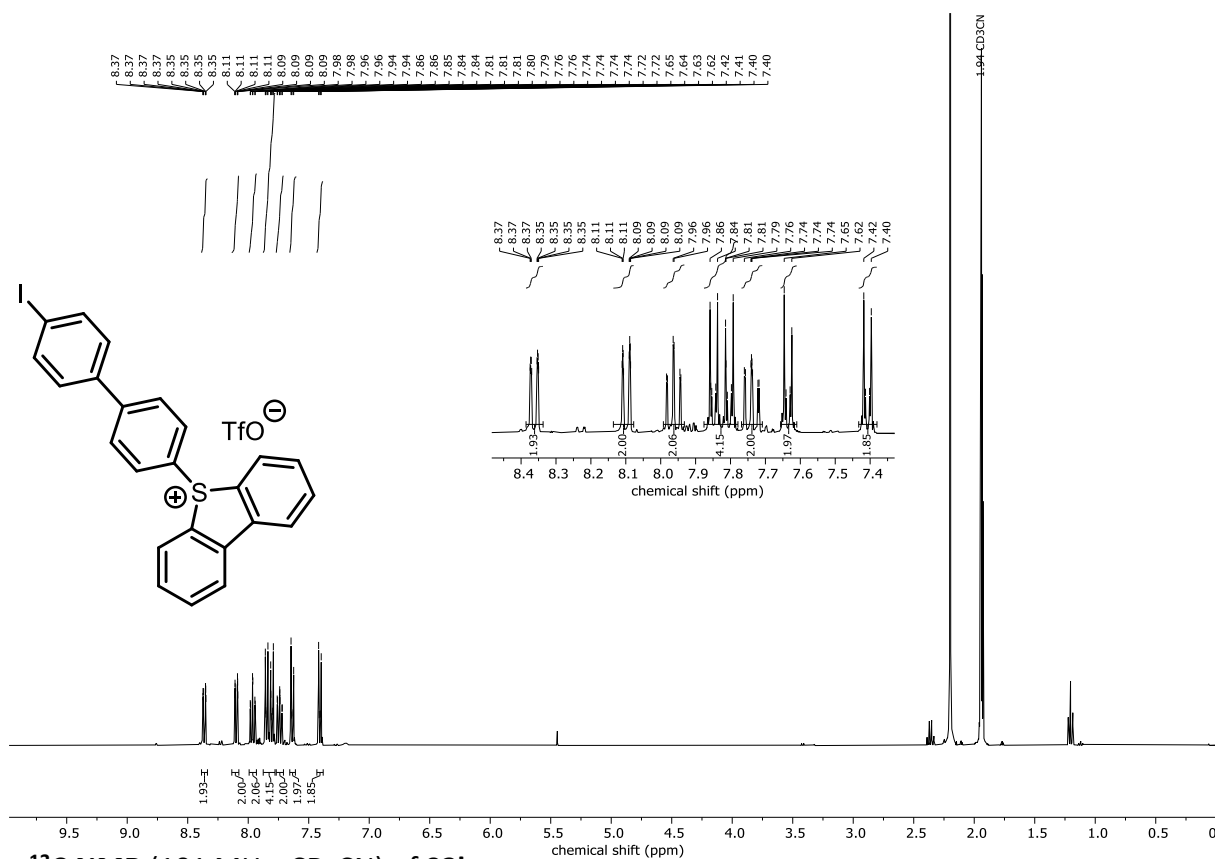
¹H NMR (400 MHz, CD₃CN) of 93j



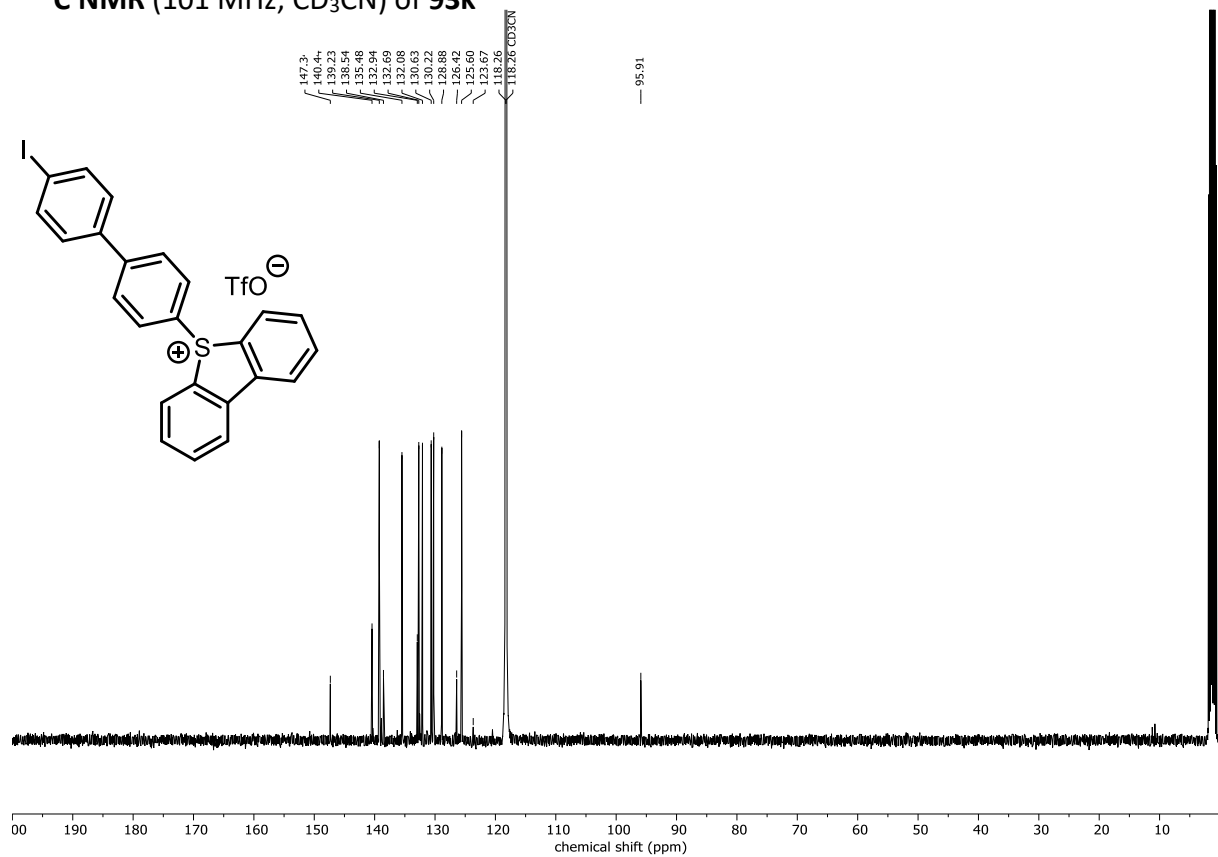
¹³C NMR (101 MHz, CD₃CN) of 93j



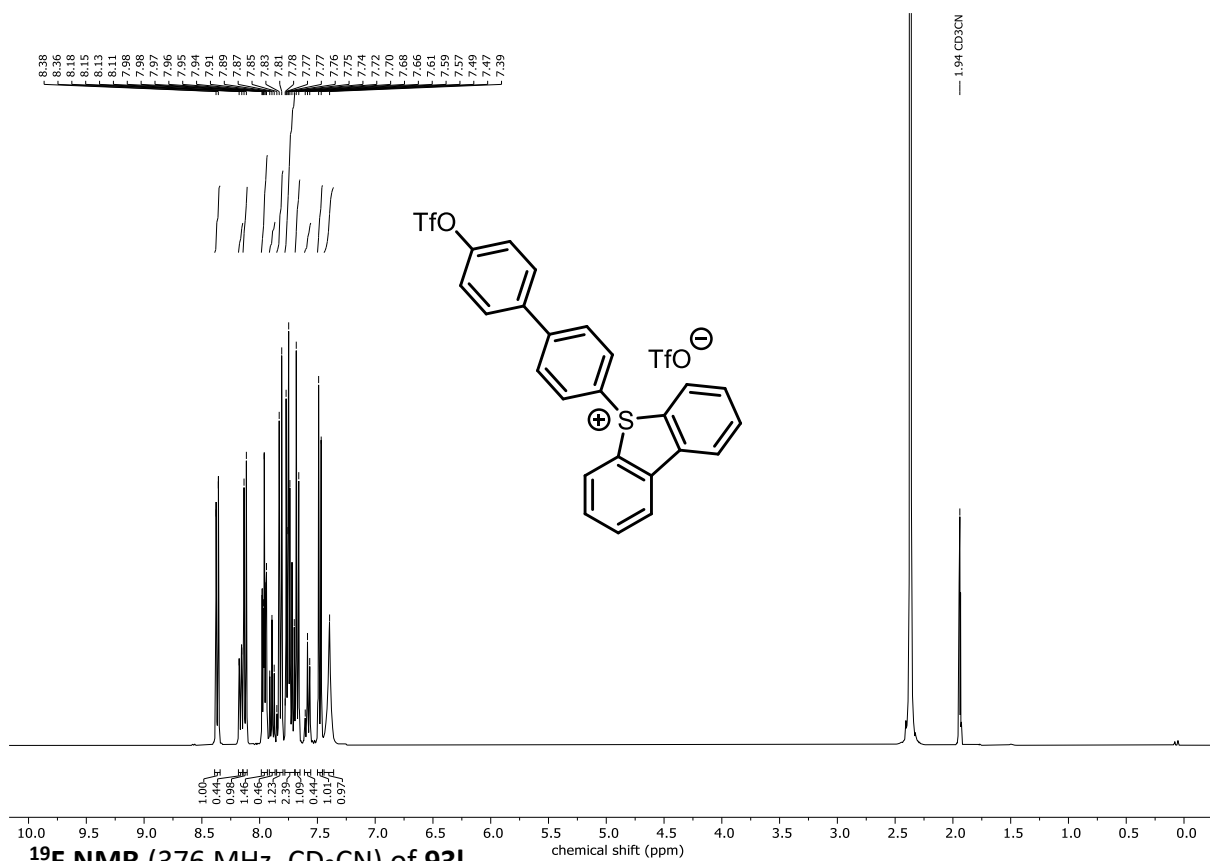
¹H NMR (400 MHz, CD₃CN) of **93k**



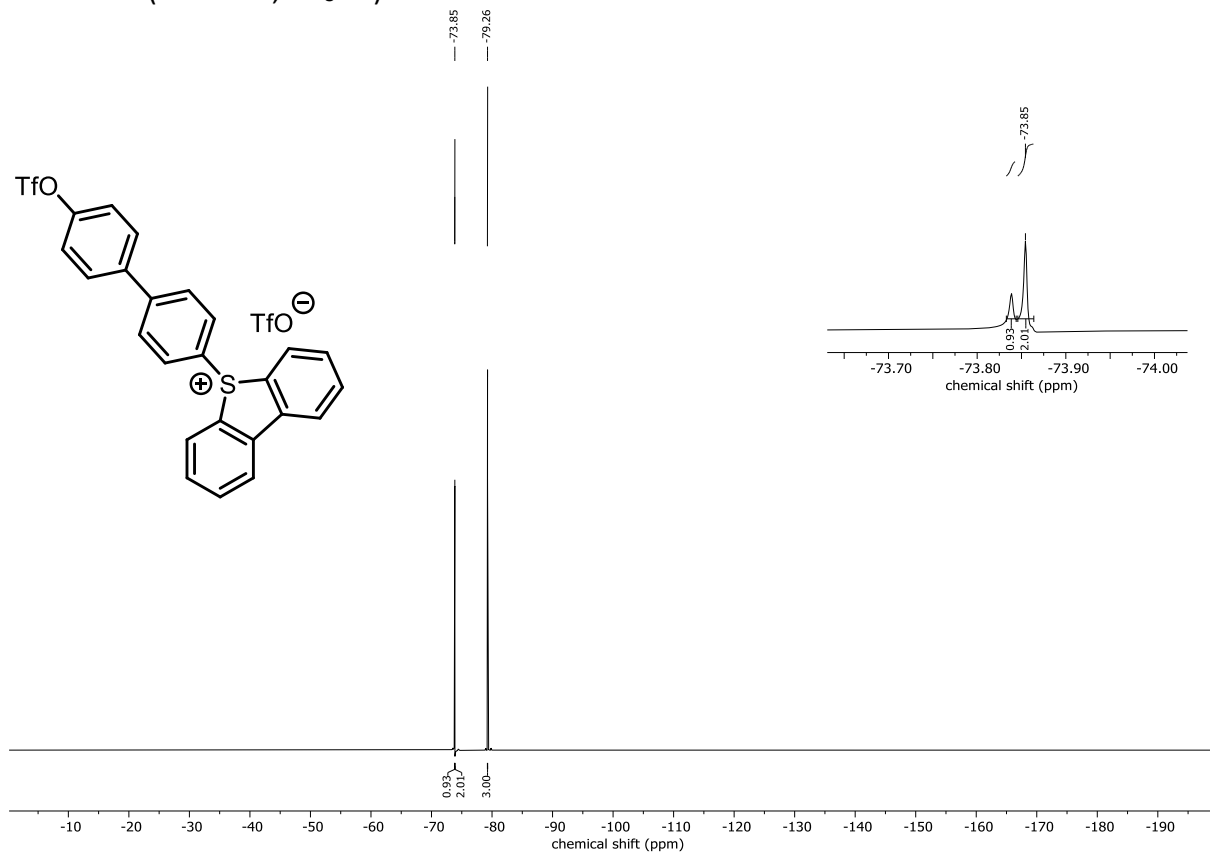
¹³C NMR (101 MHz, CD₃CN) of **93k**



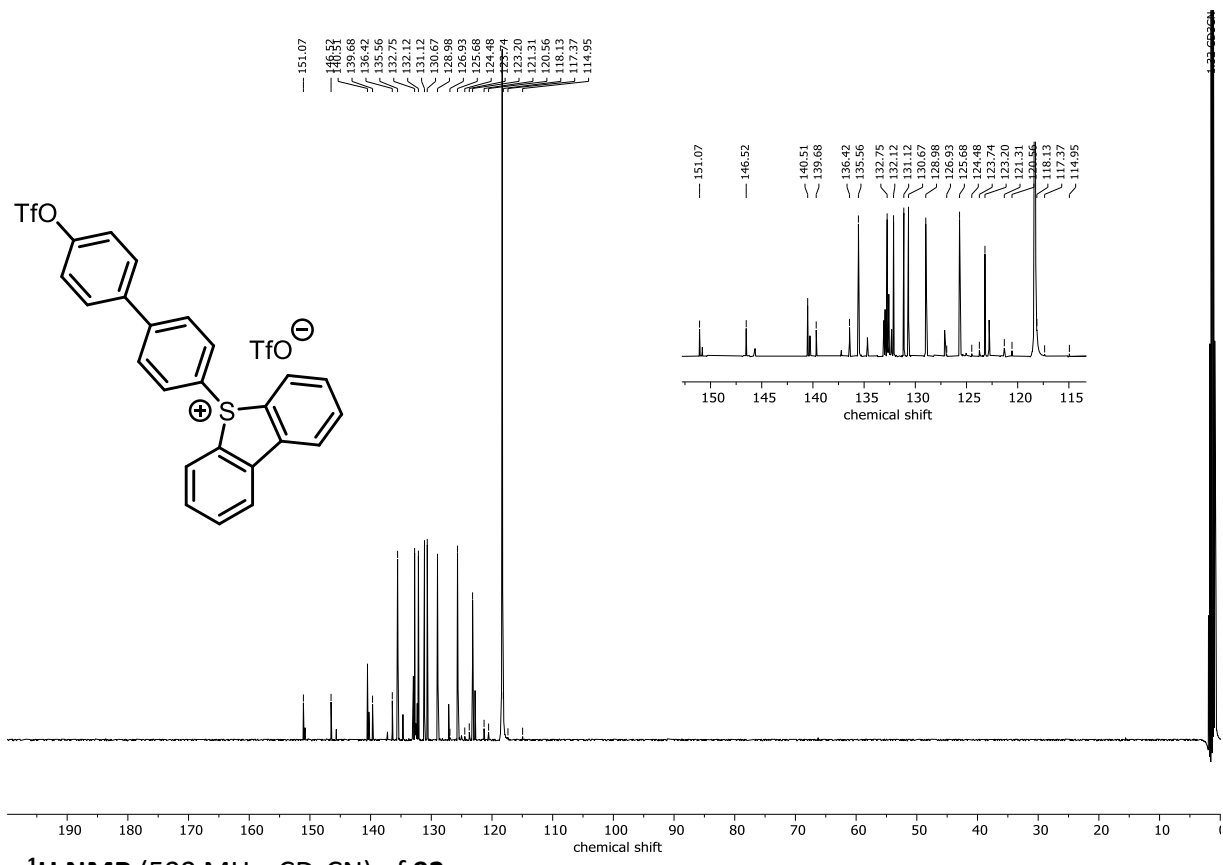
¹H NMR (400 MHz, CD₃CN) of **93I**



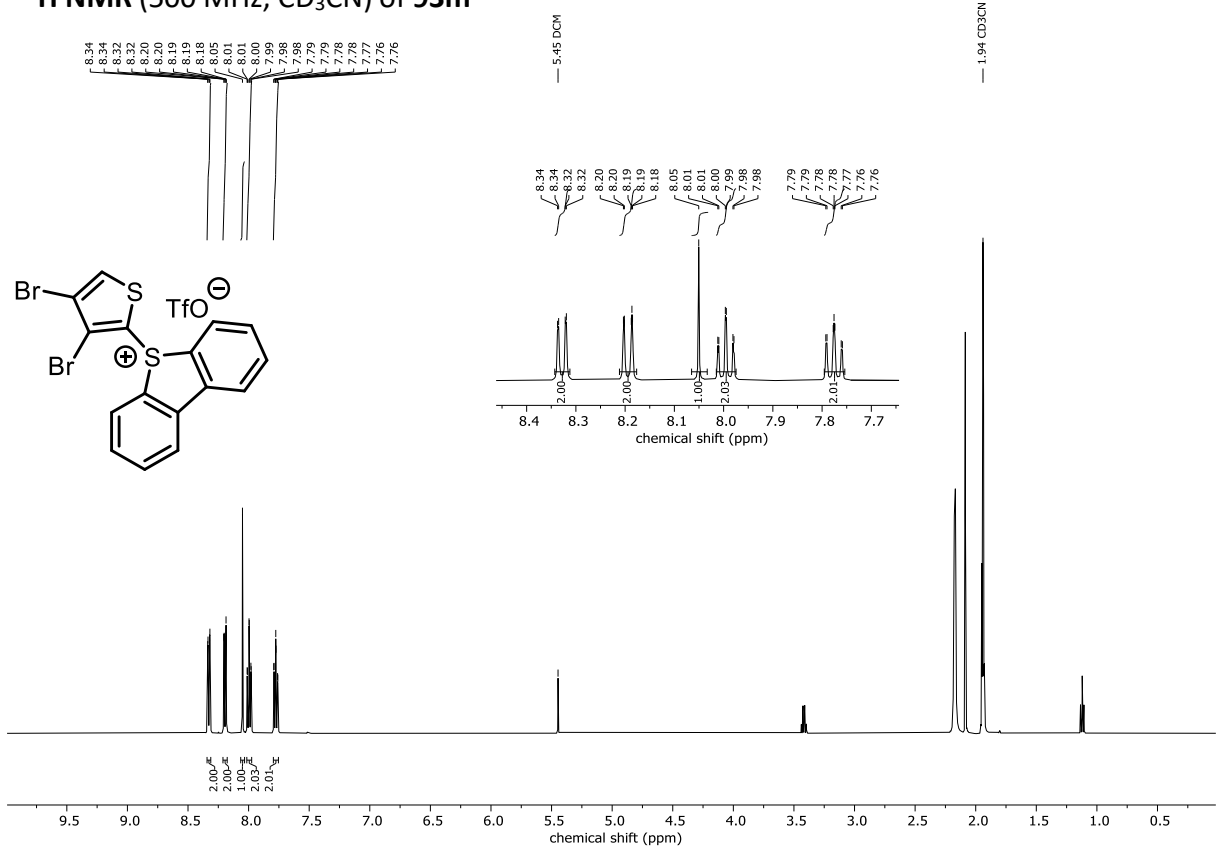
¹⁹F NMR (376 MHz, CD₃CN) of **93I**



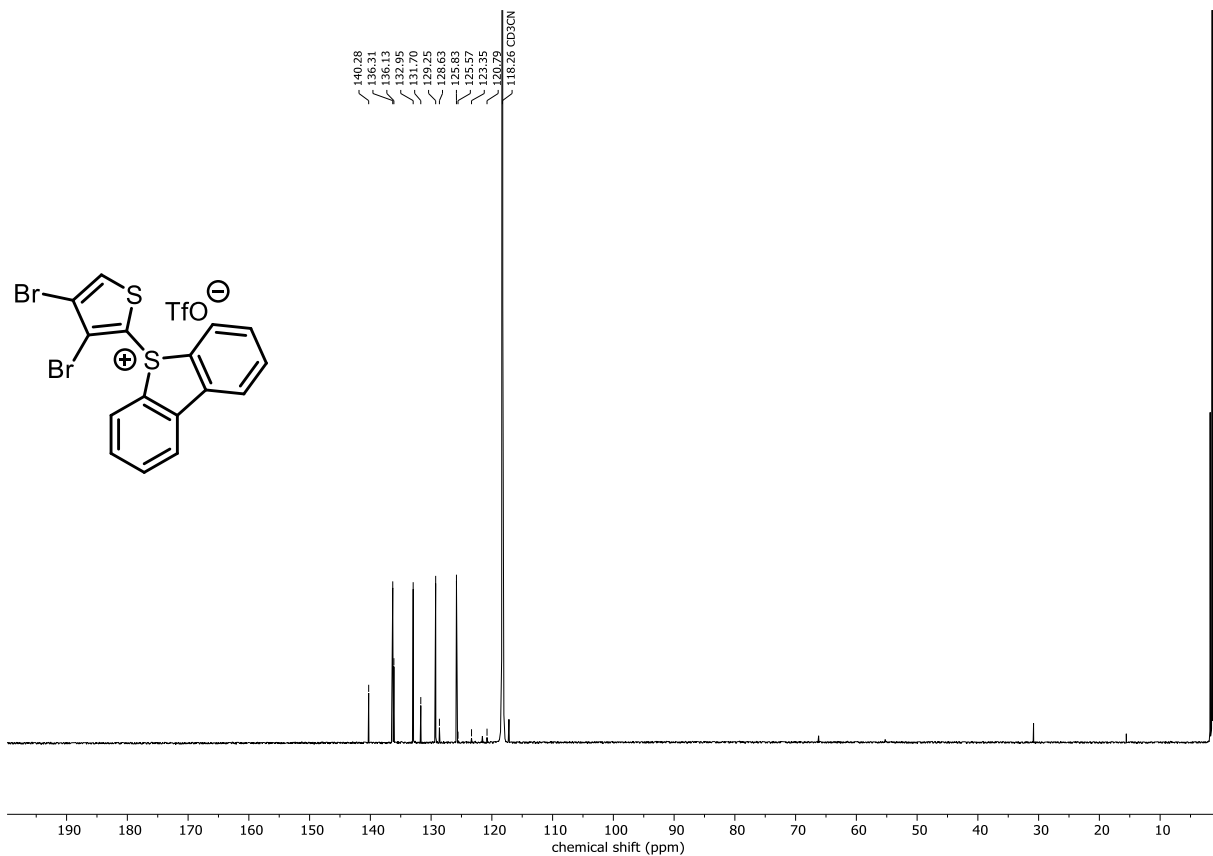
¹³C NMR (101 MHz, CD₃CN) of **93l**



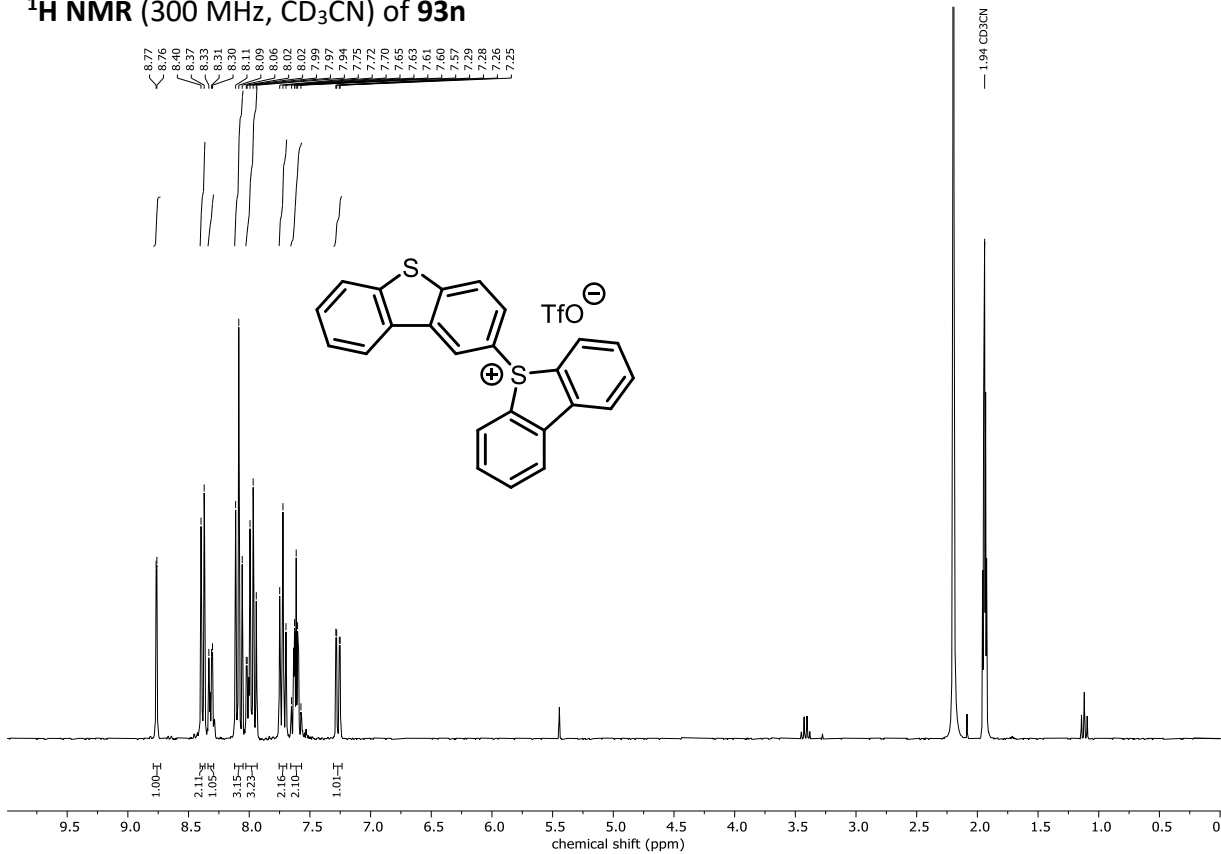
¹H NMR (500 MHz, CD₃CN) of **93m**



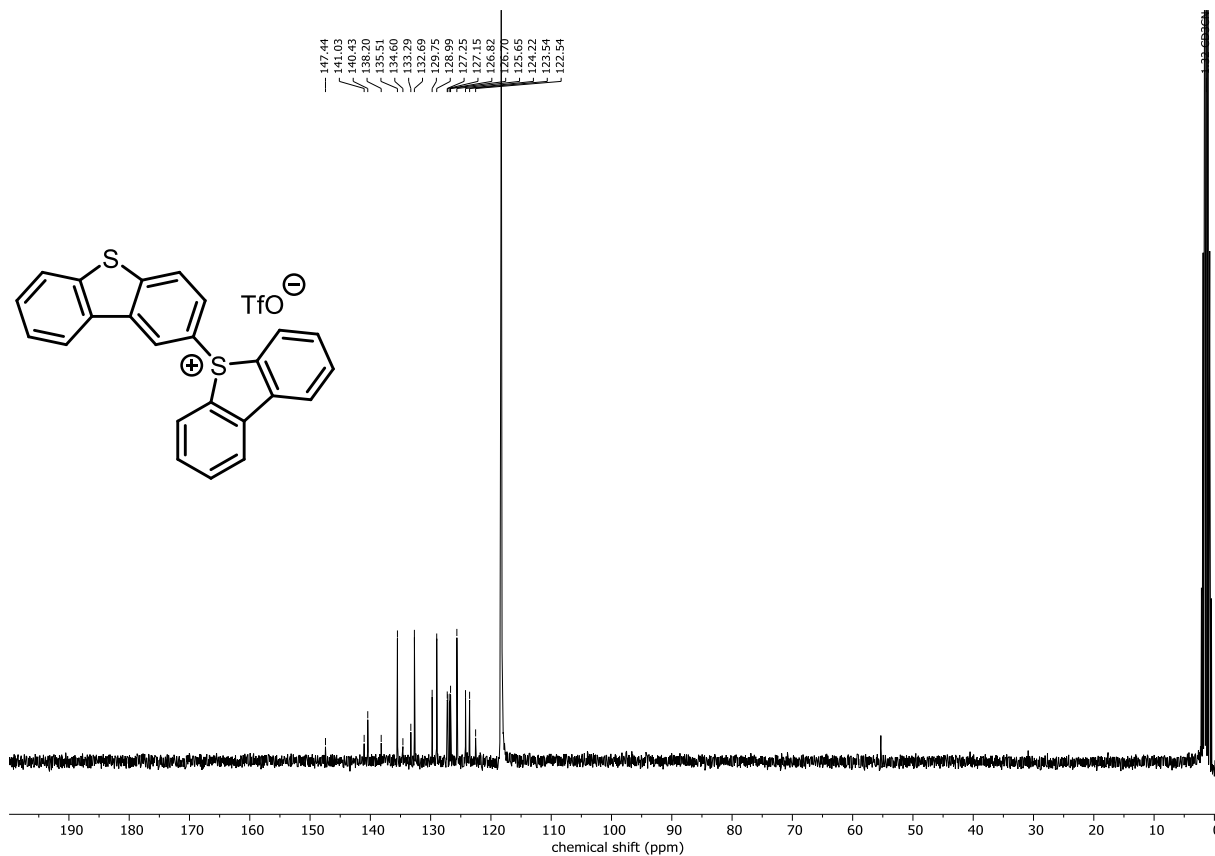
¹³C NMR (126 MHz, CD₃CN) of 93m



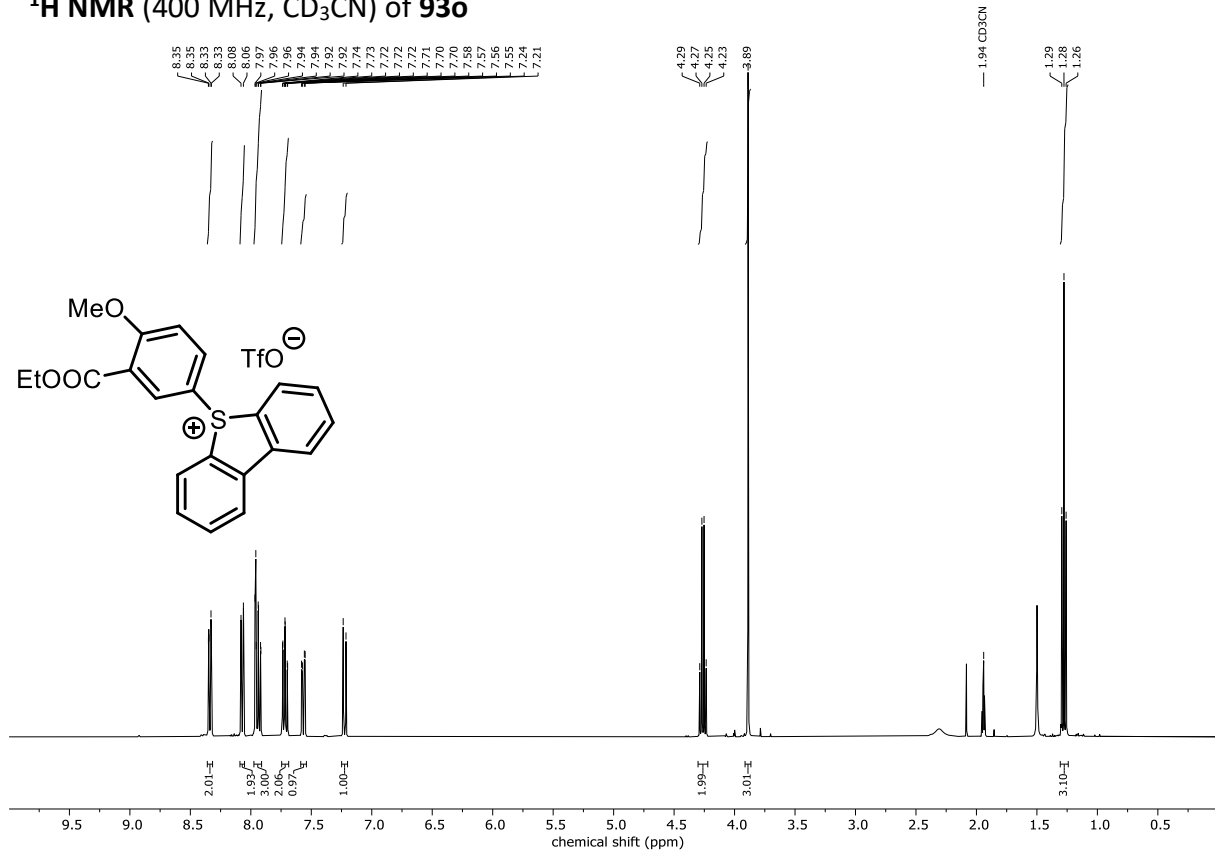
¹H NMR (300 MHz, CD₃CN) of 93n



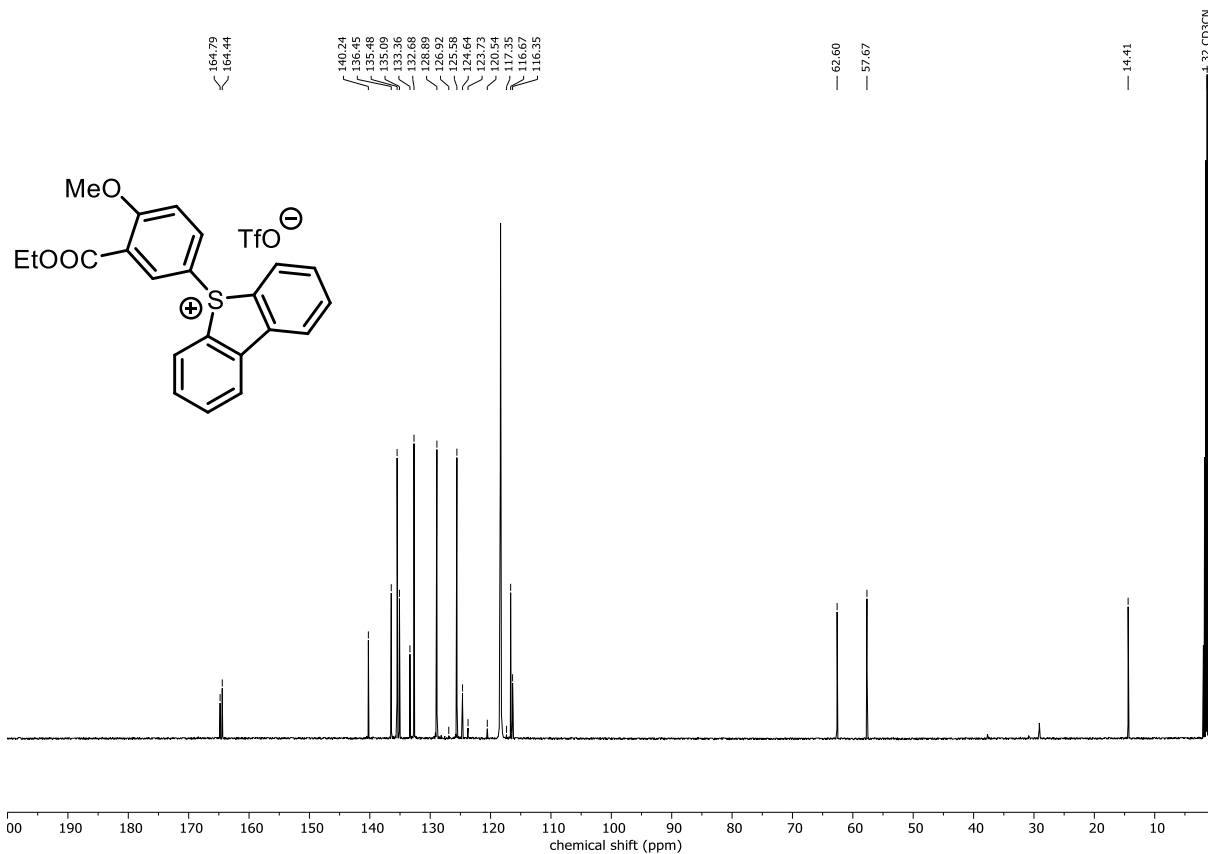
¹³C NMR (75 MHz, CD₃CN) of 93n



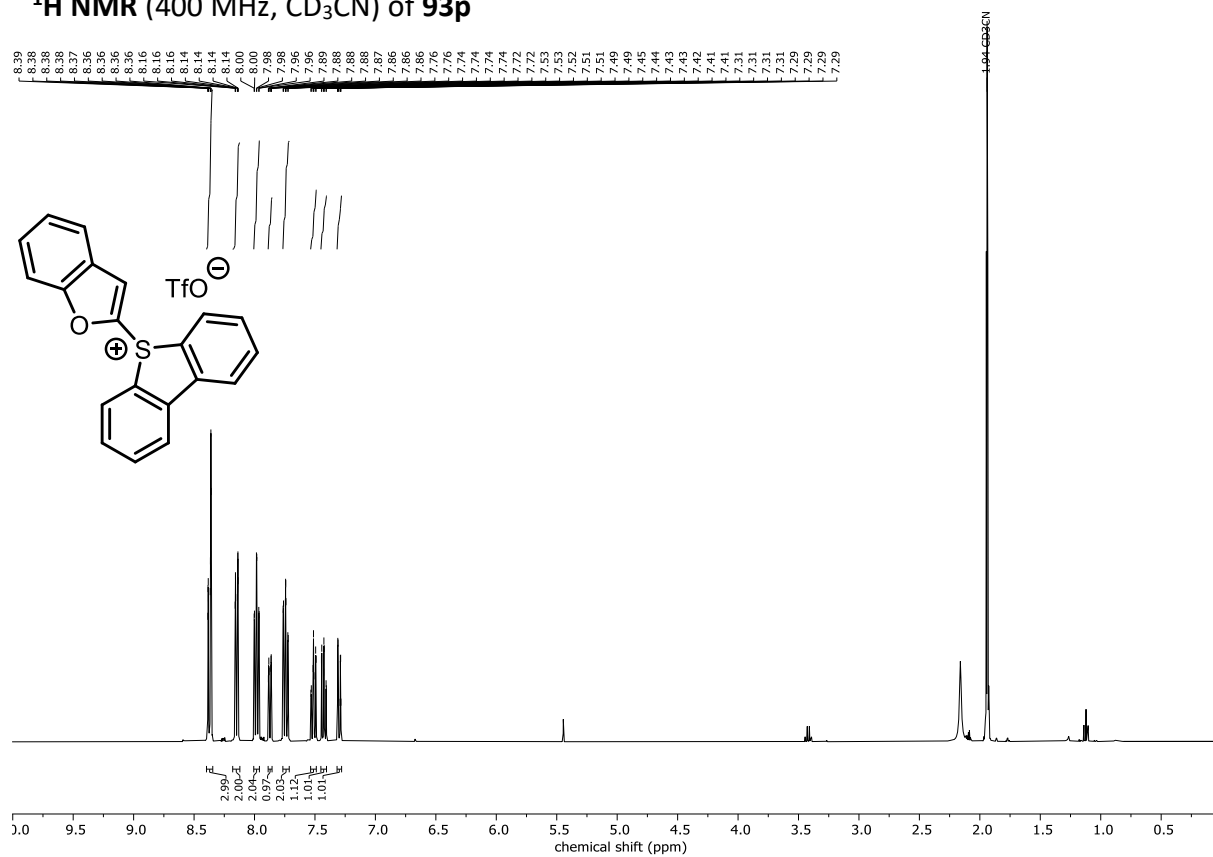
¹H NMR (400 MHz, CD₃CN) of 93o



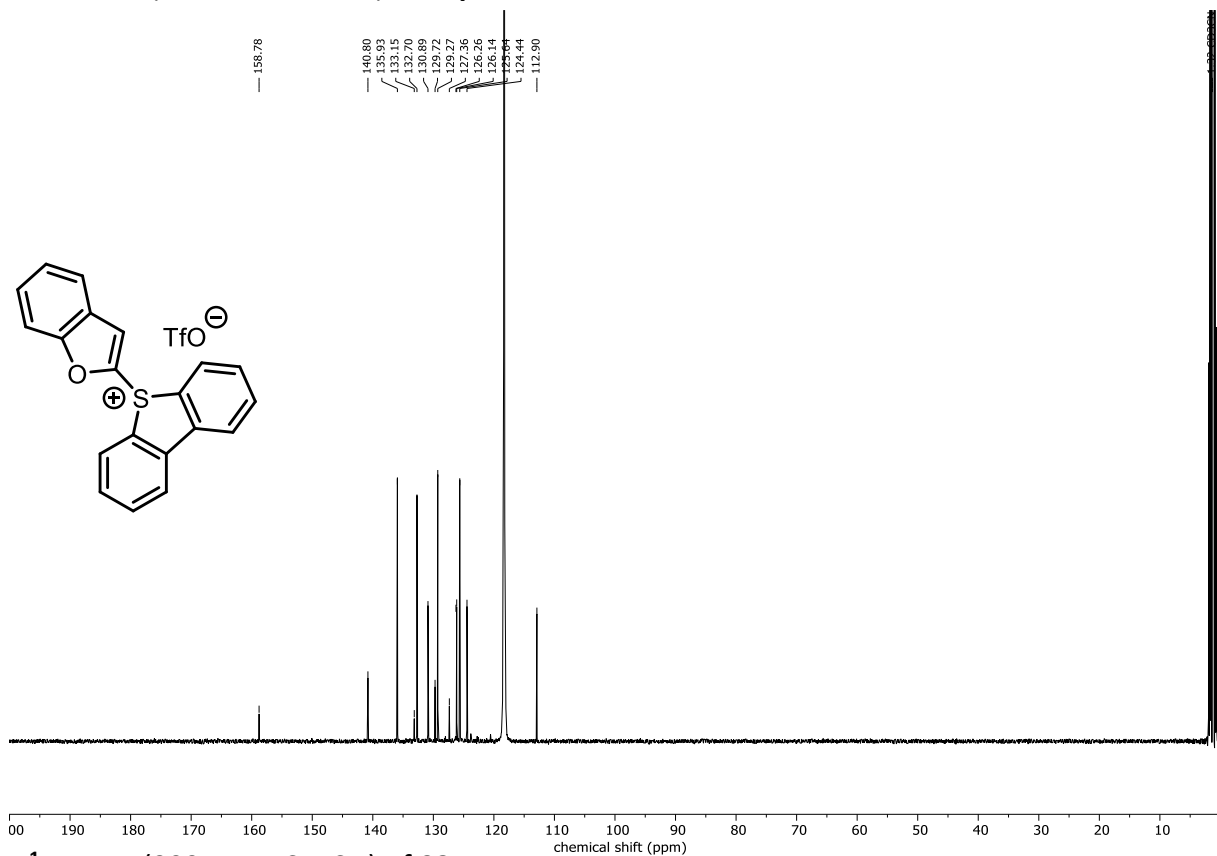
¹³C NMR (101 MHz, CD₃CN) of 93o



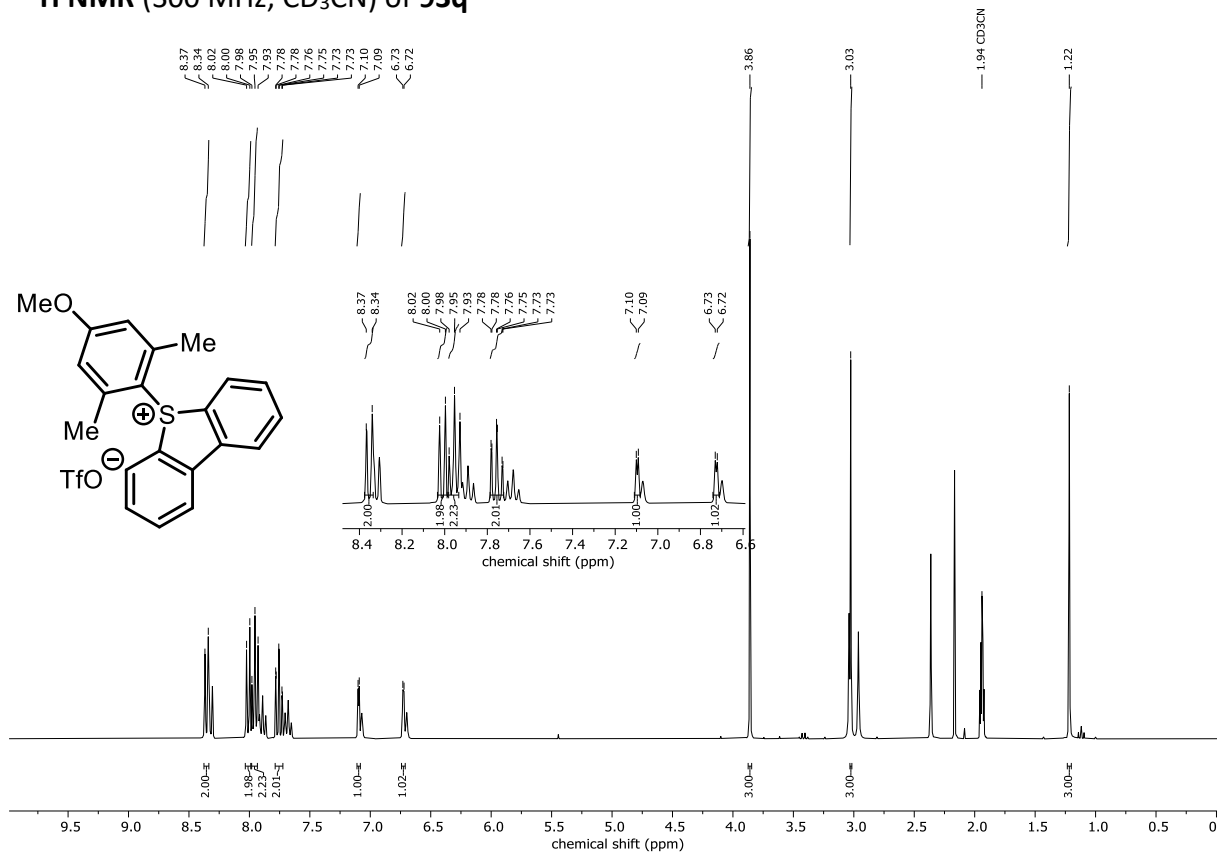
¹H NMR (400 MHz, CD₃CN) of 93p



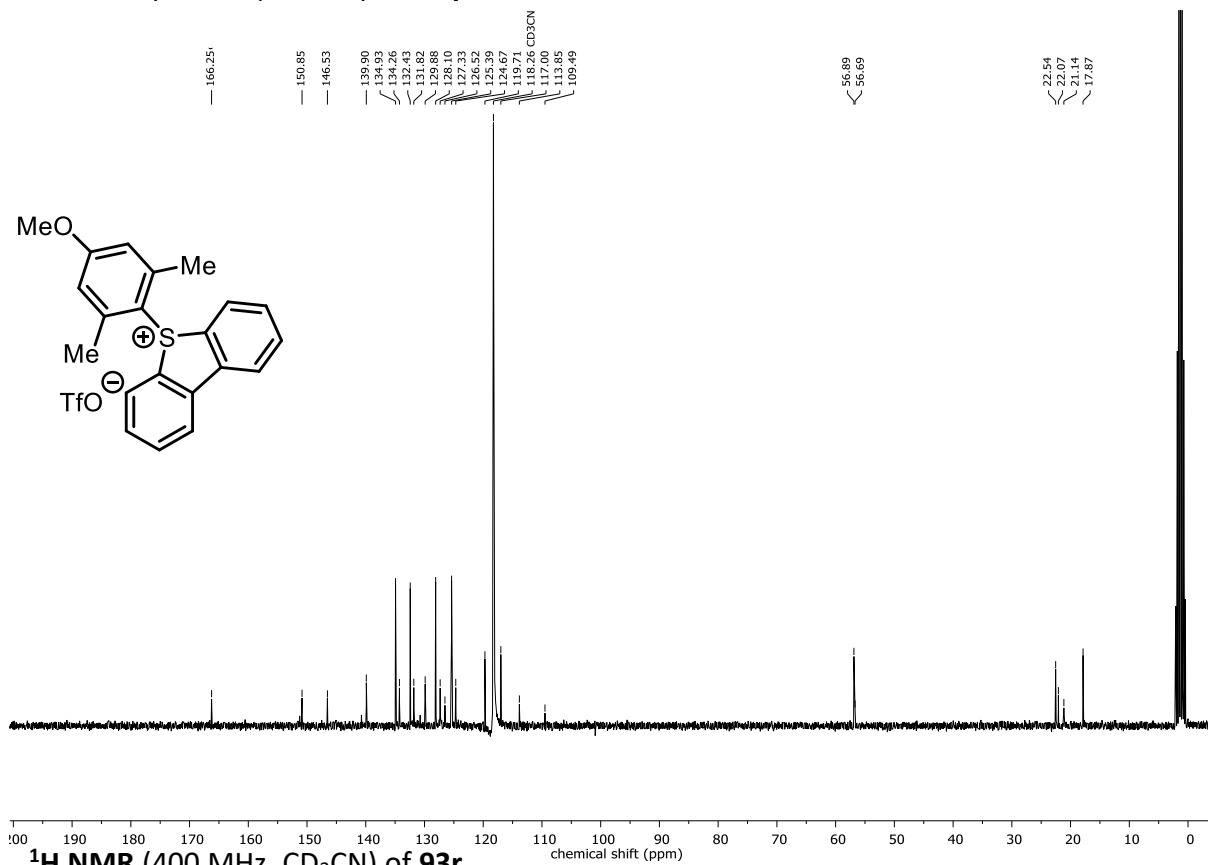
¹³C NMR (101 MHz, CD₃CN) of 93p



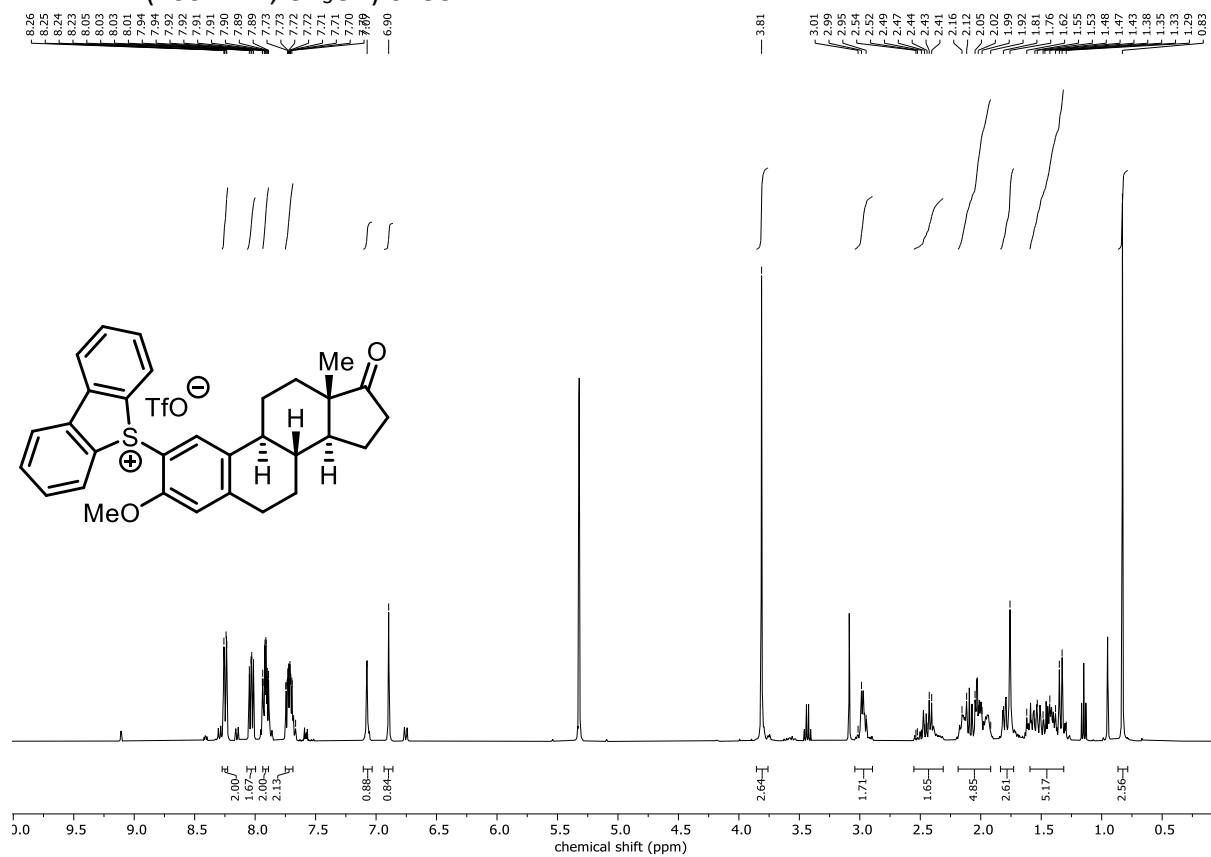
¹H NMR (300 MHz, CD₃CN) of 93q



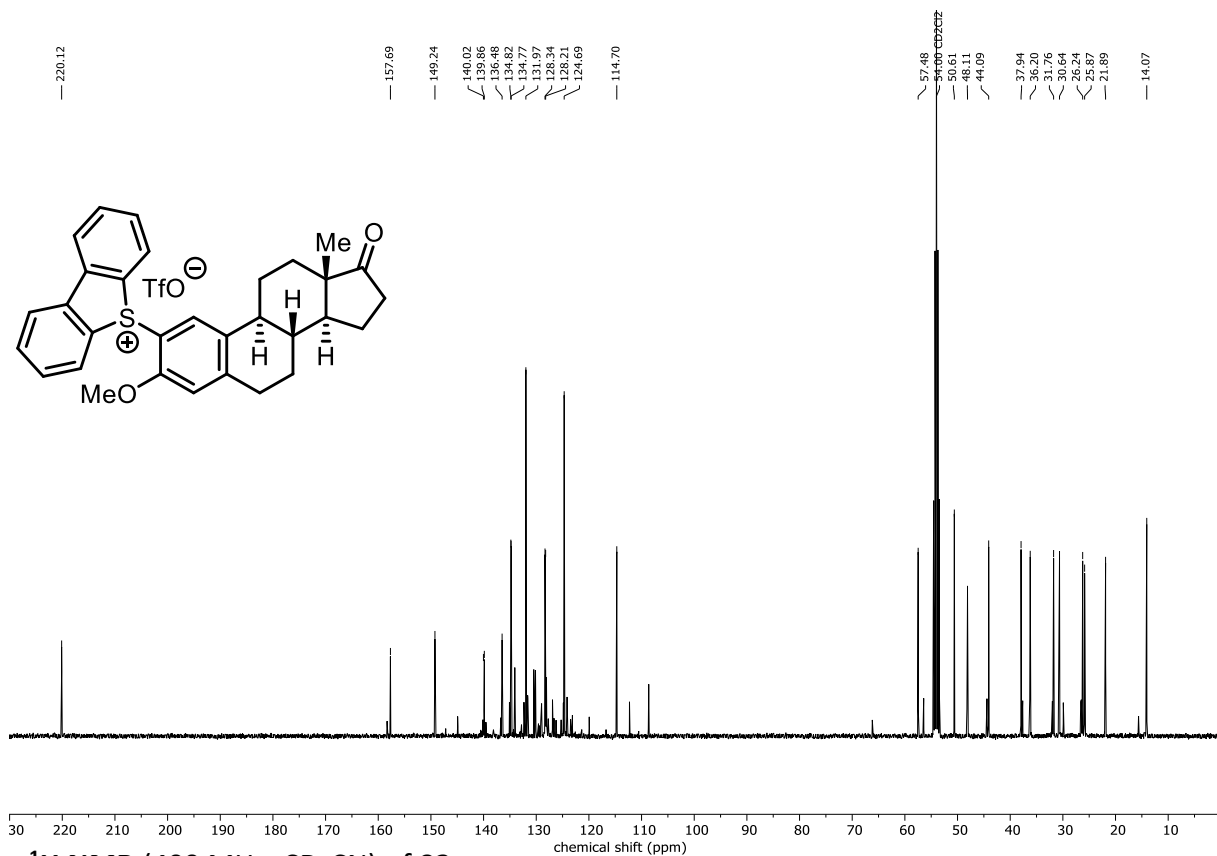
¹³C NMR (75 MHz, CD₃CN) of **93q**



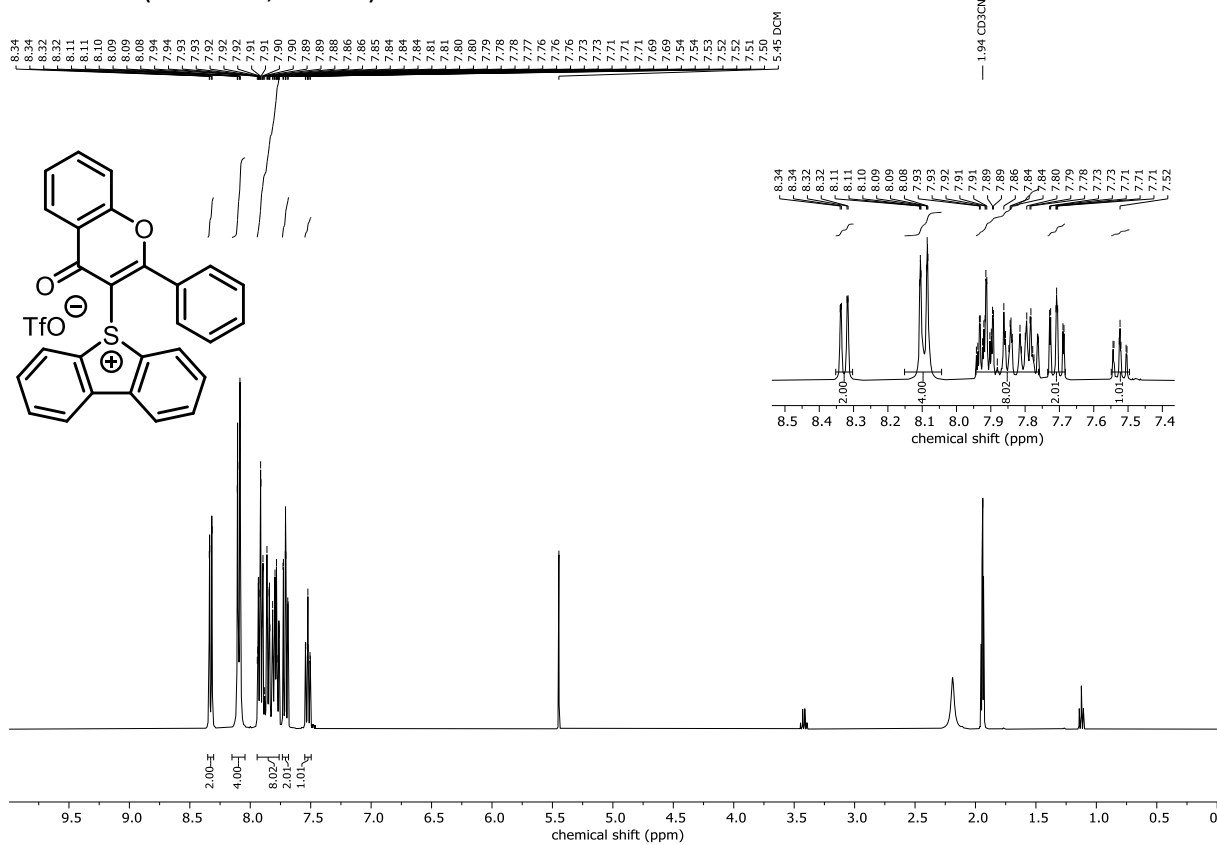
¹H NMR (400 MHz, CD₃CN) of **93r**



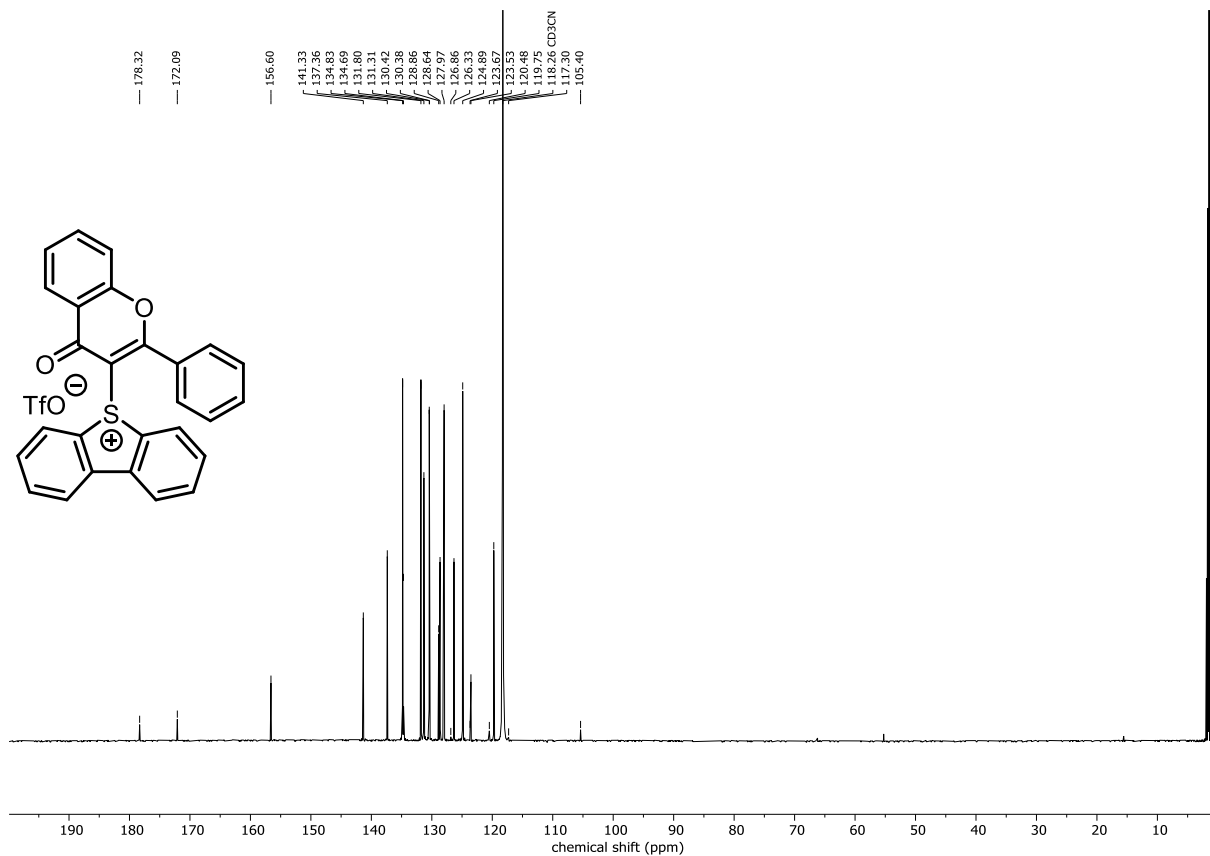
¹³C NMR (101 MHz, CD₃CN) of 93r



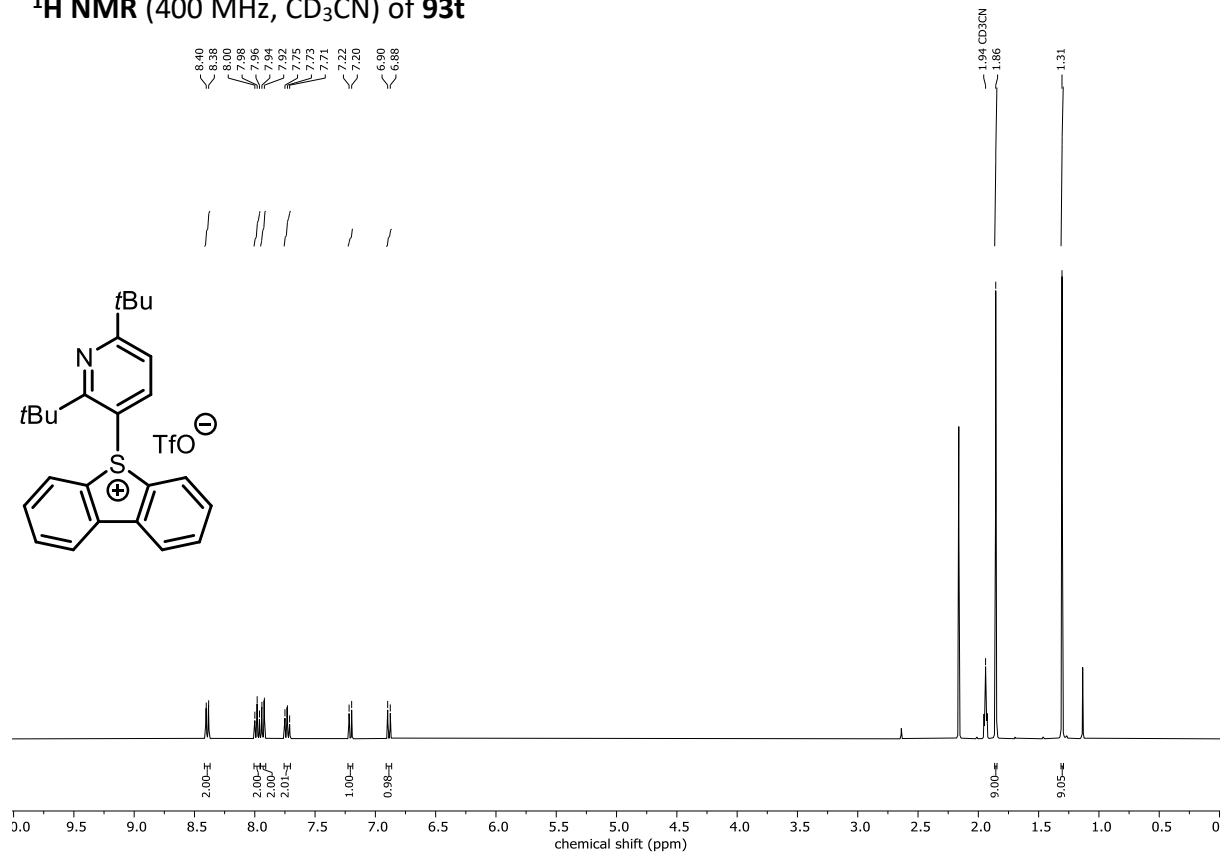
¹H NMR (400 MHz, CD₃CN) of 93s



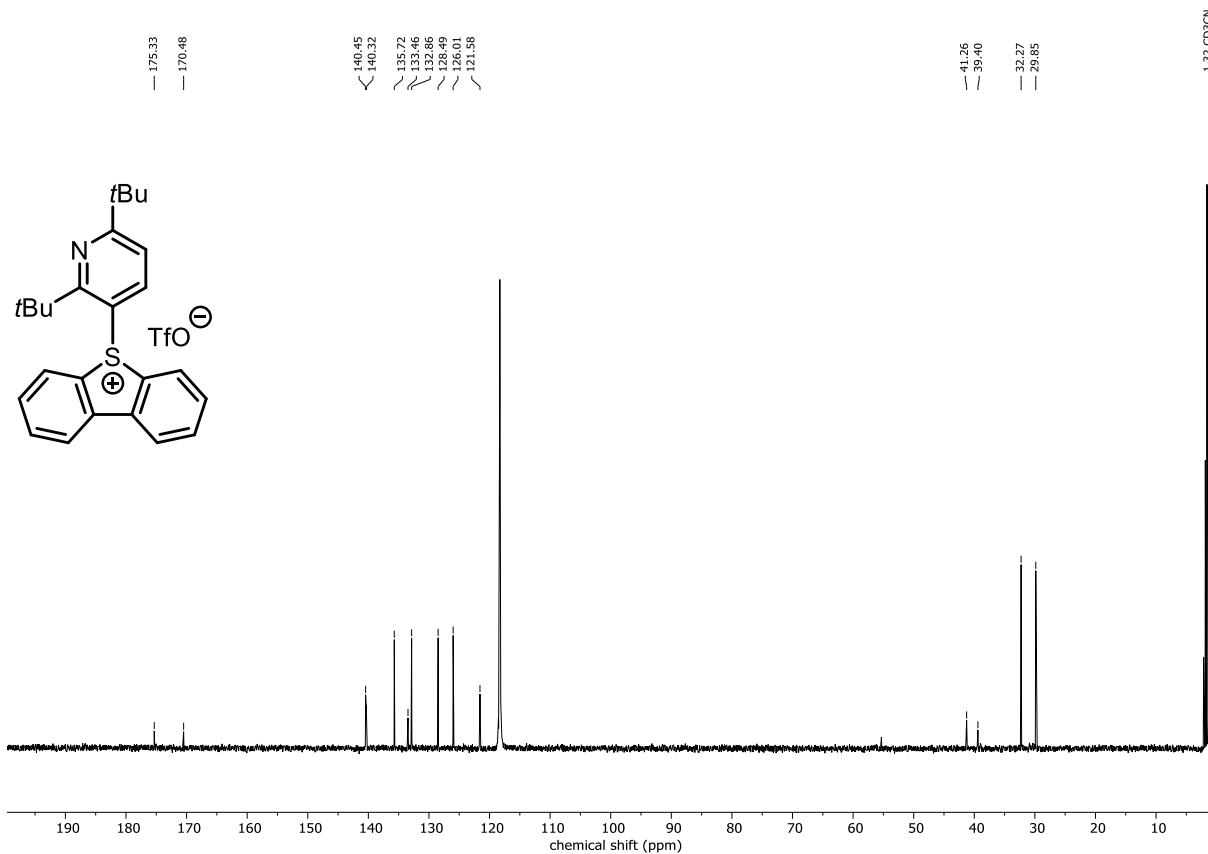
¹³C NMR (101 MHz, CD₃CN) of 93s



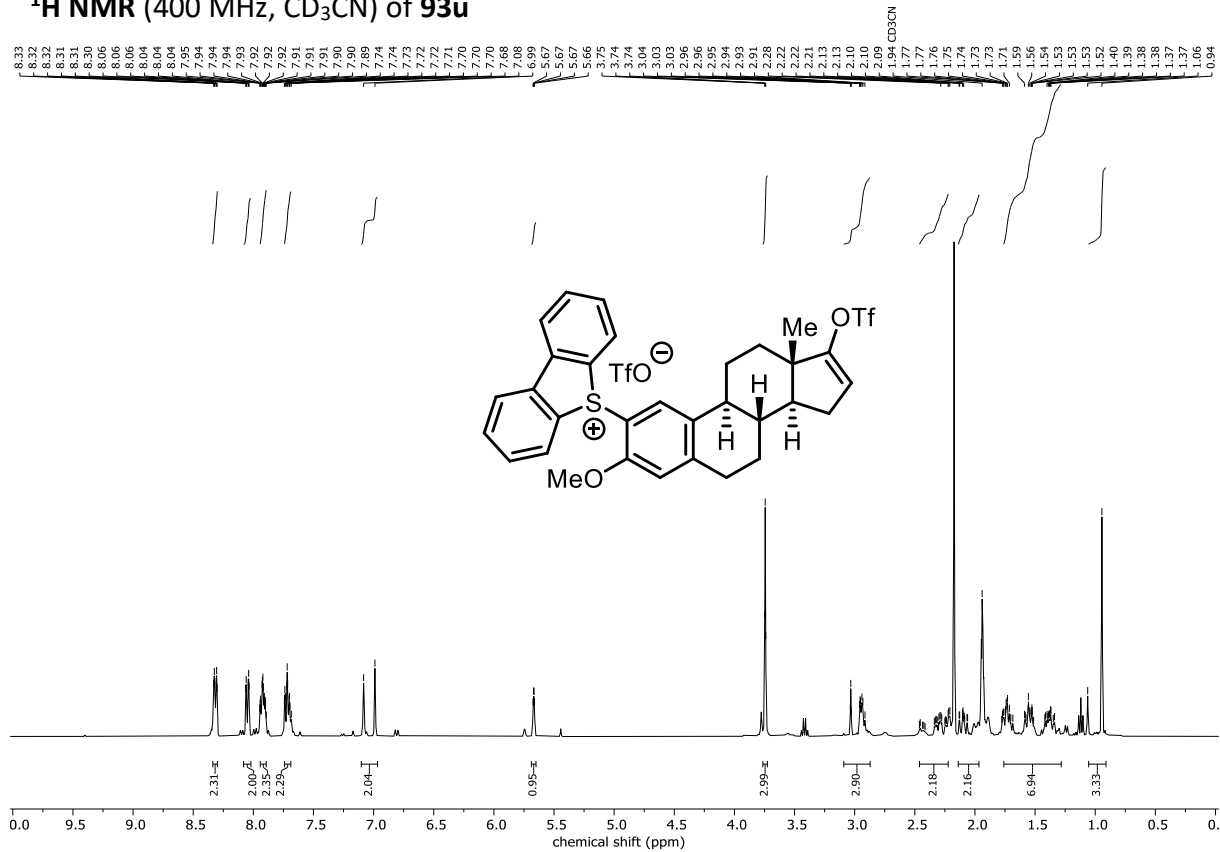
¹H NMR (400 MHz, CD₃CN) of 93t



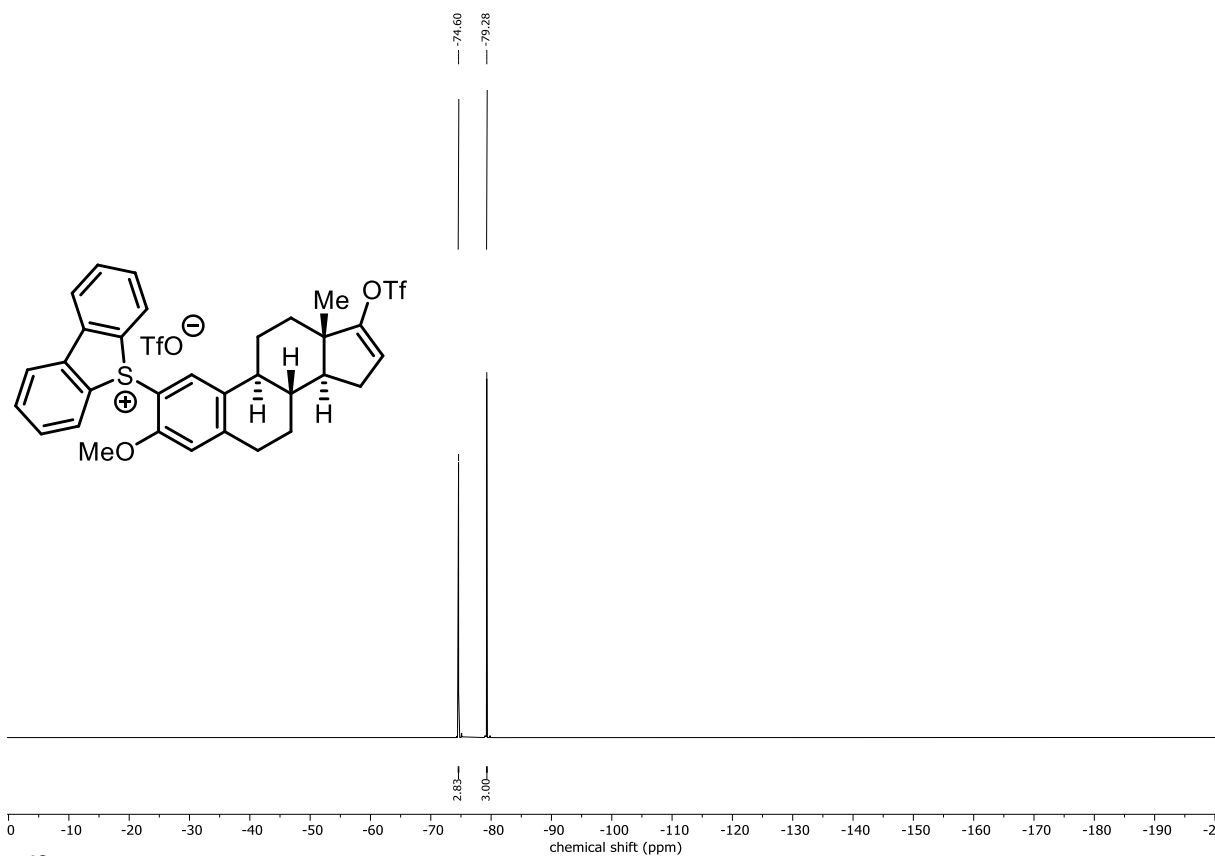
¹³C NMR (101 MHz, CD₃CN) of 93t



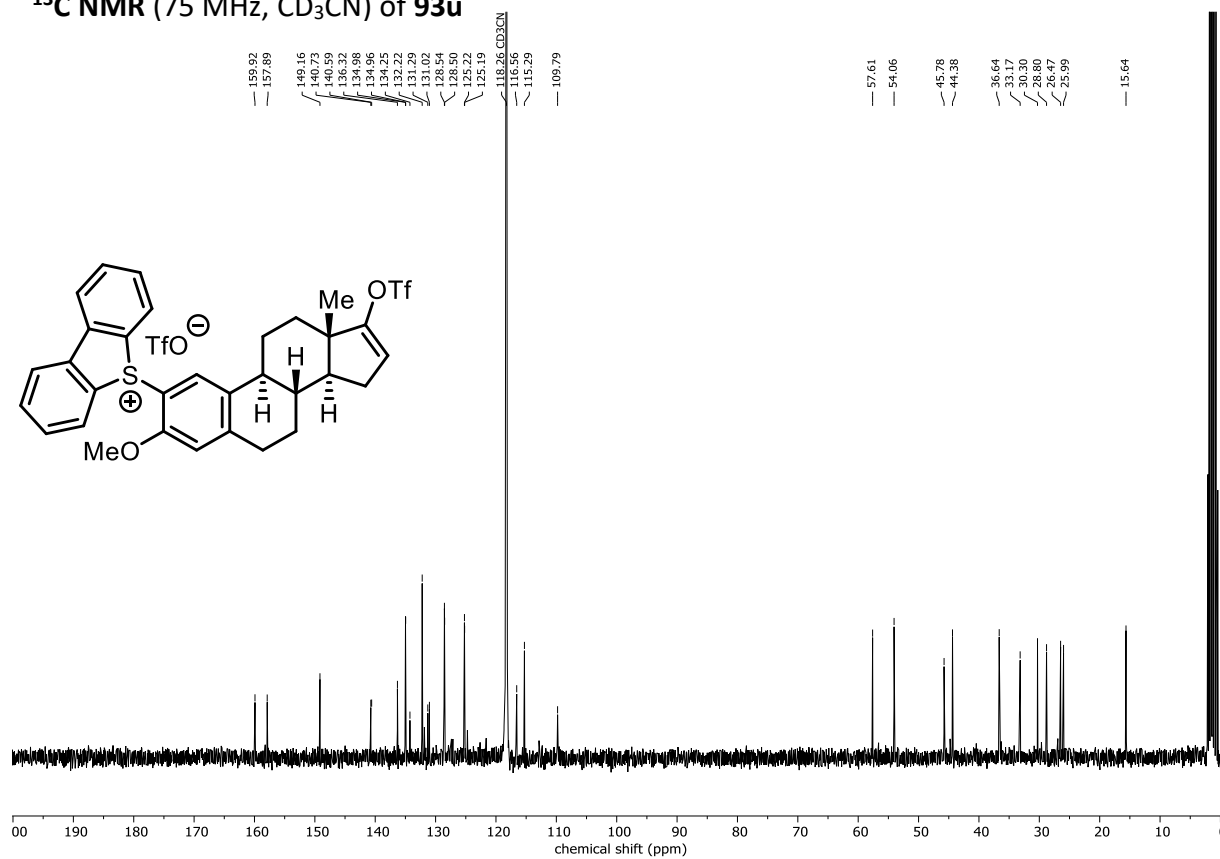
¹H NMR (400 MHz, CD₃CN) of 93u



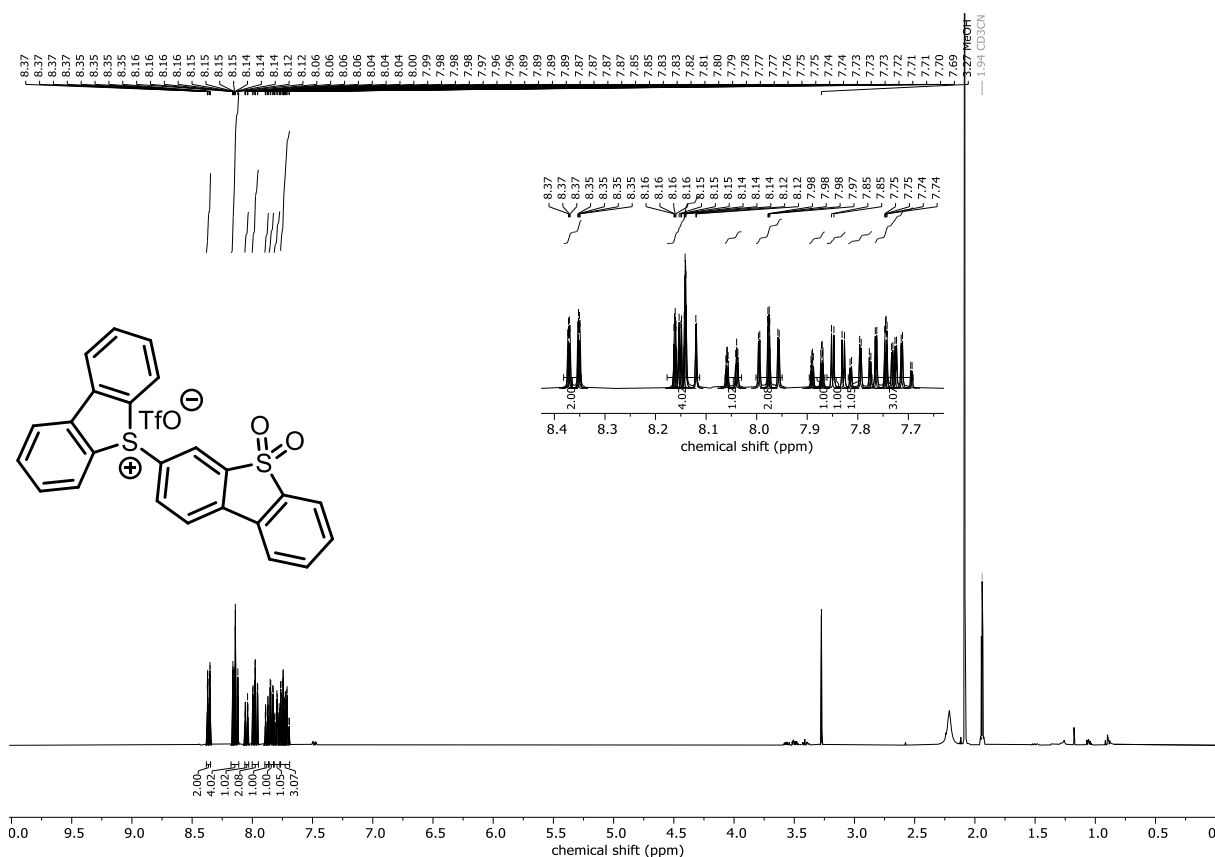
¹⁹F NMR (377 MHz, CD₃CN) of 93u



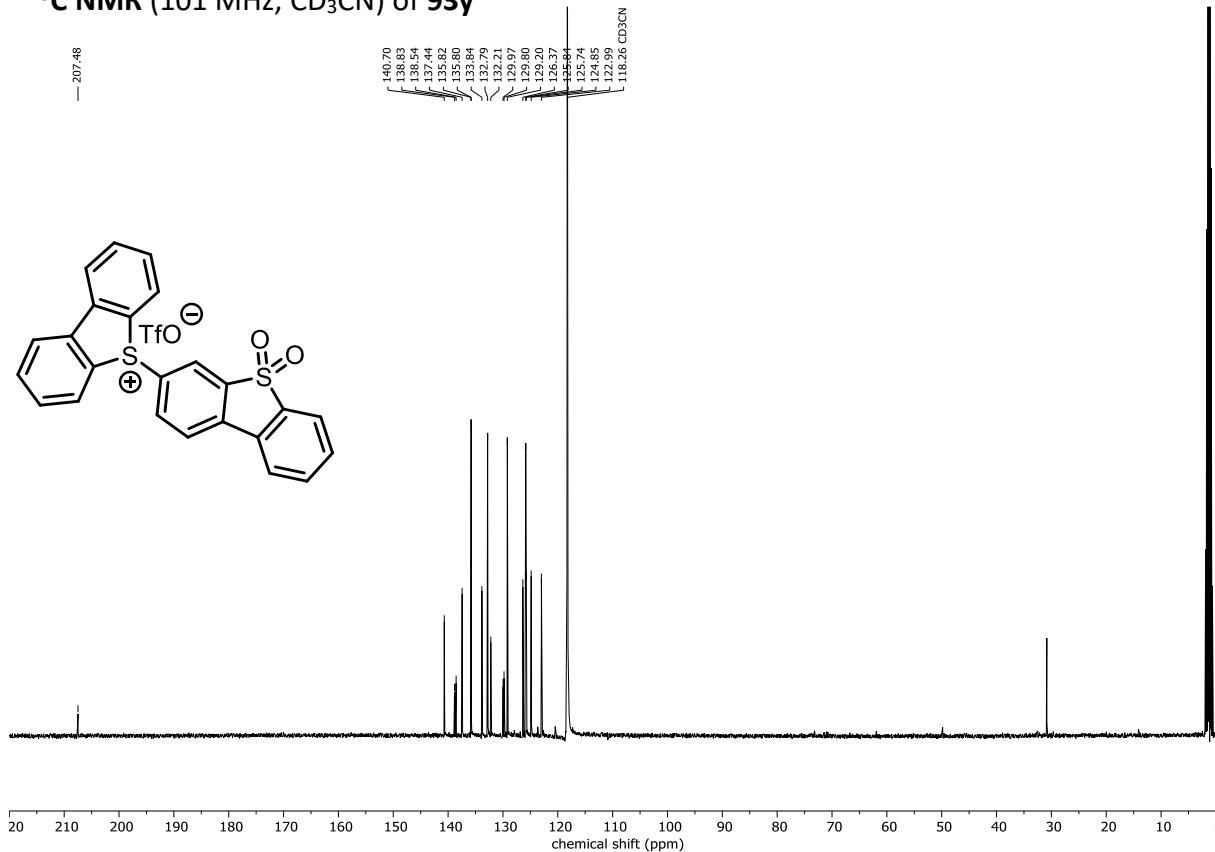
¹³C NMR (75 MHz, CD₃CN) of 93u



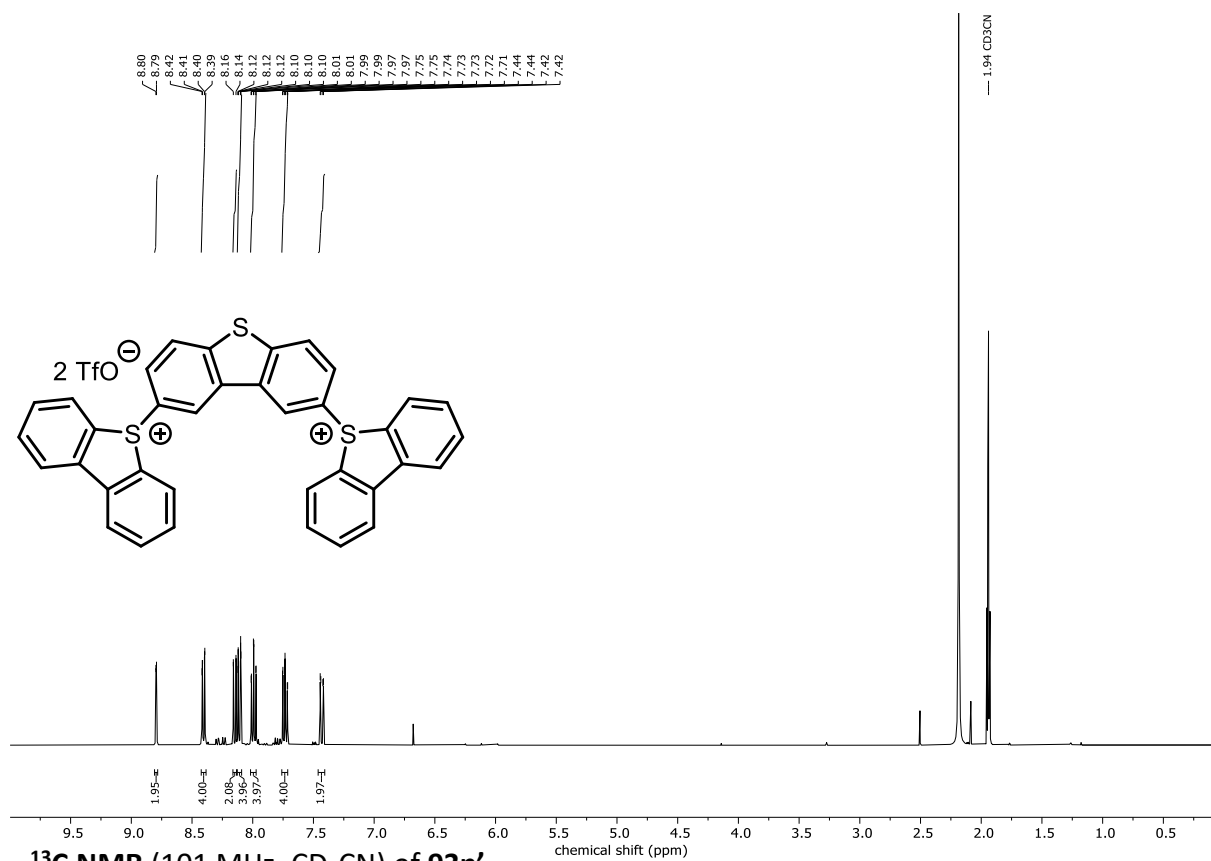
¹H NMR (400 MHz, CD₃CN) of 93y



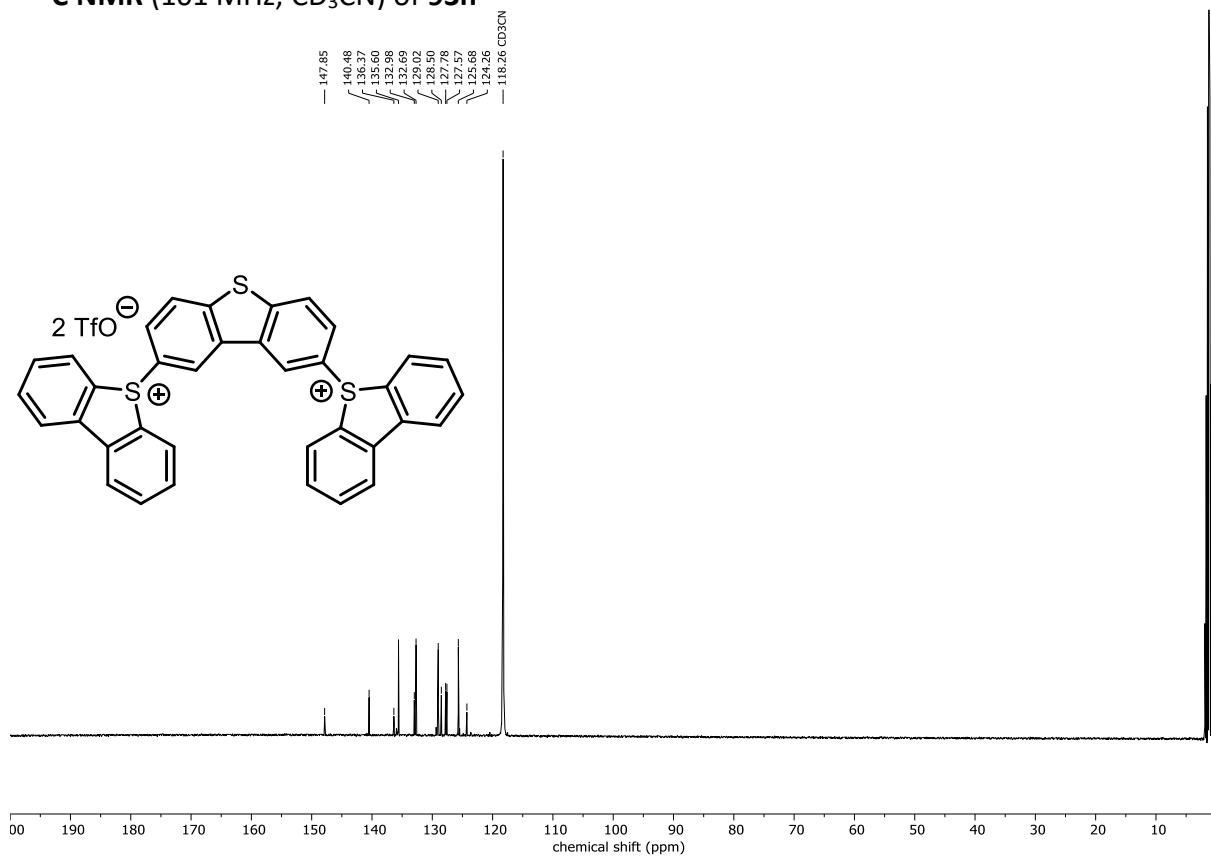
¹³C NMR (101 MHz, CD₃CN) of 93y



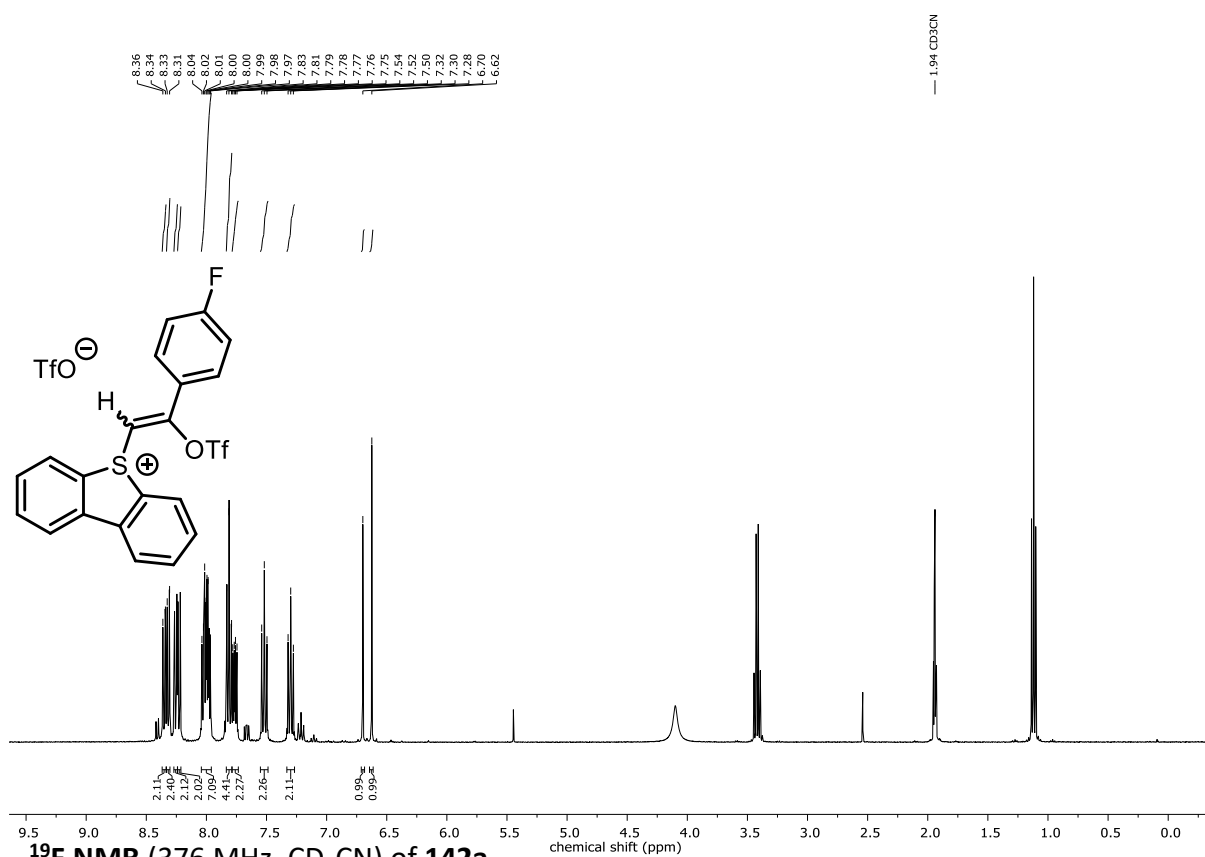
¹H NMR (400 MHz, CD₃CN) of 93n'



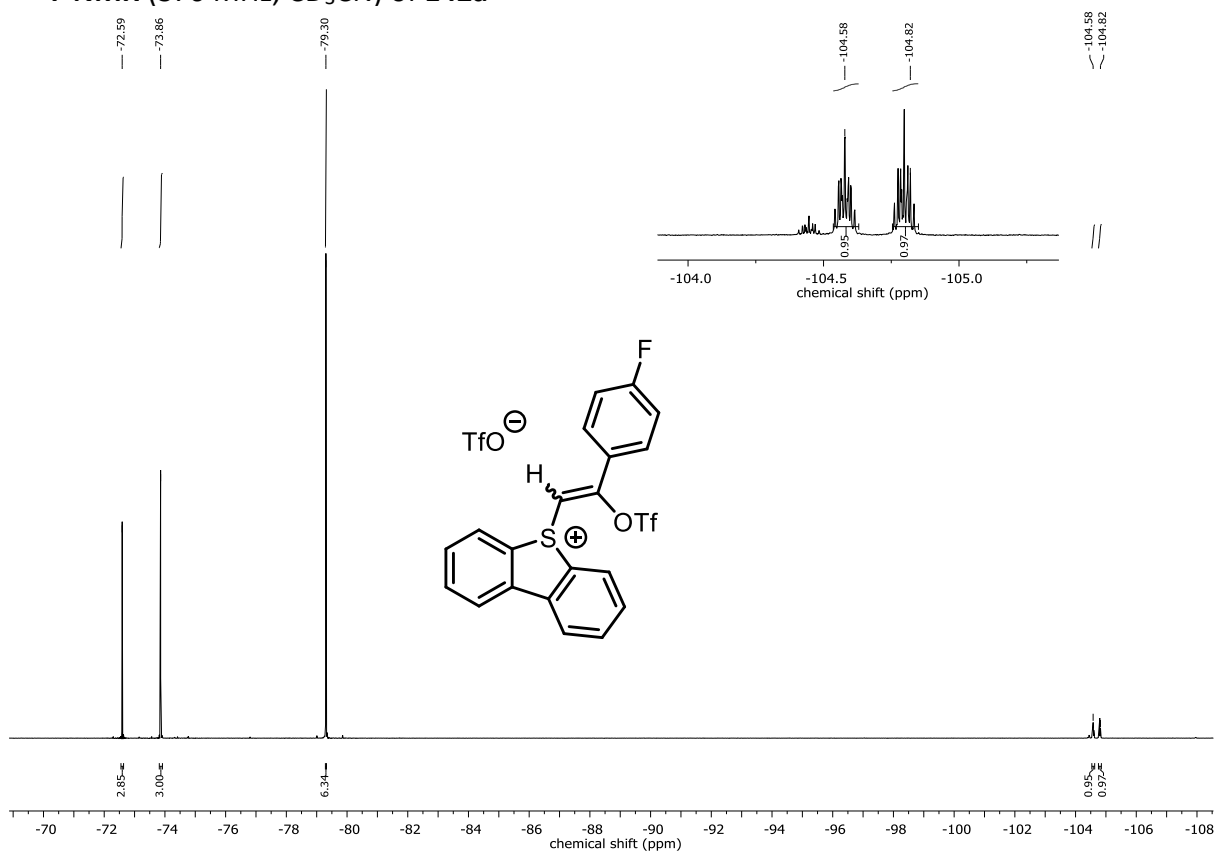
¹³C NMR (101 MHz, CD₃CN) of 93n'



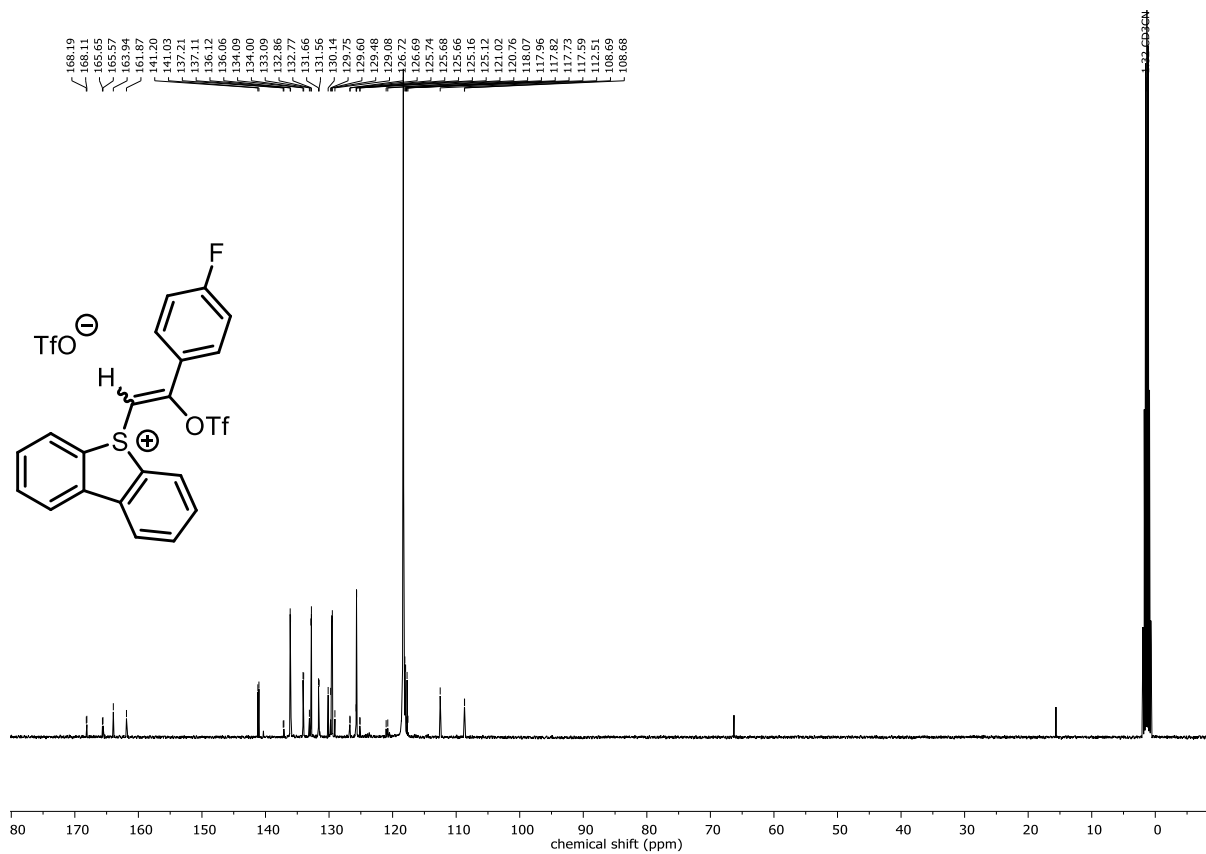
¹H NMR (400 MHz, CD₃CN) of 142a



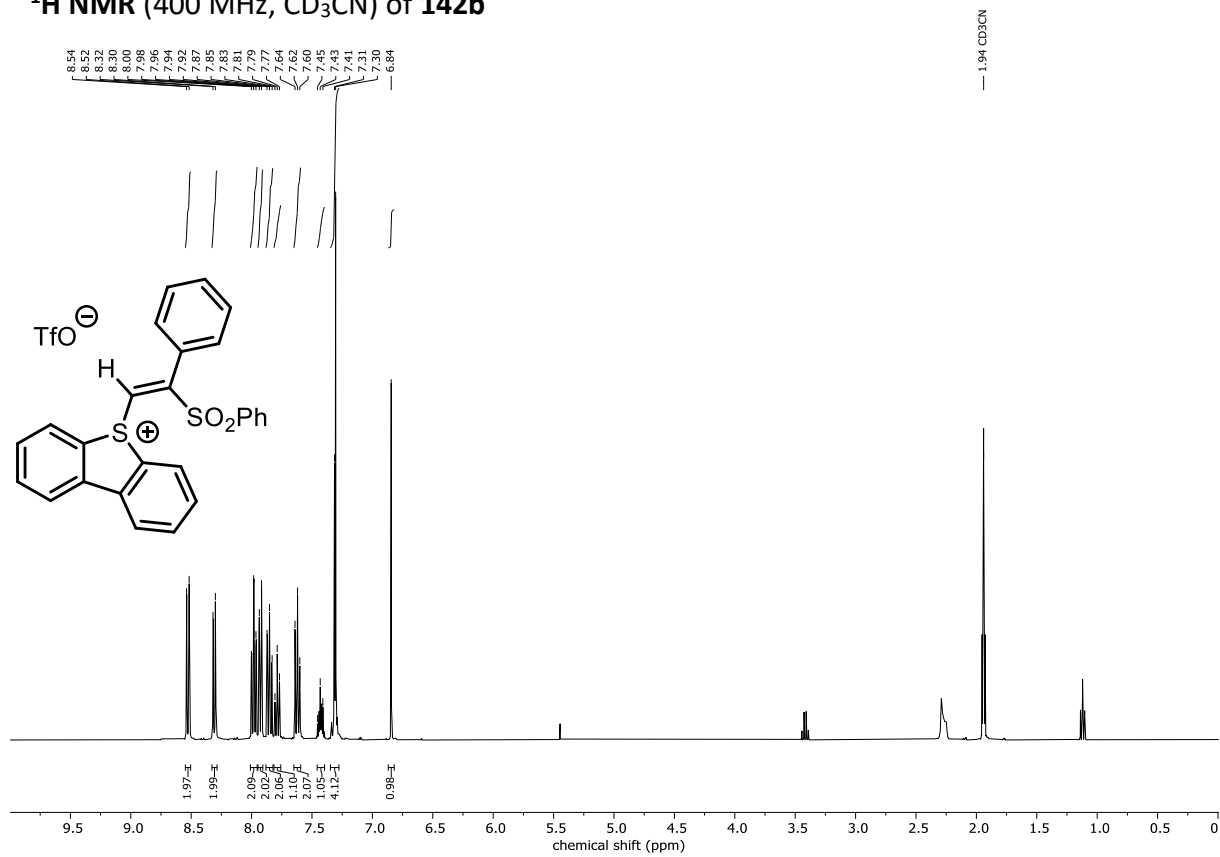
¹⁹F NMR (376 MHz, CD₃CN) of 142a



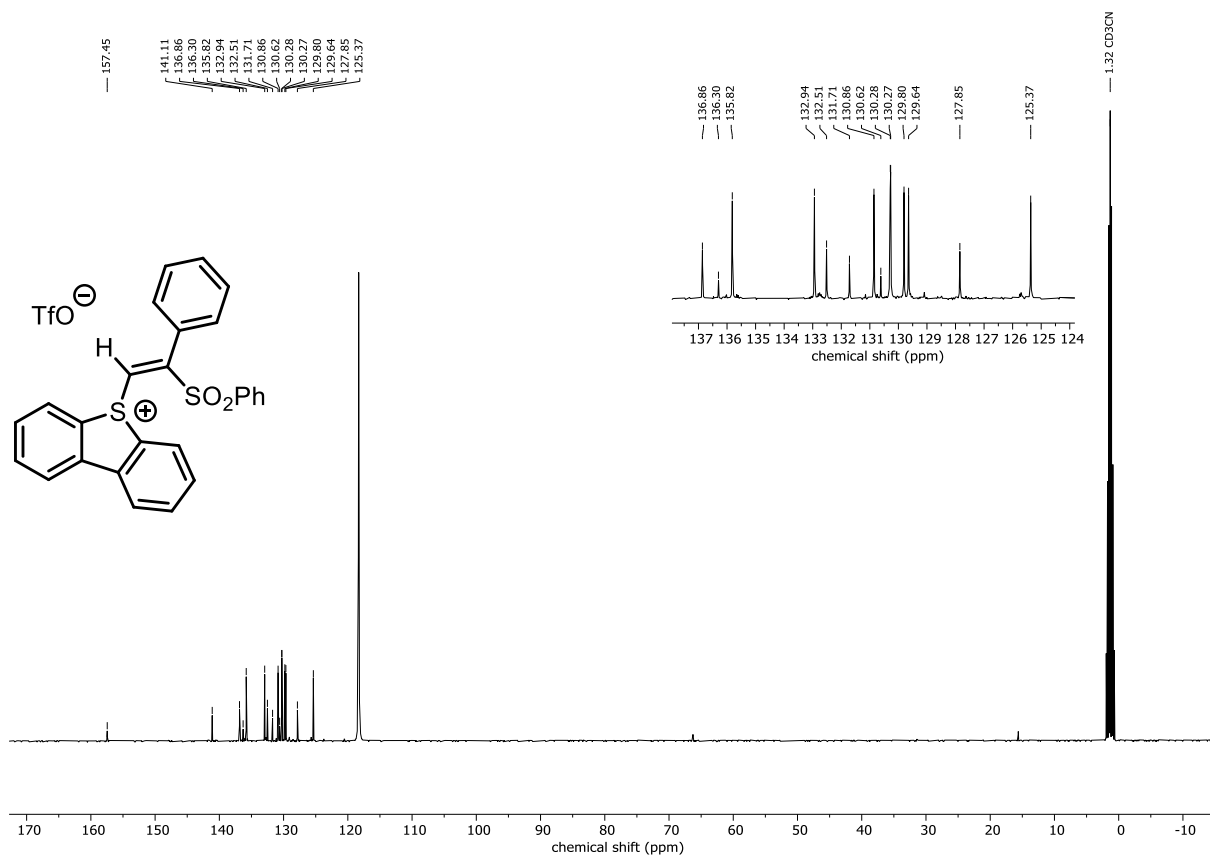
¹³C NMR (101 MHz, CD₃CN) of 142a



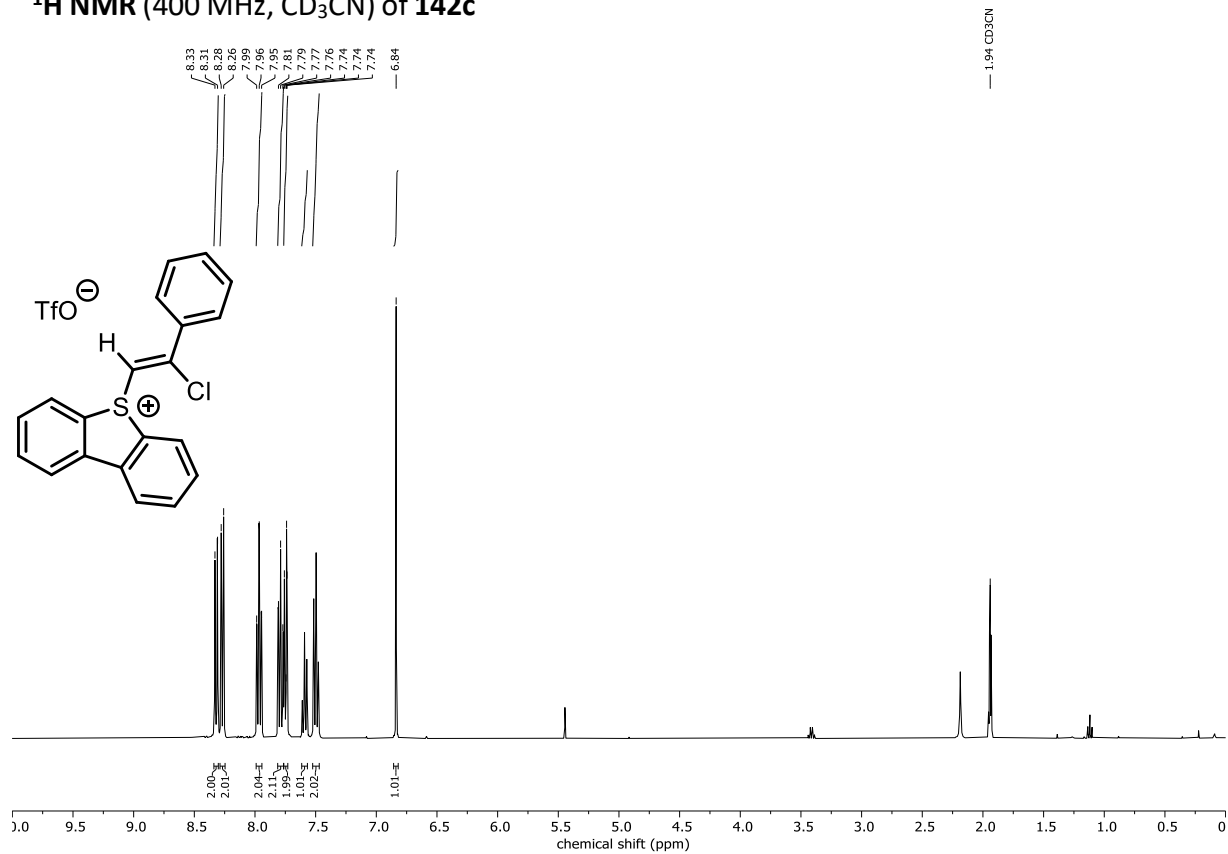
¹H NMR (400 MHz, CD₃CN) of 142b



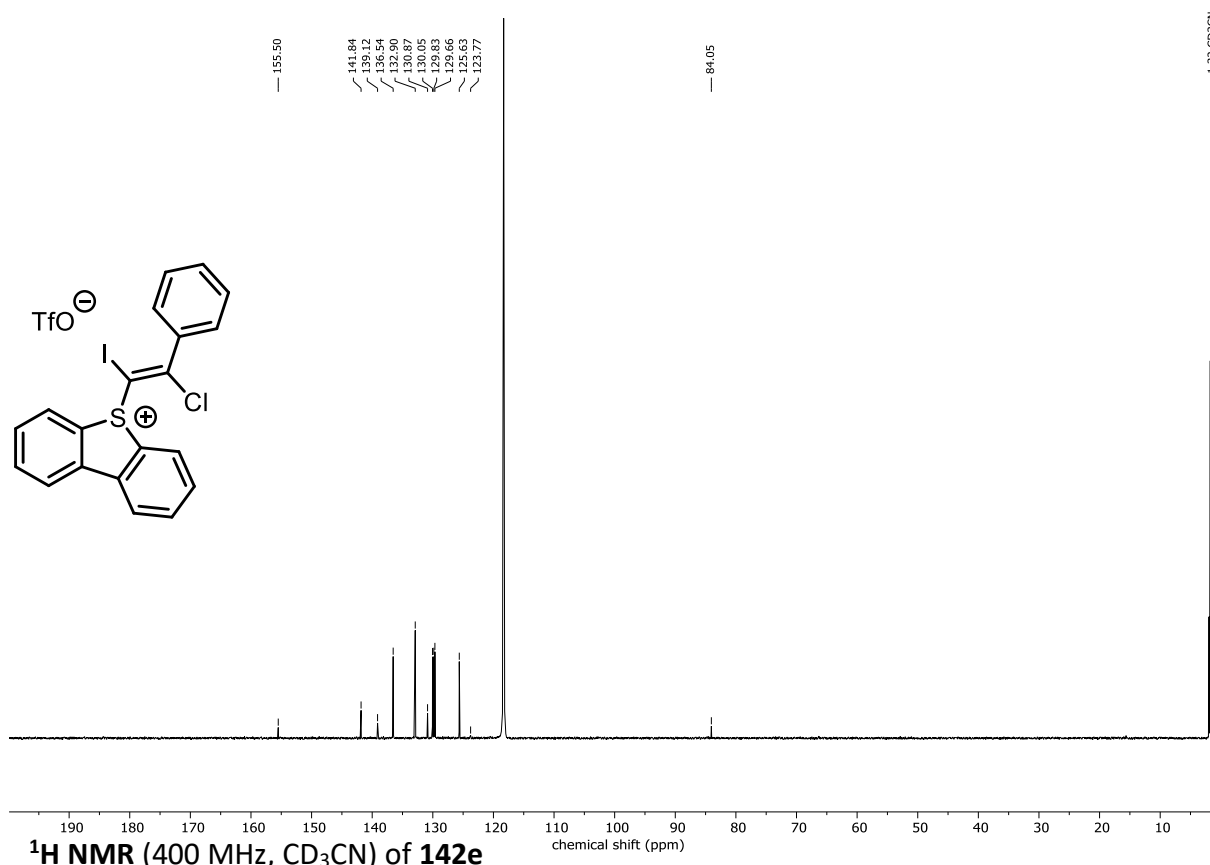
¹³C NMR (101 MHz, CD₃CN) of 142b



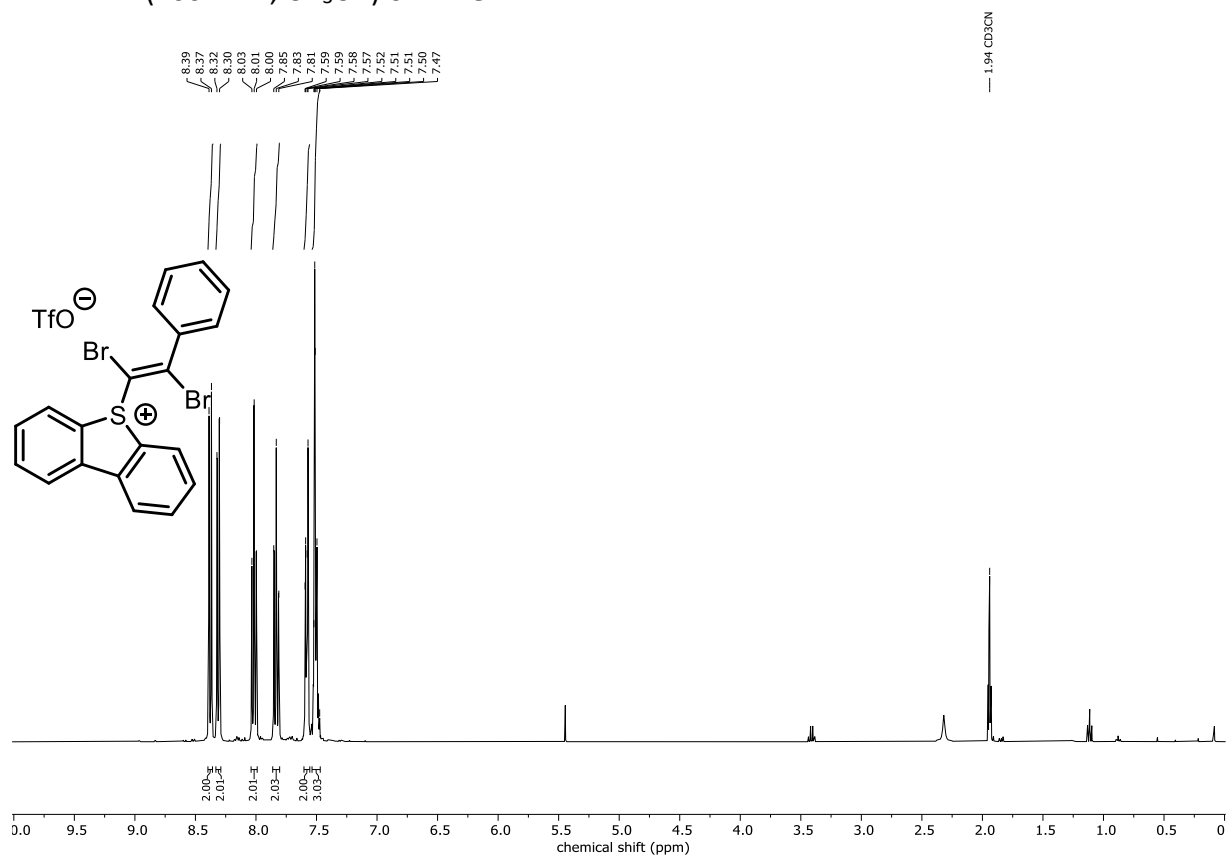
¹H NMR (400 MHz, CD₃CN) of 142c



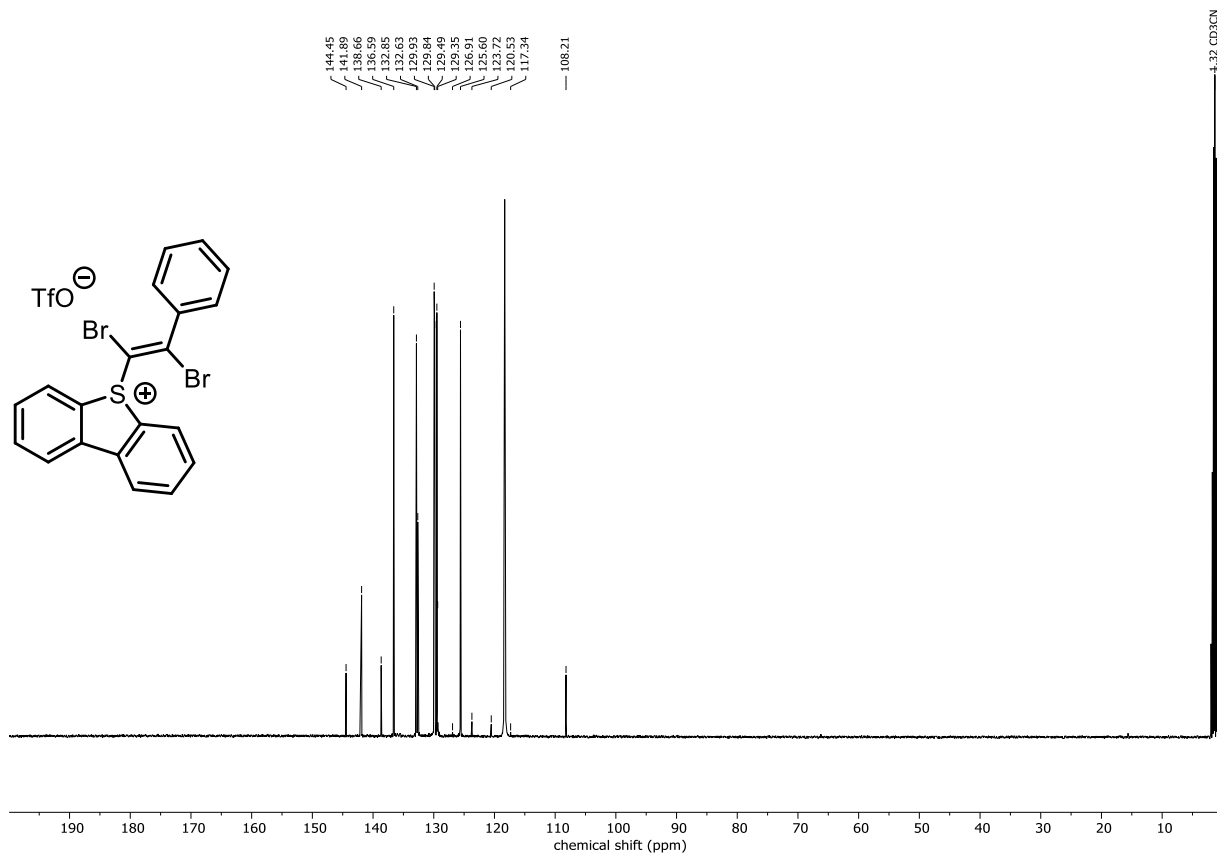
¹³C NMR (101 MHz, CD₃CN) of 142d



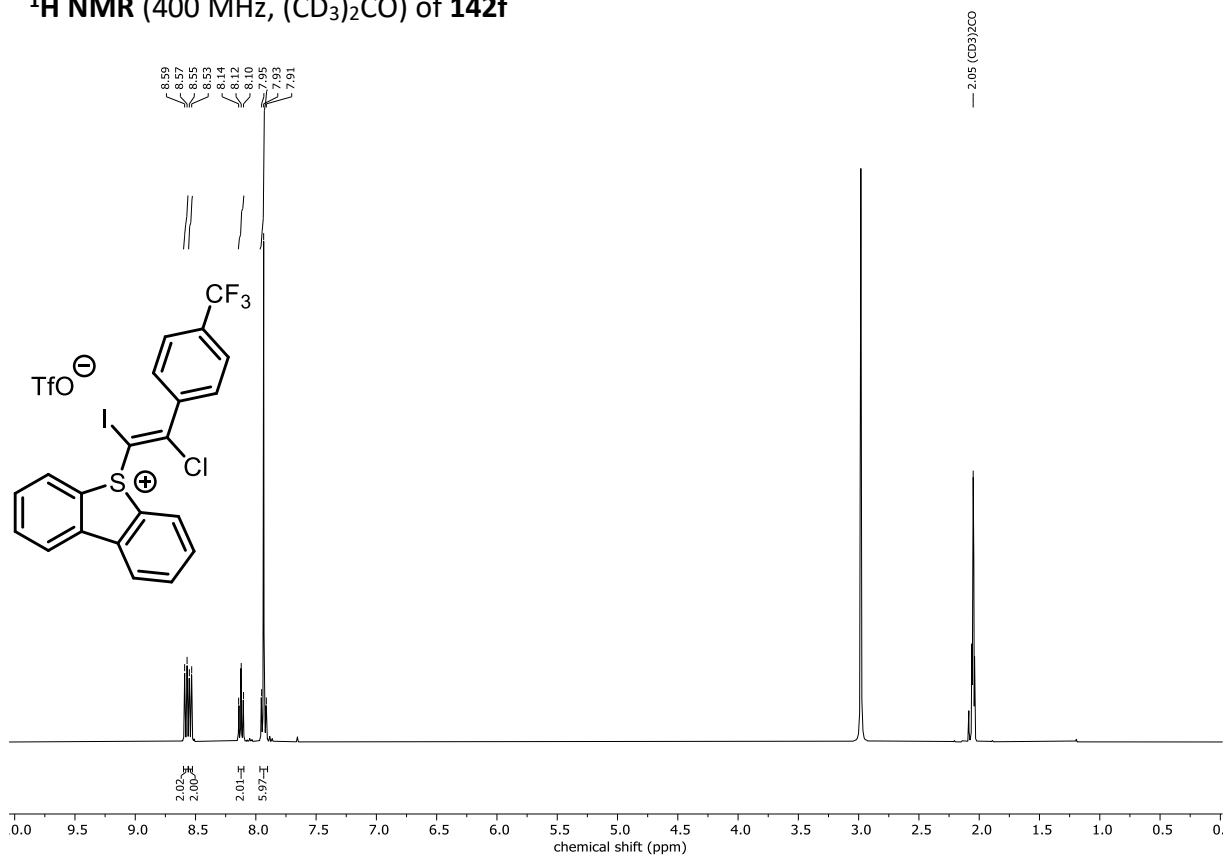
¹H NMR (400 MHz, CD₃CN) of 142e



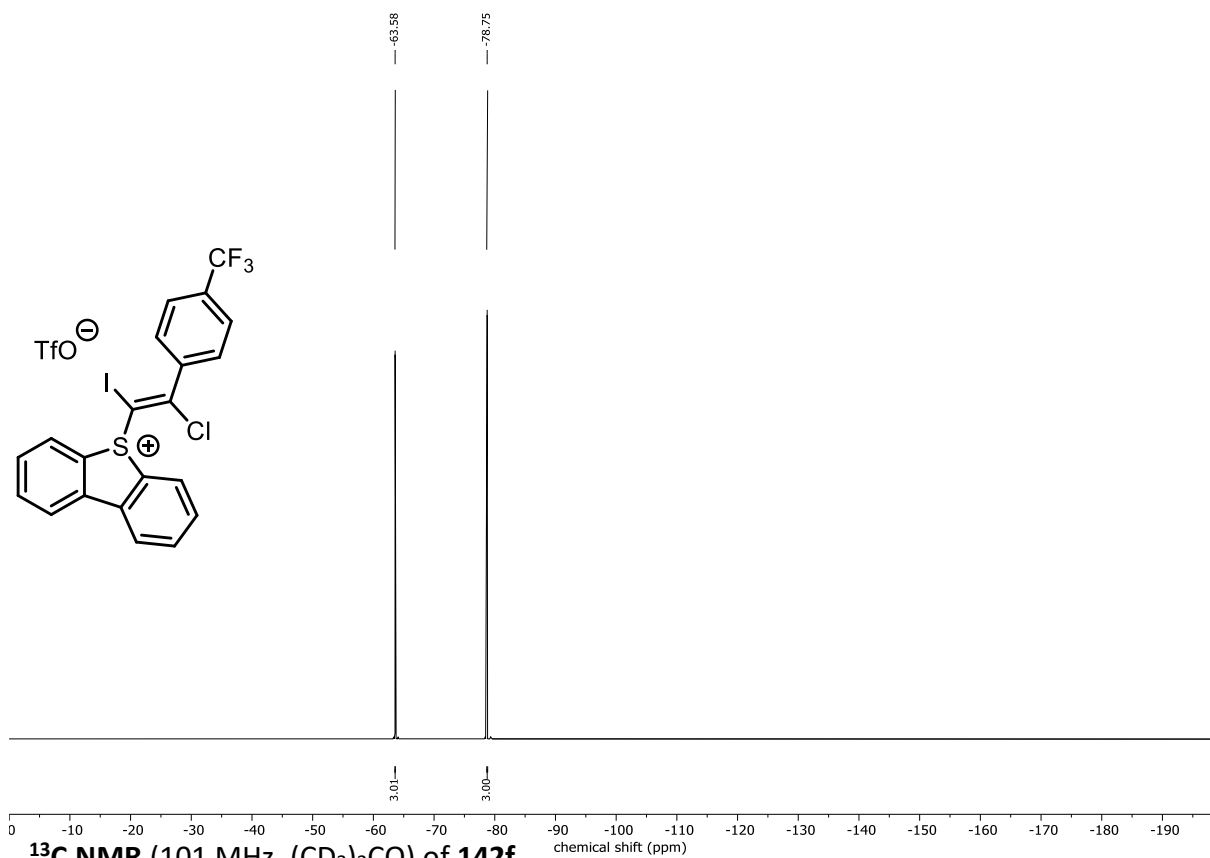
¹³C NMR (101 MHz, CD₃CN) of 142e



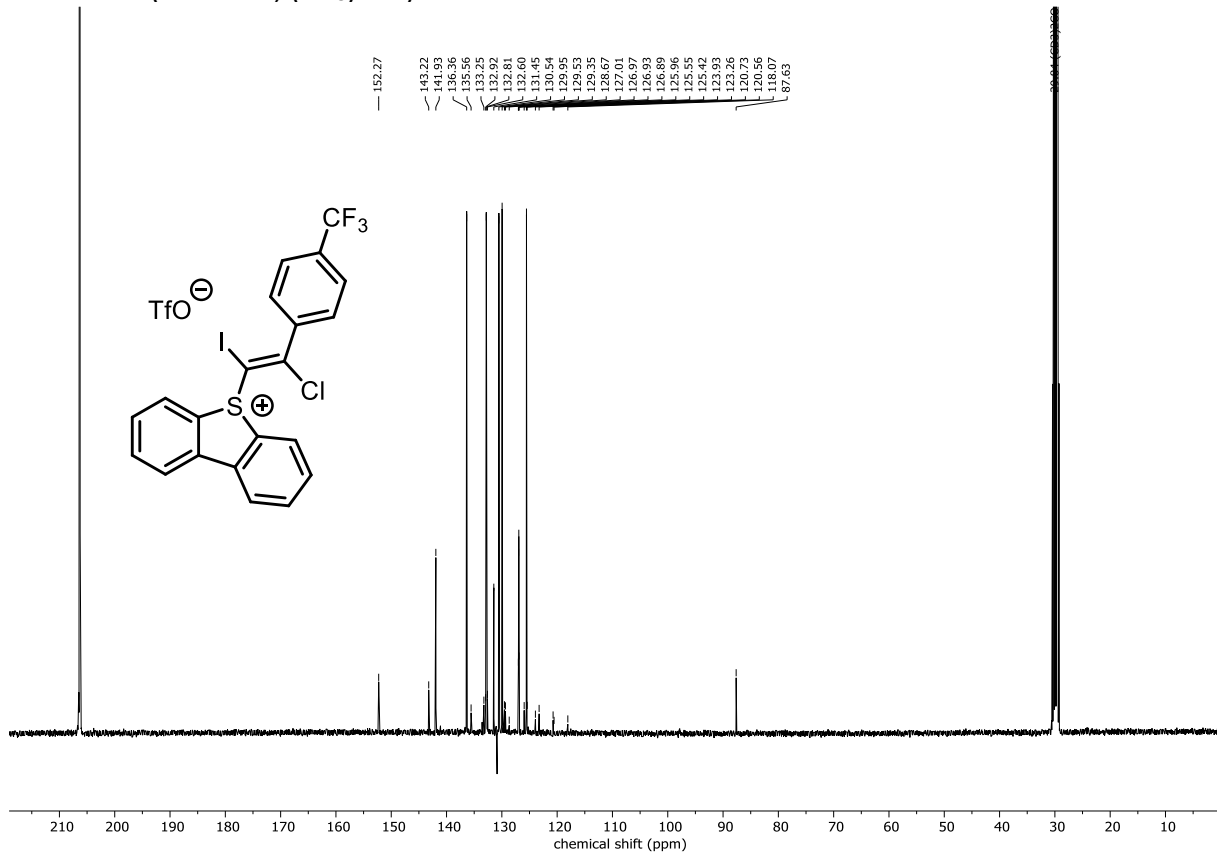
¹H NMR (400 MHz, (CD₃)₂CO) of 142f



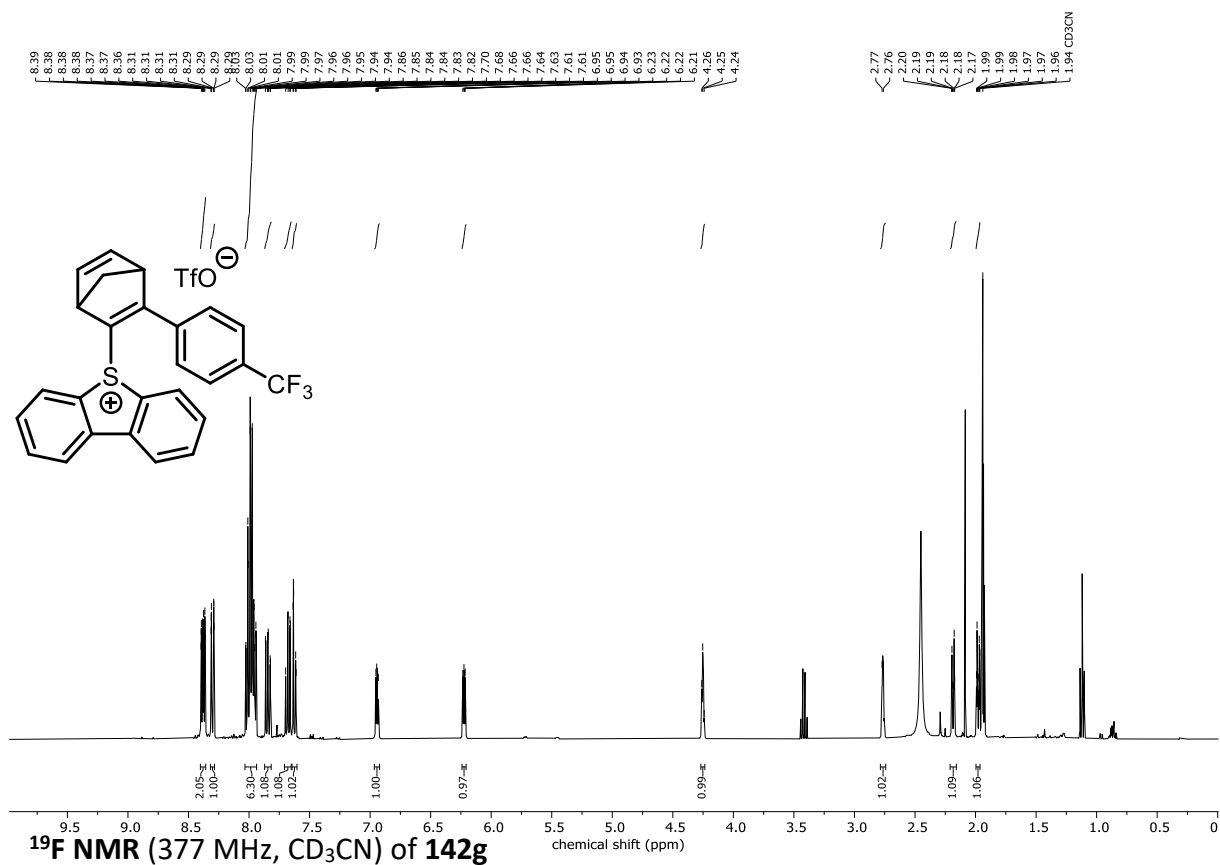
¹⁹F NMR (377 MHz, (CD₃)₂CO) of 142f



¹³C NMR (101 MHz, (CD₃)₂CO) of 142f



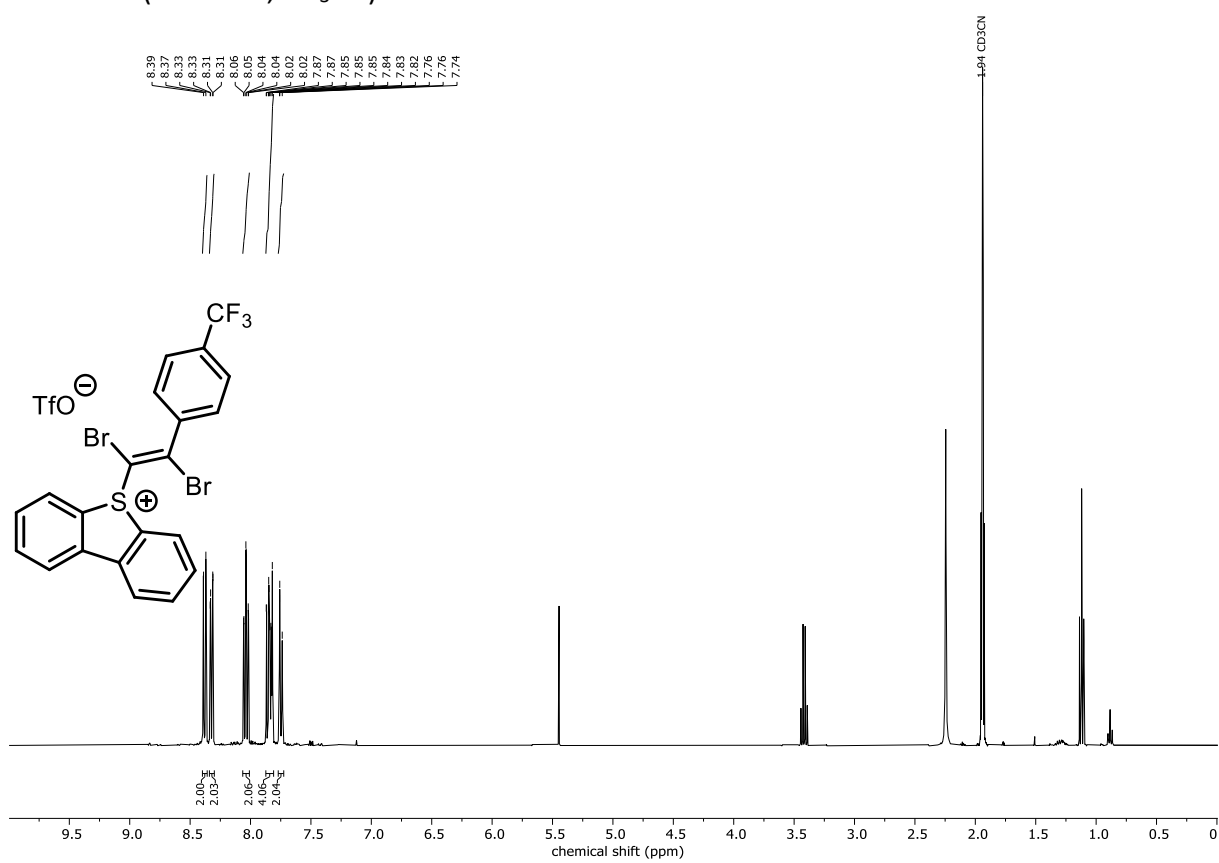
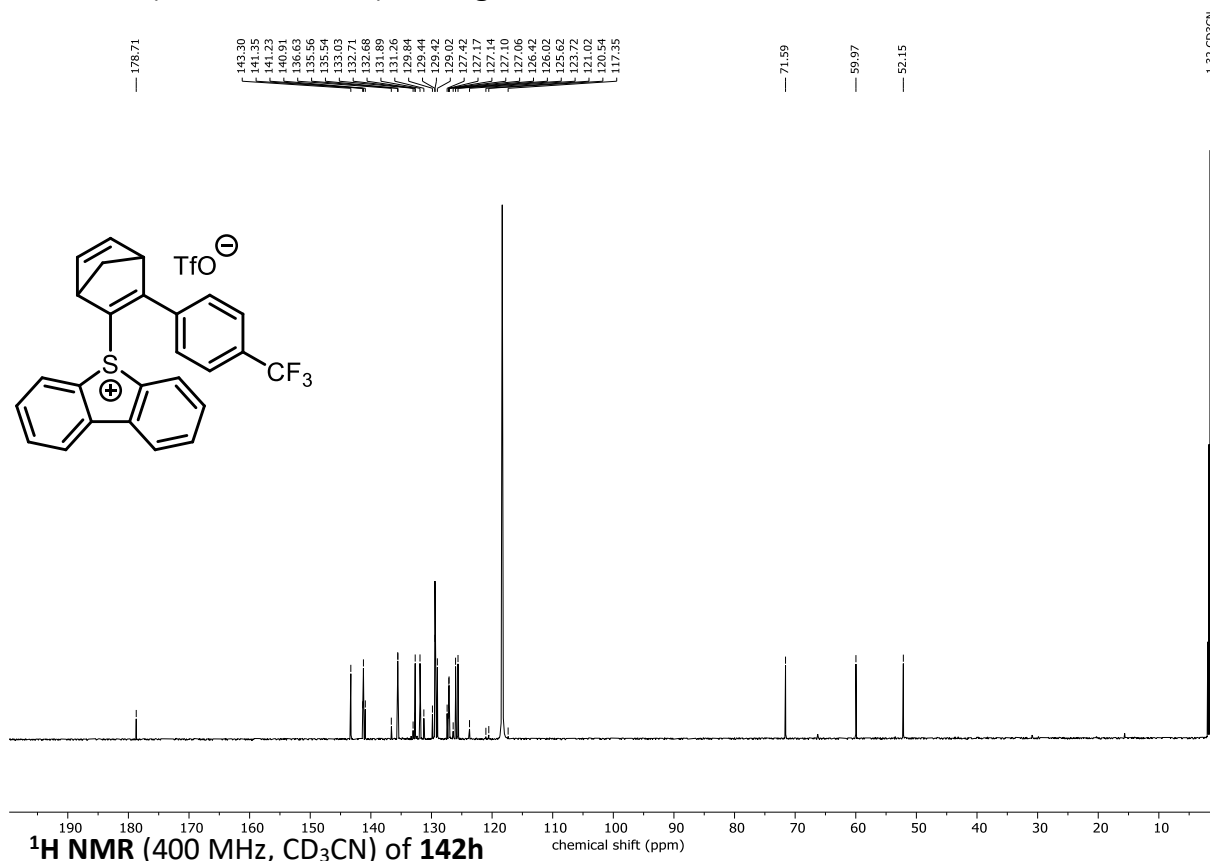
¹H NMR (400 MHz, CD₃CN) of 142g



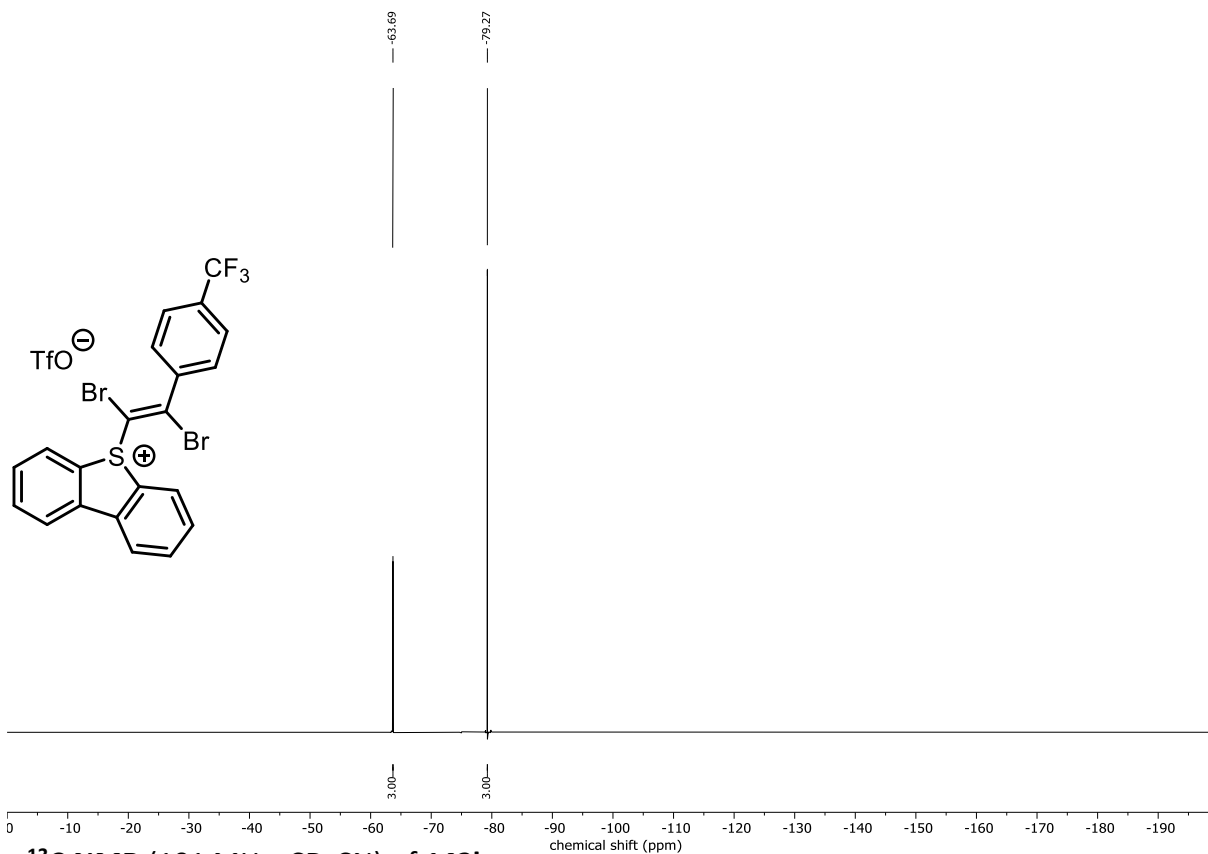
¹⁹F NMR (377 MHz, CD₃CN) of 142g



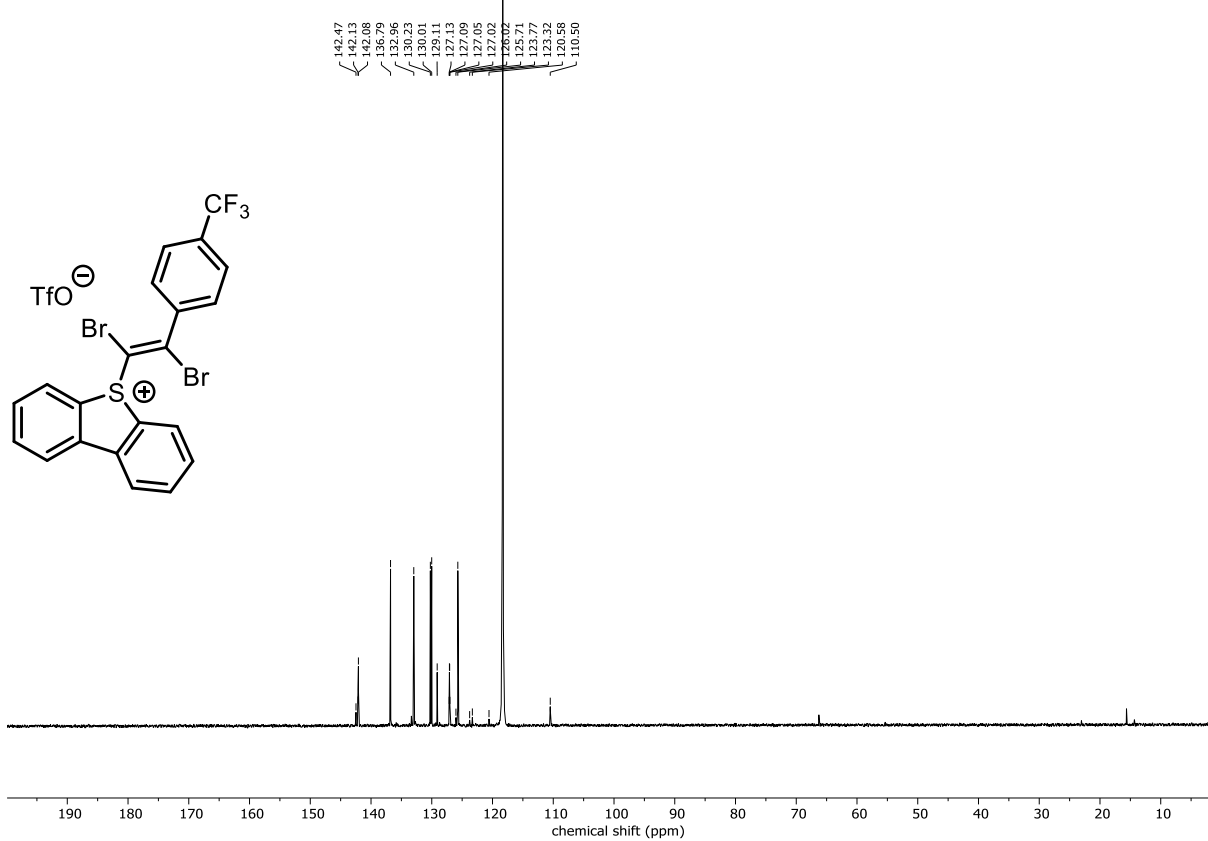
¹³C NMR (101 MHz, CD₃CN) of 142g



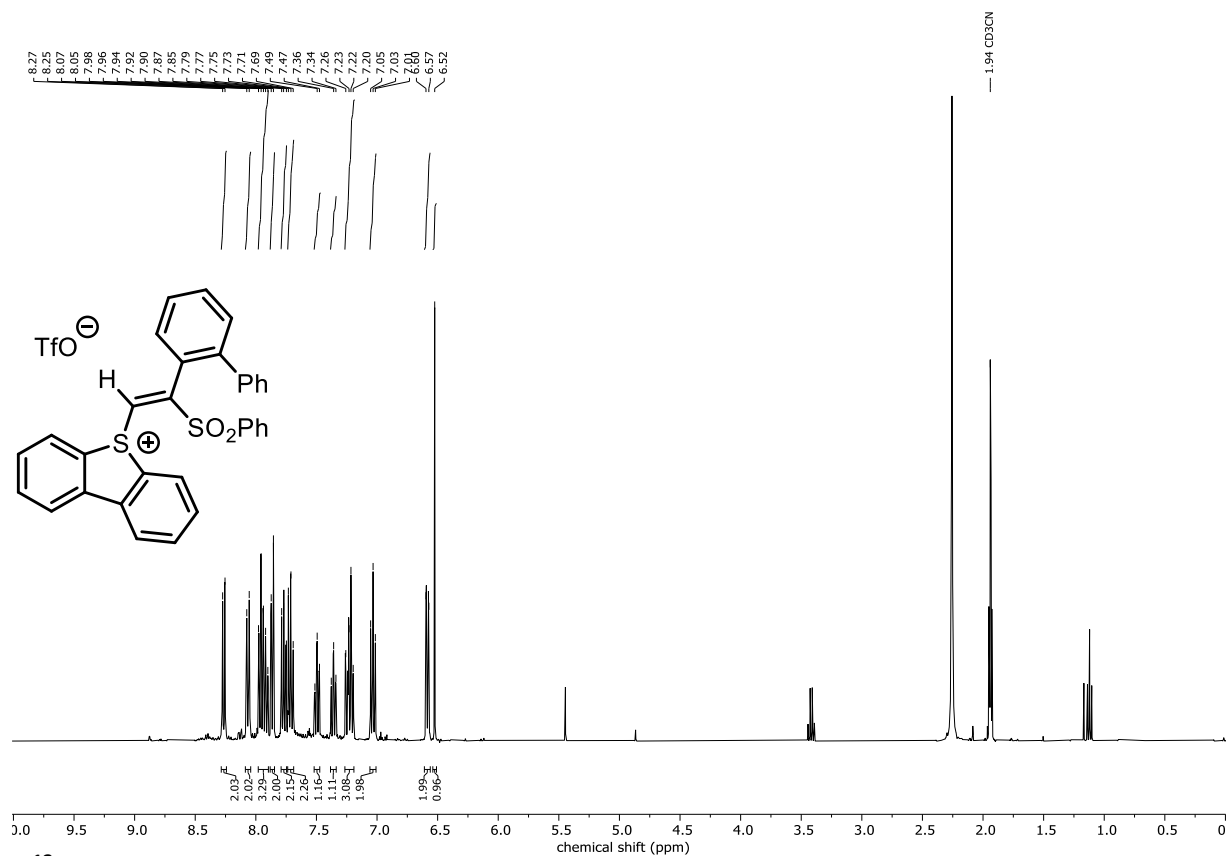
¹⁹F NMR (377 MHz, CD₃CN) of 142h



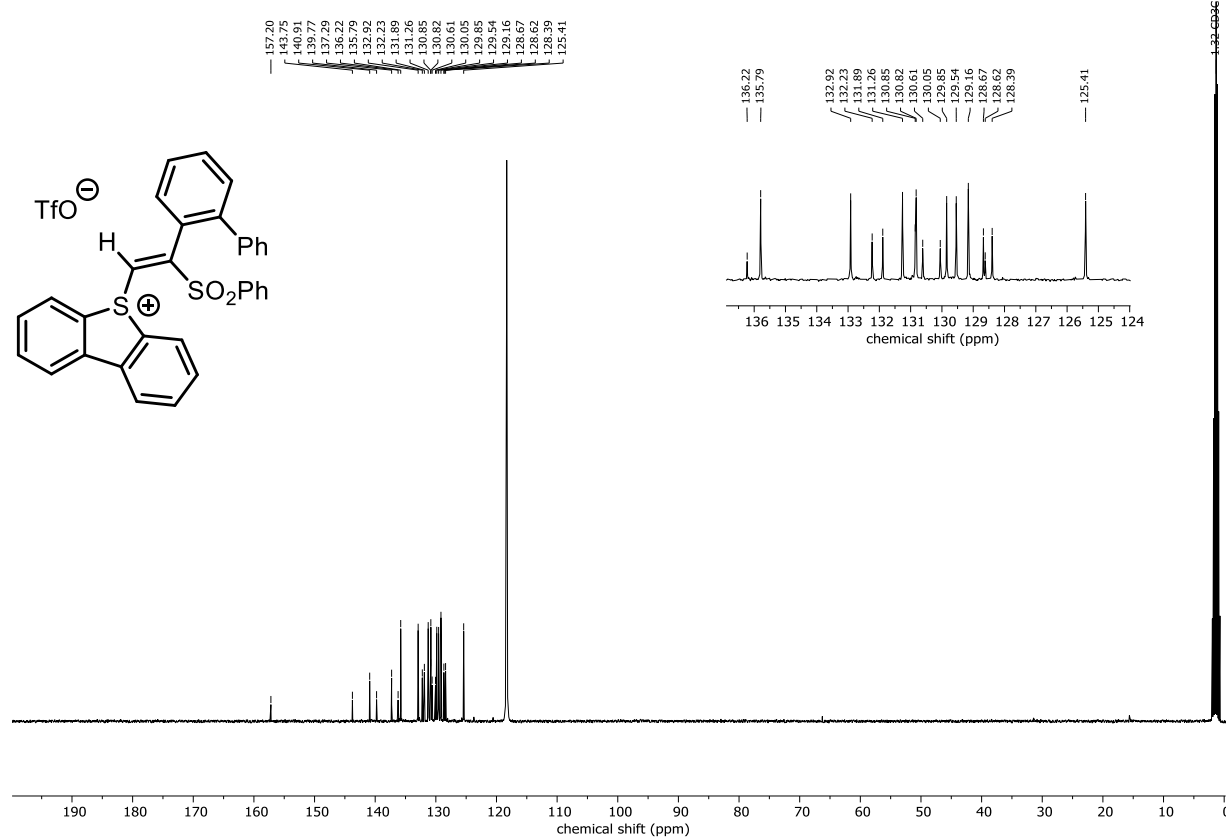
¹³C NMR (101 MHz, CD₃CN) of 142h



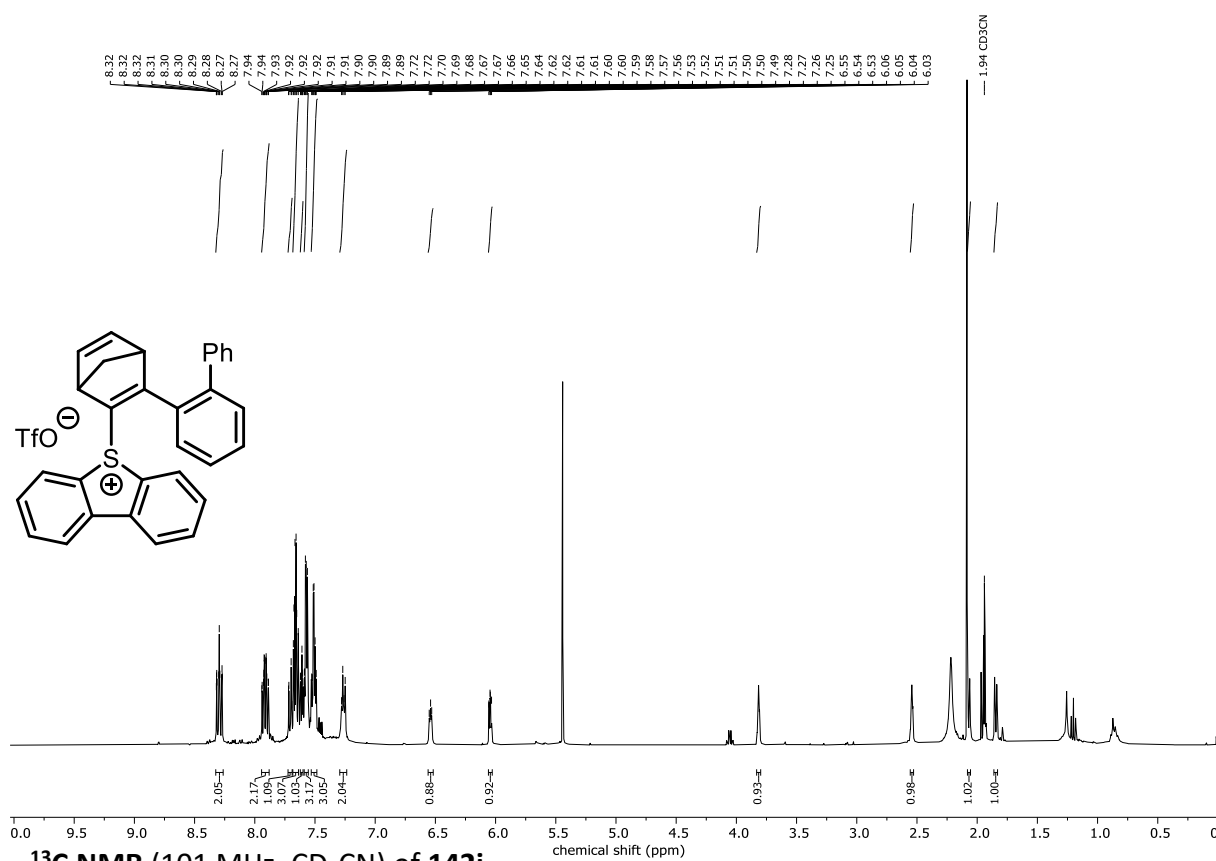
¹H NMR (400 MHz, CD₃CN) of 142i



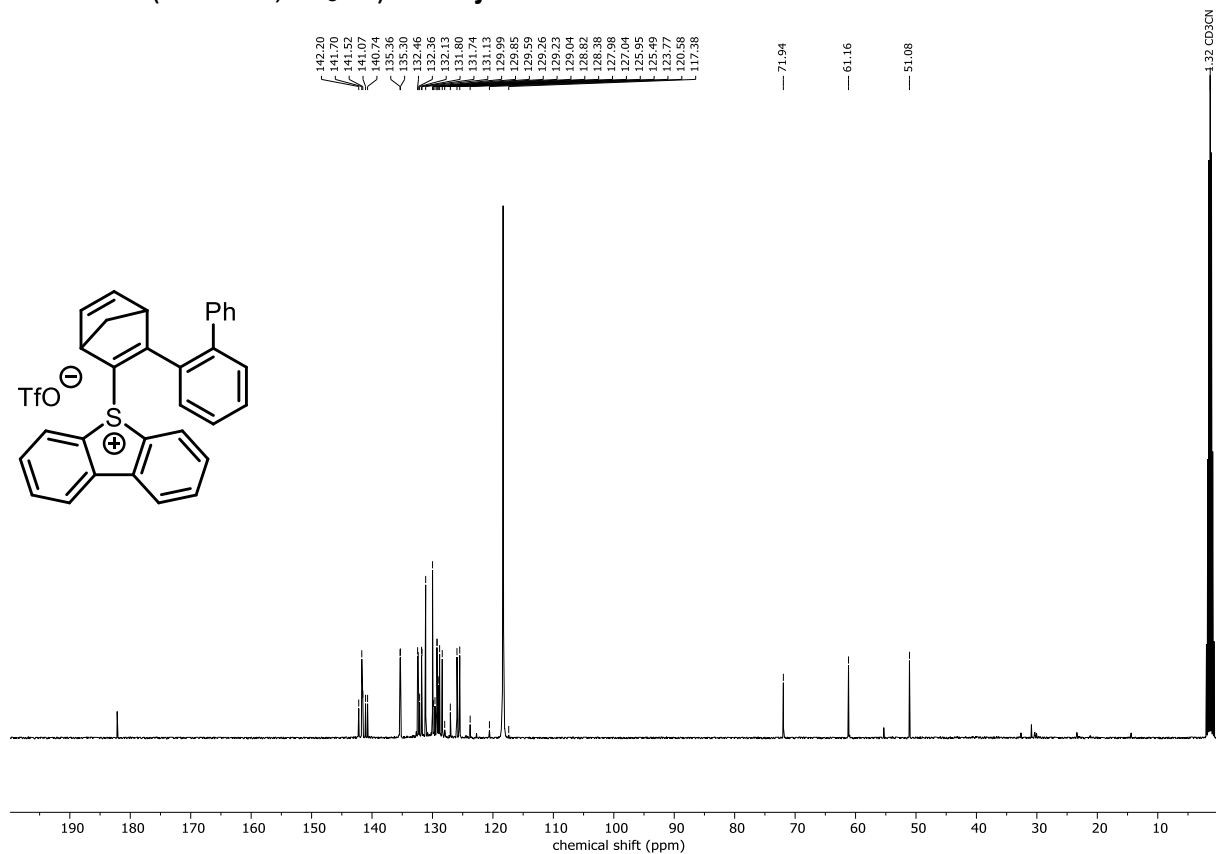
¹³C NMR (101 MHz, CD₃CN) of 142i



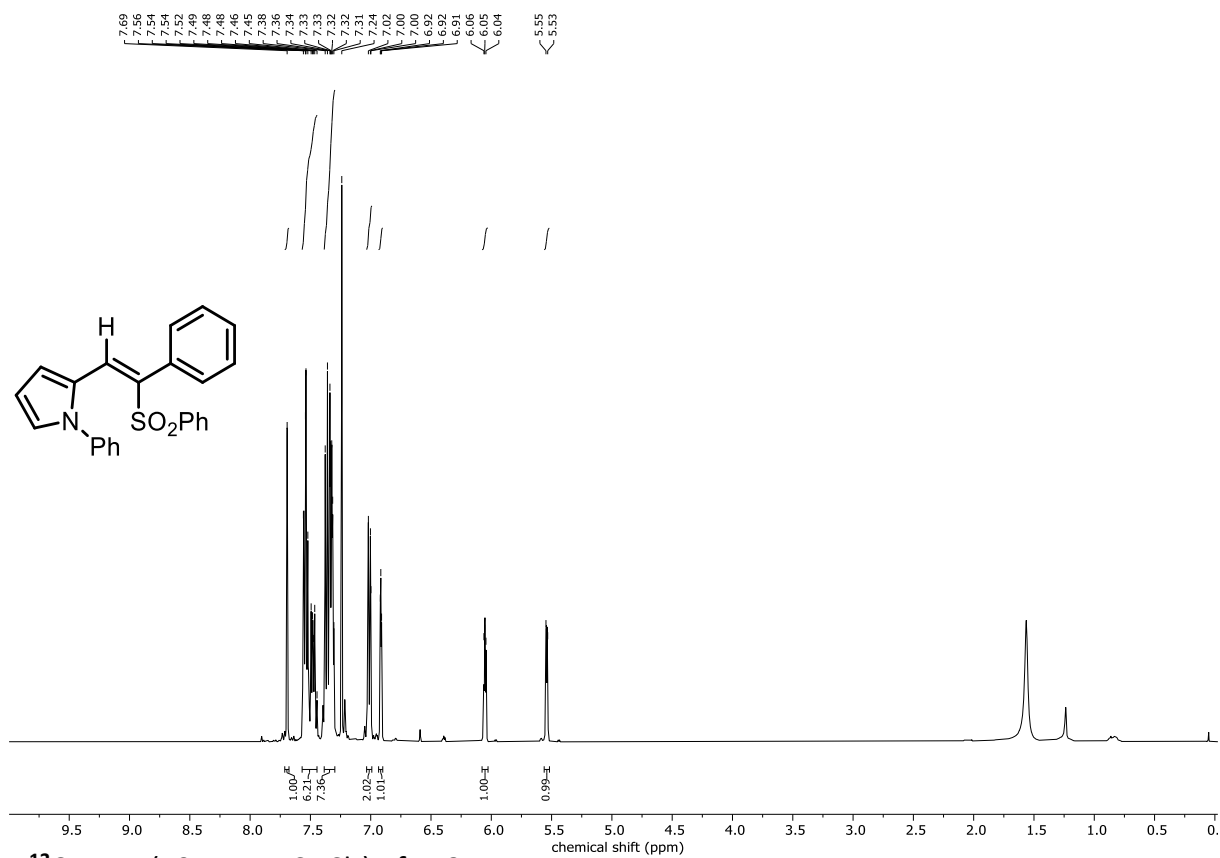
¹H NMR (400 MHz, CD₃CN) of 142j



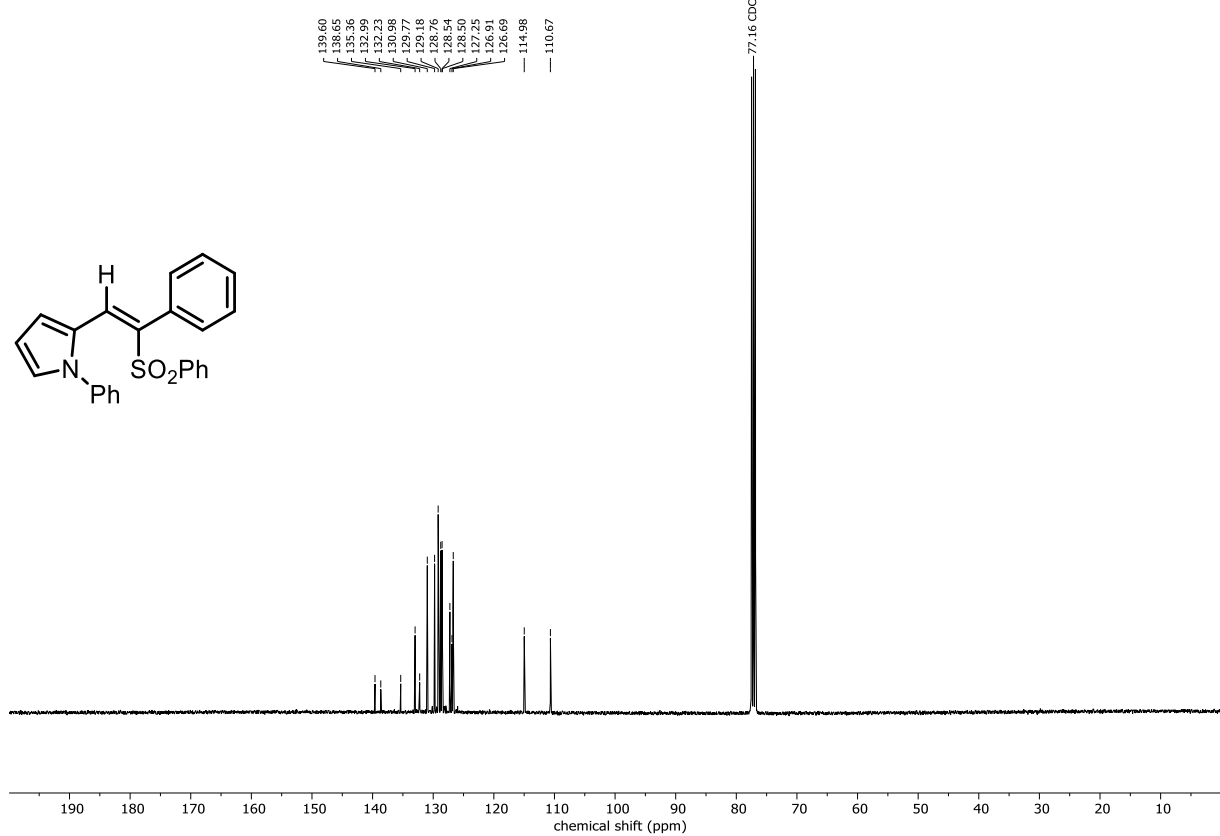
¹³C NMR (101 MHz, CD₃CN) of 142j



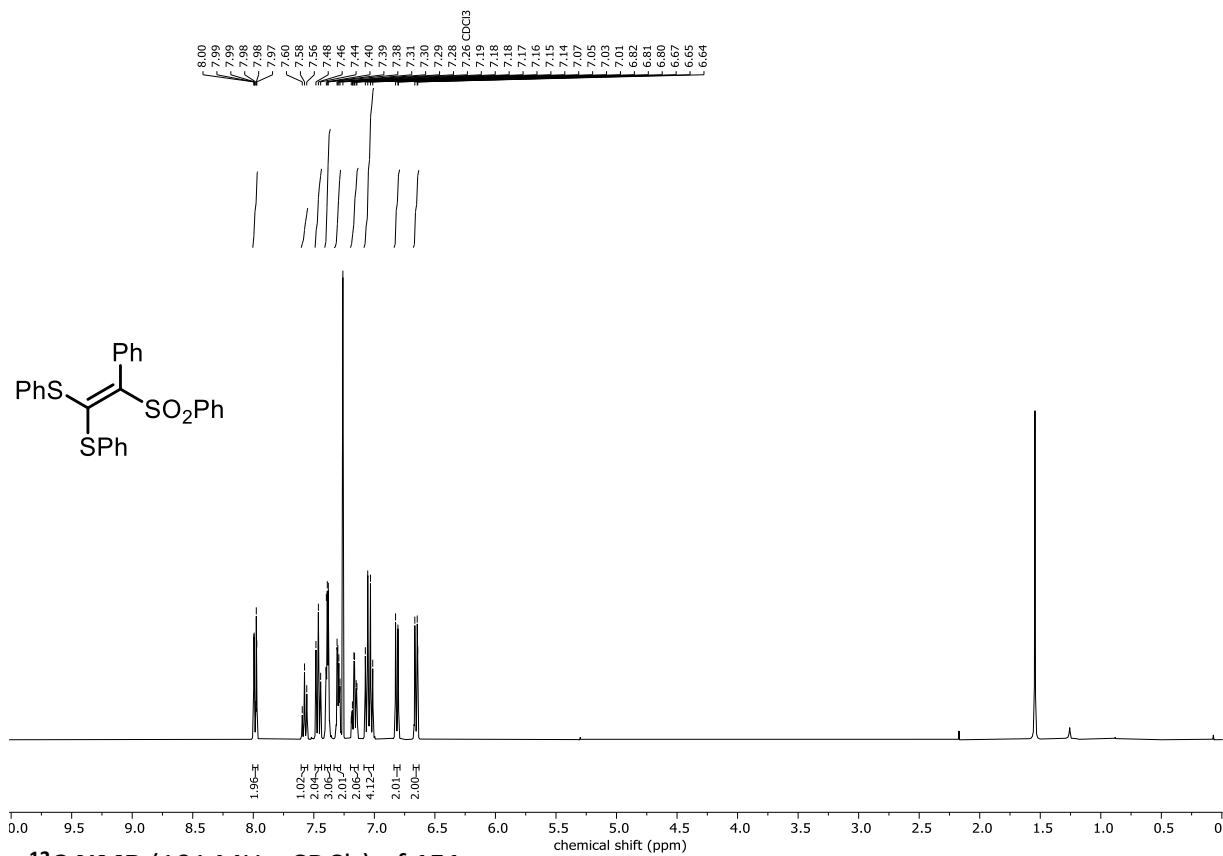
¹H NMR (400 MHz, CDCl₃) of 149



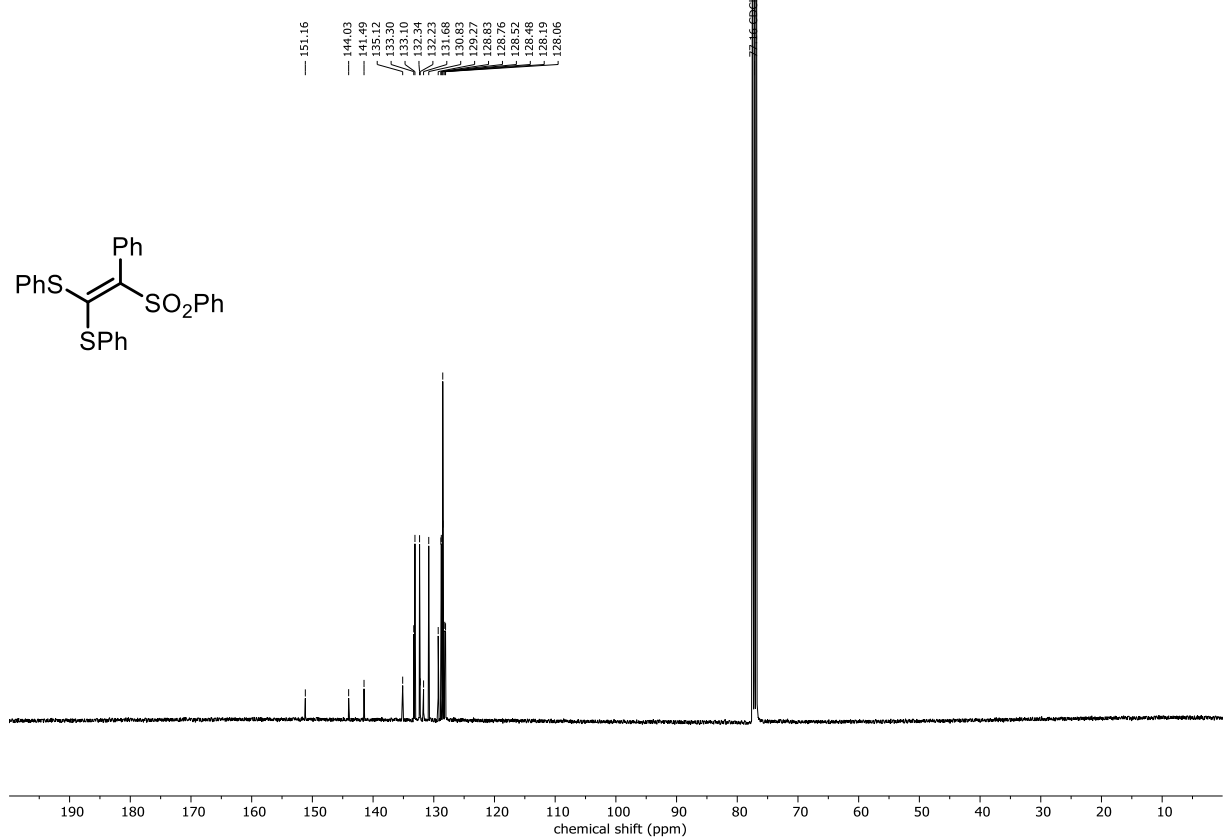
¹³C NMR (101 MHz, CDCl₃) of 149



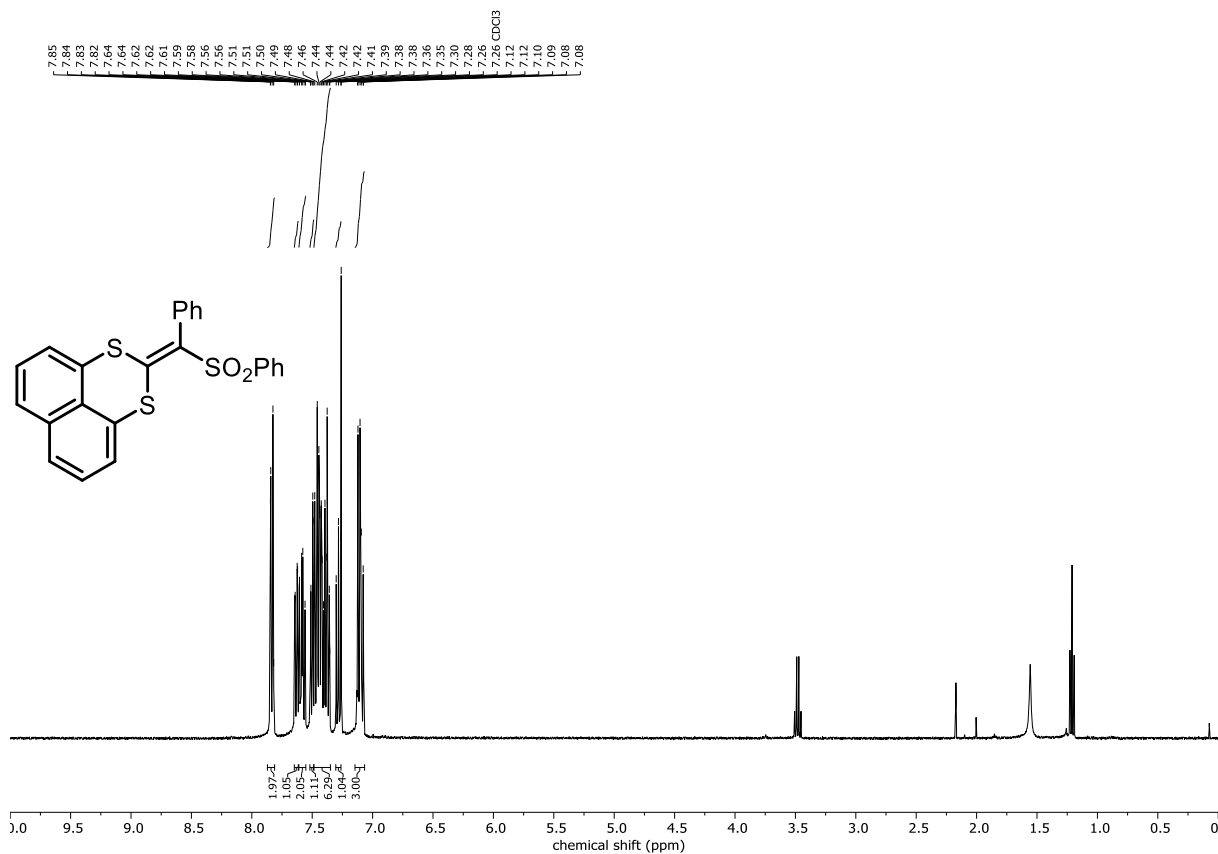
¹H NMR (400 MHz, CDCl₃) of **151a**



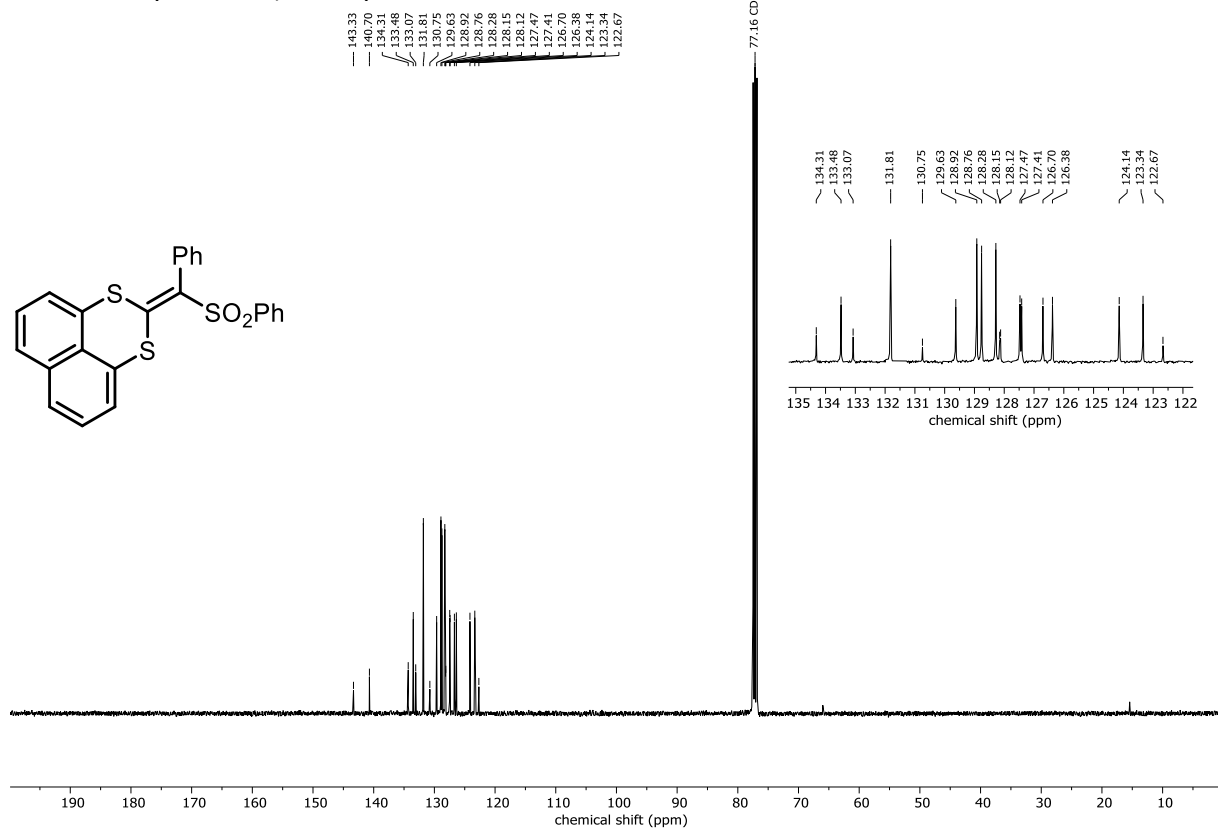
¹³C NMR (101 MHz, CDCl₃) of **151a**



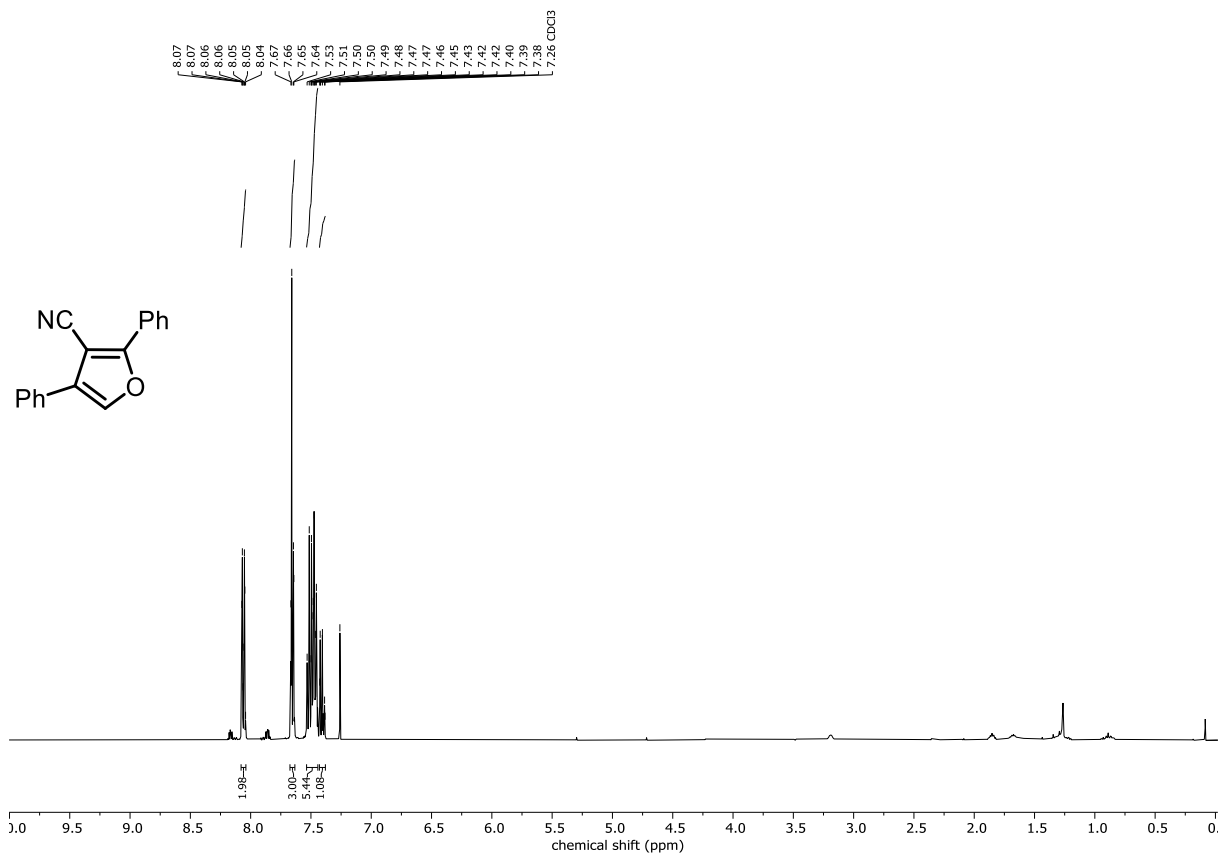
¹H NMR (400 MHz, CDCl₃) of 151b



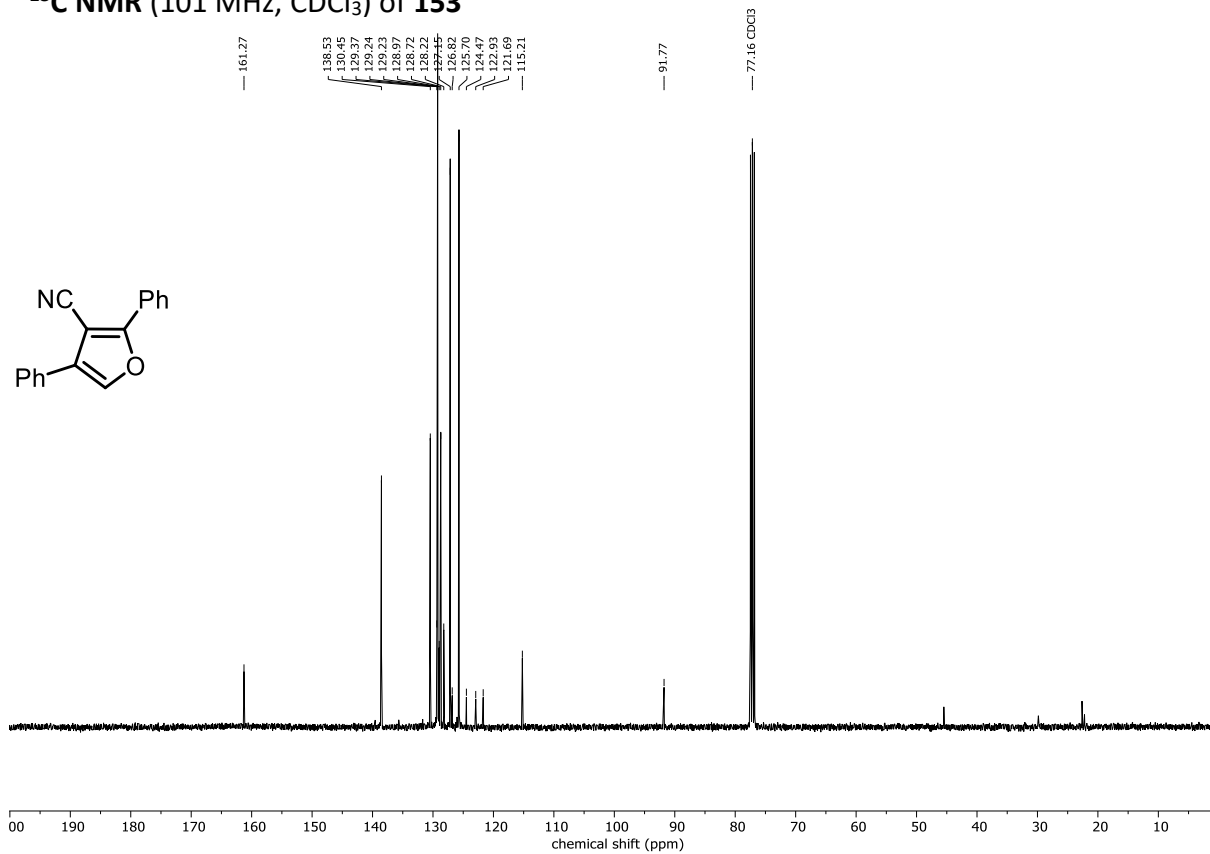
¹³C NMR (101 MHz, CDCl₃) of 151b



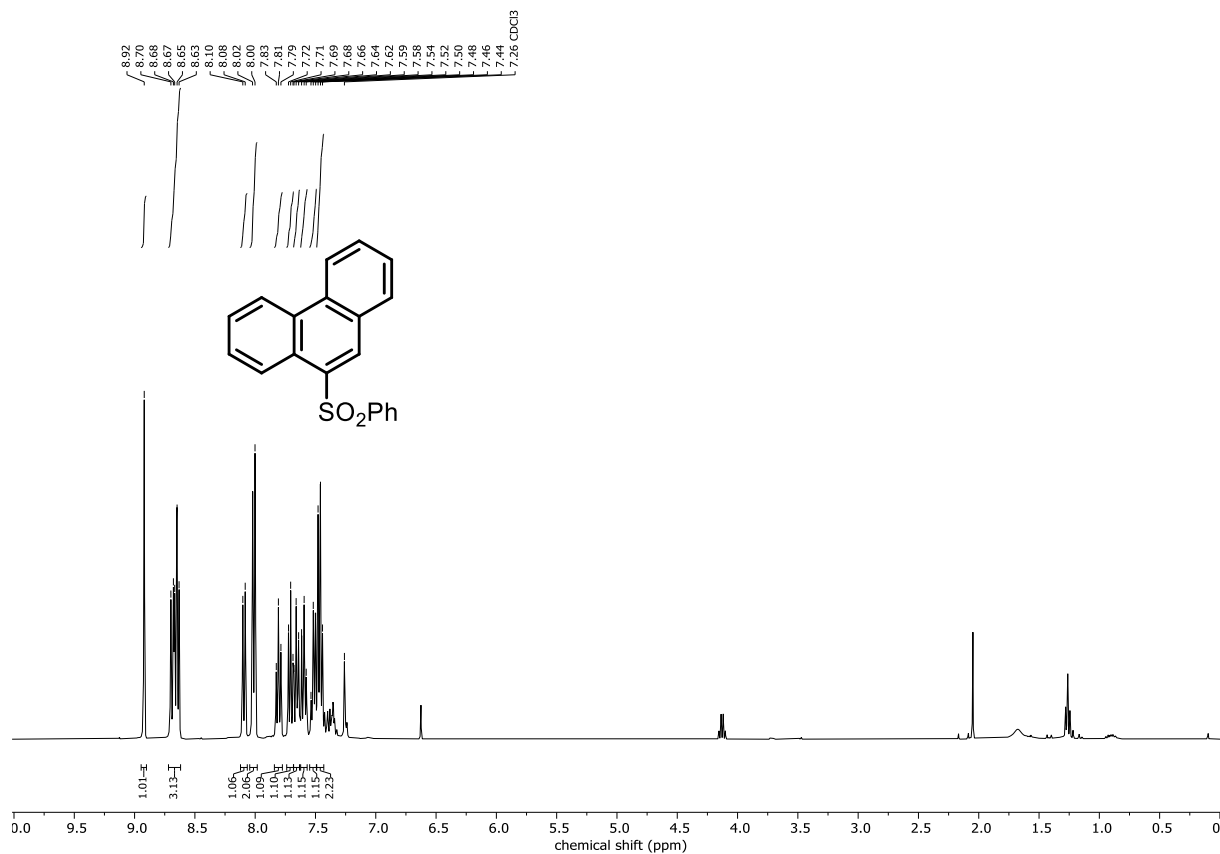
¹H NMR (400 MHz, CDCl₃) of 153



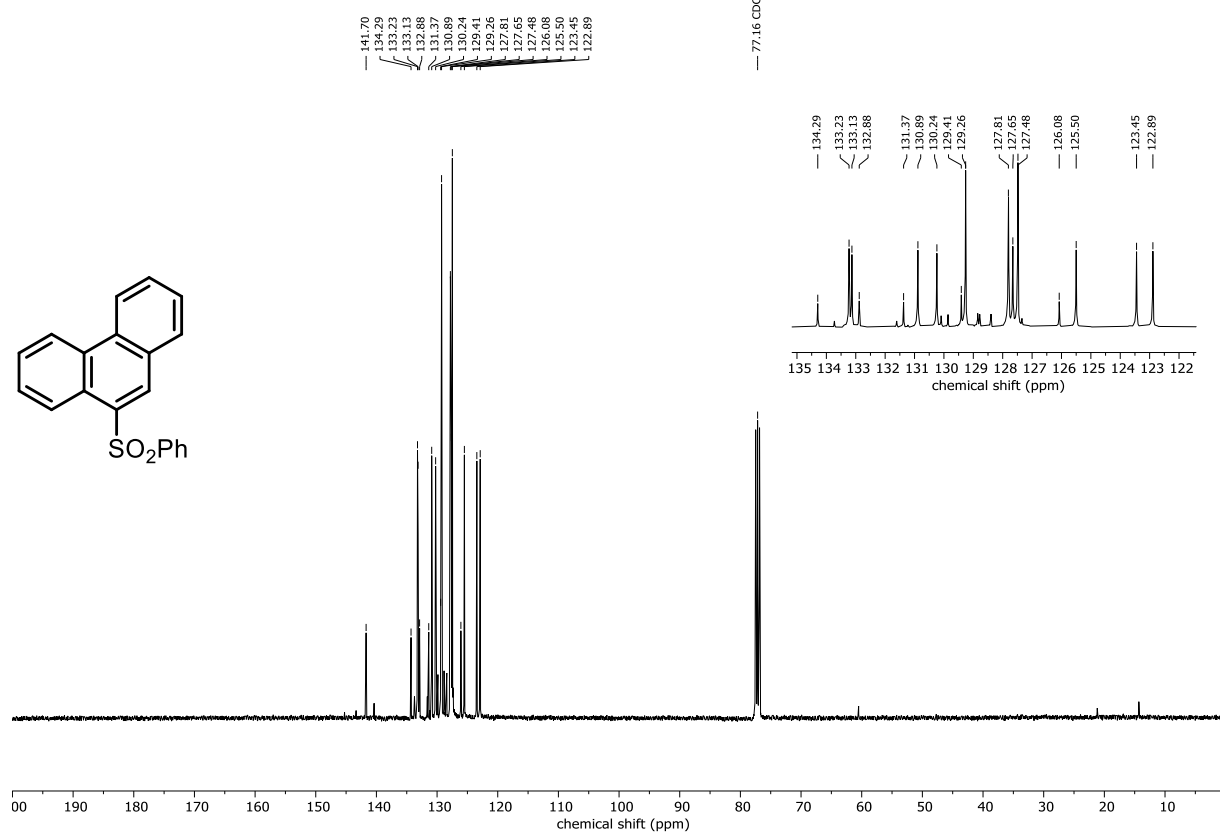
¹³C NMR (101 MHz, CDCl₃) of 153



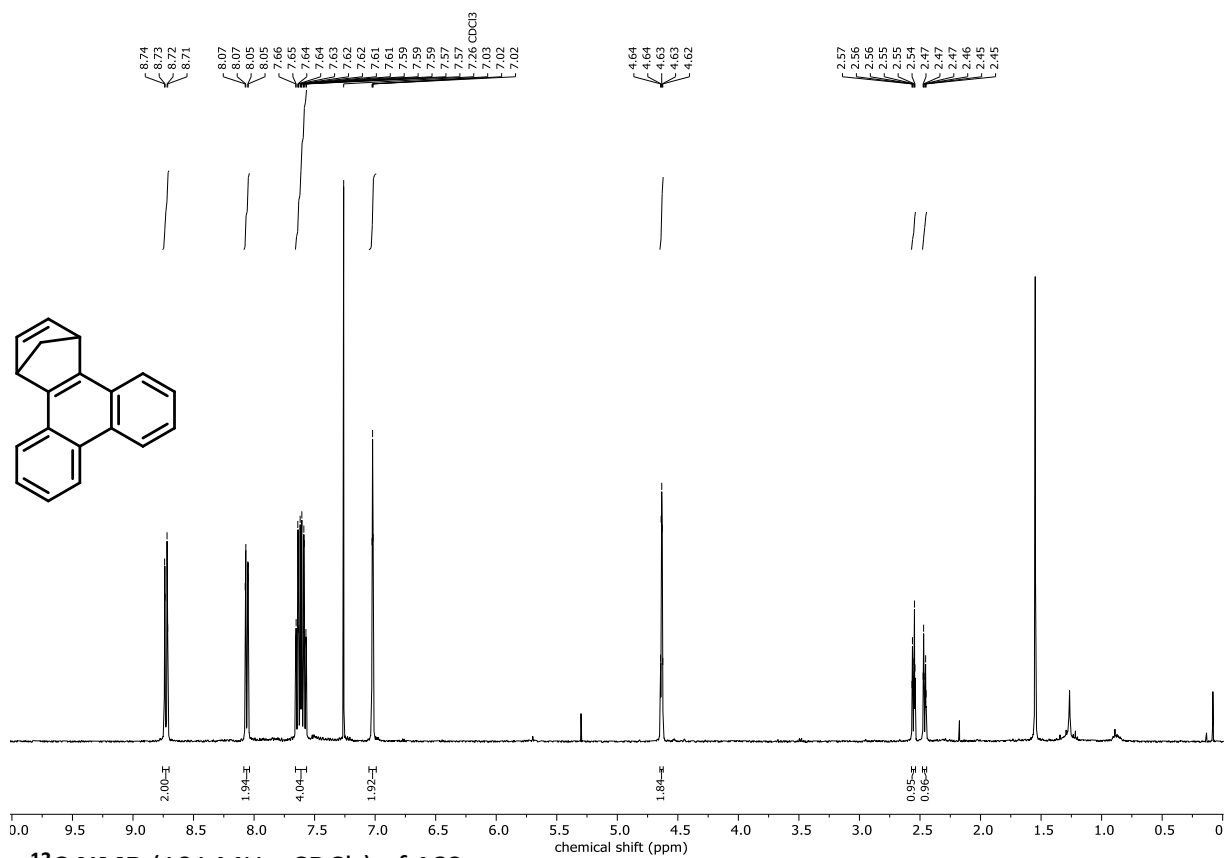
^1H NMR (400 MHz, CDCl_3) of **159**



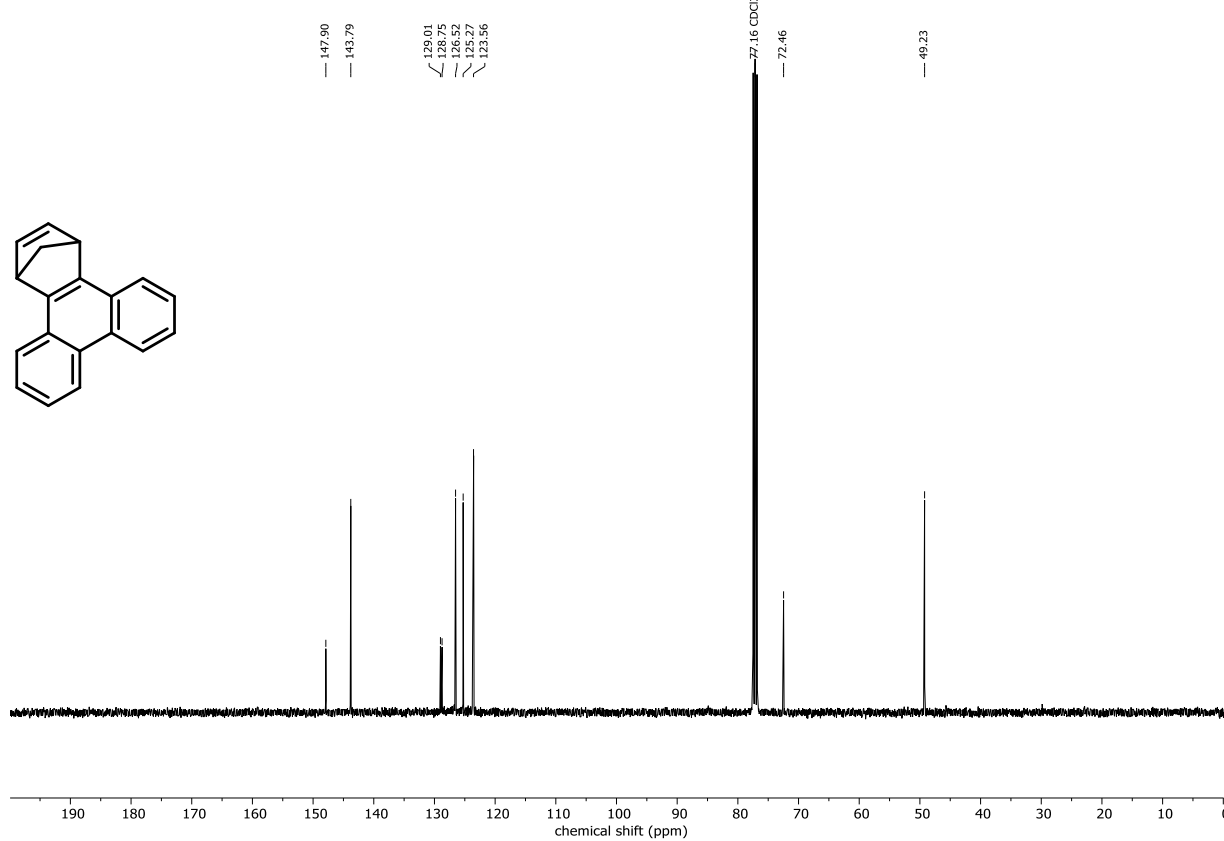
^{13}C NMR (101 MHz, CDCl_3) of **159**



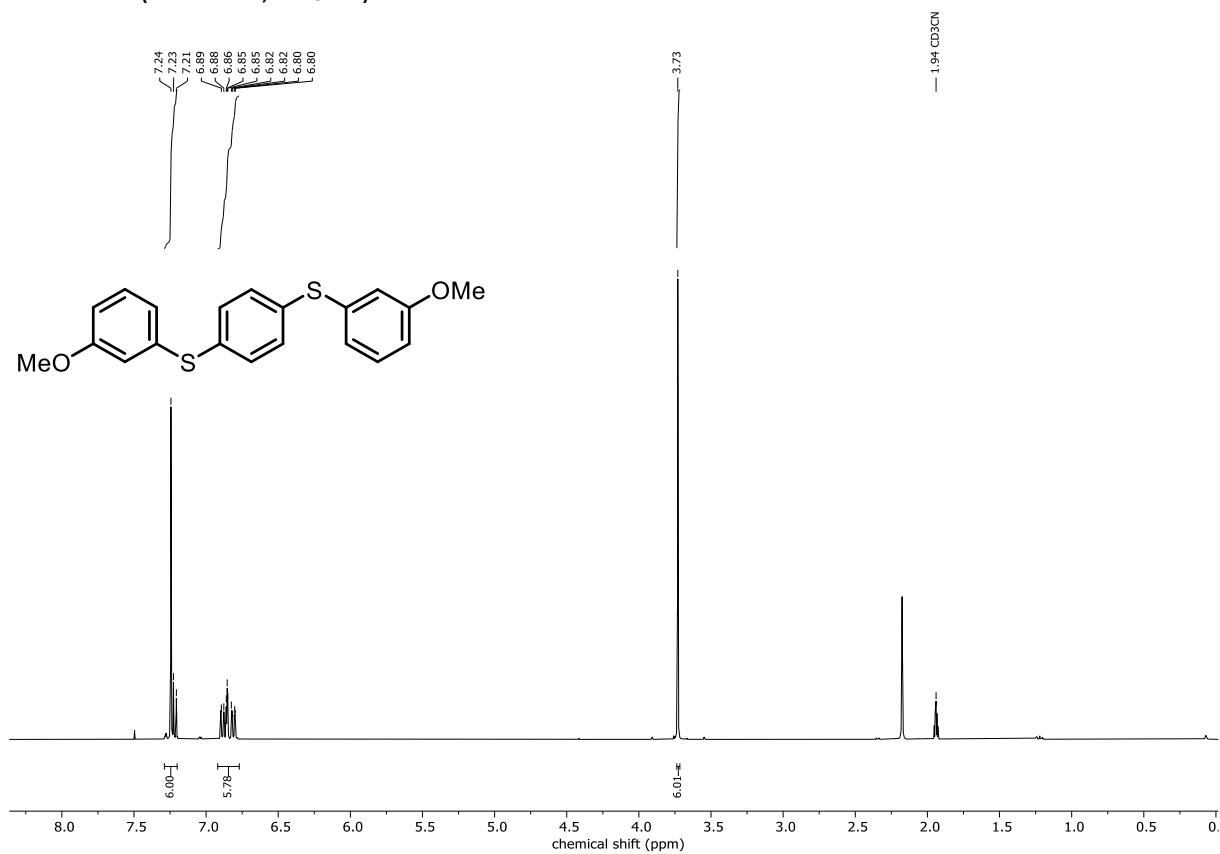
¹H NMR (400 MHz, CDCl₃) of 160



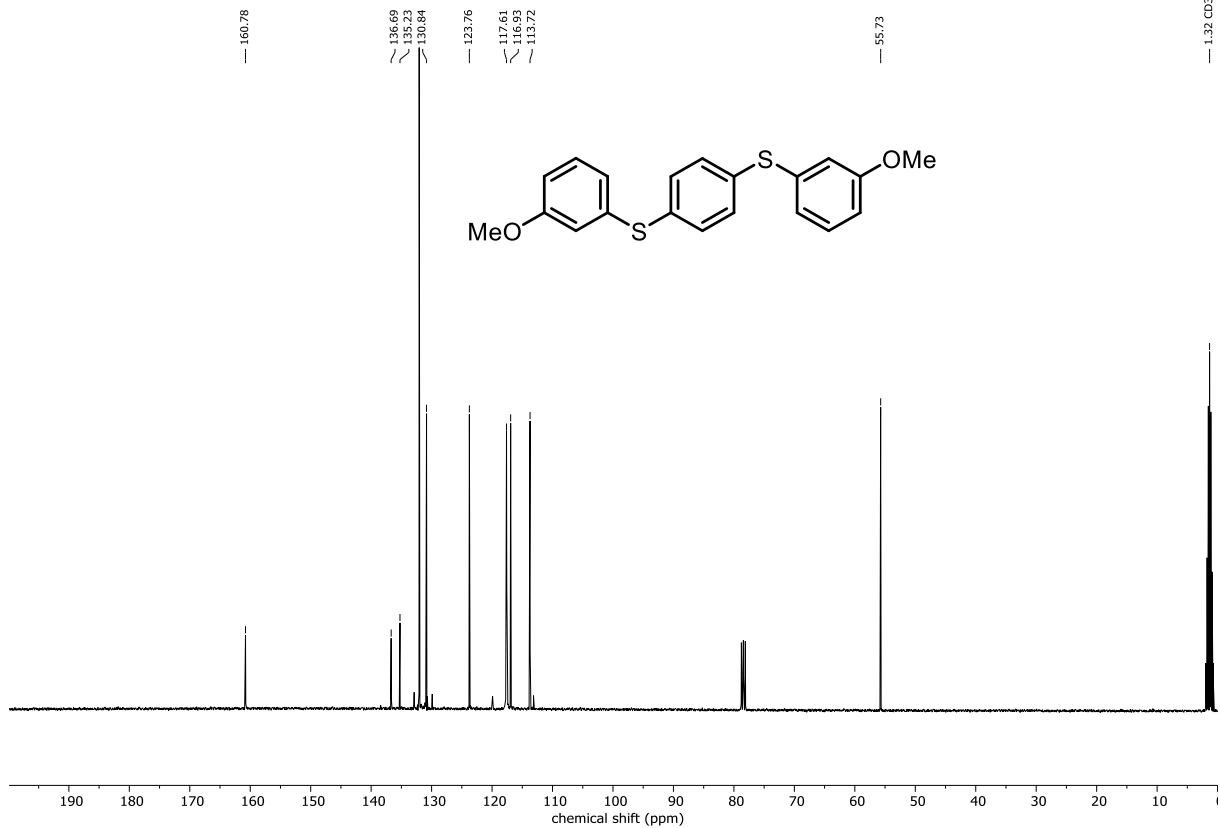
¹³C NMR (101 MHz, CDCl₃) of 160



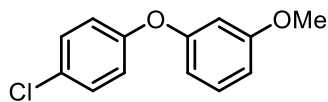
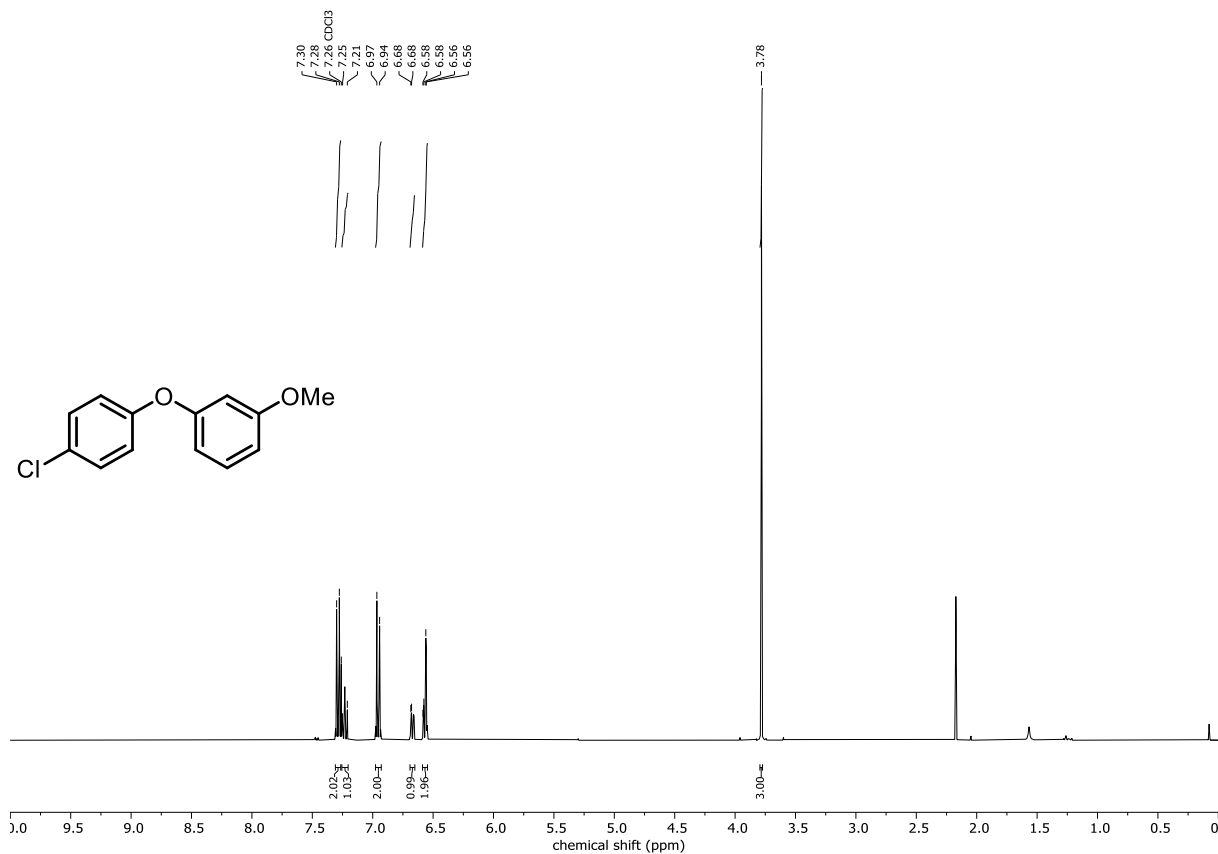
¹H NMR (400 MHz, CD₃CN) of 162a



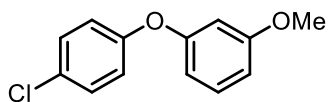
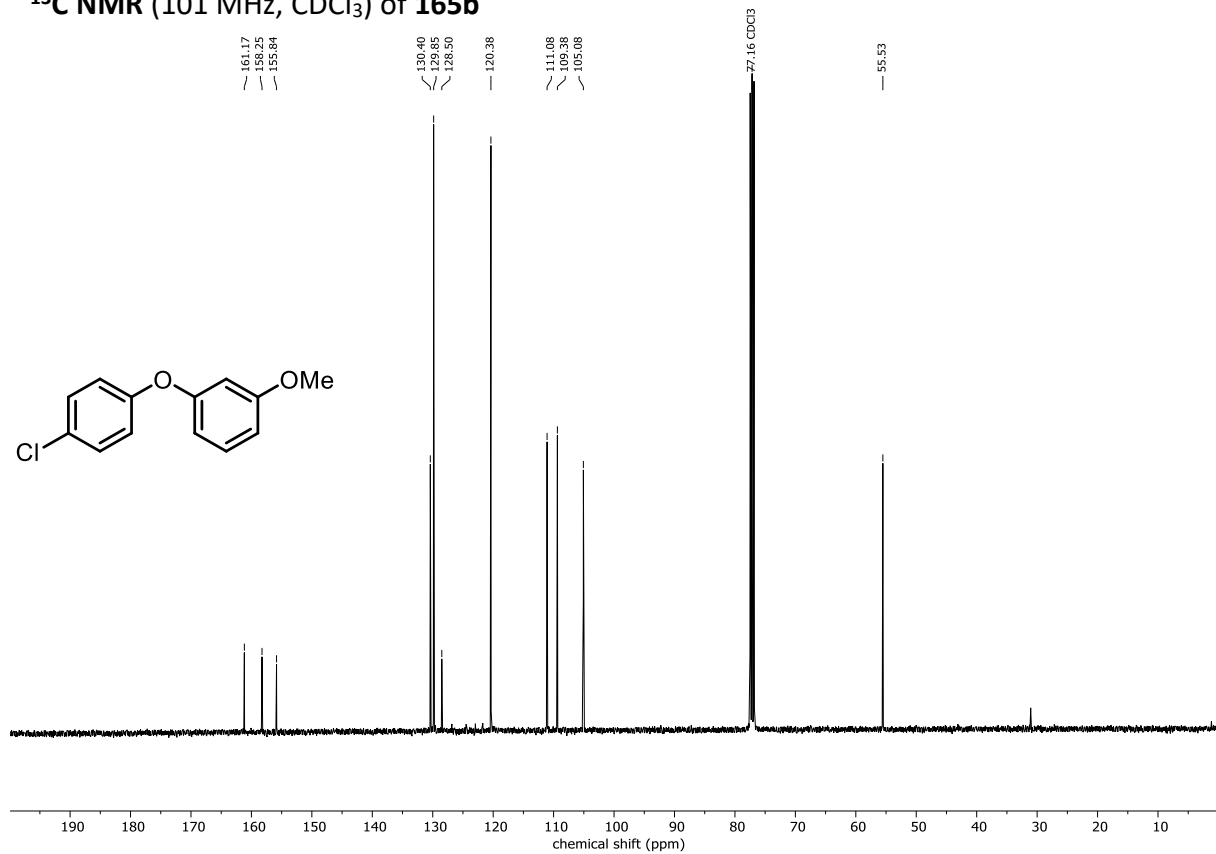
¹³C NMR (101 MHz, CD₃CN) of 162a



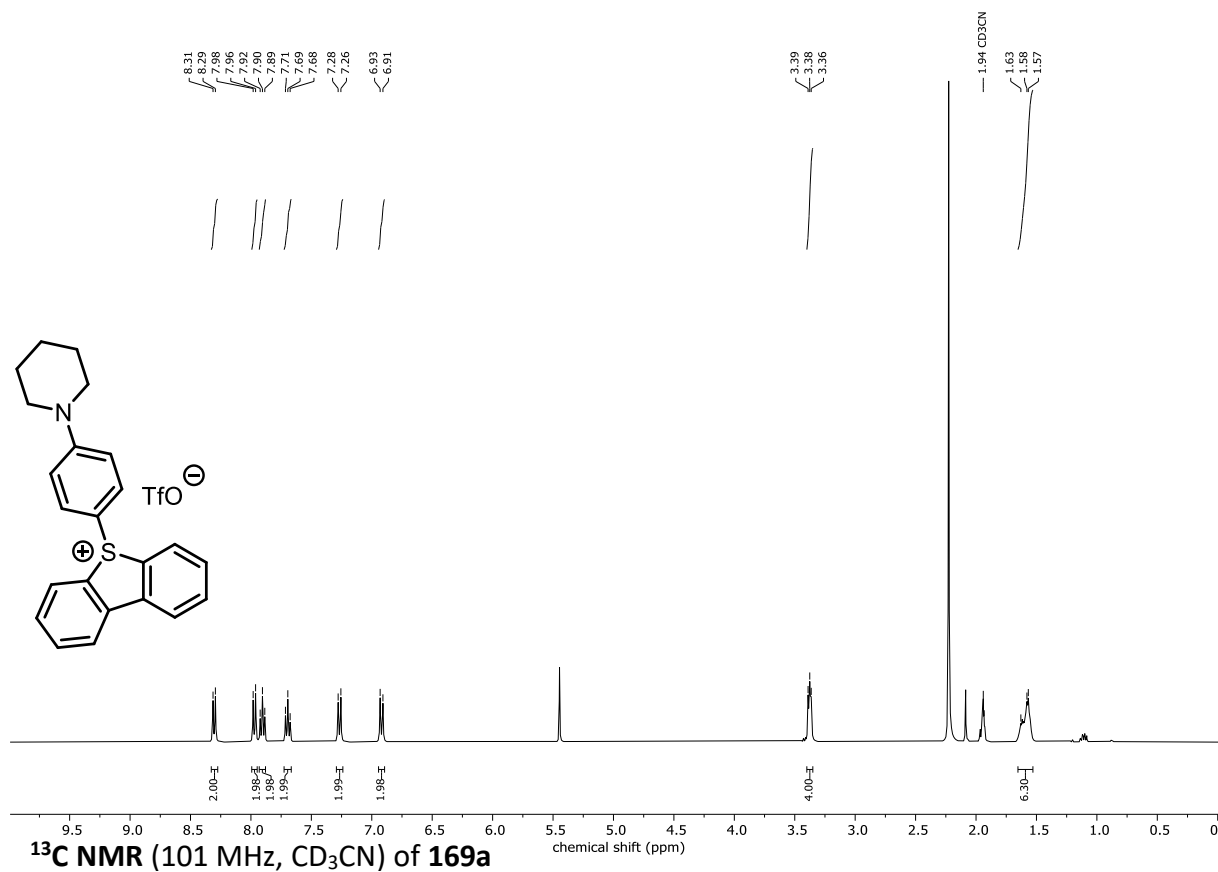
¹H NMR (400 MHz, CDCl₃) of 165b



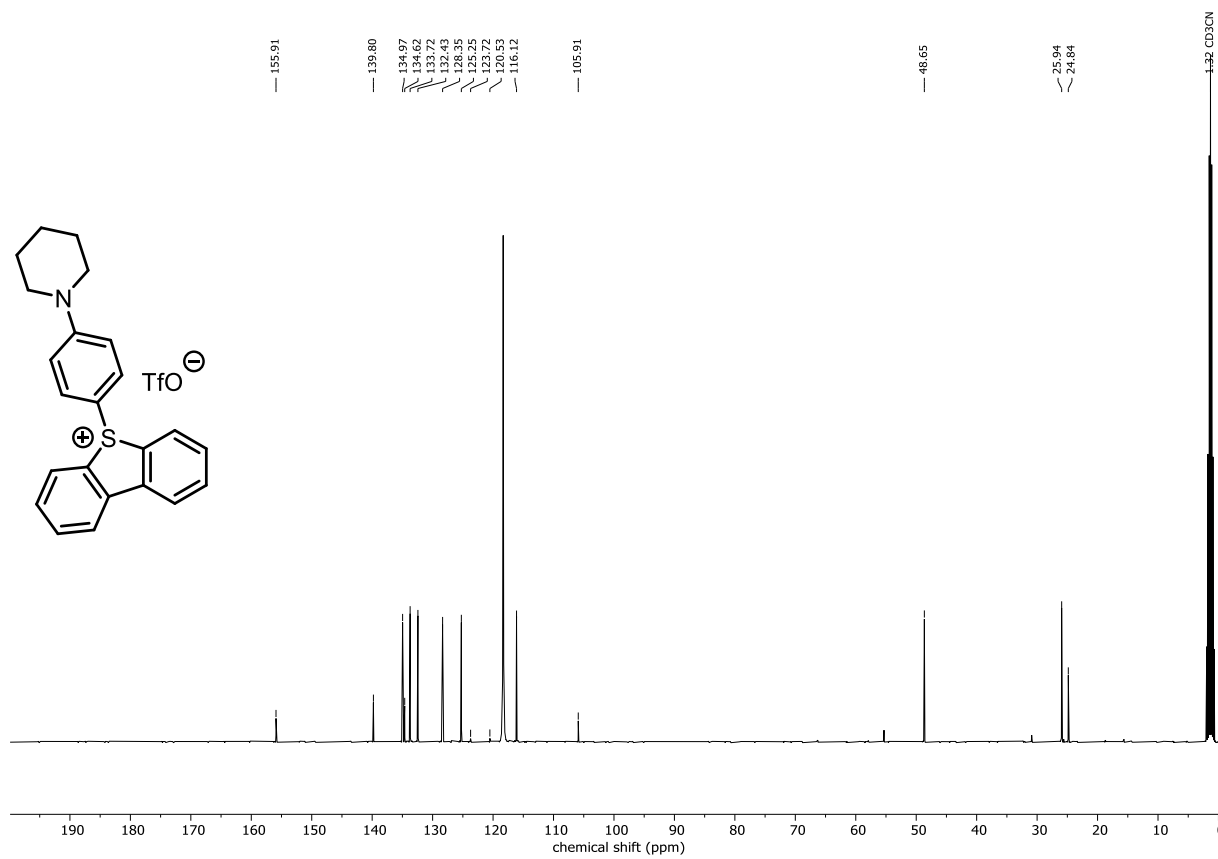
¹³C NMR (101 MHz, CDCl₃) of 165b



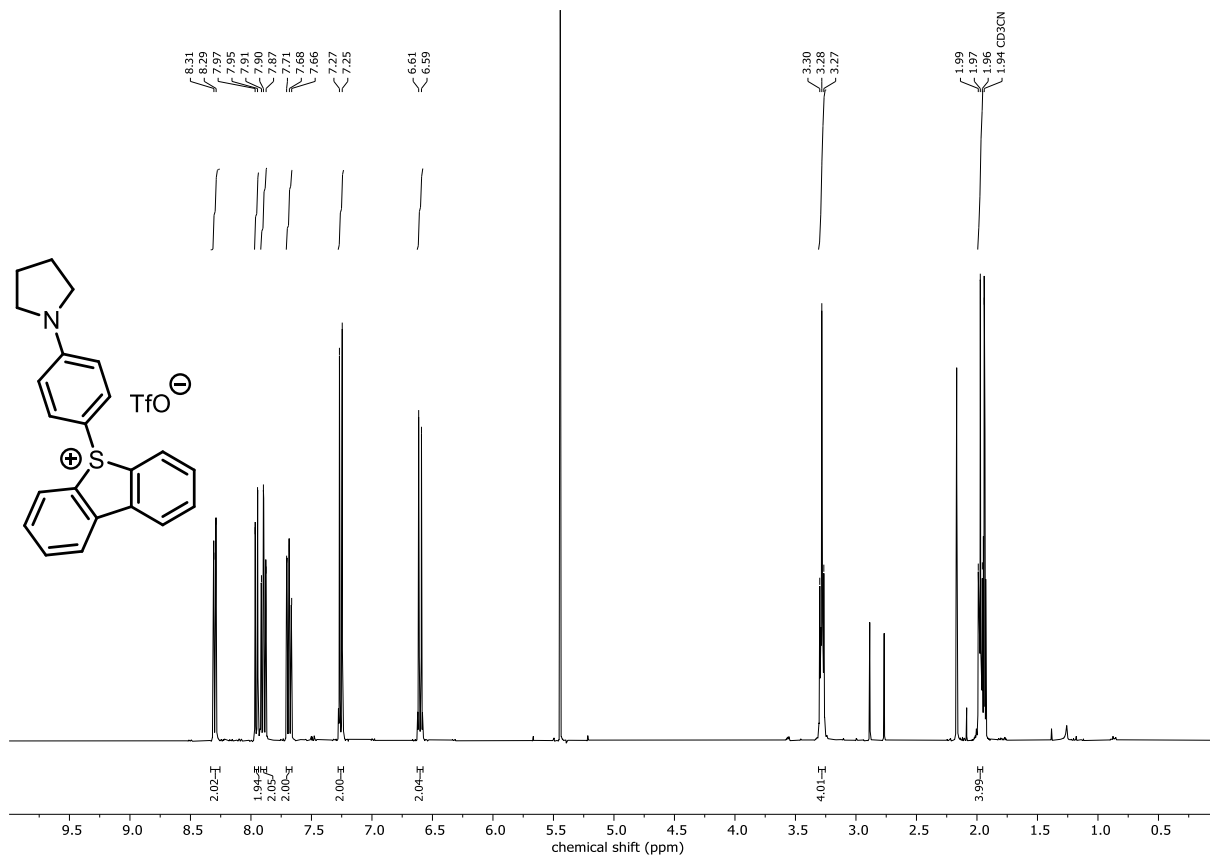
¹H NMR (400 MHz, CD₃CN) of 169a



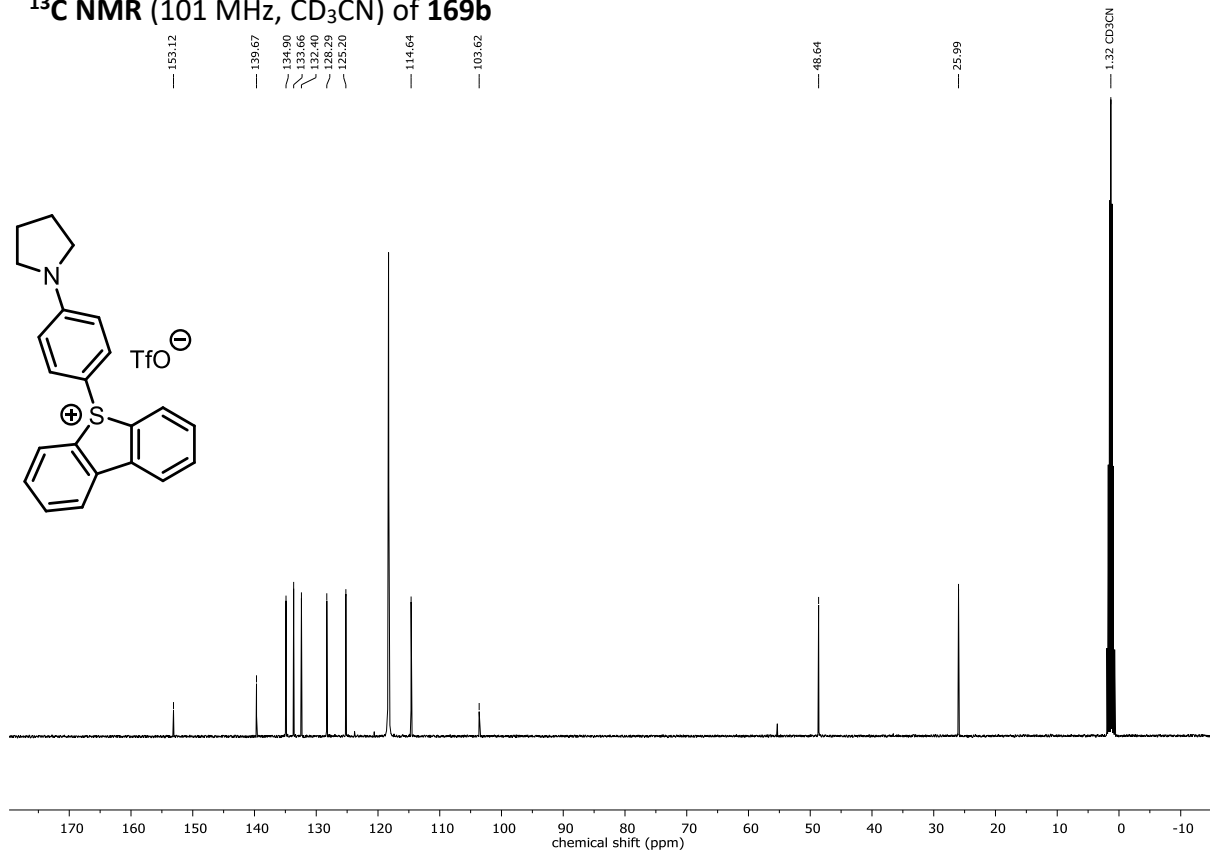
¹³C NMR (101 MHz, CD₃CN) of 169a



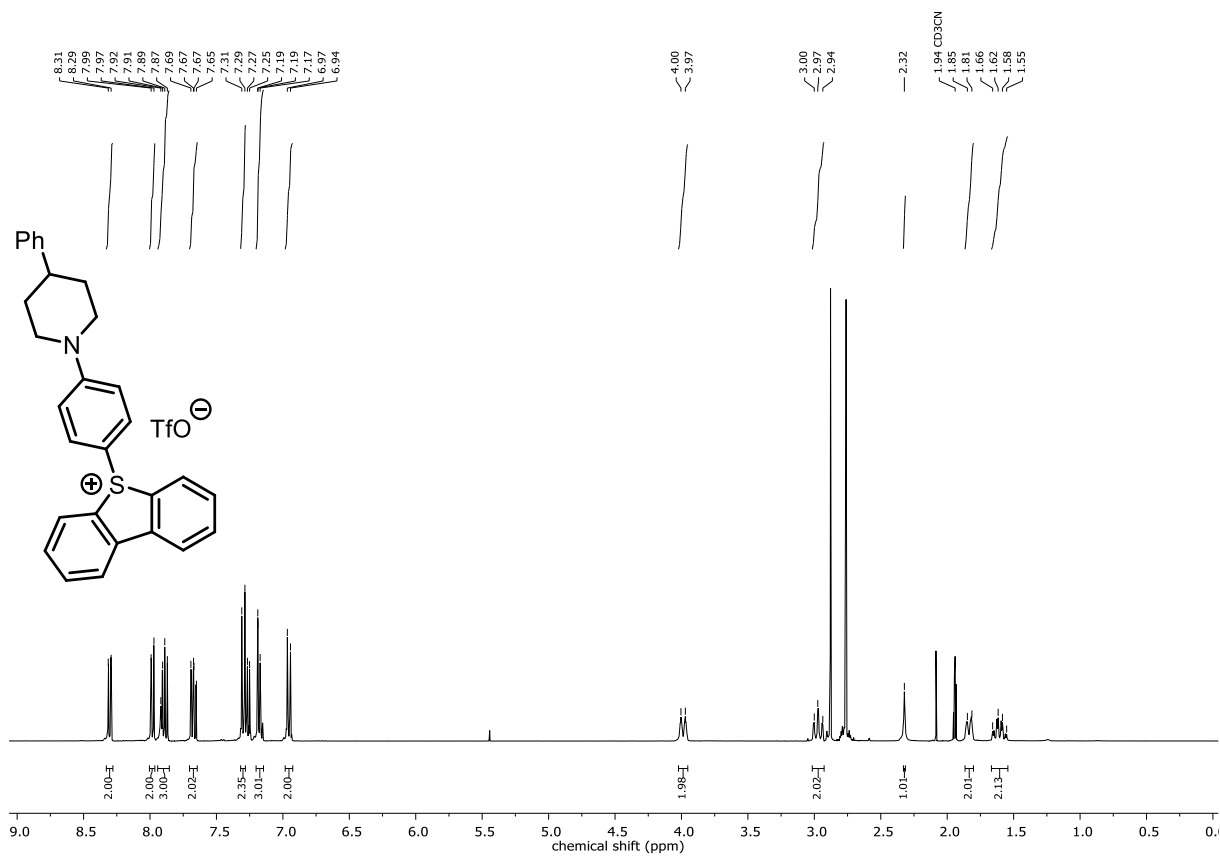
¹H NMR (400 MHz, CD₃CN) of 169b



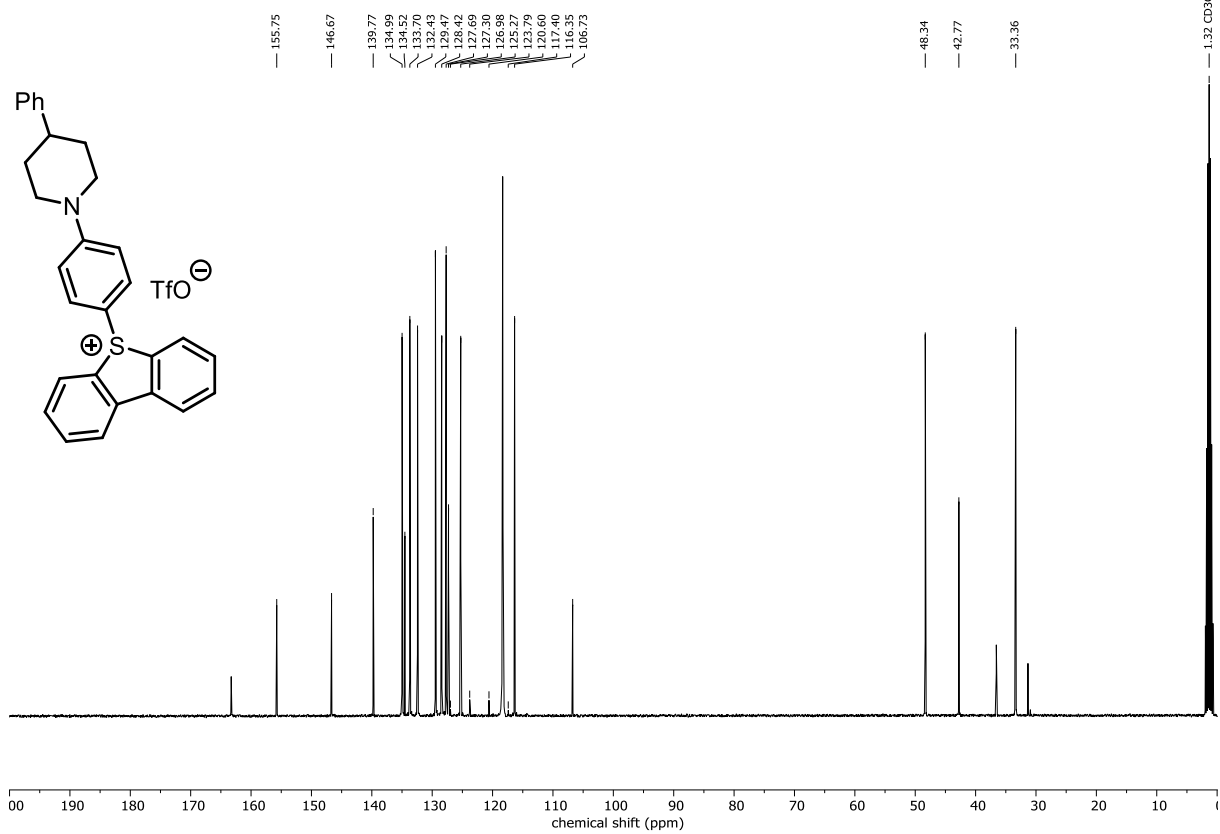
¹³C NMR (101 MHz, CD₃CN) of 169b



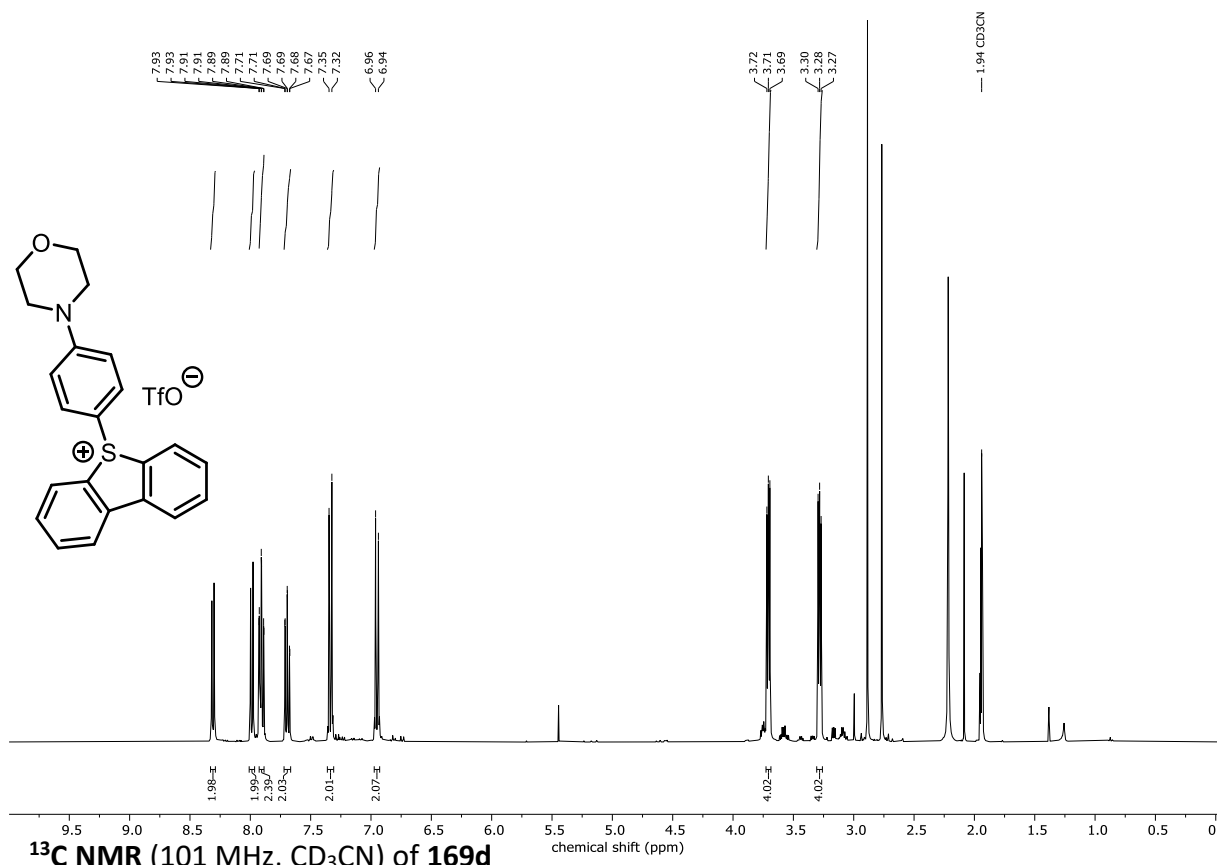
¹H NMR (400 MHz, CD₃CN) of 169c



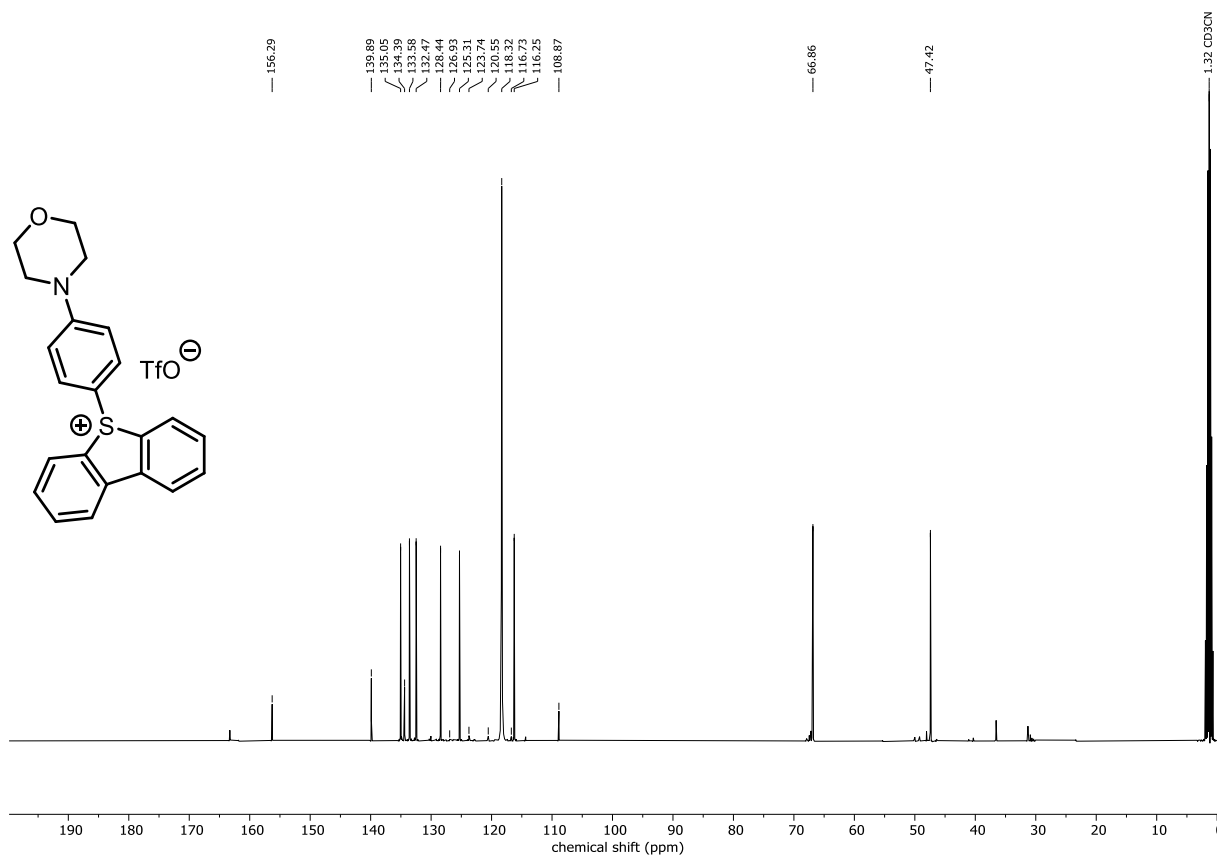
¹³C NMR (101 MHz, CD₃CN) of 169c



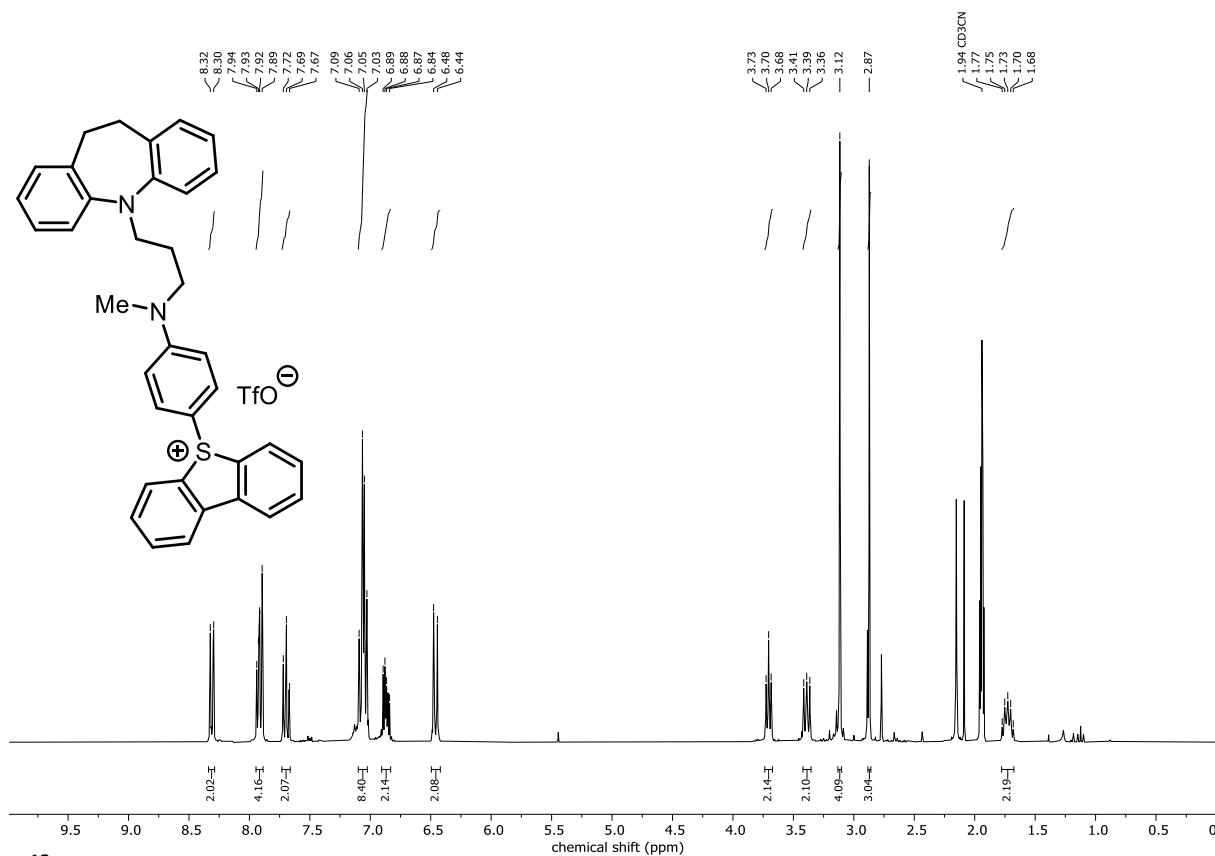
¹H NMR (400 MHz, CD₃CN) of 169d



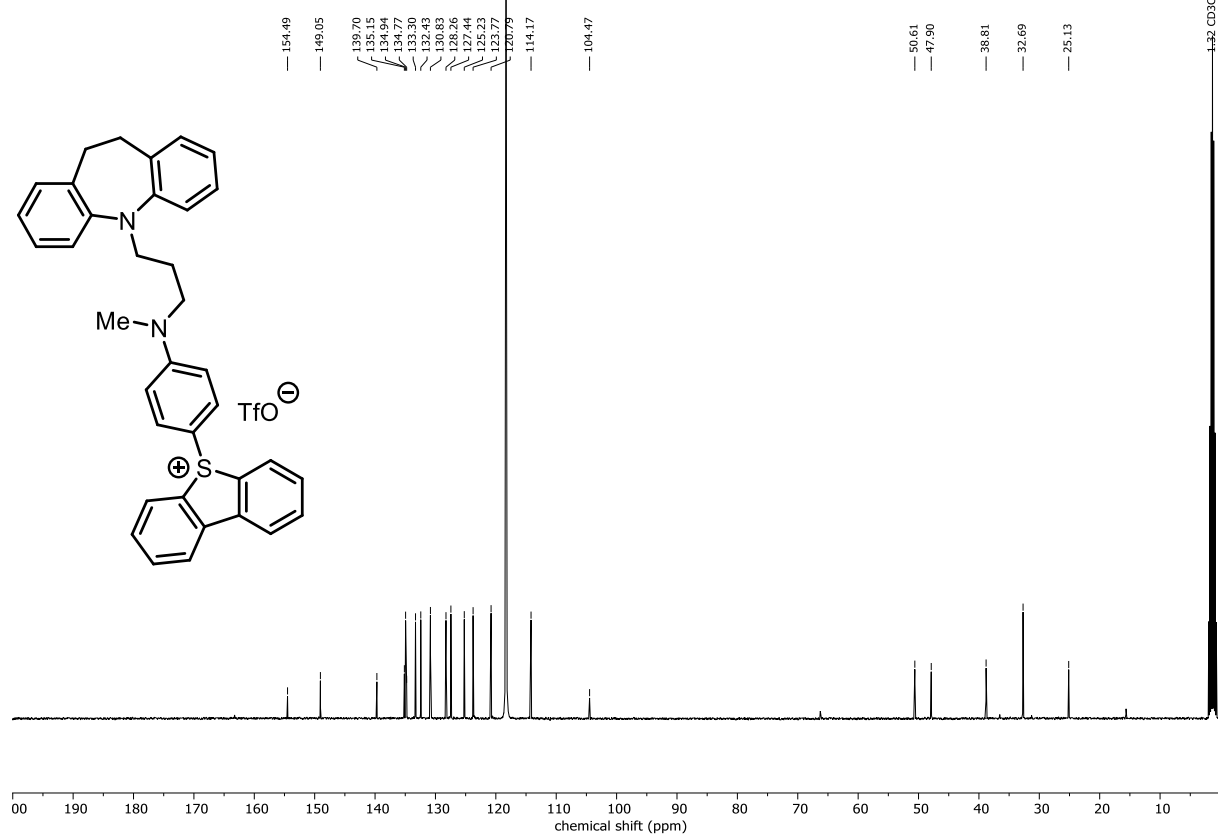
¹³C NMR (101 MHz, CD₃CN) of 169d



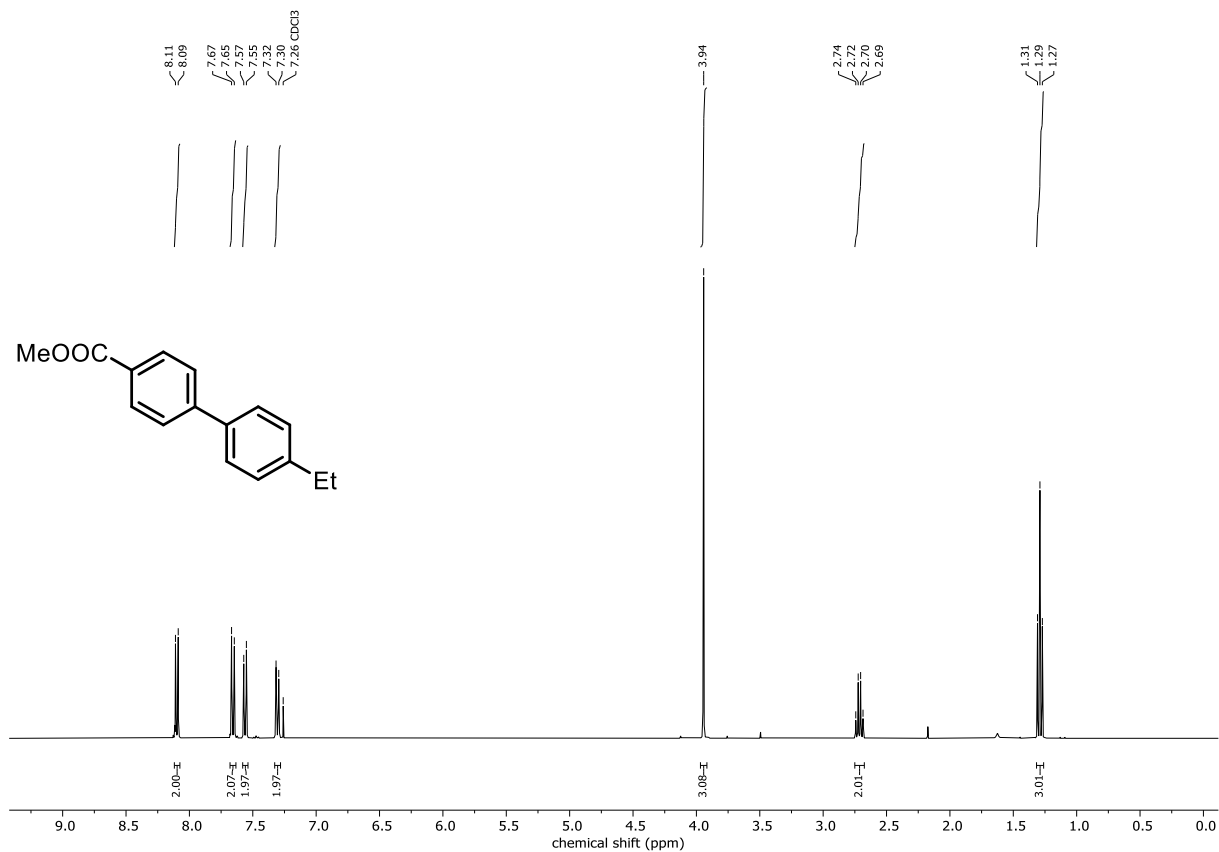
¹H NMR (400 MHz, CD₃CN) of 169e



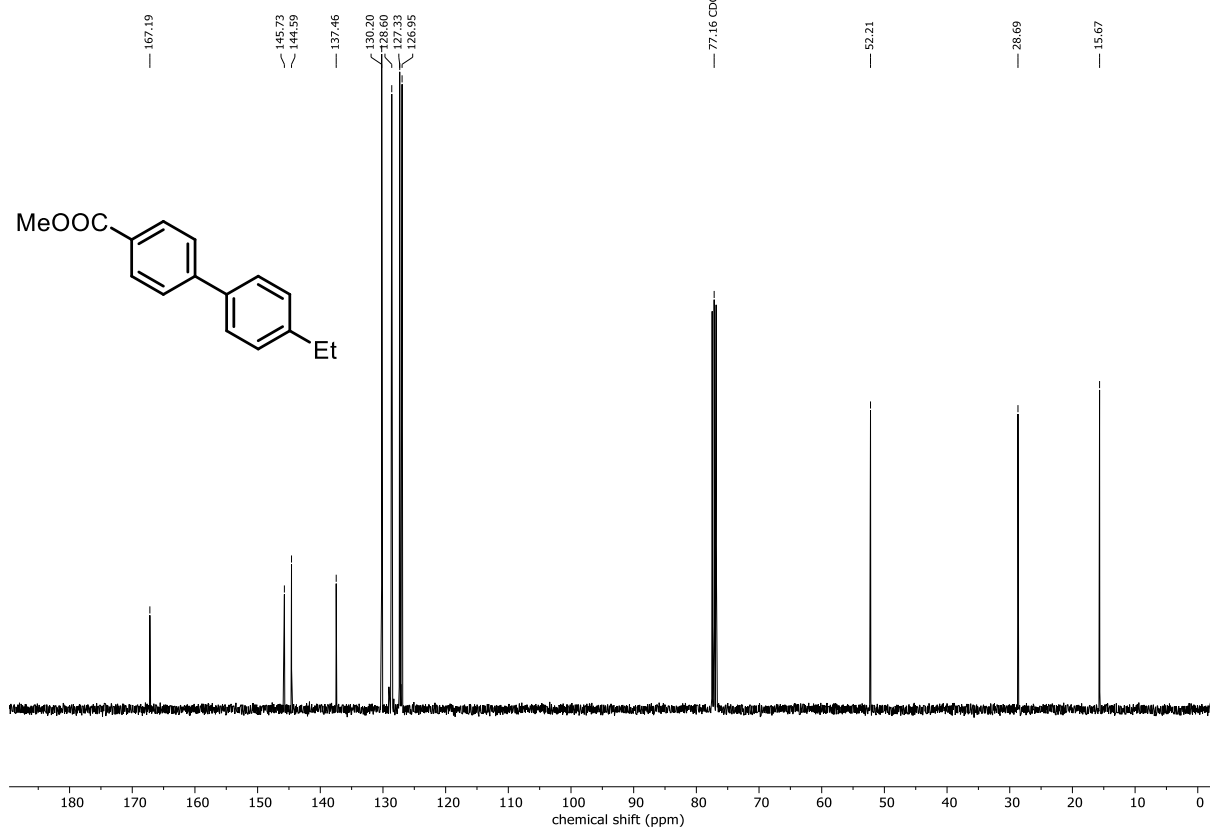
¹³C NMR (101 MHz, CD₃CN) of 169e



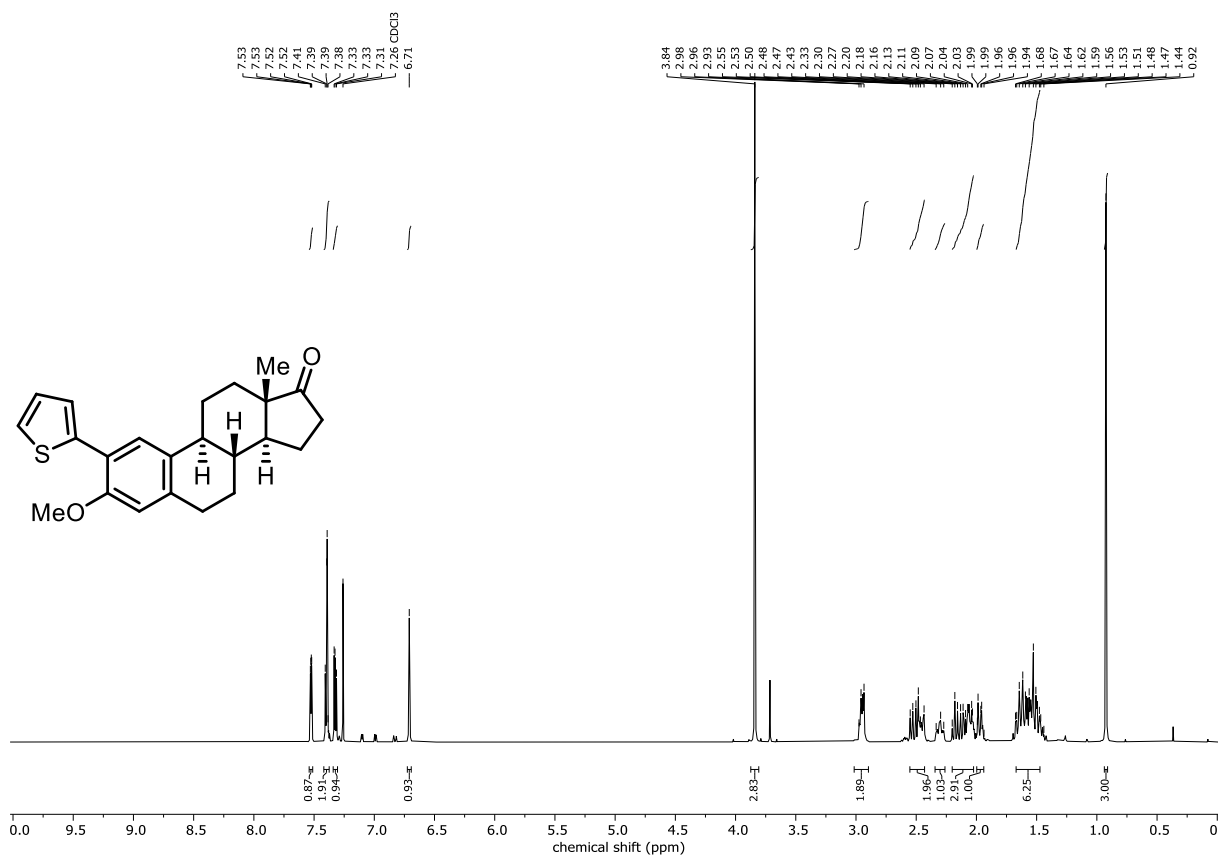
¹H NMR (400 MHz, CDCl₃) of 175



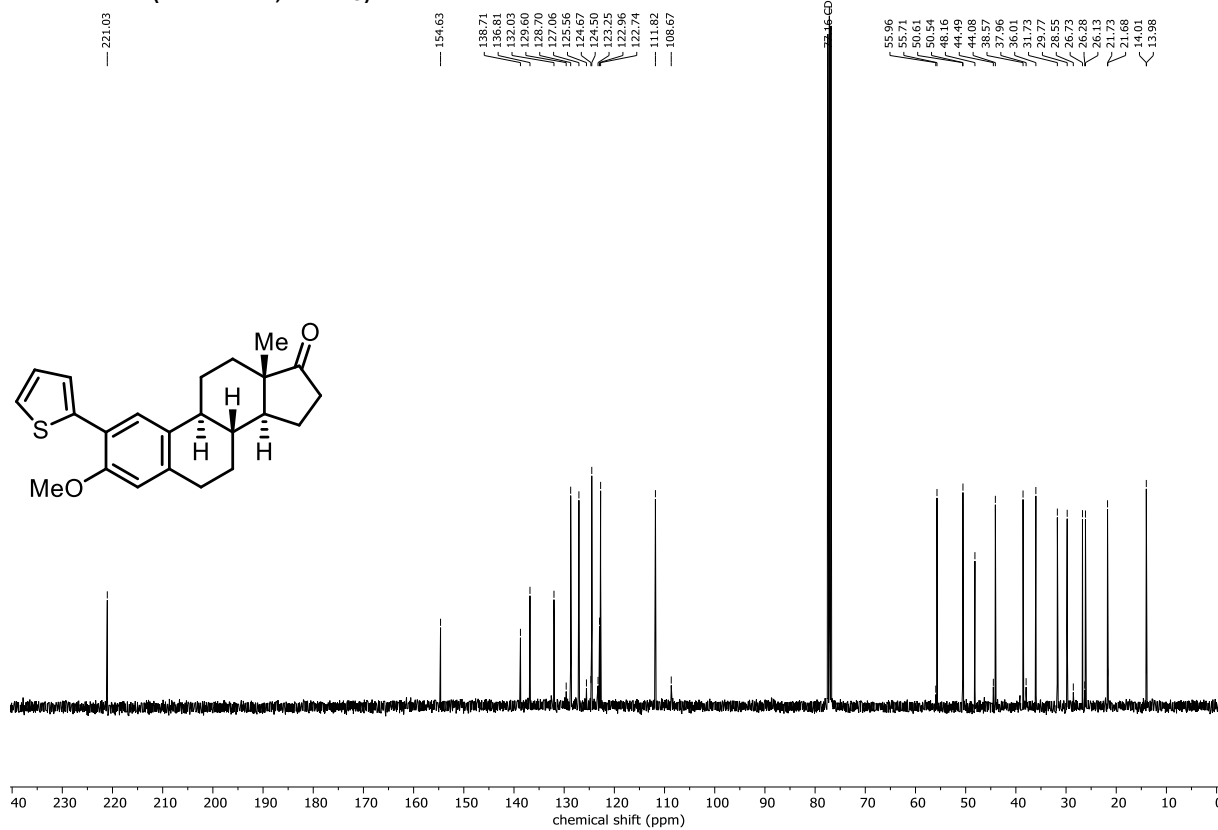
¹³C NMR (101 MHz, CDCl₃) of 175



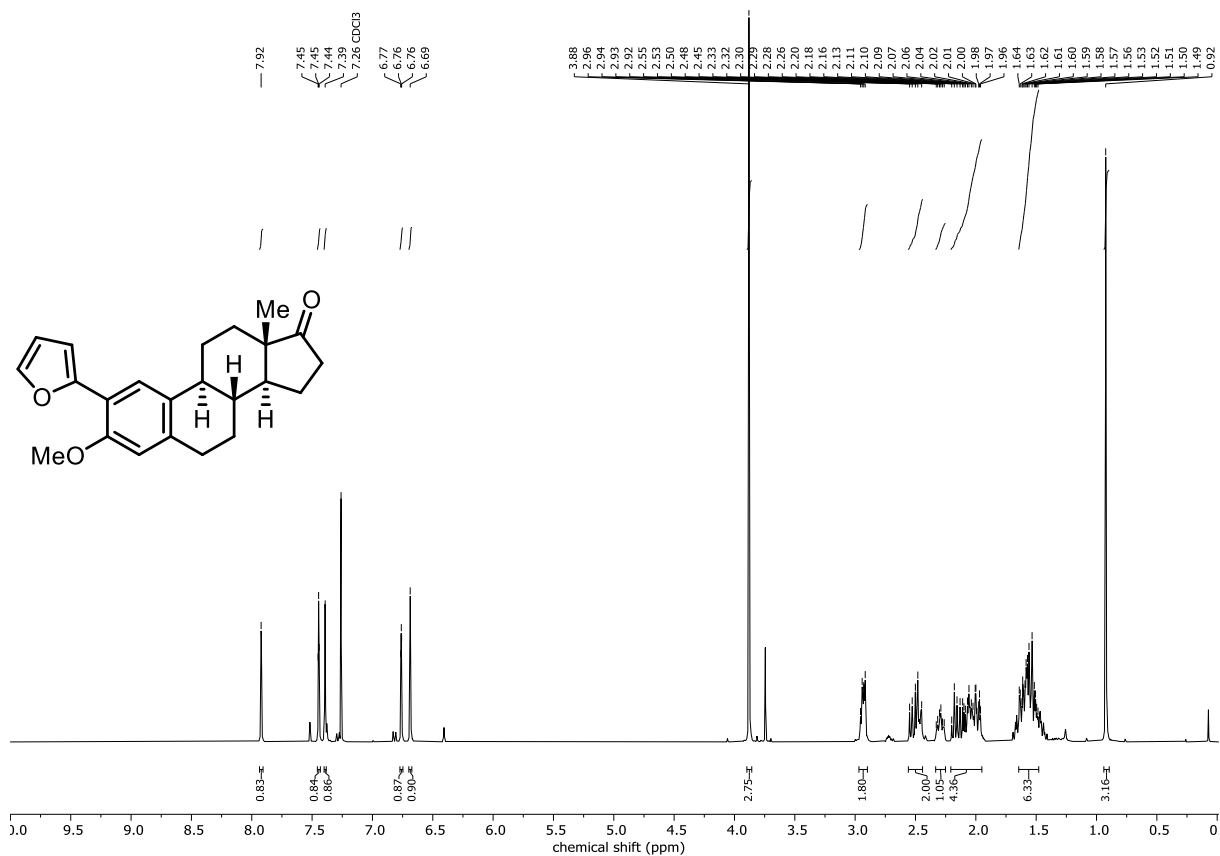
¹H NMR (400 MHz, CDCl₃) of 176a



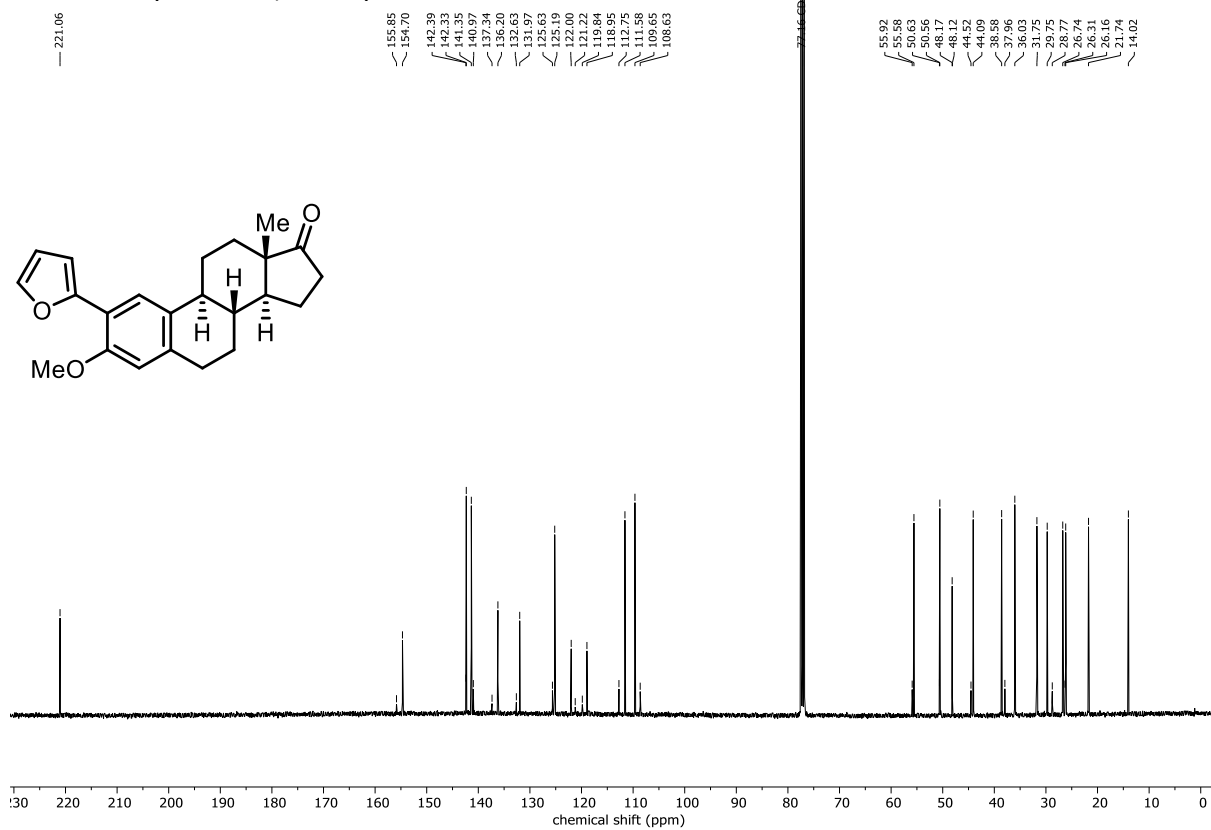
¹³C NMR (101 MHz, CDCl₃) of 176a



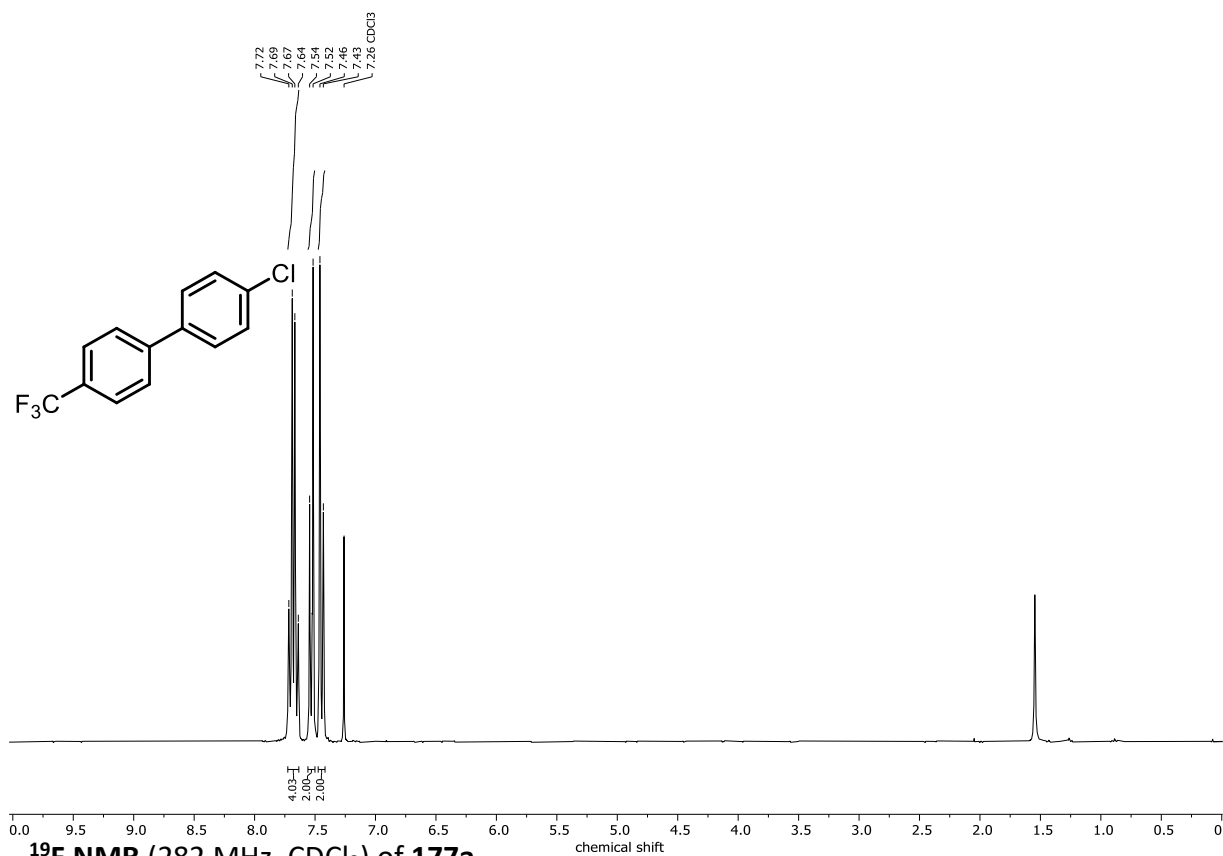
¹H NMR (400 MHz, CDCl₃) of 176b



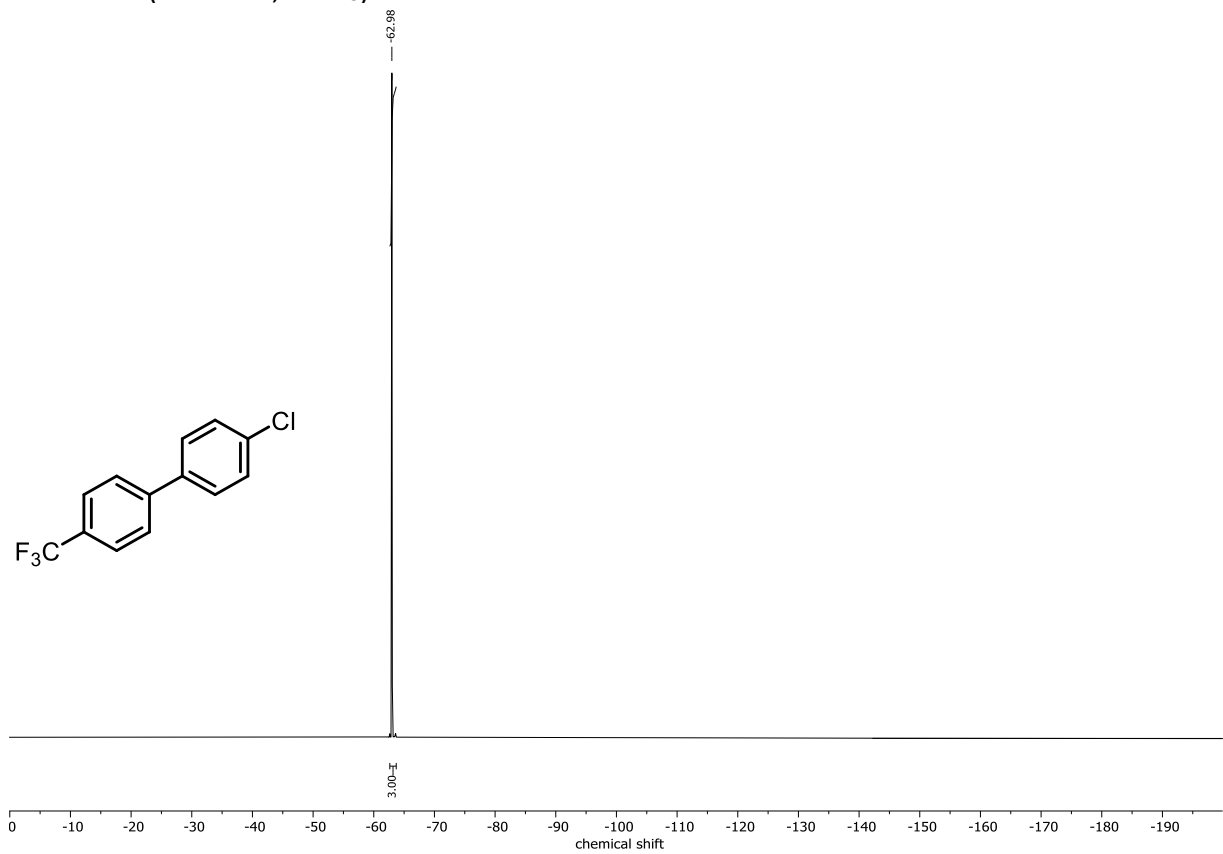
¹³C NMR (101 MHz, CDCl₃) of 176b



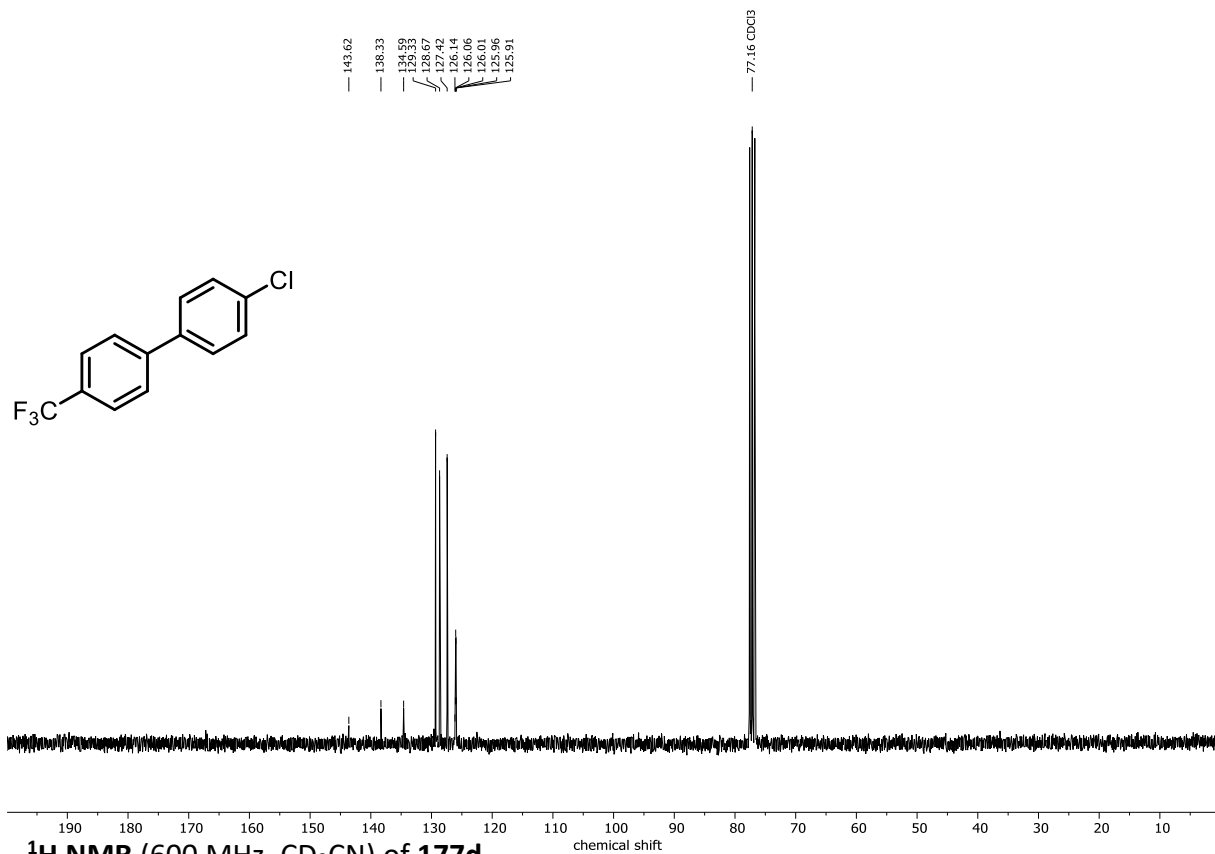
¹H NMR (300 MHz, CDCl₃) of 177a



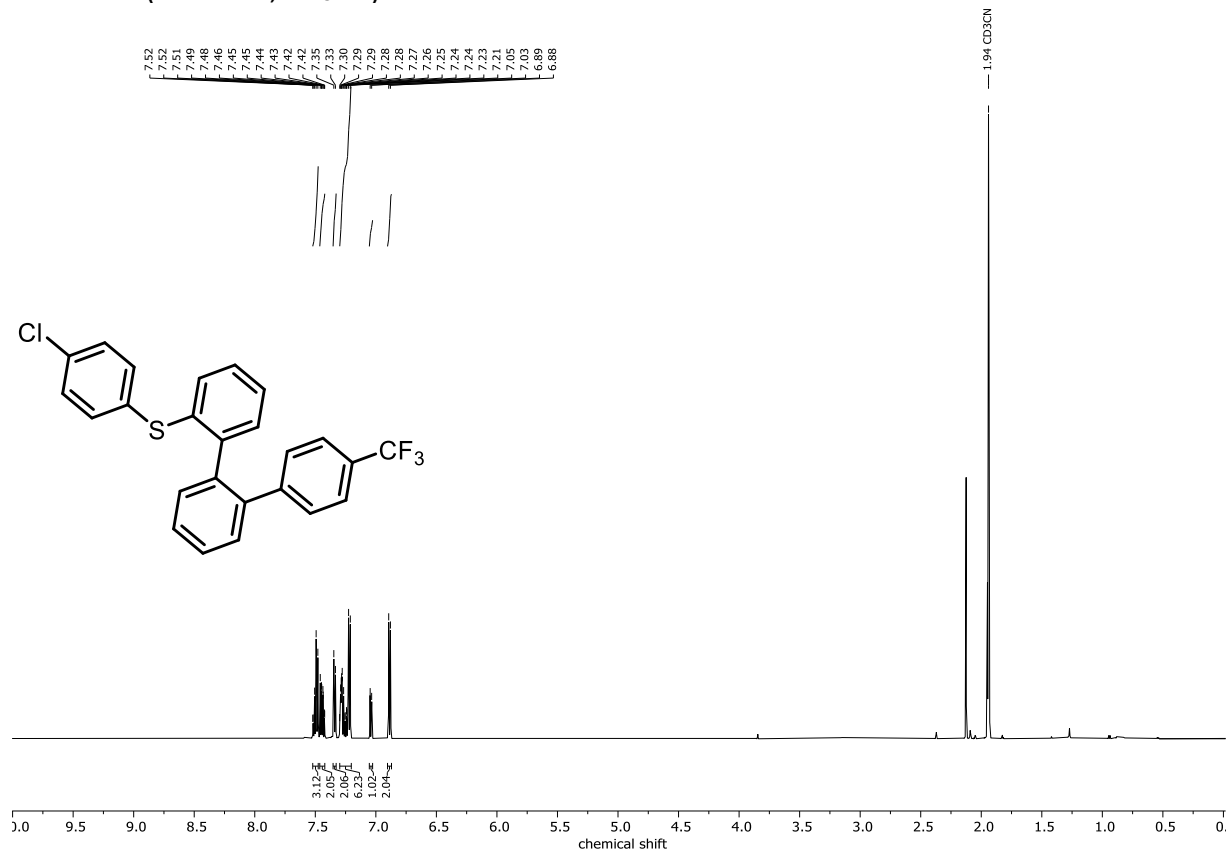
¹⁹F NMR (282 MHz, CDCl₃) of 177a



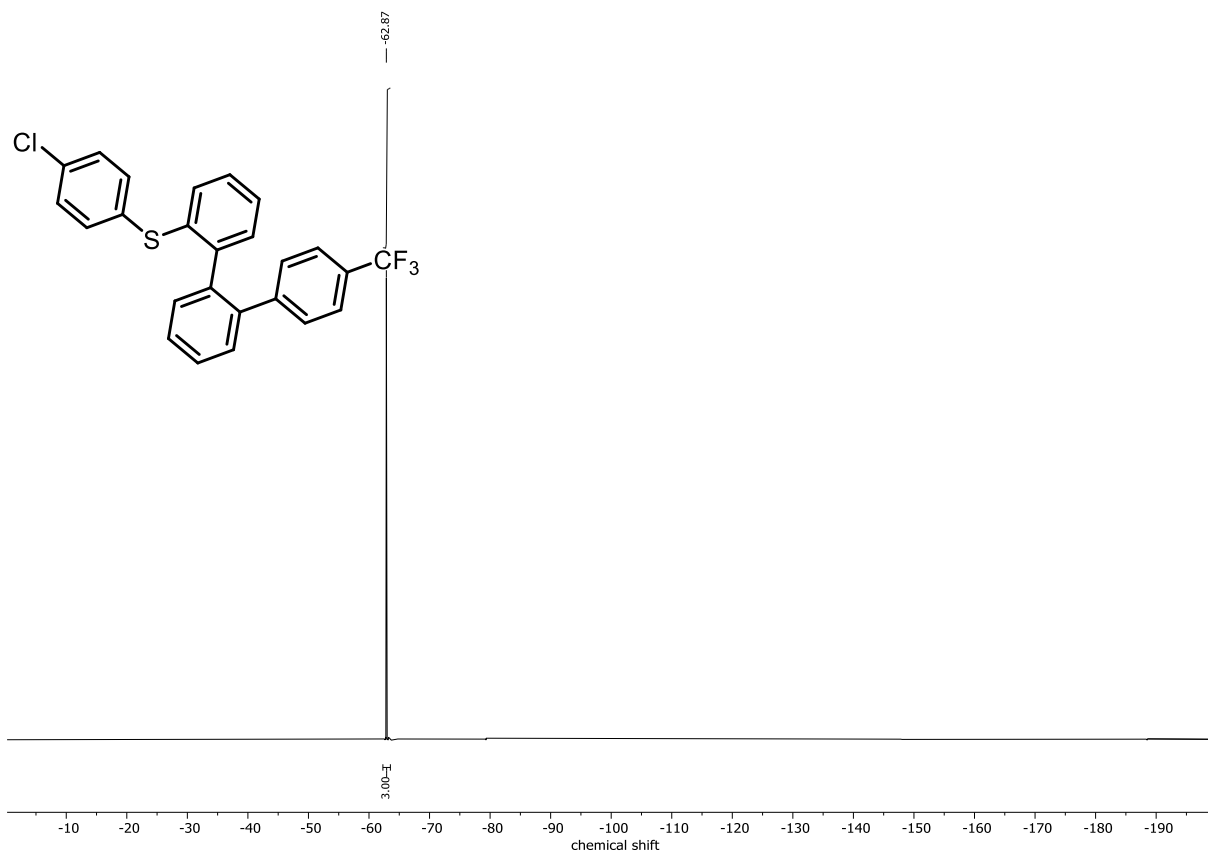
¹³C NMR (75 MHz, CDCl₃) of 177a



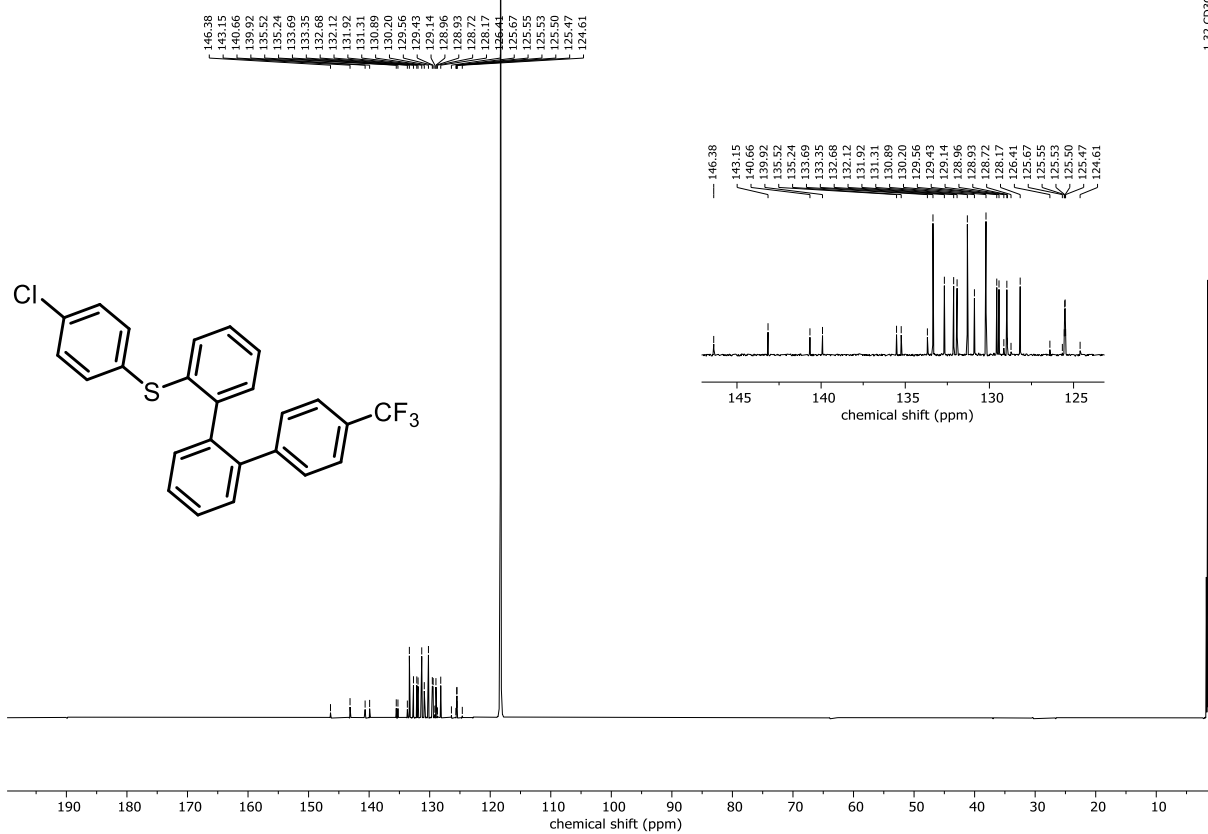
¹H NMR (600 MHz, CD₃CN) of 177d



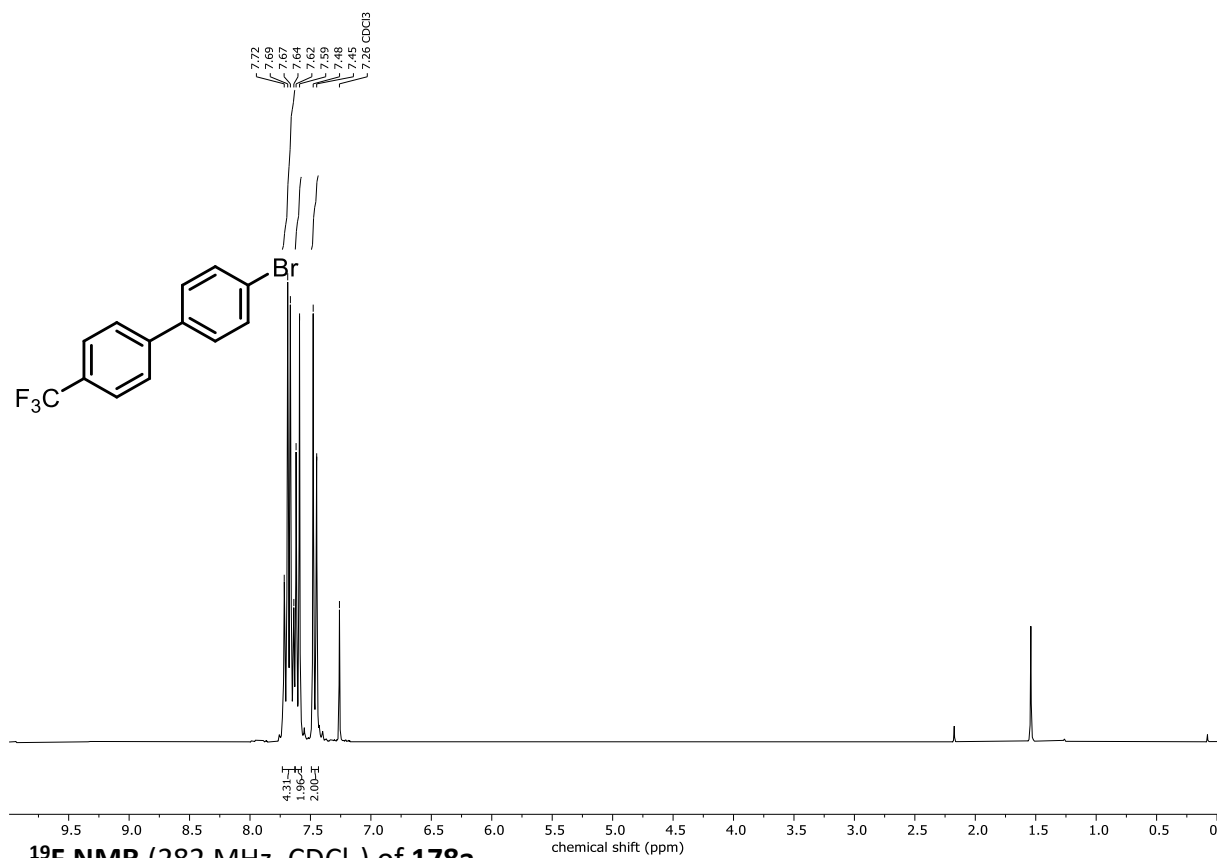
¹⁹F NMR (565 MHz, CD₃CN) of 177d



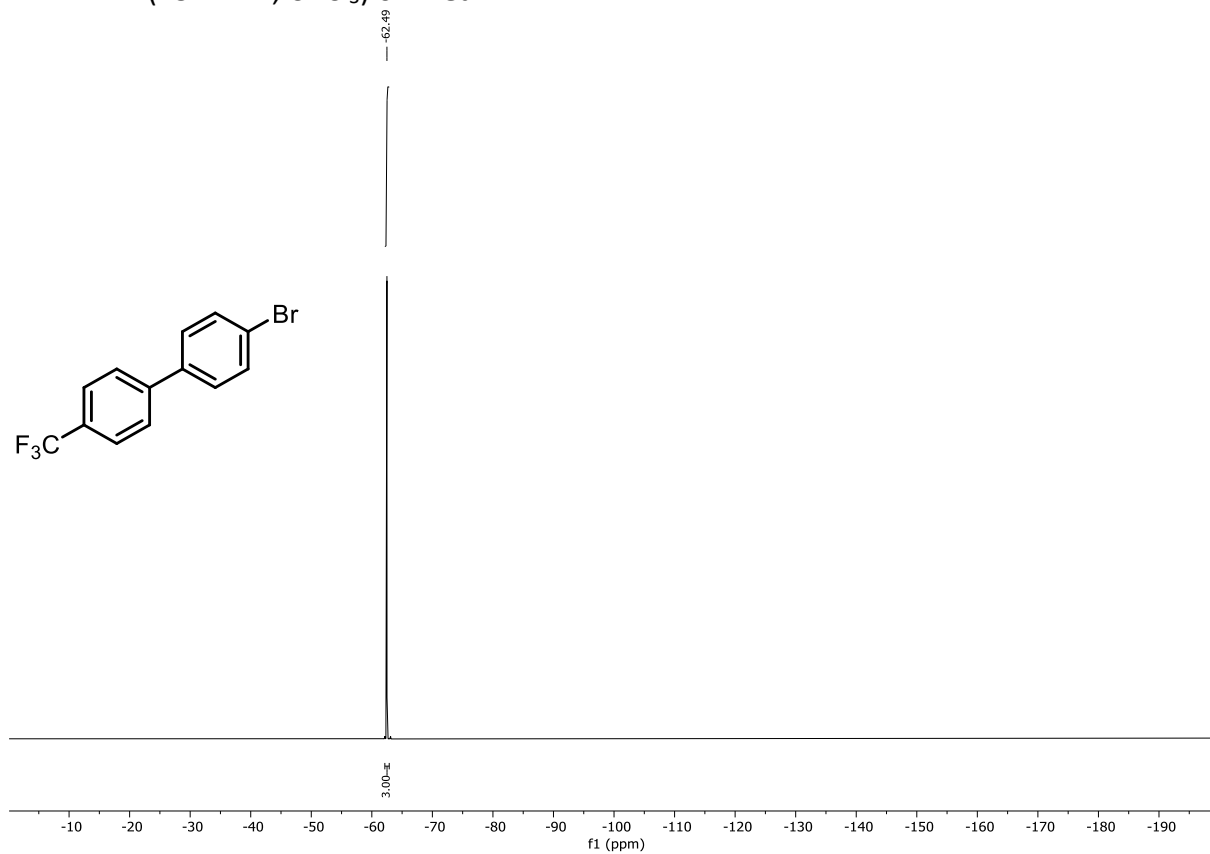
¹³C NMR (151 MHz, CD₃CN) of 177d



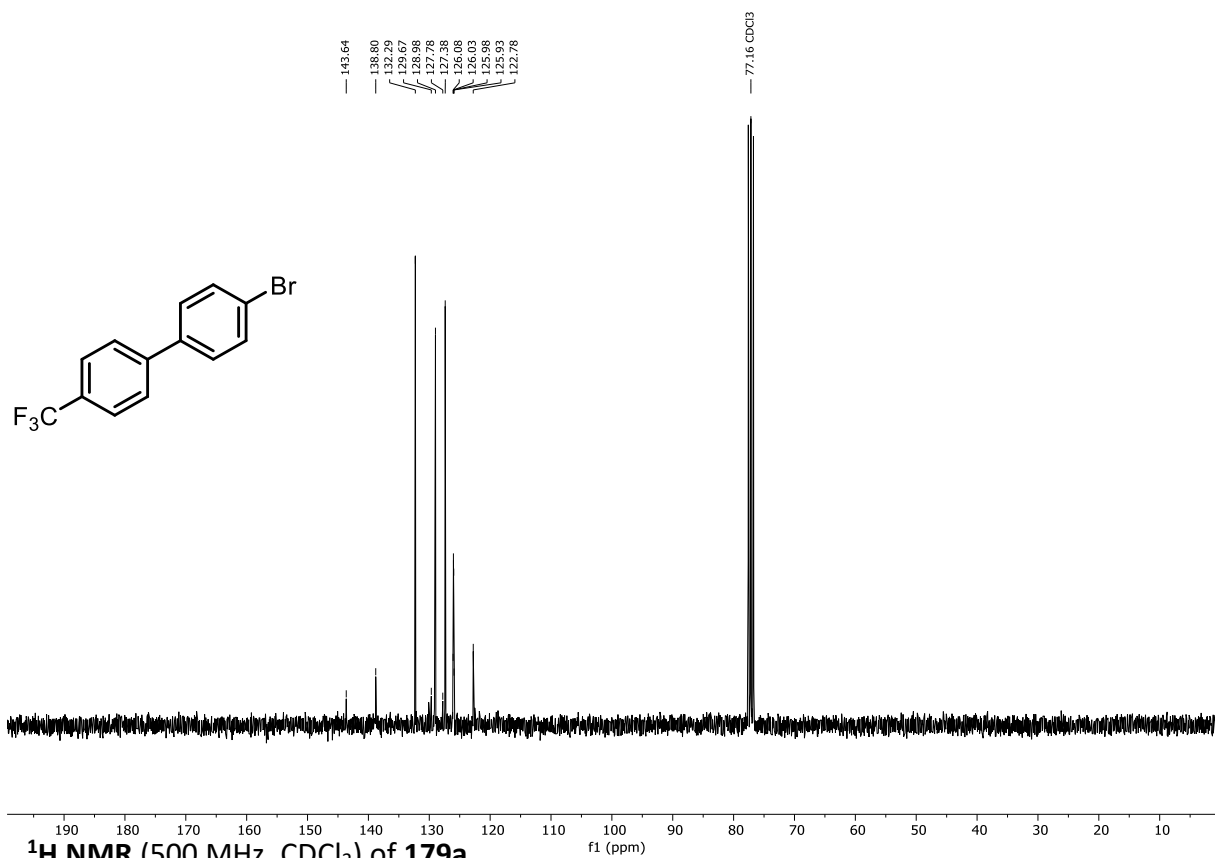
^1H NMR (300 MHz, CDCl_3) of 178a



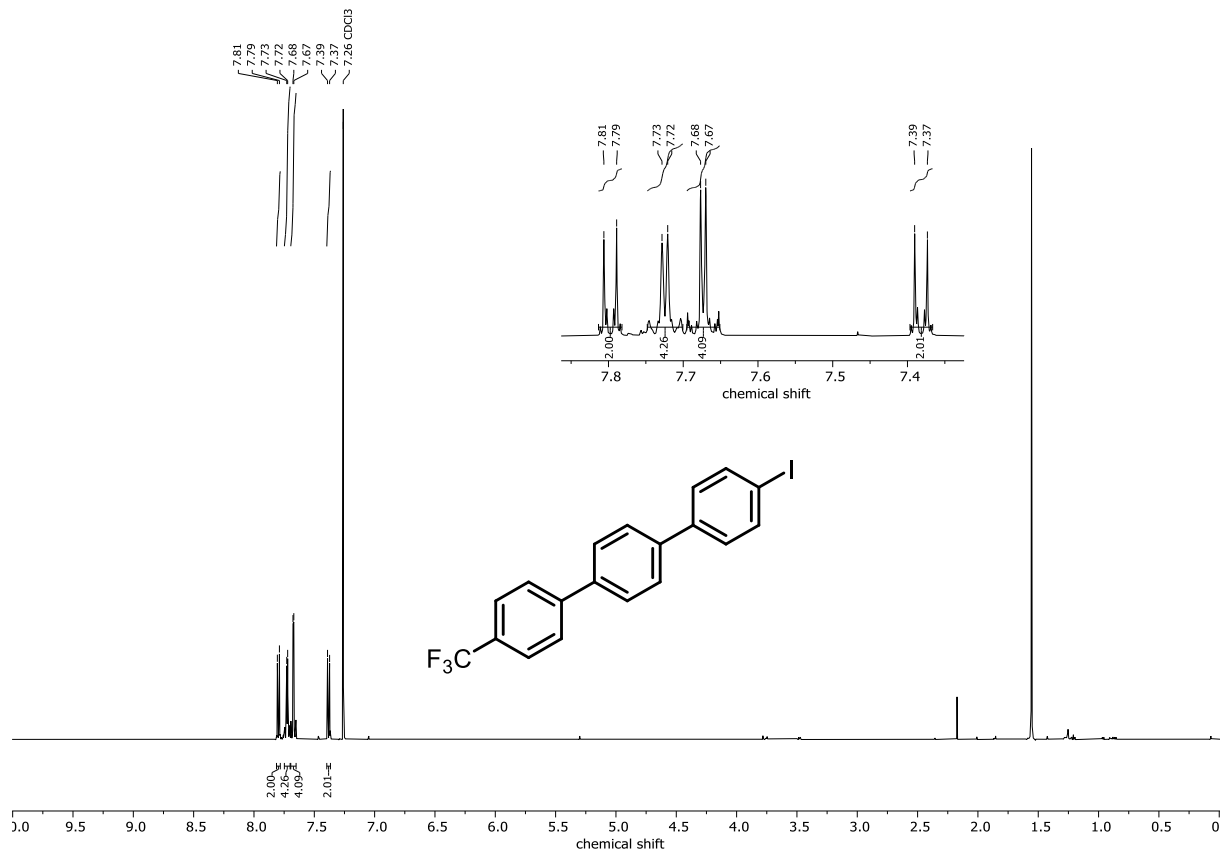
^{19}F NMR (282 MHz, CDCl_3) of 178a



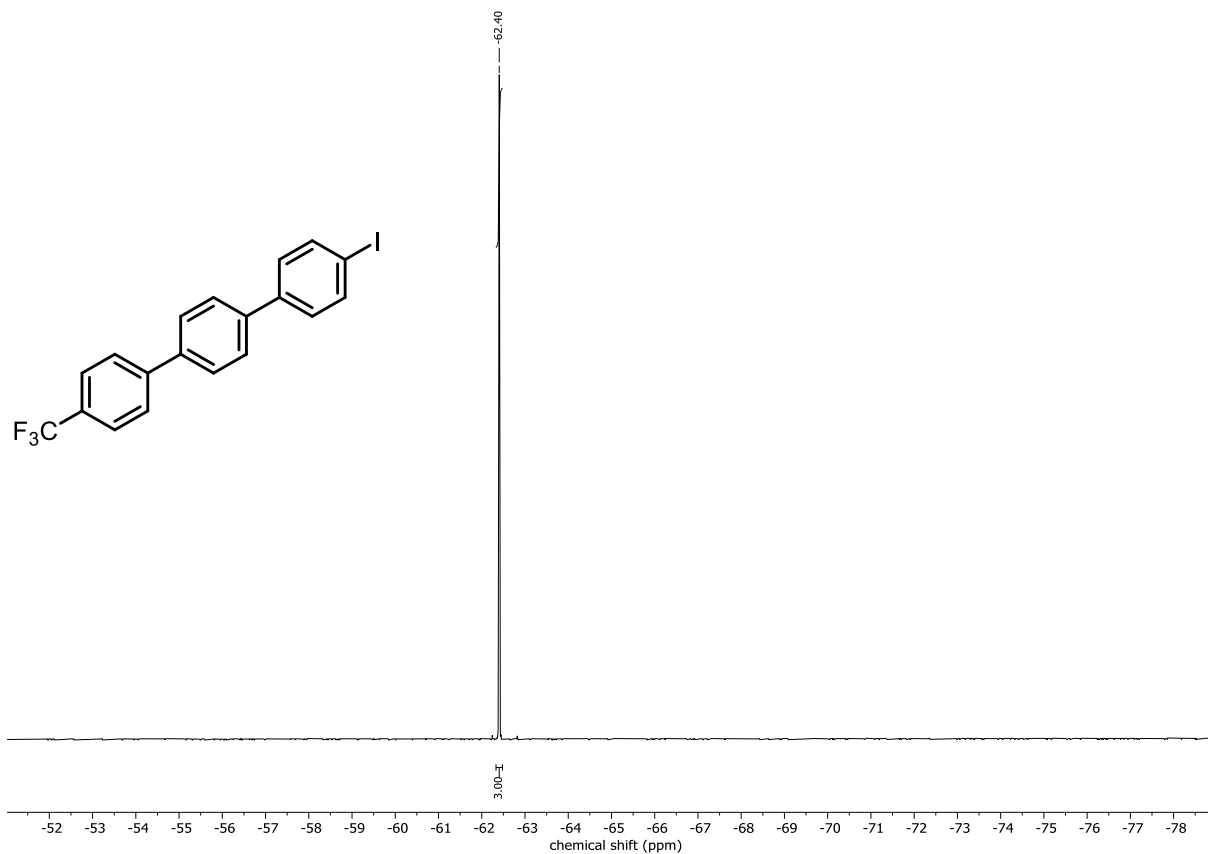
¹³C NMR (75 MHz, CDCl₃) of 178a



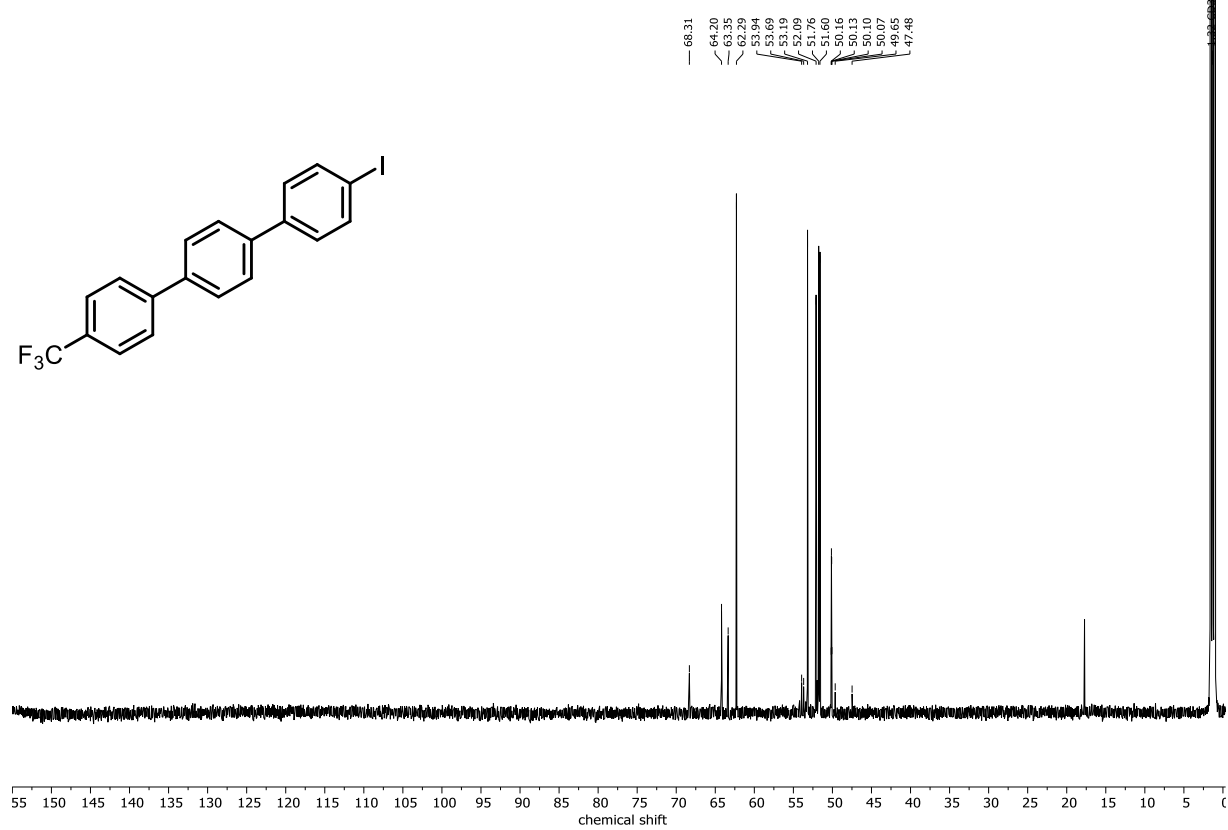
¹H NMR (500 MHz, CDCl₃) of 179a



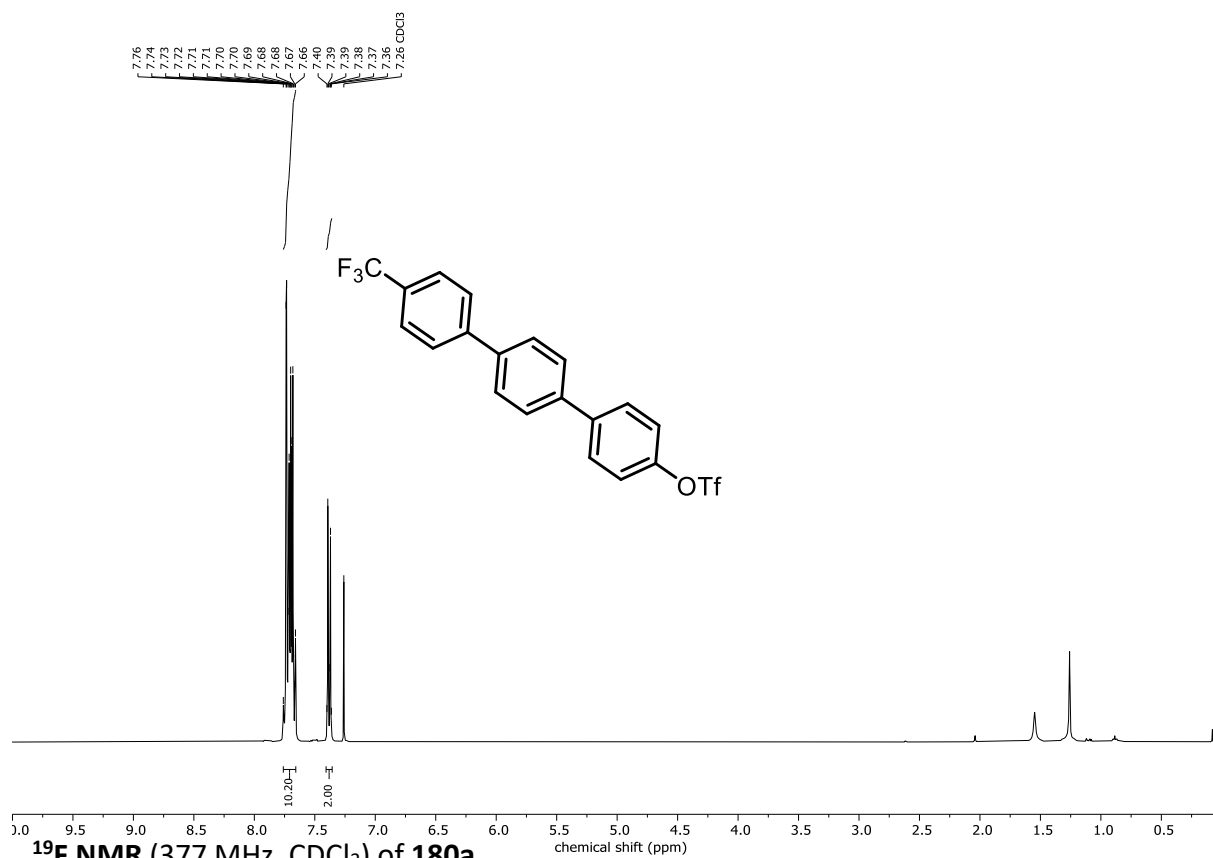
¹⁹F NMR (471 MHz, CDCl₃) of 179a



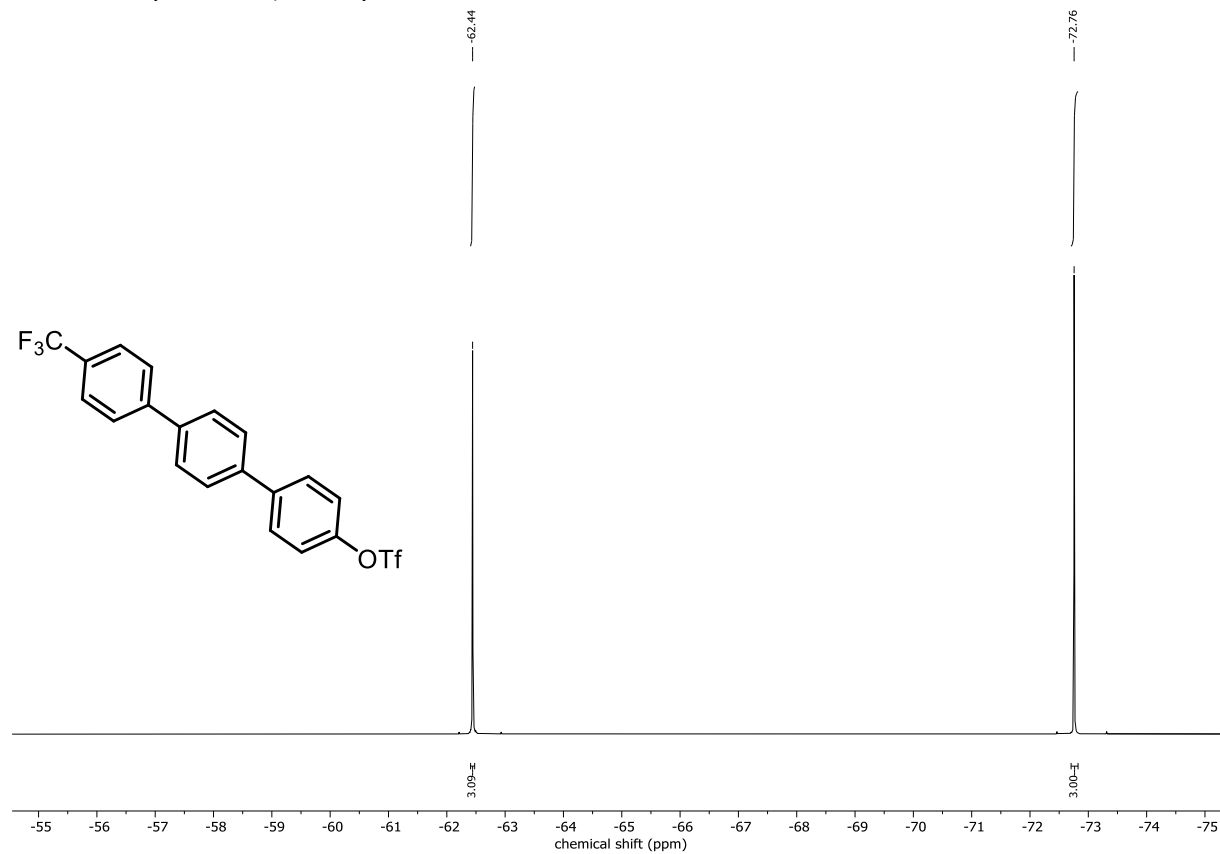
¹³C NMR (126 MHz, CDCl₃) of 179a



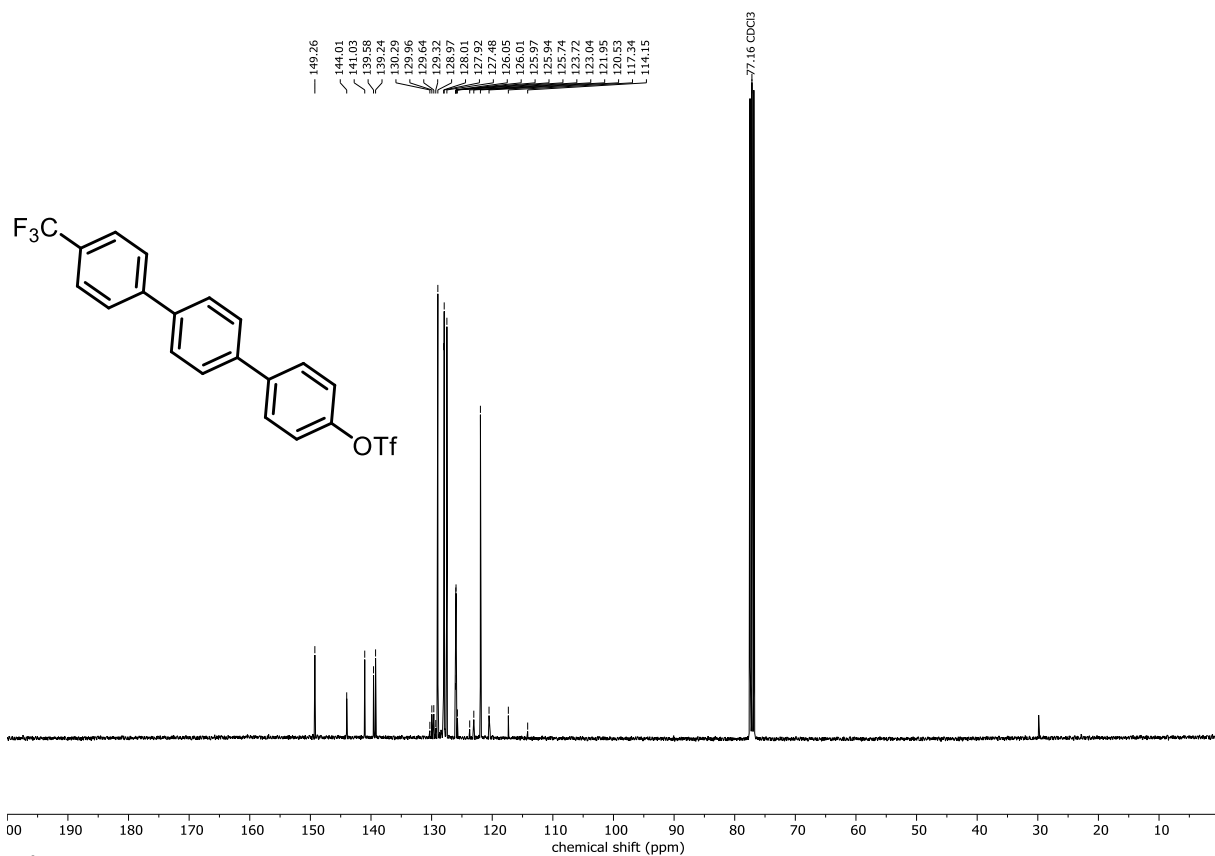
¹H NMR (400 MHz, CDCl₃) of 180a



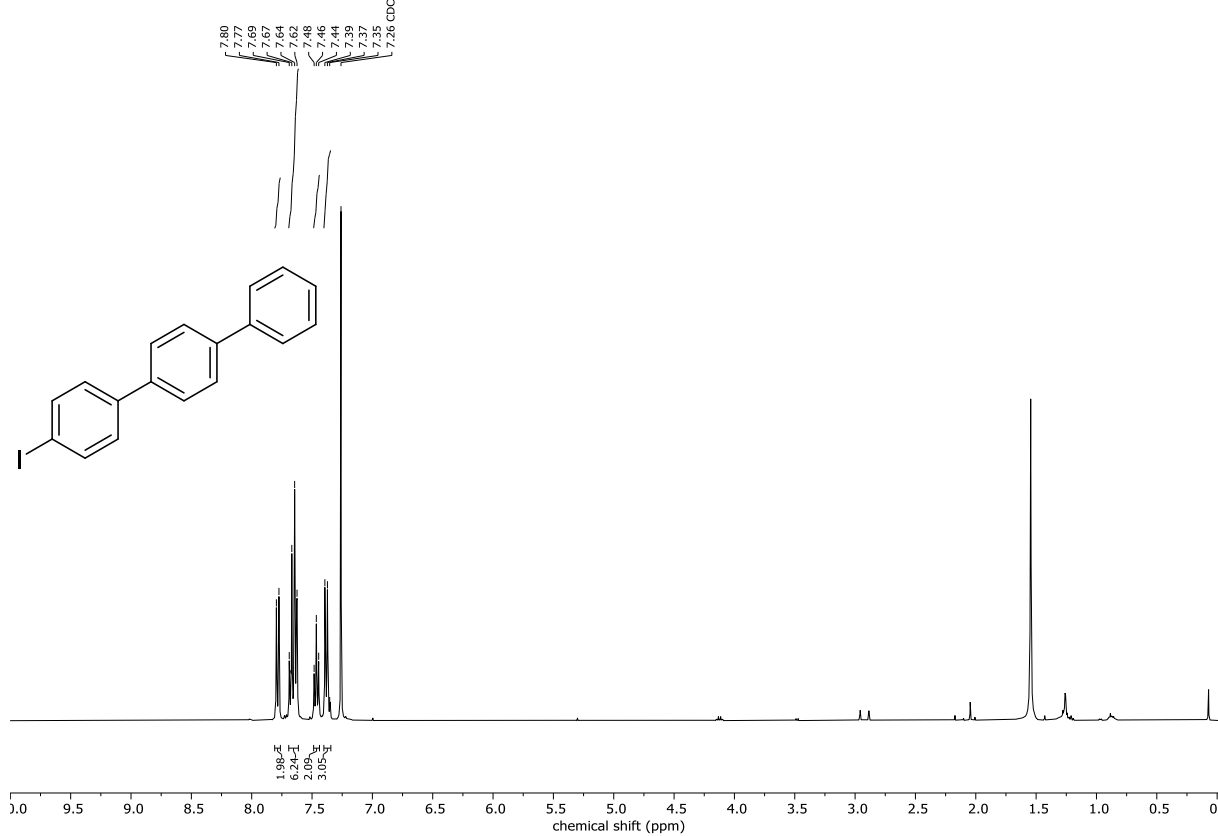
¹⁹F NMR (377 MHz, CDCl₃) of 180a



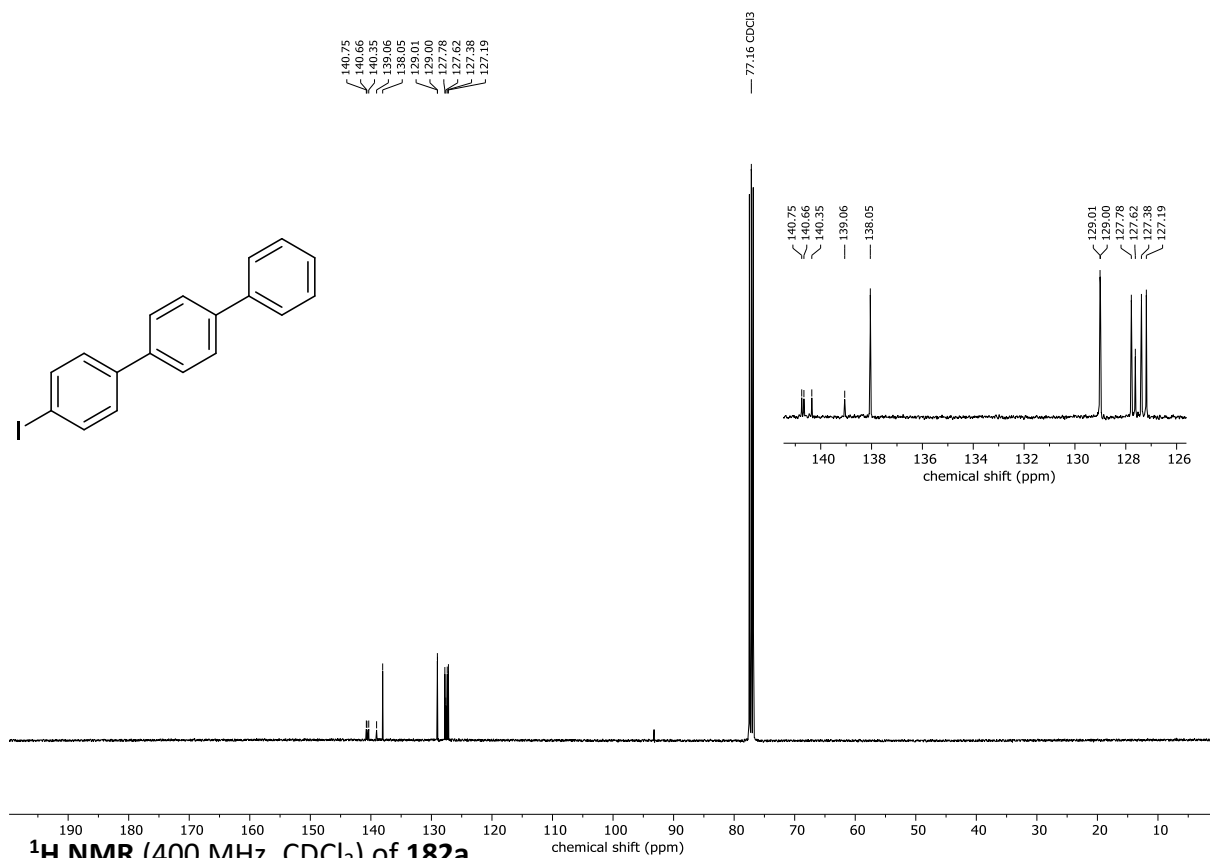
¹³C NMR (101 MHz, CDCl₃) of 180a



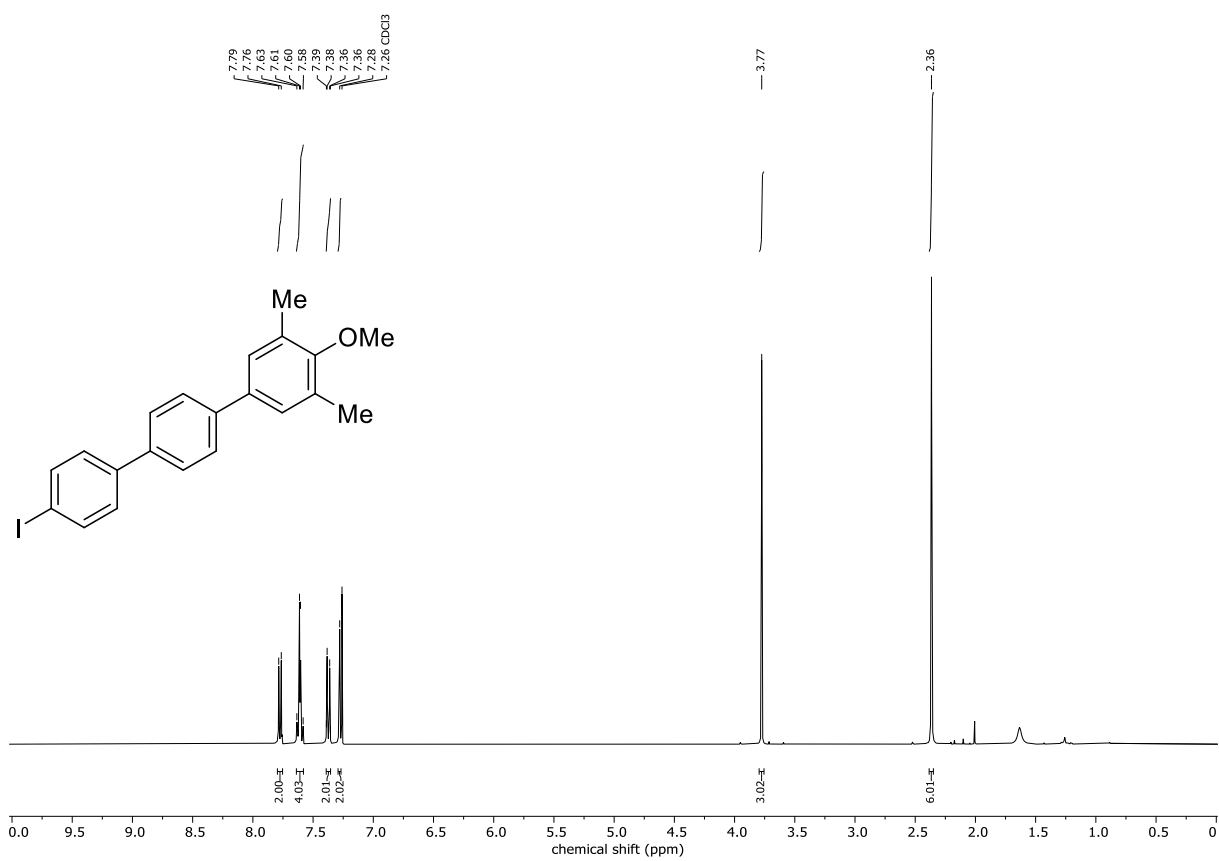
¹H NMR (400 MHz, CDCl₃) of 181a



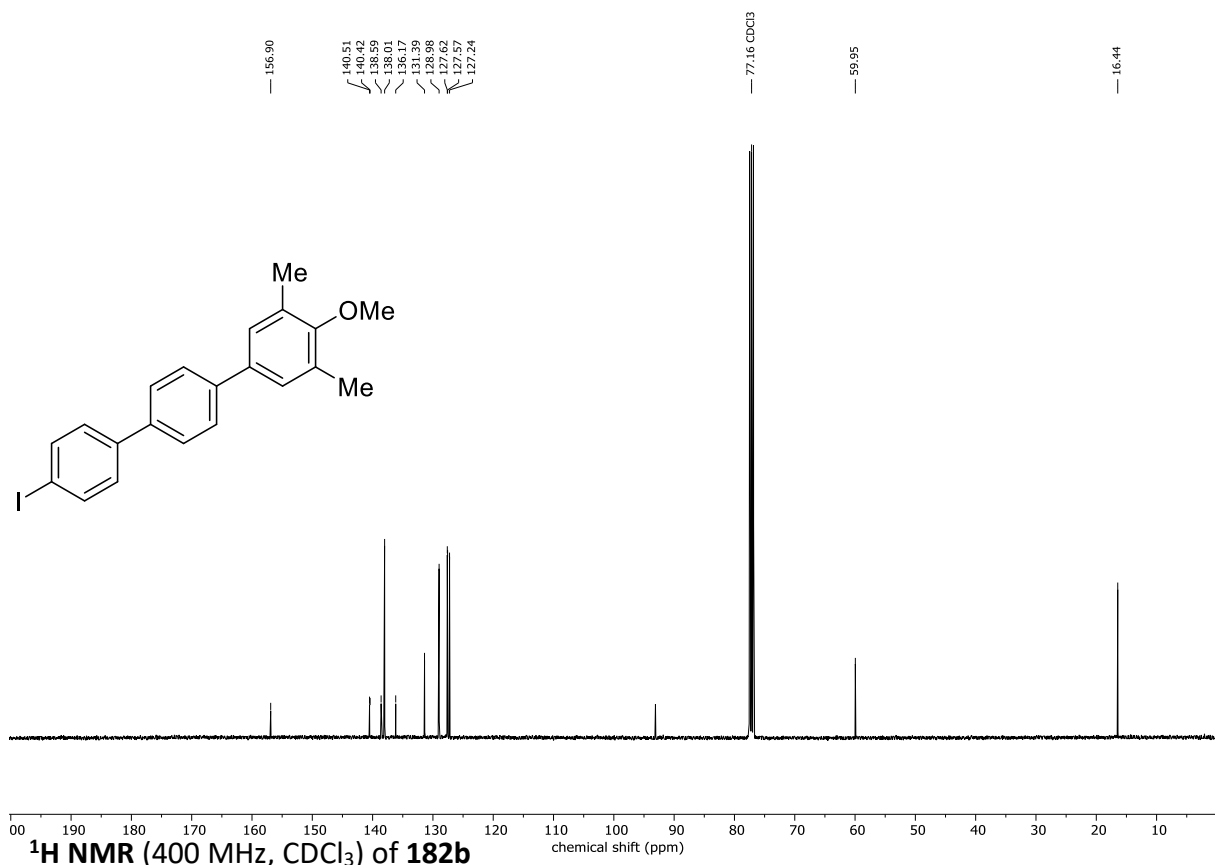
¹³C NMR (101 MHz, CDCl₃) of 181a



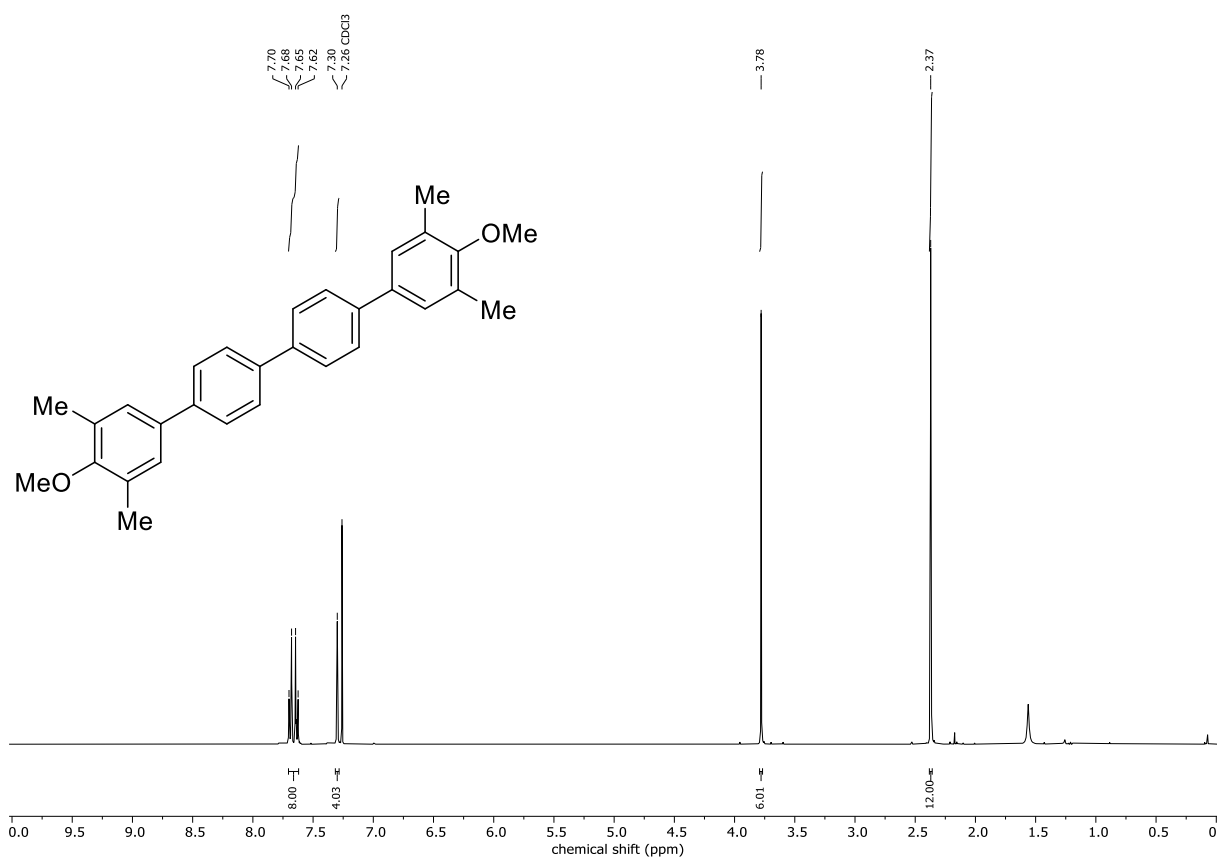
¹H NMR (400 MHz, CDCl₃) of 182a



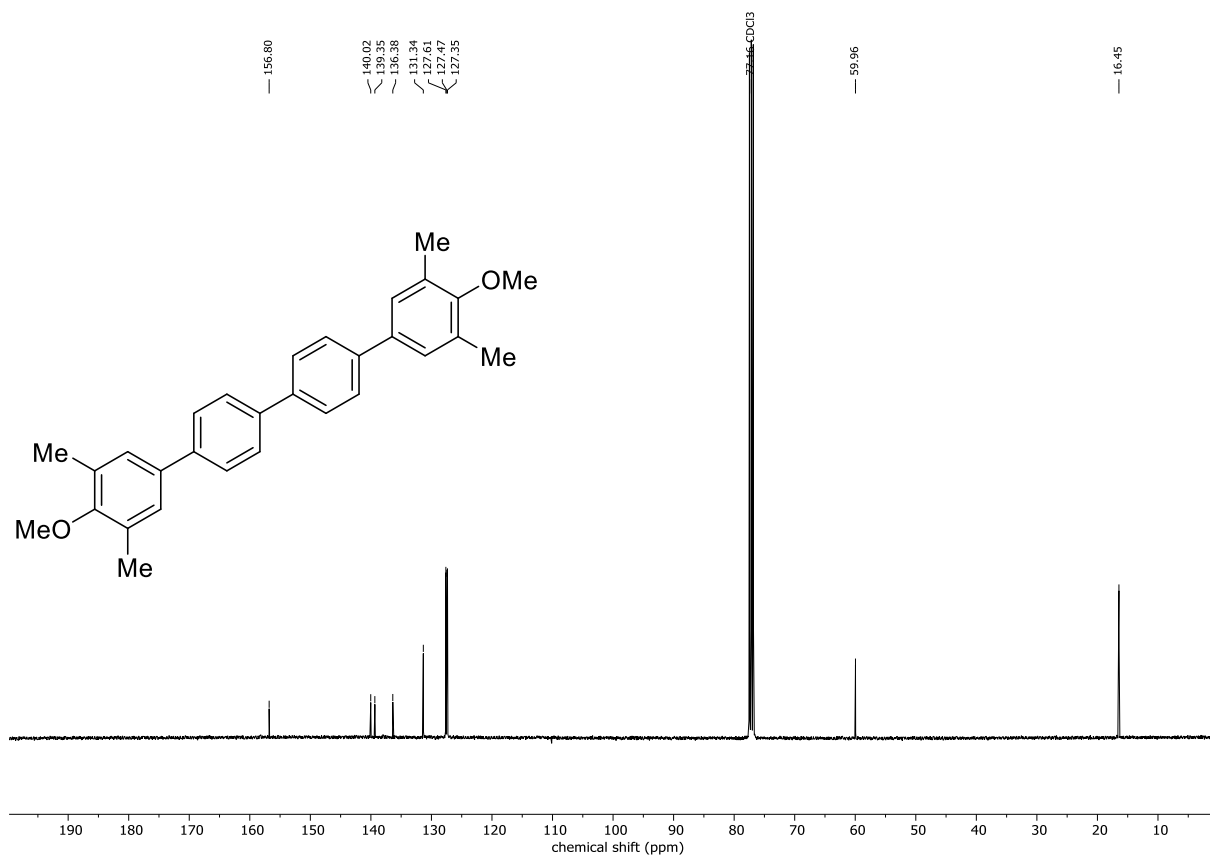
¹³C NMR (101 MHz, CDCl₃) of 182a



¹H NMR (400 MHz, CDCl₃) of 182b



¹³C NMR (101 MHz, CDCl₃) of **182b**



X-Ray Structures

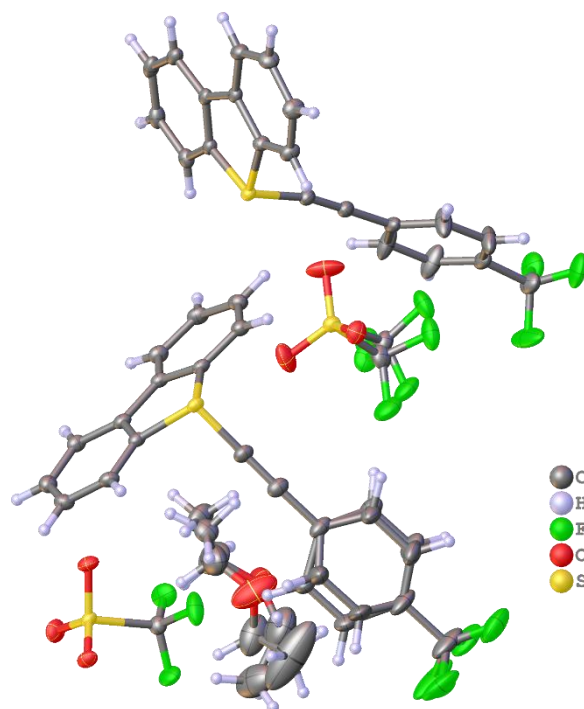


Figure 19: Crystal structure of 5c.

Table 1: Crystal data and structure refinement for 5c.

Identification code	0511_CG_0m		
Empirical formula	$C_{48}H_{34}F_{12}O_7S_4$	μ/mm^{-1}	0.308
Formula weight	1078.99	F(000)	1100.0
Temperature/K	100.01	Crystal size/ mm^3	$0.459 \times 0.218 \times 0.07$
Crystal system	triclinic	Radiation	MoK α ($\lambda = 0.71073$)
Space group	P-1	2 θ range for data collection/ $^\circ$	4.892 to 59.316
a/ \AA	8.7351(10)	Index ranges	$-12 \leq h \leq 12, -18 \leq k \leq 22, -23 \leq l \leq 23$
b/ \AA	15.8447(13)	Reflections collected	37625
c/ \AA	17.0177(19)	Independent reflections	12907 [$R_{\text{int}} = 0.0309, R_{\text{sigma}} = 0.0359$]
$\alpha/^\circ$	80.155(5)	Data/restraints/parameters	12907/193/787
$\beta/^\circ$	83.293(4)	Goodness-of-fit on F^2	1.034
$\gamma/^\circ$	89.447(4)	Final R indexes [$ I \geq 2\sigma(I)$]	$R_1 = 0.0420, wR_2 = 0.0978$
Volume/ \AA^3	2304.6(4)	Final R indexes [all data]	$R_1 = 0.0527, wR_2 = 0.1056$
Z	2	Largest diff. peak/hole / $e \text{\AA}^{-3}$	0.43/-0.49
$\rho_{\text{calc}}/\text{cm}^3$	1.555		

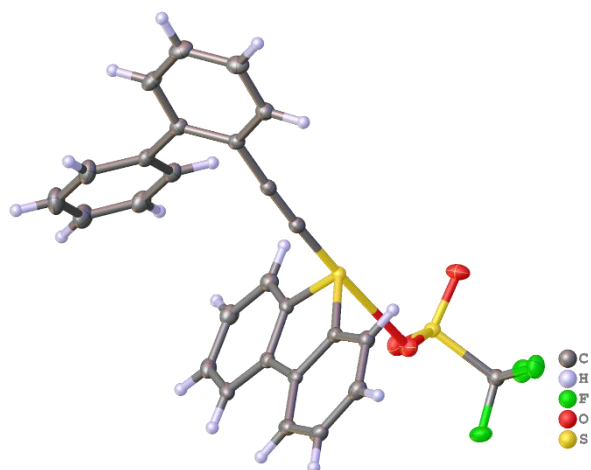


Figure 20: Crystal structure of 5j.

Table 2: Crystal data and structure refinement for 5j.

Identification code		mo_0938_CG_0m	
Empirical formula	C ₂₇ H ₁₇ F ₃ O ₃ S ₂	μ/mm^{-1}	0.289
Formula weight	510.52	F(000)	524.0
Temperature/K	100.0	Crystal size/mm ³	0.351 × 0.14 × 0.08
Crystal system	triclinic	Radiation	MoK α (λ = 0.71073)
Space group	P-1	2 θ range for data collection/°	4.57 to 59.338
a/Å	9.1125(12)	Index ranges	-12 ≤ h ≤ 12, -15 ≤ k ≤ 15, -15 ≤ l ≤ 16
b/Å	11.0838(15)	Reflections collected	115220
c/Å	11.4885(17)	Independent reflections	6406 [R _{int} = 0.0273, R _{sigma} = 0.0119]
α /°	86.788(4)	Data/restraints/parameters	6406/0/316
β /°	80.159(4)	Goodness-of-fit on F ²	1.016
γ /°	82.554(4)	Final R indexes [$ I \geq 2\sigma(I)$]	R ₁ = 0.0284, wR ₂ = 0.0763
Volume/Å ³	1133.0(3)	Final R indexes [all data]	R ₁ = 0.0299, wR ₂ = 0.0775
Z	2	Largest diff. peak/hole / e Å ⁻³	0.45/-0.35
$\rho_{\text{calc}}/\text{cm}^3$	1.497		

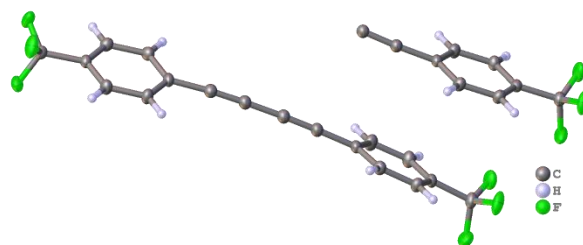


Figure 21: Crystal structure of 33c'.

Table 3: Crystal data and structure refinement for 33c'.

Identification code 0565_CG_0m

Empirical formula	C ₁₈ H ₈ F ₆	μ/mm^{-1}	0.147
Formula weight	338.24	F(000)	510.0
Temperature/K	99.97	Crystal size/mm ³	0.305 × 0.148 × 0.054
Crystal system	triclinic	Radiation	MoK α (λ = 0.71073)
Space group	P-1	2 θ range for data collection/°	5.44 to 57.738
a/Å	7.6943(14)	Index ranges	-10 ≤ h ≤ 10, -16 ≤ k ≤ 16, -17 ≤ l ≤ 17
b/Å	12.192(2)	Reflections collected	25695
c/Å	12.635(2)	Independent reflections	5322 [R _{int} = 0.0408, R _{sigma} = 0.0321]
α /°	67.297(5)	Data/restraints/parameters	5322/0/325
β /°	77.096(4)	Goodness-of-fit on F ²	1.049
γ /°	87.910(6)	Final R indexes [$I > 2\sigma(I)$]	R ₁ = 0.0443, wR ₂ = 0.1124
Volume/Å ³	1064.2(3)	Final R indexes [all data]	R ₁ = 0.0622, wR ₂ = 0.1235
Z	3	Largest diff. peak/hole / e Å ⁻³	0.48/-0.31
$\rho_{\text{calc}}/\text{cm}^3$	1.583		

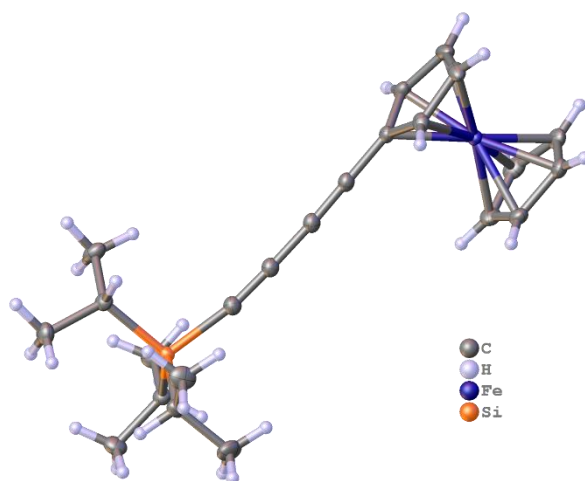


Figure 22: Crystal structure of 33h.

Table 4: Crystal data and structure refinement for 33i.

Identification code 0596_CG_0m

Empirical formula	C ₂₃ H ₃₀ FeSi	μ/mm^{-1}	0.785
Formula weight	390.41	F(000)	416.0
Temperature/K	99.99	Crystal size/mm ³	0.334 × 0.322 × 0.196
Crystal system	triclinic	Radiation	MoK α ($\lambda = 0.71073$)
Space group	P-1	2 θ range for data collection/°	4.472 to 61.126
a/Å	9.2172(6)	Index ranges	-13 ≤ h ≤ 13, -16 ≤ k ≤ 16, -16 ≤ l ≤ 16
b/Å	11.4974(7)	Reflections collected	49311
c/Å	11.6210(8)	Independent reflections	6348 [R _{int} = 0.0307, R _{sigma} = 0.0151]
α /°	104.064(2)	Data/restraints/parameters	6348/0/232
β /°	108.843(2)	Goodness-of-fit on F ²	1.055
γ /°	106.313(2)	Final R indexes [$I \geq 2\sigma(I)$]	R ₁ = 0.0227, wR ₂ = 0.0599
Volume/Å ³	1040.36(12)	Final R indexes [all data]	R ₁ = 0.0256, wR ₂ = 0.0619
Z	2	Largest diff. peak/hole / e Å ⁻³	0.40/-0.29
$\rho_{\text{calc}}/\text{cm}^3$	1.246		

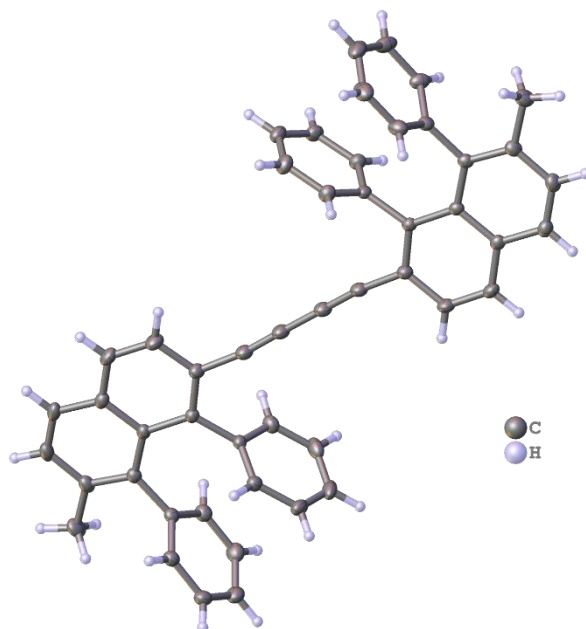


Figure 23: Crystal structure of 33i'.

Table 5: Crystal data and structure refinement for 33i'.

Identification code	0604_CG_0m		
Empirical formula	C ₅₀ H ₃₄	μ/mm^{-1}	0.070
Formula weight	634.77	F(000)	1336.0
Temperature/K	100.03	Crystal size/mm ³	0.258 × 0.256 × 0.076
Crystal system	monoclinic	Radiation	MoK α (λ = 0.71073)
Space group	P2 ₁ /n	2 θ range for data collection/°	5.316 to 59.444
a/Å	18.210(3)	Index ranges	-25 ≤ h ≤ 22, -11 ≤ k ≤ 11, -32 ≤ l ≤ 32
b/Å	8.0595(19)	Reflections collected	176883
c/Å	23.488(5)	Independent reflections	9648 [R _{int} = 0.0322, R _{sigma} = 0.0134]
α /°	90	Data/restraints/parameters	9648/0/453
β /°	98.049(7)	Goodness-of-fit on F ²	1.042
γ /°	90	Final R indexes [I >= 2 σ (I)]	R ₁ = 0.0425, wR ₂ = 0.1120
Volume/Å ³	3413.2(13)	Final R indexes [all data]	R ₁ = 0.0493, wR ₂ = 0.1176
Z	4	Largest diff. peak/hole / e Å ⁻³	0.36/-0.26
$\rho_{\text{calc}}/\text{cm}^3$	1.235		

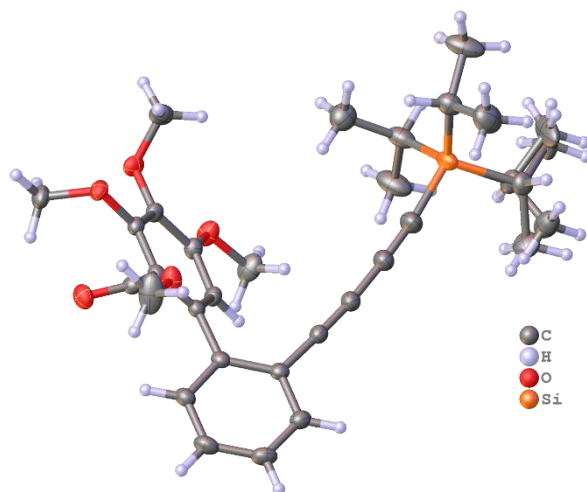


Figure 24: Crystal structure of 33j.

Table 6: Crystal data and structure refinement for 33j.

Identification code		P21c	
Empirical formula	C ₃₀ H ₃₈ O ₅ Si	μ/mm^{-1}	0.118
Formula weight	506.69	F(000)	1088.0
Temperature/K	100.02	Crystal size/mm ³	0.682 × 0.595 × 0.482
Crystal system	monoclinic	Radiation	MoK α ($\lambda = 0.71073$)
Space group	P2 ₁ /c	2 θ range for data collection/°	4.756 to 57.462
a/Å	16.2204(17)	Index ranges	-21 ≤ h ≤ 21, -23 ≤ k ≤ 23, -14 ≤ l ≤ 12
b/Å	17.1259(18)	Reflections collected	52337
c/Å	10.4293(9)	Independent reflections	7342 [R _{int} = 0.0263, R _{sigma} = 0.0163]
α /°	90	Data/restraints/parameters	7342/0/365
β /°	101.021(4)	Goodness-of-fit on F ²	1.021
γ /°	90	Final R indexes [I > 2 σ (I)]	R ₁ = 0.0451, wR ₂ = 0.1094
Volume/Å ³	2843.7(5)	Final R indexes [all data]	R ₁ = 0.0497, wR ₂ = 0.1131
Z	4	Largest diff. peak/hole / e Å ⁻³	0.91/-1.10
$\rho_{\text{calc}}/\text{cm}^{-3}$	1.183		

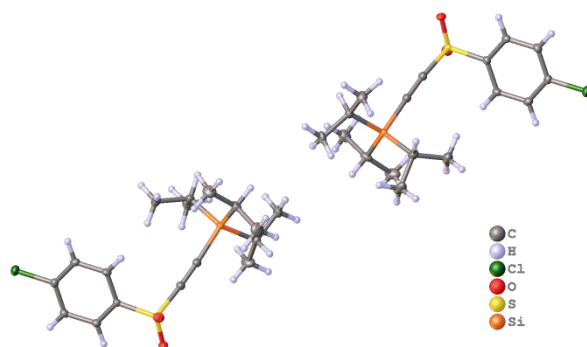


Figure 25: Crystal structure of 37e.

Table 7: Crystal data and structure refinement for 37e.

Identification code		mo_0919_CG_0m	
Empirical formula	C ₁₇ H ₂₅ ClO ₂ SSi	μ/mm^{-1}	0.384
Formula weight	356.97	F(000)	760.0
Temperature/K	100.0	Crystal size/mm ³	0.465 × 0.264 × 0.158
Crystal system	triclinic	Radiation	MoK α ($\lambda = 0.71073$)
Space group	P-1	2 θ range for data collection/°	3.798 to 57.558
a/Å	11.080(3)	Index ranges	-14 ≤ h ≤ 14, -15 ≤ k ≤ 15, -21 ≤ l ≤ 21
b/Å	11.614(3)	Reflections collected	40097
c/Å	15.962(4)	Independent reflections	9499 [R _{int} = 0.0278, R _{sigma} = 0.0257]
α /°	85.015(7)	Data/restraints/parameters	9499/0/409
β /°	80.704(7)	Goodness-of-fit on F ²	1.106
γ /°	67.483(6)	Final R indexes [I ≥ 2 σ (I)]	R ₁ = 0.0365, wR ₂ = 0.0841
Volume/Å ³	1871.8(8)	Final R indexes [all data]	R ₁ = 0.0422, wR ₂ = 0.0869
Z	4	Largest diff. peak/hole / e Å ⁻³	0.45/-0.55
$\rho_{\text{calc}}/\text{cm}^3$	1.267		

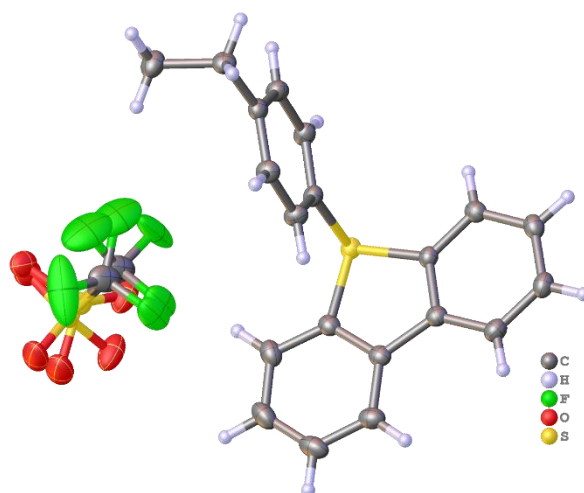


Figure 26: Crystal structure of 93b.

Table 8: Crystal data and structure refinement for 93b.

Identification code	0631_CG_0m		
Empirical formula	$C_{21}H_{17}F_3O_3S_2$	μ/mm^{-1}	0.323
Formula weight	438.46	$F(000)$	904.0
Temperature/K	99.98	Crystal size/ mm^3	$0.251 \times 0.161 \times 0.152$
Crystal system	monoclinic	Radiation	MoK α ($\lambda = 0.71073$)
Space group	$P2_1/n$	2θ range for data collection/ $^\circ$	4.838 to 59.186
$a/\text{\AA}$	9.5523(6)	Index ranges	$-12 \leq h \leq 13, -22 \leq k \leq 22, -17 \leq l \leq 17$
$b/\text{\AA}$	16.4132(12)	Reflections collected	93756
$c/\text{\AA}$	12.7116(9)	Independent reflections	5445 [$R_{\text{int}} = 0.0230, R_{\text{sigma}} = 0.0098$]
$\alpha/^\circ$	90	Data/restraints/parameters	5445/114/336
$\beta/^\circ$	103.291(2)	Goodness-of-fit on F^2	1.066
$\gamma/^\circ$	90	Final R indexes [$I \geq 2\sigma(I)$]	$R_1 = 0.0472, wR_2 = 0.1292$
Volume/ \AA^3	1939.6(2)	Final R indexes [all data]	$R_1 = 0.0489, wR_2 = 0.1307$
Z	4	Largest diff. peak/hole / $e \text{\AA}^{-3}$	0.90/-0.60
$\rho_{\text{calc}}/\text{cm}^3$	1.502		

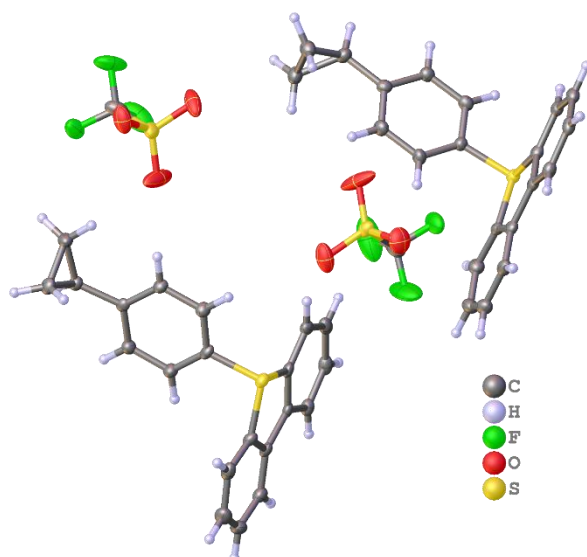


Figure 27: Crystal structure of 93c.

Table 9: Crystal data and structure refinement for 93c.

Identification code 0652_CG_0m			
Empirical formula	C ₂₂ H ₁₇ F ₃ O ₃ S ₂	μ/mm^{-1}	0.315
Formula weight	450.47	F(000)	928.0
Temperature/K	100.0	Crystal size/mm ³	0.213 × 0.18 × 0.179
Crystal system	triclinic	Radiation	MoK α (λ = 0.71073)
Space group	P-1	2 θ range for data collection/°	4.282 to 56.596
a/Å	9.804(2)	Index ranges	-12 ≤ h ≤ 12, -17 ≤ k ≤ 17, -21 ≤ l ≤ 21
b/Å	13.140(3)	Reflections collected	78677
c/Å	16.034(4)	Independent reflections	9636 [R _{int} = 0.0478, R _{sigma} = 0.0296]
α /°	89.312(7)	Data/restraints/parameters	9636/0/542
β /°	89.881(8)	Goodness-of-fit on F ²	1.169
γ /°	75.985(6)	Final R indexes [$ I \geq 2\sigma(I)$]	R ₁ = 0.0444, wR ₂ = 0.1076
Volume/Å ³	2004.0(8)	Final R indexes [all data]	R ₁ = 0.0461, wR ₂ = 0.1089
Z	4	Largest diff. peak/hole / e Å ⁻³	0.52/-0.52
$\rho_{\text{calc}}/\text{cm}^3$	1.493		

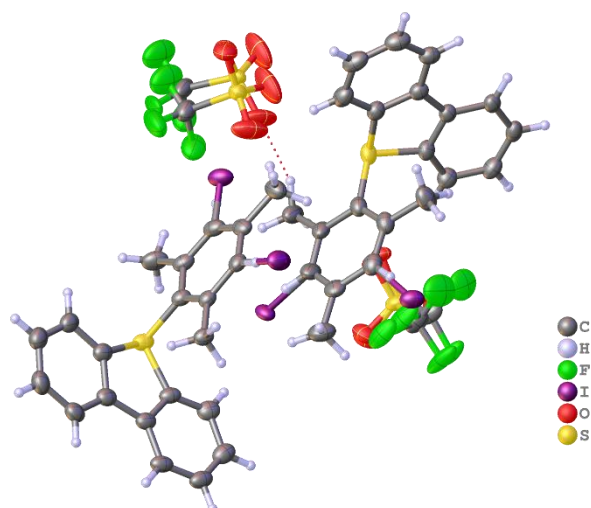


Figure 28: Crystal structure of 93d.

Table 10: Crystal data and structure refinement for 93d.

Identification code		0697_CG_100K	
Empirical formula	C ₂₂ H ₁₈ F ₃ IO ₃ S ₂	μ/mm^{-1}	1.659
Formula weight	578.38	F(000)	1144.0
Temperature/K	100.06	Crystal size/mm ³	0.352 × 0.252 × 0.11
Crystal system	triclinic	Radiation	MoK α ($\lambda = 0.71073$)
Space group	P-1	2 θ range for data collection/°	4.57 to 56.716
a/Å	9.8022(7)	Index ranges	-13 ≤ h ≤ 13, -19 ≤ k ≤ 19, -21 ≤ l ≤ 21
b/Å	14.7710(10)	Reflections collected	57665
c/Å	16.1194(10)	Independent reflections	11157 [R _{int} = 0.0243, R _{sigma} = 0.0174]
α /°	97.859(2)	Data/restraints/parameters	11157/92/731
β /°	93.882(2)	Goodness-of-fit on F ²	1.133
γ /°	102.541(2)	Final R indexes [I > 2 σ (I)]	R ₁ = 0.0481, wR ₂ = 0.1266
Volume/Å ³	2245.3(3)	Final R indexes [all data]	R ₁ = 0.0529, wR ₂ = 0.1297
Z	4	Largest diff. peak/hole / e Å ⁻³	1.68/-0.98
$\rho_{\text{calc}}/\text{cm}^3$	1.711		

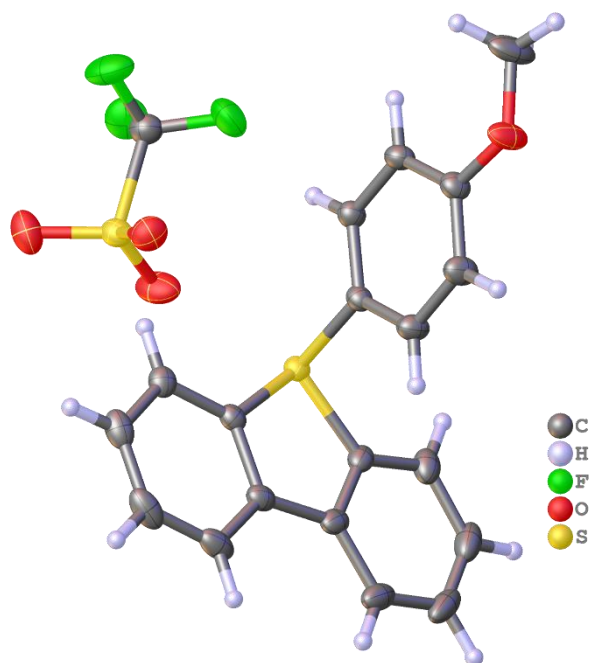


Figure 29: Crystal structure of 93e.

Table 11: Crystal data and structure refinement for 93e.

Identification code	0743_CG_0m		
Empirical formula	$C_{20}H_{15}F_3O_4S_2$	μ/mm^{-1}	0.330
Formula weight	440.44	F(000)	904.0
Temperature/K	100.01	Crystal size/ mm^3	$0.248 \times 0.122 \times 0.066$
Crystal system	monoclinic	Radiation	MoK α ($\lambda = 0.71073$)
Space group	$P2_1/n$	2θ range for data collection/ $^\circ$	4.902 to 57.45
a/ \AA	9.4127(14)	Index ranges	$-12 \leq h \leq 12, -22 \leq k \leq 22, -16 \leq l \leq 16$
b/ \AA	16.618(3)	Reflections collected	27733
c/ \AA	12.4765(18)	Independent reflections	4952 [$R_{\text{int}} = 0.0310, R_{\text{sigma}} = 0.0203$]
$\alpha/^\circ$	90	Data/restraints/parameters	4952/0/263
$\beta/^\circ$	99.220(4)	Goodness-of-fit on F^2	1.070
$\gamma/^\circ$	90	Final R indexes [$>=2\sigma(I)$]	$R_1 = 0.0358, wR_2 = 0.0870$
Volume/ \AA^3	1926.4(5)	Final R indexes [all data]	$R_1 = 0.0422, wR_2 = 0.0913$
Z	4	Largest diff. peak/hole / $e \text{\AA}^{-3}$	0.42/-0.39
$\rho_{\text{calc}}/\text{cm}^3$	1.519		

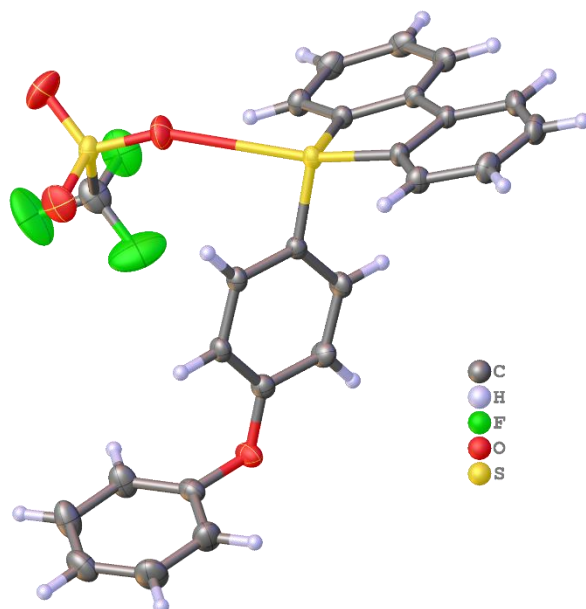


Figure 30: Crystal structure of 93f.

Table 12: Crystal data and structure refinement for 93f.

Identification code	0651_CG_0m		
Empirical formula	$C_{25}H_{17}F_3O_4S_2$	μ/mm^{-1}	0.294
Formula weight	502.50	F(000)	516.0
Temperature/K	100.03	Crystal size/ mm^3	$0.489 \times 0.06 \times 0.032$
Crystal system	triclinic	Radiation	MoK α ($\lambda = 0.71073$)
Space group	P-1	2 θ range for data collection/ $^\circ$	4.808 to 57.532
a/ \AA	10.204(4)	Index ranges	$-13 \leq h \leq 13, -14 \leq k \leq 14, -16 \leq l \leq 16$
b/ \AA	10.983(5)	Reflections collected	48304
c/ \AA	11.995(5)	Independent reflections	5801 [$R_{int} = 0.0287, R_{\sigma} = 0.0147$]
$\alpha/^\circ$	105.921(12)	Data/restraints/parameters	5801/0/307
$\beta/^\circ$	108.255(14)	Goodness-of-fit on F^2	1.023
$\gamma/^\circ$	106.854(11)	Final R indexes [$I \geq 2\sigma(I)$]	$R_1 = 0.0354, wR_2 = 0.0897$
Volume/ \AA^3	1118.8(8)	Final R indexes [all data]	$R_1 = 0.0396, wR_2 = 0.0930$
Z	2	Largest diff. peak/hole / $e \text{\AA}^{-3}$	0.44/-0.39
ρ_{calc}/cm^3	1.492		

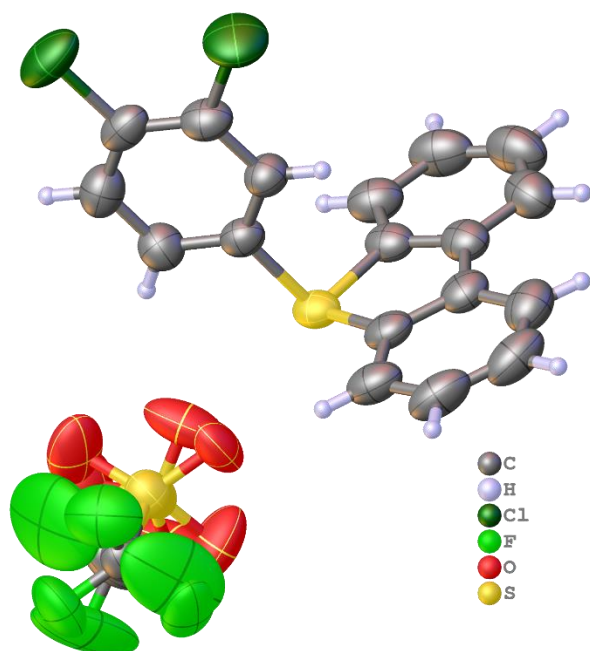


Figure 31: Crystal structure of 93g.

Table 13: Crystal data and structure refinement for 93g.

Identification code		0694_CG_0m	
Empirical formula	C ₁₉ H ₁₁ Cl ₂ F ₃ O ₃ S ₂	μ/mm^{-1}	0.563
Formula weight	479.30	F(000)	968.0
Temperature/K	275	Crystal size/mm ³	0.321 × 0.32 × 0.174
Crystal system	monoclinic	Radiation	MoK α (λ = 0.71073)
Space group	P2 ₁ /n	2 θ range for data collection/°	4.686 to 51.53
a/Å	10.2588(11)	Index ranges	-12 ≤ h ≤ 12, -19 ≤ k ≤ 20, -14 ≤ l ≤ 14
b/Å	16.5398(16)	Reflections collected	13421
c/Å	12.1788(12)	Independent reflections	3904 [R _{int} = 0.0198, R _{sigma} = 0.0189]
α /°	90	Data/restraints/parameters	3904/125/335
β /°	95.137(3)	Goodness-of-fit on F ²	1.048
γ /°	90	Final R indexes [I >= 2 σ (I)]	R ₁ = 0.0511, wR ₂ = 0.1416
Volume/Å ³	2058.2(4)	Final R indexes [all data]	R ₁ = 0.0638, wR ₂ = 0.1533
Z	4	Largest diff. peak/hole / e Å ⁻³	0.56/-0.55
$\rho_{\text{calc}}/\text{cm}^{-3}$	1.547		

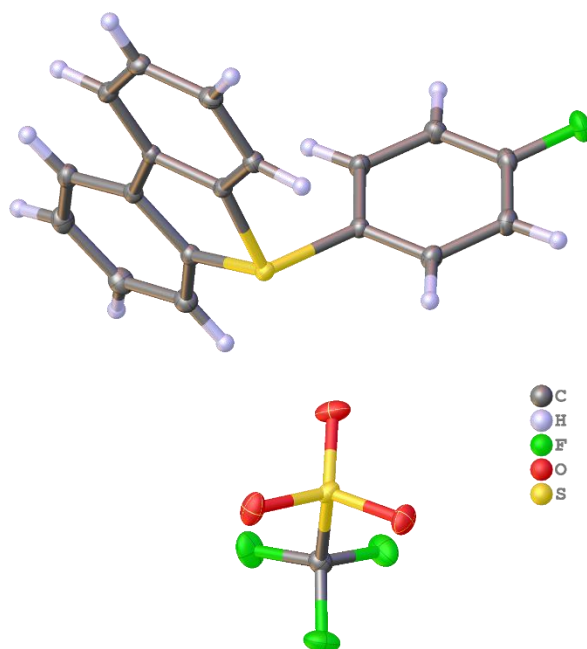


Figure 32: Crystal structure of 93h.

Table 14: Crystal data and structure refinement for 93h.

Identification code	0648_CG_0m		
Empirical formula	C ₁₉ H ₁₂ F ₄ O ₃ S ₂	μ/mm^{-1}	0.363
Formula weight	428.41	F(000)	436.0
Temperature/K	99.99	Crystal size/mm ³	0.464 × 0.343 × 0.234
Crystal system	triclinic	Radiation	MoK α ($\lambda = 0.71073$)
Space group	P-1	2 θ range for data collection/°	4.626 to 63.042
a/Å	9.6579(6)	Index ranges	-14 ≤ h ≤ 14, -15 ≤ k ≤ 15, -15 ≤ l ≤ 15
b/Å	10.4575(7)	Reflections collected	32179
c/Å	10.8774(7)	Independent reflections	5768 [R _{int} = 0.0197, R _{sigma} = 0.0159]
α /°	114.983(2)	Data/restraints/parameters	5768/0/253
β /°	95.593(2)	Goodness-of-fit on F ²	1.055
γ /°	112.240(2)	Final R indexes [$I \geq 2\sigma(I)$]	R ₁ = 0.0266, wR ₂ = 0.0714
Volume/Å ³	877.30(10)	Final R indexes [all data]	R ₁ = 0.0275, wR ₂ = 0.0720
Z	2	Largest diff. peak/hole / e Å ⁻³	0.53/-0.35
$\rho_{\text{calc}}/\text{cm}^3$	1.622		

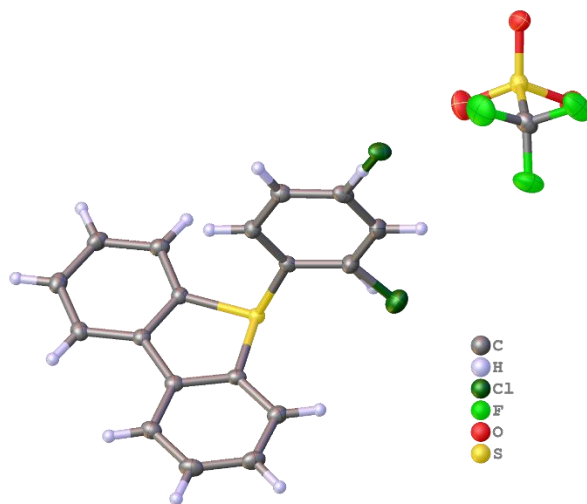


Figure 33: Crystal structure of 93i.

Table 15: Crystal data and structure refinement for 93i.

Identification code		0679_CG_0m	
Empirical formula	$C_{19}H_{12}ClF_3O_3S_2$	μ/mm^{-1}	0.487
Formula weight	444.86	F(000)	904.0
Temperature/K	99.99	Crystal size/ mm^3	$0.214 \times 0.182 \times 0.15$
Crystal system	monoclinic	Radiation	MoK α ($\lambda = 0.71073$)
Space group	$P2_1/c$	2θ range for data collection/ $^\circ$	5.026 to 57.482
a/ \AA	7.9819(5)	Index ranges	$-10 \leq h \leq 10, -21 \leq k \leq 21, -19 \leq l \leq 19$
b/ \AA	16.2116(14)	Reflections collected	78485
c/ \AA	14.0951(12)	Independent reflections	4728 [$R_{int} = 0.0247, R_{\sigma} = 0.0106$]
$\alpha/^\circ$	90	Data/restraints/parameters	4728/0/263
$\beta/^\circ$	92.114(3)	Goodness-of-fit on F^2	1.066
$\gamma/^\circ$	90	Final R indexes [$I \geq 2\sigma(I)$]	$R_1 = 0.0320, wR_2 = 0.0796$
Volume/ \AA^3	1822.7(2)	Final R indexes [all data]	$R_1 = 0.0324, wR_2 = 0.0798$
Z	4	Largest diff. peak/hole / $e \text{\AA}^{-3}$	0.62/-0.47
ρ_{calc}/cm^3	1.621		

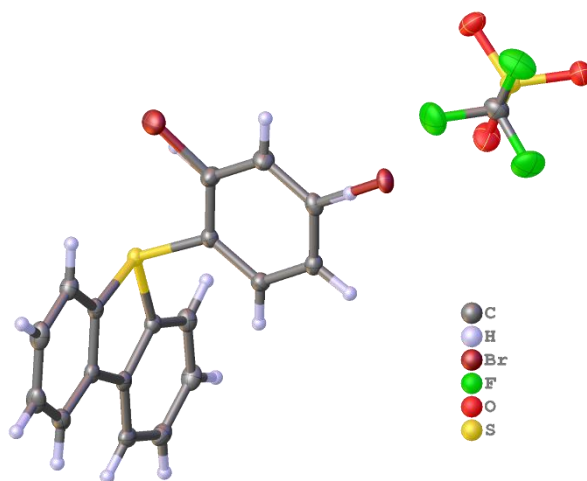


Figure 34: Crystal structure of 93j.

Table 16: Crystal data and structure refinement for 93j.

Identification code 0678_CG_0m

Empirical formula	C ₁₉ H ₁₂ BrF ₃ O ₃ S ₂	μ/mm^{-1}	2.484
Formula weight	489.32	F(000)	976.0
Temperature/K	100.0	Crystal size/mm ³	0.345 × 0.285 × 0.158
Crystal system	monoclinic	Radiation	MoK α ($\lambda = 0.71073$)
Space group	P2 ₁ /c	2 θ range for data collection/°	4.962 to 57.44
a/Å	7.9281(7)	Index ranges	-10 ≤ h ≤ 10, -22 ≤ k ≤ 19, -19 ≤ l ≤ 19
b/Å	16.4193(11)	Reflections collected	33231
c/Å	14.2964(11)	Independent reflections	4808 [R _{int} = 0.0296, R _{sigma} = 0.0173]
α /°	90	Data/restraints/parameters	4808/0/263
β /°	92.848(3)	Goodness-of-fit on F ²	1.067
γ /°	90	Final R indexes [$I > 2\sigma(I)$]	R ₁ = 0.0243, wR ₂ = 0.0615
Volume/Å ³	1858.7(3)	Final R indexes [all data]	R ₁ = 0.0257, wR ₂ = 0.0622
Z	4	Largest diff. peak/hole / e Å ⁻³	0.48/-0.52
$\rho_{\text{calc}}/\text{cm}^3$	1.749		

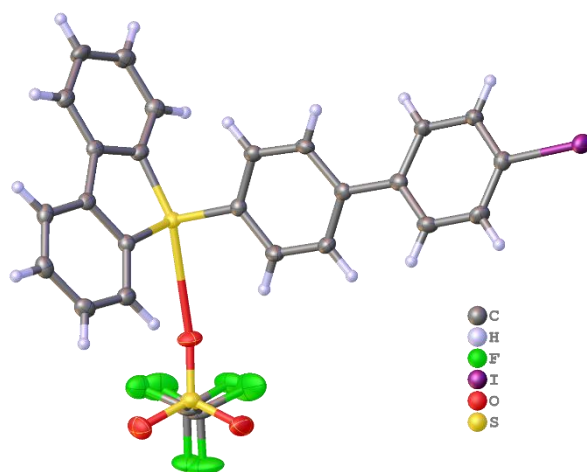


Figure 35: Crystal structure of 93k.

Table 17: Crystal data and structure refinement for 93k.

Identification code		P21c	
Empirical formula	C ₂₅ H ₁₆ F ₃ I O ₃ S ₂	μ/mm^{-1}	1.638
Formula weight	612.40	F(000)	1208.0
Temperature/K	99.99	Crystal size/mm ³	0.466 × 0.278 × 0.026
Crystal system	monoclinic	Radiation	MoK α (λ = 0.71073)
Space group	P2 ₁ /c	2 θ range for data collection/°	4.374 to 55.774
a/Å	10.413(3)	Index ranges	-13 ≤ h ≤ 13, -40 ≤ k ≤ 39, -8 ≤ l ≤ 9
b/Å	30.980(6)	Reflections collected	26467
c/Å	7.5443(12)	Independent reflections	5380 [R _{int} = 0.0335, R _{sigma} = 0.0273]
α /°	90	Data/restraints/parameters	5380/16/344
β /°	110.370(9)	Goodness-of-fit on F ²	1.195
γ /°	90	Final R indexes [$ I > 2\sigma(I)$]	R ₁ = 0.0363, wR ₂ = 0.0723
Volume/Å ³	2281.6(8)	Final R indexes [all data]	R ₁ = 0.0428, wR ₂ = 0.0744
Z	4	Largest diff. peak/hole / e Å ⁻³	0.60/-0.69
$\rho_{\text{calc}}/\text{cm}^3$	1.783		

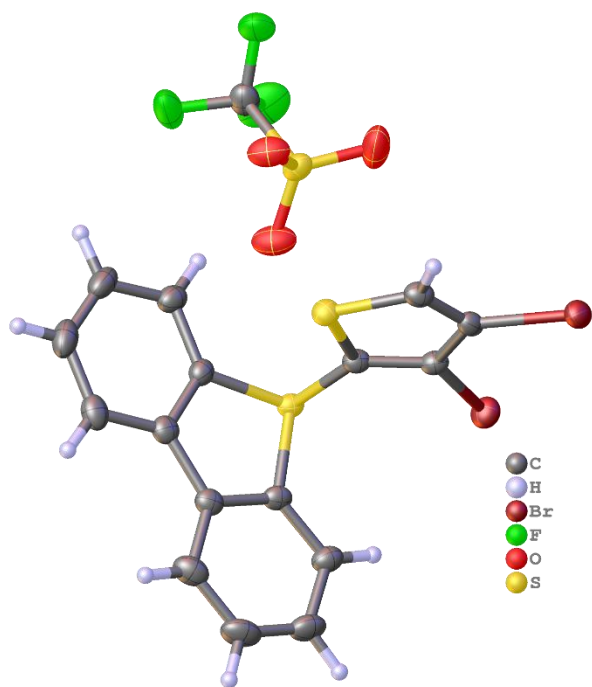


Figure 36: Crystal structure of 93m.

Table 18: Crystal data and structure refinement for 93m.

Identification code		0673_CG_0m	
Empirical formula	C ₁₇ H ₉ BrF ₃ O ₃ S ₃	μ/mm^{-1}	4.590
Formula weight	574.24	F(000)	1120.0
Temperature/K	99.99	Crystal size/mm ³	0.303 × 0.274 × 0.094
Crystal system	monoclinic	Radiation	MoK α (λ = 0.71073)
Space group	P2 ₁ /c	2 θ range for data collection/°	4.968 to 57.496
a/Å	8.0920(6)	Index ranges	-10 ≤ h ≤ 10, -22 ≤ k ≤ 22, -19 ≤ l ≤ 19
b/Å	16.3989(12)	Reflections collected	33699
c/Å	14.6855(9)	Independent reflections	4964 [R _{int} = 0.0271, R _{sigma} = 0.0169]
α /°	90	Data/restraints/parameters	4964/0/253
β /°	99.567(2)	Goodness-of-fit on F ²	1.065
γ /°	90	Final R indexes [$I \geq 2\sigma(I)$]	R ₁ = 0.0335, wR ₂ = 0.0888
Volume/Å ³	1921.7(2)	Final R indexes [all data]	R ₁ = 0.0381, wR ₂ = 0.0914
Z	4	Largest diff. peak/hole / e Å ⁻³	1.42/-0.68
$\rho_{\text{calc}}/\text{cm}^3$	1.985		

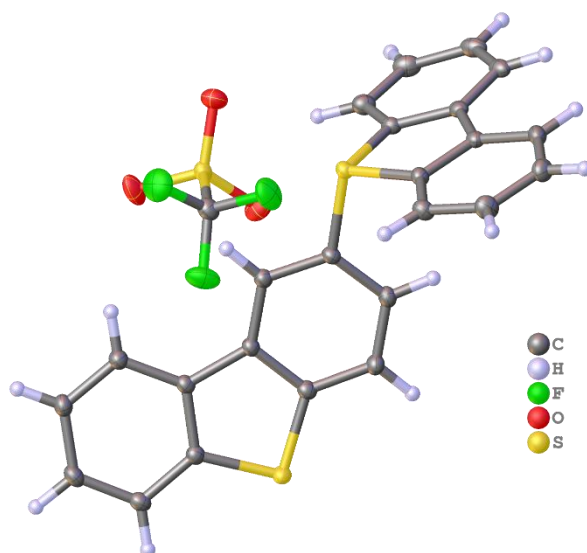


Figure 37: Crystal structure of 93n.

Table 19: Crystal data and structure refinement for 93n.

Identification code	0670_CG_0m		
Empirical formula	C ₂₅ H ₁₅ F ₃ O ₃ S ₃	μ/mm^{-1}	0.397
Formula weight	516.55	F(000)	528.0
Temperature/K	100.0	Crystal size/mm ³	0.387 × 0.362 × 0.15
Crystal system	triclinic	Radiation	MoK α (λ = 0.71073)
Space group	P-1	2 θ range for data collection/°	4.704 to 59.286
a/Å	10.1084(12)	Index ranges	-14 ≤ h ≤ 12, -13 ≤ k ≤ 14, -16 ≤ l ≤ 16
b/Å	10.5943(14)	Reflections collected	33990
c/Å	11.9529(16)	Independent reflections	6059 [R _{int} = 0.0227, R _{sigma} = 0.0167]
α /°	97.287(4)	Data/restraints/parameters	6059/0/307
β /°	105.247(4)	Goodness-of-fit on F ²	1.049
γ /°	114.652(4)	Final R indexes [$I \geq 2\sigma(I)$]	R ₁ = 0.0293, wR ₂ = 0.0775
Volume/Å ³	1080.8(2)	Final R indexes [all data]	R ₁ = 0.0316, wR ₂ = 0.0793
Z	2	Largest diff. peak/hole / e Å ⁻³	0.49/-0.35
$\rho_{\text{calc}}/\text{cm}^3$	1.587		

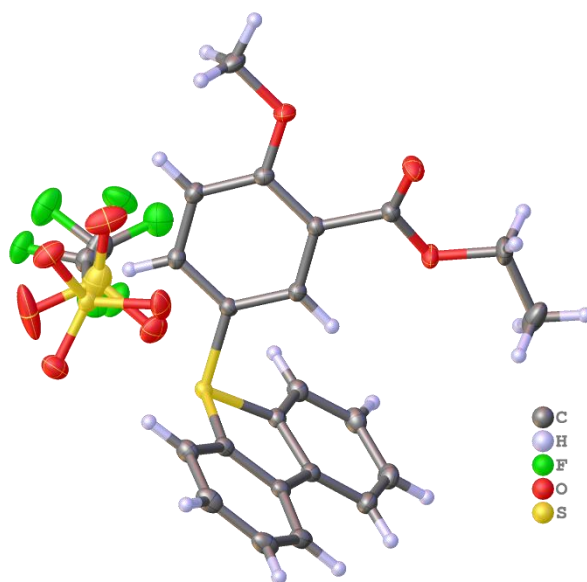


Figure 38: Crystal structure of 93o.

Table 20: Crystal data and structure refinement for 93o.

Identification code	0740_CG_0m		
Empirical formula	$C_{23}H_{19}F_3O_6S_2$	μ/mm^{-1}	0.300
Formula weight	512.50	F(000)	528.0
Temperature/K	100.02	Crystal size/ mm^3	$0.379 \times 0.364 \times 0.262$
Crystal system	triclinic	Radiation	MoK α ($\lambda = 0.71073$)
Space group	P-1	2 θ range for data collection/ $^\circ$	4.846 to 61.118
a/ \AA	9.5978(7)	Index ranges	$-13 \leq h \leq 13, -14 \leq k \leq 14, -19 \leq l \leq 19$
b/ \AA	10.4796(6)	Reflections collected	42922
c/ \AA	13.5535(9)	Independent reflections	6788 [$R_{int} = 0.0209, R_{\sigma} = 0.0157$]
$\alpha/^\circ$	94.409(2)	Data/restraints/parameters	6788/125/382
$\beta/^\circ$	107.369(2)	Goodness-of-fit on F^2	1.047
$\gamma/^\circ$	116.606(2)	Final R indexes [$I \geq 2\sigma(I)$]	$R_1 = 0.0293, wR_2 = 0.0758$
Volume/ \AA^3	1127.32(13)	Final R indexes [all data]	$R_1 = 0.0310, wR_2 = 0.0772$
Z	2	Largest diff. peak/hole / $e \text{\AA}^{-3}$	0.45/-0.30
ρ_{calc}/cm^3	1.510		

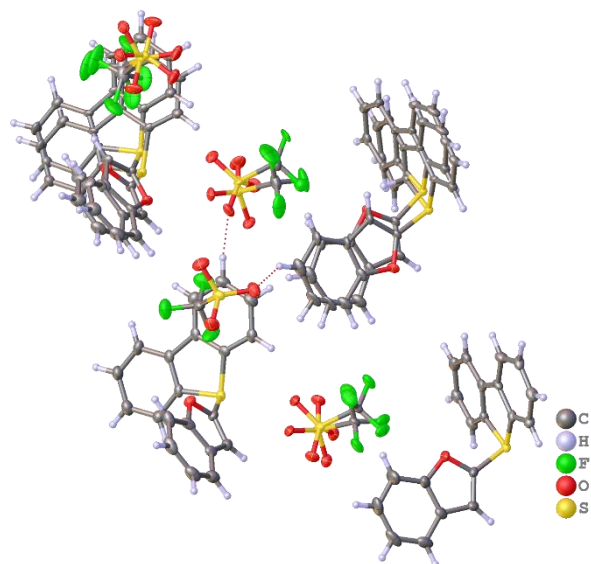


Figure 39: Crystal structure of 93p.

Table 21: Crystal data and structure refinement for 93p.

Identification code		0693_CG_0m	
Empirical formula	C ₂₁ H _{13.04} F ₃ O ₄ S ₂	μ/mm^{-1}	0.318
Formula weight	450.47	F(000)	1840.0
Temperature/K	99.99	Crystal size/mm ³	0.326 × 0.222 × 0.199
Crystal system	monoclinic	Radiation	MoK α (λ = 0.71073)
Space group	P2 ₁	2 θ range for data collection/°	4.596 to 57.53
a/Å	12.2267(9)	Index ranges	-15 ≤ h ≤ 15, -21 ≤ k ≤ 22, -27 ≤ l ≤ 27
b/Å	16.3311(14)	Reflections collected	52899
c/Å	20.1237(15)	Independent reflections	19900 [R _{int} = 0.0337, R _{sigma} = 0.0460]
α /°	90	Data/restraints/parameters	19900/477/1322
β /°	91.262(2)	Goodness-of-fit on F ²	1.078
γ /°	90	Final R indexes [$I \geq 2\sigma(I)$]	R ₁ = 0.0532, wR ₂ = 0.1426
Volume/Å ³	4017.2(5)	Final R indexes [all data]	R ₁ = 0.0586, wR ₂ = 0.1489
Z	8	Largest diff. peak/hole / e Å ⁻³	0.85/-0.60
$\rho_{\text{calc}}/\text{cm}^3$	1.490		

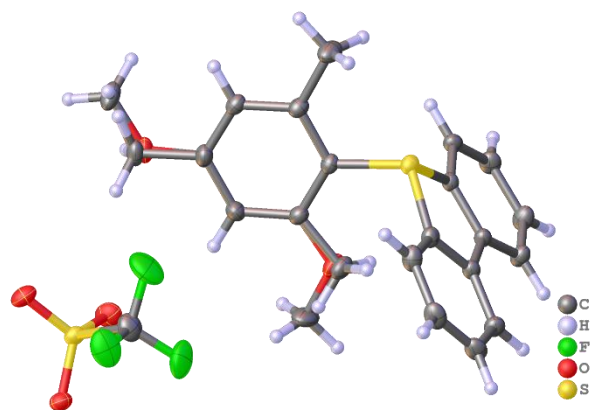


Figure 40: Crystal structure of 93q.

Table 22: Crystal data and structure refinement for 93q.

Identification code	0724_CG_0m		
Empirical formula	C ₂₂ H ₁₉ F ₃ O ₄ S ₂	μ/mm^{-1}	0.305
Formula weight	468.49	F(000)	484.0
Temperature/K	99.99	Crystal size/mm ³	0.342 × 0.198 × 0.046
Crystal system	triclinic	Radiation	MoK α (λ = 0.71073)
Space group	P-1	2 θ range for data collection/°	4.628 to 63.04
a/Å	9.1832(5)	Index ranges	-13 ≤ h ≤ 12, -15 ≤ k ≤ 16, -16 ≤ l ≤ 16
b/Å	10.9308(6)	Reflections collected	28570
c/Å	11.0290(7)	Independent reflections	6758 [R _{int} = 0.0250, R _{sigma} = 0.0169]
α /°	94.042(2)	Data/restraints/parameters	6758/12/313
β /°	102.968(2)	Goodness-of-fit on F ²	1.199
γ /°	99.192(2)	Final R indexes [$I \geq 2\sigma(I)$]	R ₁ = 0.0459, wR ₂ = 0.1041
Volume/Å ³	1058.47(11)	Final R indexes [all data]	R ₁ = 0.0483, wR ₂ = 0.1053
Z	2	Largest diff. peak/hole / e Å ⁻³	0.56/-0.36
$\rho_{\text{calc}}/\text{cm}^3$	1.470		

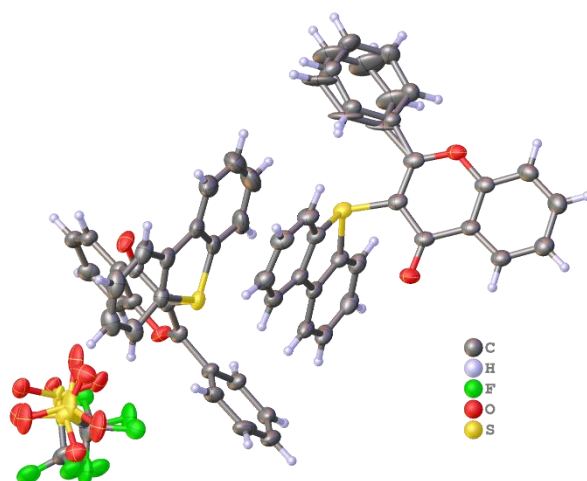


Figure 41: Crystal structure of 93s.

Table 23: Crystal data and structure refinement for 93s.

Identification code		0733_CG_0m	
Empirical formula	C _{28.5} ClF ₂ H ₁₈ O ₄ S ₃	μ/mm^{-1}	0.455
Formula weight	594.06	F(000)	1216.0
Temperature/K	100.0	Crystal size/mm ³	0.491 × 0.324 × 0.062
Crystal system	triclinic	Radiation	MoK α ($\lambda = 0.71073$)
Space group	P-1	2 θ range for data collection/°	4.622 to 55.852
a/Å	9.1333(19)	Index ranges	-12 ≤ h ≤ 12, -20 ≤ k ≤ 20, -24 ≤ l ≤ 24
b/Å	15.783(3)	Reflections collected	87633
c/Å	18.385(3)	Independent reflections	11954 [R _{int} = 0.0379, R _{sigma} = 0.0248]
α /°	96.424(6)	Data/restraints/parameters	11954/330/776
β /°	103.720(5)	Goodness-of-fit on F ²	1.038
γ /°	100.151(5)	Final R indexes [I >= 2 σ (I)]	R ₁ = 0.0745, wR ₂ = 0.2001
Volume/Å ³	2501.4(8)	Final R indexes [all data]	R ₁ = 0.0816, wR ₂ = 0.2070
Z	4	Largest diff. peak/hole / e Å ⁻³	1.50/-1.30
$\rho_{\text{calc}}/\text{cm}^3$	1.577		

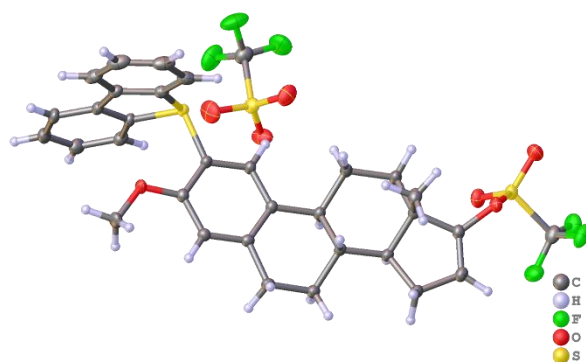


Figure 42: Crystal structure of 93u.

Table 24: Crystal data and structure refinement for 93u.

Identification code		0746_CG_0m	
Empirical formula	C ₃₃ H ₃₀ F ₆ O ₇ S ₃	μ/mm^{-1}	0.311
Formula weight	748.75	F(000)	1544.0
Temperature/K	99.98	Crystal size/mm ³	0.297 × 0.287 × 0.084
Crystal system	orthorhombic	Radiation	MoK α (λ = 0.71073)
Space group	P2 ₁ 2 ₁ 2 ₁	2 θ range for data collection/°	4.74 to 61.374
a/Å	11.0299(9)	Index ranges	-15 ≤ h ≤ 15, -17 ≤ k ≤ 17, -34 ≤ l ≤ 32
b/Å	12.3359(8)	Reflections collected	100206
c/Å	23.952(2)	Independent reflections	10025 [R _{int} = 0.0439, R _{sigma} = 0.0241]
α /°	90	Data/restraints/parameters	10025/0/444
β /°	90	Goodness-of-fit on F ²	1.046
γ /°	90	Final R indexes [$I \geq 2\sigma(I)$]	R ₁ = 0.0347, wR ₂ = 0.0981
Volume/Å ³	3259.0(4)	Final R indexes [all data]	R ₁ = 0.0358, wR ₂ = 0.0993
Z	4	Largest diff. peak/hole / e Å ⁻³	0.87/-0.34
$\rho_{\text{calc}}/\text{cm}^3$	1.526		

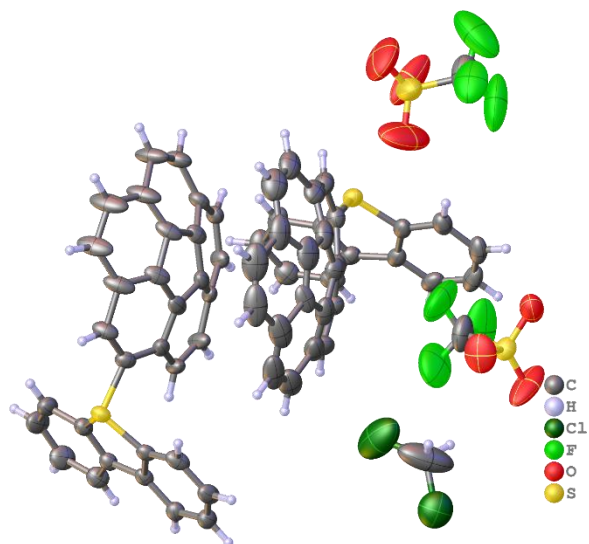


Figure 43: Crystal structure of 93v.

Table 25: Crystal data and structure refinement for 93v.

Identification code	0656_CG_0m		
Empirical formula	$C_{66.5}H_{35}ClF_6O_6S_4$	μ/mm^{-1}	0.311
Formula weight	1207.63	F(000)	2468.0
Temperature/K	100.0	Crystal size/mm ³	0.3 × 0.263 × 0.01
Crystal system	monoclinic	Radiation	MoK α ($\lambda = 0.71073$)
Space group	$P2_1/n$	2 θ range for data collection/°	4.346 to 54.316
a/Å	10.5933(15)	Index ranges	-13 ≤ h ≤ 13, -36 ≤ k ≤ 36, -22 ≤ l ≤ 22
b/Å	28.676(5)	Reflections collected	135087
c/Å	17.430(3)	Independent reflections	11682 [$R_{int} = 0.0317$, $R_{sigma} = 0.0156$]
α /°	90	Data/restraints/parameters	11682/113/748
β /°	94.731(4)	Goodness-of-fit on F^2	2.554
γ /°	90	Final R indexes [$I > 2\sigma(I)$]	$R_1 = 0.1562$, $wR_2 = 0.4878$
Volume/Å ³	5276.6(15)	Final R indexes [all data]	$R_1 = 0.1687$, $wR_2 = 0.5117$
Z	4	Largest diff. peak/hole / e Å ⁻³	3.21/-2.10
ρ_{calc}/cm^3	1.520		

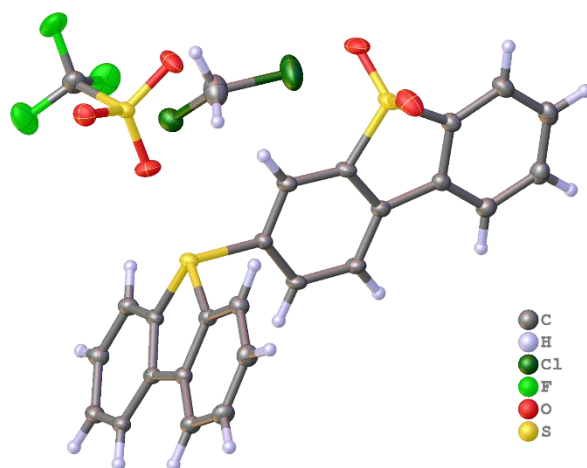


Figure 44: Crystal structure of 93y.

Table 26: Crystal data and structure refinement for 93y.

Identification code 0669_CG_0m_4			
Empirical formula	$C_{26}H_{17}Cl_2F_3O_5S_3$	μ/mm^{-1}	0.557
Formula weight	633.47	F(000)	644.0
Temperature/K	99.99	Crystal size/ mm^3	$0.189 \times 0.114 \times 0.07$
Crystal system	triclinic	Radiation	MoK α ($\lambda = 0.71073$)
Space group	P-1	2 θ range for data collection/ $^\circ$	4.438 to 59.206
a/ \AA	8.0058(3)	Index ranges	$?\leq h\leq ?, ?\leq k\leq ?, ?\leq l\leq ?$
b/ \AA	12.2505(6)	Reflections collected	7177
c/ \AA	13.9237(6)	Independent reflections	7177 [$R_{\text{int}} = 0.0$, $R_{\text{sigma}} = 0.0205$]
$\alpha/^\circ$	89.879(2)	Data/restraints/parameters	7177/0/352
$\beta/^\circ$	77.078(2)	Goodness-of-fit on F^2	1.069
$\gamma/^\circ$	75.190(2)	Final R indexes [$I \geq 2\sigma(I)$]	$R_1 = 0.0436$, $wR_2 = 0.1298$
Volume/ \AA^3	1284.57(10)	Final R indexes [all data]	$R_1 = 0.0492$, $wR_2 = 0.1332$
Z	2	Largest diff. peak/hole / $e \text{\AA}^{-3}$	0.88/-1.00
$\rho_{\text{calc}}/\text{cm}^3$	1.638		

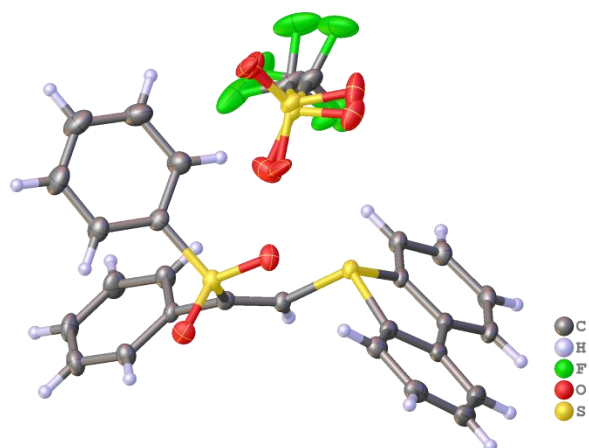


Figure 45: Crystal structure of 142b.

Table 27: Crystal data and structure refinement for 0974_P21c.

Identification code		0974_P21c	
Empirical formula	C ₂₇ H ₁₉ F ₃ O ₅ S ₃	μ/mm^{-1}	0.351
Formula weight	576.60	F(000)	1184.0
Temperature/K	100.0	Crystal size/mm ³	0.164 × 0.152 × 0.14
Crystal system	monoclinic	Radiation	MoK α ($\lambda = 0.71073$)
Space group	P2 ₁ /c	2 θ range for data collection/°	4.608 to 57.466
a/Å	15.815(2)	Index ranges	-21 ≤ h ≤ 21, -19 ≤ k ≤ 19, -15 ≤ l ≤ 15
b/Å	14.4185(16)	Reflections collected	121187
c/Å	11.1988(14)	Independent reflections	6605 [R _{int} = 0.0252, R _{sigma} = 0.0094]
α /°	90	Data/restraints/parameters	6605/131/419
β /°	92.768(4)	Goodness-of-fit on F ²	1.050
γ /°	90	Final R indexes [I >= 2 σ (I)]	R ₁ = 0.0304, wR ₂ = 0.0787
Volume/Å ³	2550.7(5)	Final R indexes [all data]	R ₁ = 0.0335, wR ₂ = 0.0814
Z	4	Largest diff. peak/hole / e Å ⁻³	0.42/-0.33
$\rho_{\text{calc}}/\text{g}/\text{cm}^3$	1.501		

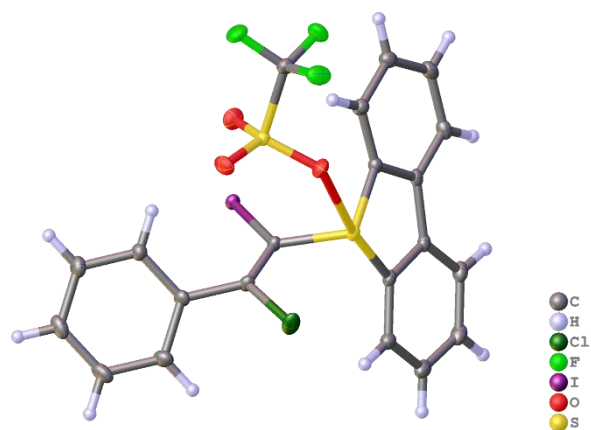


Figure 46: Crystal structure of 142d.

Table 28: Crystal data and structure refinement for 142d.

Identification code		ag_0997_CG_0m	
Empirical formula	C ₂₁ H ₁₃ ClF ₃ IO ₃ S ₂	μ/mm^{-1}	1.014
Formula weight	596.78	F(000)	1168.0
Temperature/K	100.0	Crystal size/mm ³	0.326 × 0.258 × 0.243
Crystal system	monoclinic	Radiation	AgK α (λ = 0.56086)
Space group	P2 ₁ /c	2 θ range for data collection/°	4.248 to 55.754
a/Å	7.6018(4)	Index ranges	-12 ≤ h ≤ 12, -28 ≤ k ≤ 28, -26 ≤ l ≤ 26
b/Å	17.2223(6)	Reflections collected	225496
c/Å	16.2066(8)	Independent reflections	10073 [R _{int} = 0.0347, R _{sigma} = 0.0115]
α /°	90	Data/restraints/parameters	10073/0/280
β /°	101.823(2)	Goodness-of-fit on F ²	1.068
γ /°	90	Final R indexes [I >= 2 σ (I)]	R ₁ = 0.0175, wR ₂ = 0.0406
Volume/Å ³	2076.76(17)	Final R indexes [all data]	R ₁ = 0.0217, wR ₂ = 0.0424
Z	4	Largest diff. peak/hole / e Å ⁻³	0.84/-0.64
$\rho_{\text{calc}}/\text{cm}^3$	1.909		

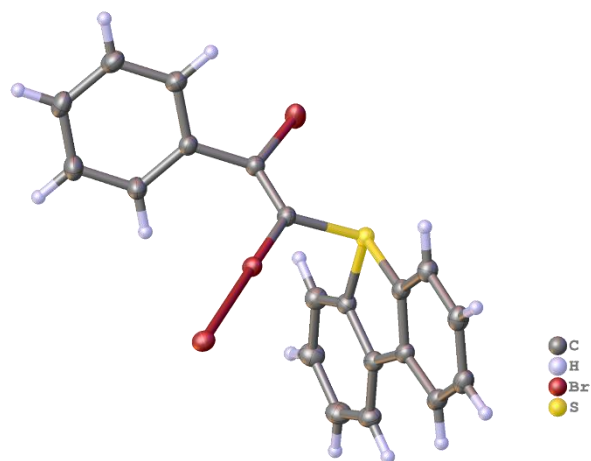


Figure 47: Crystal structure of 142e.

Table 29: Crystal data and structure refinement for 142e.

Identification code		ag_0998_CG_0m	
Empirical formula	C ₂₀ H ₁₃ Br ₃ S	μ/mm^{-1}	3.654
Formula weight	525.09	F(000)	1016.0
Temperature/K	100.0	Crystal size/mm ³	0.845 × 0.13 × 0.082
Crystal system	monoclinic	Radiation	AgK α (λ = 0.56086)
Space group	P2 ₁ /c	2 θ range for data collection/°	4.976 to 53.824
a/Å	13.4052(16)	Index ranges	-21 ≤ h ≤ 21, -11 ≤ k ≤ 11, -29 ≤ l ≤ 29
b/Å	7.3752(8)	Reflections collected	205121
c/Å	18.247(2)	Independent reflections	7919 [R _{int} = 0.0314, R _{sigma} = 0.0092]
α /°	90	Data/restraints/parameters	7919/0/217
β /°	91.642(4)	Goodness-of-fit on F ²	1.069
γ /°	90	Final R indexes [I >= 2 σ (I)]	R ₁ = 0.0182, wR ₂ = 0.0495
Volume/Å ³	1803.3(4)	Final R indexes [all data]	R ₁ = 0.0199, wR ₂ = 0.0507
Z	4	Largest diff. peak/hole / e Å ⁻³	0.99/-0.26
$\rho_{\text{calc}}/\text{cm}^3$	1.934		

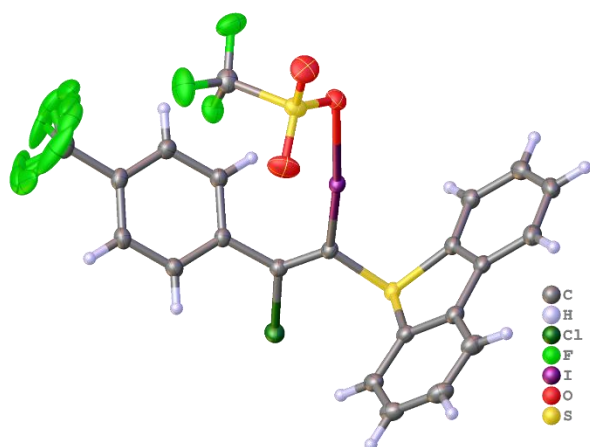


Figure 48: Crystal structure of 142f.

Table 30: Crystal data and structure refinement for 142f.

Identification code		mo_1010_CG_0m	
Empirical formula	C ₂₂ H ₁₂ ClF ₆ IO ₃ S ₂	μ/mm^{-1}	1.764
Formula weight	664.79	F(000)	648.0
Temperature/K	100.0	Crystal size/mm ³	0.333 × 0.197 × 0.052
Crystal system	triclinic	Radiation	MoK α (λ = 0.71073)
Space group	P-1	2 θ range for data collection/°	4.558 to 63.196
a/Å	8.7606(4)	Index ranges	-12 ≤ h ≤ 12, -13 ≤ k ≤ 13, -21 ≤ l ≤ 21
b/Å	9.1079(5)	Reflections collected	102665
c/Å	14.7027(8)	Independent reflections	7675 [R _{int} = 0.0274, R _{sigma} = 0.0117]
α /°	85.481(2)	Data/restraints/parameters	7675/10/373
β /°	87.424(2)	Goodness-of-fit on F ²	1.084
γ /°	79.608(2)	Final R indexes [I >= 2 σ (I)]	R ₁ = 0.0151, wR ₂ = 0.0395
Volume/Å ³	1149.74(10)	Final R indexes [all data]	R ₁ = 0.0159, wR ₂ = 0.0400
Z	2	Largest diff. peak/hole / e Å ⁻³	0.45/-0.55
$\rho_{\text{calc}}/\text{cm}^3$	1.920		

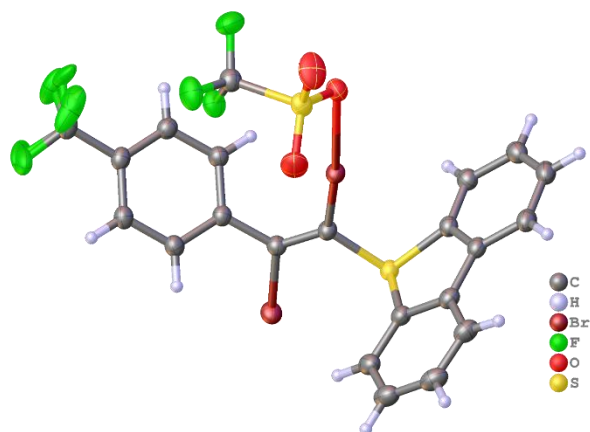


Figure 49: Crystal structure of 142h.

Table 31: Crystal data and structure refinement for 142h.

Identification code		mo_1005_CG_0m	
Empirical formula	C ₂₂ H ₁₂ Br ₂ F ₆ O ₃ S ₂	μ/mm^{-1}	3.833
Formula weight	662.26	F(000)	648.0
Temperature/K	100.0	Crystal size/mm ³	0.423 × 0.377 × 0.375
Crystal system	triclinic	Radiation	MoK α (λ = 0.71073)
Space group	P-1	2 θ range for data collection/°	4.618 to 65.464
a/Å	8.7933(5)	Index ranges	-13 ≤ h ≤ 13, -13 ≤ k ≤ 13, -22 ≤ l ≤ 22
b/Å	8.9573(4)	Reflections collected	148044
c/Å	14.6326(8)	Independent reflections	8316 [R _{int} = 0.0313, R _{sigma} = 0.0160]
α /°	85.968(2)	Data/restraints/parameters	8316/21/344
β /°	87.299(2)	Goodness-of-fit on F ²	1.121
γ /°	80.687(2)	Final R indexes [I >= 2 σ (I)]	R ₁ = 0.0250, wR ₂ = 0.0680
Volume/Å ³	1133.77(10)	Final R indexes [all data]	R ₁ = 0.0254, wR ₂ = 0.0683
Z	2	Largest diff. peak/hole / e Å ⁻³	0.71/-0.36
$\rho_{\text{calc}}/\text{cm}^3$	1.940		

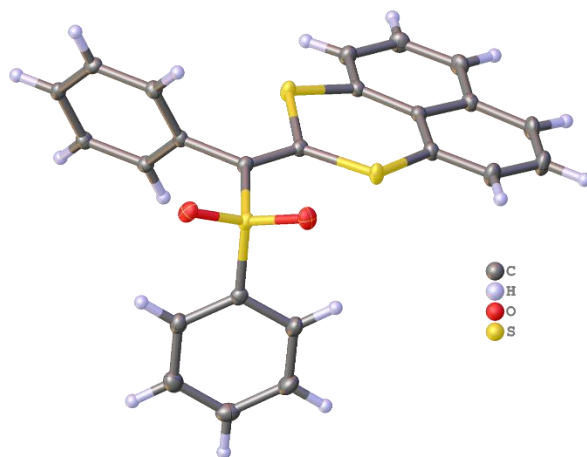


Figure 50: Crystal structure of 151b.

Table 32: Crystal data and structure refinement for 151b.

Identification code		mo_0937_CG_0m	
Empirical formula	C ₂₄ H ₁₆ O ₂ S ₃	μ/mm^{-1}	0.413
Formula weight	432.55	F(000)	896.0
Temperature/K	100.0	Crystal size/mm ³	0.256 × 0.097 × 0.074
Crystal system	monoclinic	Radiation	MoK α ($\lambda = 0.71073$)
Space group	P2 ₁ /c	2 θ range for data collection/°	4.268 to 57.468
a/Å	14.492(2)	Index ranges	-19 ≤ h ≤ 19, -7 ≤ k ≤ 7, -32 ≤ l ≤ 32
b/Å	5.4785(10)	Reflections collected	46896
c/Å	23.842(4)	Independent reflections	4899 [R _{int} = 0.0395, R _{sigma} = 0.0194]
α /°	90	Data/restraints/parameters	4899/0/262
β /°	94.389(5)	Goodness-of-fit on F ²	1.036
γ /°	90	Final R indexes [I ≥ 2 σ (I)]	R ₁ = 0.0292, wR ₂ = 0.0746
Volume/Å ³	1887.3(5)	Final R indexes [all data]	R ₁ = 0.0351, wR ₂ = 0.0793
Z	4	Largest diff. peak/hole / e Å ⁻³	0.38/-0.40
$\rho_{\text{calc}}/\text{cm}^3$	1.522		

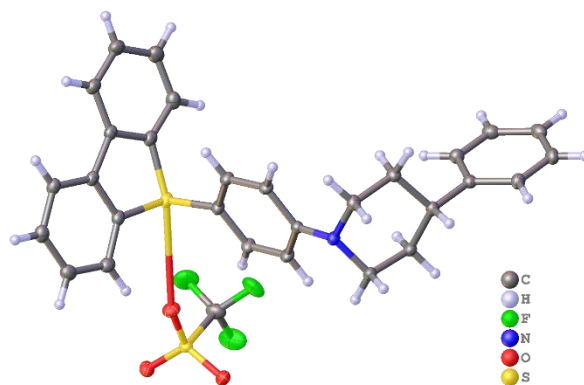


Figure 51: Crystal structure of 169c.

Table 33: Crystal data and structure refinement for 168c.

Identification code		mo_0853_CG_0m	
Empirical formula	C ₃₀ H ₂₆ F ₃ NO ₃ S ₂	μ/mm^{-1}	0.257
Formula weight	569.64	F(000)	592.0
Temperature/K	100.0	Crystal size/mm ³	0.25 × 0.25 × 0.05
Crystal system	triclinic	Radiation	MoK α ($\lambda = 0.71073$)
Space group	P-1	2 θ range for data collection/°	4.248 to 61.144
a/Å	10.1103(4)	Index ranges	-14 ≤ h ≤ 14, -17 ≤ k ≤ 17, -18 ≤ l ≤ 18
b/Å	11.9287(4)	Reflections collected	149739
c/Å	12.6966(4)	Independent reflections	8114 [R _{int} = 0.0265, R _{sigma} = 0.0099]
α /°	71.0010(10)	Data/restraints/parameters	8114/0/352
β /°	88.3590(10)	Goodness-of-fit on F ²	1.040
γ /°	66.8950(10)	Final R indexes [$ I \geq 2\sigma(I)$]	R ₁ = 0.0295, wR ₂ = 0.0818
Volume/Å ³	1323.02(8)	Final R indexes [all data]	R ₁ = 0.0305, wR ₂ = 0.0828
Z	2	Largest diff. peak/hole / e Å ⁻³	0.43/-0.47
$\rho_{\text{calc}}/\text{cm}^3$	1.430		

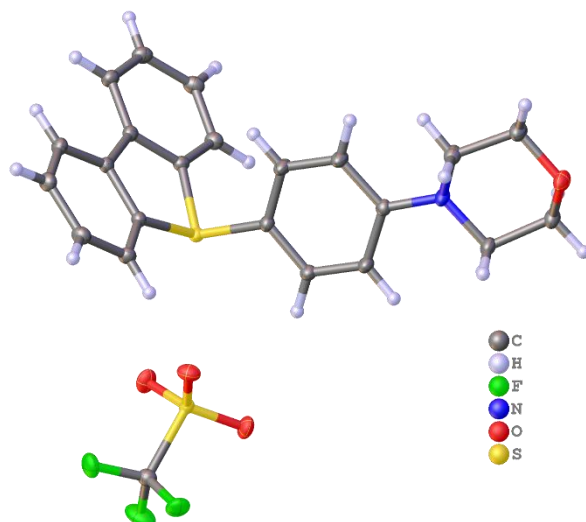


Figure 52: Crystal structure of 169d.

Table 34: Crystal data and structure refinement for 169d.

Identification code	0842_CG		
Empirical formula	C ₂₃ H ₂₀ F ₃ NO ₄ S ₂	μ/mm^{-1}	0.302
Formula weight	495.52	F(000)	1024.0
Temperature/K	100.0	Crystal size/mm ³	0.218 × 0.197 × 0.132
Crystal system	monoclinic	Radiation	MoK α (λ = 0.71073)
Space group	P2 ₁ /c	2 θ range for data collection/°	3.87 to 61.014
a/Å	15.0938(8)	Index ranges	-21 ≤ h ≤ 21, -21 ≤ k ≤ 21, -14 ≤ l ≤ 13
b/Å	15.2521(7)	Reflections collected	57634
c/Å	9.8081(5)	Independent reflections	6608 [R _{int} = 0.0211, R _{sigma} = 0.0128]
α /°	90	Data/restraints/parameters	6608/254/298
β /°	105.476(2)	Goodness-of-fit on F ²	1.033
γ /°	90	Final R indexes [$I \geq 2\sigma(I)$]	R ₁ = 0.0280, wR ₂ = 0.0747
Volume/Å ³	2176.08(19)	Final R indexes [all data]	R ₁ = 0.0303, wR ₂ = 0.0766
Z	4	Largest diff. peak/hole / e Å ⁻³	0.48/-0.37
$\rho_{\text{calc}}/\text{cm}^3$	1.513		

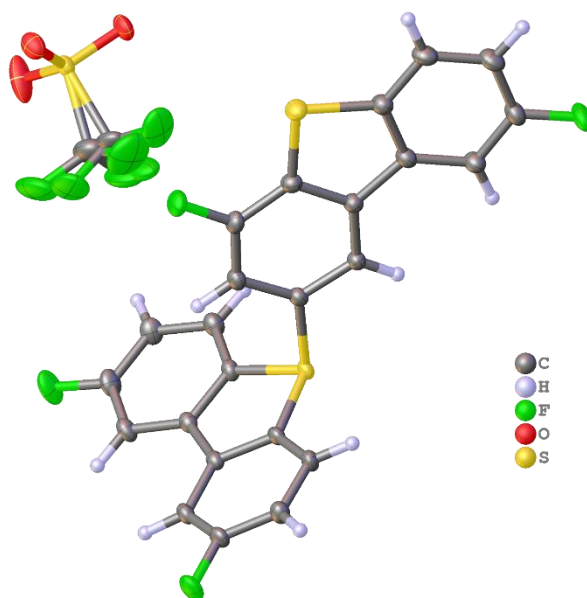


Figure 53: Crystal structure of 190.

Table 35: Crystal data and structure refinement for 190.

Identification code		0488_CG_0m	
Empirical formula	C ₂₆ Cl ₂ F ₇ H ₁₃ O ₃ S ₃	μ/mm^{-1}	0.551
Formula weight	673.44	F(000)	1352.0
Temperature/K	100	Crystal size/mm ³	0.278 × 0.113 × 0.059
Crystal system	monoclinic	Radiation	MoK α ($\lambda = 0.71073$)
Space group	P2 ₁ /n	2 θ range for data collection/°	4.308 to 59.192
a/Å	11.326(4)	Index ranges	-15 ≤ h ≤ 15, -22 ≤ k ≤ 22, -18 ≤ l ≤ 20
b/Å	16.571(4)	Reflections collected	51233
c/Å	14.507(5)	Independent reflections	7542 [R _{int} = 0.0287, R _{sigma} = 0.0191]
α /°	90	Data/restraints/parameters	7542/10/380
β /°	97.280(16)	Goodness-of-fit on F ²	1.053
γ /°	90	Final R indexes [I >= 2 σ (I)]	R ₁ = 0.0355, wR ₂ = 0.0902
Volume/Å ³	2700.7(14)	Final R indexes [all data]	R ₁ = 0.0403, wR ₂ = 0.0935
Z	4	Largest diff. peak/hole / e Å ⁻³	0.56/-0.40
$\rho_{\text{calc}}/\text{cm}^3$	1.656		

References

- (1) Fernández, I.; Khiar, N. Arylsulfonium Salts and Derivatives. In *Science of Synthesis, Vol. 31a* (Ed.: Ramsden, C. A.), Thieme, Stuttgart, **2011**, pp. 1001 ff. DOI: 10.1055/sos-SD-031-00953.
- (2) Kozhushkov, S. I.; Alcarazo, M. Synthetic applications of sulfonium salts. *Eur. J. Inorg. Chem.* **2020**, 2486–2500.
- (3) Andersen, K. K.; Cinquini, M.; Papanikolaou, N. E. Synthesis and stereochemistry of triarylsulfonium salts. *J. Org. Chem.* **1970**, *35*, 706–710.
- (4) Baechler, R. D.; Mislow, K. Effect of structure on the rate of pyramidal inversion of acyclic phosphines. *J. Am. Chem. Soc.* **1970**, *92*, 3090–3093.
- (5) Umemoto, T.; Adachi, K.; Ishihara, S. CF₃ oxonium salts, O-(trifluoromethyl)dibenzofuranium salts: *in situ* synthesis, properties, and application as a real CF₃⁺ species reagent. *J. Org. Chem.* **2007**, *72*, 6905–6917.
- (6) Aggarwal, V. K.; Harvey, J. N.; Richardson, J. Unraveling the mechanism of epoxide formation from sulfur ylides and aldehydes. *J. Am. Chem. Soc.* **2002**, *124*, 5747–5756.
- (7) a) Kaiser, C.; Trost, B. M.; Beeson, J.; Weinstock, J. Preparation of some cyclopropanes and stable sulfoxonium ylides from dimethylsulfoxonium methylide. *J. Org. Chem.* **1965**, *30*, 3972–3975. For the review on this topic see: b) Oost, R.; Neuhaus, J. D.; Merad, J.; Maulide, N. Sulfur Ylides in Organic Synthesis and Transition Metal Catalysis. In *Modern Ylide Chemistry. Structure and Bonding, Vol. 177* (Ed.: Gessner, V.), Springer, Cham **2017**.
- (8) Robiette, R. Mechanism and diastereoselectivity of aziridine formation from sulfur ylides and imines: a computational study. *J. Org. Chem.* **2006**, *71*, 2726–2734.
- (9) Pulis, A. P.; Procter, D. J. C–H Coupling reactions directed by sulfoxides: teaching an old functional group new tricks. *Angew. Chem. Int. Ed.* **2016**, *55*, 9842–9860.
- (10) Yanagi, T.; Nogi, K.; Yorimitsu, H. Recent development of *ortho*-C–H functionalization of aryl sulfoxides through [3,3] sigmatropic rearrangement. *Tetrahedron Lett.* **2018**, *59*, 2951–2959.
- (11) Waldecker, B.; Kraft, F.; Golz, C.; Alcarazo, M. 5-(Alkynyl)dibenzothiophenium triflates: sulfur-based reagents for electrophilic alkylation. *Angew. Chem. Int. Ed.* **2018**, *57*, 12538–12542.
- (12) Otsuka, S.; Nogi, K.; Rovis, T.; Yorimitsu, H. Photoredox-catalyzed alkenylation of benzylium salts. *Chem. Asian. J.* **2019**, *14*, 532–536.
- (13) Badet, B.; Julia, M.; Ramirez-Muñoz, M. Phase-transfer alkylation with sulfonium salts. *Synthesis* **1980**, 926–929.
- (14) Zhdankin, V. V. *Hypervalent Iodine Chemistry: Preparation, Structure, and Synthetic Applications of Polyvalent Iodine Compounds*; Wiley, Chichester, **2014**.

- (15) Aukland, M. H.; Šiaučiulis, M.; West, A.; Perry, G. J. P.; Procter, D. J. Metal-free photoredox-catalysed formal C–H/C–H coupling of arenes enabled by interrupted Pummerer activation. *Nat. Catal.* **2020**, *3*, 163–169.
- (16) Tian, Z.-Y.; Zhang, C.-P. Ullmann-type N-arylation of anilines with alkyl(aryl)sulfonium salts. *Chem. Comm.* **2019**, *55*, 11936–11939.
- (17) Kovatscheva, E. G.; Popova, J. G. Vorkommen von S-Methylmethionin in Pflanzen und in tierischen Produkten und dessen Beständigkeit während der Lagerung. *Nahrung* **1977**, *21*, 465–472.
- (18) Kim, W.-S.; Kim, W.-K.; Choi, N.; Suh, W.; Lee, J.; Kim, D.-D.; Kim, I.; Sung, J.-H. Development of S-methylmethionine sulfonium derivatives and their skin-protective effect against ultraviolet exposure. *Biomol. Ther.* **2018**, *26*, 306–312.
- (19) Cantoni, G. L. The nature of the active methyl donor formed enzymatically from L-methionine and adenosyltriphosphate. *J. Am. Chem. Soc.* **1952**, *74*, 2942–2943.
- (20) Ochiai, M.; Nagaoka, T.; Sueda, T.; Yan, J.; Chen, D.-W.; Miyamoto, K. Synthesis of 1-alkynyl(diphenyl)onium salts of group 16 elements via heteroatom transfer reaction of 1-alkynyl(phenyl)- λ_3 -iodanes. *Org. Biomol. Chem.* **2003**, *1*, 1517–1521.
- (21) Rangappa, P.; Shine, H. J.; Marx, J. N.; Ould-Ely, T.; Kelly, A. T.; Whitmire, K. H. Adducts of thianthrene- and phenoxathiin cation radical tetrafluoroborates to 1-alkynes. Structures and formation of 1-(5-thianthreniumyl)- and 1-(10-phenoxathiiniumyl)alkynes on alumina leading to alpha-ketoylides and alpha-ketols. *J. Org. Chem.* **2005**, *70*, 9764–9770.
- (22) Höfer, M.; Liska, R. Photochemistry and initiation behavior of phenylethynyl onium salts as cationic photoinitiators. *J. Polym. Sci. A Polym. Chem.* **2009**, *47*, 3419–3430.
- (23) Waldecker, B.; Kafuta, K.; Alcarazo, M. Preparation of 5-(triisopropylalkynyl) dibenzo[*b,d*]thiophenium triflate. *Org. Synth.* **2019**, *96*, 258–276.
- (24) Li, X.; Golz, C.; Alcarazo, M. 5-(Cyano)dibenzothiophenium triflate: a sulfur-based reagent for electrophilic cyanation and cyanocyclizations. *Angew. Chem. Int. Ed.* **2019**, *58*, 9496–9500.
- (25) Kataoka, T.; Watanabe, S.-i.; Nara, S. Synthesis of phenylethynyldibenzoselenophenium salt and its reactions with nucleophiles. *Phosphorus, Sulfur, Silicon Relat. Elem.* **1998**, *136*, 497–500.
- (26) Roy, A.; Maity, A.; Giri, R.; Bisai, A. Efficient alkynylation of 2-oxindoles with alkynyl dibenzothiophenium triflates: total synthesis of (\pm)-deoxyeseroline. *Asian J. Org. Chem.* **2020**, *9*, 226–232.
- (27) Alcarazo, M. Synthesis, structure, and applications of α -cationic phosphines. *Acc. Chem. Res.* **2016**, *49*, 1797–1805.
- (28) Beringer, F. M.; Galton, S. A. Acetylenic and ethylenic iodonium salts and their reactions with a carbanion. *J. Org. Chem.* **1965**, *30*, 1930–1934.

- (29) Ochiai, M.; Ito, T.; Takaoka, Y.; Masaki, Y.; Kunishima, M.; Tani, S.; Nagao, Y. Synthesis of ethynyl(phenyl)iodonium tetrafluoroborate. A new reagent for ethynylation of 1,3-dicarbonyl compounds. *J. Chem. Soc., Chem. Commun.* **1990**, 118–119.
- (30) Bachi, M. D.; Bar-Ner, N.; Crittell, C. M.; Stang, P. J.; Williamson, B. L. Synthesis of alkynyl(phenyl)iodonium triflates and their reaction with diethyl 2-aminomalonate. *J. Org. Chem.* **1991**, *56*, 3912–3915.
- (31) Ochiai, M.; Masaki, Y.; Shiro, M. Synthesis and structure of 1-alkynyl-1,2-benziodoxol-3(1*H*)-ones. *J. Org. Chem.* **1991**, *56*, 5511–5513.
- (32) Zhdankin, V. V.; Kuehl, C. J.; Krasutsky, A. P.; Bolz, J. T.; Simonsen, A. J. 1-(Organosulfonyloxy)-3(1*H*)-1,2-benziodoxoles: preparation and reactions with alkynyltrimethylsilanes. *J. Org. Chem.* **1996**, *61*, 6547–6551.
- (33) Fernández González, D.; Brand, J. P.; Waser, J. Ethynyl-1,2-benziodoxol-3(1*H*)-one (EBX): an exceptional reagent for the ethynylation of keto, cyano, and nitro esters. *Chem. Eur. J.* **2010**, *16*, 9457–9461.
- (34) Frei, R.; Wodrich, M. D.; Hari, D. P.; Borin, P.-A.; Chauvier, C.; Waser, J. Fast and highly chemoselective alkynylation of thiols with hypervalent iodine reagents enabled through a low energy barrier concerted mechanism. *J. Am. Chem. Soc.* **2014**, *136*, 16563–16573.
- (35) Chen, C. C.; Waser, J. Room temperature alkynylation of H-phosphi(na)tes and secondary phosphine oxides with ethynylbenziodoxolone (EBX) reagents. *Chem. Commun.* **2014**, *50*, 12923–12926.
- (36) Hari, D. P.; Caramenti, P.; Schouwey, L.; Chang, M.; Nicolai, S.; Bachert, D.; Wright, T.; Orella, C.; Waser, J. One-pot synthesis of 1-[(triisopropylsilyl)ethynyl]-1,2-benziodoxol-3(1*H*)-one (TIPS-EBX): process safety assessment and impact of impurities on product stability. *Org. Process Res. Dev.* **2020**, *24*, 106–110.
- (37) Talavera, G.; Peña, J.; Alcarazo, M. Dihalo(imidazolium)sulfuranes: a versatile platform for the synthesis of new electrophilic group-transfer reagents. *J. Am. Chem. Soc.* **2015**, *137*, 8704–8707.
- (38) Moloney, M. G.; Pinhey, J. T.; Roche, E. G. 'Alk-1-ynyllead triacetates' as alk-1-ynyl carbocation equivalents. The α -alk-1-ynylation of β -dicarbonyl compounds and nitronate salts. *Tetrahedron Lett.* **1986**, *27*, 5025–5028.
- (39) Parkinson, C. J.; Hambley, T. W.; Pinhey, J. T. The in situ generation of alk-1-ynyllead triacetates from terminal acetylenes by zinc–lead exchange and crystal structure of 2,4,7,9,13-pentamethyl-9-phenylethynyl-7,10-ethenospiro[5.5]undeca-1,4-diene-3,8-dione. *J. Chem. Soc., Perkin Trans.* **1997**, 1465–1468.

- (40) Kimbrough, R. D. Toxicity and health effects of selected organotin compounds: A Review. *Environ. Health Perspect.* **1976**, *14*, 51–56.
- (41) Dopp, E.; Rettenmeier, A. W. Tin, Toxicity. In *Encyclopedia of Metalloproteins*. (Eds.: Kretsinger, R. H., Uversky, V. N., Permyakov, E. A.), Springer, Heidelberg, **2013**; pp 2235–2239. DOI: 10.1007/978-1-4614-1533-6_118.
- (42) Ghazi, A. M.; Millette, J. R. Lead. In *Environmental Forensics: Contaminant Specific Guide* (Eds.: Morrison, R. D.; Murphy, B. L.), Academic Press, San Diego, **2006**; pp. 55–79. DOI: 10.1016/B978-012507751-4/50026-4.
- (43) Peng, J.; Zhao, Y.; Zhou, J.; Ding, Y.; Chen, C. Synthesis of dihydropyrrole derivatives by a palladium-catalyzed Heck and Suzuki cross-coupling cascade reaction. *Synthesis* **2014**, *46*, 2051–2056.
- (44) Liu, G.; Kong, L.; Shen, J.; Zhu, G. A regio- and stereoselective entry to (*Z*)- β -halo alkenyl sulfides and their applications to access stereodefined trisubstituted alkenes. *Org. Biomol. Chem.* **2014**, *12*, 2310–2321.
- (45) Zhang, J.; Li, P.; Wang, L. KOAc-promoted alkynylation of α -C–H bonds of ethers with alkynyl bromides under transition-metal-free conditions. *Org. Biomol. Chem.* **2014**, *12*, 2969–2978.
- (46) Ohmura, T.; Kijima, A.; Komori, Y.; Suginome, M. Cycloaddition-based formal C–H alkynylation of isoindoles leading to the synthesis of air-stable fluorescent 1,3-dialkynylisoindoles. *Org. Lett.* **2013**, *15*, 3510–3513.
- (47) a) Chodkiewicz, W. *Ann. Chim. Paris* **1957**, *2*, 819–869. b) Cadiot, P.; Chodkiewicz, W. In *Chemistry of Acetylenes*; (Ed.: Viehe, H. G.) Marcel Dekker, New York, **1969**, pp. 597–647.
- (48) Shen, W.; Thomas, S. A. Synthesis of 1,3-diynes via palladium-catalyzed reaction of 1,1-dibromo-1-alkenes. *Org. Lett.* **2000**, *2*, 2857–2860.
- (49) Marino, J. P.; Nguyen, H. N. Bulky trialkylsilyl acetylenes in the Cadiot-Chodkiewicz cross-coupling reaction. *J. Org. Chem.* **2002**, *67*, 6841–6844.
- (50) Peng, H.; Xi, Y.; Ronaghi, N.; Dong, B.; Akhmedov, N. G.; Shi, X. Gold-catalyzed oxidative cross-coupling of terminal alkynes: selective synthesis of unsymmetrical 1,3-diynes. *J. Am. Chem. Soc.* **2014**, *136*, 13174–13177.
- (51) Li, X.; Xie, X.; Sun, N.; Liu, Y. Gold-catalyzed Cadiot-Chodkiewicz-type cross-coupling of terminal alkynes with alkynyl hypervalent iodine reagents: highly selective synthesis of unsymmetrical 1,3-diynes. *Angew. Chem. Int. Ed.* **2017**, *56*, 6994–6998.
- (52) Banerjee, S.; Patil, N. T. Exploiting the dual role of ethynylbenziodoxolones in gold-catalyzed C(sp)-C(sp) cross-coupling reactions. *Chem. Commun.* **2017**, *53*, 7937–7940.

- (53) Schörghenmayer, J.; Waser, M. Transition metal-free coupling of terminal alkynes and hypervalent iodine-based alkyne-transfer reagents to access unsymmetrical 1,3-diynes. *Org. Biomol. Chem.* **2018**, *16*, 7561–7563.
- (54) Chen, C. C.; Waser, J. One-pot, three-component arylalkynyl sulfone synthesis. *Org. Lett.* **2015**, *17*, 736–739.
- (55) Back, T. G.; Clary, K. N.; Gao, D. Cycloadditions and cyclizations of acetylenic, allenic, and conjugated dienyl sulfones. *Chem. Rev.* **2010**, *110*, 4498–4553.
- (56) Back, T. G. The chemistry of acetylenic and allenic sulfones. *Tetrahedron* **2001**, *57*, 5263–5301.
- (57) Aziz, J.; Messaoudi, S.; Alami, M.; Hamze, A. Sulfinates derivatives: dual and versatile partners in organic synthesis. *Org. Biomol. Chem.* **2014**, *12*, 9743–9759.
- (58) Shinde, P. S.; Patil, N. T. Gold-catalyzed dehydrazinative C(sp)-S coupling reactions of arylsulfonyl hydrazides with ethynylbenziodoxolones for accessing alkynyl sulfones. *Eur. J. Org. Chem.* **2017**, 3512–3515.
- (59) Hamnett, D. J.; Moran, W. J. Improving alkynyl(aryl)iodonium salts: 2-anisyl as a superior aryl group. *Org. Biomol. Chem.* **2014**, *12*, 4156–4162.
- (60) a) Tykwinski, R. R.; Williamson, B. L.; Fischer, D. R.; Stang, P. J.; Arif, A. M. J. A new synthesis of alkynyl sulfones and single crystal x-ray structure of *p*-(tolylsulfonyl)ethyne. *J. Org. Chem.* **1993**, *58*, 5235–5237; b) Liu, Z. D.; Chen, Z. C. Hypervalent iodine in synthesis: 9. A new, effective synthesis of acetylenic sulfones. *Synth. Commun.* **1992**, *22*, 1997–2003. For the review on this topic, see: c) Zhdankin, V. V.; Stang, P. J. Alkynyliodonium salts in organic synthesis. *Tetrahedron Lett.* **1998**, *54*, 10927–10966.
- (61) Fleming, F. F. Nitrile-containing natural products. *Nat. Prod. Rep.* **1999**, *16*, 597–606.
- (62) a) Fleming, F. F.; Yao, L.; Ravikumar, P. C.; Funk, L.; Shook, B. C. Nitrile-containing pharmaceuticals: efficacious roles of the nitrile pharmacophore. *J. Med. Chem.* **2010**, *53*, 7902–7917. b) Kleemann, A.; Engel, J.; Kutscher, B.; Reichert, D. *Pharmaceutical Substances: Synthesis, Patents, Applications*. 4th Ed., Thieme, Stuttgart, **2001**, pp. 241–242, 488–489, 553, 825–826, 1154 and 1598–1599.
- (63) Pollak, P. *Fine Chemicals: The Industry and the Business*, 2nd Ed. (electronic resource), Wiley, **2011**, 312 pp. DOI: 10.1002/9780470946404.
- (64) a) Huang, S.-T.; Hsu, Y.-C.; Yen, Y.-S.; Chou, H. H.; Lin, J. T.; Chang, C.-W.; Hsu, C.-P.; Tsai, C.; Yin, D.-J. Organic dyes containing a cyanovinyl entity in the spacer for solar cells applications. *J. Phys. Chem. C* **2008**, *112*, 19739–19747. b) Miller, J. S.; Manson, J. L. Designer magnets containing cyanides and nitriles. *Acc. Chem. Res.* **2001**, *34*, 563–570.
- (65) Zil'berman, E. N. The Reactions of Nitrile-containing Polymers. *Russ. Chem. Rev.* **1986**, *55*, 39–48.

- (66) Larock, R. C. *Comprehensive Organic Transformations: A Guide to Functional Group Preparations*, 2nd Ed., Wiley-VCH, Weinheim, **2010**, pp 819–955.
- (67) a) *Chemistry of the Cyano Group* (Ed.: Rappoport, Z.), Wiley, London, **1970**, pp 121–312; b) Fatiadi, A. J. Preparation and synthetic applications of cyano compounds. In *The Chemistry of triplebonded functional groups: Part 2; The Chemistry of functional groups. Supplement C* (Eds.: Patai, S., Rappoport, Z.), Wiley, New York, **1983**, DOI: 10.1002/9780470771709.ch9.
- (68) a) Nauth, A. M.; T. Opatz, T. Non-toxic cyanide sources and cyanating agents. *Org. Biomol. Chem.* **2019**, *17*, 11–23; b) Schörgenhuber, J.; Waser, M. New strategies and applications using electrophilic cyanide-transfer reagents under transition metal-free conditions. *Org. Chem. Front.* **2016**, *3*, 1535–1540; c) Ping, Y. Ding, Q.; Peng, Y. Advances in C–CN Bond Formation via C–H Bond Activation. *ACS Catal.* **2016**, *6*, 5989–6005.
- (69) Noller, C. R. *Lehrbuch der Organischen Chemie*; Springer, Berlin-Heidelberg, **1960**. DOI: 10.1007/978-3-642-87324-9.
- (70) Wu, Y.-q.; Limburg, D. C.; Wilkinson, D. E.; Hamilton, G. S. 1-Cyanoimidazole as a mild and efficient electrophilic cyanating agent. *Org. Lett.* **2000**, *2*, 795–797.
- (71) Hughes, T. V.; Hammond, S. D.; Cava, M. P. A convenient new synthesis of 1-cyanobenzotriazole and its use as a C-cyanating reagent. *J. Org. Chem.* **1998**, *63*, 401–402.
- (72) a) Cui, J.; Song, J.; Liu, Q.; Liu, H.; Dong, Y. Transition-metal-catalyzed cyanation by using an electrophilic cyanating agent, *N*-cyano-*N*-phenyl-*p*-toluenesulfonamide (NCTS). *Chem. Asian. J.* **2018**, *13*, 482–495; b) Zhu, X.; Shen, X.-J.; Tian, Z.-Y.; Lu, S.; Tian, L.-L.; Liu, W.-B.; Song, B.; Hao, X.-Q. Rhodium-catalyzed direct bis-cyanation of arylimidazo[1,2- α]pyridine via double C–H activation. *J. Org. Chem.* **2017**, *82*, 6022–6031; c) Li, J.; Ackermann, L. Cobalt-Catalyzed C–H Cyanation of Arenes and Heteroarenes. *Angew. Chem. Int. Ed.* **2015**, *54*, 3635–3638.
- (73) Akula, R.; Xiong, Y.; Ibrahim, H. Electrophilic α -cyanation of 1,3-dicarbonyl compounds. *RSC Adv.* **2013**, *3*, 10731.
- (74) Anbarasan, P.; Neumann, H.; Beller, M. A convenient synthesis of benzonitriles via electrophilic cyanation with *N*-cyanobenzimidazole. *Chem. Eur. J.* **2010**, *16*, 4725–4728.
- (75) Anbarasan, P.; Neumann, H.; Beller, M. A novel and convenient synthesis of benzonitriles: electrophilic cyanation of aryl and heteroaryl bromides. *Chem. Eur. J.* **2011**, *17*, 4217–4222.
- (76) Zhdankin, V. V.; Kuehl, C. J.; Krasutsky, A. P.; Bolz, J. T.; Mismash, B.; Woodward, J. K.; Simonsen, A. J. 1-Cyano-3-(1H)-1,2-benziodoxols: stable cyanoiodinanes and efficient reagents for direct *N*-alkyl cyanation of *N,N*-dialkylarylamines. *Tetrahedron Lett.* **1995**, *36*, 7975–7978.
- (77) Frei, R.; Courant, T.; Wodrich, M. D.; Waser, J. General and practical formation of thiocyanates from thiols. *Chem. Eur. J.* **2015**, *21*, 2662–2668.

- (78) Le Vaillant, F.; Wodrich, M. D.; Waser, J. Room temperature decarboxylative cyanation of carboxylic acids using photoredox catalysis and cyanobenziodoxolones: a divergent mechanism compared to alkylation. *Chem. Sci.* **2017**, *8*, 1790–1800.
- (79) Declas, N.; Le Vaillant, F.; Waser, J. Revisiting the urech synthesis of hydantoins: direct access to enantiopure 1,5-substituted hydantoins using cyanobenziodoxolone. *Org. Lett.* **2019**, *21*, 524–528.
- (80) Wang, X.; Studer, A. Metal-free direct C–H cyanation of alkenes. *Angew. Chem. Int. Ed.* **2018**, *57*, 11792–11796.
- (81) Barrado, A. G.; Zieliński, A.; Goddard, R.; Alcarazo, M. Regio- and stereoselective chlorocyanation of alkynes. *Angew. Chem. Int. Ed.* **2017**, *56*, 13401–13405.
- (82) Zhao, M.; Barrado, A. G.; Sprenger, K.; Golz, C.; Mata, R. A.; Alcarazo, M. Electrophilic cyanative alkenylation of arenes. *Org. Lett.* **2020**, *22*, 4932–4937.
- (83) Johnson, A. W.; LaCount, R. B. The chemistry of ylids. VI. Dimethylsulfonium fluorenylide—a synthesis of epoxides. *J. Am. Chem. Soc.* **1961**, *83*, 417–423.
- (84) Corey, E. J.; Chaykovsky, M. Dimethyloxosulfonium methylide ((CH₃)₂SOCH₂) and dimethylsulfonium methylide ((CH₃)₂SCH₂). Formation and application to organic synthesis. *J. Am. Chem. Soc.* **1965**, *87*, 1353–1364.
- (85) Mondal, M.; Chen, S.; Kerrigan, N. J. Recent developments in vinylsulfonium and vinylsulfoxonium salt chemistry. *Molecules* **2018**, *23*, 738.
- (86) Trost, B. M. Sulfur Ylides: Emerging Synthetic Intermediates. In *Organic chemistry: A Series of Monographs* (Ed.: Melvin, L. S., Jr.), Vol. 31, Academic Press, London, **1975**, 358 pp.
- (87) Block, E. Reactions of Organosulfur Compounds. In: *Organic Chemistry: A Series of Monographs* (Eds.: Blomquist, A. T.; Wasserman, H. H.), Vol. 37, Elsevier Science, **1978**, 336 pp.
- (88) von Eggers Doering, W.; Schreiber, K. C. d-Orbital resonance. II. Comparative reactivity of vinyltrimethylsulfonium and vinyltrimethylammonium ions. *J. Am. Chem. Soc.* **1955**, *77*, 514–520.
- (89) von Eggers Doering, W.; Hoffmann, A. K. d-Orbital resonance. III. Deuterium exchange in methyl “onium” salts and in bicyclo [2.2.1]heptane-1-sulfonium iodide. *J. Am. Chem. Soc.* **1955**, *77*, 521–526.
- (90) Mitchell, K. A. R. Use of outer d orbitals in bonding. *Chem. Rev.* **1969**, *69*, 157–178.
- (91) Lehn, J.-M.; Wipff, G. Stereoelectronic effects. 5. Stereoelectronic properties, stereospecificity, and stabilization of α-oxa and α-thia carbanions. *J. Am. Chem. Soc.* **1976**, *98*, 7498–7505.
- (92) Bernardi, F.; Csizmadia, I. G.; Mangini, A.; Schlegel, H. B.; Whangbo, M.-H.; Wolfe, S. The irrelevance of d-orbital conjugation. I. α-Thiocarbanion. Comparative quantum chemical study of the static and dynamic properties and proton affinities of carbanions adjacent to oxygen and to sulfur. *J. Am. Chem. Soc.* **1975**, *97*, 2209–2218.

- (93) Streitwieser, A.; Williams, J. E. Ab initio SCF-MO calculations of thiomethyl anion. Polarization in stabilization of carbanions. *J. Am. Chem. Soc.* **1975**, *97*, 191–192.
- (94) Dobado, J. A.; Martínez-García, H.; Molina; Sundberg, M. R. Chemical bonding in hypervalent molecules revised. 3. † Application of the atoms in molecules theory to Y_3X-CH_2 (X = N, P, or As; Y = H or F) and H_2X-CH_2 (X = O, S, or Se) ylides. *J. Am. Chem. Soc.* **2000**, *122*, 1144–1149.
- (95) Ranu, B. C.; Banerjee, S. Ionic liquid as catalyst and reaction medium. The dramatic influence of a task-specific ionic liquid, [bmIm]OH, in Michael addition of active methylene compounds to conjugated ketones, carboxylic esters, and nitriles. *Org. Lett.* **2005**, *7*, 3049–3052.
- (96) Michael, A. Ueber die Addition von Natriumacetessig- und Natriummalonsäureäthern zu den Aethern ungesättigter Säuren. *J. Prakt. Chem.* **1887**, *35*, 349–356.
- (97) Brückner, R. Umsetzung von Phosphor- oder Schwefel-stabilisierten C-Nucleophilen mit Carbonylverbindungen: durch Additionen eingeleitete Kondensationen. In *Reaktionsmechanismen: Organische Reaktionen, Stereochemie, moderne Synthesemethoden*, 3. Auflage (Hrst.: Brückner, R.), Lehrbuch; Springer Spektrum: Berlin, Heidelberg, **2015**; pp. 455–483. DOI: 10.1007/978-3-662-45684-2_11.
- (98) Unthank, M. G.; Hussain, N.; Aggarwal, V. K. The use of vinyl sulfonium salts in the stereocontrolled asymmetric synthesis of epoxide- and aziridine-fused heterocycles: application to the synthesis of (-)-balanol. *Angew. Chem. Int. Ed.* **2006**, *118*, 7066–7069.
- (99) Chen, J.; Li, J.; Plutschack, M. B.; Berger, F.; Ritter, T. Regio- and stereoselective thianthrenation of olefins to access versatile alkenyl electrophiles. *Angew. Chem. Int. Ed.* **2020**, *59*, 5616–5620.
- (100) Aukland, M. H.; Talbot, F. J. T.; Fernández-Salas, J. A.; Ball, M.; Pulis, A. P.; Procter, D. J. An Interrupted Pummerer/Nickel-Catalysed Cross-Coupling Sequence. *Angewandte Chemie (International ed. in English)* **2018**, *57*, 9785–9789.
- (101) Matsuo, J.-i.; Yamanaka, H.; Kawana, A.; Mukaiyama, T. A Convenient method for the synthesis of 2-arylaziridines from styrene derivatives via 2-arylethenyl(diphenyl)sulfonium salts. *Chem. Lett.* **2003**, *32*, 392–393.
- (102) Nenajdenko, V. G.; Verteletzkiy, P. V.; Gridnev, I. D.; Shevchenko, N. E.; Balenkova, E. S. Reaction of dimethyl sulfide ditriflate with alkenes. Synthesis of sulfur derivatives of nortricyclane. *Tetrahedron* **1997**, *53*, 8173–8180.
- (103) Šiaučiulis, M.; Ahlsten, N.; Pulis, A. P.; Procter, D. J. Transition-metal-free cross-coupling of benzothiophenes and styrenes in a stereoselective synthesis of substituted (*E,Z*)-1,3-dienes. *Angew. Chem. Int. Ed.* **2019**, *58*, 8779–8783.

- (104) Yar, M.; McGarrigle, E. M.; Aggarwal, V. K. Sulfonium, Ethenyldiphenyl-, 1,1,1-Trifluoromethanesulfonate. In *Encyclopedia of reagents for organic synthesis, online* (Eds.: Paquette, L. A.; Crich, D.; Fuchs, P. L.; Molander, G. A.), Wiley, **2012**. DOI: 10.1002/047084289X.rn01409.
- (105) Jeffrey, G. A. An introduction to hydrogen bonding. Oxford University Press, New York and Oxford, **1997**, 303 pp.; as reviewed by: Dannenberg, J. J. *J. Am. Chem. Soc.* **1998**, *120* (22), 5604.
- (106) Zhou, M.; Tan, X.; Hu, Y.; Shen, H. C.; Qian, X. Highly Chemo- and regioselective vinylation of *N*-heteroarenes with vinylsulfonium salts. *J. Org. Chem.* **2018**, *83*, 8627–8635.
- (107) An, J.; Yang, Q.-Q.; Wang, Q.; Xiao, W.-J. Direct synthesis of pyrrolo[2,1-*a*]isoquinolines by 1,3-dipolar cycloaddition of stabilized isoquinolinium *N*-ylides with vinyl sulfonium salts. *Tetrahedron Lett.* **2013**, *54*, 3834–3837.
- (108) An, J.; Chang, N.-J.; Song, L.-D.; Jin, Y.-Q.; Ma, Y.; Chen, J.-R.; Xiao, W.-J. Efficient and general synthesis of oxazino[4,3- α]indoles by cascade addition-cyclization reactions of (1*H*-indol-2-yl)methanols and vinyl sulfonium salts. *Chem. Commun.* **2011**, *47*, 1869–1871.
- (109) Yar, M.; McGarrigle, E. M.; Aggarwal, V. K. An annulation reaction for the synthesis of morpholines, thiomorpholines, and piperazines from beta-heteroatom amino compounds and vinyl sulfonium salts. *Angew. Chem. Int. Ed.* **2008**, *47*, 3784–3786.
- (110) Matlock, J. V.; Svejstrup, T. D.; Songara, P.; Overington, S.; McGarrigle, E. M.; Aggarwal, V. K. Synthesis of 6- and 7-membered *N*-heterocycles using α -phenylvinylsulfonium salts. *Org. Lett.* **2015**, *17*, 5044–5047.
- (111) Fritz, S.; Moya, J.; Unthank, M.; McGarrigle, E.; Aggarwal, V. An efficient synthesis of azetidines with (2-bromoethyl)sulfonium triflate. *Synthesis* **2012**, *44*, 1584–1590.
- (112) Yar, M.; McGarrigle, E. M.; Aggarwal, V. K. Bromoethylsulfonium salt – a more effective annulation agent for the synthesis of 6- and 7-membered 1,4-heterocyclic compounds. *Org. Lett.* **2009**, *11*, 257–260.
- (113) Mao, Z.; Qu, H.; Zhao, Y.; Lin, X. A general access to 1,1-cyclopropane aminoketones and their conversion into 2-benzoyl quinolines. *Chem. Commun.* **2012**, *48*, 9927–9929.
- (114) Maeda, R.; Ooyama, K.; Anno, R.; Shiosaki, M.; Azema, T.; Hanamoto, T. Preparation and reactions of (β -trifluoromethyl)vinyl sulfonium salt. *Org. Lett.* **2010**, *12*, 2548–2550.
- (115) Srogl, J.; Allred, G. D.; Liebeskind, L. S. Sulfonium salts. Participants par excellence in metal-catalyzed carbon–carbon bond-forming reactions. *J. Am. Chem. Soc.* **1997**, *119*, 12376–12377.
- (116) Lin, H.; Dong, X.; Li, Y.; Shen, Q.; Lu, L. Highly selective activation of vinyl C-S bonds over aryl C-S bonds in the Pd-catalyzed coupling of (*E*)-(β -trifluoromethyl)vinylsulfonium salts: preparation of trifluoromethylated alkenes and dienes. *Eur. J. Org. Chem.* **2012**, 4675–4679.

- (117) Kataoka, T.; Banno, Y.; Watanabe, S.-i.; Iwamura, T.; Shimizu, H. Reactions of alkynylselenonium salts with sodium benzenesulfinate. *Tetrahedron Lett.* **1997**, *38*, 1809–1812.
- (118) Watanabe, S.-i.; Ikeda, T.; Kataoka, T.; Tanabe, G.; Muraoka, O. Development of novel diastereoselective alkenylation of enolates using alkenylselenonium salts. *Org. Lett.* **2003**, *5*, 565–567.
- (119) Watanabe, S.-i.; Nakayama, I.; Kataoka, T. The formation of cyclopropane derivatives bearing 1,2-dicarbonyl groups through tandem michael-favorskii-type reactions with (*E*)- β -styrylselenonium triflate. *Eur. J. Org. Chem.* **2005**, 1493–1496.
- (120) Watanabe, S.-i.; Yamamoto, K.; Itagaki, Y.; Iwamura, T.; Iwama, T.; Kataoka, T.; Tanabe, G.; Muraoka, O. Synthesis and reactivity of β -sulfonylvinylselenonium salts: a simple stereoselective synthesis of β -functionalized (*Z*)-vinyl sulfones. *J. Chem. Soc., Perkin Trans.* **2001**, 239–247.
- (121) Watanabe, S.-i.; Yamamoto, K.; Itagaki, Y.; Kataoka, T. A novel preparation of chiral (*Z*)-O-alkyl enol ethers from alkenylselenonium salts. *J. Chem. Soc., Perkin Trans.* **1999**, 2053–2056.
- (122) Watanabe, S.-i.; Mori, E.; Nagai, H.; Iwamura, T.; Iwama, T.; Kataoka, T. A novel stereoselective preparation of various vinyl sulfide derivatives using β -alkylthioalkenylselenonium salts. *J. Org. Chem.* **2000**, *65*, 8893–8898.
- (123) Boelke, A.; Caspers, L. D.; Nachtsheim, B. J. NH₂-Directed C–H alkenylation of 2-vinylanilines with vinylbenziodoxolones. *Org. Lett.* **2017**, *19*, 5344–5347.
- (124) Stridfeldt, E.; Seemann, A.; Bouma, M. J.; Dey, C.; Ertan, A.; Olofsson, B. Synthesis, characterization and unusual reactivity of vinylbenziodoxolones – novel hypervalent iodine reagents. *Chem. Eur. J.* **2016**, *22*, 16066–16070.
- (125) Huang, X.; Xu, X.-H. Stereospecific synthesis of (*E*)-alkenyl(phenyl)iodonium tetrafluoroborates via zirconium–iodane exchange. *J. Chem. Soc., Perkin Trans. 1* **1998**, 3321–3322.
- (126) Hinkle, R. J.; Poulter, G. T.; Stang, P. J. Palladium(II) and copper(I) cocatalyzed coupling of stereodefined alkenyl(phenyl)iodonium triflates and unsaturated tri-*n*-butylstannanes. *J. Am. Chem. Soc.* **1993**, *115*, 11626–11627.
- (127) Ochiai, M.; Uemura, K.; Oshima, K.; Masaki, Y.; Kunishima, M.; Tani, S. Michael type addition of halides to alkynyl(phenyl)iodonium tetrafluoroborates. Stereoselective synthesis of (*Z*)- β -halovinyl(phenyl)iodonium halides. *Tetrahedron Lett.* **1991**, *32*, 4753–4756.
- (128) Kitamura, T.; Furuki, R.; Taniguchi, H.; Stang, P. J. Stereoselective anti-addition of PhIO·TfOH to terminal alkynes. Preparation of *E*-(β -trifluoromethanesulfonyloxyvinyl)-iodonium triflates. *Tetrahedron Lett.* **1990**, *31*, 703–704.
- (129) Kitamura, T.; Furuki, R.; Taniguchi, H.; Stang, P. J. Electrophilic additions of iodobenzene activated by trifluoromethanesulfonic acid, [PhIO·TfOH], to alkynes. *Tetrahedron* **1992**, *48*, 7149–7156.

- (130) Ochiai, M.; Oshima, K.; Masaki, Y. Nucleophilic vinylic substitutions of (Z)-(β-(phenylsulfonyl)-alkenyl)iodonium tetrafluoroborates with tetrabutyl-ammonium halides: retention of configuration. *Tetrahedron Lett.* **1991**, *32*, 7711–7714.
- (131) Williamson, B. L.; Stang, P. J.; Arif, A. M. Preparation, molecular structure, and Diels-Alder cycloaddition chemistry of β-functionalized alkynyl(phenyl)iodonium salts. *J. Am. Chem. Soc.* **1993**, *115*, 2590–2597.
- (132) Ochiai, M.; Sumi, K.; Nagao, Y.; Fujita, E. Vinyliodonium salts : their stereospecific synthesis and reactions as the activated vinyl halides. *Tetrahedron Lett.* **1985**, *26*, 2351–2354.
- (133) Okuyama, T.; Fujita, M. Generation of cycloalkynes by hydro-iodonio-elimination of vinyl iodonium salts. *Acc. Chem. Res.* **2005**, *38*, 679–686.
- (134) Fujita, M.; Kim, W. H.; Sakanishi, Y.; Fujiwara, K.; Hirayama, S.; Okuyama, T.; Ohki, Y.; Tatsumi, K.; Yoshioka, Y. Elimination-addition mechanism for nucleophilic substitution reaction of cyclohexenyl iodonium salts and regioselectivity of nucleophilic addition to the cyclohexyne intermediate. *J. Am. Chem. Soc.* **2004**, *126*, 7548–7558.
- (135) Radiation Curing in Polymer Science and Technology; (Eds.: Fouassier, J.-P.; Rabek, J. F.), Elsevier Applied Science, London, **1993**, 653 pp.
- (136) Dektar, J. L.; Hacker, N. P. Photochemistry of triarylsulfonium salts. *J. Am. Chem. Soc.* **1990**, *112*, 6004–6015.
- (137) Ito, H.; Marty, J. D.; Mauzac, M. Microlithography. Molecular imprinting. In *Adv. Polymer Sci.*, Vol. 172 (Ed.: Kobayashi, T.), Springer, Berlin-Heidelberg, **2005**. DOI: 10.1007/b14099.
- (138) Ito, H.; Willson, C. G. Chemical amplification in the design of dry developing resist materials. *Polym. Eng. Sci.* **1983**, *23*, 1012–1018.
- (139) Crivello, J. V. Applications of photoinitiated cationic polymerization to the development of new photoresists. In *Polymers in electronics: Based on a symposium sponsored by the Division of Organic Coatings and Plastics Chemistry at the 185. ACS Meeting, Seattle, Washington, March 20–25, 1983; ACS Symposium Series, Vol. 242* (Ed.: Davidson, T.), American Chemical Society, **1984**, pp 3–10. DOI: 10.1021/bk-1984-0242.ch001.
- (140) Saeva, F. D.; Breslin, D. T.; Luss, H. R. Intramolecular photoinduced rearrangements via electron-transfer-induced, concerted bond cleavage and cation radical/radical coupling. *J. Am. Chem. Soc.* **1991**, *113*, 5333–5337.
- (141) Péter, Á.; Perry, G. J. P.; Procter, D. J. Radical C–C Bond Formation using Sulfonium Salts and Light. *Adv. Synth. Catal.* **2020**, *362*, 2135–2142.
- (142) Beak, P.; Sullivan, T. A. One-electron chemical reductions of phenylalkylsulfonium salts. *J. Am. Chem. Soc.* **1982**, *104*, 4450–4457.

- (143) Saeva, F. D. The mechanism of electrocleavage reactions and photorearrangements of some sulfonium salt derivatives. *Tetrahedron* **1986**, *42*, 6123–6129.
- (144) Chung, S.-K.; Sasamoto, K. Reactions of a triarylsulphonium salt with alkoxide nucleophiles: involvement of radical intermediates. *J. Chem. Soc., Chem. Commun.* **1981**, 346–347.
- (145) Wang, X.; Saeva, F. D.; Kampmeier, J. A. Photosensitized reduction of sulfonium salts: evidence for nondissociative electron transfer. *J. Am. Chem. Soc.* **1999**, *121*, 4364–4368.
- (146) Donck, S.; Baroudi, A.; Fensterbank, L.; Goddard, J.-P.; Ollivier, C. Visible-light photocatalytic reduction of sulfonium salts as a source of aryl radicals. *Adv. Synth. Catal.* **2013**, *355*, 1477–1482.
- (147) *Visible light photocatalysis in organic chemistry* (Eds.: Stephenson, C.; Yoon, T.; MacMillan, D. W. C.); Wiley-VCH, Weinheim, Germany, 2018.
- (148) Crivello, J. V.; Lam, J. H. W. A new preparation of triarylsulfonium and -selenonium salts *via* the copper(II)-catalyzed arylation of sulfides and selenides with diaryliodonium salts. *J. Org. Chem.* **1978**, *43*, 3055–3058.
- (149) Zhang, L.; Li, X.; Sun, Y.; Zhao, W.; Luo, F.; Huang, X.; Lin, L.; Yang, Y.; Peng, B. Mild synthesis of triarylsulfonium salts with arynes. *Org. Biomol. Chem.* **2017**, *15*, 7181–7189.
- (150) Li, X.; Sun, Y.; Huang, X.; Zhang, L.; Kong, L.; Peng, B. Synthesis of *o*-aryloxy triarylsulfonium salts *via* aryne insertion into diaryl sulfoxides. *Org. Lett.* **2017**, *19*, 838–841.
- (151) Andersen, K. K.; Papanikolaou, N. E. Synthesis of triarylsulfonium salts from diarylethoxysulfonium salts. *Tetrahedron Lett.* **1966**, *7*, 5445–5449.
- (152) Miller, R. D.; Renaldo, A. F.; Ito, H. Deoxygenation of sulfoxides promoted by electrophilic silicon reagents: preparation of aryl-substituted sulfonium salts. *J. Org. Chem.* **1988**, *53*, 5571–5573.
- (153) Imazeki, S.; Sumino, M.; Fukasawa, K.; Ishihara, M.; Akiyama, T. Facile method for the preparation of triarylsulfonium bromides using grignard reagents and chlorotrimethylsilane as an activator. *Synthesis* **2004**, 1648–1654.
- (154) Akhtar, S. R.; Crivello, J. V.; Lee, J. L. Synthesis of aryl-substituted sulfonium salts by the phosphorus pentoxide-methanesulfonic acid promoted condensation of sulfoxides with aromatic compounds. *J. Org. Chem.* **1990**, *55*, 4222–4225.
- (155) *Ligand Coupling Reactions with Heteroatomic Compounds*, 1st Ed. (Ed.: Finet, J.-P.), Tetrahedron Organic Chemistry series, Vol. 18, Elsevier Science, Oxford, **2011**, 308 pp.
- (156) Kafuta, K.; Korzun, A.; Böhm, M.; Golz, C.; Alcarazo, M. Synthesis, structure, and reactivity of 5-(aryl)dibenzothiophenium triflates. *Angew. Chem. Int. Ed.* **2020**, *59*, 1950–1955.
- (157) Xu, P.; Zhao, D.; Berger, F.; Hamad, A.; Rickmeier, J.; Petzold, R.; Kondratiuk, M.; Bohdan, K.; Ritter, T. Site-selective late-stage aromatic [¹⁸F]Fluorination *via* aryl sulfonium salts. *Angew. Chem. Int. Ed.* **2020**, *59*, 1956–1960.

- (158) Ye, F.; Berger, F.; Jia, H.; Ford, J.; Wortman, A.; Börgel, J.; Genicot, C.; Ritter, T. Aryl sulfonium salts for site-selective late-stage trifluoromethylation. *Angew. Chem. Int. Ed.* **2019**, *58*, 14615–14619.
- (159) Berger, F.; Plutschack, M. B.; Riegger, J.; Yu, W.; Speicher, S.; Ho, M.; Frank, N.; Ritter, T. Site-selective and versatile aromatic C-H functionalization by thianthrenation. *Nature* **2019**, *567*, 223–228.
- (160) Fernández-Salas, J. A.; Pulis, A. P.; Procter, D. J. Metal-free C–H thioarylation of arenes using sulfoxides: a direct, general diaryl sulfide synthesis. *Chem. Commun.* **2016**, *52*, 12364–12367.
- (161) a) Ming, X.-X.; Tian, Z.-Y.; Zhang, C.-P. Base-mediated *O*-arylation of alcohols and phenols by triarylsulfonium triflates. *Chem. Asian. J.* **2019**, *14*, 3370–3379. For the review on single electron transfer, see: b) Zhang, N.; Samanta, S. R.; Rosen, B. R.; Percec, V. Single electron transfer in radical ion and radical-mediated organic, materials and polymer synthesis. *Chem. Rev.* **2014**, *114*, 5848–5958.
- (162) Oae, S.; Khim, Y. H. Alkaline decomposition of triarylsulfonium halides with various bases. *Bull. Chem. Soc. Japan* **1969**, *42*, 3528–3535.
- (163) Kitamura, T.; Miyaji, M.-a.; Soda, S.-i.; Taniguchi, H. Complete retention of configuration in the nucleophilic substitution of 1-phenylbenzo[*b*]thiophenium salts by alkoxide anions. *J. Chem. Soc., Chem. Commun.* **1995**, 1375.
- (164) Kim, K. S.; Ha, S. M.; Kim, J. Y.; Kim, K. 5-Arylthianthreniumyl perchlorates as a benzyne precursor. *J. Org. Chem.* **1999**, *64*, 6483–6486.
- (165) Knapczyk, J. W.; McEwen, W. E. Photolysis of triarylsulfonium salts in alcohol. *J. Org. Chem.* **1970**, *35*, 2539–2543.
- (166) Zhao, J.-N.; Kayumov, M.; Wang, D.-Y.; Zhang, A. Transition-metal-free aryl-heteroatom bond formation via C-S bond cleavage. *Org. Lett.* **2019**, *21*, 7303–7306.
- (167) Mu, L.; Fischer, C. R.; Holland, J. P.; Becaud, J.; Schubiger, P. A.; Schibli, R.; Ametamey, S. M.; Graham, K.; Stellfeld, T.; Dinkelborg, L. M.; Lehmann, L. ¹⁸F-Radiolabeling of aromatic compounds using triarylsulfonium salts. *Eur. J. Org. Chem.* **2012**, 889–892.
- (168) Sander, K.; Galante, E.; Gendron, T.; Yiannaki, E.; Patel, N.; Kalber, T. L.; Badar, A.; Robson, M.; Johnson, S. P.; Bauer, F.; Mairinger, S.; Stanek, J.; Wanek, T.; Kuntner, C.; Kottke, T.; Weizel, L.; Dickens, D.; Erlandsson, K.; Hutton, B. F.; Lythgoe, M. F.; Stark, H.; Langer, O.; Koepp, M.; Årstad, E. Development of fluorine-18 labeled metabolically activated tracers for imaging of drug efflux transporters with positron emission tomography. *J. Med. Chem.* **2015**, *58*, 6058–6080.
- (169) Tian, Z.-Y.; Wang, S.-M.; Jia, S.-J.; Song, H.-X.; Zhang, C.-P. Sonogashira reaction using arylsulfonium salts as cross-coupling partners. *Org. Lett.* **2017**, *19*, 5454–5457.
- (170) Wang, X.-Y.; Song, H.-X.; Wang, S.-M.; Yang, J.; Qin, H.-L.; Jiang, X.; Zhang, C.-P. Pd-catalyzed Suzuki–Miyaura cross-coupling of [Ph₂SR][OTf] with arylboronic acids. *Tetrahedron Lett.* **2016**, *72*, 7606–7612.

- (171) Cowper, P.; Jin, Y.; Turton, M. D.; Kociok-Köhn, G.; Lewis, S. E. Azulenesulfonium salts: accessible, stable, and versatile reagents for cross-coupling. *Angew. Chem. Int. Ed.* **2016**, *55*, 2564–2568.
- (172) Wang, S.-M.; Song, H.-X.; Wang, X.-Y.; Liu, N.; Qin, H.-L.; Zhang, C.-P. Palladium-catalyzed Mizoroki-Heck-type reactions of Ph₂SR_nOTf with alkenes at room temperature. *Chemical Communications* **2016**, *52*, 11893–11896.
- (173) Vasu, D.; Yorimitsu, H.; Osuka, A. Palladium-assisted "aromatic metamorphosis" of dibenzothiophenes into triphenylenes. *Angew. Chem. Int. Ed.* **2015**, *54*, 7162–7166.
- (174) Engl, P. S.; Häring, A. P.; Berger, F.; Berger, G.; Pérez-Bitrián, A.; Ritter, T. C-N Cross-couplings for site-selective late-stage diversification via aryl sulfonium salts. *J. Am. Chem. Soc.* **2019**, *141*, 13346–13351.
- (175) Hedstrand, D. M.; Kruizinga, W. H.; Kellogg, R. M. Light induced and dye accelerated reductions of phenacyl onium salts by 1,4-dihydropyridines. *Tetrahedron Lett.* **1978**, *19*, 1255–1258.
- (176) van Bergen, T. J.; Hedstrand, D. M.; Kruizinga, W. H.; Kellogg, R. M. Chemistry of dihydropyridines. 9. Hydride transfer from 1,4-dihydropyridines to sp³-hybridized carbon in sulfonium salts and activated halides. Studies with NAD(P)H models. *J. Org. Chem.* **1979**, *44*, 4953–4962.
- (177) Hari, D. P.; Schroll, P.; König, B. Metal-free, visible-light-mediated direct C–H arylation of heteroarenes with aryl diazonium salts. *J. Am. Chem. Soc.* **2012**, *134*, 2958–2961.
- (178) Comprehensive organic name reactions and reagents (Ed.: Wang, Z.), Wiley, Hoboken, **2010**, 3824 pp. DOI: 10.1002/9780470638859.
- (179) Sang, R.; Korkis, S. E.; Su, W.; Ye, F.; Engl, P. S.; Berger, F.; Ritter, T. Site-selective C–H oxygenation via aryl sulfonium salts. *Angew. Chem. Int. Ed.* **2019**, *58*, 16161–16166.
- (180) Li, J.; Chen, J.; Sang, R.; Ham, W.-S.; Plutschack, M. B.; Berger, F.; Chhabra, S.; Schnegg, A.; Genicot, C.; Ritter, T. Photoredox catalysis with aryl sulfonium salts enables site-selective late-stage fluorination. *Nat. Chem.* **2020**, *12*, 56–62.
- (181) Huang, C.; Feng, J.; Ma, R.; Fang, S.; Lu, T.; Tang, W.; Du, D.; Gao, J. Redox-neutral borylation of aryl sulfonium salts via C-S activation enabled by light. *Org. Lett.* **2019**, *21*, 9688–9692.
- (182) Trost, B. M.; Bogdanowicz, M. J. Preparation of cyclopropyldiphenylsulfonium and 2-methylcyclopropyldiphenylsulfonium fluoroborate and their ylides. Stereochemistry of sulfur ylides. *J. Am. Chem. Soc.* **1973**, *95*, 5298–5307.
- (183) Kemp, D. S.; Vellaccio, F. Studies toward practical thioxanthene-derived protective groups. 9,10-Propanothioxanthylum salts. *J. Org. Chem.* **1981**, *46*, 1807–1810.
- (184) Aggarwal, V. K.; Thompson, A.; Jones, R. V.H. Synthesis of sulfonium salts by sulfide alkylation; an alternative approach. *Tetrahedron Lett.* **1994**, *35*, 8659–8660.

- (185) Andersen, K. K.; Caret, R. L.; Ladd, D. L. Synthesis of optically active dialkylarylsulfonium salts from alkyl aryl sulfoxides. *J. Org. Chem.* **1976**, *41*, 3096–3100.
- (186) Umemoto, T. Electrophilic perfluoroalkylating agents. *Chem. Rev.* **1996**, *96*, 1757–1778.
- (187) Umemoto, T.; Ishihara, S. Power-variable electrophilic trifluoromethylating agents. S-, Se-, and Te-(trifluoromethyl)dibenzothio-, -seleno-, and -tellurophenium salt system. *J. Am. Chem. Soc.* **1993**, *115*, 2156–2164.
- (188) Teruo, U.; Sumi, I. Power-variable trifluoromethylating agents, (trifluoromethyl)dibenzothio- and -selenophenium salt system. *Tetrahedron Lett.* **1990**, *31*, 3579–3582.
- (189) Shibata, N.; Matsnev, A.; Cahard, D. Shelf-stable electrophilic trifluoromethylating reagents: A brief historical perspective. *Beilstein J. Org. Chem.* **2010**, *6*, No. 65.
- (190) Matsnev, A.; Noritake, S.; Nomura, Y.; Tokunaga, E.; Nakamura, S.; Shibata, N. Efficient access to extended Yagupolskii-Umemoto-type reagents: triflic acid catalyzed intramolecular cyclization of *ortho*-ethynylaryltrifluoromethylsulfanes. *Angew. Chem. Int. Ed.* **2010**, *49*, 572–576.
- (191) Miyatake, K.; Yamamoto, K.; Endo, K.; Tsuchida, E. Superacidified reaction of sulfides and esters for the direct synthesis of sulfonium derivatives. *J. Org. Chem.* **1998**, *63*, 7522–7524.
- (192) Liu, B.; Shine, H. J. Reactions of 5-(alkyl)thianthrenium and other sulfonium salts with nucleophiles. *J. Phys. Org. Chem.* **2001**, *14*, 81–89.
- (193) Burtoloso, A. C. B.; Dias, R. M. P.; Leonarczyk, I. A. Sulfoxonium and sulfonium ylides as diazocarbonyl equivalents in metal-catalyzed insertion reactions. *Eur. J. Org. Chem.* **2013**, 5005–5016.
- (194) Lu, L.-Q.; Li, T.-R.; Wang, Q.; Xiao, W.-J. Beyond sulfide-centric catalysis: recent advances in the catalytic cyclization reactions of sulfur ylides. *Chem. Soc. Rev.* **2017**, *46*, 4135–4149.
- (195) Li, A.-H.; Dai, L.-X.; Aggarwal, V. K. Asymmetric ylide reactions: epoxidation, cyclopropanation, aziridination, olefination, and rearrangement. *Chem. Rev.* **1997**, *97*, 2341–2372.
- (196) Umemura, K.; Matsuyama, H.; Kamigata, N. Alkylation of Several Nucleophiles with Alkylsulfonium Salts. *BCSJ* **1990**, *63*, 2593–2600.
- (197) Varga, B.; Gonda, Z.; Tóth, B. L.; Kotschy, A.; Novák, Z. A Ni-Ir dual photocatalytic Liebeskind coupling of sulfonium salts for the synthesis of 2-benzylpyrrolidines. *Eur. J. Org. Chem.* **2020**, 1466–1471.
- (198) Wang, X.; Truesdale, L.; Yu, J.-Q. Pd(II)-catalyzed *ortho*-trifluoromethylation of arenes using TFA as a promoter. *J. Am. Chem. Soc.* **2010**, *132*, 3648–3649.
- (199) Simkó, D. C.; Elekes, P.; Pázmándi, V.; Novák, Z. Sulfonium salts as alkylating agents for palladium-catalyzed direct *ortho* alkylation of anilides and aromatic ureas. *Org. Lett.* **2018**, *20*, 676–679.

- (200) Tóth, B. L.; Béke, F.; Egyed, O.; Bényei, A.; Stirling, A.; Novák, Z. Synthesis of multifunctional aryl(trifloxyalkenyl)iodonium triflate salts. *ACS omega* **2019**, *4*, 9188–9197.
- (201) Al-huniti, M. H.; Lepore, S. D. Zinc(II) catalyzed conversion of alkynes to vinyl triflates in the presence of silyl triflates. *Org. Lett.* **2014**, *16*, 4154–4157.
- (202) Stang, P. J. Polyvalent iodine in organic chemistry. *J. Org. Chem.* **2003**, *68*, 2997–3008.
- (203) Mantina, M.; Chamberlin, A. C.; Valero, R.; Cramer, C. J.; Truhlar, D. G. Consistent van der Waals radii for the whole main group. *The journal of physical chemistry. A* **2009**, *113*, 5806–5812.
- (204) McCulla, R. D.; Jenks, W. S. Deoxygenation and other photochemical reactions of aromatic selenoxides. *J. Am. Chem. Soc.* **2004**, *126*, 16058–16065.
- (205) MacFarquhar, J. K.; Broussard, D. L.; Melstrom, P.; Hutchinson, R.; Wolkin, A.; Martin, C.; Burk, R. F.; Dunn, J. R.; Green, A. L.; Hammond, R.; Schaffner, W.; Jones, T. F. Acute selenium toxicity associated with a dietary supplement. *Arch. Int. Med.* **2010**, *170*, 256–261.
- (206) a) Bach, R. D.; Badger, R. C.; Lang, T. J. Theoretical studies on E2 elimination reactions. Evidence that syn elimination is accompanied by inversion of configuration at the carbanionic center. *J. Am. Chem. Soc.* **1979**, *101*, 2845–2848; b) Johnson, J. E.; Morales, N. M.; Gorczyca, A. M.; Dolliver, D. D.; McAllister, M. A. Mechanisms of acid-catalyzed Z/E isomerization of imines. *J. Org. Chem.* **2001**, *66*, 7979–7985. c) Strain parameter of cyclopropane = 1.36, of Et is only 0.86: Beckhaus, H.-D. *Sf* Parameters – a measure of the front strain of alkyl groups. *Angew. Chem. Int. Ed. Engl.* **1978**, *17*, 593–594; d) Fischer, P.; Taylor, R. Electrophilic aromatic substitution. Part 26. The effect of the cyclopropyl substituent in aromatic detritiation. *J. Chem. Soc., Perkin Trans 2* **1980**, 781–785.
- (207) Denis, J. N.; Krief, A. New Synthesis of ketene thioacetals, vinylsulfides and their seleno analogues. *Tetrahedron Lett.* **1982**, *23*, 3407–3410.
- (208) Denis, J. N.; Desauvage, S.; Hevesi, L.; Krief, A. New synthetic routes to vinyl sulfides, ketene thioacetals and their seleno analogues from carbonyl compounds. *Tetrahedron Lett.* **1981**, *22*, 4009–4012.
- (209) Kataoka, T.; Watanabe Si, S.-i.; Yamamoto, K.; Yoshimatsu, M.; Tanabe, G.; Muraoka, O. Reactions of diphenyl(phenylethynyl)selenonium salts with active methylene compounds and amides: first isolation of oxyselenuranes 10-Se-4(C3O) as a reaction intermediate. *J. Org. Chem.* **1998**, *63*, 6382–6386.
- (210) Ochiai, M.; Kunishima, M.; Nagao, Y.; Fuji, K.; Shiro, M.; Fujita, E. Tandem Michael-carbene insertion reactions of alkynyliodonium salts. Extremely efficient cyclopentene annulations. *J. Am. Chem. Soc.* **1986**, *108*, 8281–8283.
- (211) Kim, Y. H.; Lee, H.; Kim, Y. J.; Kim, B. T.; Heo, J.-N. Direct one-pot synthesis of phenanthrenes via Suzuki-Miyaura coupling/aldol condensation cascade reaction. *J. Org. Chem.* **2008**, *73*, 495–501.

- (212) Feng, B.; Yang, Y.; You, J. Palladium-catalyzed denitrative Sonogashira-type cross-coupling of nitrobenzenes with terminal alkynes. *Chem. Commun.* **2020**, *56*, 790–793.
- (213) Shen, H.-C.; Tang, J.-M.; Chang, H.-K.; Yang, C.-W.; Liu, R.-S. Short and efficient synthesis of coronene derivatives via ruthenium-catalyzed benzannulation protocol. *J. Org. Chem.* **2005**, *70*, 10113–10116.
- (214) Cho, H. Y.; Ajaz, A.; Himali, D.; Waske, P. A.; Johnson, R. P. Microwave flash pyrolysis. *J. Org. Chem.* **2009**, *74*, 4137–4142.
- (215) Yamamoto, Y.; Matsui, K.; Shibuya, M. A combined experimental and computational study on the cycloisomerization of 2-ethynylbiaryls catalyzed by dicationic arene ruthenium complexes. *Chem. Eur. J.* **2015**, *21*, 7245–7255.
- (216) Zhao, Z.; Britt, L. H.; Murphy, G. K. Oxidative, iodoarene-catalyzed intramolecular alkene arylation for the synthesis of polycyclic aromatic hydrocarbons. *Chem. Eur. J.* **2018**, *24*, 17002–17005.
- (217) Wei, Y.; Duan, A.; Tang, P.-T.; Li, J.-W.; Peng, R.-M.; Zhou, Z.-X.; Luo, X.-P.; Kurmoo, M.; Liu, Y.-J.; Zeng, M.-H. Remote and selective C(sp²)-H olefination for sequential regioselective linkage of phenanthrenes. *Org. Lett.* **2020**, *22*, 4129–4134.
- (218) Tang, J.; Sivaguru, P.; Ning, Y.; Zanoni, G.; Bi, X. Silver-catalyzed tandem C≡C bond hydroazidation/radical addition/cyclization of biphenyl acetylene: one-pot synthesis of 6-methyl sulfonylated phenanthridines. *Org. Lett.* **2017**, *19*, 4026–4029.
- (219) Kitamura, T.; Tanaka, T.; Taniguchi, H.; Stang, P. Selective coupling reactions of alkynyl(phenyl)iodonium tosylates with alkynyl, copper reagents. *J. Chem. Soc., Perkin Trans. 1* **1991**, 2892–2893.
- (220) Han C. H., McEwen W. E. Exchange and redox reactions of diaryl sulfides with aromatic hydrocarbons. *Tetrahedron Lett.* **1970**, *11*, 2629–2632.
- (221) Knapczyk, J. W.; McEwen, W. E. Reactions of triarylsulfonium salts with bases. *J. Am. Chem. Soc.* **1969**, *91*, 145–150.
- (222) Tian, Z.-Y.; Ming, X.-X.; Teng, H.-B.; Hu, Y.-T.; Zhang, C.-P. Transition-metal-free *N*-arylation of amines by triarylsulfonium triflates. *Chem. Eur. J.* **2018**, *24*, 13744–13748.
- (223) Sanger, F. The free amino groups of insulin. *The Biochemical journal* **1945**, *39*, 507–515.
- (224) Hooshmand, S. E.; Heidari, B.; Sedghi, R.; Varma, R. S. Recent advances in the Suzuki-Miyaura cross-coupling reaction using efficient catalysts in eco-friendly media. *Green Chem.* **2019**, *21*, 381–405.
- (225) Wilson, K.; Murray, J.; Jamieson, C.; Watson, A. Cyrene as a bio-based solvent for the Suzuki-Miyaura cross-coupling. *Synlett* **2018**, *29*, 650–654.
- (226) Smith, K.; El-Hiti, G. A. Use of zeolites for greener and more *para*-selective electrophilic aromatic substitution reactions. *Green Chem.* **2011**, *13*, 1579–1608.

- (227) Samanta, R. C.; Yamamoto, H. Selective halogenation using an aniline catalyst. *Chem. Eur. J.* **2015**, *21*, 11976–11979.
- (228) Frantz, D. E.; Weaver, D. G.; Carey, J. P.; Kress, M. H.; Dolling, U. H. Practical synthesis of aryl triflates under aqueous conditions. *Org. Lett.* **2002**, *4*, 4717–4718.
- (229) Kégl, T. R.; Kollár, L.; Kégl, T. DFT Study on the oxidative addition of 4-substituted iodobenzenes on Pd(0)-phosphine complexes. *Adv. Phys. Chem.* **2015**, 1–6.
- (230) Kotha, S.; Chakraborty, K.; Brahmachary, E. A general and simple method for the synthesis of star-shaped thiophene derivatives. *Synlett* **1999**, 1621–1623.
- (231) Blakemore, D. C. Suzuki-Miyaura coupling. In *Synthetic methods in drug discovery, Vol. 1* (Eds.: Blakemore, D. C.; Doyle, P. M.; Fobian, Y. M.), Royal Society of Chemistry, Cambridge, **2016**, pp. 1–89.
- (232) Wolfe, J. P.; Singer, R. A.; Yang, B. H.; Buchwald, S. L. Highly active palladium catalysts for suzuki coupling reactions. *J. Am. Chem. Soc.* **1999**, *121*, 9550–9561.
- (233) Stille, J. K.; Lau, K. S. Y. Mechanisms of oxidative addition of organic halides to Group 8 transition-metal complexes. *Acc. Chem. Res.* **1977**, *10*, 434–442.
- (234) Umemoto, T.; Zhang, B.; Zhu, T.; Zhou, X.; Zhang, P.; Hu, S.; Li, Y. Powerful, thermally stable, one-pot-preparable, and recyclable electrophilic trifluoromethylating agents: 2,8-difluoro- and 2,3,7,8-tetrafluoro-S-(trifluoromethyl)dibenzothiophenium salts. *J. Org. Chem.* **2017**, *82*, 7708–7719.
- (235) Murugan, K.; Nainamalai, D.; Kanagaraj, P.; Nagappan, S. G.; Palaniswamy, S. Green-synthesized nickel nanoparticles on reduced graphene oxide as an active and selective catalyst for suzuki and Glaser-Hay coupling reactions. *Appl. Organomet. Chem.* **2020**, *34*, e5778.
- (236) Chassaing, S.; Alix, A.; Boningari, T.; Sani Souna Sido, K.; Keller, M.; Kuhn, P.; Louis, B.; Sommer, J.; Pale, P. Copper(I)-zeolites as new heterogeneous and green catalysts for organic synthesis. *Synthesis* **2010**, 1557–1567.
- (237) Gao, C.; Nakao, S.; Blum, S. A. Borylative heterocyclization without air-free techniques. *J. Org. Chem.* **2020**, *85*, 10350–10368.
- (238) Feng, L.; Hu, T.; Zhang, S.; Xiong, H.-Y.; Zhang, G. Copper-mediated deacylative coupling of ynones via C–C bond activation under mild conditions. *Org. Lett.* **2019**, *21*, 9487–9492.
- (239) Sakamoto, R.; Kume, S.; Nishihara, H. Visible-light photochromism of triarylamine- or ferrocene-bound diethynylethenes that switches electronic communication between redox sites and luminescence. *Chem. Eur. J.* **2008**, *14*, 6978–6986.
- (240) Aragonès, A. C.; Darwish, N.; Ciampi, S.; Jiang, L.; Roesch, R.; Ruiz, E.; Nijhuis, C. A.; Díez-Pérez, I. Control over near-ballistic electron transport through formation of parallel pathways in a single-molecule wire. *J. Am. Chem. Soc.* **2019**, *141*, 240–250.

- (241) Paixão, D. B.; Rampon, D. S.; Salles, H. D.; Soares, E. G. O.; Bilheri, F. N.; Schneider, P. H. Trithiocarbonate anion as a sulfur source for the synthesis of 2,5-disubstituted thiophenes and 2-substituted benzobthiophenes. *J. Org. Chem.* **2020**, *85*, 12922–12934.
- (242) Mallory, F. B.; Mallory, C. W. Photocyclization of Stilbenes and Related Molecules. In *Organic reactions*; Wiley Online Library **2004**-; pp 1–456. DOI: 10.1002/0471264180.or030.01.
- (243) Landarani-Isfahani, A.; Mohammadpoor-Baltork, I.; Mirkhani, V.; Moghadam, M.; Tangestaninejad, S.; Amiri Rudbari, H. Palladium nanoparticles immobilized on a nano-silica triazine dendritic polymer: a recyclable and sustainable nanoreactor for C–S cross-coupling. *RSC Adv.* **2020**, *10*, 21198–21205.
- (244) Zhang, Q.; Wang, D.; Wang, X.; Ding, K. (2-Pyridyl)acetone-promoted Cu-catalyzed *O*-arylation of phenols with aryl iodides, bromides, and chlorides. *J. Org. Chem.* **2009**, *74*, 7187–7190.
- (245) Chen, X.-Y.; Nie, X.-X.; Wu, Y.; Wang, P. *para*-Selective arylation and alkenylation of monosubstituted arenes using thianthrene S-oxide as a transient mediator. *Chem. Commun.* **2020**, *56*, 5058–5061.
- (246) Malapit, C. A.; Ichiishi, N.; Sanford, M. S. Pd-catalyzed decarbonylative cross-couplings of aroyl chlorides. *Org. Lett.* **2017**, *19*, 4142–4145.
- (247) Mizuta, S.; Stenhagen, I. S. R.; O'Duill, M.; Wolstenhulme, J.; Kirjavainen, A. K.; Forsback, S. J.; Tredwell, M.; Sandford, G.; Moore, P. R.; Huiban, M.; Luthra, S. K.; Passchier, J.; Solin, O.; Gouverneur, V. Catalytic decarboxylative fluorination for the synthesis of tri- and difluoromethyl arenes. *Org. Lett.* **2013**, *15*, 2648–2651.
- (248) Unroe, M. R.; Reinhardt, B. A. One pot synthesis of *p*-polyphenyls *via* the intramolecular cyclization of 3-dimethyl-amino-hex-5-en-1-ynes. *Synthesis* **1987**, 981–986.